DTIC FILE COPY

(2)

AD-A208 925

AFWAL-TR-89-2008

LUBRICANT EVALUATION AND PERFORMANCE

Costandy S. Saba
Hoover A. Smith
Michael A. Keller
Robert E. Kauffman
Vinod K. Jain

University of Dayton Research Institute
Dayton, Ohio 45469

April 1989

Final Technical Report for Period January 1987 - June 1988

APPROVED FOR PUBLIC RELEASE; DISTRIBUTION UNLIMITED

DTIC
ELECTE
JUN 12 1989
H

AERO PROPULSION LABORATORY
AIR FORCE WRIGHT AERONAUTICAL LABORATORIES
AIR FORCE SYSTEMS COMMAND
WRIGHT-PATTERSON AIR FORCE BASE, OHIO 45433-6563

89 6 12 003

NOTICE

When Government drawings, specifications, or other data are used for any purpose other than in connection with a definitely related Government procurement operation, the United States Government thereby incurs no responsibility nor any obligation whatsoever; and the fact that the government may have formulated, furnished, or in any way supplied the said drawings, specifications, or other data, is not to be regarded by implication or otherwise as in any manner licensing the holder or any other person or corporation, or conveying any rights or permission to manufacture use, or sell any patented invention that may in any way be related thereto.

This report has been reviewed by the Office of Public Affairs (ASD/PA) and is releasable to the National Technical Information Service (NTIS). At NTIS, it will be available to the general public, including foreign nations.

This technical report has been reviewed and is approved for publication.

Lynne M. Schoen

LYNNE M. SCHOEN
Lubrication Branch
Fuels and Lubrication Division
Aero Propulsion and Power Laboratory

Ronald D. Dayton

RONALD D. DAYTON, Acting Chief
Lubrication Branch
Fuels and Lubrication Division
Aero Propulsion and Power Laboratory

FOR THE COMMANDER

Benito P. Botteri

BENITO P. BOTTERI, Assistant Chief
Fuels and Lubrication Division
Aero Propulsion and Power Laboratory

If your address has changed, if you wish to be removed from our mailing list, or if the addressee is no longer employed by your organization please notify WRDC/POSL, *W-PAFB, OH 45433 to help us maintain a current mailing list.*

Copies of this report should not be returned unless return is required by security considerations, contractual obligations, or notice on a specific document.

REPORT DOCUMENTATION PAGE

Form Approved OMB No. 0704-0188

1a. REPORT SECURITY CLASSIFICATION: UNCLASSIFIED	1b. RESTRICTIVE MARKINGS: None
2a. SECURITY CLASSIFICATION AUTHORITY: N/A	3. DISTRIBUTION/AVAILABILITY OF REPORT: Approved for Public Release; Distribution Unlimited
2b. DECLASSIFICATION/DOWNGRADING SCHEDULE: N/A	
4. PERFORMING ORGANIZATION REPORT NUMBER(S): UDR-TR-88-95	5. MONITORING ORGANIZATION REPORT NUMBER(S): AFWAL-TR-89-2008
6a. NAME OF PERFORMING ORGANIZATION: University of Dayton Research Institute; 6b. OFFICE SYMBOL (If applicable):	7a. NAME OF MONITORING ORGANIZATION: Aero Propulsion Laboratory (AFWAL/POSL) Air Force Wright Aeronautical Laboratories
6c. ADDRESS (City, State, and ZIP Code): 300 College Park Dayton, Ohio 45469	7b. ADDRESS (City, State, and ZIP Code): Wright-Patterson AFB, Ohio 45433-6563
8a. NAME OF FUNDING/SPONSORING ORGANIZATION; 8b. OFFICE SYMBOL (If applicable):	9. PROCUREMENT INSTRUMENT IDENTIFICATION NUMBER: F33615-85-C-2507
8c. ADDRESS (City, State, and ZIP Code):	10. SOURCE OF FUNDING NUMBERS: PROGRAM ELEMENT NO. 62203F; PROJECT NO. 3048; TASK NO. 06; WORK UNIT ACCESSION NO. 41

11. TITLE (Include Security Classification)

Lubricant Evaluation and Performance

12. PERSONAL AUTHOR(S)

Saba, Costandy S., Smith, Hoover A., Keller, Michael A., Kauffman, Robert E., Jain, Vinod K.

13a. TYPE OF REPORT	13b. TIME COVERED	14. DATE OF REPORT (Year, Month, Day)	15. PAGE COUNT
Final	FROM Jan 87 TO Jun 88	April 1989	553

16. SUPPLEMENTARY NOTATION

17. COSATI CODES			18. SUBJECT TERMS (Continue on reverse if necessary and identify by block number)
FIELD	GROUP	SUB-GROUP	Lubricant Degradation, Deposition, Wear, Load Carrying Capacity, Foaming, Lubricant Monitoring, Wear Metal Analysis,
11	08		
14	02		

19. ABSTRACT (Continue on reverse if necessary and identify by block number)

This effort involved the development of improved methods for defining and measuring turbine engine lubricant performance and the development of improved techniques for lubricant monitoring, lubrication system health monitoring, investigating antiwear characteristics and load carrying capacities of lubricants.

In Task I, Arrhenius plots were developed for describing the effective life of MIL-L-7808, MIL-L-23699 and 4 cSt viscosity candidate lubricants as a function of time and temperature for selected limiting values of changes in physical and chemical properties. Relative ranking of the lubricants was established with respect to their stability which depended to some degree on the specific selected limiting test values. Stabilities of some high temperature lubricants were also investigated using Corrosion/Oxidation testing. Some of these fluids exhibited less than 50% viscosity (40°C) change and no corrosion of metal coupons when tested at 320°C for over 400 hours. Ranking of new

20. DISTRIBUTION/AVAILABILITY OF ABSTRACT	21. ABSTRACT SECURITY CLASSIFICATION	
☒ UNCLASSIFIED/UNLIMITED ☐ SAME AS RPT. ☐ DTIC USERS	UNCLASSIFIED	
22a. NAME OF RESPONSIBLE INDIVIDUAL: Lynne M. Schoen	22b. TELEPHONE (Include Area Code): (513) 255-3100	22c. OFFICE SYMBOL: AFWAL/POSL

18. (Concluded)
Atomic Emission, Atomic Absorption, Spectrometric Oil Analysis, Gas Chromatography, Microfiltration, Wear Particle Analyzer, Remaining Useful Lubricant Life.

19. (Concluded)
lubricants with respect to their deposit forming characteristics using the AFAPL Static Coker was in general similar to the MCRT and coking propensity tests. Thermal and oxidative stressing changed the ranking of the lubricants. Foaming characteristics of MIL-L-7808 lubricants were investigated using static foam testing with various air dispersers, air flow rates and sample volume for developing a 25 mL sample volume test. The 25 mL test using 13/16 inch diameter 5 micron rated pore size sparger correlated the best with Test Method 3213 for lubricants having distinct oil/foam interfaces.

In Task II, significant improvement in AE spectrometer sensitivity for analyzing wear metal particles was achieved when using a cup-tip electrode with the reversible polarity pin stand. A 6-gallon capacity microfiltration test rig was designed and constructed under Phase I of this program to simulate fine filtration in gas turbine engine lubrication systems. Six microfiltration tests were conducted using samples from a wear metal generator, T56 gearboxes, J57 engine simulator and other used oils. The 3 micron filtration system was effective in removing wear debris $\geq$ microns. The capability of the wear particle analyzer (WPA) was evaluated for the analysis of metallic iron in lubricants and responded to changes in concentrations of ferromagnetic wear debris.

In Task III, the COBRA, a dielectric constant (DC) tester and a dielectric breakdown strength device were evaluated as lubricant monitoring devices. Relationships between chemical changes in the lubricants and their respective COBRA and DC tester readings were investigated. The dielectric breakdown strength did not correlate well with lubricant condition.

In Tasks IV and V, an assessment of the literature on lubricant load carrying capacity (LCC) test methods was made. Various wear test configurations were investigated as possible techniques for determining the LCC of MIL-L-7808 MIL-L-7808, MIL-L-23699 and some high temperature lubricants. Effects of load, speed and lubricant formulations containing various concentrations of TCP on wear scar size and wear volume rates were determined

In Task VI, a software system was developed and implemented on the Zenith Z-100 microcomputer for storage, retrieval and correlation of MIL-L-7808 lubricant qualification data.

In Task VII, the remaining useful life of a lubricant evaluation rig (RULLER) was developed for MIL-L-7808 and MIL-L-23699 type lubricants and was based on reductive cyclic voltammetry. A single board voltammograph was developed to reduce the size and cost of the RULLER. The RULLER candidates are being field tested and data to date indicats satisfactory capability for assessing the remaining useful lives of used lubricants.

FOREWORD

This report describes the research conducted by personnel of the University of Dayton Research Institute on Contract No. F33615-85-C-2507. The work was conducted at the Aero Propulsion Laboratory, Air Force Wright Aeronautical Laboratories, Wright-Patterson AFB, Ohio.

The work was accomplished under Project 3048, Task 304806, Work Unit 30480641, Lubricant Evaluation and Performance, with Ms. Lynne M. Schoen as the project monitor.

The work reported herein was performed during 18 January 1987 to 17 June 1988.

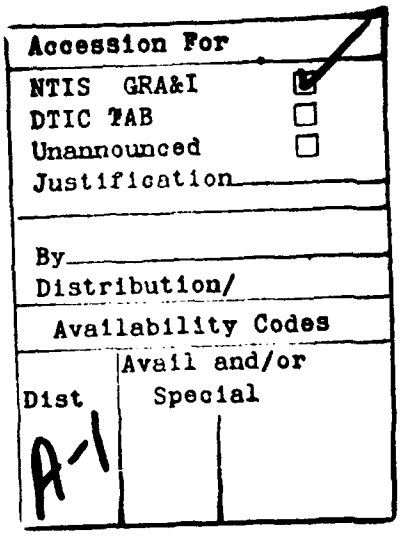

TABLE OF CONTENTS

SECTION		PAGE
I	INTRODUCTION	1
II	DEVELOPMENT OF IMPROVED METHODS FOR MEASURING LUBRICANT PERFORMANCE	5
	1. LUBRICANT OXIDATIVE STABILITY	5
	a. Introduction	5
	b. Test Apparatus	5
	c. Test Procedure	5
	d. Test Lubricants and Test Conditions	5
	e. Results and Discussion	7
	f. Summary	34
	2. LUBRICANT CONFINED HEAT STABILITY	35
	a. Introduction	35
	b. Test Apparatus	35
	c. Test Procedure	35
	d. Test Lubricants and Test Conditions	36
	e. Results and Discussion	36
	f. Summary	44
	3. CORROSIVENESS AND OXIDATIVE STABILITY	45
	a. Introduction	45
	b. Test Apparatus	45
	c. Test Procedure	46
	d. Test Lubricants and Conditions	46
	e. Results and Discussion	47
	(1) MIL-L-23699 Lubricants	47

TABLE OF CONTENTS (CONTINUED)

SECTION				PAGE
II		(2)	High Temperature Fluids	50
			(a) General	50
			(b) Comparison of Data Using D 4871 Tubes and Squires Tubes	51
			(c) Thermal Stressing Study	53
			(d) Effect of Nascent Wear Metal on 5P4E Oxidative Stability	55
			(e) Long Term Oxidative Testing of O-67-1 Fluid	59
			(f) Weak Acid Number Determinations of Polyphenyl Ether Fluid	63
			(g) Effect of Additive A Concentration and Other Materials on Corrosion and Oxidative Stability of 5P4E Fluid O-77-6	70
			(h) Basestock Analysis of New and Stressed O-67-1 and O-77-6 Lubricants	76
			(i) Evaluation of Other Polyphenyl Ether Lubricants	98
			(j) Evaluation of Chemical and Electrical Oxidation Stressing Techniques for Monitoring Polyphenyl Ether Lubricants	103
		f.	Summary	115
	4.		ADDITIVE ANALYSIS	117
		a.	Gas Chromatographic Analysis of Additive A in PPE During Oxidation Testing	118
		b.	Tin Analysis of Oxidized Formulated PPEs by Spectrophotometry	118
		c.	Filtration of Oxidatively Stressed Formulated PPEs	121

TABLE OF CONTENTS (CONTINUED)

SECTION			PAGE
II	d.	Identification of Intermediate Tin Species in Oxidatively Stressed Formulated PPEs	123
		(1) Production of Sn Species	123
		(2) X-ray Diffraction (XD) Analyses	124
		(3) Thermogravimetric Analyses	127
		(4) Infrared Spectroscopic Analyses	130
		(5) X-ray Photoelectron Spectrometric Technique	133
		(6) Mossbauer Analysis	142
		(7) Summary	144
	5.	LUBRICANT DEPOSITION STUDIES	144
	a.	AFAPL Static Coker Study	144
		(1) Introduction	144
		(2) Apparatus and Procedure	145
		(3) Test Lubricants	146
		(4) Results and Discussion	146
		(a) Coking Study of Correlation Lubricant OP-369	146
		(b) Effect of Brass Test Specimens on Deposits	146
		(c) Effect of Wear Debris on Lubricant Coking	151
		(d) Solubility Study of Deposits	151
		(e) Effect of Confined Heat and Oxidative Stressing on AFAPL Static Coker Deposits	154
		(f) Static Coker Deposits as a Function of Test Time and Temperature	154

TABLE OF CONTENTS (CONTINUED)

SECTION			PAGE
II		(g) AFAPL Static Coker Testing of High Temperature Lubricant O-67-1	160
		(5) Summary	162
	b.	Micro Carbon Residue Tester (MCRT)	163
		(1) Introduction	163
		(2) Test Apparatus and Procedure	164
		(3) Test Lubricants	164
		(4) Results and Discussion	164
		(5) Summary	172
	c.	Coking Propensity Test	172
		(1) Introduction	172
		(2) Test Apparatus	172
		(3) Test Procedure	173
		(4) Test Lubricants	173
		(5) Results and Discussion	174
		(6) Summary	177
	6.	LUBRICANT FOAMING STUDY	177
	a.	Introduction	177
	b.	Test Apparatus	178
	c.	Test Procedure	178
	d.	Test Lubricants	178
	e.	Results and Discussion	180
		(1) Repeatability of Test Data Between Phase 1 and Phase 2 for Lubricants Having Distinct Foaming Characteristics	180

TABLE OF CONTENTS (CONTINUED)

SECTION			PAGE
II		(2) Correlation of Test Method 3213 Foam Test Data with 25 mL Volume Foam Test Data	180
	f.	Summary	185
III	DEVELOPMENT OF IMPROVED LUBRICATION SYSTEM HEALTH MONITORING TECHNIQUES		190
	1.	INTRODUCTION	190
	2.	BACKGROUND	191
	3.	ATOMIC EMISSION SPECTROMETER	193
	a.	Rotating Disk Electrode Ashing Study	193
		(1) Introduction	193
		(2) Procedure	193
		(3) Effect of Exposure Time and Spark Intensity	193
		(4) Effect of Surface Density on Emission Signal	196
	b.	Electronic Spark Source with Reversible Polarity Pin Stand	196
		(1) Introduction	196
		(2) Procedure	198
		(a) Electrodes	198
		(b) Emission Spectrometer Parameters	199
		(3) Results and Discussion	201
		(4) Conclusions	207
	4.	MICROFILTRATION	207
	a.	Introduction	207
	b.	Background	208
	c.	Apparatus	209

TABLE OF CONTENTS (CONTINUED)

SECTION			PAGE
III	d.	Test Lubricants	209
	e.	Results and Discussion	211
		(1) Wear Debris Generated Within Filtration Test Rig	211
		(2) Wear Metal Generator	213
		(3) Operating and Test Parameters for the Filtration Test Rig	215
		(4) Microfiltration Testing	219
		(a) Test No. 1	219
		(b) Test No. 2	228
		(c) Test No. 3	236
		(d) Test No. 4	242
		(e) Test No. 5	248
		(f) Test No. 6	254
		(5) Correlation of Microfiltration Testing	261
		(6) Conclusions	266
		(7) Recommendations	268
	5.	DETERMINATION OF METALLIC IRON IN WEAR DEBRIS USING A WEAR PARTICLE ANALYZER	269
	a.	Introduction	269
	b.	Instrumentation	270
		(1) WPA	270
		(2) Magnetometer	271
		(3) Acid Dissolution Method (ADM)	271
		(4) Solvent Extraction/Atomic Absorption (SE/AA)	271

TABLE OF CONTENTS (CONTINUED)

SECTION			PAGE
III	c.	Samples	272
		(1) 325 Mesh Fe Powder	272
		(2) Sieved Fe Powder	272
		(3) Fe_3O_4 Powder	273
		(4) Pin-On-Disk Samples	273
		(5) Used Engine Oil Samples	273
	d.	Analytical Procedures	273
		(1) WPA Calibration	273
		(2) Typical Sample Analysis on the WPA	273
		(3) Quantitative Collection of the Filtrate	274
		(4) Particle Size Distribution	274
		(5) Modified Sample Introduction Technique	275
	e.	Results and Discussion	275
		(1) Effect of Particle Size and Filter Fiber Size	275
		(2) Effect of Sample Volume	277
		(3) Particle Size Limitation	279
		(4) Modified Sample Introduction System	282
		(5) Effect of Flow Rate	284
		(6) Comparative Analyses	287
		(7) Analysis of Used Oils	289
	f.	Summary	292
	g.	Conclusions	292
IV	INVESTIGATION OF LUBRICANT MONITORING TECHNIQUES		294
	1.	INTRODUCTION	294

TABLE OF CONTENTS (CONTINUED)

SECTION			PAGE
IV	2.	MONITORING OF LUBRICANTS BY DIELECTRIC CONSTANT	294
		a. Theory and Design of Instrument	294
		b. Lubri Sensor Analysis of Degraded Turbine Engine Lubricants	295
		(1) Confined Heat Stability Test Lubricants	296
		(2) Squires Oxidative Test Samples	296
		(3) Corrosion and Oxidation Test Samples	302
		c. Lubri Sensor Analysis of Lubricant with Simulated Wear Particles	307
		d. Calibration Standards	308
		e. Lubri Sensor Analysis of Oxidized Polyphenyl Ethers	309
		f. Summary	311
	3.	COMPLETE OIL BREAKDOWN RATE ANALYZER	312
		a. Introduction	312
		b. Effect of Dielectric Constant Changes on COBRA Response	313
		c. Nature of Charge Carrier in COBRA Active Lubricants	313
		(1) Adsorption Chromatography of Degraded Lubricants	316
		(2) Other COBRA Active Compounds	326
		d. Conclusions	329
	4.	DIELECTRIC BREAKDOWN STRENGTH OF MIL-L-7808 LUBRICANTS	330
V		LUBRICANT LOAD CARRYING CAPABILITY TEST ASSESSMENT	332
	1.	INTRODUCTION	332
	2.	TEST PROCEDURES	333
	3.	RESULTS AND DISCUSSION	334
		a. Extreme Pressure Test	334

TABLE OF CONTENTS (CONTINUED)

SECTION			PAGE
V		b. Gear Simulation Test	349
		c. Comparison of Different Test Methods	351
	4.	CONCLUSION	356
VI	DEVELOPMENT OF SPECIFICATION WEAR TEST		358
	1.	INTRODUCTION	358
	2.	EXPERIMENTAL	358
		a. Apparatus and Procedures	358
		b. Analysis	359
	3.	RESULTS AND DISCUSSION	362
		a. Accuracy	362
		b. Load Effects	362
		c. Speed Effects	367
		d. Differences in Wear Prevention Properties of Lubricants	370
		e. One Hour Versus Twenty Hour Testing	370
	4.	SUMMARY	380
	5.	CONCLUSIONS	380
VII	DEVELOPMENT OF LUBE DATA STORAGE AND RETRIEVAL SYSTEM		382
VIII	RULLER DEVELOPMENT		383
	1.	INTRODUCTION	383
	2.	EXPERIMENTAL	384
		a. Instrumentation	384
		(1) Universal Single Board Voltammograph	384
		(2) Microcomputer System	384
		(3) Atomic Emission Spectrometer-Multichannel Capacitor System	385

TABLE OF CONTENTS (CONTINUED)

SECTION				PAGE
VIII		(4)	Gas Chromatograph	385
	b.		Electrode System	385
	c.		Laser 128 Microcomputer Software	387
	d.		Chemicals	387
	e.		Lubricating Oils	387
		(1)	Laboratory Stressed MIL-L-23699 Oil Samples	387
		(2)	Used MIL-L-7808 Oils Obtained from Engine Test Stand	387
		(3)	Used MIL-L-7808 and MIL-L-23699 Oil Samples Obtained for Evaluating the RULLER Candidate	388
		(4)	Used Gas Turbine Lubricating Oils Obtained from RULLER Field Test	388
	f.		Reductive Cyclic Technique	389
	3.		RESULTS AND DISCUSSION	389
	a.		Development of RULLER Candidate for MIL-L-7808 and MIL-L-23699 Lubricating Oils	389
		(1)	Introduction	389
		(2)	Effects of Lubricating Oil Formulation on the SBV-IIe RULLER Candidate's RUL Evaluations	390
			(a) Introduction	390
			(b) Cyclic Voltammetric Analyses of the Fresh MIL-L-23699 Lubricating Oils	391
			(c) Optimization of the RCV Analyses for the MIL-L-23699 Lubricating Oils	394
			(d) Reduction Voltammograms Produced by the Fresh and Laboratory Stressed 0-79-18 Oils	394

TABLE OF CONTENTS (CONTINUED)

SECTION			PAGE
VIII		(e) Mathematical Relationships Among the SBV-IIe RULLER Candidate's Results and the RUL of the MIL-L-23699 Oils	395
		(f) Summary	399
	(3)	SBV-IIe RULLER Candidate Evaluations of Authentic Used MIL-L-7808 and MIL-L-23699 Oil Samples	399
		(a) Introduction	399
		(b) Failure Oil Sample Series Analyses	400
		(c) Hit Oil Sample Series Analyses	407
		(d) Routine Oil Sample Series Analyses	414
		(e) Summary	416
	b.	Production and Evaluation of RULLER Demonstration Devices	418
		(1) Introduction	418
		(2) Production of the RULLER Demonstration Devices	419
		(3) Evaluation of the RULLER Demonstration Devices	420
		(4) Summary	423
	c.	Field Testing of RULLER Demonstration Devices	423
		(1) Introduction	423
		(2) Air Force Base "A" RULLER Results	423
		(3) UDRI RULLER Results	426
		(4) Air Force Base "B" RULLER Results	427
		(5) AFWAL/POSL C-130 RULLER Results	429
		(6) Air Force Base "C" RULLER Results	429
		(7) Summary	429

TABLE OF CONTENTS (CONCLUDED)

SECTION		PAGE
VIII	d. Conclusions	430
IX	RECOMMENDATIONS	431
APPENDIX A	LUBRICANT PERFORMANCE TEST DATA	439
APPENDIX B	IRON CONCENTRATIONS AND PARTICLE SIZE DISTRIBUTIONS OF MICROFILTRATION SAMPLES	494
APPENDIX C	SCHEMATIC FOR RULLER CANDIDATE	500
APPENDIX D	CHARACTERIZATION OF STRESSED MIL-L-23699 TYPE OIL SAMPLES FOR RULLER STUDIES	507
REFERENCES		513

LIST OF ILLUSTRATIONS

FIGURE		PAGE
1.	Effect of Temperature on Lubricant Life Using DERD Method No. 9, Total Acid Number Increase Limit of 1.0	8
2.	Effect of Temperature on Lubricant Life Using DERD Method No. 9, Total Acid Number Increase Limit of 1.5	9
3.	Effect of Temperature on Lubricant Life Using DERD Method No. 9, Total Acid Number Increase Limit of 3.0	10
4.	Effect of Temperature on Lubricant Life Using DERD Method No. 9, Total Acid Number Increase Limit of 1.0 (4 cSt Fluids)	12
5.	Effect of Temperature on Lubricant Life Using DERD Method No. 9, Total Acid Number Increase Limit of 1.5 (4 cSt Fluids)	13
6.	Effect of Temperature on Lubricant Life Using DERD Method No. 9, Total Acid Number Increase Limit of 3.0 (4 cSt Fluids)	14
7.	Effect of Temperature on Lubricant Life Using DERD Method No. 9, Viscosity Increase Limit of 15%	16
8.	Effect of Temperature on Lubricant Life Using DERD Method No. 9, Viscosity Increase Limit of 25%	17
9.	Effect of Temperature on Lubricant Life Using DERD Method No. 9, Viscosity Increase Limit of 35%	18
10.	Effect of Temperature on Lubricant Life Using DERD Method No. 9, Viscosity Increase Limit of 15% (4 cSt Fluids)	19
11.	Effect of Temperature on Lubricant Life Using DERD Method No. 9, Viscosity Increase Limit of 25% (4 cSt Fluids)	20
12.	Effect of Temperature on Lubricant Life Using DERD Method No. 9, Viscosity Increase Limit of 35% (4 cSt Fluids)	21
13.	Effect of Temperature on Lubricant Life Using DERD Method No. 9, Volatilization Loss Limit of 15%	24
14.	Effect of Temperature on Lubricant Life Using DERD Method No. 9, Volatilization Loss Limit of 25%	25

LIST OF ILLUSTRATIONS (CONTINUED)

FIGURE		PAGE
15.	Effect of Temperature on Lubricant Life Using DERD Method No. 9, Volatilization Loss Limit of 35%	26
16.	Effect of Temperature on Lubricant Life Using DERD Method No. 9, Volatilization Loss Limit of 15% (4 cSt Fluids)	27
17.	Effect of Temperature on Lubricant Life Using DERD Method No. 9, Volatilization Loss Limit of 25% (4 cSt Fluids)	28
18.	Effect of Temperature on Lubricant Life Using DERD Method No. 9, Volatilization Loss Limit of 35% (4 cSt Fluids)	29
19.	Effect of Temperature on Lubricant Life Using DERD Method No. 1 (Confined Heat Stability), Total Acid Number Increase Limit of 2.0	38
20.	Effect of Temperature on Lubricant Life Using DERD Method No. 1 (Confined Heat Stability), Total Acid Number Increase Limit of 4.0	39
21.	Effect of Temperature on Lubricant Life Using DERD Method No. 1 (Confined Heat Stability), Total Acid Number Increase Limit of 6.0	40
22.	Effect of Temperature on Lubricant Life Using DERD Method No. 1 (Confined Heat Stability), Total Acid Number Increase Limit of 2.0 (4 cSt Fluids)	41
23.	Effect of Temperature on Lubricant Life Using DERD Method No. 1 (Confined Heat Stability), Total Acid Number Increase Limit of 4.0 (4 cSt Fluids)	42
24.	Viscosity Increase Versus Test Hours During Corrosion and Oxidation Testing of Lubricant O-67-1 Using D 4871 Tubes, 100 ml Samples, 320°C Test Temperature and 10 L/h Airflow	61
25.	Titration Curve of Phenol with TBAH in Acetonitrile	68
26.	Effect of Additive A Content on 40°C Viscosity Change During Corrosion and Oxidation Testing of O-77-6 at 320°C and 10 L/h Airflow	73
27.	Varnish and Coke Deposits Inside of Air Tubes of 5P4E Fluid Containing Various Concentrations of Additive A	75

LIST OF ILLUSTRATIONS (CONTINUED)

FIGURE		PAGE
28.	Effect of Various Materials and Concentrations on 40°C Viscosity Change During Corrosion and Oxidation Testing of O-77-6 at 320°C and 10 L/h Airflow	78
29.	Gas Chromatogram of O-67-1 Lubricant	80
30.	Gel Permeation Chromatogram of O-67-1 Lubricant	81
31.	Log Molecular Weight vs. GPC Retention Time for Three Polyphenyl Ether Calibration Standards	82
32.	BASIC Program for GPC Molecular Weight Calculations	84
33.	GPC Chromatogram of O-67-1 from the Corrosion and Oxidation Test at 320°C, 48 Hours	87
34.	Relative Rates of Oxidation of Three Components During 192 Hour Corrosion and Oxidation Test of O-67-1 at 320°C by Gas Chromatography	90
35.	Infrared Spectrum of Fresh 5P4E Polyphenyl Ether (Top) and Acetonitrile Insolubles from Oxidized 5P4E Polyphenyl Ether (Bottom)	94
36.	Reverse Phase Liquid Chromatogram of Isolated Biphenyl Dimer from Oxidized Polyphenyl Ether	96
37.	Percent Acetonitrile Insolubles in O-67-1 Stressed in the Corrosion and Oxidation Test at 320°C	97
38.	Gel Permeation Chromatograms of O-67-1 Stressed in the Corrosion and Oxidation Test at 320°C for 240 Hours. a) After Filtration, b) Before Filtration	99
39.	Viscosity Change of Lubricants TEL-8039, TEL-8040 and O-77-6 with 75 Relative Percent of Additive A at 40°C and 100°C	102
40.	Plots of BDN Solution Decoloration Versus Hydroperoxide Reaction Time for the Blank, Fresh (250 and 500 μL) O-67-1, 48-Hour (Air and N_2 at 320°C) Stressed O-67-1 Oils and Additive A[2]	106
41.	Plots of the Precipitate Weight (mg) Produced by the RULLER Solvent, the Percent Weight Loss, and Percent Change in Viscosity Versus Stressing Time (Hours) at 320°C for the O-67-1 Polyphenyl Ether Based Lubricating Oil	108

FIGURE		PAGE
42.	Gel Permeation Chromatograms of the 120 Hour Stressed O-67-1 Oil (320°C) Diluted with Acetone and with $LiClO_4$/Acetone Solution and of the Precipitate Produced by the 120 Hour Stressed O-67-1 Oil Diluted with $LiClO_4$/Acetone Solution	110
43.	Successive Cyclic Voltammograms (1st-5th Scans) of the Fresh O-67-1 Oil in Acetone Using a Glassy Carbon Working Electrode	113
44.	Successive Cyclic Voltammograms (1st-5th Scans) of the 240 Hour, 320°C, Stressed O-67-1 Oil in Acetone Using a Glassy Carbon Working Electrode	114
45.	Gas Chromatogram of Additive A in Polyphenyl Ether	119
46.	Tin Concentration in Formulated PPE from the Corrosion and Oxidation Test at 320°C Using AA and AE Analysis	120
47.	Percent Filterable Tin in Formulated PPE Stressed in the Corrosion and Oxidation Test at 320°C	122
48.	X-ray Diffraction Spectra Versus 2 X Degree of Angle for Additive A and the Isolated Sn Species from 3% Additive/ O-77-6 Fluid Samples Stressed at 320°C for 8 Hours in Argon, for 1 Hour in Air and 18 Hours in Air	125
49.	Thermogravimetric Analysis of the Isolated Sn Species from 3% Additive A/O-77-6 Stressed in Air (20°C/minute)	128
50.	Thermogravimetric Analysis of Fresh O-77-6 and O-67-1 Fluids (20°C/min in Nitrogen)	129
51.	Infrared Spectra of the Isolated Sn Species from 3% Additive A in O-77-6 Stressed 18 Hours at 320°C in Air, 5P4E Polyphenyl Ether (O-77-6) and SnO_2	131
52.	Infrared Spectra of the Isolated Sn Species from 3% Additive A in O-77-6 Stressed 18 Hours at 320°C in Air After Repeated THF Washings (Top) and the Precipitate Produced by Diluting the 120 Hour Stressed O-67-1 Oil Sample with the $LiClO_4$/Acetone Solution (Bottom)	132

LIST OF ILLUSTRATIONS (CONTINUED)

FIGURE		PAGE
53.	Oxygen 1s XPS Spectra of the Isolated Sn Species from Additive A in O-77-6 Stressed for 1 and 18 Hours in Air at 320°C	137
54.	Oxygen 1s XPS Spectrum of Solid Filtered from O-67-1 Stressed 120 Hours in the Corrosion and Oxidation Test at 320°C	141
55.	Mossbauer Spectra of O-67-1 Stressed in the Corrosion and Oxidation Test at 320°C for 24 Hours	143
56.	AFAPL Static Coker Deposits for Lubricant OP-369 (180 min Test Time)	148
57.	AFAPL Static Coker Deposits for Lubricant O-85-1 Before and After Pentane Solubility Test	153
58.	Solubility of AFAPL Static Coker Deposits for Lubricant O-85-1	153
59.	Correlation of AFAPL Static Coker Deposits with MCRT Deposits (New Oil)	167
60.	Correlation of AFAPL Static Coker Deposits with MCRT Deposits (Stressed Oil)	170
61.	Correlation Between Fed. Test Method 3213 and 25 mL Volume Foam Test for Lubricants with Oil/Foam Interface and Lubricants Having Severe Aeration and No Oil/Foam Interface	184
62.	Effect of Airflow on Degree of Aeration and Foaming for Lubricants O-82-2 and O-79-20 (13/16" Diameter 5 Micron Sparger Used for 25 mL Test)	186
63.	Effect of Airflow on Degree of Aeration and Foaming for Lubricants O-82-14 and O-79-17 (13/16" Diameter 5 Micron Sparger Used for 25 mL Test)	187
64.	Effect of Airflow on Degree of Aeration and Foaming for Lubricant O-79-16 (13/16" Diameter 5 Micron Sparger Used for 25 mL Test)	188
65.	Top View and Side View of DC Arc Bottom Electrodes Configuration Having (a) Concave Dip with a Rise in the Center and (b) Concave Dip	199
66.	Cup-Tip Electrode	200

LIST OF ILLUSTRATIONS (CONTINUED)

FIGURE		PAGE
67.	Side View of Cup-Tip Electrode Sharpener	200
68.	Atomic Emission Intensities Using Fe Conostan Standards and Three Types of Lower Electrodes	204
69.	Emission Intensities for Fe Standards Using Coated and Uncoated Cup-Tip Electrodes	205
70.	Variation of the Ratio L/S (Large Particle/Small Particle) with the Product of Load and Speed for Wear Debris Generated from Pin-on-Disk Wear Tests	216
71.	Iron Concentration of Pre- and Post-filter Samples for the First, Second, Third and Fourth Passes of Microfiltration Test No. 1 Using AA, AE and ADM	221
72.	Particle Size Distribution of Iron Wear Debris in Pre- and Post-filter Samples from Microfiltration Test No. 1 Using ADM, PWMA and AE	223
73.	Iron Concentration of Pre- and Post-filter Samples for the First, Second and Third Passes of Microfiltration Test No. 2 Using AA, AE and ADM	230
74.	Particle Size Distribution of Iron Wear Debris in Pre- and Post-filter Samples from Microfiltration Test No. 2 Using ADM, PWMA and AE	231
75.	Comparison of L/S Values for the Analytical and DR Ferrograph	235
76.	Iron Concentration of Pre- and Post-filter Samples for the First, Second and Third Passes of Microfiltration Test No. 3 Using AA, AE and ADM	238
77.	Particle Size Distribution of Iron Wear Debris in Pre- and Post-filter Samples from Microfiltration Test No. 3 Using ADM, PWMA and AE	240
78.	Iron Concentration of Pre- and Post-filter Samples for the First, Second, Third and Fourth Passes of Microfiltration Test No. 4 Using AA, AE, ADM and PWMA	244
79.	Particle Size Distribution of Iron Wear Debris in Pre- and Post-filter Samples from Microfiltration Test No. 4 Using ADM and AE	245

LIST OF ILLUSTRATIONS (CONTINUED)

FIGURE		PAGE
80.	Iron Concentration of Pre- and Post-filter Samples for the First, Second, Third and Fourth Passes of Microfiltration Test No. 5 Using AA, AE, ADM and PWMA	250
81.	Particle Size Distribution of Iron Wear Debris in Pre- and Post-filter Samples from Microfiltration Test No. 5 Using ADM and AE	251
82.	Iron Concentration of Pre- and Post-filter Samples for the First, Second, Third and Fourth Passes of Microfiltration Test No. 6 Using AA, AE, ADM and PWMA	256
83.	Particle Size Distribution of Iron Wear Debris in Pre- and Post-filter Samples from Microfiltration Test No. 6 Using ADM, PWMA and AE	257
84.	Correlation of % Iron Greater than 3 Microns with % Iron Captured by the MFR 3 Micron Filter and % Decrease in L/S Values Using the Analytical and DR Ferrograph with % Iron Being Determined by ADM	262
85.	Correlation of % Iron Greater than 3 Microns with % Iron Captured by the MFR 3 Micron Filter and % Decrease in L/S Values Using the Analytical and DR Ferrographs with % Iron Being Determined by AE	264
86.	Correlation of % Iron Greater than 3 Microns with % Iron Captured by the MFR 3 Micron Filter and % Decrease in L/S Values Using the Analytical and DR Ferrographs with % Iron Being Determined by the PWMA	265
87.	Correlation of % Iron Greater than 3 Microns Determined by ADM with % Iron Captured by the MFR as Determined by AE, PWMA and AA Analyses	267
88.	ADM and WPA Analyses of Two Pin-On-Disk Samples	280
89.	ADM and WPA Analyses of Pin-On-Disk #6 and Used Engine Oil	281
90.	Iron Results of Engine Simulator Test Samples Using ADM and WPA Techniques	291
91.	Lubri Sensor Readings for MIL-L-7808 and MIL-L-23699 Lubricants Stressed in the Confined Heat Stability Test	297
92.	Lubri Sensor Reading vs. TAN Increase for MIL-L-7808 and MIL-L-23699 Lubricants Stressed in the Confined Heat Stability Test	298

LIST OF ILLUSTRATIONS (CONTINUED)

FIGURE		PAGE
93.	Lubri Sensor Readings for MIL-L-7808 and MIL-L-23699 Lubricants Stressed in the Squires Oxidative Test	299
94.	Volatility Weight Loss for MIL-L-7808 and MIL-L-23699 Lubricants Stressed in the Squires Oxidative Test	301
95.	Lubri Sensor Readings for MIL-L-23699 Lubricants Stressed in the Corrosion and Oxidation Test	303
96.	Lubri Sensor vs. TAN Increase for MIL-L-23699 Lubricants Stressed in the Corrosion and Oxidation Test	305
97.	Lubri Sensor Reading vs. Viscosity Increase of MIL-L-23699 Lubricants Stressed in the Corrosion and Oxidation Test	306
98.	Time Dependency of Lubri Sensor Readings for Polyphenyl Ethers	310
99.	COBRA Reading vs. Volume Percent of Various Basestocks Added to O-76-5 Plus 1% PANA and 1% DODPA from Squires Oxidative Test at 190°C, 120 Hours	314
100.	COBRA Reading vs. Volume Percent of Various Basestocks Added to O-77-1 Plus 1% PANA and 1% DODPA from the Squires Oxidation Test at 190°C, 48 Hours	315
101.	GC-FID Trace of Hexane Fraction of O-77-1 Plus 1% PANA and 1% DODPA from the 48 Hour Squires Oxidation Test	319
102.	GC-FID Trace of Acetone Fraction of O-77-1 Plus 1% PANA and 1% DODPA from the 48 Hour Squires Oxidation Test at 190°C	320
103.	RPLC Traces of a) Hexane Fraction and b) Acetone Fraction of O-77-1 Plus 1% PANA and 1% DODPA from the 48 Hour Squires Oxidation Test at 190°C	321
104.	GC-FID Trace of Hexane Fraction of O-76-5A Plus 1% PANA and 1% DODPA from the 48 Hour Squires Oxidation Test at 190°C	322

LIST OF ILLUSTRATIONS (CONTINUED)

FIGURE		PAGE
105.	GC-FID Trace of Acetone Fraction of O-76-5A Plus 1% PANA and 1% DODPA from the 48 Hour Squires Oxidation Test at 190°C	323
106.	COBRA Reading vs. Weight Percent p-Nitrophenol in O-76-5 and O-77-1	328
107.	Four-Ball Seizure Test Sequence for O-79-20 Oil. Seizure Load = 1890 N, Final Scar Diameter = 0.11 Inch	336
108.	Four-Ball Seizure Test Sequence Showing the Effects of Frictional Heating on Chamber Temperature for Oil O-79-20	337
109.	Four-Ball Seizure Test Sequence for O-72-9 Oil. Seizure Load = 2669+ N, Final Scar Diameter = 0.12 Inch	339
110.	Four-Ball Seizure Test Sequence for O-76-1 Oil. Seizure Load = 2669+ N, Final Scar Diameter = 0.12 Inch	340
111.	Four-Ball Seizure Test Sequence for O-79-20 Oil. Seizure Load = 1890 N, Final Scar Diameter = 0.12 Inch	341
112.	Four-Ball Seizure Test Sequence for O-82-2 Oil. Seizure Load = 1557 N, Final Scar Diameter = 0.09 Inch	342
113.	Four-Ball Seizure Test Sequence for O-82-14 Oil. Seizure Load = 1112 N, Final Scar Diameter = 0.15 Inch	343
114.	Four-Ball Seizure Test Sequence for O-85-1 Oil. Seizure Load = 1334 N, Final Scar Diameter = 0.11 Inch	344
115.	Four-Ball Seizure Test Sequence for O-86-2 Oil. Seizure Load = 1112 N, Final Scar Diameter = 0.10 Inch	345
116.	LVDT Versus Time for Six Tests in Four-Ball Seizure Sequence 3. First Test was 60 Minutes at 400 N Load. Subsequent Tests were 10 Minutes at 670, 890, 1115, 1335 and 1560 N	347
117.	Coefficient of Friction Versus Time for Six Tests in Four-Ball Seizure Sequence 3. First Test was 60 Minutes. Subsequent Tests were 10 Minutes each	348
118.	Normalized Results of Four Test Methods on Eight MIL-L-7808 Lubricants, % of Best vs. Test Method	353
119.	Normalized Results of Four Test Methods on Eight MIL-L-7808 Lubricants, % of Best vs. Oil Type	354

FIGURE		PAGE
120.	Variation of Scar Diameter with Height as a Function of Load	361
121.	Comparison of WSD Calculated from One 20 Hour Test with the Results of Eleven Discrete Tests	363
122.	Calculated Wear Scar Volume Versus Time for Seven Four-Ball Tests Using Lubricant O-79-20 (Loadings in N)	365
123.	Least Squares Curve Fit to Wear Rate Versus Load Data in the Four-Ball Wear Test Using Oil O-79-20	366
124.	Computed Wear Scar Volume (WSV) Versus Time for Oil O-79-20	368
125.	Final Wear Scar Diameter (WSD) Versus Speed in Oil O-79-20	369
126.	Calculated Wear Scar Volume Versus Time for Seven Lubricants Producing Scar Sizes Greater than 0.9 mm	373
127.	Calculated Wear Scar Volume Versus Time for Six Lubricants Producing Scar Sizes Greater than 0.9 mm	374
128.	Final Scar Diameter for Various Oils at 1 Hour and 20 Hour Test Durations. Conditions: 145 N Load, 75°C Temp., 1200 rpm	375
129.	Final Scar Diameter for Various Oils at 1 Hour and 20 Hour Test Durations. Conditions: 392 N Load, 75°C Temp., 1200 rpm	376
130.	Calculated Scar Diameter from Test of O-76-1. Figure Illustrates Errors Present During Initial Portion of Wear Test. Dashed Line is Estimated Wear Path from Known Diameter at Time Zero	378
131.	Calculated Scar Volume from Test of O-76-1. Figure Illustrates a Constant Wear Rate During Second Half of Wear Test	379
132.	First and Successive Cyclic Voltammograms of the Fresh O-71-6 and O-77-15 MIL-L-23699 Lubricating Oils in the -0.4 to 1.2 V Scan Range	392
133.	First and Successive Cyclic Voltammograms of the Fresh TEL-7004 and O-79-18 MIL-L-23699 Lubricating Oil in the -0.4 to 1.2 V Scan Range	393

FIGURE		PAGE
134.	Reduction Voltammograms Produced by the Fresh and the 24, 48, 192 and 480 Hours Laboratory Stressed O-79-18 Oil Samples	396
135.	Plots of the ln of the Reduction Wave Area Versus Hours of Remaining Useful Life at 370°F for the Fresh and Laboratory Stressed O-71-6, O-77-15, TEL-7004, O-79-18 (MIL-L-23699) and TEL-4004 (MIL-L-7808) Oils	398
136.	Plots of the % Remaining Useful Life Versus Hours of Operation Prior to Engine Failure for the Used MIL-L-23699 (F50, F51 and F53) Oil Sample Series	401
137.	Example Difference Plots (2 Sec) of the Multichannel Capacitor System Connected to the Fe, Ag, Ni and Cu Channels for the F50A-C Used MIL-L-23699 Oil Samples Produced by the Direct Analysis Method on the A/E35U-1 Spectrometer	403
138.	Example Difference Plots (2 Sec) of the Multichannel Capacitor System Connected to the Fe, Ni and Cu Channels for the F51A-D Used MIL-L-23699 Oil Samples Produced by the Direct Analysis Method on the A/E35U-1 Spectrometer	404
139.	Example Difference Plots (2 Sec) of the Multichannel Capacitor System Connected to the Fe, Ag, Ni and Cu Channels for the F53A-D Used MIL-L-23699 Oil Samples Produced by the Direct Analysis Method on the A/E35U-1 Spectrometer	405
140.	Example Difference Plots (2 Sec) of the Multichannel Capacitor System Connected to the Fe, Ag, Ni and Cu Channels for the C12-10 Standard Produced by the Direct Analysis Method on the A/E35U-1 Spectrometer	406
141.	Plots of the % Remaining Useful Life Versus Hours of Operation Prior to Engine Removal (Air Force OAP Recommended) for the Used MIL-L-7808 (H99 and H100) and MIL-L-23699 (H95, H97 and H98) Oil Sample Series	408
142.	Example Difference Plots (2 Sec) of the Multichannel Capacitor System Connected to the Fe and Cu Channels for the H95A-C Used MIL-L-23699 Oil Samples Produced by the Direct Analysis Method on the A/E35U-1 Spectrometer	409

FIGURE		PAGE
143.	Example Difference Plots (2 Sec) of the Multichannel Capacitor System Connected to the Fe and Cu Channels for the H97A-D Used MIL-L-23699 Oil Samples Produced by the Direct Analysis Method on the A/E35U-1 Spectrometer	410
144.	Example Difference Plots (2 Sec) of the Multichannel Capacitor System Connected to the Fe and Cu Channels for the H98A-D Used MIL-L-23699 Oil Samples Produced by the Direct Analysis Method on the A/E35U-1 Spectrometer	411
145.	Example Difference Plots (2 Sec) of the Multichannel Capacitor System Connected to the Fe and Cu Channels for the H99A-D Used MIL-L-7808 Oil Samples Produced by the Direct Analysis Method on the A/E35U-1 Spectrometer	412
146.	Example Difference Plots (2 Sec) of the Multichannel Capacitor System Connected to the Fe and Cu Channels for the H100A-D Used MIL-L-7808 Oil Samples Produced by the Direct Analysis Method on the A/E35U-1 Spectrometer	413
147.	Plots of the Percent Remaining Useful Life, Viscosity (40°C) and Total Acid Number (TAN) Measurements Versus the Hours of Operation for the MIL-L-7808J Oil Samples Obtained from a Normal Operating Test Stand Engine	415
148.	Example Difference Plots (2 Sec) of the Multichannel Capacitor System Connected to the Fe and Cu Channels for the 10, 60, 110 and 170 Hours Stressed (Test Stand Engine) MIL-T 7808 Oil Samples Produced by the Direct Analysis Method on the A/E35U-1 Spectrometer	417
149.	Photograph of RULLER - Microcomputer System Setup	421
150.	Photograph of RULLER Box (Packaged Universal Single Board Voltammograph) and Developed Electrode System	422
151.	Plots of the Percent Remaining Useful Life Versus the Hours Since Last Oil Change for Used Oil Sample Series Obtained from Normal and Abnormal Operating A-10 Aircraft Engines	425
152.	Plots of the Percent Remaining Useful Life Versus the Hours Since Last Oil Change for Used Oil Samples Series Obtained from C-130 Aircraft Engines	428

LIST OF ILLUSTRATIONS (CONCLUDED)

FIGURE		PAGE
C-1.	Schematic of Universal Single Board Voltammograph	501
C-2.	Parts Diagram of Universal Single Board Voltammograph	502
C-3.	Wiring Diagram of the Digital-to-Analog Microchip Connected to the Input of the Universal Single Board Voltammograph	503
C-4.	Wiring Diagram of the Analog-to-Digital Microchip Connected to the Output of the Universal Single Board Voltammograph	504
C-5.	Wiring Connections of the Parallel Interface Connected to the Digital-to-Analog (AD565A) and Analog-to-Digital (AD570) Microchips and to the Electrode Switch (Relay) of the Universal Single Board Voltammograph	505
C-6.	Laser Microcomputer Memory Map	506
D-1.	Plots of the Viscosity (40°C) and Total Acid Number (TAN) Versus Hours of Stressing Time at 370°F for the Fresh and Stressed O-71-6 and O-77-15 MIL-L-23699 Type Oils	508
D-2.	Plots of the Viscosity (40°C) and Total Acid Number (TAN) Versus Hours of Stressing Time at 370°F for the Fresh and Stressed TEL-7004 MIL-L-23699 Type Oil	509
D-3.	Plots of the Viscosity (40°C) and Total Acid Number (TAN) Versus Hours of Stressing Time at 370°F for the Fresh and Stressed O-79-18 MIL-L-23699 Type Oil	511

LIST OF TABLES

TABLE		PAGE
1.	Description of Test Fluids Used for Oxidative Stability Study	6
2.	Effective Lubricant Life, DERD Method No. 9 (no Dilution), Acidity Increase Limits	15
3.	Effective Lubricant Life, DERD Method No. 9 (no Dilution), Viscosity Increase Limits	22
4.	Effective Lubricant Life, DERD Method No. 9 (no Dilution), Volatilization Loss Limits	30
5.	Comparison of Squires Oxidative Test Data for Lubricants O-85-1 and O-86-2	31
6.	Effect of Condensate Return on Squires Oxidation Test for Lubricant O-79-18 at 215°C Test Temperature	32
7.	Effect of Condensate Return on Squires Oxidation Test for Lubricant O-85-1 at 215°C Test Temperature	32
8.	Effect of Condensate Return on Squires Oxidation Test for Lubricants O-79-18 and O-85-1 at 205°C, 72 Test Hours	33
9.	Effective Lubricant Life, DERD Method No. 1 (Confined Heat Stability), Acidity Increase Limits	43
10.	Comparison of Confined Heat Test Data for Lubricants O-85-1 and O-86-2	44
11.	Description of Test Fluids Used for Corrosiveness and Oxidative Stability Study	47
12.	Results of Reflux Corrosion/Oxidation Test, Lubricant O-79-18	48
13.	Results of Reflux Corrosion/Oxidation Test, Lubricant TEL-7004	49
14.	Temperature Profile of Aluminum Block Bath Using D 4871 Tubes	50
15.	Temperature Profile of Aluminum Block Bath Using Aluminum Inserts for Small Volume Test Cells	51
16.	Corrosion and Oxidation Test Data for Polyphenyl Ethers, 320°C, 48 Test Hours, 10 L/H Airflow	52

LIST OF TABLES (CONTINUED)

TABLE		PAGE
17.	Effect of Test Variables on Corrosion and Oxidation Stability of O-67-1, 320°C, 48 Test Hours, 10 L/H Airflow	54
18.	Properties and Test Conditions of Four-Ball Wear Test Samples No. 195 and No. 200 and the Mixture of These Samples Used for Corrosion and Oxidation Study	57
19.	Chromatographic Analysis of O-67-1 Four-Ball Wear Test Lubricants	58
20.	Corrosion and Oxidation Test Data For Lubricant O-67-1 at 320°C Using D 4871 Tubes (100 ML Sample), 10 L/H Airflow (Sample Container X)	60
21.	Corrosion and Oxidation Test Data for Lubricant O-67-1 (Can B, Top Sample) at 320°C Using D 4871 Tubes and 100 ML Samples and 10 L/H Airflow	64
22.	Corrosion and Oxidation Test Data for Lubricant O-67-1 (Can B, Top Sample) at 320°C Using a D 4871 Tube and 150 ML Sample with Intermediate Sampling and 10 L/H Airflow	65
23.	Repeatability of Corrosion and Oxidation Testing of Lubricant O-67-1 at 320°C Using D 4871 Tubes with and without Intermediate Sampling	66
24.	Potentiometric Titration of Weak Acid in O-67-1 Stressed in the Corrosion/Oxidation Test at 320°C	69
25.	Effect of Additive A Content on Corrosion and Oxidation Stability of Polyphenyl Ether O-77-6 at 320°C Using D 4871 Tubes and Intermediate Sampling	71
26.	Comparison of 320°C Corrosion and Oxidation Stability of Optimum and Excessive Concentrations of Additive A	74
27.	Corrosion and Oxidation Stability of Polyphenyl Ether O-77-6 Containing Various Additives at 320°C Using D 4871 Tubes, Intermediate Sampling and 10 L/H Airflow	77
28.	GPC Molecular Weight Analysis of Polyphenyl Ethers from Corrosion/Oxidation Test for 48 Hours	85
29.	Molecular Weight Analysis of O-67-1 from Corrosion/ Oxidation Test at 320°C by GPC	85

LIST OF TABLES (CONTINUED)

TABLE		PAGE
30.	Component Distribution of O-67-1 Samples	91
31.	Composition of New and 320°C, 240 Hour C&O Stressed O-77-6 Fluid Containing Various Additive A Content	91
32.	Composition of New and Condenser Washings from 320°C, 240 Hour C&O Stressed O-77-6 (5P4E) Fluid Containing Various Additive A Content	92
33.	Corrosion and Oxidation Data for Lubricants TEL-8039 and TEL-8040 (320°C, D 4871 Tubes, 10 L/H Airflow)	100
34.	XPS Results for Precipitate Obtained from Stressed O-67-1 Oil	112
35.	Corrected Sn $3d_{5/2}$ Binding Energies and Atomic Formula Derived from XPS Analyses of Sn Containing Compounds	134
36.	Description of Test Fluids Used in Coking Study	147
37.	AFAPL Static Coker Test Data for Lubricant OP-369 (180 Min Test Time)	149
38.	Description of AFAPL Static Coker Deposits for Lubricant OP-369 (180 Min Test Time)	150
39.	Comparison of AFAPL Static Coker Test Deposits Using Brass and Shim Stock Test Specimens at 315°C and 180 Min Test Time	151
40.	Effects of Confined Heat and Oxidative Stressing on AFAPL Static Coker Deposits	155
41.	Effect of Test Temperature and Test Time on AFAPL Static Coker Deposits for Lubricant O-85-1	157
42.	Rate of Change in AFAPL Static Coker Deposits with Time for Lubricant O-85-1	158
43.	Effect of Test Temperature and Test Time on AFAPL Static Coker Deposits for Lubricant O-87-3	159
44.	AFAPL Static Coker Deposits for New and Stressed O-67-1 (5P4E) Lubricant at 355°C	161
45.	AFAPL Static Coker Data and MCRT Coking Data for Various Lubricants	165

LIST OF TABLES (CONTINUED)

TABLE		PAGE
46.	Effects of Confined Heat and Oxidative Stressing on MCRT Deposits	168
47.	MCRT and AFAPL Static Coker Deposits for New and Stressed O-67-1 Lubricant	171
48.	Lubricants Used in Coking Propensity Study	173
49.	Lubricant Coking Propensity Test Data, 235°C Test Temperature	175
50.	Lubricant Coking Propensity Test Data, 260°C Test Temperature	176
51.	Lubricants and Fluids Used for Foaming and Aeration Study	179
52.	Repeatability of Foam Testing	181
53.	Comparison of Foam Test Data Using Fed. Method 3213 and 25 ML Volume Test for Various Air Dispersers and 1000 CC/Min Airflow	182
54.	Effect of Spark Intensity on Emission Signal of Fe Particles Using 10 Sec Exposure Time and 75 μL Sample Volume	194
55.	Effect of Spark Intensity on Emission Signal of Fe Particles Using 20 Sec Exposure Time and 75 μL Sample Volume	195
56.	Effect of Disk Electrode Surface Density on the Fe Emission Analytical Signal	197
57.	Effect of Cup Geometry of the DC Arc Stand on Fe Emission Signal	202
58.	Atomic Emission Intensities for Uncoated and Coated Cup Tip Electrodes	206
59.	Description of Microfiltration Test Fluids	210
60.	Description of Nomenclature of Microfiltration Test Samples	210
61.	Ferrographic Analysis of MFR Gear Pump Test Samples	212
62.	Analysis of Wear Debris from Small Gear Pump	213

LIST OF TABLES (CONTINUED)

TABLE		PAGE
63.	Direct Reading Ferrograph Results for the Pin-On-Disk Wear Test Samples	214
64.	Variation of Oil Flow and Pressure in Filter Housing with and without the Filter Element	217
65.	Parameters Monitored During the Microfiltration Test Rig Operation	218
66.	Optical Density Readings of Analytical Ferrograms for Microfiltration Test No. 1 (Standard 3 ML Sample)	225
67.	Optical Density Readings of Analytical Ferrograms for Microfiltration Test No. 1 (1 ML and Diluted Samples)	226
68.	DR Ferrograph Data for Microfiltration Test No. 1	227
69.	Optical Density Readings of Analytical Ferrograms for Microfiltration Test No. 2 (1 ML and Diluted Samples)	232
70.	DR Ferrograph Data for Microfiltration Test No. 2	233
71.	L/S Values for Microfiltration Tests No. 1 and No. 2 Based on 5 Micron Filtration and ADM Iron Analysis	234
72.	Optical Density Readings of Analytical Ferrograms for Microfiltration Test No. 3	241
73.	DR Ferrograph Data for Microfiltration Test No. 3	241
74.	Optical Density Readings of Analytical Ferrograms and L/S Values for Samples Obtained from Microfiltration Test No. 4	247
75.	Direct Reading Ferrograph Data for Microfiltration Test No. 4	248
76.	Optical Density Readings of Analytical Ferrograms and L/S Values for Samples Obtained from Microfiltration Test No. 5	252
77.	Direct Reading Ferrograph Data for Microfiltration Test No. 5	253
78.	Particle Size Distribution of Fe, Cu, Mg, Si and Zn in Microfiltration Test No. 6 Samples Using AE	259
79.	Particle Size Distribution of Fe, Cu, Mg and Si in Microfiltration Test No. 6 Samples Using PWMA	259

LIST OF TABLES (CONTINUED)

TABLE		PAGE
80.	Optical Density Readings of Analytical Ferrograms and L/S Values for Samples Obtained from Microfiltration Test No. 6	260
81.	Direct Reading Ferrograph Data for Microfiltration Test No. 6	261
82.	Efficiency of Filters Using Various Particle Sizes of Fe Powders and Pin-On-Disk #1 Sample	276
83.	Effect of Sample Volume on WPA Readout Using Pin-On-Disk #2 and Used Engine Oil Samples with Various Size WPA Filters	278
84.	Repeatability of the Wear Particle Analyzer for Different Sample Volumes and Filters Using Pin-On-Disk #3 Oil Sample	283
85.	Particle Size Distribution of Fe in Pin-On-Disk Sample #4 Using Acid Dissolution Method (ADM), Solvent Extraction/Atomic Absorption (SE/AA), Magnetometer and Wear Particle Analyzer (WPA)	283
86.	Results of Modified Sample Introduction System in the WPA	285
87.	Effect of Flow Rate on WPA Response	286
88.	Iron Concentration Obtained from Using ADM, WPA and Magnetometer	288
89.	Comparative Results Using the Wear Particle Analyzer and a Solvent Extraction Method for Iron in Used Turbine Engine Oils	290
90.	Effect of Condensate Return on Lubri Sensor Readings	302
91.	Lubri Sensor Readings for O-79-16 with Suspended Iron Powder	307
92.	Lubri Sensor Readings of Fresh MIL-L-7808 and MIL-L-23699 Lubricants	308
93.	COBRA Readings of Degraded Lubricants after Adsorption Chromatography	317
94.	IR Absorptions of Fractionated MIL-L-7808 Lubricants	325
95.	Effect of Additive A-658 on COBRA Readings of Stressed Lubricants	329

LIST OF TABLES (CONCLUDED)

TABLE		PAGE
96.	Dielectric Breakdown Voltage Measurements	331
97.	Comparison of Ryder, IAE and FZG Test Parameters	333
98.	Four-Ball Seizure Test Results for MIL-L-7808 Type Lubricants	338
99.	Conditions of Four-Ball Seizure Test Sequence 1	349
100.	Conditions of Four-Ball Seizure Test Sequence 3	349
101.	Wear and COF Results of Gear Simulation Tests	351
102.	Results of Various Test Methods	352
103.	Normalized Results of Various Wear Tests	355
104.	Ranking of Oils by the Various Wear Tests	355
105.	Results of Four-Ball Wear Tests Using O-79-20 Lubricant	364
106.	Characterization of Various Lubricants Based on Scar Size Produced from 20 Hr Test at 75°C, 1200 RPM, 145 N Load	371
107.	Calculated Wear Rates of Oils with Scar Sizes Greater Than 0.9 MM	372
108.	Engine Test Condition	388
109.	OAP Wear Metal Concentrations for NC-141 Aircraft Engines	427
A-1.	Squires Oxidative Test Data	440
A-2.	Squires Confined Heat Test Data	447
A-3.	AFAPL Static Coker Test Data	453
A-4.	MCRT Coking Test Data	476
A-5.	Lubricant Foaming Test Data	482
A-6.	Variable Airflow Foaming Test Data	487
B-1.	Summary of Various Analytical Techniques Used to Evaluate Effect of Microfiltration on Iron Concentration	495
B-2.	Particle Size Distribution of Iron Particles from Microfiltration Test as Determined by ADM, PWMA and AE	497

SECTION I

INTRODUCTION

This work describes the second half of research conducted for developing improved methods for defining and predicting lubricant performance in gas turbine engines. This includes development of lubrication system health monitoring techniques, methods and techniques for lubricant condition monitoring, the efficient storage, correlation and display of current and historical lubricant performance data and development of a diagnostic candidate instrument for evaluating the remaining useful life of a lubricant. Methods were investigated and developed during this program to better define and predict lubricant performance and for evaluating physical and chemical properties as related to lubricant performance. These investigations and studies involved various types of lubricating fluids including current ester type lubricants and potential high temperature candidate fluids.

Section II (Task I), "The Development of Improved Methods for Measuring Lubricant Performance," was directed towards determining lubricant stability, lubricant coking and lubricant foaming characteristics. Lubricant stability was studied using various high temperature degradation techniques including existing oxidation, confined heat and corrosion/oxidation tests and various modifications of these techniques.

These techniques were used to study the stabilities of lubricants up to temperatures of 320^{o}C and for test periods up to 408 hours, depending upon the test fluid and test conditions. Evaluation and correlation of test results were based on changes in composition, acidity, viscosity, volatility and electrochemical characteristics of the stressed lubricants. Arrhenius plots were developed for the ester base fluids describing the performance

capabilities based on selected levels of degradation in terms of time and temperature.

The lubricant coking characteristics were investigated with respect to the effects of time, temperature, sample volume, lubricant composition, and test specimen material on the deposition tendencies of various lubricants. The effects of wear debris and lubricant degradation on lubricant deposition characteristics were also studied. The AFAPL Static Coker, Micro Carbon Residual Tester (MCRT) and the Rolls-Royce Coking Propensity Tests were used for the various coking studies. The physical properties of the coke deposits were studied and the deposit values obtained from the various tests were compared and evaluated with respect to each other as well as other deposition tests such as the bearing deposition and tube deposition tests.

The third area of Task I was concerned with the study of different size and types of air dispersers, airflow rates, glassware design and other variables required for the development of a static foaming test requiring 25 mL or less sample and which would correlate with the Fed. Test Method 3213.

Section III (Task II), "Development of Improved Lubrication System Health Monitoring Techniques," involved determining the morphology of wear debris present in used oils, the effects of wear debris morphology and the impact of fine filtration on oil analysis techniques. The particle size detection capabilities of different analytical techniques such as the wear particle analyzer, atomic absorption and atomic emission spectroscopy were determined for wear metal debris of various composition and morphology. The impact of using fine filtration (3 micron absolute) in aircraft lubrication systems was evaluated with regard to present Air Force SOAP wear metal monitors using a microfiltration test rig designed and built to simulate microfiltration in gas turbine engine lubrication systems. The efficiency of

fine filtration as well as the particle size distributions were determined for wear metals in the pre- and post-filtered samples. Comparative analyses were performed on pre- and post-filtered samples using flame and graphite furnace atomic absorption, rotating disk atomic emission, ferrography and a wear particle analyzer.

Section IV (Task III), "Investigation of Lubricant Monitoring Techniques," involved an investigation into the electrochemical properties of synthetic turbine lubricants. This investigation included a systematic study involving the effects of various basestock and additive package combinations and of different degrees of thermal and oxidative stressing on the electrochemical properties of synthetic turbine lubricants. The Complete Oil Breakdown Rate Analyzer, a dielectric constant device and other applicable instruments for measuring conductivity and dielectric breakdown voltage were used to measure and study the changes in the lubricants' electrochemical properties.

Section V (Task IV), "Lubricant Load Carrying Capability Test Assessment," involved an investigation of alternative techniques for measuring load carrying capacity. Specifically, the FZG-Ryder and IAE were assessed as alternatives to replace the Ryder gear test. Factors included in the assessment were test conditions and materials for testing lubricants. The four ball wear test was investigated for determining the load carrying capacity of lubricants. Extreme pressure testing using the four ball wear test was also examined along with a gear simulation test involving a roll/slide wear surface configuration.

Section VI (Task V), "Development of Specification Wear Test," began with a review of existing techniques and test rigs used for measuring wear. The techniques and test rigs with the potential of being developed into a

specification test for measuring wear prevention characteristics of synthetic turbine lubricants were ranked according to test time and repeatability. The ability of each test rig or technique to detect changes in the wear prevention characteristics of different lubricants produced by minor formulation changes was determined. A wear rate calculation method was developed to characterize the wear prevention properties of lubricants and a recommendation for using these techniques was made for evaluating the wear characteristics of MIL-L-7808 and MIL-L-23699 lubricants.

Section VII (Task VI), "Development of Lube Data Storage and Retrieval System," resulted in the implementation and demonstration of a microcomputer system for lubricant test data storage, retrieval, correlation, and evaluation. The developed system incorporated generated data for MIL-L-7808, MIL-L-23699, and other laboratory formulated lubricants for determining and defining lubricant performance using a Zenith Z-100 microcomputer.

Section VIII (Task VII), "RULLER DEVELOPMENT" was conducted to develop a reductive cyclic voltammetric technique (RCV) for the determination of the remaining useful life of lubricants. Optimizing experimental parameters of the RCV for determining the remaining useful life of used MIL-L-7808 and MIL-L-23699 was completed. RULLER candidates were developed and are being field tested. Data to date collected from four locations indicates that the RULLER is successful in assessing the remaining useful life of lubricants.

SECTION II

DEVELOPMENT OF IMPROVED METHODS FOR MEASURING LUBRICANT PERFORMANCE

1. LUBRICANT OXIDATIVE STABILITY

a. Introduction

The objective of this phase of the program was to investigate the oxidative stability of selected turbine engine lubricants under various temperature conditions, and define stability in terms of their effective lubricant life based upon selected limiting values of various physical and chemical properties. Properties monitored during lubricant stressing included volatility, acidity, viscosity, toluene insolubles, electrochemical characteristics and composition. Arrhenius curves describing effective lubricant life as a function of temperature were developed using only the changes in total acid number (TAN), viscosity and lubricant loss (volatility).

b. Test Apparatus

The oxidation test apparatus has been previously described in the Interim Technical Report[1] for Phase 1 of this study. This test is essentially an oxidation test without use of metal test specimens. Limited oxidation testing was also conducted on selected lubricants using condensers with modified air inlet tubes for providing condensate return.

c. Test Procedure

The test procedure has also been previously described in a technical report[1] and applies to the use of condensate return as well as no condensate return.

d. Test Lubricants and Test Conditions

A total of five lubricants were examined during the second phase of

this study. Table 1 presents a listing of the lubricants including a MIL-L-7808 lubricant which was included in the previous technical report[1] and which will be used for comparative purposes in Phase 2 of this study.

TABLE 1

DESCRIPTION OF TEST FLUIDS USED FOR OXIDATIVE STABILITY STUDY

Test Fluid	Description
O-71-6	MIL-L-23699 Lubricant
O-77-15	MIL-L-23699 Lubricant
O-79-16	MIL-L-7808 Lubricant
O-79-18	MIL-L-23699 Lubricant
O-85-1	4 cSt Candidate Lubricant
O-86-2	4 cSt Candidate Lubricant (Different Lot of O-85-1)
O-87-3	4 cSt Candidate Lubricant
TEL-7043	MIL-L-23699 Lubricant (Different Lot of O-71-6)

Lubricants were stressed at temperatures ranging from 190°C (374°F) to 215°C (419°F). Test durations ranged from 24 hours to 720 hours depending upon the test temperature and the specific fluid being tested. Testing was discontinued for each test fluid after severe degradation or very high lubricant loss had occurred. Lubricant make-up due to volatility oil loss during test was not made prior to analysis of stressed samples which may be done using DERD METHOD NO. 9 if desired.

Total acid numbers and COBRA measurement were conducted on the same day the samples were removed from the test bath since these properties can change with time after being stressed and stored at room temperature.

e. Results and Discussion

The rate of degradation can be expressed by the Arrhenius equation $K = Ae^{-E/RT}$ where

K = rate constant

A = pre-exponential factor (constant)

E = activation energy (cal/mole)

R = gas constant (cal/deg mole)

T = absolute temperature (^{o}K)

Lubricant life is inversely proportional to the rate of degradation and can be expressed as $D = (1/A)e^{-E/RT}$. Representing E/R log e by C, the logarithmic form to base 10 of this equation is log D = C/T log A. Using this equation and plotting effective lubricant life against reciprocal degrees Kelvin using semilogarithmic graph paper provides a linear relationship between temperature and lubricant life. Appendix A, Table A-1 provides all the Squires Oxidative test data developed during Phase 2 of this study and from which Arrhenius plots were developed.

Lubricant life must be defined in terms of limiting values for selected properties. For all the lubricants, Arrhenius plots were developed using the following criteria as limiting values.

Total Acid Number Changes of 1, 1.5 and 3

Viscosity Increases at 100^{o}C of 15%, 25% and 35%

Volatilization Losses of 15%, 25% and 35%

Figures 1 thru 3 show Arrhenius plots for three MIL-L-23699 lubricants and one 4 cSt candidate lubricant using TAN increase as the limiting life criterion. At the low levels of TAN increase (1.0 and 1.5) two of the MIL-L-23699 lubricants are very similar while the other MIL-L-23699 fluid and the 4 cSt candidate fluid are very similar. At the TAN increase

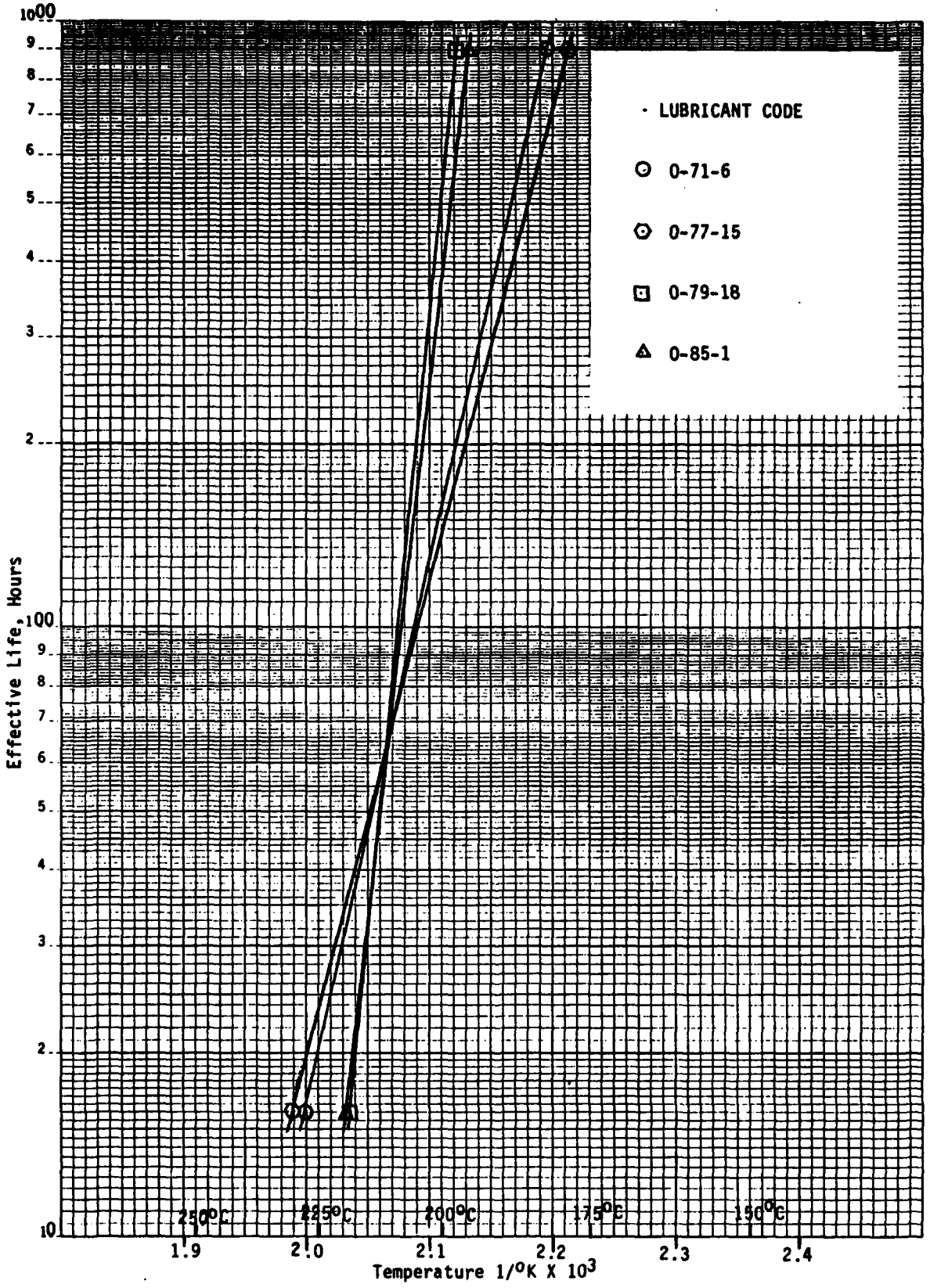

Figure 1. Effect of Temperature on Lubricant Life Using DERD Method No. 9, Total Acid Number Increase Limit of 1.0

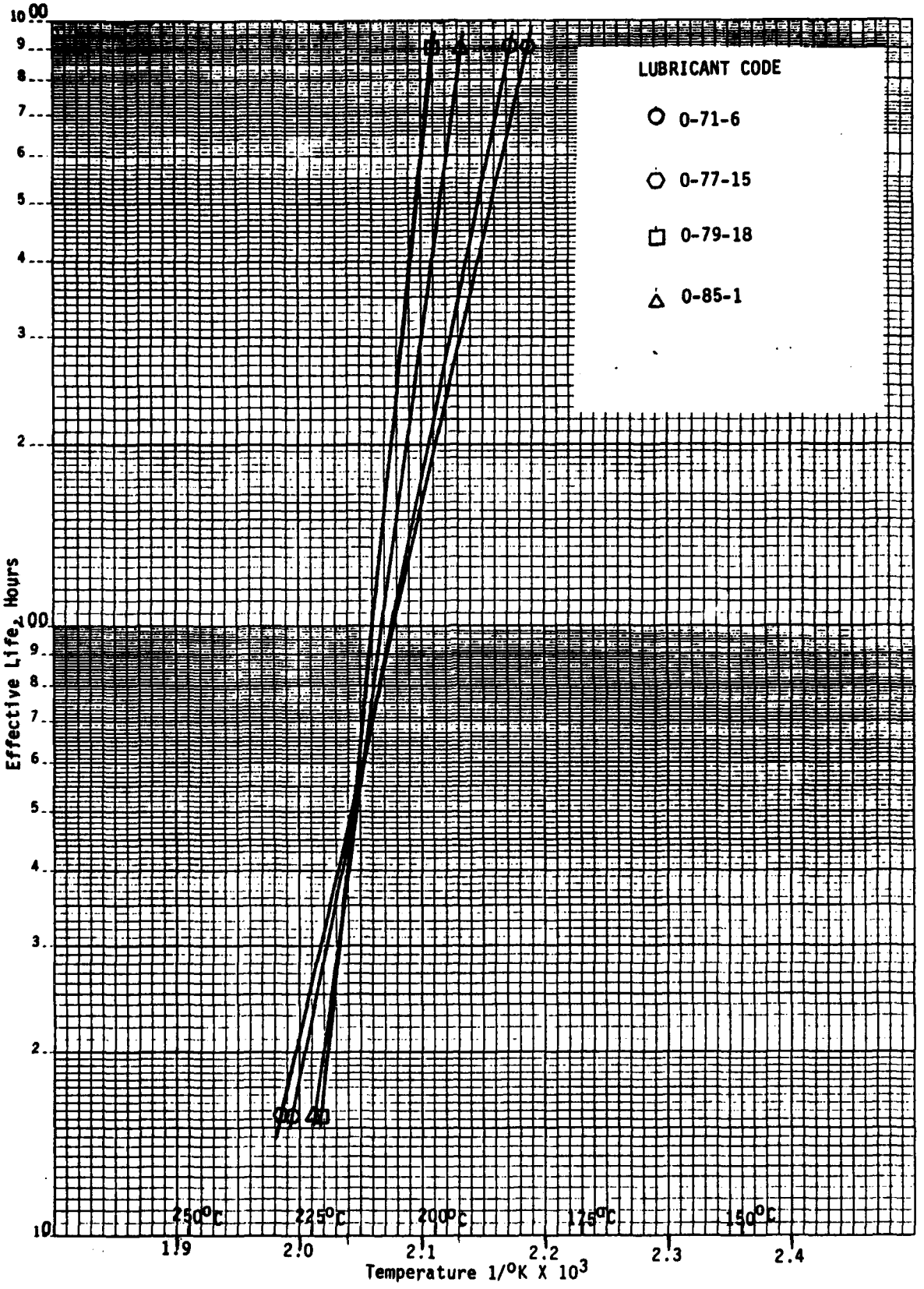

Figure 2. Effect of Temperature on Lubricant Life Using DERD Method No. 9, Total Acid Number Increase Limit of 1.5

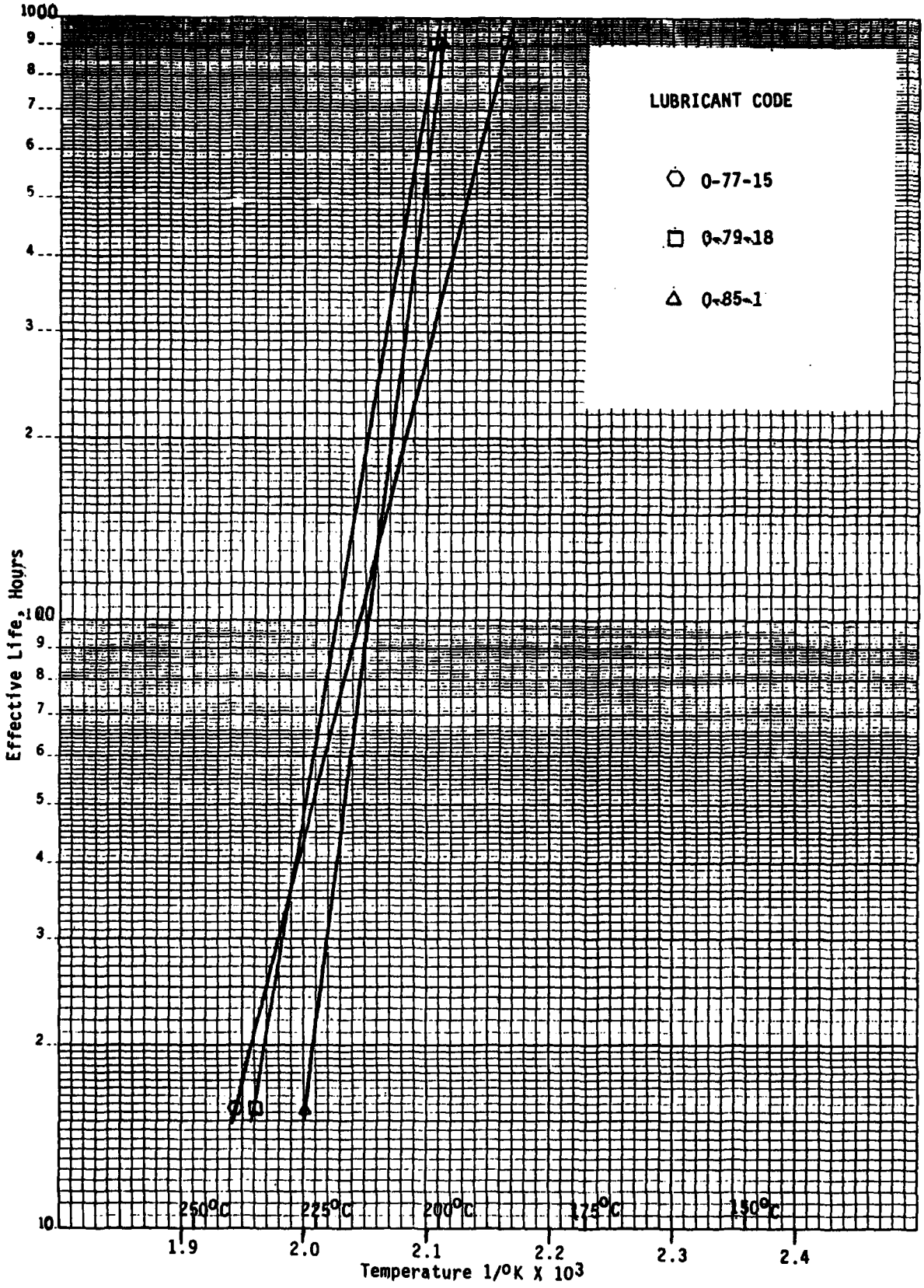

Figure 3. Effect of Temperature on Lubricant Life Using DERD Method No. 9, Total Acid Number Increase Limit of 3.0

level of 3.0, the lubricants did not fall into any grouping with the ranking of the lubricants depending very much on the test temperature. Figures 4 thru 6 show Arrhenius plots for the two 4 cSt candidate lubricants using TAN increase as the limiting life criterion. Lubricant O-85-1 shows a much greater effective life for all the three limiting TAN values and for all test temperatures. The differences in effective life of all the lubricants including the MIL-L-7808 lubricant evaluated in Phase 1 are shown in Table 2 for test temperatures of 175°C, 200°C, and 225°C for the three limiting TAN values. This data shows that the MIL-L-23699 lubricant O-79-18 and the 4 cSt candidate lubricant O-85-1 have the best overall effective lubricant life. The data in Table 2 also shows the ranking of the lubricants with respect to lubricant life depends to some extent on the selected TAN increase limit.

Figures 7 thru 9 show the Arrhenius plots for three MIL-L-23699 lubricants and the 4 cSt fluid using viscosity increase as the limiting life criterion. As expected, relative ranking of the lubricants depends upon the temperature and level of viscosity increase selected for the comparison parameter. Less difference existed between the lubricants using limiting viscosity increase values of 25% and 35% than the 15% viscosity increase value.

Figures 10 thru 12 show Arrhenius plots for the two 4 cSt lubricants using viscosity increase as the limiting life criterion. For temperatures up to 175°C and the 15% and 25% limiting viscosity increase values, lubricant O-87-3 showed the largest effective life. For stress temperatures above 175°C, lubricant O-85-1 shows the largest effective life at all three viscosity increase values.

The difference in the effective life of all the lubricants is shown in Table 3 for test temperatures of 175°C, 200°C, 225°C for the three

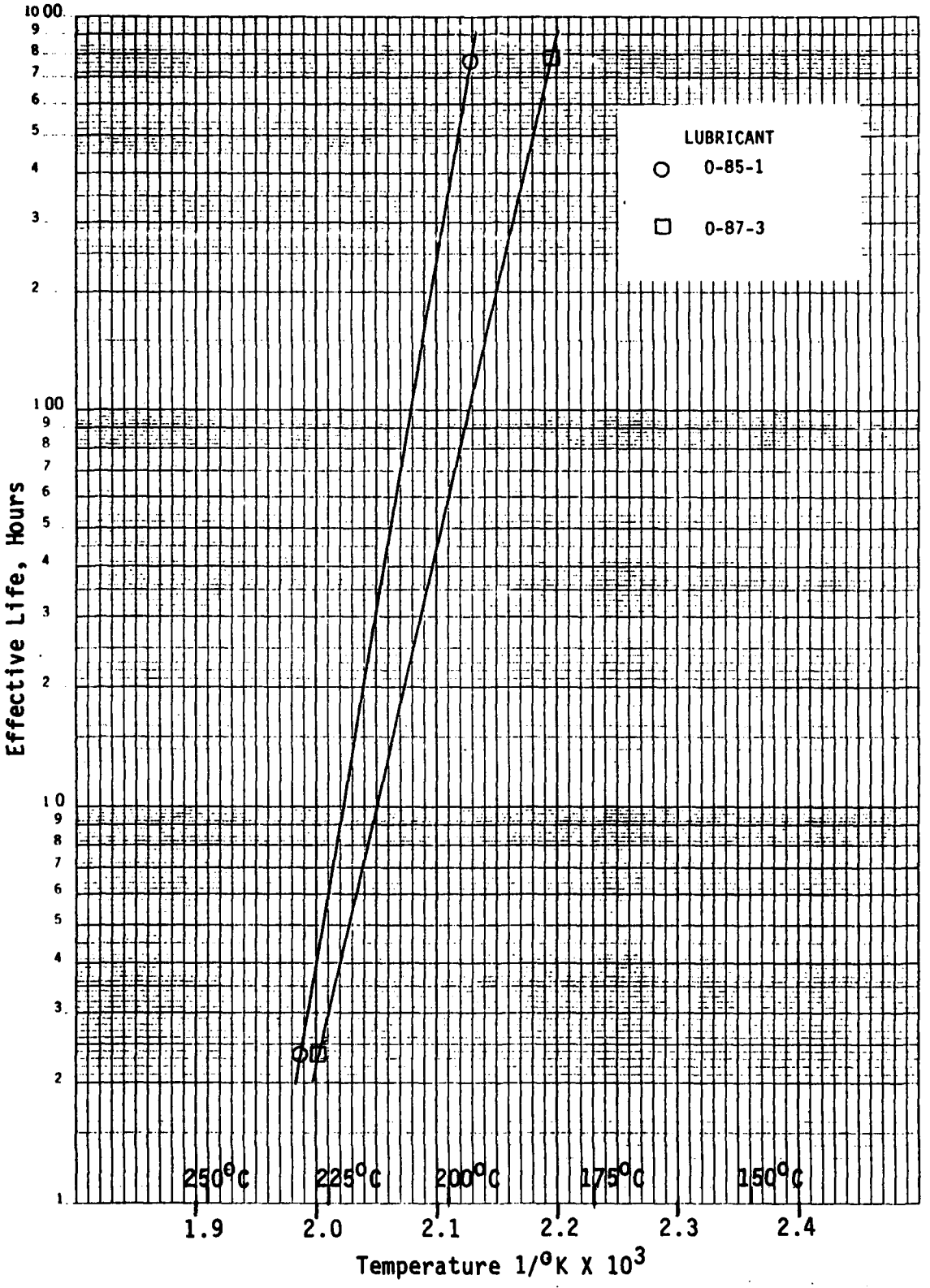

Figure 4. Effect of Temperature on Lubricant Life Using DERD Method No. 9, Total Acid Number Increase Limit of 1.0 (4 cSt Fluids)

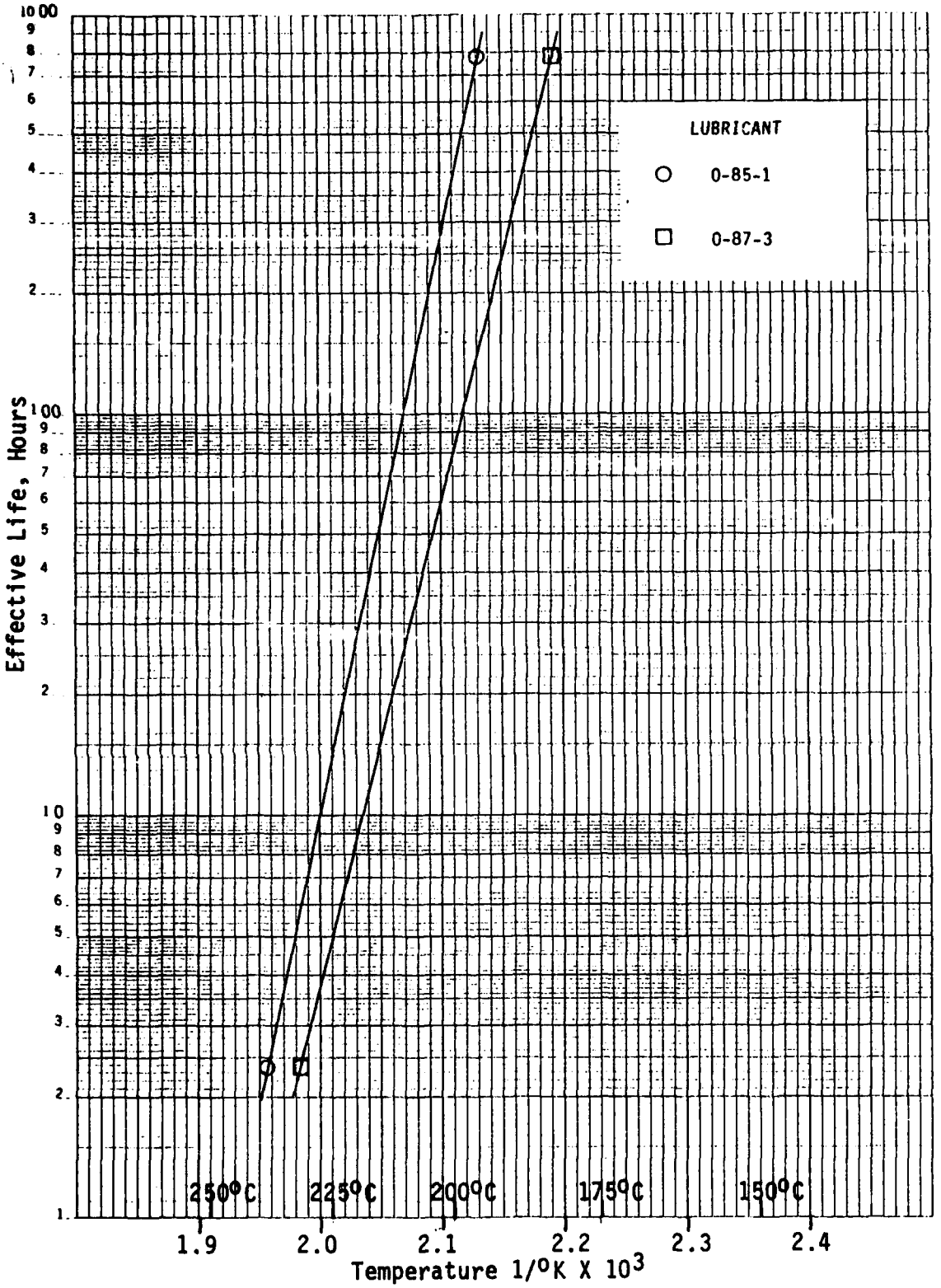

Figure 5. Effect of Temperature on Lubricant Life Using DERD Method No. 9, Total Acid Number Increase Limit of 1.5 (4 cSt Fluids)

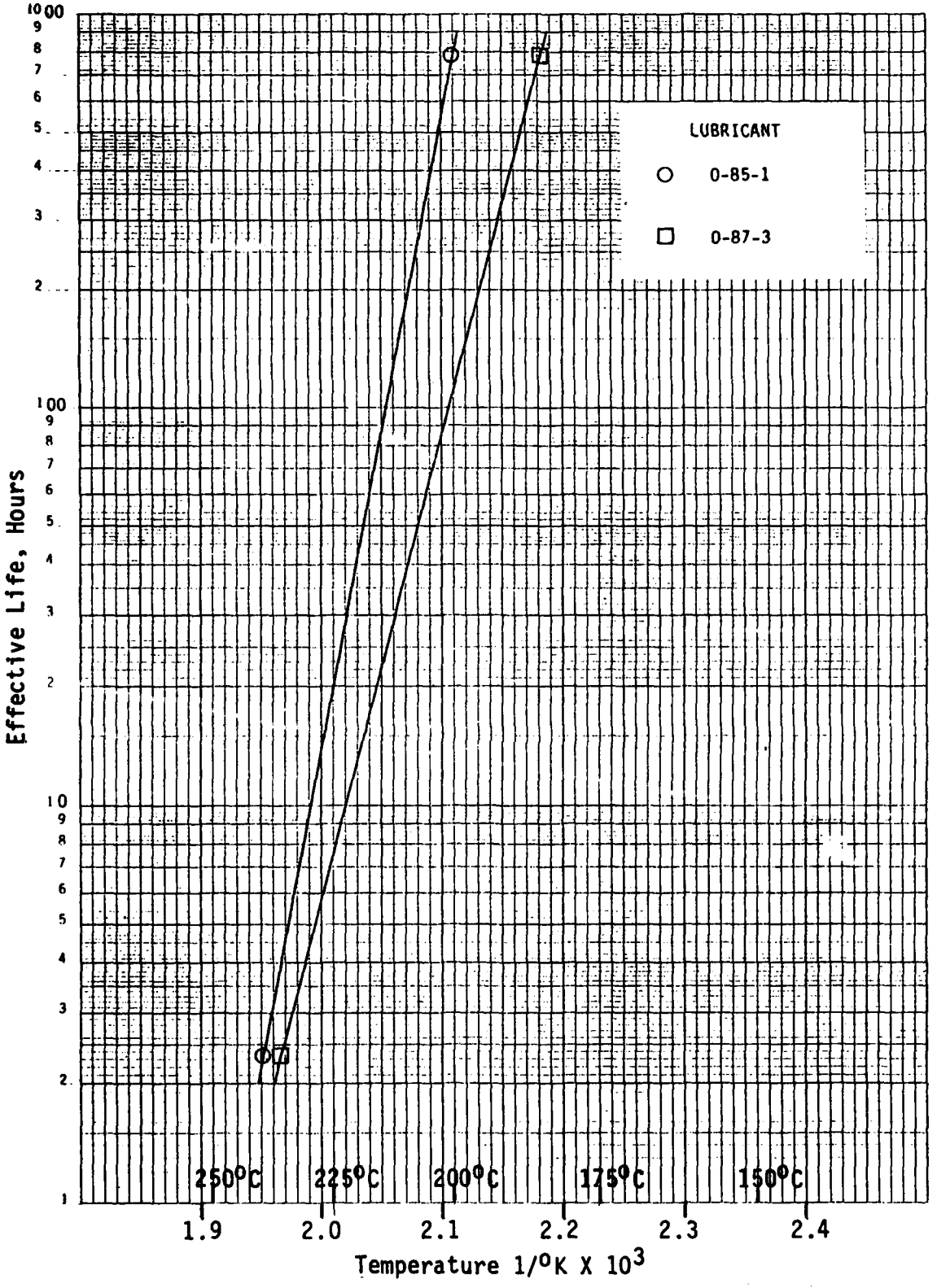

Figure 6. Effect of Temperature on Lubricant Life Using DERD Method No. 9, Total Acid Number Increase Limit of 3.0 (4 cSt Fluids)

TABLE 2

EFFECTIVE LUBRICANT LIFE
DERD METHOD NO. 9 (NO DILUTION)
ACIDITY INCREASE LIMITS

TAN Increase Limit of 1.0
Lubricant Life, Hours

Lubricant	0-79-16	0-71-6	0-77-15	0-79-18	0-85-1	0-87-3
175°C	2500	2000	1300	10,000	10,000	2000
200°C	100	155	140	520	350	60
225°C	7	20	24	5	6	3

TAN Increase Limit of 1.5
Lubricant Life, Hours

Lubricant	0-79-16	0-71-15	0-77-15	0-79-18	0-85-1	0-87-3
175°C	2800	2700	2000	10,000	10,000	2300
200°C	149	215	190	800	380	80
225°C	15	22	26	13	14	5

TAN Increase Limit of 3.0
Lubricant Life, Hours

Lubricant	0-79-16	0-71-6	0-77-15	0-79-18	0-85-1	0-87-3
175°C	3300	3200	3000	10,000	10,000	3000
200°C	278	308	330	1,000	800	115
225°C	35	44	52	61	20	6

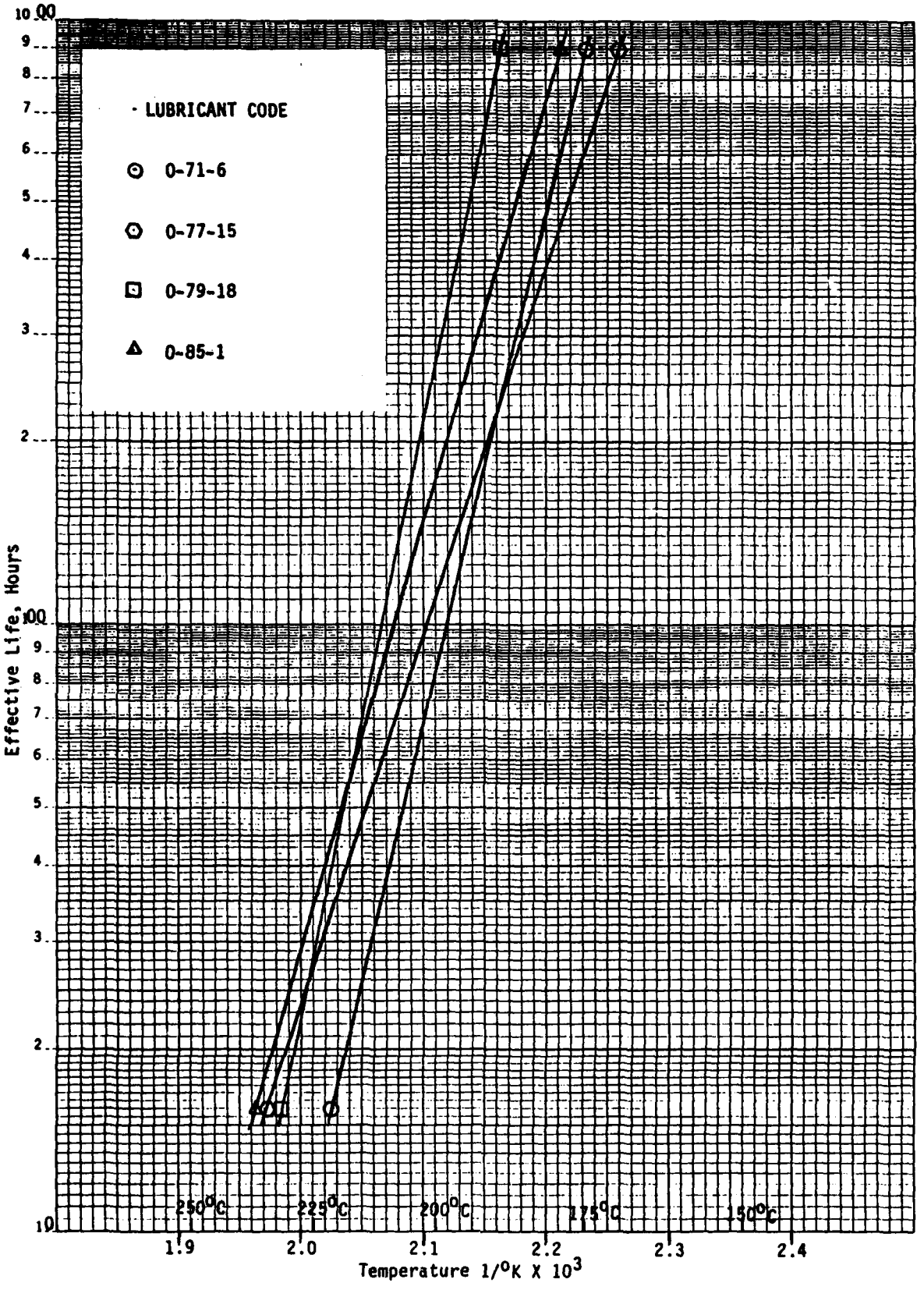

Figure 7. Effect of Temperature on Lubricant Life Using DERD Method No. 9, Viscosity Increase Limit of 15%

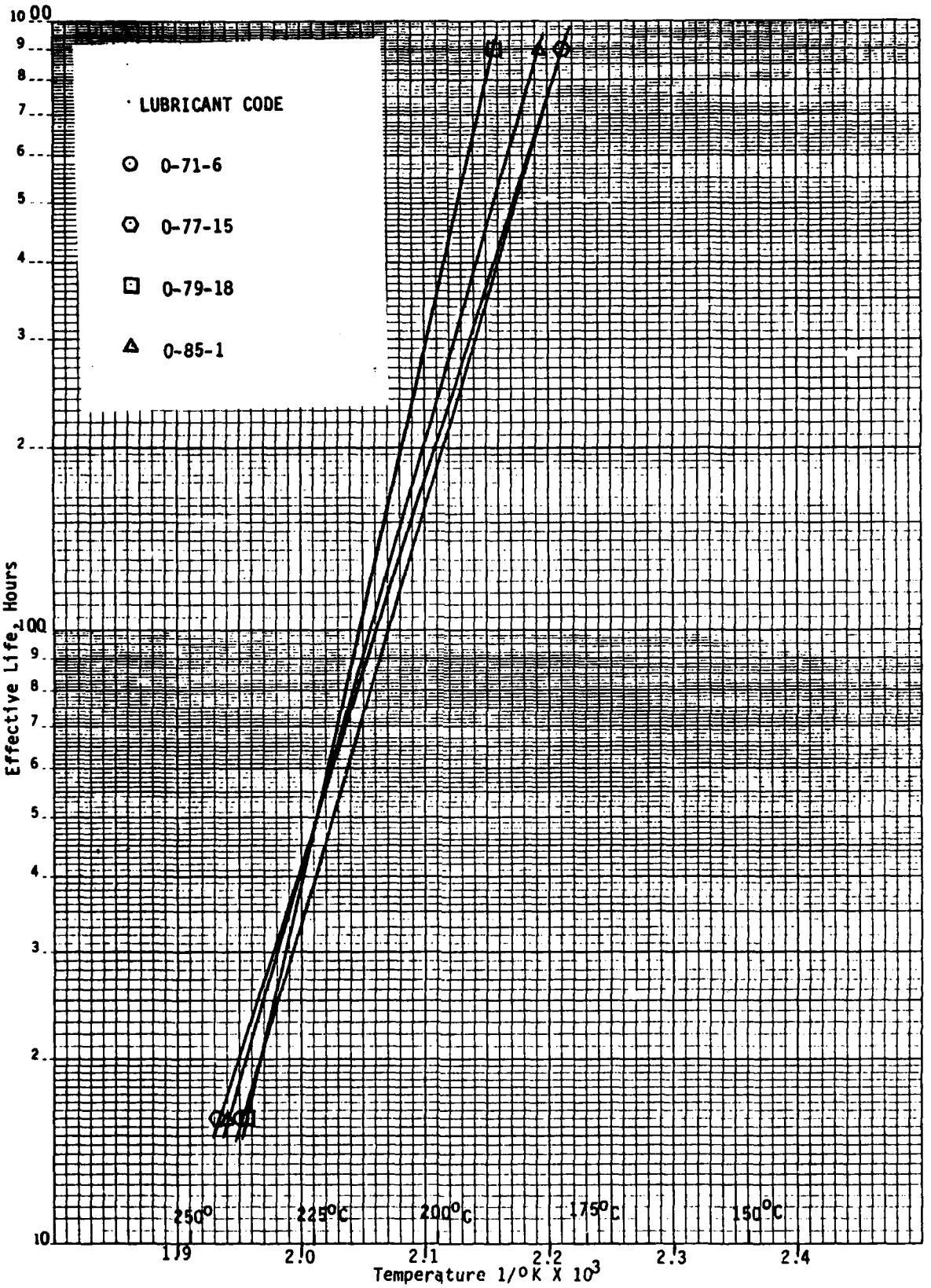

Figure 8. Effect of Temperature on Lubricant Life Using DERD Method No. 9, Viscosity Increase Limit of 25%

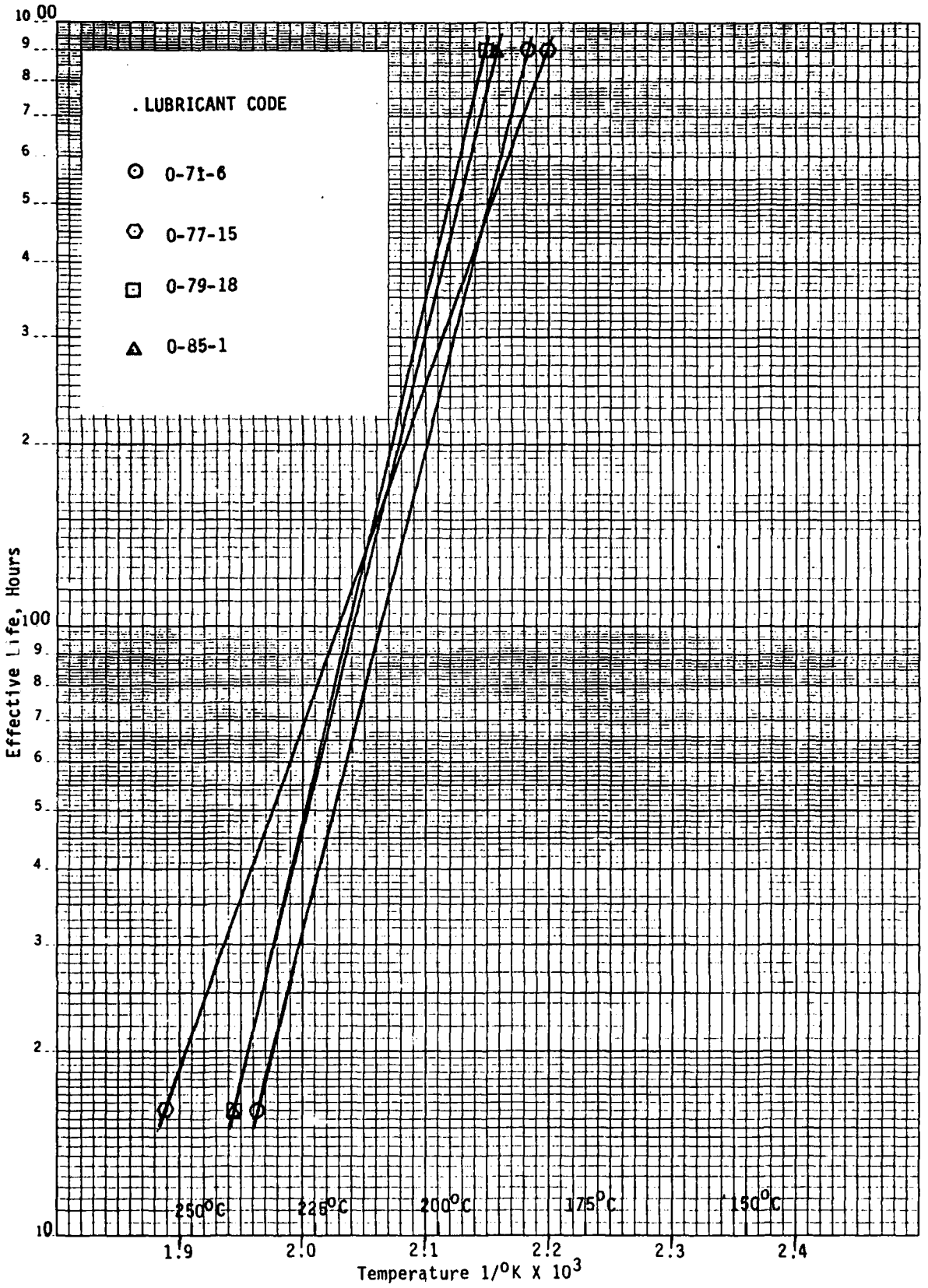

Figure 9. Effect of Temperature on Lubricant Life Using DERD Method No. 9, Viscosity Increase Limit of 35%

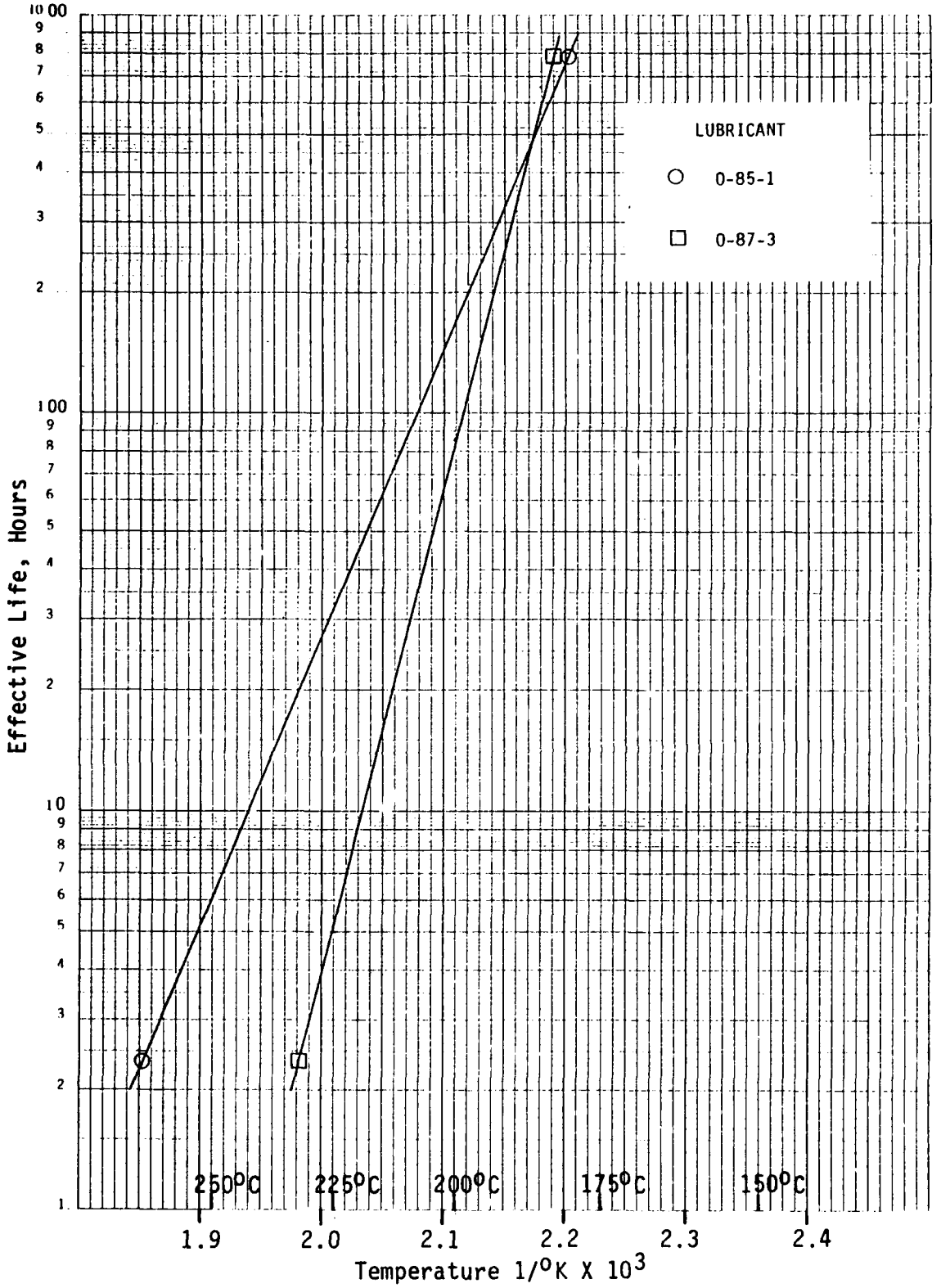

Figure 10. Effect of Temperature on Lubricant Life Using DERD Method No. 9, Viscosity Increase Limit of 15% (4 cSt Fluids)

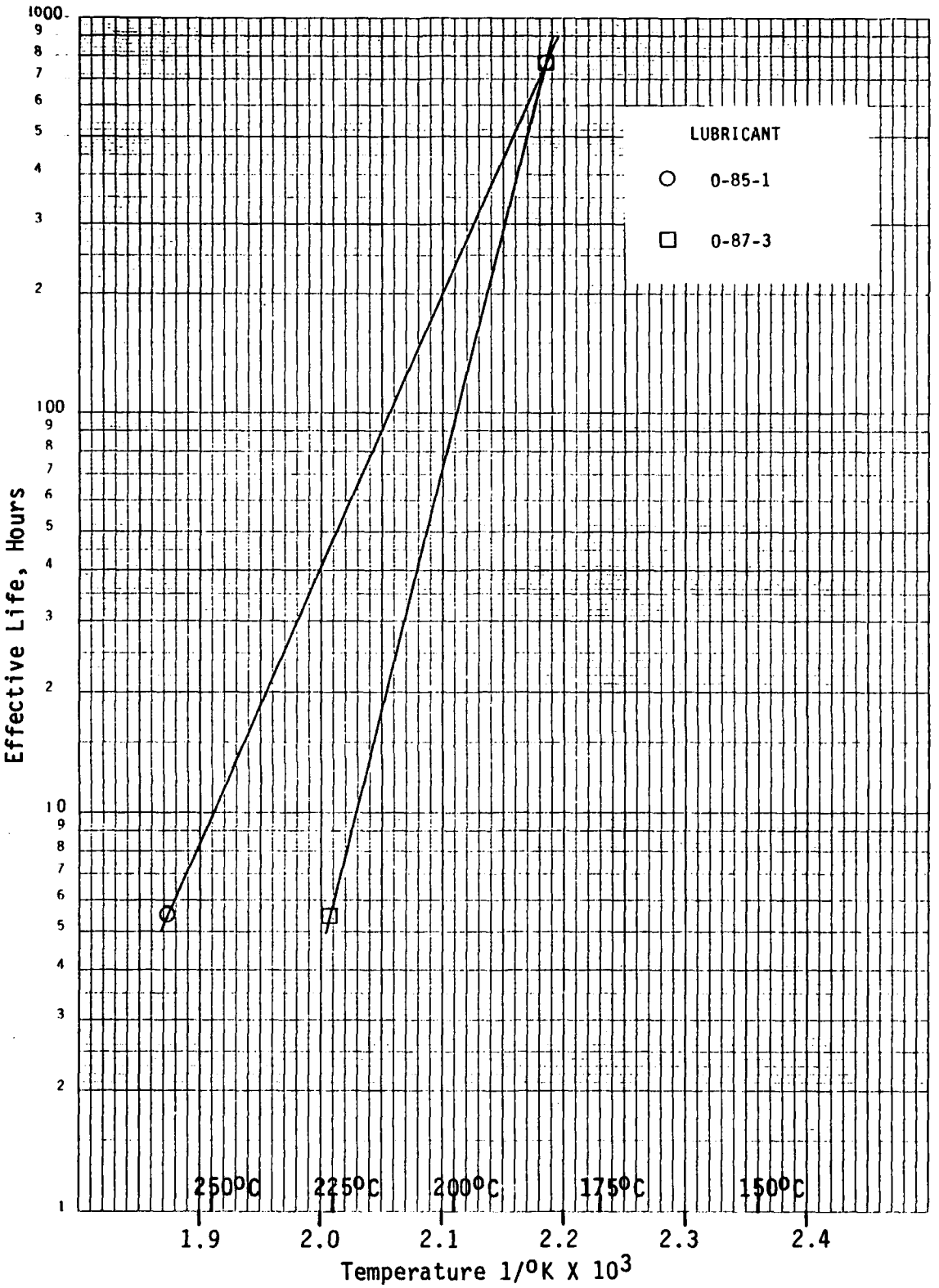

Figure 11. Effect of Temperature on Lubricant Life Using DERD Method No. 9, Viscosity Increase Limit of 25% (4 cSt Fluids)

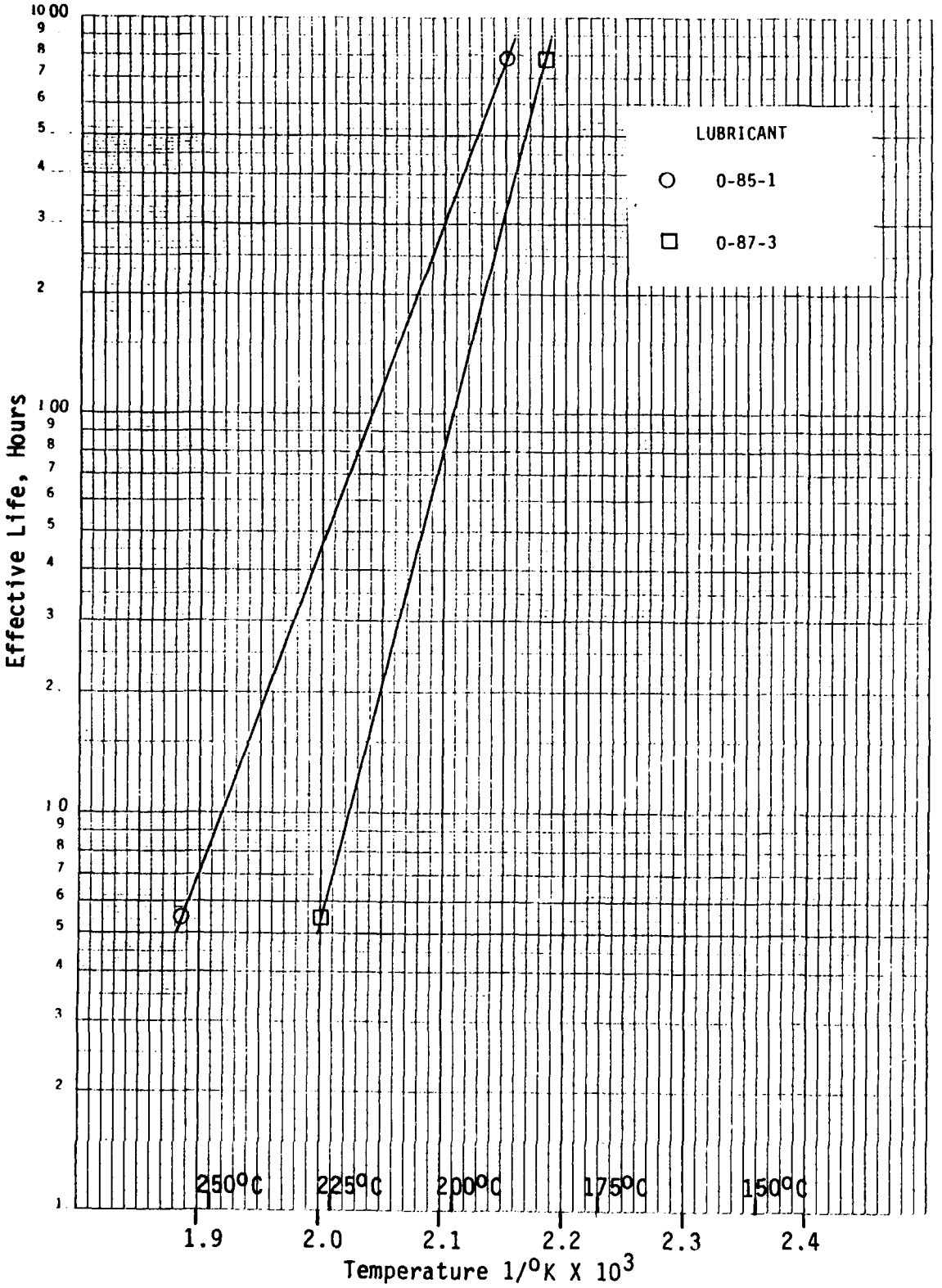

Figure 12. Effect of Temperature on Lubricant Life Using DERD Method No. 9, Viscosity Increase Limit of 35% (4 cSt Fluids)

TABLE 3

EFFECTIVE LUBRICANT LIFE
DERD METHOD NO. 9 (NO DILUTION)
VISCOSITY INCREASE LIMITS

Viscosity Increase Limit of 15%
Lubricant Life, Hours

Lubricant	O-71-6	O-77-15	O-79-18	O-85-1	O-87-3
175°C	840	590	4500	1250	2400
200°C	82	120	270	165	85
225°C	12	27	27	33	5

Viscosity Increase Limit of 25%
Lubricant Life, Hours

Lubricant	O-71-6	O-77-15	O-79-18	O-85-1	O-87-3
175°C	1250	1200	4000	1650	2850
200°C	190	200	350	235	95
225°C	38	49	48	48	6

Viscosity Increase Limit of 35%
Lubricant Life, Hours

Lubricant	O-71-6	O-77-15	O-79-18	O-85-1	O-87-3
175°C	2200	1350	4800	3500	2900
200°C	235	280	417	365	103
225°C	37	77	57	56	7

limiting viscosity increase values. This data shows that the two lubricants (O-79-18 and O-85-1) having the highest effective life based on acidity (TAN increase limits) have the highest overall effective life based on viscosity increase. The effective life of all the lubricants based on viscosity increases are lower than the effective life based on TAN increases which is mostly due to volatility and loss of the lighter (lower viscosity) esters.

Figures 13 thru 15 show the Arrhenius plots for the three MIL-L-23699 lubricants and the 4 cSt fluid using volatilization loss as the limiting life criterion and in general show the same relationship between effective life and stress temperature as was shown by the Arrhenius plots for these lubricants using selected viscosity increase values.

Figures 16 thru 18 show Arrhenius plots for the two 4 cSt lubricants using volatilization loss as the limiting life criterion. These Arrhenius plots are similar to those developed from viscosity change with O-85-1 showing slightly greater effective life at temperatures above 175°C to 200°C than O-87-3 and slightly lower effective lives at temperatures below these values for the 15%, 25% and 35% volatilization limits. The differences in effective life of all the lubricants are given in Table 4 for temperatures of 175°C, 200°C and 225°C. Lubricant O-79-18 shows a greater overall effective life based on volatilization loss than the other lubricants especially at temperatures of 200°C and below.

The evaluation of lubricant O-86-2 which is a different lot of the 4 cSt lubricant O-85-1 was evaluated at a test temperature of 210°C using DERD Method No. 9 for comparative purposes. Comparison of the test data is given in Table 5 and shows that very little difference exists in the oxidative stability of the two lubricants based on volatility, total acid number change, viscosity change or COBRA readings.

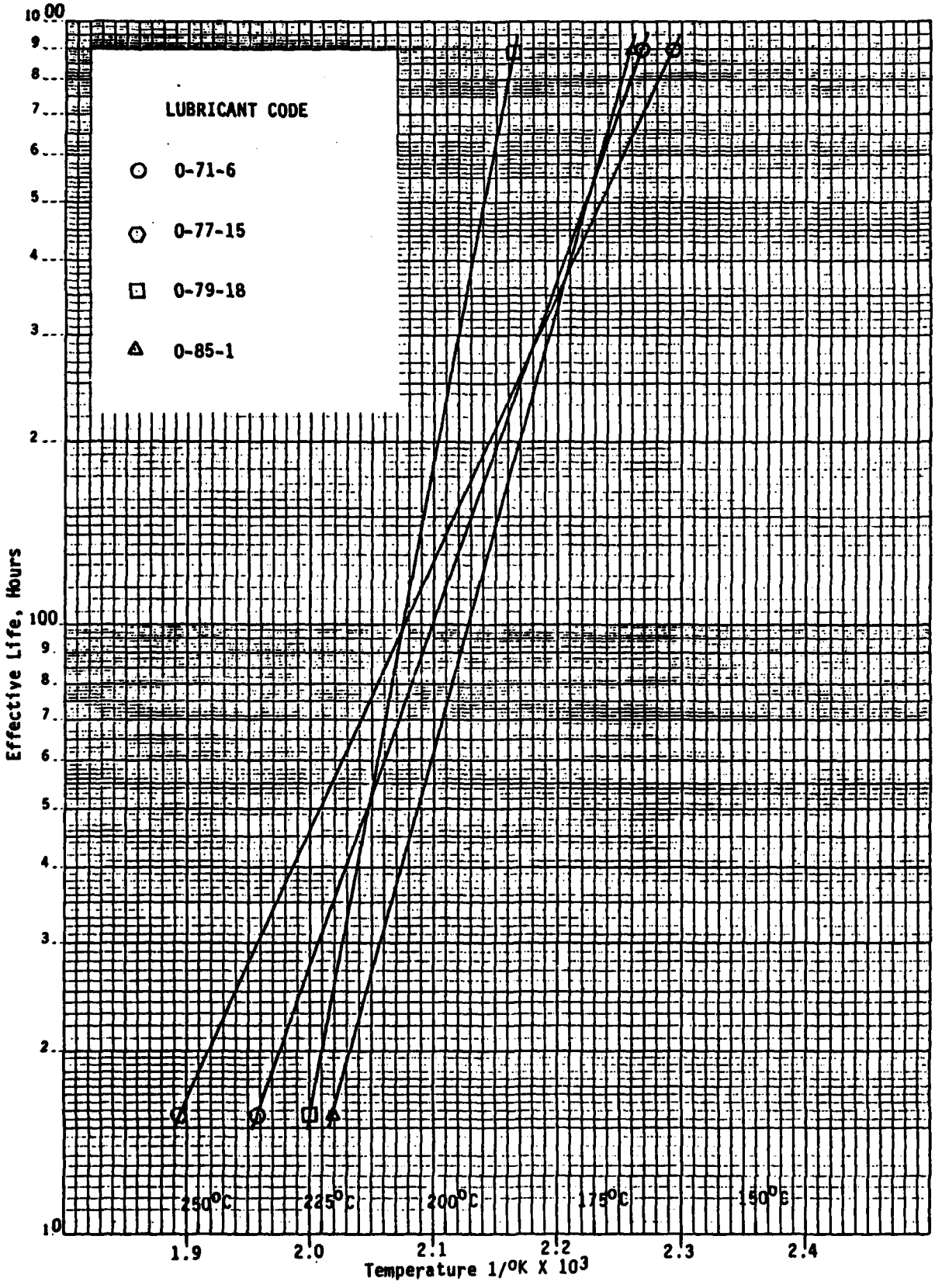

Figure 13. Effect of Temperature on Lubricant Life Using DERD Method No. 9, Volatilization Loss Limit of 15%

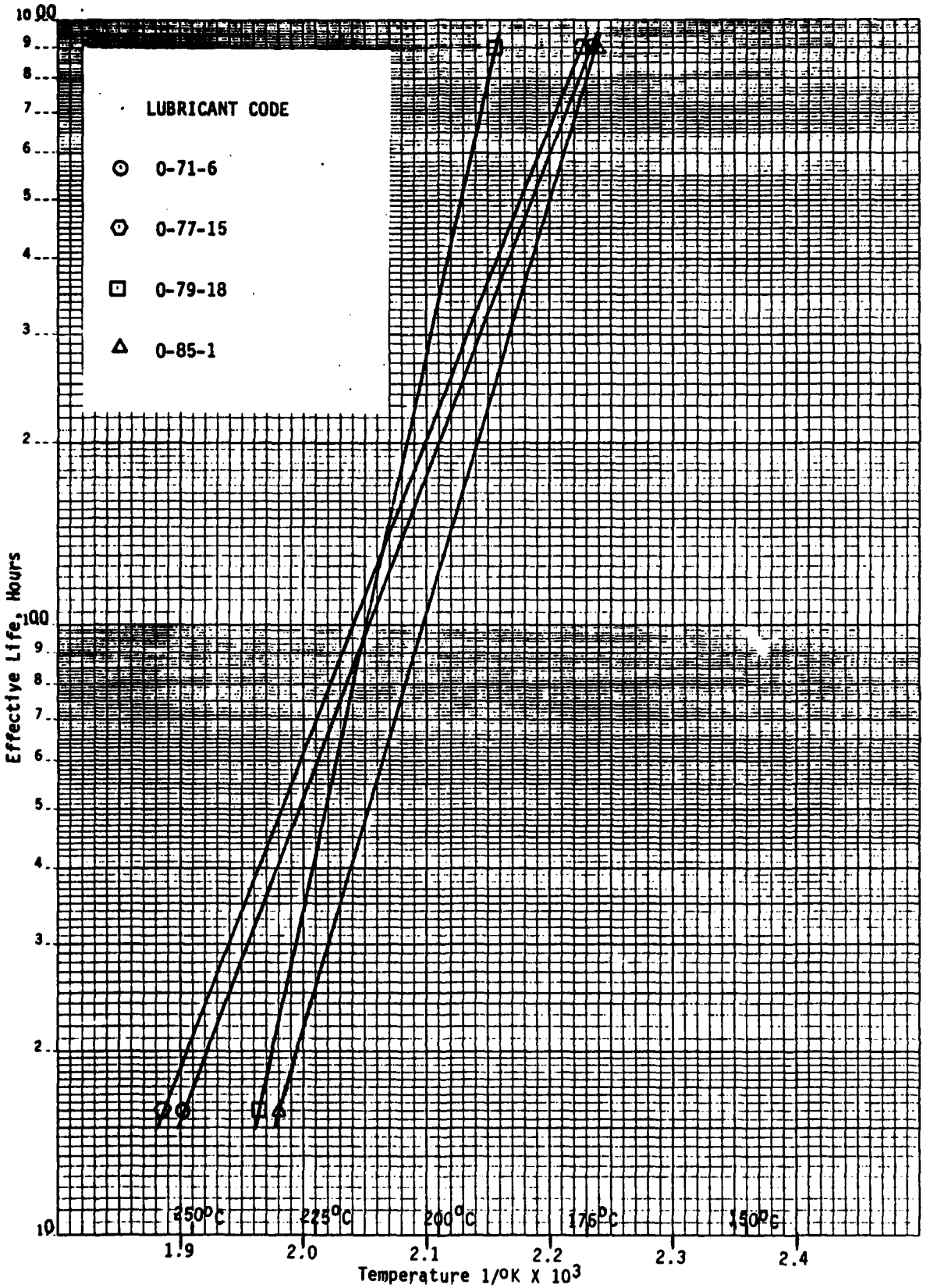

Figure 14. Effect of Temperature on Lubricant Life Using DERD Method No. 9, Volatilization Loss Limit of 25%

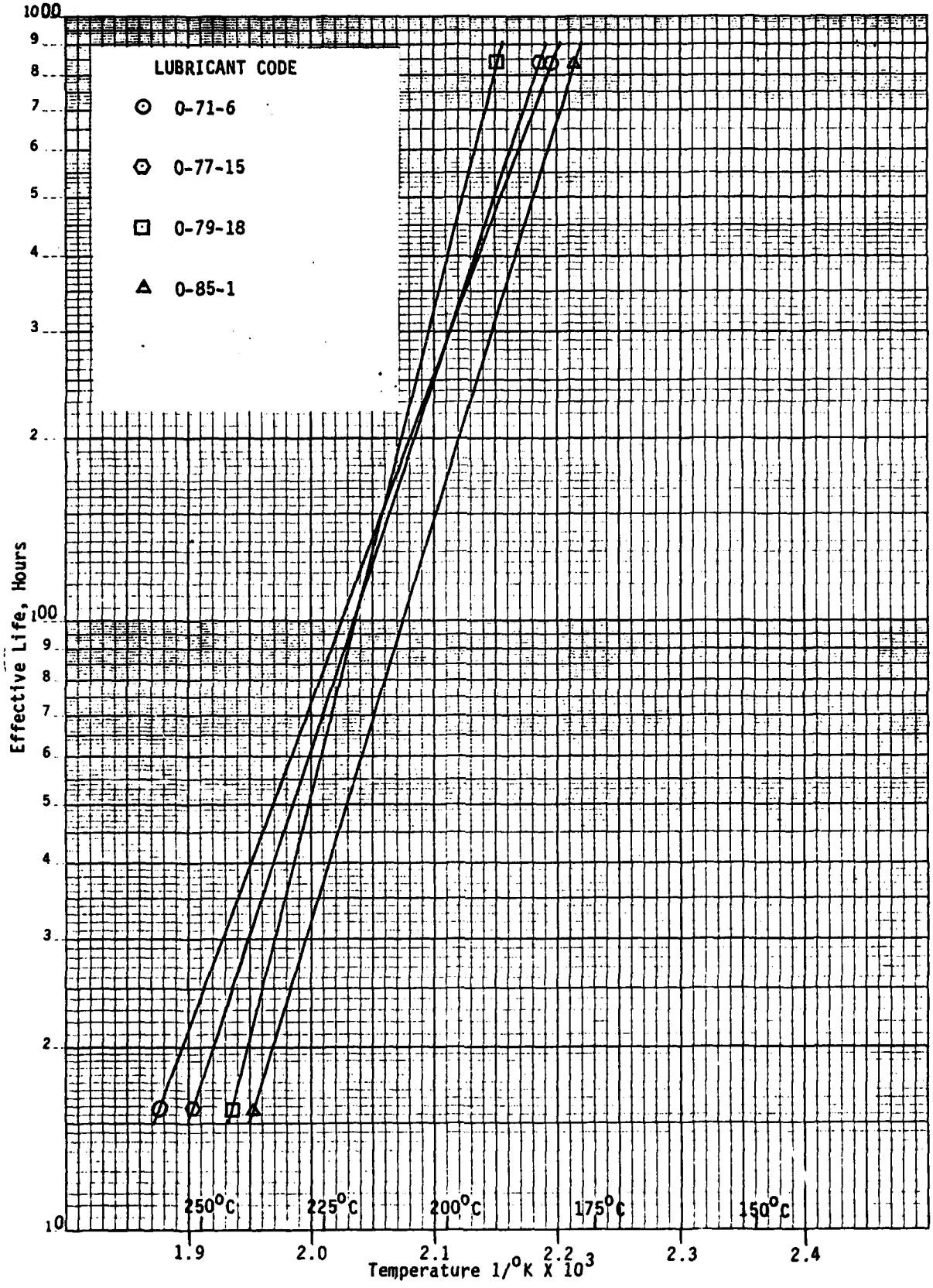

Figure 15. Effect of Temperature on Lubricant Life Using DERD Method No. 9, Volatilization Loss Limit of 35%

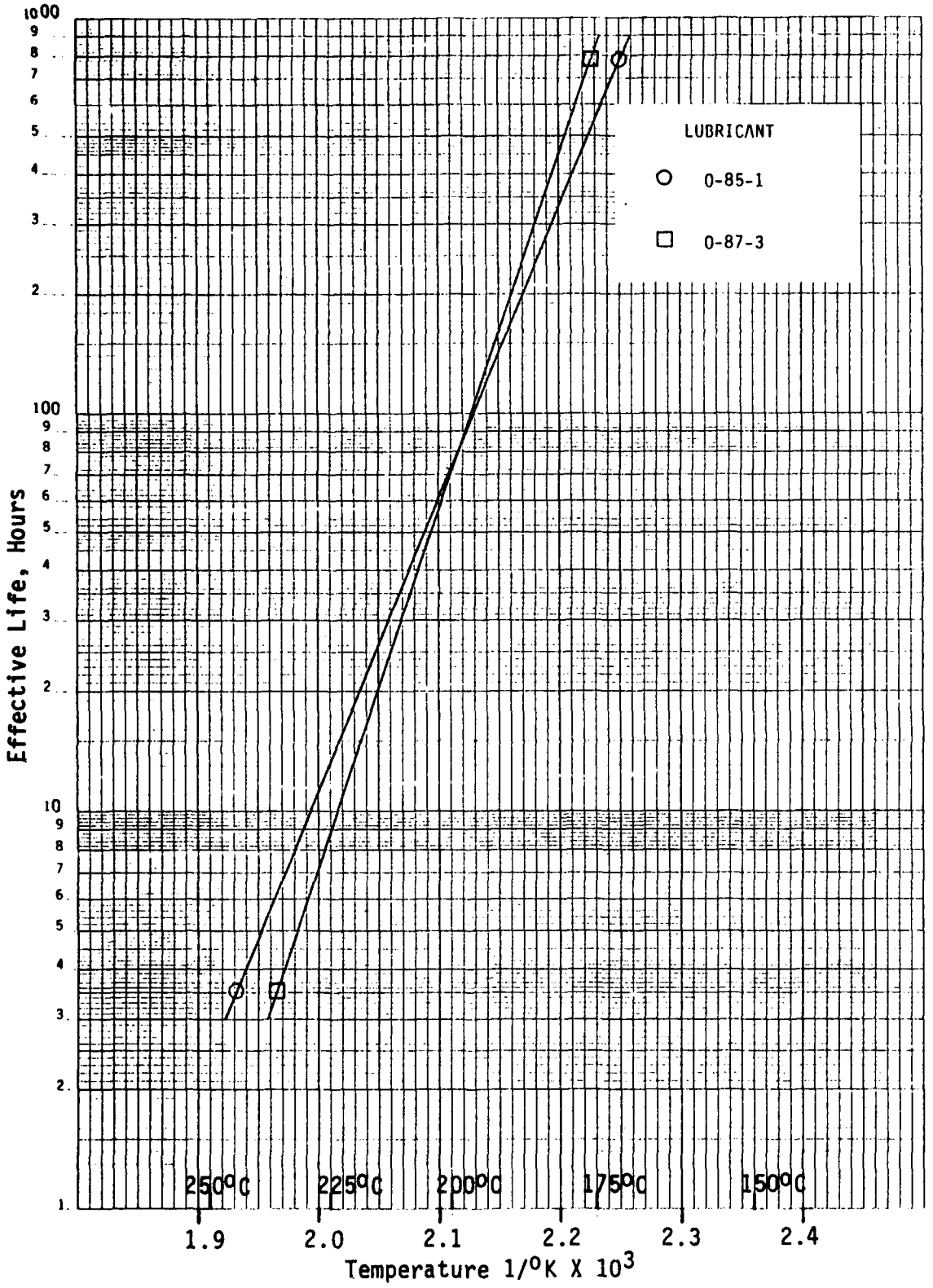

Figure 16. Effect of Temperature on Lubricant Life Using DERD Method No. 9, Volatilization Loss Limit of 15% (4 cSt Fluids)

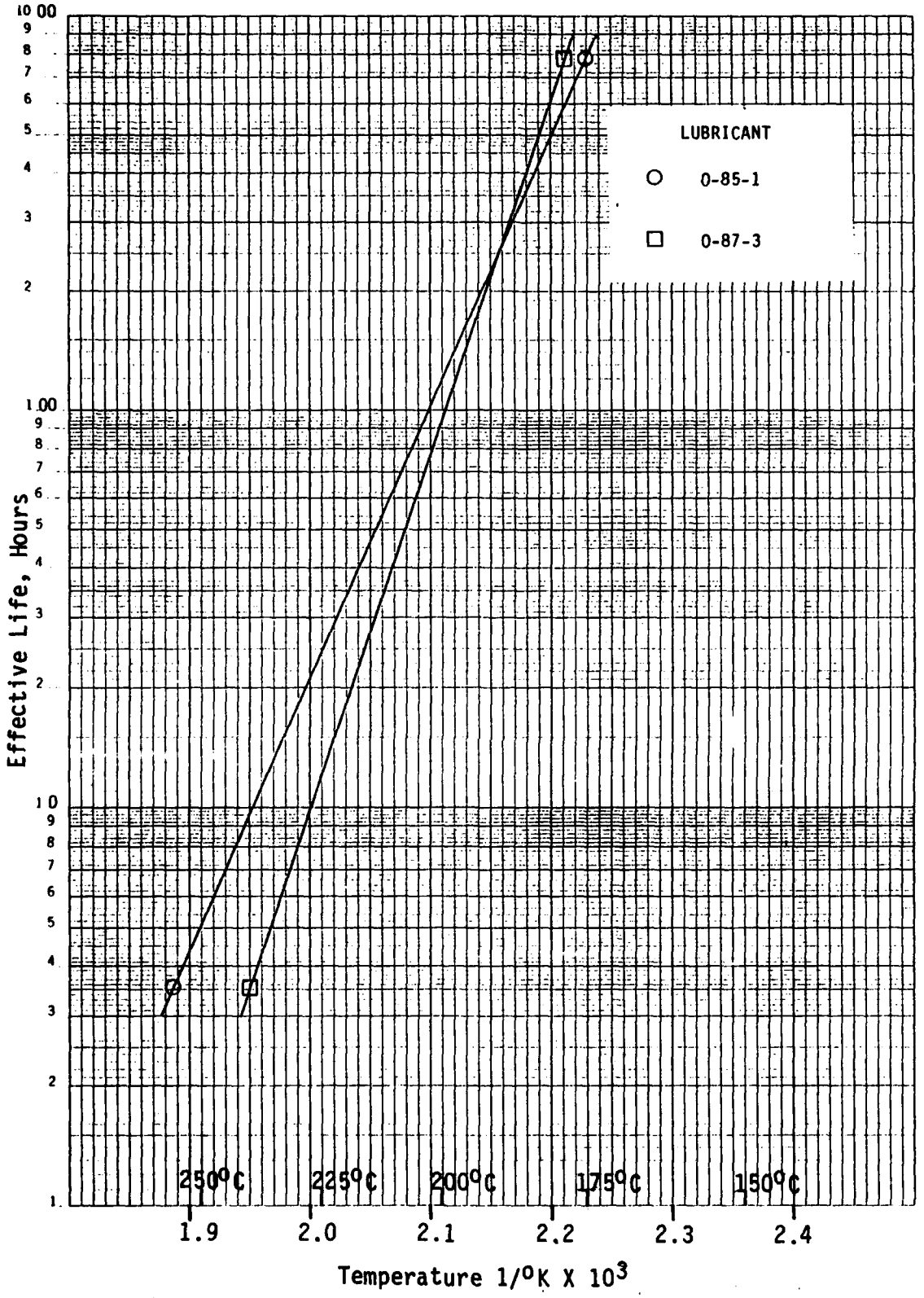

Figure 17. Effect of Temperature on Lubricant Life Using DERD Method No. 9, Volatilization Loss Limit of 25% (4 cSt Fluids)

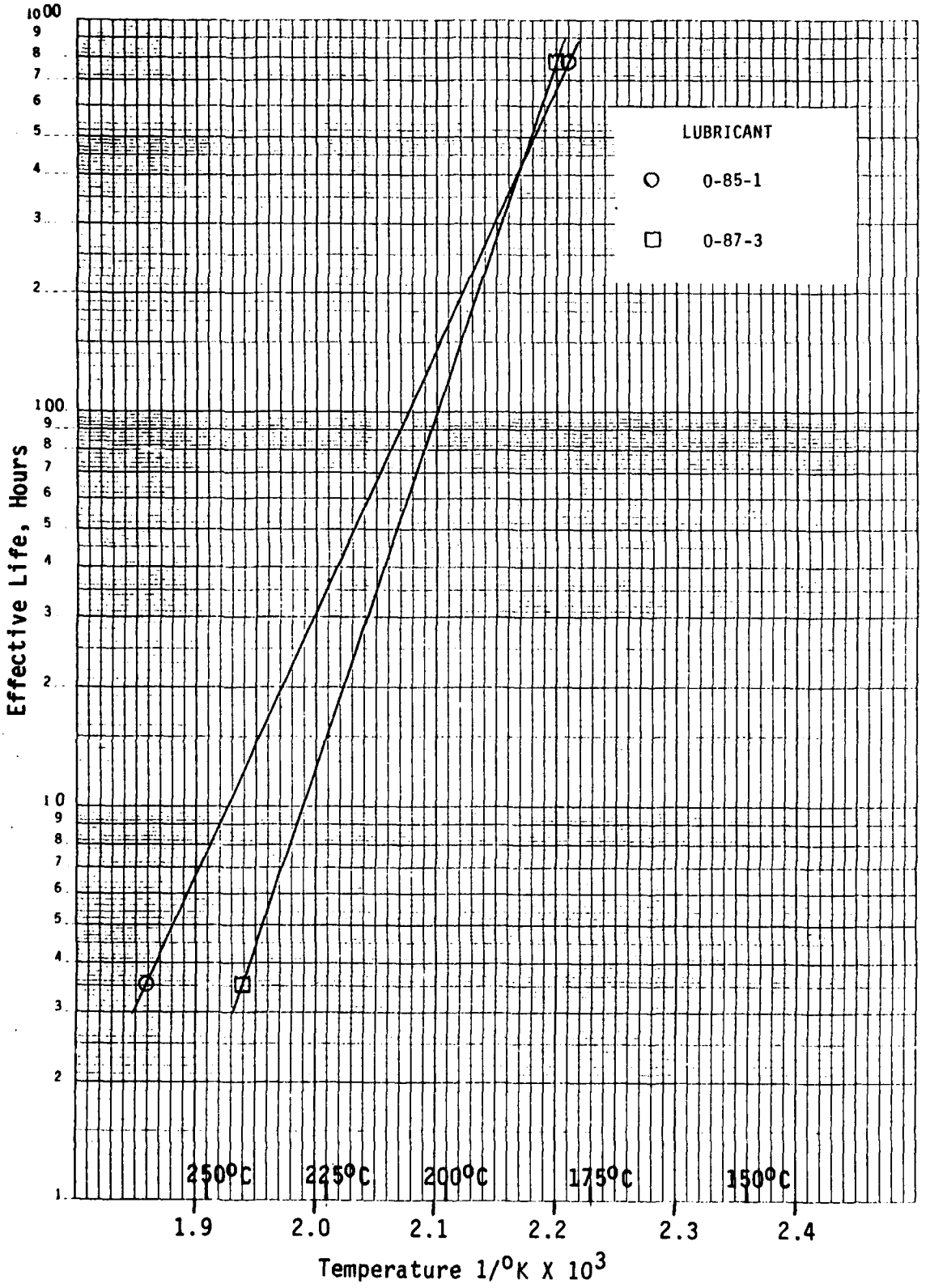

Figure 18. Effect of Temperature on Lubricant Life Using DERD Method No. 9, Volatilization Loss Limit of 35% (4 cSt Fluids)

TABLE 4

EFFECTIVE LUBRICANT LIFE
DERD METHOD NO. 9 (NO DILUTION)
VOLATILIZATION LOSS LIMITS

Volatilization Loss Limit of 15%
Lubricant Life, Hours

Lubricant	0-71-6	0-77-15	0-79-18	0-85-1	0-87-3
175°C	550	480	3600	550	840
200°C	115	145	230	72	73
225°C	32	52	21	14	9

Volatilization Loss Limit of 25%
Lubricant Life, Hours

Lubricant	0-71-6	0-77-15	0-79-18	0-85-1	0-87-3
175°C	850	930	3800	800	1200
200°C	195	220	325	120	95
225°C	57	66	40	25	12

Volatilization Loss Limit of 35%
Lubricant Life, Hours

Lubricant	0-71-6	0-77-15	0-79-18	0-85-1	0-87-3
175°C	1250	1650	4000	1100	1450
200°C	275	275	390	165	121
225°C	80	67	61	37	15

TABLE 5

COMPARISON OF SQUIRES OXIDATIVE TEST
DATA FOR LUBRICANTS O-85-1 AND O-86-2

Lubricant	O-85-1	O-86-2
Test Temp., °C	210	210
Test Hours	116	120
Weight Loss, %	44.8	44.8
COBRA Reading	123	129
Total Acid No.	1.70	2.05
Viscosity at 100°C, cSt	4.94	5.03
Viscosity Change, %	22.3	25.4

Testing of the 4 cSt lubricant O-85-1 and the MIL-L-23699 lubricant O-79-18 was conducted using DERD Method No. 9 test equipment modified by adding a condenser. This testing was conducted for comparing lubricant stability as determined with and without condensate return using 50 mL samples and the "Squires" sample tube.

The data in Table 6 shows the effect of condensate return on Squires oxidation testing of lubricant O-79-18 at a test temperature of 215°C. This data shows that condensate return has a considerable effect on changes in COBRA value, total acid number (TAN) and viscosity change. The COBRA value triples and the TAN value doubles using condensate return after only 24 hours of oxidative stressing. The 48 hour test using condensate return showed a much higher degree of degradation than the 72 hour test without condensate return. The much higher weight loss for the 48 hour test and the large increase in viscosity for the 48 hour condensate return test show that the effect of condensate return involves mechanisms other than mere condensation of esters and breakdown products but subsequent degradation and polymerization of the condensed material and a catalytic effect of condensate material on increasing the rate of lubricant degradation.

TABLE 6

EFFECT OF CONDENSATE RETURN ON SQUIRES OXIDATION TEST FOR LUBRICANT O-79-18 AT 215°C TEST TEMPERATURE

	Test Hours					
	24		48		72	
	Condensate Return		Condensate Return		Condensate Return	
	No	Yes	No	Yes	No	Yes
Weight Loss, %	6.8	8.3	-	39.8	20.9	-
COBRA Reading	65	200+	-	200+	92	-
Lubri Sensor Reading (μA)	+15	+50	-	+50	+33	-
Total Acid No.	0.91	1.81	-	4.73	1.60	-
Vis. at 100°C, cSt	5.43	5.62	-	11.02	6.14	-
Vis. Change, %	2.6	6.2	-	108.2	16.1	-

The data in Table 7 shows the effect of condensate return on Squires oxidation testing of lubricant O-85-1 at a test temperature of 215°C. This data shows that condensate return has much less effect on this lubricant than on O-79-18 and that the effect of condensate return is merely condensation which decreases the viscosity and increases the TAN slightly.

TABLE 7

EFFECT OF CONDENSATE RETURN ON SQUIRES OXIDATION TEST FOR LUBRICANT O-85-1 AT 215°C TEST TEMPERATURE

	Test Hours					
	24		48		72	
	Condensate Return		Condensate Return		Condensate Return	
	No	Yes	No	Yes	No	Yes
Weight Loss, %	13.4	9.8	24.7	14.7	35.2	26.1
COBRA Reading	56	71	104	161	115	200+
Lubri Sensor Reading (μA)	+10	+15	+21	+50	+25	+50
Total Acid No.	0.62	0.47	1.20	1.76	1.86	3.83
Vis. at 100°C, cSt	4.23	4.13	4.46	4.23	4.73	4.62
Vis. Change, %	4.7	2.2	10.4	4.7	17.0	14.4

Testing was conducted for comparing lubricant stability as determined with and without condensate return at a temperature lower than 215°C which gave severe degradation for the condensate return testing. The data in Table 8 shows the effect of condensate return on Squires oxidation testing of lubricants O-79-18 and O-85-1 at a temperature of 205°C.

TABLE 8

EFFECT OF CONDENSATE RETURN ON SQUIRES OXIDATION TEST FOR LUBRICANTS O-79-18 AND O-85-1 AT 205°C, 72 TEST HOURS

Lubricant	O-79-18		O-85-1	
	Condensate Return		Condensate Return	
	No	Yes	No	Yes
Weight Loss, %	9.7	38.5	17.6	13.6
COBRA Reading	75	200+	72	200+
Total Acid No.	0.50	17.53	0.40	4.97
Vis. at 100°C, cSt	5.67	very viscous	4.29	4.24
Vis. Change, %	7.1	-	6.3	5.0

The data in Table 8 shows that condensate return can have a considerable effect on changes in COBRA value, total acid number and viscosity as did the data in Table 6. The data in Tables 6 and 8 also shows that the use of condensate return can greatly increase the weight loss and that the effects of condensate return include mechanisms other than mere condensation of esters and breakdown products but involves subsequent degradation and polymerization of the condensed material and a catalytic effect of condensate material on increasing the rate of lubricant degradation. The data in Table 8 for lubricant O-85-1 is more similar to that obtained at the test temperature of 215°C showing much less effect of condensate return on this lubricant which is merely condensation of volatiles that decreases the viscosity and increases the TAN slightly.

The data in Tables 6 thru 8 show that the effect of condensate return on lubricant properties after oxidative degradation is highly lubricant formulation dependent.

f. Summary

Effective lubricant lives of three MIL-L-23699 lubricants and two 4 cSt candidate lubricants were established using different levels of limiting values for changes in TAN, viscosity and weight loss as the maximum permissible degree of degradation occurring during oxidative stressing using DERD Method No. 9. One MIL-L-23699 lubricant and one of the 4 cSt candidate lubricants were found to have similar and superior lubricant effective lives than the other lubricants studied including those reported in the Interim Technical Report.[1] Relative ranking of the lubricants within each group depended on the criteria for defining maximum permissible degradation.

Evaluation of two lots of the same 4 cSt lubricant at 210°C using the Squires oxidation test gave good repeatability for changes in TAN, viscosity, COBRA reading and weight loss.

Condensate return has been shown to have a considerable effect on changes in TAN, viscosity, COBRA values and weight loss during oxidative stressing and that mechanisms other than mere condensation of esters and breakdown products occur. Other mechanisms involve subsequent degradation and polymerization of the condensed material and a catalytic effect of condensate material on increasing the rate of degradation. The effect of condensate return on post test properties is also highly lubricant formulation dependent.

2. LUBRICANT CONFINED HEAT STABILITY

a. Introduction

The purpose of this study was to determine the confined heat stability of selected turbine engine lubricants under various temperatures, and to provide a measure of their stability in terms of effective lubricant life. The effective life was determined by selecting limiting values for various physical and chemical properties, and monitoring these properties during lubricant stressing. Properties monitored included weight loss due to volatility, acidity increase, viscosity increase, toluene insolubles, electrochemical properties, and composition. Only the acidity increases and viscosity increases were significant enough to provide data required for the development of Arrhenius plots, which graphically depict the effective life of a lubricant as a function of temperature.

b. Test Apparatus

The confined heat stability test apparatus has been previously described in the Interim Technical Report[1] for Phase 1 of this study.

Prior to each test the vessels were degreased with V.M.&P. naphtha. The vessels were then polished with a cotton pad which had been dampened in heptane and dipped into 3 micron size corundum powder. The condenser tube, aluminum washer and vessel cover were cleaned in the same manner. A small brush with the scouring mixture was used to clean inside the vent tube. The entire vessel was then rinsed and washed with Alconox detergent. Using distilled water and isopropanol as final rinses, the vessels were then blown dry with clean dry air.

c. Test Procedure

The vessel was filled to approximately two-thirds of its volume with 85 mL of the sample fluid. The lid, aluminum washer, and condenser tube were

assembled, screwed firmly into place, and weighed to the nearest 0.1 gram. The apparatus was placed into the heating bath which had been heated to the required test temperature. At the end of the specified test period, the vessels were removed and allowed to cool to room temperature.

The vessels were then wiped with a lint-free towel, washed with V.M.&P. naphtha and reweighed. The percent weight loss was calculated and the test assembly was opened and inspected for deposits. The test fluid was poured into an amber bottle and sealed with a Polyseal cap.

The total acid number, viscosity, toluene insolubles and electrochemical properties were determined as described in Section II.1.c. of the previous technical report[1].

d. Test Lubricants and Test Conditions

A total of five lubricants were examined during Phase 2 of this study. Table 1, Section II.1.d, presents a listing and description of these lubricants.

Lubricants were stressed at temperatures ranging from 190°C to 215°C with test durations ranging from 24 hours to 336 hours depending upon the test temperature and the specific fluid being tested. Testing of each fluid was discontinued after severe degradation had occurred. Total acid numbers and COBRA measurements were conducted on the same day the samples were removed from the test bath since these properties can change with time after lubricant stressing.

e. Results and Discussion

Lubricant lives of the thermally stressed lubricants were developed using Total Acid Number (TAN) increases of 2.0, 4.0 and 6.0 as the effective life limiting values. No viscosity increase or volatility loss criterion was used for describing effective lubricant life since only very small viscosity

change or lubricant loss occurred within the test hours required for providing TAN increases above 6. Appendix A, Table A-2 provides all the Squires Confined Heat test data developed during Phase 2 of this study and from which Arrhenius plots were developed.

Arrhenius plots showing effective lubricant life using selected acidity increase limits of 2.0, 4.0 and 6.0 are shown in Figures 19 through 21. The Arrhenius plots for lubricants O-77-15, O-85-1 and TEL-7043 are very similar to the Arrhenius plots for the MIL-L-7808 fluids shown by Figures 15 and 16 (pages 37 and 38) of the Interim Technical Report[1]. The Arrhenius plots for lubricant O-79-18 vary considerably from the Arrhenius plots of all other MIL-L-7808 or MIL-L-23699 lubricants and the 4 cSt fluid O-85-1 established from confined heat testing and using acidity increase limits as the limiting life criteria. The effective lubricant life for lubricant O-79-18 was very much lower than that for the other lubricants at temperatures below 200°C. However, for temperatures above 200°C lubricant O-79-18 showed the greatest effective lubricant life of all lubricants investigated.

Figures 22 and 23 show Arrhenius plots for the two 4 cSt lubricants using TAN increase limits of 2.0 and 4.0 as the limiting life criteria. The two lubricants show similar effective lives for both TAN limits except at temperatures below 175°C where lubricant O-85-1 displays a much greater effective life than lubricant O-87-3.

Differences in effective life of the three MIL-L-23699 fluids O-77-15, O-79-18 and TEL-7043 and the 4 cSt fluids O-85-1 and O-87-3 are shown in Table 9 for test temperatures of 175°C, 200°C, and 225°C for limiting TAN increase values. This data is very similar to the data shown by Table 8 of the Interim Technical Report[1] for the MIL-L-7808 type fluids

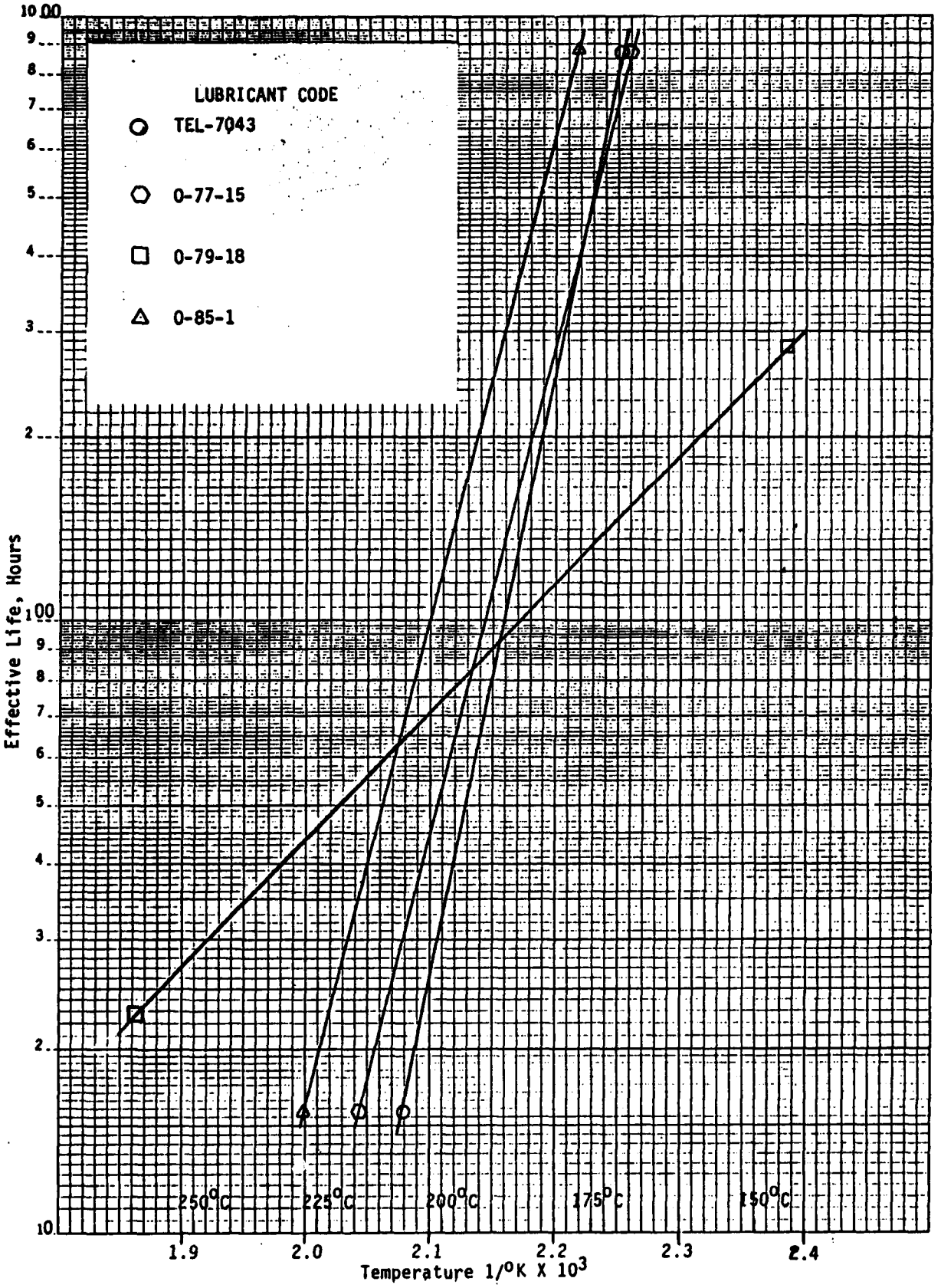

Figure 19. Effect of Temperature on Lubricant Life Using DERD Method No. 1 (Confined Heat Stability), Total Acid Number Increase Limit of 2.0

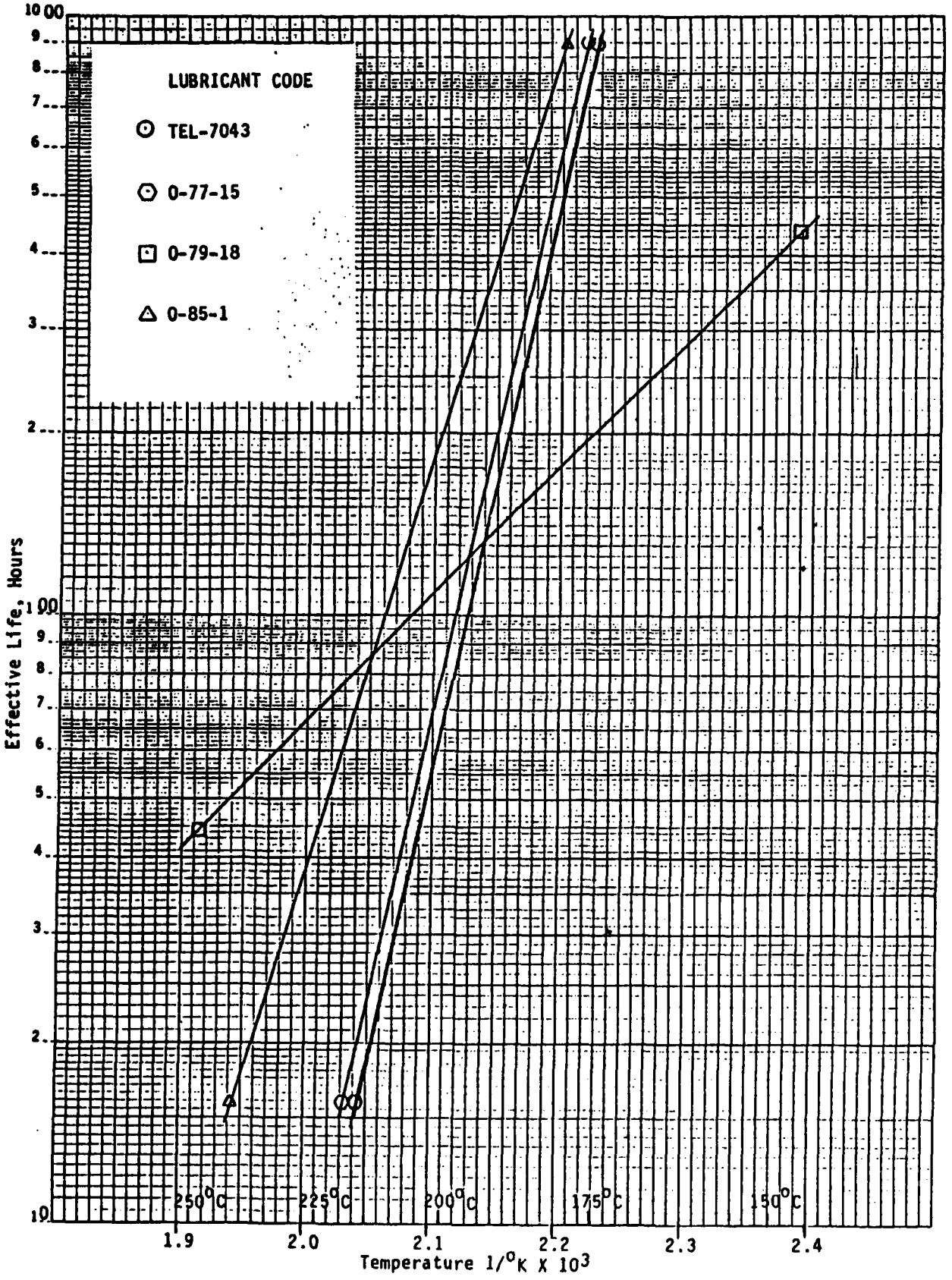

Figure 20. Effect of Temperature on Lubricant Life Using DERD Method No. 1 (Confined Heat Stability), Total Acid Number Increase Limit of 4.0

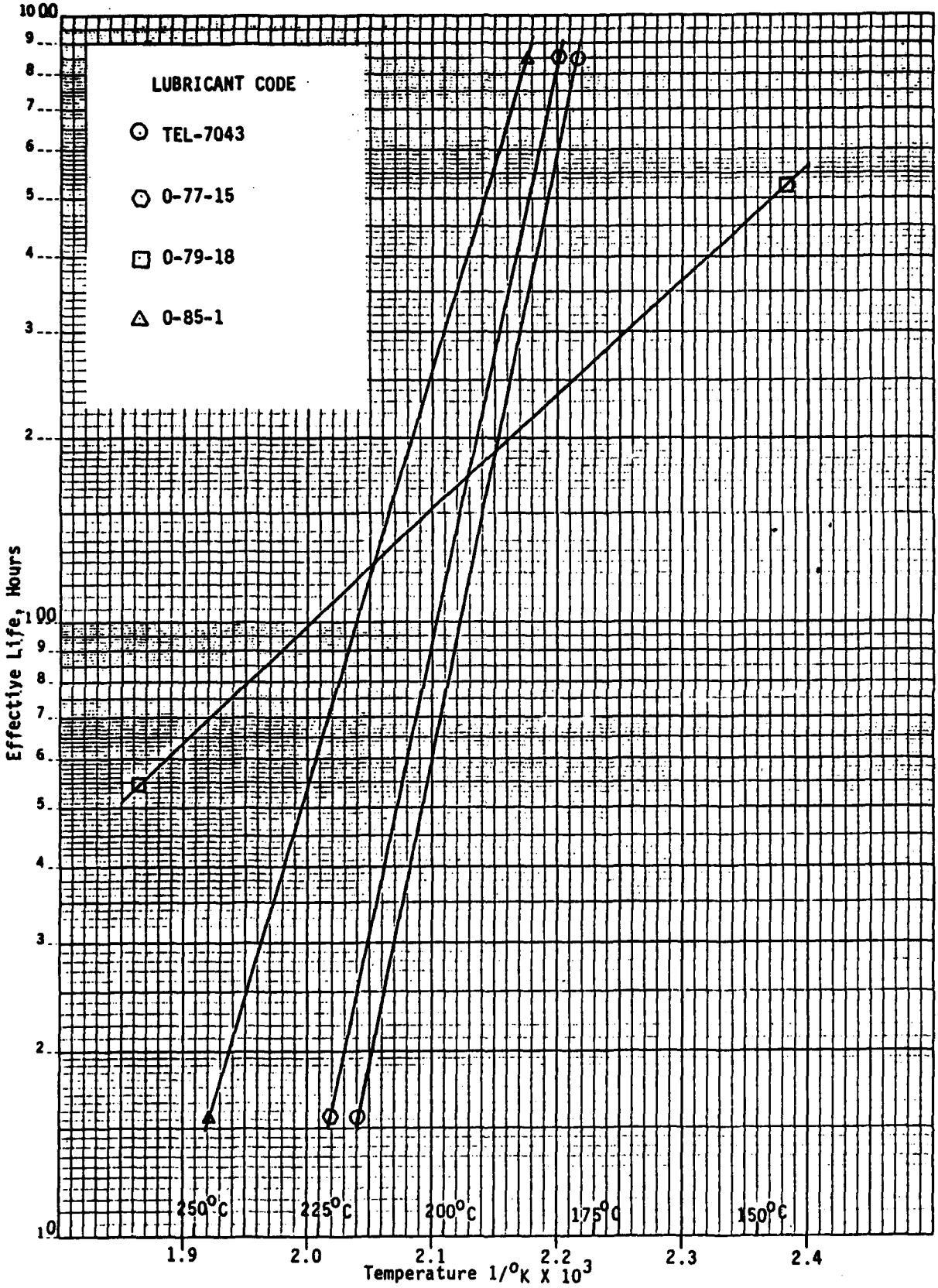

Figure 21. Effect of Temperature on Lubricant Life Using DERD Method No. 1 (Confined Heat Stability), Total Acid Number Increase Limit of 0.0

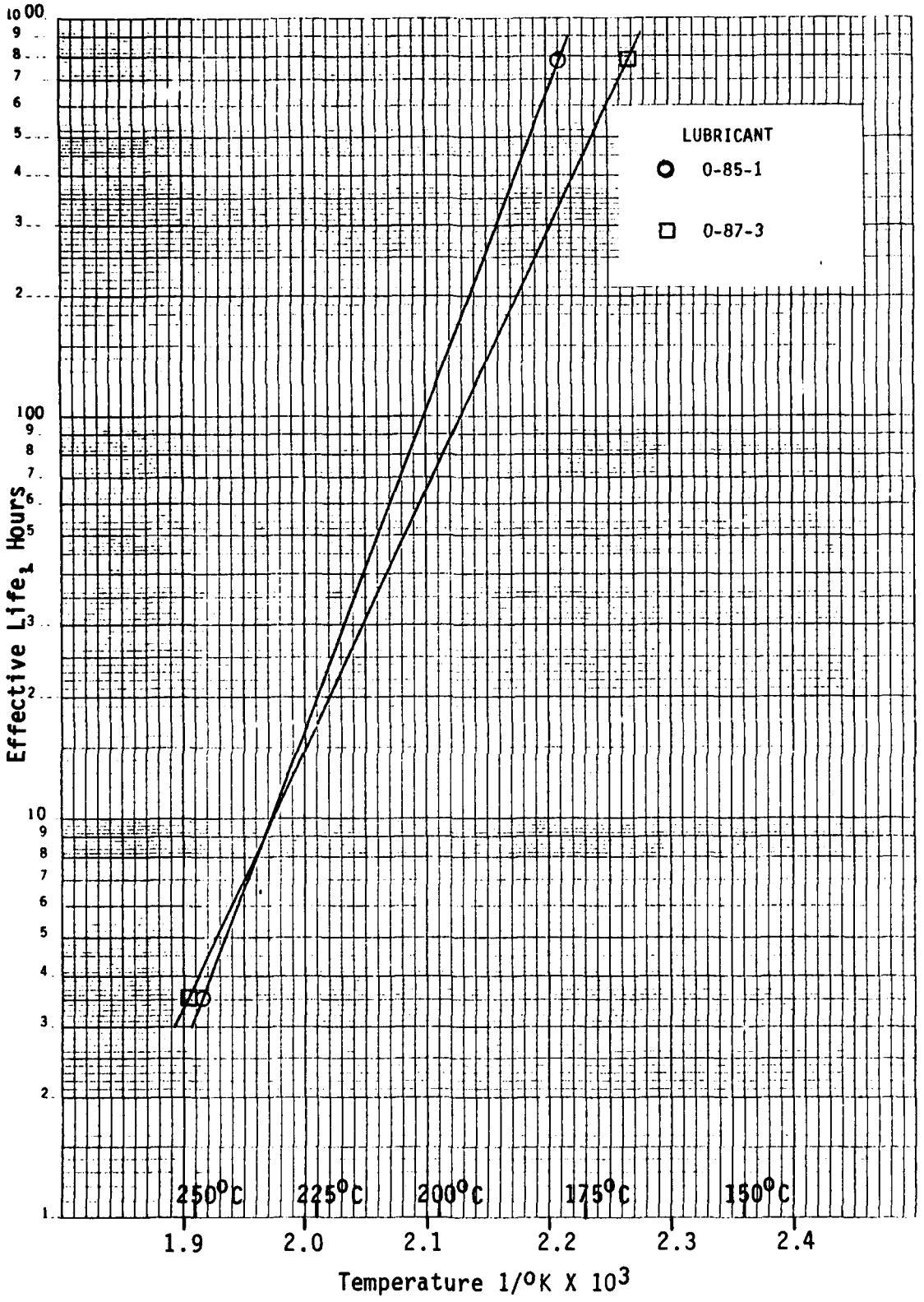

Figure 22. Effect of Temperature on Lubricant Life Using DERD Method No. 1 (Confined Heat Stability), Total Acid Number Increase Limit of 2.0 (4 cSt Fluids)

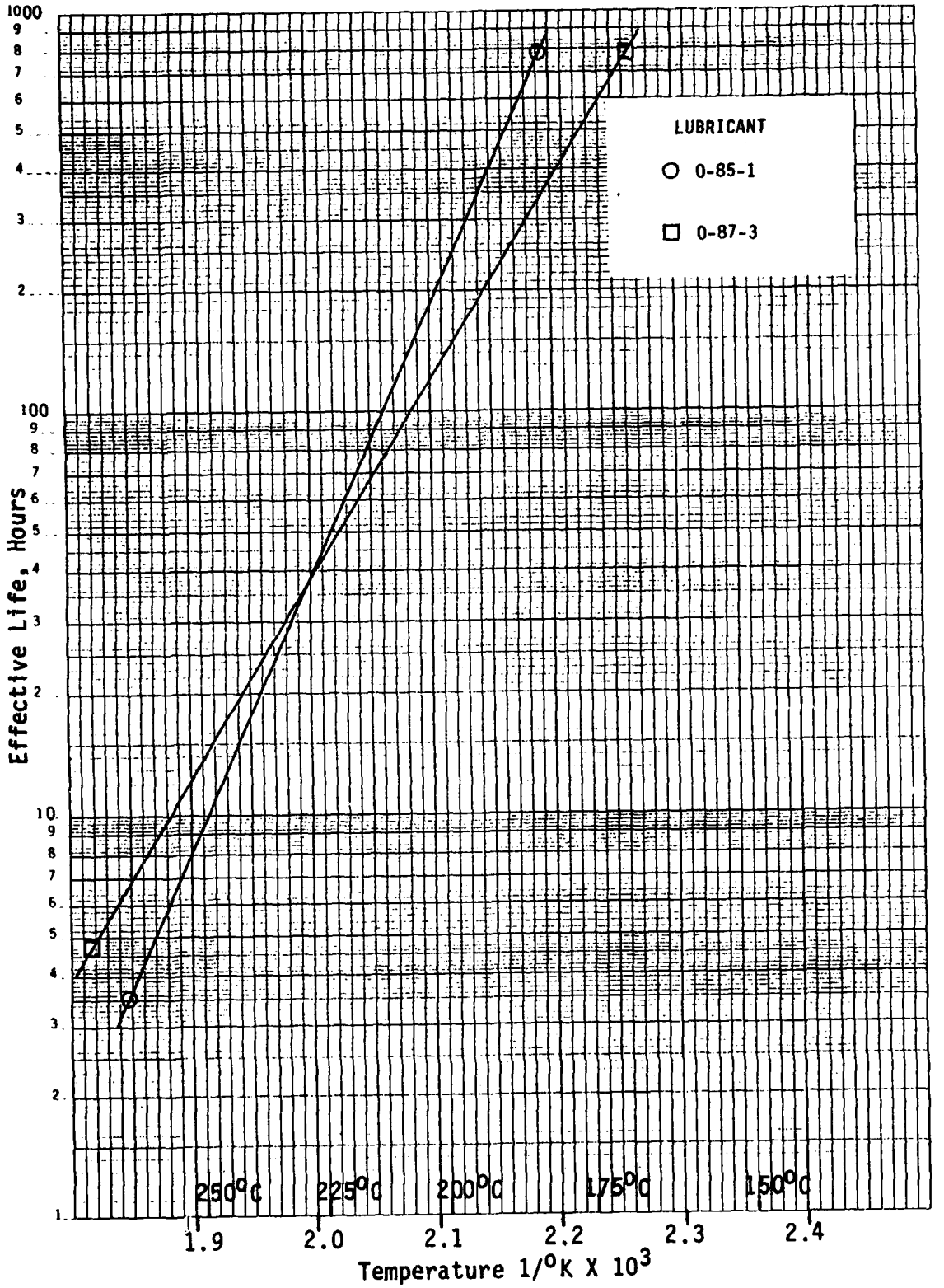

Figure 23. Effect of Temperature on Lubricant Life Using DERD Method No. 1 (Confined Heat Stability), Total Acid Number Increase Limit of 4.0 (4 cSt Fluids)

TABLE 9

EFFECTIVE LUBRICANT LIFE
DERD METHOD NO. 1 (CONFINED HEAT STABILITY)
ACIDITY INCREASE LIMITS

TAN Increase Limit of 2.0
Lubricant Life, Hours

Lubricant	O-77-15	O-79-18	O-85-1	TEL-7043	O-87-3
175°C	490	132	1100	490	445
200°C	53	72	120	32	75
225°C	9	46	19	3	17

TAN Increase Limit of 4.0
Lubricant Life, Hours

Lubricant	O-77-15	O-79-18	O-85-1	TEL-7043	O-87-3
175°C	1100	205	1400	950	530
200°C	84	115	212	56	135
225°C	10	71	45	6	43

TAN Increase Limit of 6.0
Lubricant Life, Hours

Lubricant	O-77-15	O-79-18	O-85-1	TEL-7043	O-87-3
175°C	1600	265	2100	1400	-
200°C	125	160	300	77	-
225°C	14	105	63	8	-

except for lubricant O-79-18 which shows greater stability at 225°C but less stability at 200°C and 175°C. Relative ranking of the four lubricants remained the same for all TAN limiting values at each temperature. Lubricant O-85-1 has the best overall confined heat stability based on acidity increase than any of the MIL-L-7808 or MIL-L-23699 lubricants evaluated.

This data also shows that ranking of the lubricants with respect to effective life depends not only on the lubricant formulation but also on the test temperature and the selected limiting TAN increase value.

Comparison of the data in Tables 2 and 9 show that ranking of the lubricants with respect to effective life based on acidity increase is also much different between oxidative stressing and confined heat stressing.

The evaluation of lubricant O-86-2 (different lot of O-85-1) was evaluated at a test temperature 210°C, 168 test hours using DERD Method No. 1 for comparative purposes. Comparison of the test data is given in Table 10 and shows very little difference in the confined heat stability of the two lubricants based on changes in acidity, viscosity or COBRA readings.

TABLE 10

COMPARISON OF CONFINED HEAT TEST
DATA FOR LUBRICANTS O-85-1 AND O-86-2

Lubricant	O-85-1	O-86-2
Test Temp., °C	210	210
Test Hours	168	168
Weight Loss, %	0.4	0.0
COBRA Reading	99	99
Total Acid No.	6.93	6.76
Viscosity at 100°C, cSt	4.11	4.10
Viscosity Change, %	1.7	2.2

f. Summary

Effective lubricant lives of three MIL-L-23699 lubricants and two 4 cSt lubricants under confined heat (thermal) conditions were determined using

different levels of limiting values for changes in TAN as the maximum permissible degree of degradation. Arrhenius plots were developed describing effective life as a function of temperature. The lubricant having the overall highest effective life under confined heat conditions (O-85-1) also had the highest effective life under oxidative conditions. The MIL-L-23699 lubricant O-79-18 showed slightly better confined heat oxidative stability above 225°C but much worse at temperatures below 225°C.

This data shows that ranking of the lubricants with respect to confined heat effective life depends not only on the lubricant formulation but on the test temperature and selected limiting life value.

Evaluation of two lots of the same 4 cSt lubricant at 210°C and 168 test hours showed very little difference existed between the two lots with respect to confined heat stability.

3. CORROSIVENESS AND OXIDATIVE STABILITY

a. Introduction

During Phase 2 of this study corrosion and oxidation testing was directed towards (1) providing stressed MIL-L-23699 fluids for RULLER (Remaining Useful Lubricant Life Evaluation Rig) development and (2) investigating the corrosion and oxidation stability of potential high temperature lubricants.

b. Test Apparatus

Test apparatus used for the corrosion and oxidation testing of the MIL-L-23699 fluids is described by Federal Test Method Std. 791, Method 5307 and will not be repeated in this report.

Test apparatus used for the corrosion and oxidation studies of the high temperature fluids consisted of an aluminum block bath and glassware described as a Universal Oxidation/Thermal Stability Test Apparatus (FN1) by

the ASTM Committee D02 and Subcommittee D02.09 (Method D 4871). Modifications were also made to the bath by adding machined aluminum inserts and insulating tops which would accommodate a smaller size oxidation tube ("Squires" tube used in Section II.2) for the evaluation of small samples. Corrosion test specimens used consisted of those specified by specification MIL-L-87100.[2]

c. Test Procedure

The test procedure used for the testing of the MIL-L-23699 fluids has been previously described.[1] The test procedure used for the evaluation of the high temperature was very similar to that described by Federal Test Method Std. 791, Method 5307 with modifications such as type of metal test specimens, test glassware, test temperatures and test times, intermediate sampling periods, sample size and post test analyses. The modifications used depended on the type fluid being evaluated and the purpose of the evaluation.

The post test analyses included total acid number, viscosity changes, volatility and the amount of corrosion all of which have been previously described.[1] Gas chromatography and gel permeation chromatography were used for the analysis of basestock composition and changes occurring in the composition during stressing. Chromatography conditions such as type columns, detectors, etc cannot be given due to proprietary reasons. Mass spectrometry was also used for the identification of a high molecular weight compound formed during oxidative stressing of lubricant O-67-1 and will also be discussed with the test data.

d. Test Lubricants and Conditions

Table 11 presents a listing and description of the fluids used during the high temperature oxidation study.

TABLE 11

DESCRIPTION OF TEST FLUIDS USED FOR
CORROSIVENESS AND OXIDATIVE STABILITY STUDY

Test Fluid	Description
O-78-18	MIL-L-23699 Lubricant
TEL-7004	MIL-L-23699 Lubricant
O-67-1	Inhibited Polyphenyl Ether
O-77-6	Uninhibited Polyphenyl Ether
O-77-6 (Inhibited)	Blends Containing Various Concentration of Additive A
O-77-6 (Inhibited)	O-77-6 plus SnO_2
O-77-6 (Inhibited)	O-77-6 plus Sn
TEL-8039	Polyphenyl Ether
TEL-8040	Polyphenyl Ether

The MIL-L-23699 lubricants were stressed at 188°C (370°F) for test durations up to 696 hours with intermediate sampling. The high temperature fluids were stressed at 320°C (608°F) for various test periods up to 408 hours with intermediate sampling, with and without metal test specimens and with various airflows.

e. Results and Discussion

(1) MIL-L-23699 Lubricants

Corrosion and oxidation testing of two MIL-L-23699 lubricants (O-79-18 and TEL-7004) was conducted for providing stressed lubricant samples for "RULLER" development. Lubricant TEL-7004 reached its "breakpoint" at approximately 528 test hours which is 100 test hours longer than the two MIL-L-23699 lubricants (O-71-6 and O-77-15) previously tested.[1] Lubricant O-79-18 did not show a viscosity breakpoint but showed TAN and COBRA

TABLE 12

RESULTS OF REFLUX CORROSION/OXIDATION TEST
LUBRICANT O-79-18

Sample	Viscosity cSt/40°C	40°C Viscosity Increase, %	Neut. No. mg KOH/g	Neut. No. Increase	COBRA
Initial	27.19	-	0.07	-	3
24	28.00	3.0	0.37	0.30	20
48	28.33	4.2	0.42	0.35	30
192	29.54	8.6	1.03	0.96	75
312	30.68	12.8	1.22	1.15	112
336	31.28	15.0	0.96	0.87	127
360	31.20	14.8	1.09	1.02	121
384	31.40	15.5	0.82	0.75	127
408	31.65	16.4	1.15	1.08	126
456	32.81	20.7	1.53	1.46	132
480	33.17	22.0	1.20	1.13	128
504	33.50	23.2	1.33	1.26	139
528	33.37	22.8	0.97	0.90	114
552	34.49	26.8	0.90	0.83	131
576	34.47	26.8	1.13	1.06	130
600	34.85	28.2	1.03	0.96	120
624	34.89	28.3	1.07	1.00	120
648	36.11	32.8	1.31	1.24	131
672	36.87	35.6	1.31	1.24	113
696	37.77	38.9	4.32	4.25	160

METAL SPECIMEN DATA

Metal Type	Visual Appearance
Aluminum	no change
Silver	no change
Bronze	sl. tarnish
Mild Steel	bluish
M-50 Steel	bluish
Magnesium	sl. discoloration
Titanium	no change

TEST CELL DATA

Tube Deposits:	small area of varnish above oil level
Condenser Deposits:	none

TEST CONDITIONS

Sample Volume	250 mL per each of 2 tubes
Air Rate	10 L/h
Test Temp.	188°C (370°F)

TABLE 13

RESULTS OF REFLUX CORROSION/OXIDATION TEST
LUBRICANT TEL-7004

Sample	Viscosity cSt/40°C	40°C Viscosity Increase, %	Neut. No. Mg KOH/g	Neut. No. Increase	COBRA
Initial	25.43	-	0.11	-	1
24	26.97	6.0	0.16	0.05	7
48	27.57	8.4	0.33	0.22	24
192	28.92	13.7	0.83	0.92	89
240	29.55	16.2	0.93	0.82	111
336	29.96	17.8	0.84	0.73	131
360	30.11	18.4	0.92	0.81	126
384	30.33	19.3	0.65	0.54	119
408	30.88	21.4	0.89	0.78	127
456	31.21	22.7	1.12	1.01	124
480	31.94	25.6	1.60	1.49	96
504	32.00	25.8	1.37	1.26	95
528	45.13	77.5	10.34	10.23	140

METAL SPECIMEN DATA

Metal Type	Visual Appearance
Aluminum	no change
Silver	no change
Bronze	sl. tarnish
Mild Steel	bluish
M-50 Steel	bluish
Magnesium	sl discoloration
Titanium	no change

TEST CELL DATA

Tube Deposits:	small area of varnish above oil level
Condenser Deposits:	orange crystals

TEST CONDITIONS

Sample Volume	250 mL per each of 2 tubes
Air Rate	10 L/h
Test Temp.	188°C (370°C)

breakpoints at approximately 692 test hours. Tables 12 and 13 show the results of the viscosity, total acid number, COBRA values and corrosion test data obtained on the intermediate samples taken during the test.

(2) High Temperature Fluids

(a) General

Prior to initiating high temperature corrosion and oxidation studies, a temperature profile of the aluminum block bath was conducted for determining temperature uniformity of the bath. This was accomplished by using D 4871 tubes containing 100 mL of 5P4E fluid, fitted with condensers and "J" thermocouples using a Doric Model 402 temperature indicator for measuring the temperature and using 10 L/h airflow. Data is given in Table 14. The D 4871 tubes are smaller than the tubes used in FTM. 5307.

TABLE 14

TEMPERATURE PROFILE OF ALUMINUM BLOCK BATH USING D 4871 TUBES

Bath Indicator Temp	Test Cell Temperature, °C Cell Number											
°C	1	2	3	4	5	6	7	8	9	10	Avg	Spread
20	21	21	21	21	21	21	21	21	21	21	21	0
100	99	99	99	99	100	99	99	99	99	100	100	1
150	151	151	151	150	152	151	151	150	151	150	151	2
200	201	202	202	201	202	200	200	201	201	201	201	2
250	251	250	251	250	251	251	251	250	251	252	251	2
300	300	299	301	299	302	299	300	299	301	301	300	3
350	352	350	352	350	351	353	351	353	352	353	352	3

The data given in Table 14 shows good temperature uniformity between the test cells considering measurement conditions and considering temperature measurement repeatability.

A temperature profile was also made using the aluminum inserts, small sample tubes and insulation rings with the same procedure used without the inserts. Measurements were only on the front 5 cells since access and ease of using all 10 cells is difficult with the bath being located in a hood. Table 15 shows the temperature measurements obtained.

TABLE 15

TEMPERATURE PROFILE OF ALUMINUM BLOCK BATH USING ALUMINUM INSERTS FOR SMALL VOLUME TEST CELLS

Temp Control Setting °C	Indicator Temp °C	Test Cell Temperature, °C Cell Number 7	8	9	10	1	Cell Avg °C	Max Cell Spread °C
20	20	20	20	20	20	20	20	0
50	50	49	48	48	48	48	48	1
100	100	96	97	97	97	97	97	1
150	150	147	149	148	147	149	148	2
200	200	196	198	196	197	198	197	2
250	250	247	250	248	248	249	248	3
300	300	297	299	298	297	298	298	2

The data given in Table 15 shows the same degree of temperature uniformity as that obtained without the inserts. The data in Table 15 also shows that a slightly higher bath indicator temperature is required to provide desired cell temperature.

(b) Comparison of Data Using D 4871 Tubes and Squires Tubes

Initial testing of the high temperature fluids involved testing polyphenyl ether (5P4E) fluids in the D 4871 tubes using a 100 mL sample and the Squires tubes using a 30 mL sample for a test period of 48 hours and at 320°C. Lubricants O-67-1 and O-77-6 were tested in each type of tube with the test data being given in Table 16. The change in viscosity for lubricant O-67-1 using the D 4871 tube is very close to the viscosity increase of approximately 15% at 37.8°C (100°F) and 7% at 98.9°C (210°F)

TABLE 16

CORROSION AND OXIDATION TEST DATA FOR POLYPHENYL ETHERS
320°C, 48 TEST HOURS, 10 L/H AIRFLOW

	Lubricant O-67-1 (5P4E with Additive)		Lubricant O-77-6 (5P4E without Additive)	
	Squires Tube (30 mL Sample)	D 4871 Tube (100 mL Sample)	Squires Tube (30 mL Sample)	D 4871 Tube (100 mL Sample)
Viscosity @ 40°C (Initial), cSt	285.4	285.4	276.2	Oil semi-solidified
Viscosity @ 40°C (Final), cSt	318.1	333.3	534.5	
% Viscosity Change at 40°C	11.5	16.8	93.4	
Viscosity @ 100°C (Initial), cSt	12.69	12.69	12.45	
Viscosity @ 100°C (Final), cSt	13.28	13.43	17.05	
% Viscosity Change at 100°C	4.6	5.8	36.9	
TAN (Initial)	0.00	0.00	0.00	
TAN (Final)	0.00	0.00	0.00	
TAN Increase	0.00	0.00	0.00	
Weight Loss, %	4.4	1.5	7.5	2.6
Tube Deposits	None	None	None	
Corrosion of Metal Specimens, mg/cm^2				
Aluminum	0.0	-0.06	-0.16	
Silver	0.0	-0.08	-0.12	
Mild Steel	-0.04	0.00	+0.02	
M-50 Steel	-0.08	-0.02	-0.06	
Waspaloy	-0.12	-0.06	-0.06	
Titanium	-0.08	-0.20	-0.06	

previously reported[3] using Fed. Test Method 5307. This testing used 200 mL samples and only Al, Ti, Ag and steel test specimens. The viscosity data for O-67-1 using the Squires tube (30 mL sample) showed slightly less degradation than the D 4871 tube testing. The data for lubricant O-77-6 shows this fluid to have a much lower oxidative stability than O-67-1 as expected and that the D 4871 tube (100 mL) test was much more severe than the 30 mL test which also occurred for lubricant O-67-1.

Different airflows and sample volumes were investigated for determining if changing the ratio of airflow to sample volume would account for the D 4871 test being more severe. The data from this study is given in Table 17 including data from thermal prestressing and the effect of nascent wear metal. The effect of changing airflow (3, 7 and 10 L/h) using the Squires tube had very little effect on the change in degradation except that the 3 L/h airflow rate gave less weight loss as would be expected. The increase in sample volume from 30 mL to 60 mL using the standard 10 L/h airflow gave a slightly lower change in viscosity. This data shows that some variable other than the ratio of airflow to sample volume causes more degradation with the D 4871 tubes when measured by changes in viscosity. No TAN values are given in Table 17 due to the lack of significant increases in TAN occurring during thermal and oxidative stressing of polyphenyl ethers. Potentiometric Titration of weak acids will be discussed in subsection (f).

(c) Thermal Stressing Study

Gas chromatography analysis of the new and stressed 5P4E containing additive A discussed in detail in Subsection 4 (Additive Analysis) showed that the initial additive concentration was practically 0.0% after a very short test time (less than 24 hours) during oxidative stressing. Thermal stressing of O-67-1 using nitrogen was conducted for studying the

TABLE 17

EFFECT OF TEST VARIABLES ON CORROSION AND OXIDATION STABILITY OF O-67-1, 320°C, 48 TEST HOURS, 10 L/H AIRFLOW

Type Tube	Sample Size ml	Type Gas and Flow Rate	Vis. at 40°C cSt	Vis. Change %	Vis. at 100°C cSt	Vis. Change %	Weight Loss %	Corrosion
Squires	30	air, 3 L/h	317.2	11.1	13.38	5.4	1.1	Nil
Squires	30	air, 7 L/h	318.5	11.6	13.37	5.4	4.7	Nil
Squires	30	air, 10 L/h	318.1	11.5	13.28	4.6	4.4	Nil
Squires	60	air, 10 L/h	306.4	7.4	13.20	4.0	5.0	Nil
Squires	30[a]	air, 10 L/h	425.0	46.1	15.68	23.4	3.1	Nil
D 4871	100	air, 10 L/h	333.3	16.8	13.43	5.8	1.5	Nil
D 4871	100	air, 10 L/h	328.0	14.9	13.47	6.1	2.0	Nil
D 4871	100	N2, 10 L/h	294.6	3.2	12.75	0.4	2.3	Nil
D 4871	100	N2, 10 L/h for 48 h air, 10 L/h	320.7	12.4	13.33	5.0	4.4	Nil

[a]Sample from 4-Ball wear tests No. 195 (approximately 25%) and No. 200 (approximately 75%). Reference Table 18 for wear test conditions and lubricant properties after wear testing

mechanism of the additive degradation. The test was conducted using the D 4871 tube, 10 L/h nitrogen flow, 320°C for 48 test hours. The change in physical property test data is included in Table 17 and shows that only a small change in any of the properties occurred except for weight loss which was about the same as that obtained using the 10 L/h airflow. One change noted in the sample after the nitrogen test was a turbidity of the lubricant indicating the presence of particles which were identified as a tin compound using atomic emission spectroscopy. Phase contrast microscopy showed the particles to be 1 micron and below in size. No additive was present after the 48 hour thermal stressing.

A corrosion and oxidation test was conducted on lubricant O-67-1 after being subjected to the 48 hour corrosion and thermal (nitrogen) test. Data from this test is also given in Table 17 and shows less degradation as measured by viscosity change than the two 48 hour oxidation tests without the prior thermal stressing. This difference could be due to test repeatability or loss of lubricant impurities during the thermal stressing which contribute to the degree of degradation during the normal oxidation test. This test does show that the chemical change of the additive did not have a detrimental effect on oxidative stability of the lubricant. This test also showed twice the weight loss as the two 48 hour oxidative tests or the 48 hour nitrogen test which indicates that fluid volatility is the major factor in weight loss and not the loss of degradation products.

(d) Effect of Nascent Wear Metal on 5P4E Oxidative Stability

A corrosion and oxidation test was conducted on lubricant O-67-1 after being used in 4-Ball wear testing for the purpose of determining the effects of nascent wear particles on the rate of degradation of

polyphenyl ether. Lubricant from two wear tests had to be used to provide sufficient sample for the corrosion and oxidation test. Table 18 shows the wear tests' conditions and the viscosity change and iron content after the wear tests. Table 18 also shows the calculated properties of the mixed oil (25% Test No. 195 and 75% Test No. 200). The results of the corrosion and oxidation test on the mixed sample are given in Table 17 and shows the iron wear debris from the wear testing greatly increased the amount of degradation. The viscosity measurements made on the two wear test samples before the corrosion and oxidation test given in Table 17 shows the great increase in viscosity after the corrosion and oxidation test occurred during the corrosion and oxidation testing and not during the 4-Ball testing.

Analysis of O-67-1 from the four-ball wear tests before and after the 48 hour corrosion and oxidation test at 320°C was made by gel permeation chromatography (GPC) and gas chromatography (GC), the results of which are shown in Table 19. The molecular weight averages (by GPC) indicate that there is no change in the basestock due to the four ball wear test procedure (1 or 3 hours at 250°C). However, analysis of the lubricants by GC reveals that the additive level is nearly depleted and the combined lubricant (75% Test #200, 25% Test #195) used in the corrosion and oxidation test had an estimated relative level of 25%, a 75% reduction from the original additive level in the fresh lubricant. Since the mechanism of inhibition of the additive or the nature of its intermediate products is not known it could not be established whether the relatively higher degree of degradation observed in the C&O tested four-ball wear test lubricant is due only to the effect of wear generated iron or that the processes involved in the four ball wear test "inactivated" the additive in some way.

TABLE 18

PROPERTIES AND TEST CONDITIONS OF FOUR-BALL WEAR TEST SAMPLES NO. 195 AND NO. 200 AND THE MIXTURE OF THESE SAMPLES USED FOR CORROSION AND OXIDATION STUDY

	Wear Test Sample		
	No. 195	No. 200	Mixed Oil[a]
Test Load, lb	32.5	32.5	-
Test RPM	1200	1200	-
Test Temperature, °C	250	250	-
Test Time, h	1	3	-
Iron Content after Test, ppm	29	86	72
Vis. at 40°C after Test, cSt	283.9	293.4	291.0
Vis. Change at 40°C, %	-0.5	2.8	2.0
Vis. at 100°C after Test, cSt	12.61	12.71	12.68
Vis. Change at 100°C, %	-0.2	0.60	0.0

[a]Calculated properties of mixed oil for corrosion and oxidation study consisting of 25% (volume) of test No. 195 and 75% of test No. 200

TABLE 19

CHROMATOGRAPHIC ANALYSIS OF O-67-1 FOUR-BALL WEAR TEST LUBRICANTS

Lubricant	GPC Data Mn	GPC Data Mw	GPC Data D	GC DATA Relative % Additive A
Fresh	451	456	1.01	100
Four Ball Wear Test #200 (250°C, 3 h)	445	451	1.01	15
Four Ball Wear Test #195 (250°C, 1 h)	450	458	1.02	50
Combined, Test #195, #200 C&O at 320°C, 48 h)	487	561	1.15	5
Fresh Lubricant C&O at 320°C, 48 h	454	480	1.06	5

Since the lubricants obtained from four-ball wear testing and used for corrosion and oxidation testing showed a 75% reduction in the additive content after wear testing and prior to the corrosion and oxidation testing, a study was conducted for determining the cause for the decrease in the initial additive content. Two 52100 steel balls were placed in each of two test tubes and approximately 10 mL of O-67-1 was added to each tube which covered the balls. The tubes were then heated at 250°C using a forced air circulating oven. One tube was removed from the oven after one hour and the other after 3 hours. The tubes were cooled to room temperature and the additive content of each sample was determined by gas chromatography. No decrease in additive content occurred for either sample and the 52100 steel balls did not exhibit "bluing" as those used in the 250°C wear testing. This indicates that the loss of additive in the wear test samples is due to factors other than just the 250°C test temperature. These factors could be wear processes or the presence of wear debris, contact temperatures higher

than 250°C or aeration during the four ball wear testing.

(e) Long Term Oxidative Testing of O-67-1 Fluid

Long term oxidative testing of the O-67-1 fluid was conducted due to the small degree of degradation during the 48 hour testing and the decrease in rate of degradation shown by the 48 hour viscosity data compared to the 24 hour viscosity data. Lubricant O-67-1 sample from 5 gal. container No. X was stressed for 240 hours at 320°C using D 4871 tubes, 100 mL samples, (no intermediate sampling) and 10 L/h airflow. The test data presented in Table 20 shows a normal small weight loss, a moderate increase in refractive index and very little corrosion for any of the metal corrosion test specimens. The largest change occurred for the increase in viscosity which is shown graphically in Figure 24. At 240 test hours the lubricant is undergoing a very rapid increase in viscosity.

Examination of O-67-1 fluid (Container A) was made using phase contrast and polarized light microscopy showed the presence of "needle habit" (shape) anisotropic crystals. A microscope slide prepared from this sample of O-67-1 was heated at a controlled rate using a Mettler hot stage and 100X polarized light. The crystals showed initial dissolving at 50.8°C and complete dissolving at 56.7°C. Since a number of quart samples had been removed from the 5 gal can "A", a top, middle and bottom sample was taken from an unopened 5 gal container ("B") without any agitation using a glass "thief" and standard vacuum flask. The top and middle samples contained a few crystals while the bottom sample contained so many crystals the fluid was cloudy. These crystals were removed from 50 mL of the 5P4E fluid by filtering through a 10 micron Teflon filter. The crystals were washed with cold toluene and dried. A melting point determination of the washed crystals gave a melting point range of 223.1°C to 228.6°C. The Composition of the

TABLE 20
CORROSION AND OXIDATION TEST DATA FOR
LUBRICANT O-67-1 AT 320°C USING D 4871 TUBES (100 ML SAMPLE)
10 L/h AIRFLOW (SAMPLE CONTAINER X)

Test Hours	Viscosity at 40°C cSt	Viscosity Chg at 40°C, %	Viscosity at 100°C cSt	Viscosity Chg at 100°C, %
0	285.4	-	12.69	-
24	312.6	9.5	13.20	4.0
48	328.0	14.9	13.47	6.1
72	337.2	18.1	13.67	7.7
96	358.4	25.6	13.96	10.0
120	367.3	28.7	14.18	11.7
168	401.8	40.8	14.77	16.4
192	434.6	52.3	15.26	20.3
240	529.1	85.4	16.78	32.2

Test Hours	TAN	Weight Loss %	Tube Deposits	Ref. Index at 25°C
0	0.00	-	-	1.6290
24	0.00	1.2	None	1.6290
48	0.00	2.0	None	1.6293
72	0.00	1.7	None	1.6297
96	-	1.9	Slight Stain	1.6303
120	-	3.6	Slight Stain	1.6306
168	-	3.3	None	1.6324
192	-	3.5	Slight Stain	1.6325
240	-	4.7	Slight Stain	1.6344

Test Hours	Corrosion of Metal Specimens, mg/cm^2					
	Al	Ag	M.Steel	M-50 Steel	Waspaloy	Ti
24	+0.06	0.00	+0.10	+0.06	+0.06	+0.10
48	+0.02	-0.02	-0.08	+0.02	+0.06	+0.08
72	+0.02	-0.04	+0.06	+0.04	-0.02	+0.02
96	+0.08	+0.04	+0.16	+0.08	+0.06	+0.06
120	+0.04	+0.02	+0.10	+0.02	+0.04	+0.06
168	+0.04	-0.06	+0.10	+0.04	+0.10	+0.04
192	+0.00	-0.06	+0.12	+0.04	+0.02	+0.04
240	+0.00	-0.01	+0.00	+0.00	+0.00	+0.00

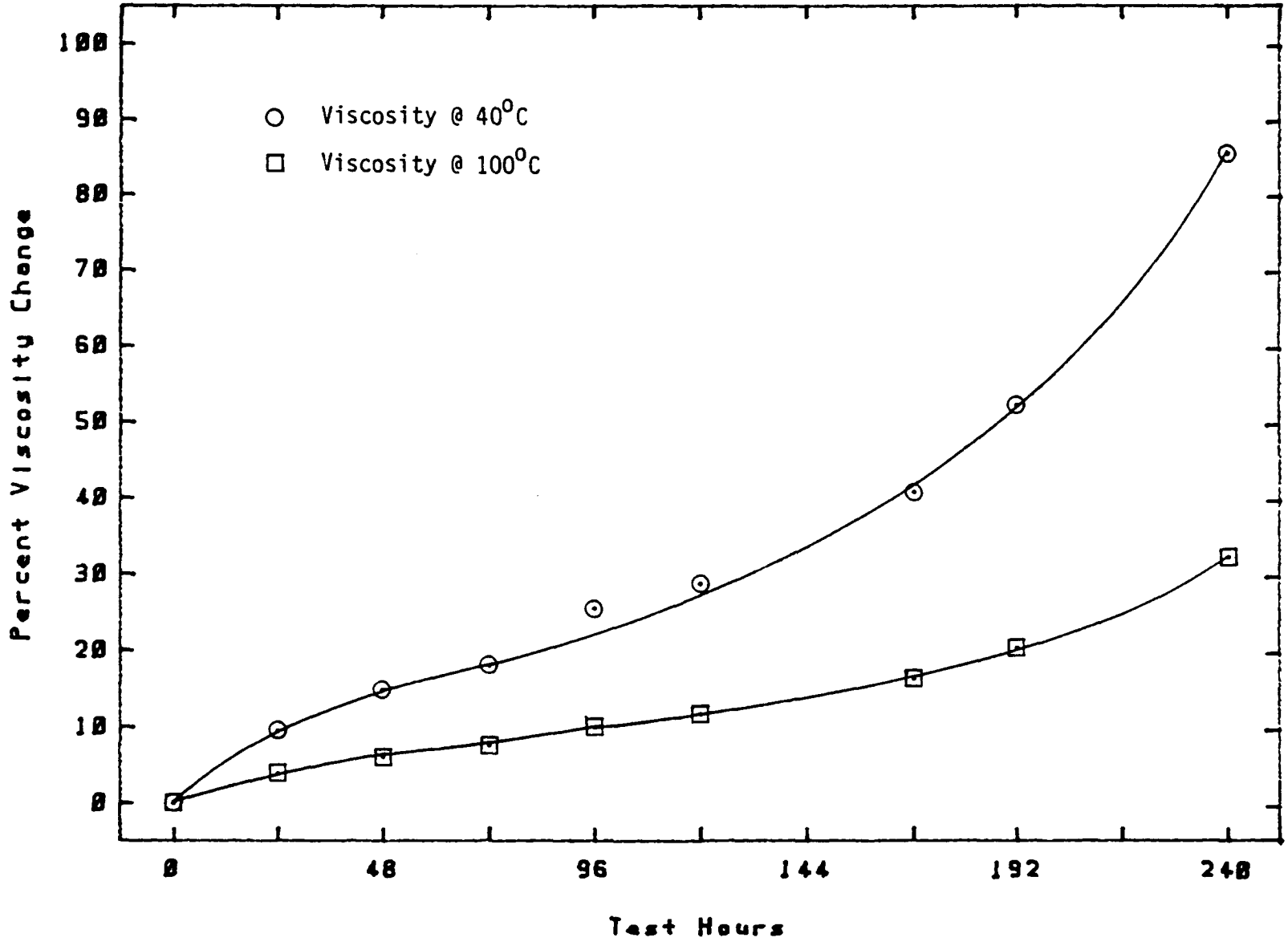

Figure 24. Viscosity Increase Versus Test Hours During Corrosion and Oxidation Testing of Lubricant O-67-1 Using D 4871 Tubes, 100 mL Samples, 320°C Test Temperature and 10 L/h Airflow

crystals were identified by gas chromatography as additive A.

A microscopic slide prepared from the bottom sample of Can B was heated at a controlled rate and for intermittent isothermal soak periods. The test sequence along with microscopic observations are as follows:

Heating rate of 3°C/min. to 61°C	Indication of crystal solubility at 61°C
Heating rate of 3°C/min. to 75°C	Slight increase in crystal solubility
Held at 75°C for 5 min.	No apparent increase in solubility
Heating rate of 3°C/min. to 80°C and held for 10 min.	Increased solubility but not complete crystal solubility
Heating rate 30°C/min. to 85°C and held for 10 min.	Complete solubility
Cooling rate 10°C/min. to 75°C and held for 20 min.	No crystallization
Cooled to room temperature (22°C)	
After 5 min.	No crystallization
After 90 min.	No crystallization
After 16 h	Seven crystals approximately 100 microns long and 10 microns thick

The above data indicates that the temperature required for redissolving the crystals in the various samples of O-67-1 depends upon the quantity of crystals present as would be expected and the solubility limit of the additive in the 5P4E.

Corrosion and oxidation testing of lubricant O-67-1 (Can B, Top Sample) containing slightly higher additive content than container X as determined by gas chromatography (internal standard procedure) was conducted at 320°C using 100 mL samples in D 4871 tubes for 24, 48, 72 and 96 hour test periods. A D 4871 tube containing 150 mL sample was also tested using intermediate sampling of approximately 10 to 15 mL at 24, 48, 72 and 96 test hours. Oxidative stressing of the remaining lubricant was continued for a

total of 168 test hours. Data obtained from testing without intermediate sampling is given in Table 21 and data obtained from testing with intermediate sampling is given in Table 22. The data in Tables 21 and 22 shows very little degradation has occurred for test times up to 96 hours. The 168 hour sample (Table 22) shows a significant increase in viscosity after 168 hours. Very little corrosion occurred for any of the metal specimens. Tube deposits consisted of a slight stain over a small area of the test tube.

The repeatability of corrosion and oxidation testing of lubricant O-67-1 at 320°C using two different samples (Can X and Can B) and with and without intermediate sampling is shown in Table 23. Only viscosity data is shown since the other measured properties (Tables 20 and 21) exhibit very little change. The correlation of the data in Table 22 is very good with the exception of the data for the 168 test hour samples. The change in 40°C viscosity was 40.8% for the sample from 5 gal Can "X" and 49.3% for sample from 5 gal Can "B" (Top). These two samples also showed a difference in the initial viscosity prior to stressing. The difference in the viscosity change of the two 168 hour samples could be due to different samples or to effects caused by intermediate sampling.

(f) Weak Acid Number Determinations of Polyphenyl Ether Fluid

The TAN of all oxidized polyphenyl ethers have been found to be very low (less than 0.05) and in most cases 0.00 even after severe degradation based on viscosity increase. The reason for this may be due to the fact that the type of oxidation products produced in degraded polyphenyl ether may be too low to be titrated by the standard method (eg. pK_b of phenol = 10). A procedure was used for titrating the very weak acids that may be produced (such as phenols) in such lubricants. Briefly,

TABLE 21

CORROSION AND OXIDATION TEST DATA
FOR LUBRICANT O-67-1 (CAN B, TOP SAMPLE) AT 320°C
USING D 4871 TUBES, 100 ML SAMPLES AND 10 L/h AIRFLOW

Test Hours	Viscosity at 40°C cSt	Viscosity Chg. at 40°C, %	Viscosity at 100°C cSt	Viscosity Chg. at 100°C, %
0	280.4	-	12.61	-
24	310.8	10.7	13.15	4.3
48	324.2	15.5	13.47	6.8
72	338.2	20.4	13.73	8.9
96	349.9	24.6	13.89	10.2

Test Hours	TAN	Weight Loss %	Tube Deposits	Refrac. Index at 25°C
0	0.00	-	-	1.6290
24	-	1.4	Slight Stain	1.6296
48	-	1.7	Slight Stain	1.6299
72	-	2.4	Slight Stain	1.6300
96	-	3.5	Slight Stain	1.6307

Test Hours	Corrosion of Metal Specimens, mg/cm^2					
	Al	Ag	M.Steel	M-50 Steel	Waspaloy	Ti
24	+0.02	+0.02	+0.10	+0.06	+0.10	+0.12
48	-0.02	+0.02	+0.08	+0.10	+0.04	0.00
72	+0.04	-0.06	+0.06	+0.06	+0.08	+0.04
96	+0.06	-0.08	+0.04	+0.08	+0.06	+0.02

TABLE 22

CORROSION AND OXIDATION TEST DATA FOR LUBRICANT
0-67-1 (CAN B, TOP SAMPLE) AT 320°C USING A D 4871 TUBE
AND 150 ML SAMPLE WITH INTERMEDIATE SAMPLING AND
10 L/h AIRFLOW

Test Hours	Viscosity at 40°C cSt	Viscosity Chg at 40°C, %	Viscosity at 100°C cSt	Viscosity Chg. at 100°C, %
0	280.8	-	12.61	-
24	308.5	9.9	13.11	4.0
48	322.0	14.7	13.42	6.4
72	337.7	20.3	13.68	8.5
96	353.0	25.7	13.97	10.8
168	419.2	49.3	15.11	19.8

Test Hours	TAN	Weight Loss %	Tube Deposits	Refrac. Index at 25°C
0	0.00	N/A	N/A	1.6290
24	-	N/A	N/A	1.6296
48	-	N/A	N/A	1.6299
72	-	N/A	N/A	1.6301
96	-	N/A	N/A	1.6305
168	-	N/A	Slight Stain	1.6318

Test Hours	Corrosion of Metal Specimen, mg/cm^2					
	Al	Ag	M.Steel	M-50 Steel	Waspaloy	Ti
168 (End of Test)	+0.04	-0.08	+0.10	+0.06	0.00	+0.02

TABLE 23

REPEATABILITY OF CORROSION AND OXIDATION TESTING OF LUBRICANT O-67-1 AT 320°C USING D 4871 TUBES WITH AND WITHOUT INTERMEDIATE SAMPLING

	Sample Can X		Sample Can B (Top)			
	No Intermediate Sampling (100 mL Sample)		No Intermediate Sampling (100 mL Sample)		Intermediate Sampling (150 mL Sample)	
Test Hours	Viscosity at 40°C cSt	% Change	Viscosity at 40°C cSt	% Change	Viscosity at 40°C cSt	% Change
0	285.4	-	280.8	-	280.8	-
24	312.6	9.5	310.8	10.7	308.5	9.9
48	328.0	14.9	324.2	15.5	322.0	14.7
72	337.2	18.1	338.2	20.4	337.7	20.3
96	358.4	25.6	349.9	24.6	353.0	25.7
168	401.8	40.8	-	-	419.2	49.3

Test Hours	Viscosity at 100°C cSt	% Change	Viscosity at 100°C cSt	% Change	Viscosity at 100°C cSt	% Change
0	12.64	-	12.61	-	12.61	-
24	13.20	4.0	13.15	4.3	13.11	4.0
48	13.47	6.1	13.47	6.8	13.42	6.4
72	13.67	7.7	13.73	8.9	13.68	8.5
96	13.96	10.0	13.89	10.2	13.97	10.8
168	14.77	16.4	-	-	15.11	19.8

this procedure uses potentiometric titration with tetrabutylammonium hydroxide as the titrant in a nonaqueous solvent. For this study acetonitrile was the solvent and phenol was used for the weak acid.

The results reported by Cundiff and Markunas[4] for a similar procedure showed that using the above specified conditions gave a titration curve for phenol with a very sharp end point. The results of this experiment, as shown in Figure 25, are considerably different. Figure 25 shows that, after an initial early mV rise due to titration of the acidic impurities in the solvent, the end point is very weak and finally levels off at about -4.10 mV. A sharp end point, however, is not a requirement for titration of an oxidized lubricant since it is expected to contain a large variety of titratable species all with separate pK_a's. So like the TAN procedure, titration is done to a particular pH (or in this case mV reading). Titration of a blank yielded a -4.1 mV endpoint of 0.07 mL using a 0.117 M titrant. Using this procedure, a titration of 2.36 grams of O-67-1 stressed in the corrosion/oxidation at 320°C for 48 hours was conducted. This titration, however, was essentially the same as the blank indicating that there was nothing titratable in the sample despite the fact there was 20.5% increase in viscosity. The reason for this could be due to solubility problems in the acetonitrile. Although 5P4E polyphenyl ether is soluble in acetonitrile, it was noted that not all of the degraded lubricant dissolved in the solvent. Gel permeation chromatography analysis of the acetonitrile insoluble fraction revealed it to be all high molecular weight compounds which may have titratable components.

The procedure was repeated using 2:1 acetonitrile:THF as the solvent. This solvent mix not only was able to dissolve all parts of the oxidized lubricant but it also had a large effect on the titration results.

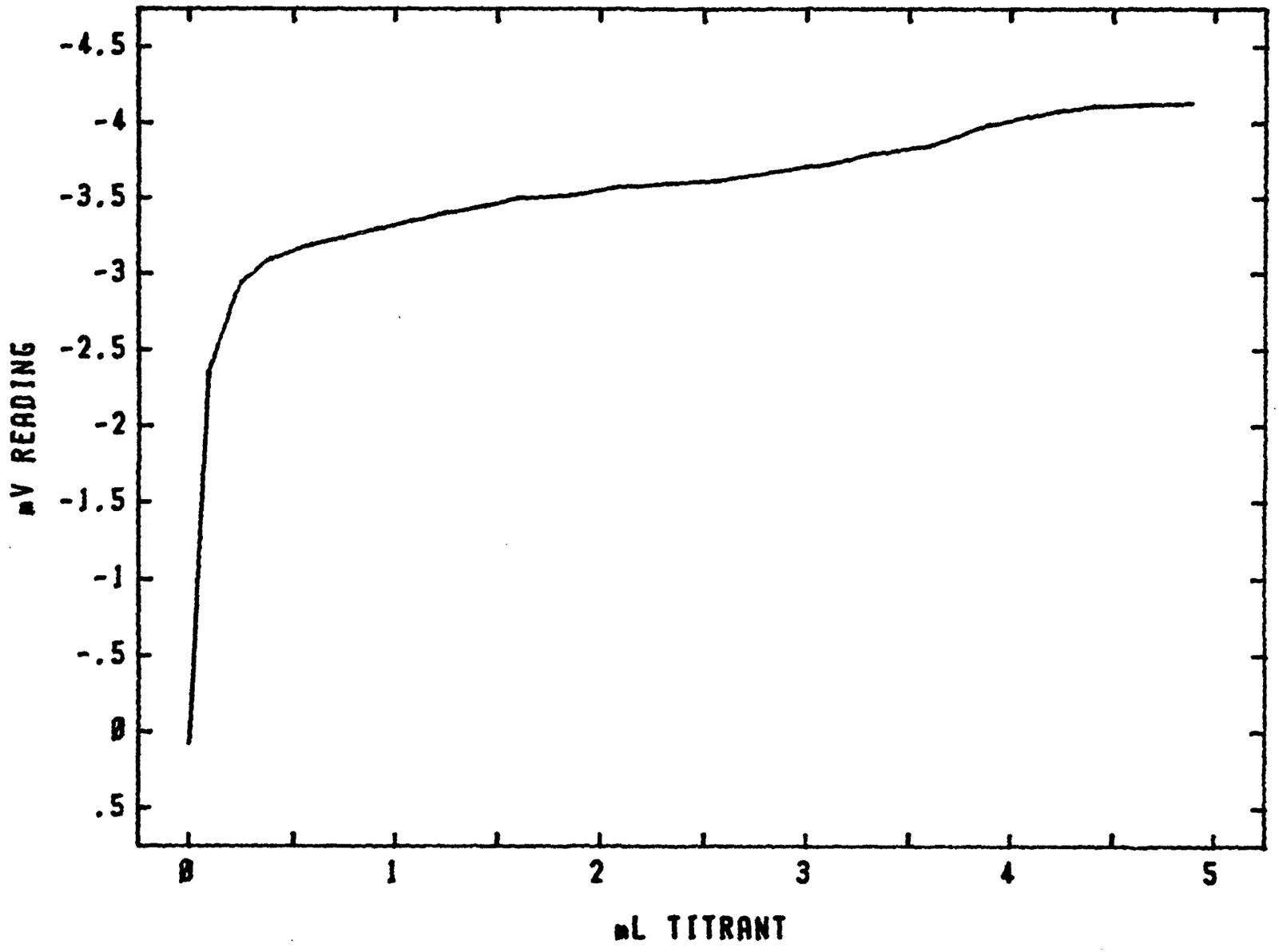

Figure 25. Titration Curve of Phenol with TBAH in Acetonitrile

A small but definite acid number, that increased with stressing time, was observed. Acid numbers from this procedure were calculated exactly as TAN in ASTM D 664 and is represented in Table 24 as WAN (weak acid number). Actually this procedure titrates for strong and weak acids but since the TAN of all oxidized polyphenyl ethers was found to be zero, it is equivalent to a weak acid number.

TABLE 24

POTENTIOMETRIC TITRATION OF WEAK ACIDS IN O-67-1 STRESSED IN THE CORROSION/OXIDATION TEST AT 320°C

Test Hours	WAN*
0	0.05
24	0.17
48	0.17
72	0.28
96	0.32
120	0.38
168	0.63
192	0.49

*Weak Acid Number

The data in Table 24 shows that the WAN of oxidized polyphenyl ethers does not reach the high values of TAN commonly seen in oxidized ester lubricants. This data also is in line with the viscosity change and GPC molecular weight increase data in that it shows a more or less stepwise increase in WAN with time. Since it was found that one of the principal oxidation products from O-67-1 was a biphenyl dimer, which is a neutral species, it is not surprising that there are not many titratable compounds present. It seems likely that much of what is produced is among the small evaporative weight losses reported (3.5% at 192 hours). Wilson[5] reported that cold trapped volatiles from the oxidation of uninhibited m,m-4P3E consisted of a high proportion of phenol (29%) and m-phenoxyphenol

(12-16%) in addition to 4P3E, 3P2E, water and carbon dioxide. No analyses were conducted on the corrosion/oxidation volatiles.

(g) Effect of Additive A Concentration and Other Materials on Corrosion and Oxidative Stability of 5P4E Fluid O-77-6

Corrosion and oxidation testing of O-77-6 (Can A) with 25, 50, 75, and 100 relative percents additive A concentration of O-67-1 was conducted for determining if an optimum concentration of additive exists which provides a maximum in oxidation stability and for determining if concentrations above the optimum value causes a reduction in oxidative stability, which has been indicated by previous researchers.[6,7] Testing was conducted at 320°C, 10 L/h airflow, D 4871 Tubes with 120 mL initial sample size and with intermediate sampling. Table 25 shows the data obtained from this testing which includes viscosity measurements at 40°C, % viscosity increase, refractive index and corrosion of the 6 metal test specimens for "end-of-test" or "final" samples for the various tests. The change in viscosity is also shown graphically in Figure 26. This data shows that polyphenyl ethers do not exhibit a sharp "breakpoint" during oxidative stressing at 320°C but a gradual change in the rate of viscosity increase. The data also shows that significant increase in oxidative stability exists for the 75 relative percent blend compared to the 50 relative percent blend. No significant difference in viscosity change occurred between the 75 and 100 relative percent blends. The data in Table 25 shows only a small increase in refractive index for any of the stressed samples and very little corrosion occurred for any of the metal test specimens with the maximum being a loss of Ag of 0.14 mg/cm^2 and 0.16 mg/cm^2 for the 75 and 100 relative percent blends respectively and a gain of 0.16 mg/cm^2 for the mild steel specimen with the 50 and 75 relative percent blends. Microscopic examination of the various

TABLE 25

EFFECT OF ADDITIVE A CONTENT ON CORROSION AND OXIDATION STABILITY OF POLYPHENYL ETHER O-77-6 AT 320°C USING D 4871 TUBES AND INTERMEDIATE SAMPLING

Lubricant Formulation	Test Hours	Viscosity at 40°C cSt	Viscosity Chg at 40°C, %	Refractive Index at 25°C
O-77-6	0	280.8	-	1.6290
	24	565.3	101.3	1.6340
O-77-6 + 25 Relative % Additive A	0	279.5	-	1.6290
	24	303.3	8.5	1.6290
	48	324.9	16.2	1.6300
	72	353.3	26.4	1.6306
	96	405.8	45.2	1.6312
	120	465.2	66.2	1.6328
	144	555.2	98.6	1.6337
O-77-6 + 50 Relative % Additive A	0	279.1	-	1.6290
	24	300.9	7.8	1.6291
	48	315.7	13.1	1.6294
	72	330.3	18.3	1.6299
	96	348.8	25.0	1.6307
	120	370.0	32.6	1.6307
	144	398.2	42.7	1.6314
	168	436.0	56.2	1.6321
	192	475.3	70.3	1.6327
	216	540.1	93.5	1.6335
	240	617.4	121.2	1.6345
O-77-6 + 75 Relative % Additive A	0	280.3	-	1.6290
	24	301.7	7.6	1.6293
	48	312.8	11.6	1.6296
	72	326.6	16.5	1.6302
	96	346.5	23.6	1.6302
	120	360.9	28.8	1.6305
	144	384.1	37.0	1.6305
	168	411.4	46.8	1.6314
	192	434.1	54.9	1.6325
	216	455.2	62.4	1.6325
	240	495.3	76.7	1.6332
O-77-6 + 100 Relative % Additive A	0	279.5	-	1.6290
	24	-	-	-
	48	318.0	13.8	1.6301
	72	332.5	19.0	1.6303
	96	-	-	-
	120	-	-	-
	144	380.7	36.2	1.6313
	168	406.2	45.3	1.6317
	192	427.6	53.0	1.6320
	216	460.1	64.6	1.6326
	240	494.0	76.7	1.6335

TABLE 25 (CONT'D)

EFFECT OF ADDITIVE A CONTENT ON CORROSION AND OXIDATION STABILITY OF POLYPHENYL ETHER O-77-6 AT 320°C USING D 4871 TUBES AND INTERMEDIATE SAMPLING

Lubricant Formulation	Test Hours	Corrosion of Metal Specimens mg/cm^2					
		Al	Ag	Mild Steel	M-50 Steel	Waspaloy	Ti
O-77-6 + 25 Rel. % Additive A	72	+0.06	-0.04	+0.08	+0.02	0.00	-0.02
	144	+0.04	0.00	+0.12	+0.06	0.00	+0.04
O-77-6 + 50 Rel. % Additive A	72	-0.04	-0.06	+0.02	-0.02	-0.02	-0.02
	192	+0.10	+0.04	+0.16	+0.12	+0.04	+0.04
	240	-0.08	-0.12	-0.02	-0.02	-0.06	-0.06
O-77-6 + 75 Rel. % Additive A	72	0.00	-0.08	+0.04	+0.02	-0.04	-0.04
	192	+0.08	+0.06	+0.16	+0.10	+0.06	+0.08
	240	-0.06	-0.14	-0.02	-0.06	-0.10	0.00
O-77-6 + 100 Rel. % Additive A	240	-0.08	-0.16	-0.04	-0.08	-0.08	-0.12

Testing conducted using 10 L/h airflow

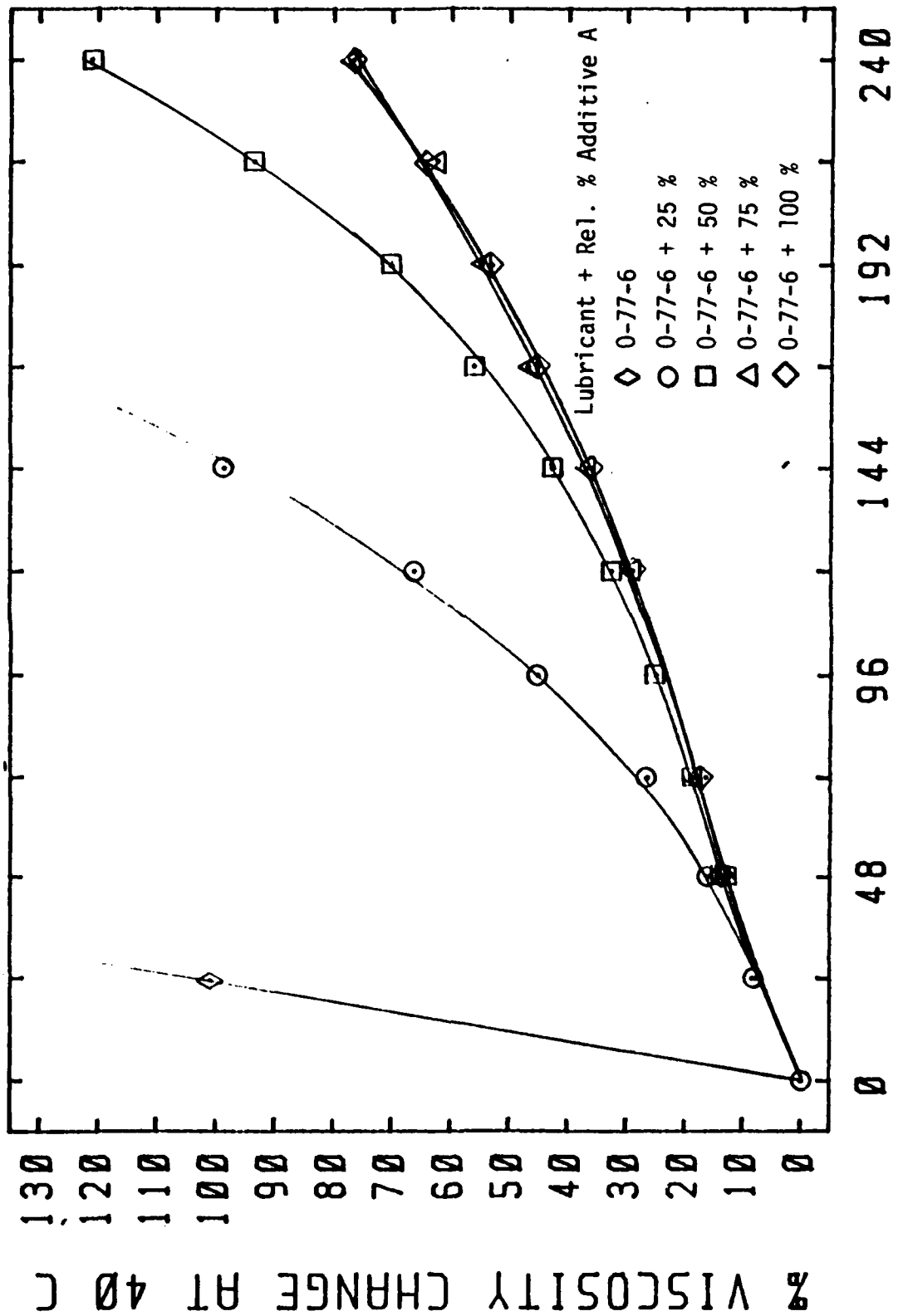

Figure 26. Effect of Additive A Content on 40°C Viscosity Change During Corrosion and Oxidation Testing of 0-77-6 at 320°C and 10 L/h Airflow

O-77-6/additive blends after standing at room temperature (22°C) for several days indicated the solubility of additive A in the 5P4E fluid O-77-6 is close to being 75% of initial concentration.

Corrosion and oxidation testing of O-77-6 with 250 relative percent additive A was conducted for investigating the effects of excessive antioxidant since 75 and 100 relative percent blends gave similar viscosity change during the 240 hours of oxidative stressing. This increase of additive A had very little effect on the stability of the 5P4E fluid O-77-6 as shown in Table 26.

TABLE 26

COMPARISON OF 320°C CORROSION AND OXIDATION STABILITY OF OPTIMUM AND EXCESSIVE CONCENTRATIONS OF ADDITIVE A

Test Hours	Viscosity Change at 40°C, %		
	75 Rel. %	100 Rel. %	250 Rel. %
48	11.6	13.8	19.7
144	37.0	36.2	35.7
240	76.7	76.7	72.3

The air tubes used during the testing of O-77-6 additive A contained various amounts of varnish and coke inside the air tubes. The tube used for O-77-6 did not contain any coke or varnish. The amount of these deposits within the air tubes depended on the concentration of additive as is shown in Figure 27. These deposits must be forming inside of the air tubes due to the occurrence of very thin oil films providing for optimum oxygen absorption. Only light stains were formed on the test tubes during any of these tests.

Corrosion and oxidation testing of O-77-6 containing 100

End View

A B C D E

Side View

Figure 27. Varnish and Coke Deposits Inside of Air Tubes of 5P4E Fluid Containing Various Concentrations of Additive A (A = 0, B = 50, C = 75, D = 100, E = 250 Relative Percent)

relative % of additive A at a test temperature of 320°C without metal test specimens was conducted with the test data being given in Table 27. The data shows a small improvement in viscosity change when testing without the metal specimens. For example, at 240 test hours a 40°C viscosity change of 63.7% occurred without the metal specimens and 76.7% 40°C viscosity increase with the metal specimens.

Since studies showed that additive A changes to tin oxide at a very fast rate (less than 24 hours) at 320°C, corrosion and oxidation testing of O-77-6 plus SnO_2 and O-77-6 plus Sn was conducted. The concentrations were selected to provide equivalent tin content of 75 relative percent of additive A. The particle size of the Sn and SnO_2 was below 5 microns. Test data obtained from this testing is also given in Table 27 and shown graphically in Figure 28. The Sn and SnO_2 provided very little improvement in oxidative stability of O-77-6. This could be due to particle size or to the "contamination" or "deactivation" of the surface of the Sn and SnO_2 used. The viscosity change obtained using 25 and 75 relative percent of additive A is included in Figure 27 for comparison.

(h) Basestock Analysis of New and Stressed O-67-1 and O-77-6 Lubricants

Gas chromatography and gel permeation chromatography methods of analyses were developed for characterizing and analyzing new and stressed polyphenyl ethers including additives and breakdown products. This section discusses primarily the basestock analyses and changes therein. Additive analyses are presented in Section II.4. However, some references will be made to additive content in this section since some of the developed analysis techniques determines and identifies both the basestock and additives.

TABLE 27

CORROSION AND OXIDATION STABILITY
OF POLYPHENYL ETHER O-77-6 CONTAINING
VARIOUS ADDITIVES AT 320°C USING D 4871
TUBES, INTERMEDIATE SAMPLING AND 10 L/h AIRFLOW

Lubricant Formulation	Test Hours	Viscosity 40°C	Viscosity Change at 40°C, %
O-77-6 + 250 Rel. % Additive A	0	285.4	-
	48	341.5	19.7
	144	387.4	35.7
	240	491.7	72.3
O-77-6 + 100 Rel. % Additive A (No metal specimens)	0	279.5	-
	48	322.5	15.4
	144	359.2	28.5
	240	457.6	63.7
O-77-6 + SnO_2 (<5 microns in size)	0	279.7	
	24	421.4	50.7
	48	3461.0	1137.4
O-77-6 + Sn (<5 microns in size)	0	278.7	-
	24	449.3	61.2
	48	4223.6	1415.2

Lubricant Formulation	Test Hours	Corrosion of Metal Specimens, mg/cm^2 Al	Ag	Mild Steel	M-50 Steel	Waspaloy	Ti
O-77-6 + 250 Rel. % Additive A	240	+0.10	-0.10	+0.14	+0.12	+0.08	+0.08
O-77-6 + SnO_2[1]	48	+0.06	+0.16	+0.18	+0.18	+0.08	+0.10
O-77-6 + Sn[1]	48	+0.08	+0.16	+0.24	+0.28	+0.12	+0.12

[1]Equivalent to 75 relative percent Additive A with respect to tin content of O-67-1

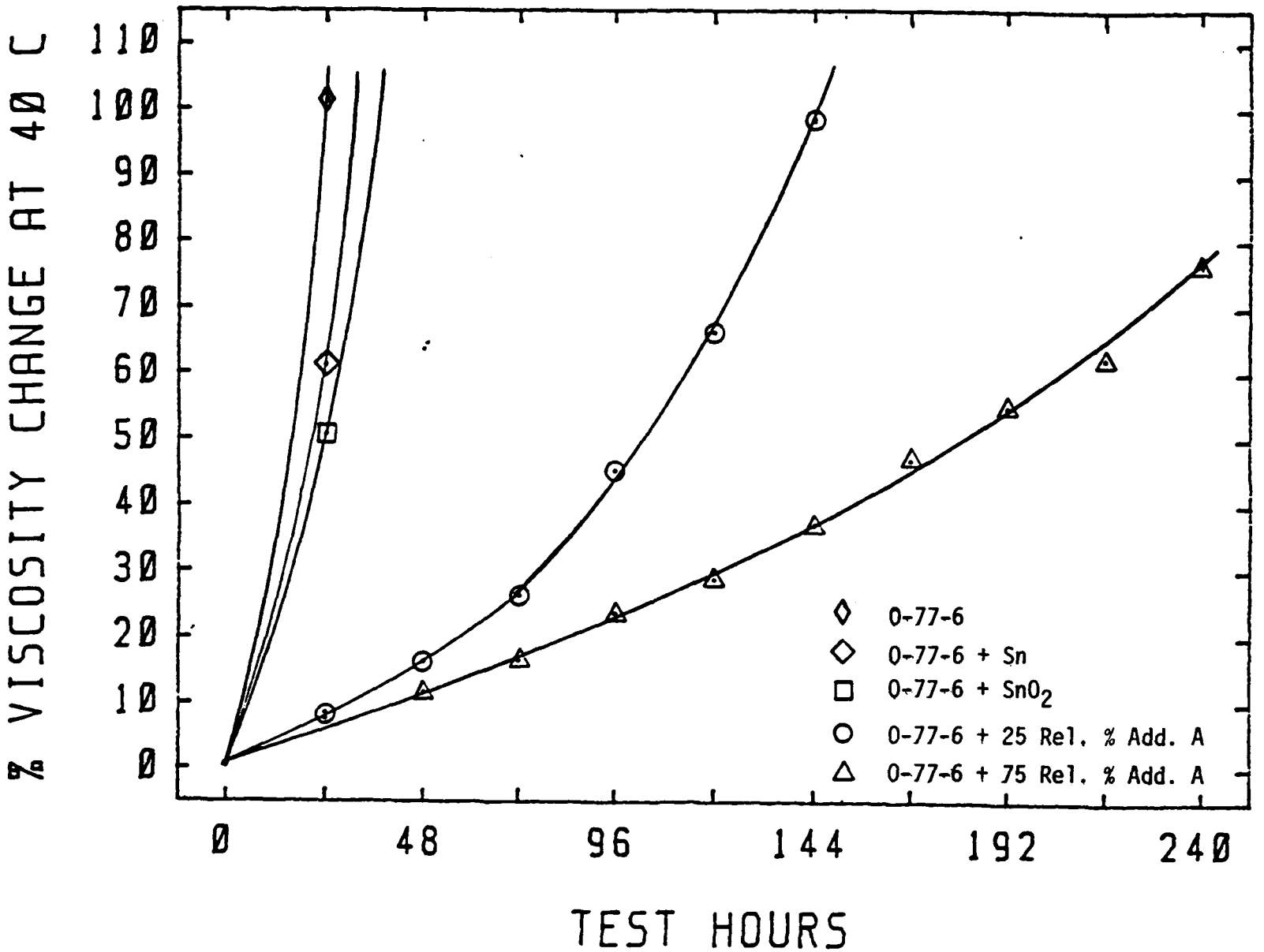

Figure 28. Effect of Various Materials and Concentrations on 40°C Viscosity Change During Corrosion and Oxidation Testing of O-77-6 at 320°C and 10 L/h Airflow

In order to characterize the basestock and additive A in O-67-1, a gas chromatographic method using flame ionization detection (GC-FID) was developed. Figure 29 shows the GC-FID chromatogram of O-67-1 basestock components. The three basestock components were found to be in approximately the % area ratio of 62.5 : 32.5 : 5.0. The small peak at 7.26 minutes is additive A.

Polyphenyl ethers are UV active and can be easily analyzed by gel permeation chromatography (GPC) with an ultraviolet detector. Figure 30 shows the GPC chromatogram of O-67-1. The particular set of columns cover a molecular weight range of about 200 to 20,000 (size equivalent to polystyrene). Although O-67-1 consists of three different basestock components the difference in their molecular size is insignificant and beyond the resolution of the column and appear as one peak.

Since GPC can be used to calculate average molecular weights, owing to the linear relationship of log molecular weight and retention time, such a program was developed for polyphenyl ethers in accordance with ASTM D-3536, "Molecular Weight Averages and Molecular Weight Distribution of Polystyrene by Liquid Exclusion Chromatography (Gel Permeation Chromatography - GPC)." Briefly, the columns are calibrated with three polyphenyl ethers (6P5E, 5P4E, 4P3E) and the log of their molecular weights are plotted vs. their respective retention times. The plot of this calibration is shown in Figure 31 along with the slope (m), intercept (b) and correlation coefficient (r), and as expected shows excellent linearity. From this calibration data it is possible to calculate molecular weight averages from the peak heights at various retention times. The three statistical averages commonly used in such work are number average (M_n) and weight average (M_w) molecular weights and dispersion (D) and are mathematically

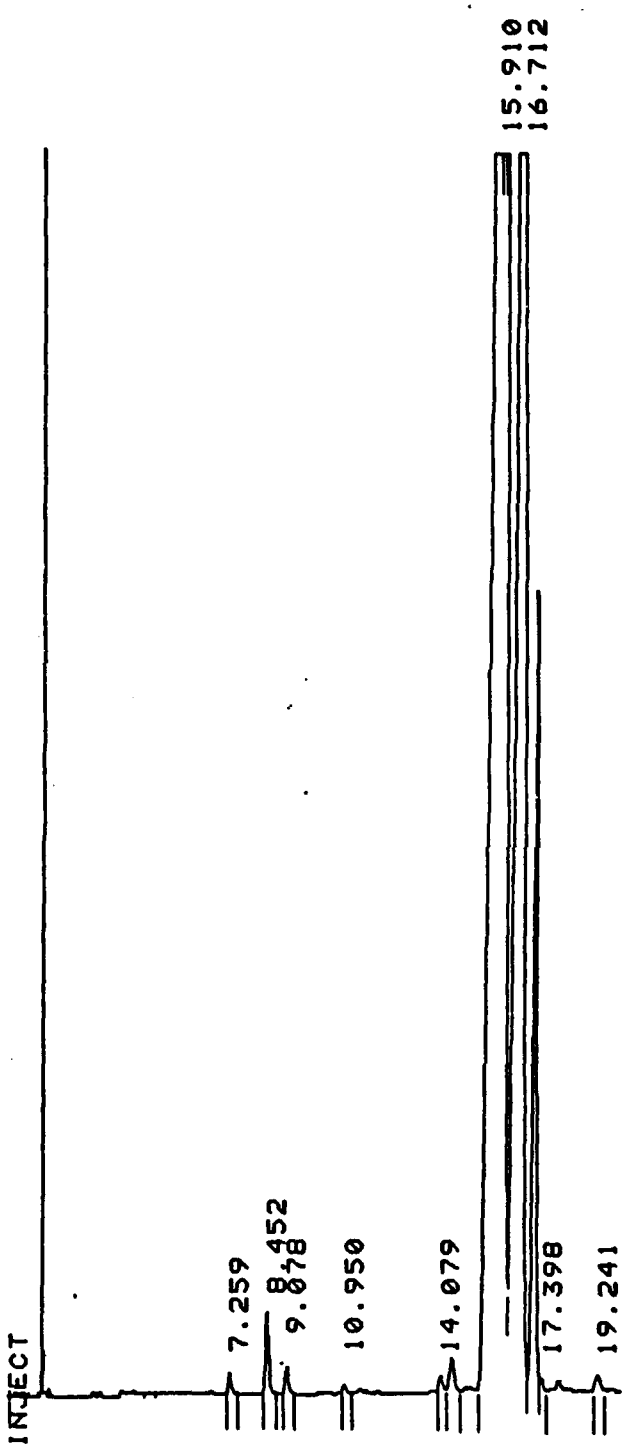

Figure 29. Gas Chromatogram of O-67-1 Lubricant

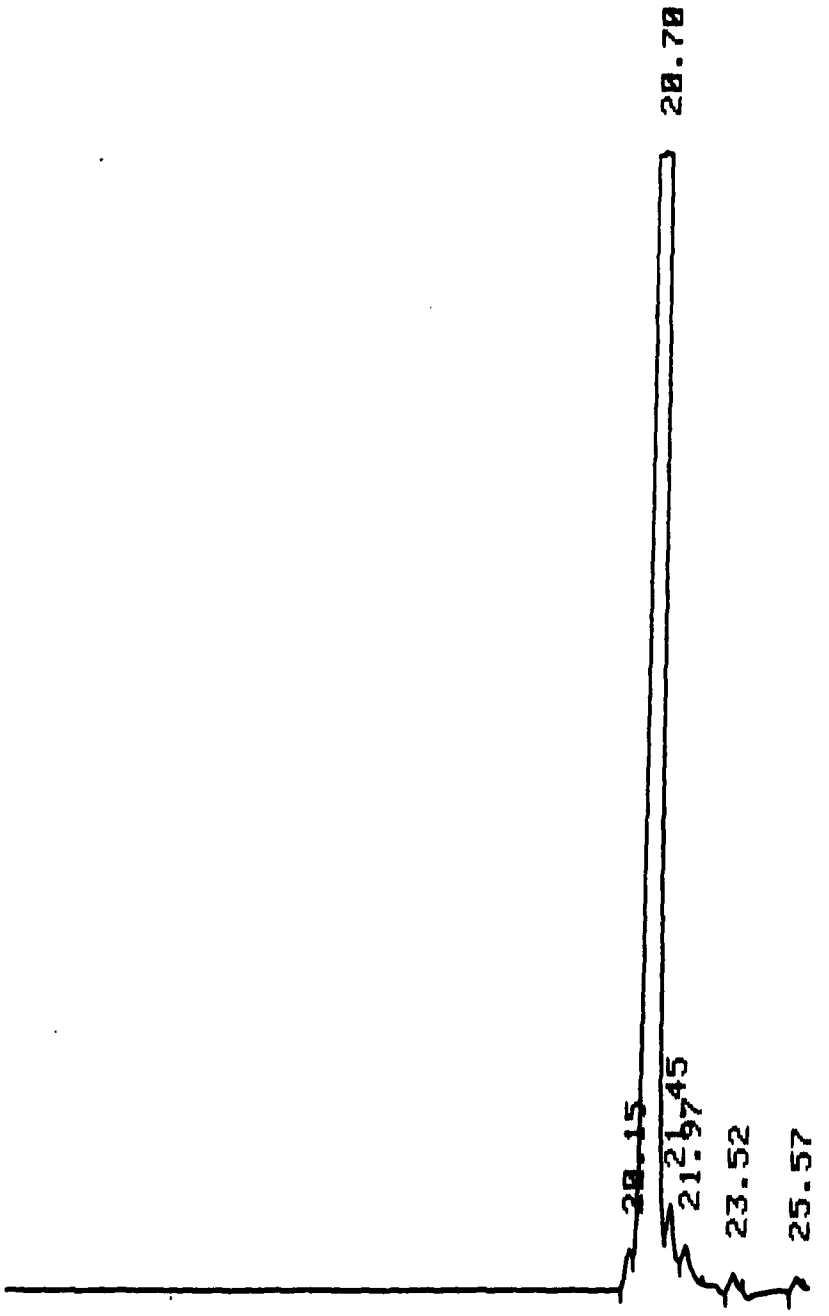

Figure 30. Gel Permeation Chromatogram of O-67-1 Lubricant

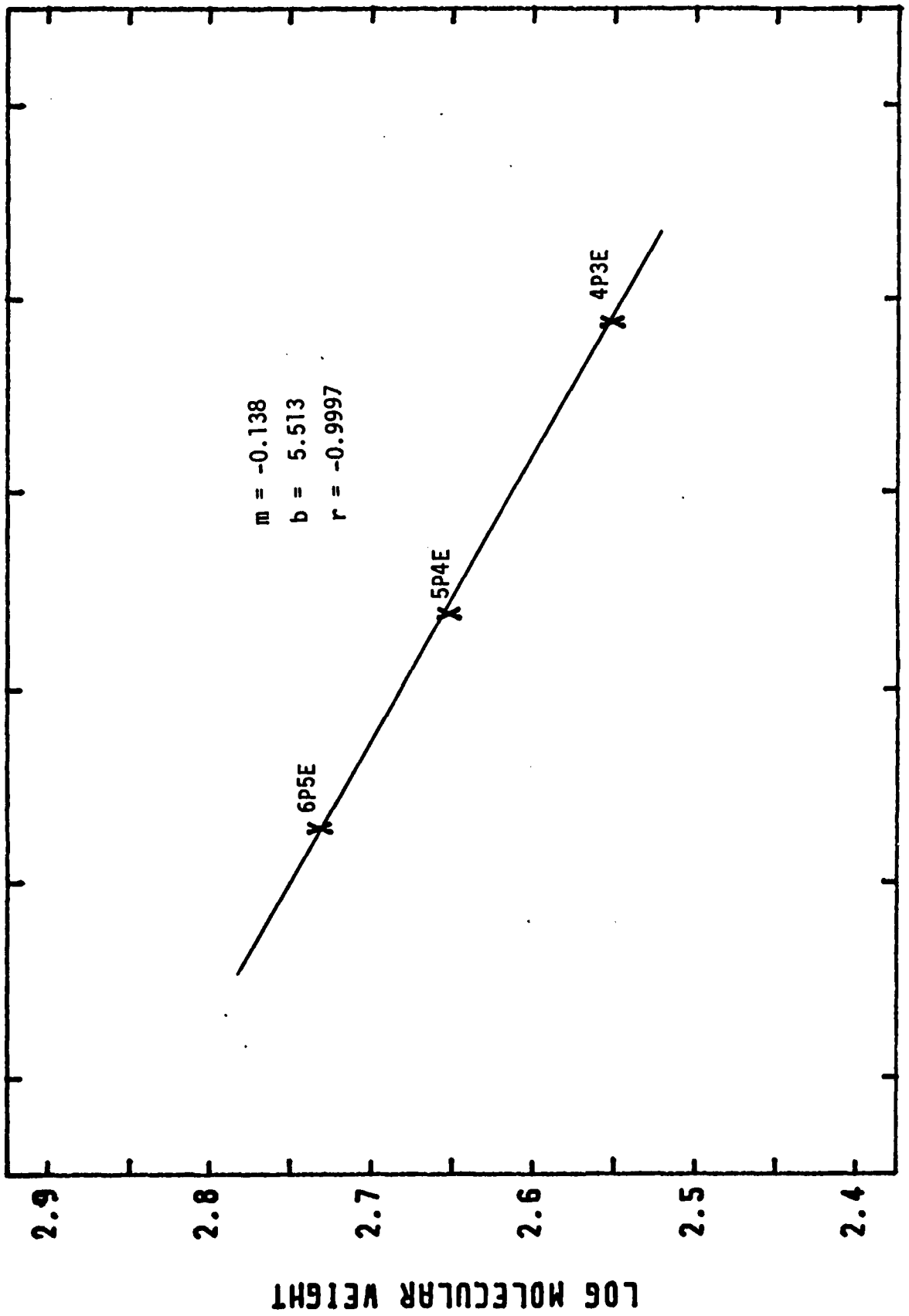

Figure 31. Log Molecular Weight vs. GPC Retention Time for Three Polyphenyl Ether Calibration Standards

defined as follows:

$$M_n = \frac{\sum_{i=1}^{N} H_i}{\sum_{i=1}^{N} (H_i/M_i)} \qquad M_w = \frac{\sum_{i=1}^{N} (H_i \times M_i)}{\sum_{i=1}^{N} H_i} \qquad D = \frac{M_w}{M_n}$$

where = H_i = peak height at time i and M_i = Molecular weight at time i (from calibration curve).

Both M_n and M_w are measures of the average molecular weight of the sample and their significance can be shown by a simple example. If monodisperse polymers of 50,000 and 100,000 molecular weight are combined in equal molar amounts, M_n would be equal to 75,000 and if they were combined in equal weights, M_w would be equal to 75,000. Dispersion (D) is a measure of the range of molecular weights and is equal to 1.0 for a monodisperse sample (one molecular weight). The HP 79850B data integrator was set to take area slices (the system cannot do heights) at 0.25 minute intervals from 13 to 22 minutes (a range of approximately 300 to 5000 molecular weight). This data is put into a text file such as PeachText or Edlin and the necessary calculations made by a BASIC program (See Figure 32).

Using this system, molecular weight averages were determined on two polyphenyl ether lubricants stressed in the corrosion and oxidation test at 320°C for 48 hours with their molecular weight average data shown in Table 28.

```
  5 'MWD.BAS
6 'GPC MOLECULAR WEIGHT CALCULATION PROGRAM
10 CLEAR 100
20 CLS
25 M!=-.138:B!=5.513 'M=SLOPE AND B=INTERCEPT FROM GPC CALIB CURVE
30 DIM TSD!(2,100) 'ARRAY FOR GPC TIME SLICE DATA
40 INPUT "NAME OF FILE: ",A$ 'NAME OF PEACHTEXT OR EDLIN FILE CN. DATA
50 OPEN A$ FOR INPUT AS #1
60 A=1
70 INPUT #1,TSD!(1,A),TSD!(2,A)
80 A=A+1
90 IF EOF(1) THEN 92
91 GOTO 70
92 CLOSE #1
93 N=A-1 'NUMBER OF POINTS IN FILE
99 SUM!=0
100 FOR A=1 TO N
110 SUM!=SUM!+TSD!(2,A) 'SUMMATION OF AREAS
120 NEXT A
125 SUMA!=0:SUMB!=0
130 FOR A=1 TO N
140 LMW!=M!*TSD!(1,A)+B! 'GET LN MOL WT. FROM SLOPE AND INT. AND RET. TIME
150 LMW!=LMW!*2.30259  'CHANGE TO LOG MW
160 MOLWT!=EXP(LMW!)  'GET MOLECULAR WEIGHT
170 SUMA!=SUMA!+(TSD!(2,A)/MOLWT!) 'SUMMATION OF (AREA/MW)
171 SUMB!=SUMB!+(TSD!(2,A)*MOLWT!) 'SUMMATION OF (AREA X MW)
180 NEXT A
190 MN!=INT(SUM!/SUMA!) 'NUMBER AVERAGE MOL. WT.
191 MW!=INT(SUMB!/SUM!) 'WEIGHT AVERAGE MOL. WT.
192 CLS
193 PRINT "MN="MN! 'PRINT NUMBER AVERAGE MW.
194 PRINT "MW="MW! 'PRINT WEIGHT AVERAGE MW.
195 PRINT "D="INT(100*MW!/MN!)/100 'PRINT DISPERSION FACTOR
200 END
```

Figure 32. BASIC Program for GPC Molecular Weight Calculations

TABLE 28

GPC MOLECULAR WEIGHT ANALYSIS OF POLYPHENYL ETHERS FROM CORROSION/OXIDATION TEST FOR 48 HOURS

Lubricant	Test Temp°C	Type Tube	Visc. Change at 40°C, %	Molecular Weight Averages* Mn	Mw	D
O-67-1	320	Squires	11.5	451	467	1.03
O-67-1	320	D 4871	16.8	454	476	1.05
O-77-6	320	Squires	93.4	502	608	1.21
O-77-6	320	D 4871	Solid	740	1364	1.84

*M_n is the number average, Mw is the weight average and D is dispersion

The stressed O-67-1 lubricant showed slight increases in viscosity and molecular weight averages at the higher temperatures. Also, the lubricant tested in the D 4871 tube showed slightly greater increases in physical properties relative to that in the Squires tube at the same temperature.

Gel permeation chromatography (GPC) was used to analyze O-67-1 from the 192 hour corrosion/oxidation test at 320°C. The results of these analyses are shown in Table 29.

TABLE 29

MOLECULAR WEIGHT ANALYSIS OF O-67-1 FROM CORROSION/OXIDATION TEST AT 320°C BY GPC

Test Hours	Molecular Weight Averages Mn	Mw	D
0	451	456	1.01
24	452	468	1.03
48	454	480	1.06
72	461	494	1.07
96	476	522	1.09
120	483	531	1.09
168	489	547	1.11
192	499	564	1.13

During the oxidation of polyphenyl ether (5P4E) a high molecular weight compound is formed, as evidenced by the appearance of a peak with a retention time of 18.8 minutes in the GPC chromatogram. Since this compound reaches a fairly high concentration during oxidation (>3%) and is fairly well separated from other components (Figure 33), a sample of this compound was collected by preparative GPC and submitted for direct probe mass spectrometry. Based on the molecular ion (M^+ = 890) and the various molecular ion fragments it would appear that this compound is a dimer of 5P4E probably with a biphenyl linkage. A probable mechanism for the formation of this dimer is as follows. Formation of a phenyl radical would occur by abstraction of a hydrogen by some type of radical (X) or perhaps molecular oxygen.

This radical could then attack another polyphenyl ether molecule.

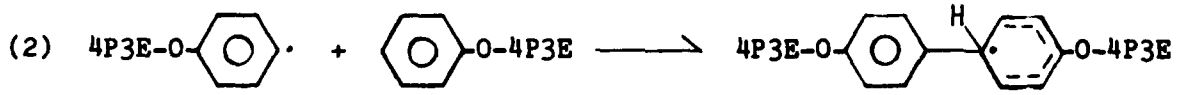

The dimer radical could form the final dimer by disproportionation with another radical (R).

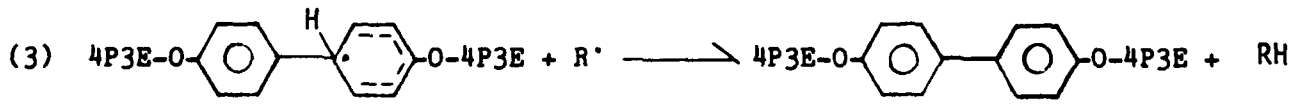

This reaction is very similar to that which produces dimerization of secondary aromatic amine antioxidants such as PANA.

Although the oxidation of polyphenyl ethers has been

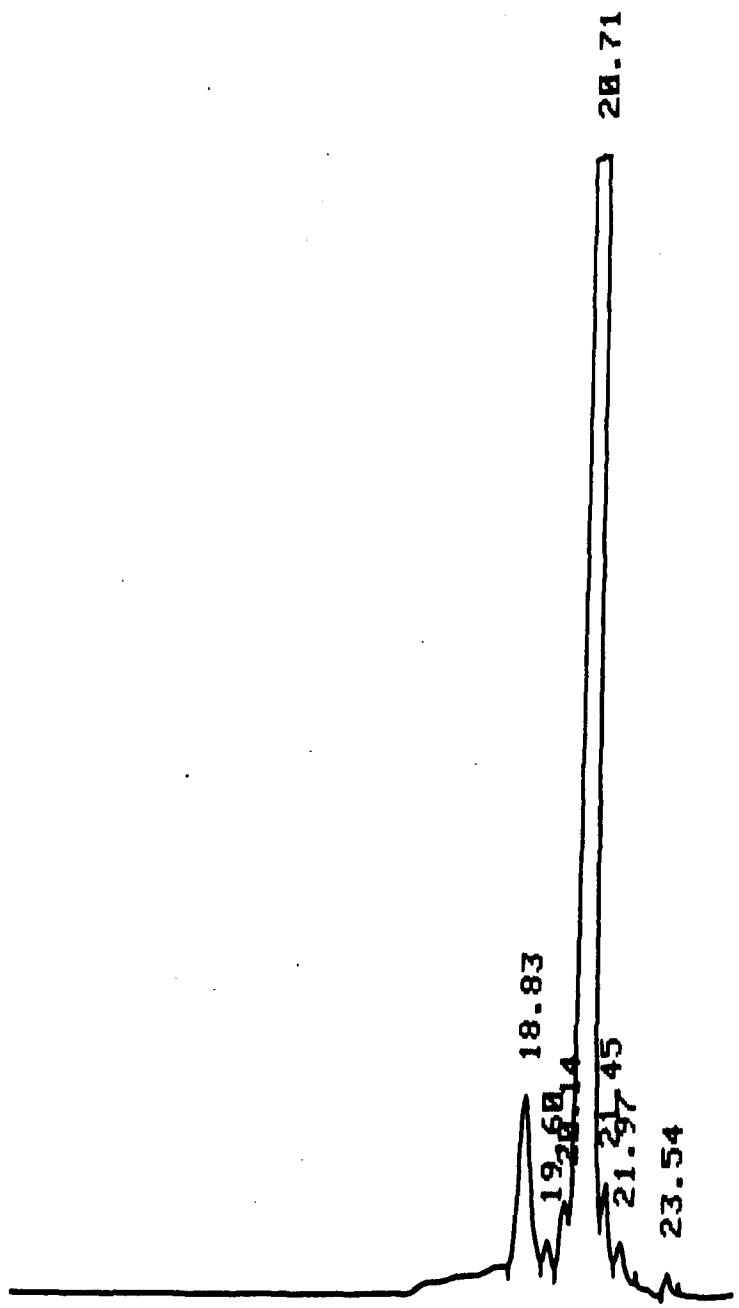

Figure 33. GPC Chromatogram of O-67-1 from the Corrosion and Oxidation Test at 320°C, 48 Hours

investigated,[5,8] the mechanism does not seem to be as well proven as that for other organic materials such as hydrocarbons and esters. Most reaction schemes proposed involve direct attack of molecular oxygen on C-O-C bonds with subsequent cleavage to form phenoxy type radicals. Normally, radicals of the type produced in reaction (1) would be expected to insert molecular oxygen to create peroxy radicals.

(4)

These peroxy radicals can then abstract a hydrogen thus acting as a chain transfer agent and produce a compound (hydroperoxide) that is thermally unstable which produces more radicals. This may very well be occurring in the oxidation of polyphenyl ethers but the dimerization process of reactions (2) and (3) is apparently very competitive.

In order to determine whether or not this dimer is a thermal reaction product, a 48 hour corrosion and thermal stability test at 320°C was run on O-67-1. This test is identical to the corrosion and oxidation test except that nitrogen is substituted for air. Analysis of this sample by gel permeation chromatography revealed the sample to be virtually unchanged from the fresh sample. Likewise the viscosity of the lubricant only shows minimal increases (Table 17). It would appear that the dimer seen in the corrosion and oxidation test is solely an oxidation product.

Polyphenyl ether lubricant O-67-1 consists primarily of three main components with the relative percent composition of the three being 62.5, 32.5 and 5.0% respectively as determined by gas chromatography. It had been reported by Archer and Bozer[9] that based on the results of oxygen

consumption in a modified Dornte oxidation apparatus that a "meta-enriched" 4P3E polyphenyl ether was considerably less stable than the para 4P3E polyphenyl ether. In order to determine the relative oxidative stability of the three components present in O-67-1, their relative percent areas were determined by gas chromatography for samples from the 192 hour corrosion and oxidation test at 320°C. Figure 34 shows the absolute percent change in the relative component distribution in O-67-1 during this test. Identical rates of oxidation would result in the curves for the three components in Figure 34 to stay at 0% throughout the test (assuming equal rates of evaporation). The actual plot shows, despite some fluctuations, a somewhat higher rate of oxidation for components B and C relative to component A. However, if one considers the reproducibility of the data, approximately $\pm$ 0.10%, this difference is not as significant as it may seem. Based on this data, there does not seem to be a great difference in the oxidative stability of the three components of polyphenyl ether.

Gas Chromatographic analysis of the three 5P4E components was made on several samples of O-67-1 taken from 5 gal can "A" and 5 gal can "B." These results are given in Table 30.

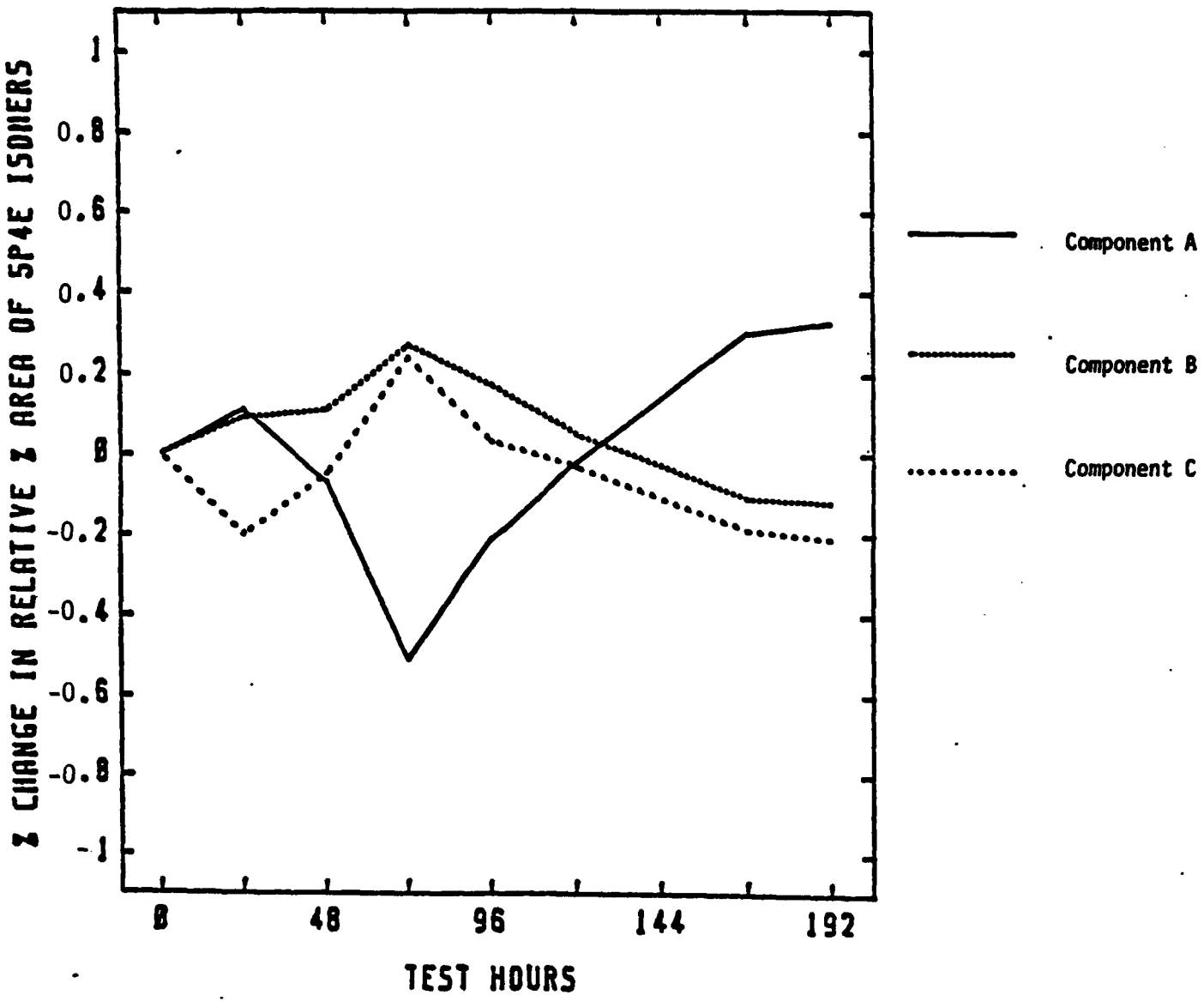

Figure 34. Relative Rates of Oxidation of Three Components During 192 Hour Corrosion and Oxidation Test of O-67-1 at 320°C by Gas Chromatography

TABLE 30

COMPONENT DISTRIBUTION OF O-67-1 SAMPLES

Sample	Component, % (Peak Area) A	B	C
Can "B", Top	65.2	30.5	4.3
Can "B", Middle	65.9	30.0	4.1
Can "B", Bottom	64.5	31.0	4.5
Can "B", Bottom (Filtered)	64.6	30.9	4.5
Mean	65.1	30.6	4.4
Std. Dev.	0.6	0.4	0.2
Can "A" (Sampled 9 Dec 87)	62.3	32.7	5.0
Can "A" (Sampled Sept 87)	62.5	32.5	5.0
Mean	62.4	32.6	5.0
Std. Dev.	0.1	0.1	0.0

The data in Table 30 shows that the two different 5 gal cans of O-67-1 lubricant have a different composition and were not blended as one "batch" or "lot."

Table 31 shows the change in component distribution for new O-77-6 and various O-77-6/additive A blends after 320°C, 240 hour corrosion and oxidation testing and Table 32 shows the change in component distribution of the "condenser washings" after the corrosion and oxidation testing.

TABLE 31

COMPOSITION OF NEW AND 320°C, 240 HR C&O STRESSED
O-77-6 FLUID CONTAINING VARIOUS ADDITIVE A CONTENT

Fluid	% Wt. Component Distribution A	B	C
New O-77-6	62.2	32.7	5.2
Stressed O-77-6 plus 50 Rel. % Additive A	63.6	31.9	4.5
Stressed O-77-6 plus 75 Rel. % Additive A	63.5	32.2	4.3
Stressed O-77-6 plus 100 Rel. % Additive A	63.3	32.2	4.4

TABLE 32

COMPOSITION OF NEW AND CONDENSER WASHINGS FROM 320°C, 240 HOUR C&O STRESSED O-77-6 (5P4E) FLUID CONTAINING VARIOUS ADDITIVE A CONTENT

Fluid	Component, % Wt A	B	C
New O-77-6	62.2	32.7	5.2
Stressed O-77-6 50 Rel. % Additive A	66.9	29.3	3.9
Stressed O-77-6 75 Rel. % Additive A	66.7	29.3	4.0
Stressed O-77-6 100 Rel. % Additive A	68.6	28.1	3.3

The data in Tables 31 and 32 shows that changes do occur in the composition during stressing for both series of samples and with the "condenser" samples showing a much greater change than the "C&O tube" samples after the stressing period. Since the standard deviation based on duplicate analysis of new O-77-6 fluid was 0.49 for component A, 0.14 for component B, and 0.35 for component C, the data in both tables show that "A" is increasing, "B" and "C" are decreasing and with the percent decrease being much greater for "C" than for "B."

An investigation was made into the chemical nature of the oxidation products of polyphenyl ethers. It was found that an oxidized polyphenyl ether could be fractionated by extraction with acetonitrile into a light orange colored soluble liquid fraction and a black solid insoluble fraction. Analysis of these two fractions by gel permeation chromatography reveal the insoluble portion to be high molecular weight oxidation products while the soluble portion consists of the basestock and the previously discussed dimer.

These two fractions were analyzed by infrared spectroscopy (IR), the soluble portion as a neat smear on NaCl plates and the insoluble

portion as a 2% KBr pellet. The IR spectra of the soluble portion was essentially identical to the fresh basestock. It was not anticipated that the weakly absorbing C-C biphenyl bond from the dimer that is present in this fraction would be obscured in this matrix. The IR spectra of the insoluble fraction displayed some significant differences from the fresh basestock (Figure 35). In addition to considerable band broadening that is typical of complex higher molecular weight materials, absorptions at 1770, 1740 and 1660 cm^{-1} are present. Although the 1660 cm^{-1} absorption may be due to a quinone type structure, the other two absorptions are not easily assignable. There are also some quantitative decreases in the absorption band at 760 cm^{-1}. This band is a result of aromatic substitution patterns, possibly meta substitution, but the complexity of the matrix makes a precise assignment impossible.

The two fractions were analyzed by ^{1}H and ^{13}C NMR spectroscopy. The results for the soluble fraction were identical to that of the fresh basestock. It was hoped that this analysis would confirm the presence of the C-C biphenyl link that should exist in the dimer that is present in this fraction at about 10% concentration. The lack of an absorption is probably due to the fact that the dimer is not a single compound but a complex mixture of isomers. Since the dimer is a result of a radical reaction, which generally produces random substitution patterns, the number of structural isomers is likely very large. Since the ^{13}C NMR chemical shift for each of these dimeric compounds would be slightly different, the small signals resulting from each compound would be lost in background noise or in the stronger absorption of the monomer compounds. The complexity of the dimer is revealed by its reverse phase liquid chromatogram (C-18 column, isocratic acetonitrile, UV detection). The chromatogram

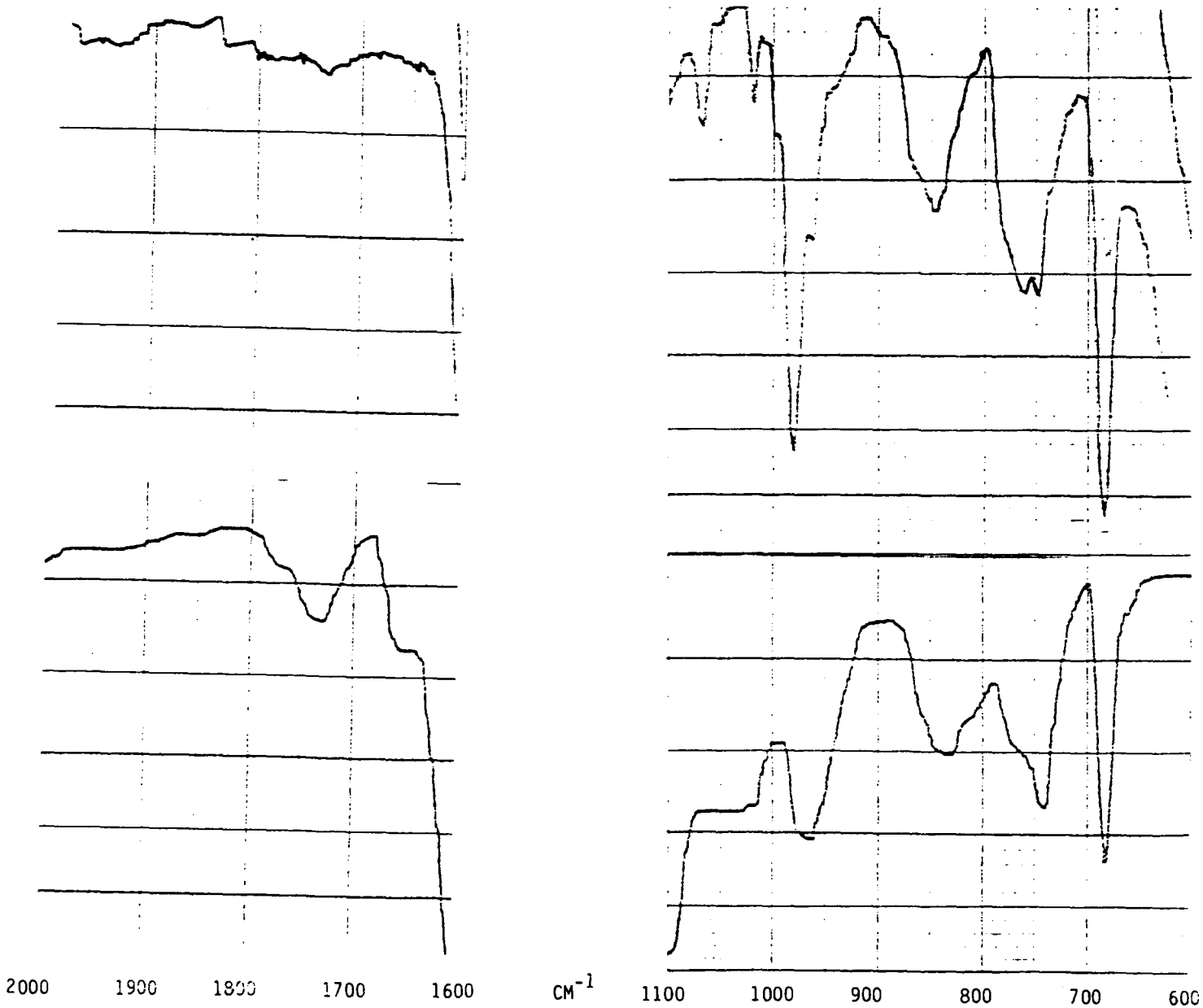

Figure 35. Infrared Spectrum of Fresh 5P4E Polyphenyl Ether (Top) and Acetonitrile Insolubles from Oxidized 5P4E Polyphenyl Ether (Bottom)

(Figure 36) of the GPC isolated dimer would at first glance appear to consist of only three major components but the presence of numerous shoulders and a general asymmetry of peaks indicate the presence of numerous unresolved compounds. It was not possible to analyze the isolated dimer by ^{13}C NMR due to the large sample requirements of this technique (minimum of 100 mg). The NMR of the insoluble fraction displayed large broadening of absorptions due to the complexity of the material and possibly due to the presence of paramagnetic impurities. The ^{1}H NMR indicated the presence of aliphatic compounds but since there is no logical source for such compounds from the oxidation of polyphenyl ethers it must be assumed that these absorptions are due to residual solvent. Because of a poor signal to noise ratio, the ^{13}C NMR of this fraction did not yield any significant information.

A procedure was developed for quantitating the amount of acetonitrile insoluble materials in oxidized polyphenyl ethers. The procedure used was very similar to that in the Toluene Insoluble Matter test (DERD Test Method No. 1)[1] with certain necessary changes. Because considerably more insoluble material is produced with the acetonitrile based test it was necessary to greatly reduce the amount of oxidized lubricant used (100 mg in 20 mL acetonitrile vs. 10 g in 100 mL toluene normally used). This was done to prevent the 5.0 micron filter from plugging and the amount of lubricant used was determined empirically. Also, because acetonitrile is not as strong a solvent as toluene, it was necessary to use an ultrasonic bath for about 15 minutes in order to break up the oil droplets to maximize extraction of the soluble components. This agitation was very important for the heavily oxidized oils. Figure 37 shows the plot of the % insoluble material from the 320°C oxidation and corrosion test of O-67-1 (PPE with additive). The results show an incremental increase in insolubles until a

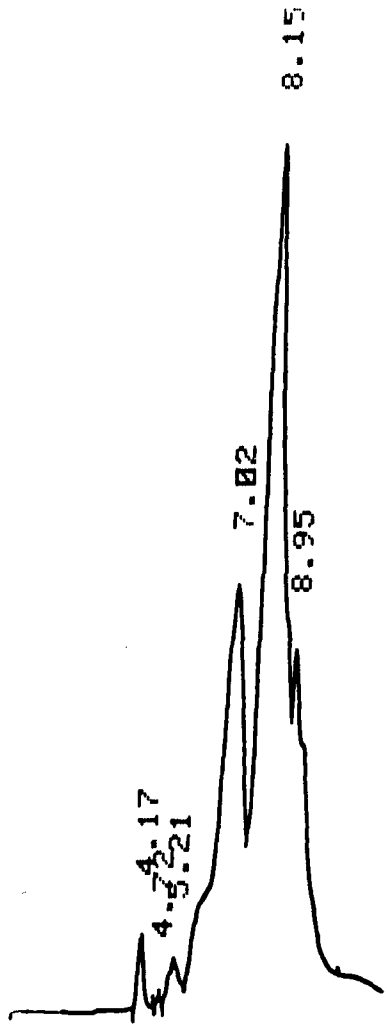

Figure 36. Reverse Phase Liquid Chromatogram of Isolated Biphenyl Dimer from Oxidized Polyphenyl Ether

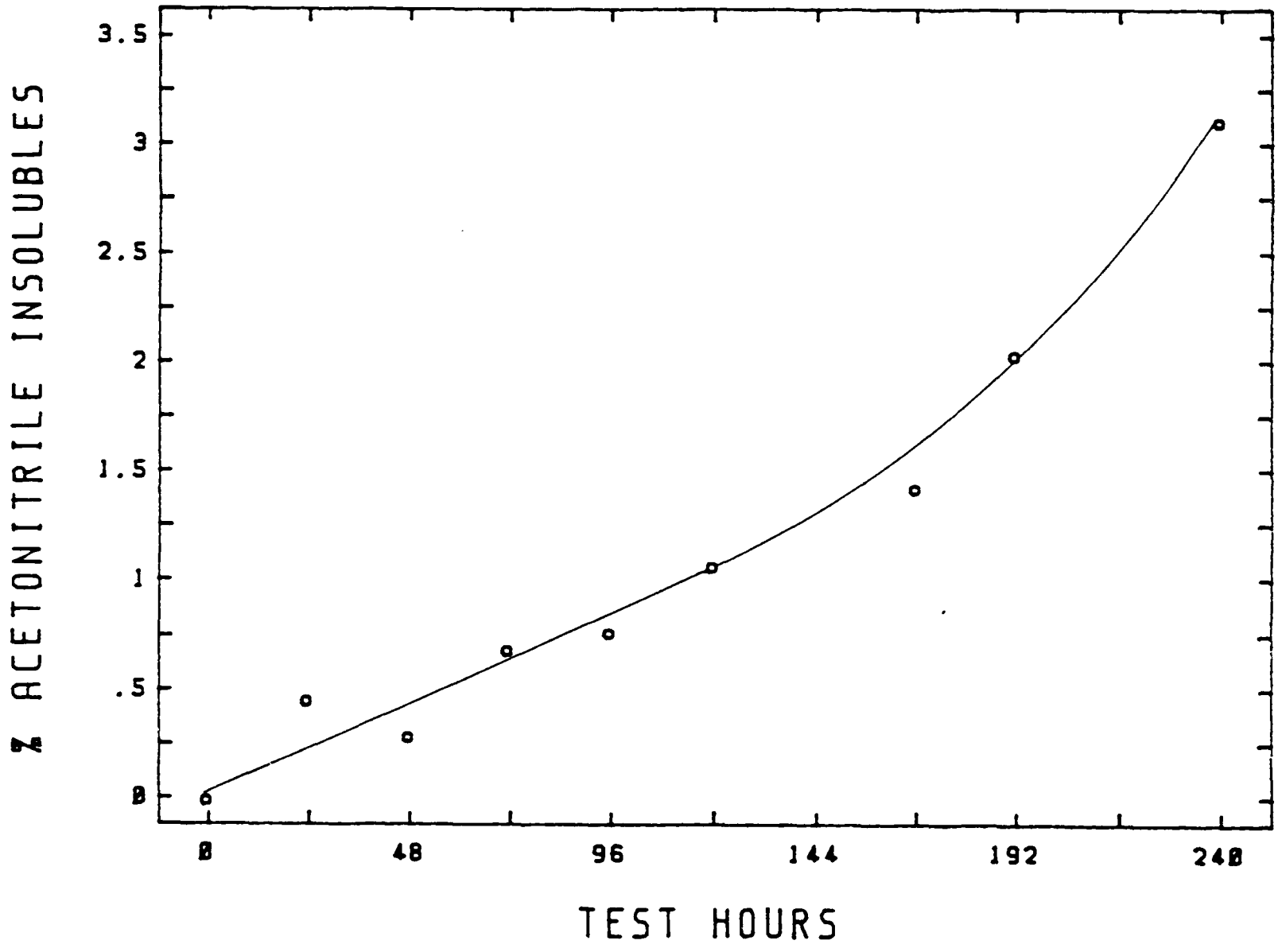

Figure 37. Percent Acetonitrile Insolubles in O-67-1 Stressed in the Corrosion and Oxidation Test at 320°C

sudden rise at the end of the test. This data correlates well with the viscosity and molecular weight increases found previously for this stressed lubricant. In order to determine the efficiency of the filtration, the filtrate from the 240 hour test sample was evaporated to remove the acetonitrile and the residual oil was analyzed by gel permeation chromatography (GPC) and compared to the unfiltered sample. The chromatogram (Figure 38) shows an almost complete loss of the early eluting (higher molecular weight) components compared to the unfiltered sample, as anticipated. It should be noted that the biphenyl dimer (at 18.9 minutes retention time), which is one of the major oxidation products from PPE, is almost completely unaffected by the filtration. The results show that quantitation of acetonitrile insolubles in the oxidized PPE oils studied correlates well with the condition of the oil. Also, because the filtered material represents the nonvolatile components of the oxidized PPE it would be expected to correlate well with the increase in coking tendency of the lubricant.

(i) Evaluation of Other Polyphenyl Ether Lubricants

Corrosion and Oxidation testing of two additional polyphenyl ether formulated lubricants was conducted at 320°C, 10 L/h airflow and for 408 test hours. Data obtained from this testing is given in Table 33 and shows that these two lubricants have a much greater oxidative stability than O-67-1 or the O-77-6 blended fluids. The superior oxidative stability is shown graphically by Figure 39. The viscosity change is 65% less than lubricant O-77-6 containing 75 relative percent of additive A after 240 test hours. No significant corrosion of the metal test specimens occurred with either lubricant considering the long test time. No visual appearance of etching or pitting existed for any of the metal test specimens.

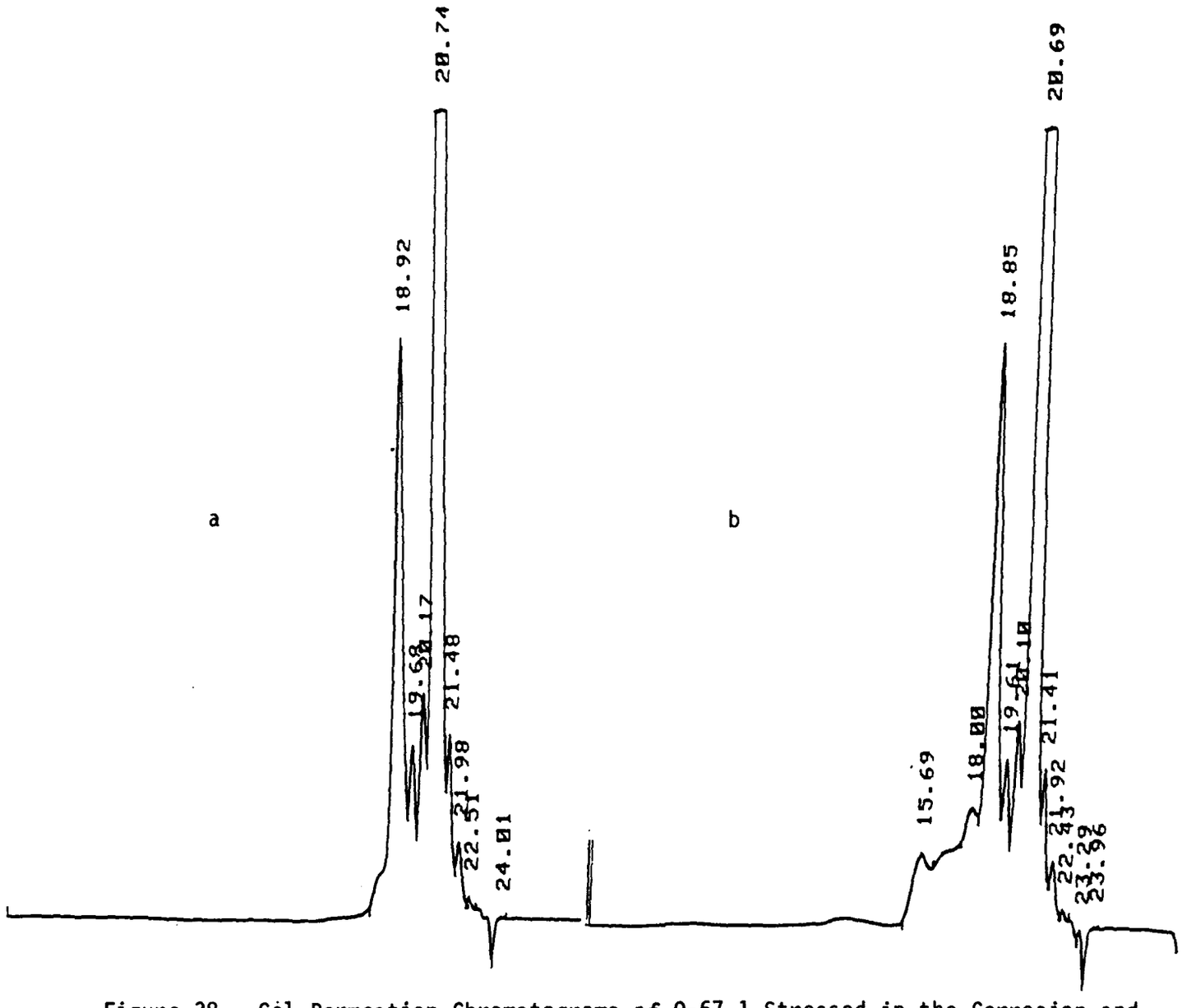

Figure 38. Gel Permeation Chromatograms of O-67-1 Stressed in the Corrosion and Oxidation Test at 320°C for 240 Hours. (a) After Filtration, (b) Before Filtration

TABLE 33

CORROSION AND OXIDATION DATA
FOR LUBRICANTS TEL-8039 AND TEL-8040
(320°C, D 4871 TUBES, 10 L/H AIRFLOW)

Lubricant	Test Hours	Viscosity @ 40°C, cSt	Viscosity Chg @ 40°C, %	Viscosity @ 100°C, cst	Viscosity Chg @ 100°C, %	Refractive Index @ 25°C
TEL-8039	0	291.2	-	12.77	-	1.6283
	48	308.8	6.0	13.05	2.2	1.6284
	144	334.4	14.8	13.49	5.6	1.6294
	240	362.5	24.5	13.92	9.0	1.6297
	264	368.4	26.5	14.06	10.1	1.6299
	312	381.9	31.1	14.32	12.1	1.6301
	336	393.9	35.3	14.53	13.8	1.6302
	360	401.3	37.8	14.69	15.0	1.6302
	384	412.7	41.7	14.87	16.4	1.6303
	408	421.7	44.8	14.95	17.1	1.6304
TEL-8040	0	284.9	-	12.79	-	1.6278
	48	310.7	7.9	13.09	2.3	1.6282
	144	335.8	16.6	13.56	6.0	1.6292
	240	363.0	26.1	13.95	9.1	1.6296
	264	366.2	27.2	14.01	9.5	1.6300
	312	382.2	32.8	14.23	11.3	1.6301
	336	407.1	44.1	14.76	15.4	1.6303
	360	412.3	43.2	14.83	15.9	1.6302
	384	424.6	47.5	15.01	17.4	1.6304
	408	433.0	50.4	15.20	18.8	1.6305

TABLE 33 (CONCLUDED)

CORROSION AND OXIDATION DATA
FOR LUBRICANTS TEL-8039 AND TEL-8040
(320°C, D 4871 TUBES, 10 L/H AIRFLOW)

	Corrosion Test Data, mg/cm^2					
	Aluminum	Silver	Mild Steel	M-50 Steel	Waspaloy	Titanium
TEL-8039[a]	0.00	+0.02	+0.24	+0.10	0.00	+0.04
TEL-8040[a]	+0.04	+0.24	+0.30	+0.08	+0.02	+0.04
TEL-8039[b]	-0.02	-0.04	+0.16	+0.04	-0.04	0.00
TEL-8040[b]	-0.04	+0.02	+0.20	+0.08	0.00	0.00

[a]For test samples up to 336 hours

[b]For test samples from 336 to 408 hours

No visual appearance of etching or pitting on any of the specimens

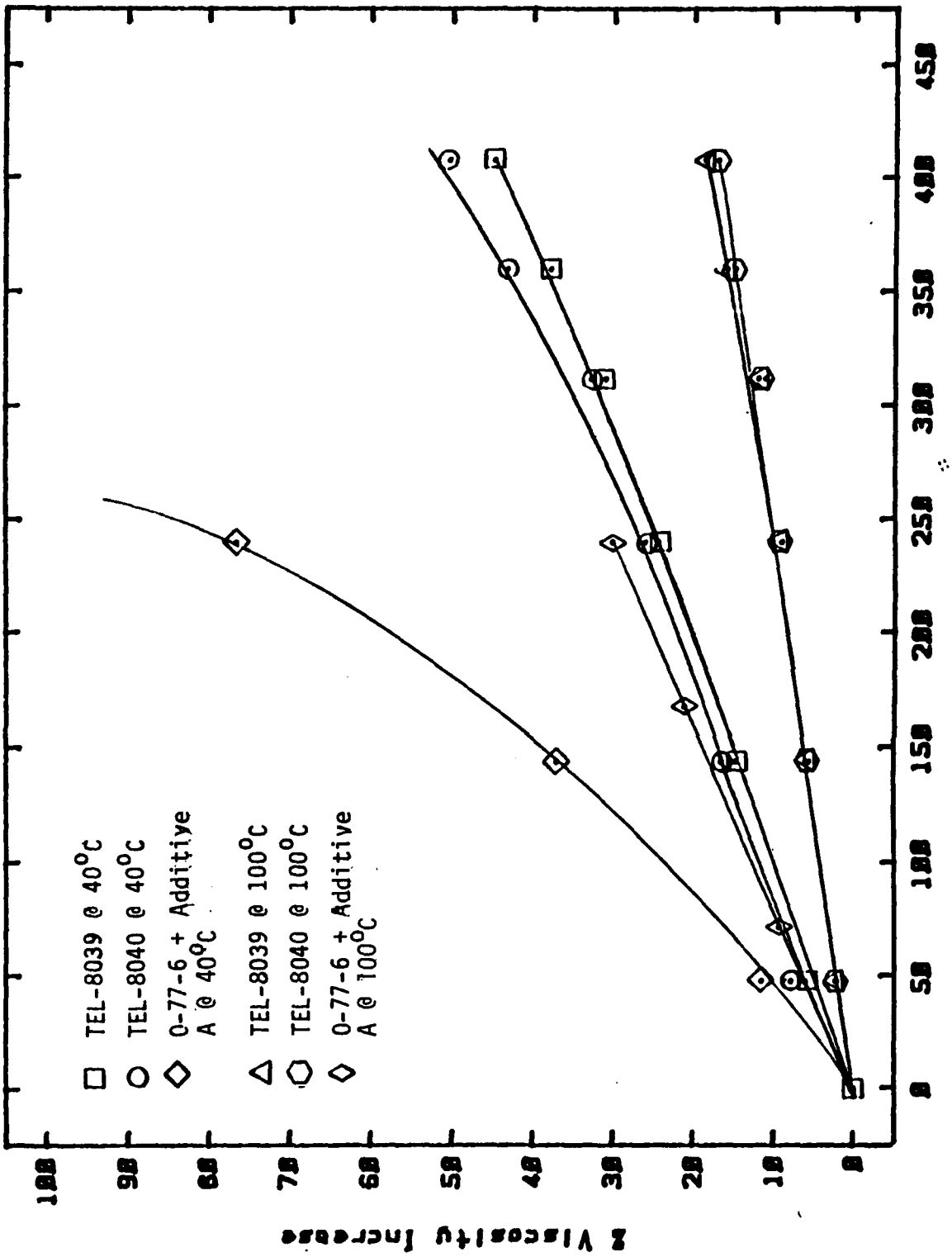

Figure 39. Viscosity Change of Lubricants TEL-8039, TEL-8040 and 0-77-6 with 75 Relative % of Additive A at 40°C and 100°C

(j) Evaluation of Chemical and Electrical Oxidation Stressing Techniques for Monitoring Polyphenyl Ether Lubricants

Analytical techniques based on chemical and electrical oxidation stressing were used to study the additives and degradation products in new and stressed polyphenyl ether lubricants. The chemical-oxidative stressing techniques determine the oxidation stability of the oil. These techniques include free radical trapping (FRT), hydroperoxide decomposing (HPD) methods, and the oxidation-precipitation (OP) method. The electro-oxidation stressing technique determines the concentration(s) and oxidation potential(s) of the antioxidant species in the lubricant.

The RULLER (Remaining Useful Lubricant Life Evaluation Rig) has been previously described[1] and involves the use of voltammetry for determining a fluid's antioxidation capability and degree of degradation of the fluid during thermal and oxidative stressing. Although the RULLER was developed primarily for use with ester base lubricants, an evaluation of the technique and modifications thereof was conducted for determining its potential for monitoring polyphenyl ether lubricants.

In the FRT method, the antioxidant species in the oil sample are titrated with peroxy radicals in an air tight system. The peroxy radicals are created at a constant rate by the thermal decomposition of the free radical initiator, azobisisobutyronitrile (AIBN) at 60°C. Once the antioxidant species have been depleted through reaction with the peroxy radicals, an easily oxidizable compound, benzaldehyde, undergoes rapid oxidation absorbing oxygen. The length of time before the rapid oxygen consumption begins (induction time) is then used to determine the FRT capability of the antioxidant system in the oil sample.

To study the FRT capabilities of the polyphenyl ether based

fluids and oils, the oil sample (20 µl) was added to the AIBN (0.5 g)/chlorobenzene (4.0 mL)/benzaldehyde (0.5 mL) solution. Upon heating to 65°C, the AIBN decomposes to form free radicals and peroxy radicals which react with the oil's additive species and then the benzaldehyde resulting in oxygen absorption (pressure decreases in the air tight system). Regardless of the stressing time at 320°C (24-240 hours), the O-77-6 oil/benzaldehyde/AIBN solution absorbed oxygen at the same rate as the blank (benzaldehyde/AIBN) solution (no induction time). When the fresh O-67-1 oil was added to the benzaldehyde/AIBN solution, the test solution absorbed oxygen at a faster rate than the blank solution. These results indicate the formulated oil and its oxidation product do not have FRT capability and that the additive acts as a free radical promoter.

In the HPD method, the oil sample is first diluted with a solution of bis[(dimethylamino)dithiobenzil] nickel (BDN). When cumene hydroperoxide is added to the oil/BDN solution, the antioxidant species in the oil compete with the BDN complex for reaction with the cumene hydroperoxide. As the BDN complex reacts, the solution becomes colorless, so that the reaction rate of the BDN complex can be measured by its decoloration rate. Since the decoloration rate of the oil/BDN solution is dependent upon the ability of the oils' additive species to inhibit the BDN complex from reacting with the cumene hydroperoxide, the decoloration rate is used to determine the HPD capability of the antioxidant system in the oil sample.

The HPD capability of the polyphenyl ether based fluids and oils was studied by adding cumene hydroperoxide (0.5 mL) to the oil (250 µL)/BDN (3 mL) solution. The test was run at room temperature and the decoloration of the oil/BDN/cumene hydroperoxide solution was monitored with a UV-VIS spectrophotometer (wavelength set to 632.8 nm). The photomultiplier

tube output was plotted versus hydroperoxide reaction time using a strip chart recorder.

As an initial test of the O-67-1 oils' HPD capabilities, fresh and 48 hour stressed (320°C in air and nitrogen) O-67-1 oils were studied. The BDN solution decoloration versus hydroperoxide reaction time plots for the fresh, 48 hour stressed in air, and 48 hour stressed in nitrogen O-67-1 oils and for the blank BDN/cumene hydroperoxide solution (no oil) are shown in Figure 40. The BDN solution decoloration versus hydroperoxide reaction time plots for 500 µL of fresh O-67-1 oil and for 0.1 g of additive A (added to blank BDN/cumene hydroperoxide solution) are also presented in Figure 40. The BDN solution decoloration plots show that the fresh and 48 hour stressed (in nitrogen) O-67-1 oils decolorize at the same rate as the blank. When increased from 250 to 500 µL, the fresh O-67-1 oil inhibits the decoloration of the BDN solution during the initial 30 seconds of reaction with the cumene hydroperoxide. After the induction period, the decoloration rate for the 250 and 500 µL quantities of the fresh O-67-1 oil are similar. Even though 0.1 gram of additive A represents the equivalent of over 10 mL of fresh O-67-1 oil, the decoloration plot of the additive decreases at the same rate as the blank after a 45 second induction period. Of the decoloration plots shown in Figure 40, the plot produced by the O-67-1 oil stressed 48 hours in air exhibits the longest induction time (60 seconds) and the slowest decoloration rate.

In addition to the formulated O-67-1 oils, O-77-6 polyphenyl ether fluid which had been stressed 48 hours in air was studied with the BDN/cumene hydroperoxide system. In contrast to the formulated oils, the 48 hour stressed O-77-6 fluid produced a BDN decoloration plot with an induction time over 5 minutes. As a point of reference, MIL-L-7808 oils

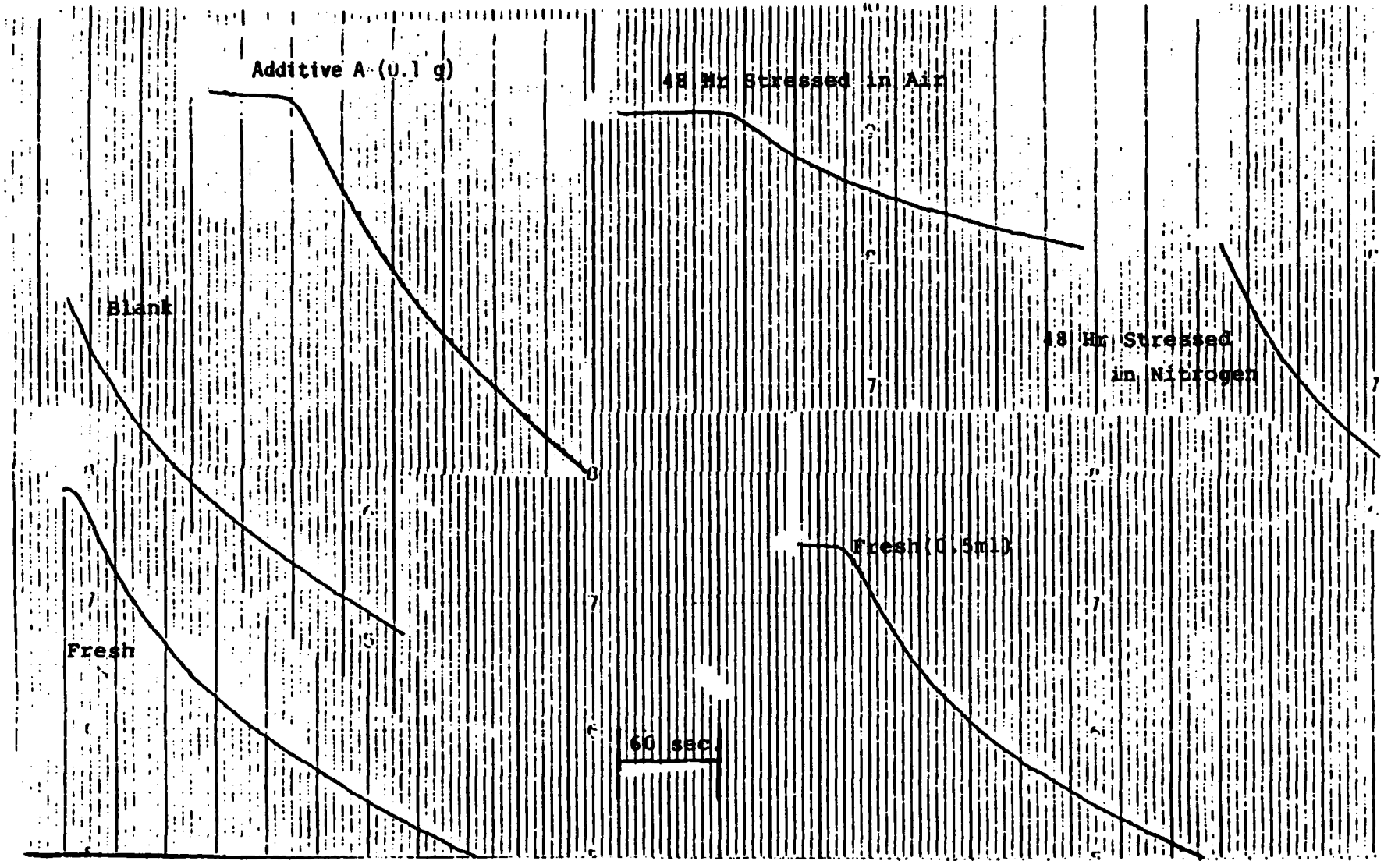

Figure 40. Plots of BDN Solution Decoloration Versus Hydroperoxide Reaction Time for the Blank, Fresh (250 and 500 µL) O-67-1, 48-Hour (Air and N_2 at 320°C) Stressed O-67-1 Oils and Additive A

(15 μL samples) produced induction times over 15 minutes when studied at room temperature.

These results indicate that antioxidant species with HPD capabilities are produced by the initial stages of oxidative stressing, but not by thermal stressing, of the O-67-1 polyphenyl ether based lubricating oil. The additive has poor HPD capabilities at high or low concentrations. In addition to the initial species with HPD capabilities, degradation products are produced in the later stages of thermal oxidation which actually increase the HPD capabilities of the severely stressed O-77-6 fluid. Although the stressed O-67-1 oils have measurable HPD capabilities, the O-67-1 oils' HPD capabilities are very limited in comparison to the HPD capabilities of MIL-L-7808 or MIL-L-23699 ester-based lubricating oils.

In the oxidation-precipitation (OP) method, the lubricant sample (100 μL) is diluted with RULLER solvent (0.5 M $LiClO_4$ in acetone). Upon the addition of the solvent, a reddish brown precipitate forms and settles out of solution. The precipitate is isolated from the oil/acetone solution, dried and weighed. The OP method was used to study the fresh and stressed (24-240 hours) O-67-1 oils and the O-77-6 polyphenyl ether fluid stressed for 24 hours (100% viscosity increase). The weights of the isolated solids were then plotted versus their corresponding stressing times at 320°C for the O-67-1 oil as shown in Figure 41. The percent viscosity change at 40°C and percent weight loss versus stressing time are also included in Figure 41.

The plots in Figure 41 demonstrate that the solid's weight and the viscosity of the oil sample undergo similar increases with increasing stressing time. The solid's weight and viscosity both show some changes in rate of change around 168-192 hours of stressing. However, the shape of the

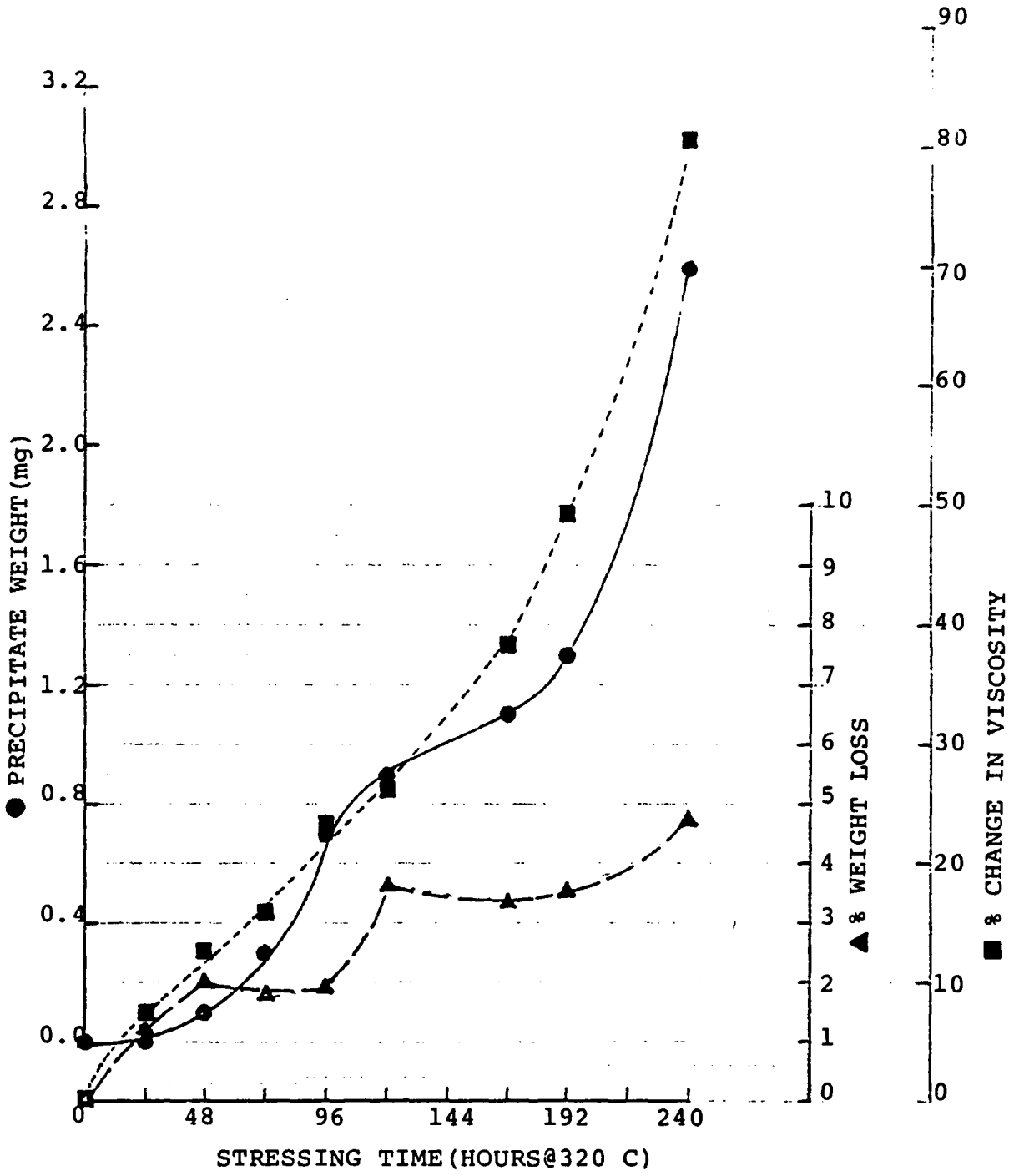

Figure 41. Plots of the Precipitate Weight (mg) Produced by the RULLER Solvent, the Percent Weight Loss, and the Percent Change in Viscosity Versus Stressing Time (Hours) at 320°C for the O-67-1 Polyphenyl Ether Based Lubricating Oil

solid's weight versus stressing time plot in Figure 41 is more closely related to the percent weight loss plot than the viscosity plot.

The 24 hour oxidatively stressed O-77-6 fluid was studied for determining if the precipitate formation in the presence of the RULLER solvent is a function of the additive species. When dissolved in the RULLER solvent, the 24 hour stressed O-77-6 fluid (100% viscosity increase) produced 3.1 mg of precipitate which is in good agreement with the 2.6 mg precipitate (Figure 41) produced by the 240 hour stressed O-67-1 lubricant (80% viscosity increase). Consequently, the precipitate appeared to be mainly dependent on the thermal-oxidation products of the polyphenyl ethers since the amounts of precipitate were similar for the stressed O-77-6 and O-67-1 fluids.

To identify the source of the precipitate, the stressed O-67-1 oils (100 µL) were diluted with 3 mL of acetone or with 3 mL of 0.5 M LiCl in acetone in place of the RULLER solvent. When acetone was the diluent, no precipitates were formed from the O-67-1 oils with less than 192 hours of stressing. For the 192 and 240 hour stressed O-67-1 oils, and the 24 hour stressed O-77-6 fluid, very small amounts (below 0.1 mg) of a precipitate formed. Similar results were obtained when the 0.5 M LiCl in acetone solution was used. The 120 hour stressed O-67-1 oil (100 µL) was then dissolved in acetone (clear solution) and in the RULLER solvent (precipitate). For the RULLER solvent, the precipitate was removed by filtration to produce a clear solution. The clear acetone and RULLER solvent based solutions were then analyzed by GPC to produce the chromatograms in Figure 42. Except for the high molecular weight (MW = 3300 to 1000) oxidation products (RT = 15.0 to 18.0 minutes), the chromatograms produced by the acetone and RULLER solvent in Figure 38 are identical. The presence of $LiClO_4$ in the RULLER solvent lowered the concentration of the highest

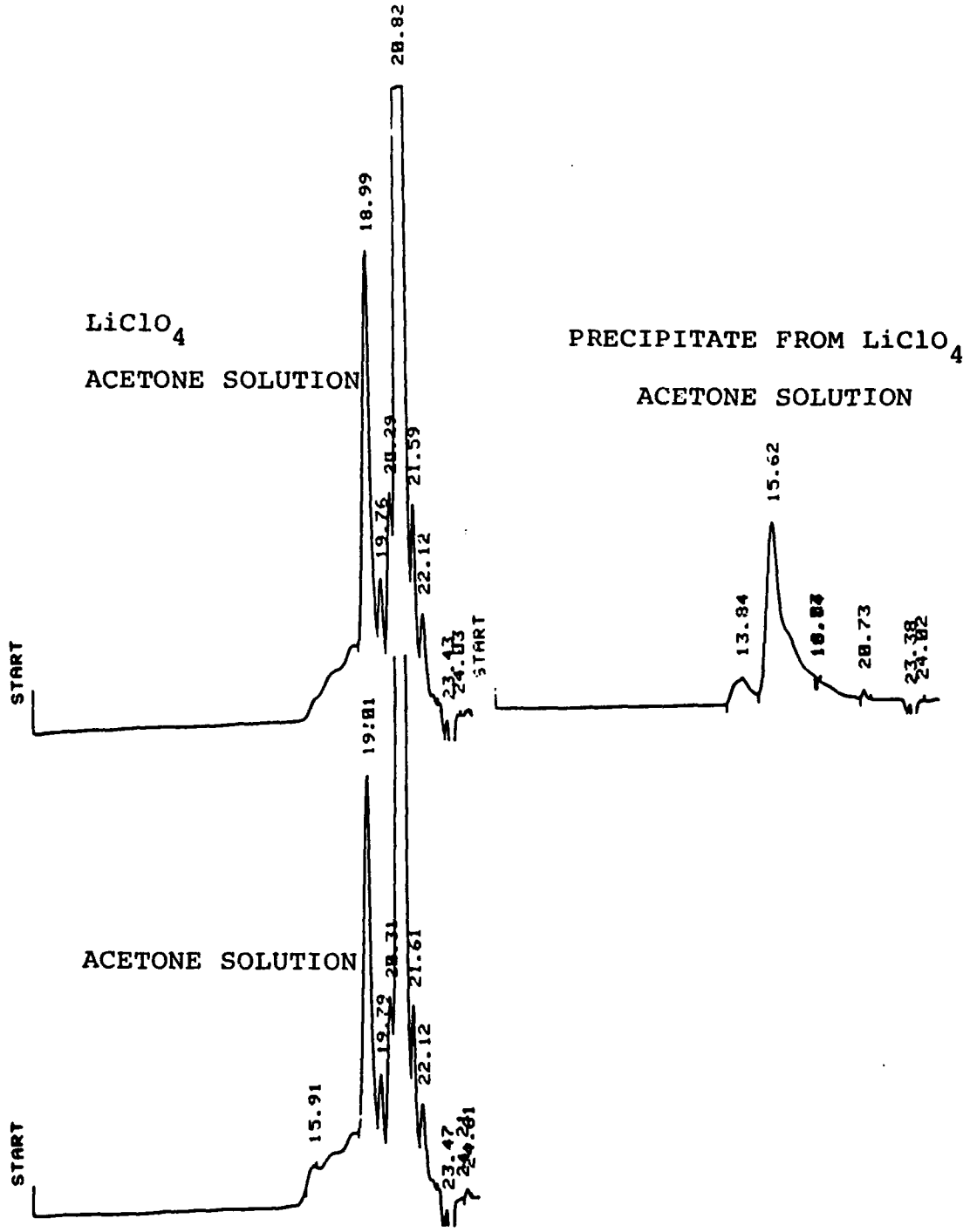

Figure 42. Gel Permation Chromatograms of the 120 Hour Stressed 0-67-1 Oil (320°C) Diluted with Acetone and with $LiClO_4$/Acetone Solution and of the Precipitate Produced by the 120 Hour Stressed 0-67-1 Oil Diluted with $LiClO_4$/Acetone Solution

molecular weight species in respect to acetone. These results indicate that the precipitate produced by the RULLER solvent might be formed from the high molecular weight thermal oxidation products of the polyphenyl ether fluid. Since the precipitate is formed in the presence of $LiClO_4$ (oxidizing agent) but not in the presence of LiCl (non-oxidizing agent) or in pure acetone, the results indicate that the $LiClO_4$ is oxidizing the thermal-oxidation products making them insoluble in acetone.

To determine the molecular weight(s) of the precipitate formed by the RULLER solvent, the dried precipitate formed from the 120 hour stressed O-67-1 oil using the RULLER solvent was dissolved in THF and analyzed by GPC and is also shown in Figure 42. These chromatograms show that the precipitate formed from the 120 hour stressed O-67-1 oil is very similar in molecular weight (MW about 2300, RT = 15.6 minutes) to the highest molecular weight compounds produced by the stressed oil in acetone. The main difference among the chromatograms is the peak at a retention time of 13.84 minutes (MW about 4000) produced by the precipitate from the 120 hour stressed O-67-1 oil. These results also indicate that the $LiClO_4$ is oxidizing the thermal-oxidation products of the polyphenyl ether fluid to higher molecular weights causing them to become insoluble in the acetone of the RULLER solvent.

Final characterization of the precipitate formed from the stressed 5P4E fluids was performed using X-ray Photoelectron Spectroscopy (XPS) analyses. The percent atomic weight determined by XPS for the precipitate obtained from the oxidatively 120 hour stressed O-67-1 lubricant is given in Table 34. These results show that the precipitate does not contain Li or Cl which would be expected if the precipitate was comprised of salts or complexes of $LiClO_4$.

TABLE 34

XPS RESULTS FOR PRECIPITATE OBTAINED FROM STRESSED O-67-1 OIL

Element	Atomic Percentage	Type of Bonding
C	6.5	C = O
	17.7	C - O
	55.3	C - H
O	19.7	
Other	0.8	

In contrast to the chemical-oxidation stressing methods, the electro-oxidation method is based on the current-voltage-time relationships at the surfaces of microelectrodes. The electro-oxidation techniques determine the amount of electrons flowing to or from the microelectrode surface as the electroactive (antioxidant) species undergo oxidation or reduction. These techniques monitor the electron flow as the potential of the microelectrode is varied versus time or is held constant at a preselected value capable of oxidizing the species. The amount of electron flow is then used to quantitate the antioxidant species in the oil sample and the potential(s) at which the electron flow(s) occurs is used to determine the type(s) of antioxidant species present in the oil sample.

To initially study electro-oxidation stressing techniques for use with polyphenyl ether fluids, cyclic voltammetry was used to analyze fresh and 240 hour stressed O-67-1 oil using the RULLER solvent system (375 ppm pyridazine and 0.5 M $LiClO_4$ in acetone) and a 0.5 V/sec scan rate. The voltammograms produced by successive cyclic scans of the fresh and stressed O-67-1 oils are shown in Figures 43 and 44. The similar oxidation and reduction waves of Figures 43 and 44 show that reduction waves are not produced during the first scan and that the species which produce reduction

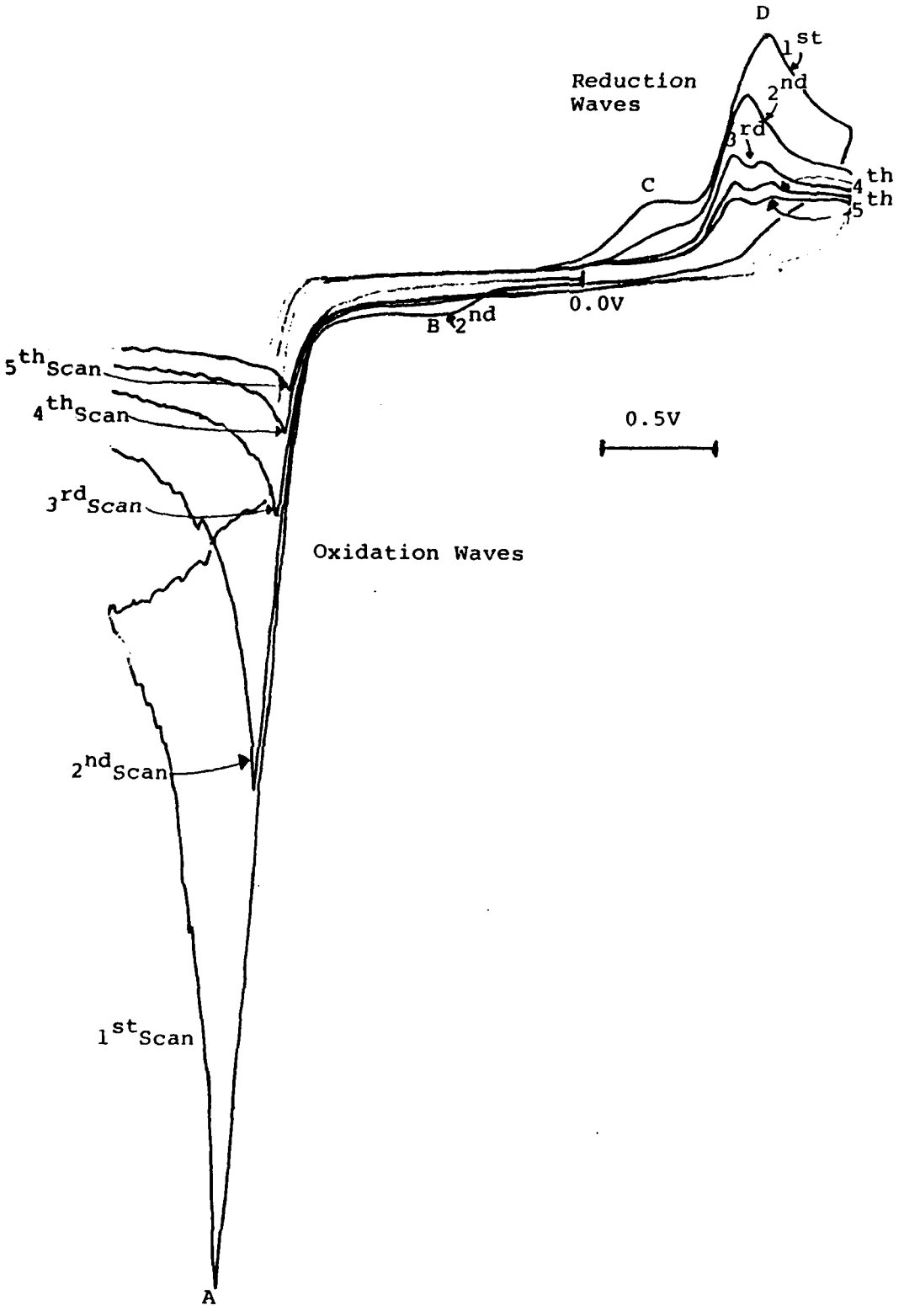

Figure 43. Successive Cyclic Voltammograms (1st-5th Scans) of the Fresh O-67-1 Oil in Acetone Using a Glassy Carbon Working Electrode

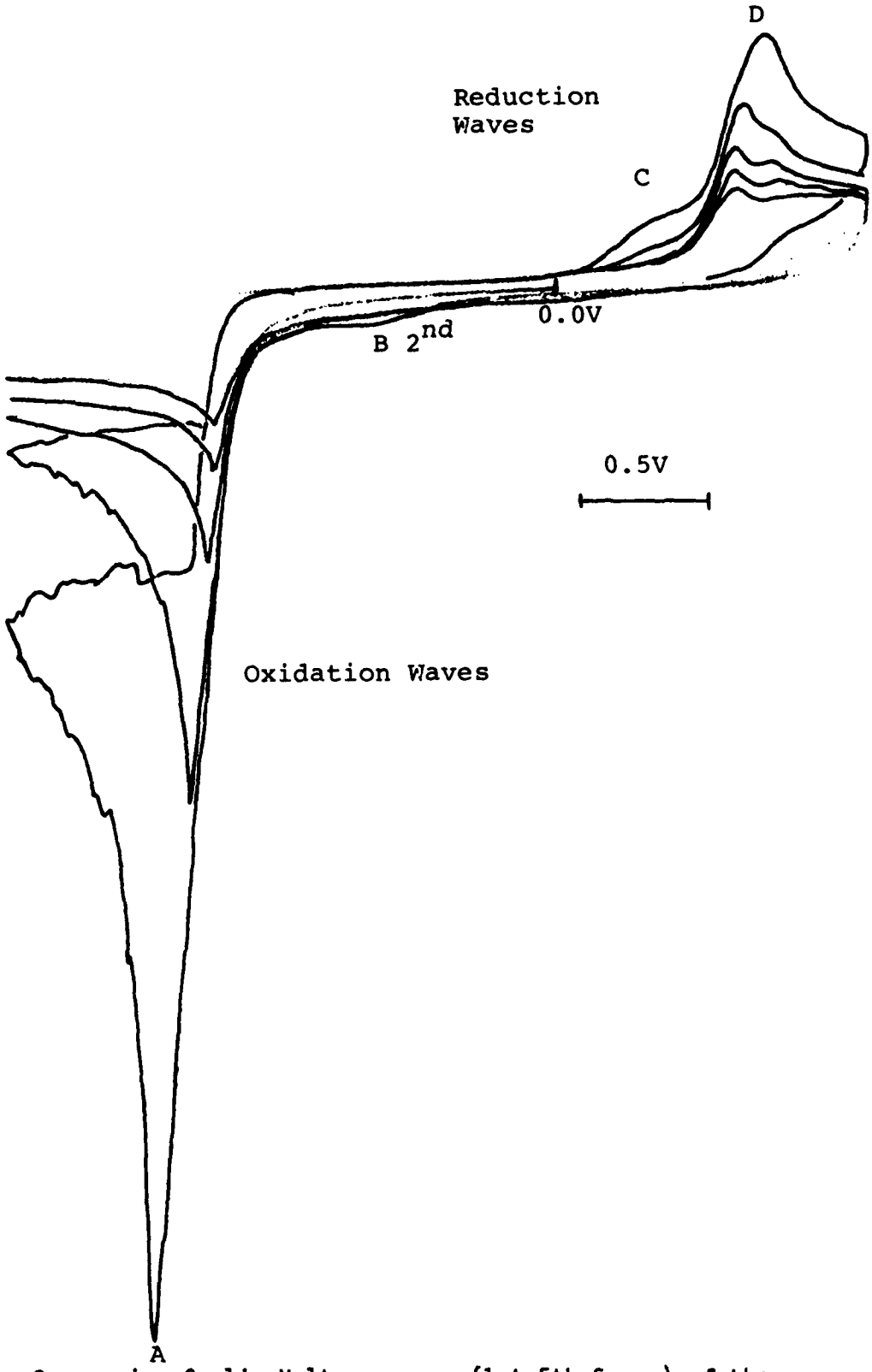

Figure 44. Successive Cyclic Voltammograms (1st-5th Scans) of the 240 Hour, 320°C, Stressed 0-67-1 Oil in Acetone Using a Glassy Carbon Working Electrode

waves in subsequent scans are not present in the fresh or stressed oils. This indicates that the oxidation waves are due to electrooxidation of lubricant impurities and not by oxidation products.

Since the species in O-67-1 oils analyzable by cyclic voltammetry do not change in concentration with increasing stressing time, this technique does not have potential as a lubricant analysis technique for polyphenyl ether based lubricating oils.

f. Summary

Corrosion and oxidation testing using Federal Test Method Standard No. 791, Method 5307.1 with modified intermediate sampling frequencies was completed for two MIL-L-23699 lubricants for extended test times up to 696 hours at a test temperature of 188°C. This testing provided long term stressed lubricants for "RULLER" development for ester base lubricants.

Corrosion and oxidation studies of the high temperature lubricant basestock (5P4E) and formulated high temperature lubricants using 5P4E have shown the following.

(1) Good temperature uniformity of the aluminum block bath was obtained for temperatures up to 350°C using D 4871 tubes and aluminum inserts using the small volume sample tubes (Squires Tubes).

(2) The use of D 4871 tubes (100 to 150 mL sample size) gives a higher degree of degradation based on viscosity change than the Squires Tubes with 30 mL samples. Changing sample size or airflow rate did not explain the difference nor did close monitoring of the test temperature.

(3) Prior thermal stressing of the formulated lubricant O-67-1 improved the oxidative stability of the lubricant.

(4) Additive A changes form in less than 24 hours at 320°C using either thermal or oxidative test conditions. The change in structure did not

affect its antioxidant capability.

(5) Lubricants O-67-1 and O-77-6 (5P4E basestock) with additive A showed good oxidative stability up to approximately 192 test hours at 320°C with no increase in TAN, insignificant corrosion and a gradually increasing rate of change in viscosity.

(6) The solubility of additive A in 5P4E is approximately 75 relative percent of the O-67-1 concentration

(7) Corrosion and oxidation stability of O-67-1 lubricant obtained from the four-ball test showed a great increase in degradation which occurred during the C&O testing at 320°C. The additive content of the oil from the four-ball wear test showed a decrease of 75%. An oven test at 250°C using 52100 balls showed no change in additive content. Thus, the exact effect of nascent wear debris on the wear test fluid is not well identified.

(8) Stressed polyphenyl ether lubricants having a 0.00 TAN (Total Acid Number) had WAN (Weak Acid Number) values up to 0.50.

(9) The optimum concentration of additive A in 5P4E was found to be near the solubility limit at room temperature.

(10) The use of Sn and SnO_2 powders having particle sizes below 5 microns did not significantly improve the oxidative stability of the uninhibited 5P4E fluid.

(11) Corrosion and Oxidation testing of O-77-6 plus additive A at 320°C without metal test specimens gave a small improvement in viscosity change compared to equivalent testing using metal test specimens.

(12) Small changes occur in the basestock composition during corrosion and oxidation testing of 5P4E fluids especially in the condenser washings.

(13) GPC analysis of oxidatively stressed PPEs indicate the formation

of higher molecular weight compounds. Fractionation of oxidized PPEs using acetonitrile and analysis by various techniques revealed a biphenyl dimer to be a main oxidation product. Other high molecular weight compounds could not be identified due to the complexity of the matrix. Quantitation of acetonitrile insolubles shows a good correlation with other physical property changes.

(14) The corrosion and oxidation stability of two specific formulated polyphenyl ethers is at least twice as good as the other polyphenyl ether fluids studied.

(15) Chemical-oxidative stressing methods (free radical trapping and hydroperoxide decomposing) and electro-oxidative stressing methods (cyclic voltammetry) are incapable of evaluating the remaining oxidation stability of 5P4E fluids.

4. ADDITIVE ANALYSIS

Additive A used in polyphenyl ethers is among a group of metal containing compounds including phenyl nitrosalicyamine adducts of nickel and cobalt[6], oxides, hydroxides and carbonates of alkali metals and barium[8], phenoxide salts of barium, strontium and potassium[10], and various tin compounds[6] that have been reported to be effective oxidation inhibitors in PPEs. The mechanism of inhibition has not been established for these compounds but has been speculated to be due to radical scavenging by the metal[6] or, in the case of the more basic metal salts, transformation of peroxy radicals to superoxides.[10] Since the efficacy of additive A as an oxidation inhibitor in PPEs was clearly established in work conducted under this contract, an investigation was made into the nature of its mechanism.

a. Gas Chromatographic Analysis of Additive A in PPE During Oxidation Testing

A procedure for quantitating additive A in PPE by gas chromatography was developed in order to follow changes in its concentration during oxidative stressing. Using an internal standard method (with diphenylphthalate), quantitation of additive A over the range of 2.5 to 250 relative percent of O-67-1 was possible. A chromatogram showing the separation of additive A is given in Figure 45. Analysis of formulated PPEs from the corrosion and oxidation test of 320°C revealed that the additive was depleted by the first sample taken (24 hours). In fact, it was found that exposing the formulated PPE in an open test tube to a circulating air oven at 320°C resulted in depletion of additive A in less than one hour. Since depletion of additive A is very rapid and the oxidation inhibition effect resulting from the formulation of this additive in the PPE extends far beyond this period, it must be concluded that additive A itself possesses no oxidation inhibition properties. Therefore, it seems likely that additive A is chemically changed into a specie or species which are the active oxidation inhibitors.

b. Tin Analysis of Oxidized Formulated PPEs by Spectrophotometry

In order to determine if the tin present in formulated PPEs changes concentration during oxidation testing, via deposition or initial evaporation of the additive atomic absorption (AA) and Atomic emission (AE) spectrophotometric analyses were made on a formulated PPE from a corrosion and oxidation test at 320°C for various intervals up to 168 hours. The AE results (Figure 46) show that after an initial drop at 24 hours, the percent tin remains fairly constant, indicating the possibility of evaporation of the additive. However, the AA results show a slight rise in the tin level

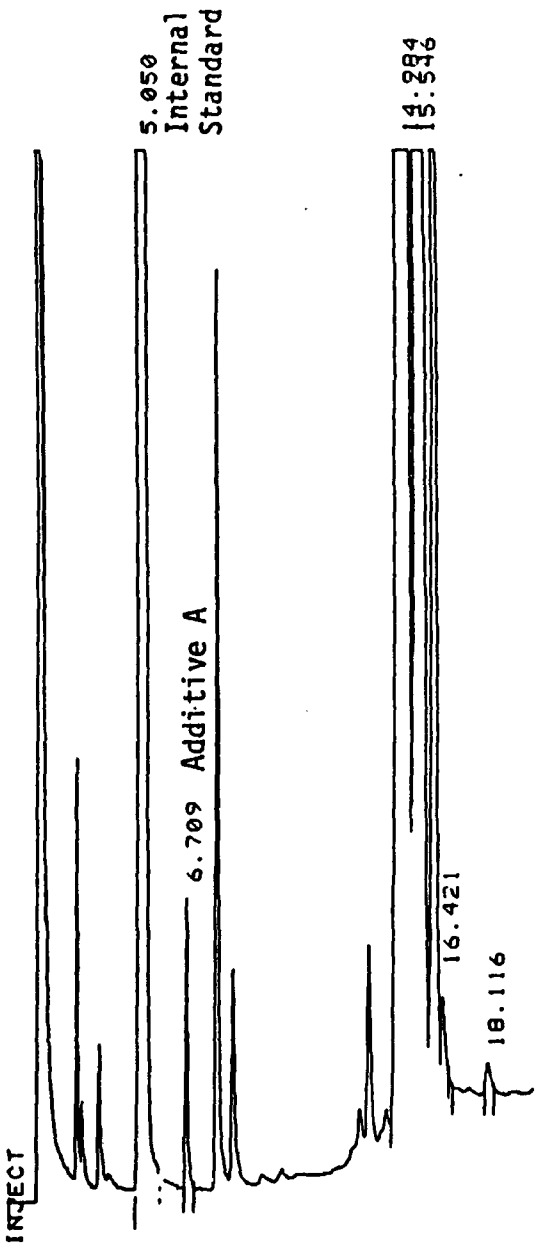

Figure 45. Gas Chromatogram of Additive A in Polyphenyl Ether

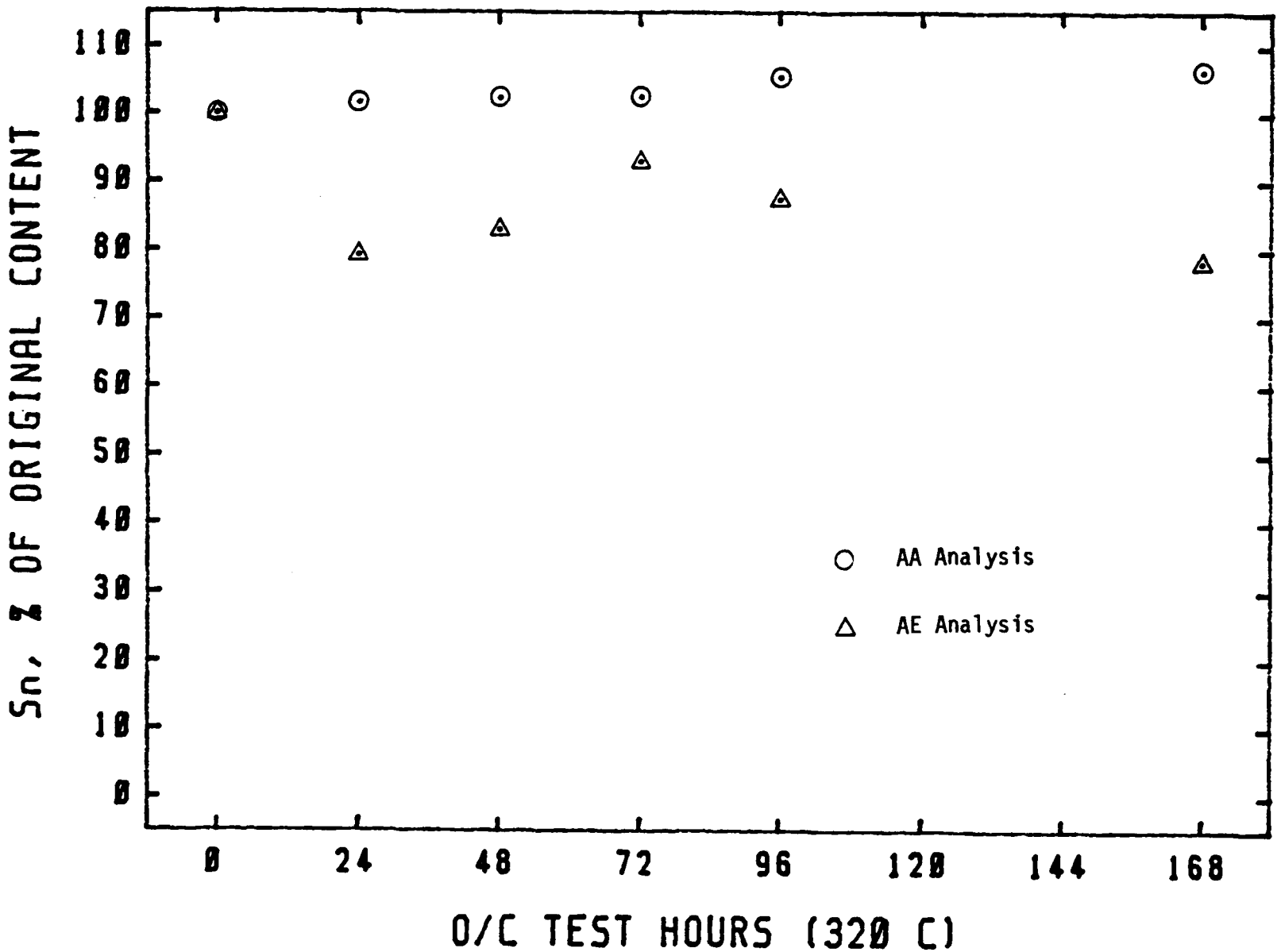

Figure 46. Tin Concentration in Formulated PPE from the Corrosion and Oxidation Test at 320°C Using AA and AE Analysis

probably due to the small evaporation of PPE components observed in this test. The difference in results between the two methods may be due to sample handling differences inherent in each technique. The AE method, which introduces the neat sample via a rotating disk electrode, may be more particle size dependent than the AA method, which aspirates an MIBK diluted oil sample. Because of these results and the fact that no additive was found in the condenser tubes, it appears that evaporative loss of additive is insignificant. Also, loss of tin by deposition is not observed.

c. Filtration of Oxidatively Stressed Formulated PPEs

Since it had been shown that additive A decomposes rapidly under oxidative conditions at 320°C, the possibility of the formation of an insoluble tin compound(s) was examined by filtration experiments. Because of the high viscosity of the PPE lubricants, it was necessary to dilute the samples in toluene (2 g diluted to 10 mL) prior to filtration and AA analysis. Thus, the diluted formulated PPEs samples from the corrosion and oxidation test at 320°C (up to 168 hours) were filtered through 0.22 micron Durapore filters (polyvinylidene difluoride) and both pre- and post-filtration samples were analyzed by AA for tin content. The results (Figure 47) show that the percent of filterable tin (i.e. particles greater than 0.22 microns) is large initially (24 hours) and decreases constantly throughout the test (note that the fresh 0 hour lubricant did not lose any tin by filtration). Also indicated in Figure 47, are the results of filtration of a second corrosion and oxidation test as well as filtration using a 0.22 micron MF-65 filter (mixed cellulose acetate and nitrate). Since the results show basically the same trend as the first filtration experiment, it would appear that the observed decrease in particle size is not test or filter media dependent. Since these results indicate that the

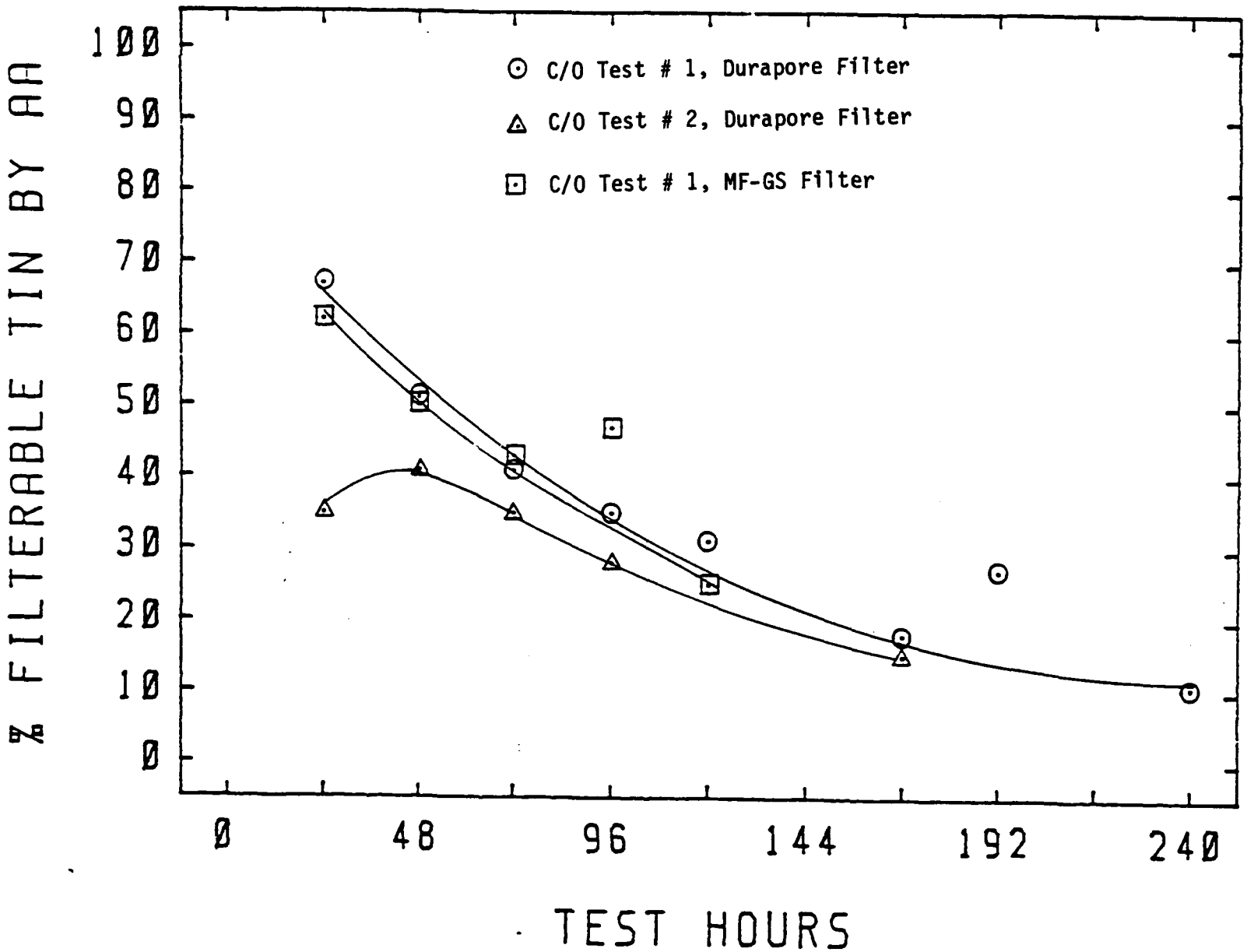

Figure 47. Percent Filterable Tin in Formulated PPE Stressed in the Corrosion and Oxidation Test at 320°C

additive is oxidatively changed into insoluble tin species, it seems likely that the mechanism of inhibition would be as a heterogenous catalyst. The significance of the decreasing particle size observed in samples from the oxidation and corrosion test is not obvious.

d. Identification of Intermediate Tin Species in Oxidatively Stressed Formulated PPEs

Since previous research indicated that the tin present in oxidatively stressed polyphenyl ethers formulated with additive A may be a chemically altered insoluble tin containing compound(s), an investigation was made to identify these species. The tin species and polyphenyl ether degradation products isolated from the stressed fluids were studied using GC, GPC, SEM/EDS, XPS, and XD analytical techniques. Also, an in situ analysis was made on a stressed PPE sample formulated with additive A using Mossbauer spectroscopy.

(1) Production of Sn Species

Due to the low concentration of Sn in the fresh and stressed O-67-1 oils (350 ppm), the isolation of the Sn species from the oils for analysis would be impractical. To obtain 0.1 g of Sn for analysis, 290 g of oil would have to be filtered. The solid material isolated from the stressed O-67-1 oils would also contain polyphenyl ether degradation products further complicating the identification of the Sn species.

To obtain suitable amounts of Sn species from the stressed polyphenyl ether fluids, O-77-6 fluids containing 1-6% of additive A were prepared. Upon heating to 200°C, the additive became completely soluble in the O-77-6 fluid. If allowed to cool back to room temperature without thermal-oxidative stressing at 305°C, the additive (identified by GC, XPS,

and XD) would recrystallize. Thus, heating to 200°C did not alter the chemical composition of the additive.

In another experiment the additive was dissolved in cumene and heated to 150°C (refluxing cumene) in the presence of cumene hydroperoxide (strong oxidizing agent) or AIBN (free radical producer). After 8 hours of refluxing the concentration of the additive (monitored by GC) was not affected. Thus, additive does not appear to possess hydroperoxide decomposing or free radical trapping capabilities at temperatures below 150°C in agreement with the HPD and FRT methods' results [Section(2)(J)].

Since the low temperature stressing was incapable of decomposing the additive, the 1 to 6% additive/O-77-6 polyphenyl ether solutions were heated for 2 to 24 hours at about 305°C in the presence and absence of air. The additive concentration in the O-77-6 fluid was monitored using GC. Once the additive was no longer detectable by the GC technique, the stressed solution was sampled at 1- to 2-hour intervals up to 24 hours. The Sn species were isolated from the stressed samples using either filtration or dilution with toluene.

(2) X-ray Diffraction (XD) Analyses

To perform the XD analyses on the additive A and isolated Sn species, the solids were ground to less than 325 mesh and pressed into pellets. The XD spectra produced by additive A, the Sn species isolated from the 3% additive A solutions stressed for 1 hour and 18 hours in air, and the Sn species isolated from the 3% solution stressed for 8 hours in argon are shown in Figure 48. Since these spectra are based upon the crystal structure of the solids and not their chemical compositions, the conclusions derived were verified by other analytical techniques (discussed in the following paragraphs).

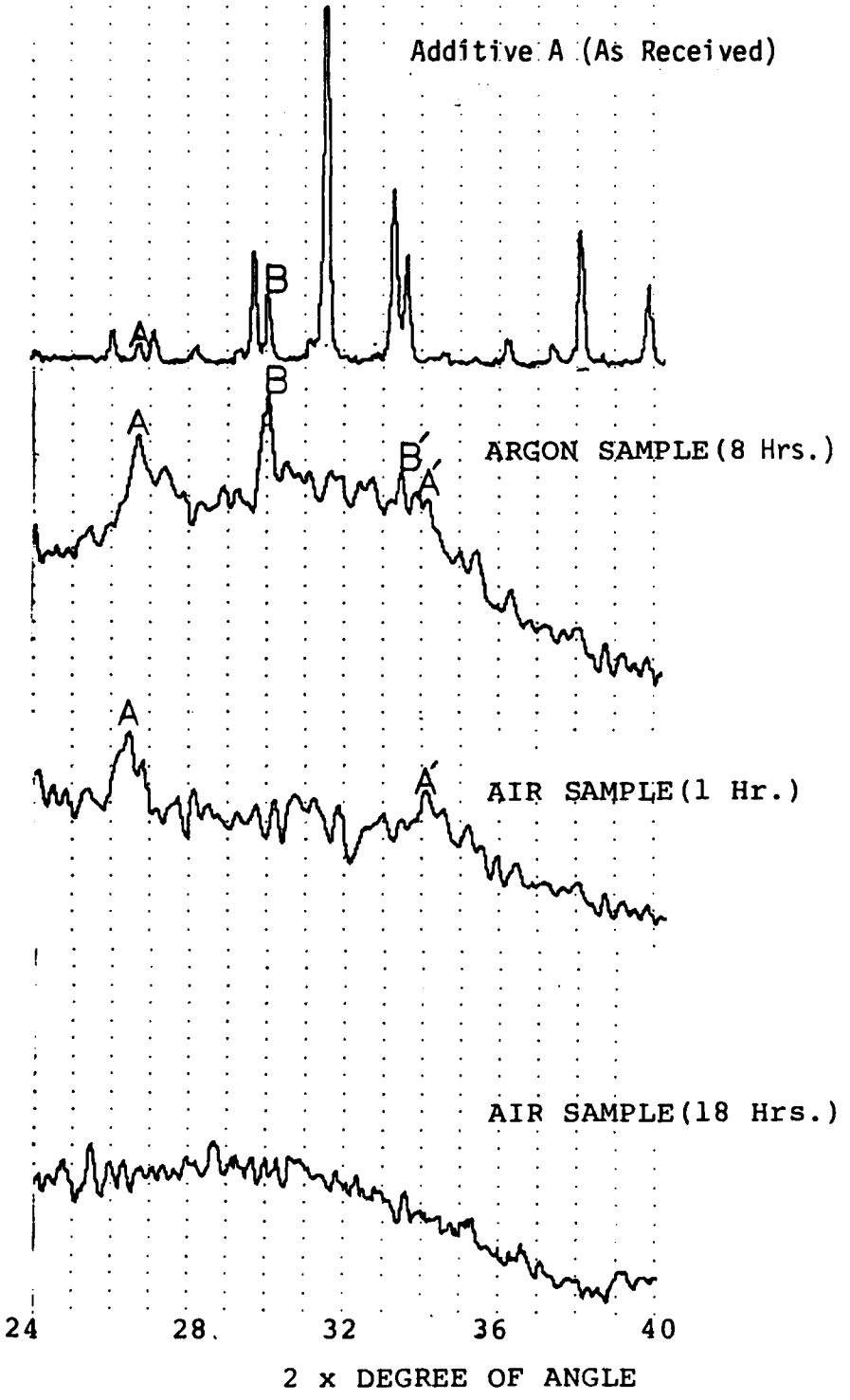

Figure 48. X-ray Diffraction Spectra Versus 2 X Degree of Angle for Additive A and the Isolated Sn Species from the 3% Additive/O-77-6 Fluid Samples Stressed at 320°C for 8 Hours in Argon, for 1 Hour in Air and 18 Hours in Air

The XD spectra in Figure 48 show that additive A is not present in the Sn species isolated from the stressed O-77-6 fluids (shown by GC). The broadness of the spectra produced by the Sn species isolated from the stressed samples is a result of the 1000 angstrom (0.1 micron) particle size (verified by SEM) of the isolated solids. For every series of stressed additive (1-6%)/O-77-6 solution (air or argon stressing atmosphere), the spectra produced by the isolated Sn species did not match the spectrum of additive A and the peaks of the Sn species were broad and decreasing in intensity with stressing time.

The peaks labeled A in the spectra of the 1 hour (air) and 8 hour (argon) samples match the primary peak of SnO_2. The spectrum of the 8 hour sample also contains a peak (B) which matches the primary peak of SnO. However, the corresponding secondary (60% intensity of primary) peaks (A' and B') for SnO_2 and SnO are less definite due to the noise level of the spectra. The spectrum of additive A also contains minor peaks which match the primary peaks of SnO_2 and SnO. The lack of detectable peaks in the spectrum of the 18 hour sample may be a result of the tin oxides' crystal structures being altered through reactions with the polyphenyl ether degradation products. However, the lack of detectable peaks in the spectrum of the 18 hour sample is more likely due to the increased concentration of polyphenyl ether degradation products in the 18 hour sample in comparison to the 1 hour sample (verified by XPS).

Thus, the initial XD results indicate that additive A is thermally (argon) degraded or oxidized (air) in polyphenyl ether at 305°C to form Sn oxide species with particle sizes of approximately 1000 A. The XD results also demonstrate that the Sn oxide species produced from the additive A are present as contaminants in the additive (A.C.S. Certified Grade) which

was added to the O-77-6 fluid.

(3) Thermogravimetric Analyses

To study the thermal and thermal oxidative stabilities of the tin species isolated from the stressed O-77-6 fluids, thermogravimetric analyses were performed on the isolated solids in nitrogen and air, respectively. The thermograms in Figure 49 are representative of the thermograms produced by the thermogravimetric analyses of the Sn species isolated from the different O-77-6 fluids stressed in air. The Sn species were thermally stable (less than 2% weight loss) up to 400°C and underwent a slow rate of weight loss when heated to 700°C. In contrast to the thermal stabilities, the isolated Sn species were oxidatively stable up to 200°C and underwent a rapid weight loss at 400°C. Above 400°C the Sn species heated in air did not undergo further weight loss up to 700°C. Whether heated in nitrogen or air, the Sn species underwent total weight losses of 15-25% to produce SnO_2.

For comparison to the Sn species, thermogravimetric analyses of O-77-6 fluid and O-67-1 oil were performed in nitrogen and are shown in Figure 50. The results demonstrate that the presence of additive A may inhibit the formation of thermal degradation polymers which undergo a weight loss at 500°C in the O-67-1 thermogram.

Thus, the initial thermogravimetric analytical results indicate that the Sn species isolated from thermally or oxidatively stressed 3% additive A in O-77-6 are approximately 75-85% SnO_2, are thermally stable at stressing temperatures below 400°C and are readily oxidized at stressing temperatures above 320°C. Thermograms produced by the O-77-6 fluid and O-67-1 oil show that the composition of the organics present with the isolated Sn species are most likely high molecular weight PPE oxidation

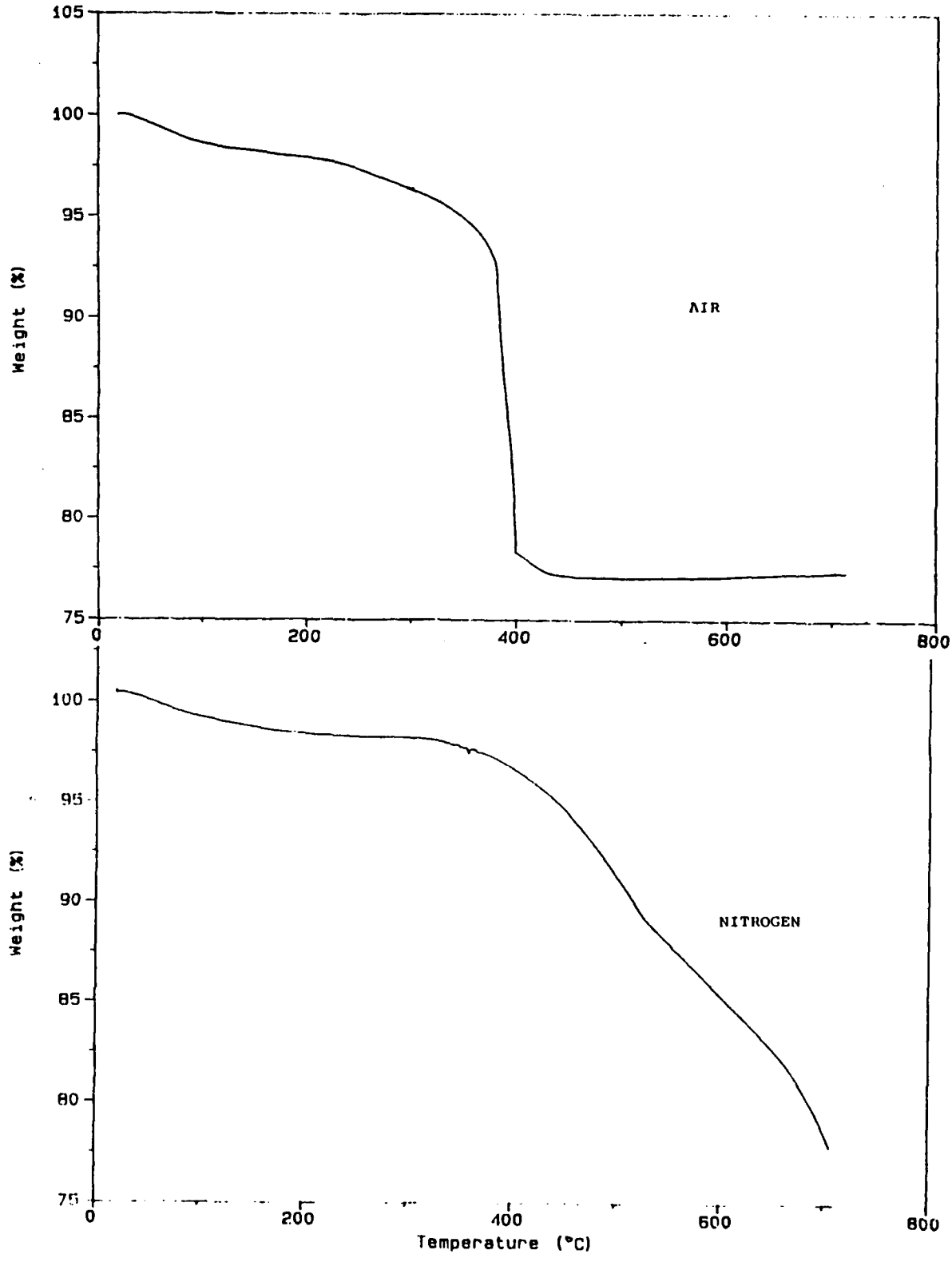

Figure 49. Thermogravimetric Analysis of the Isolated Sn Species from 3% Additive A/O-77-6 Stressed in Air (20°C/minute)

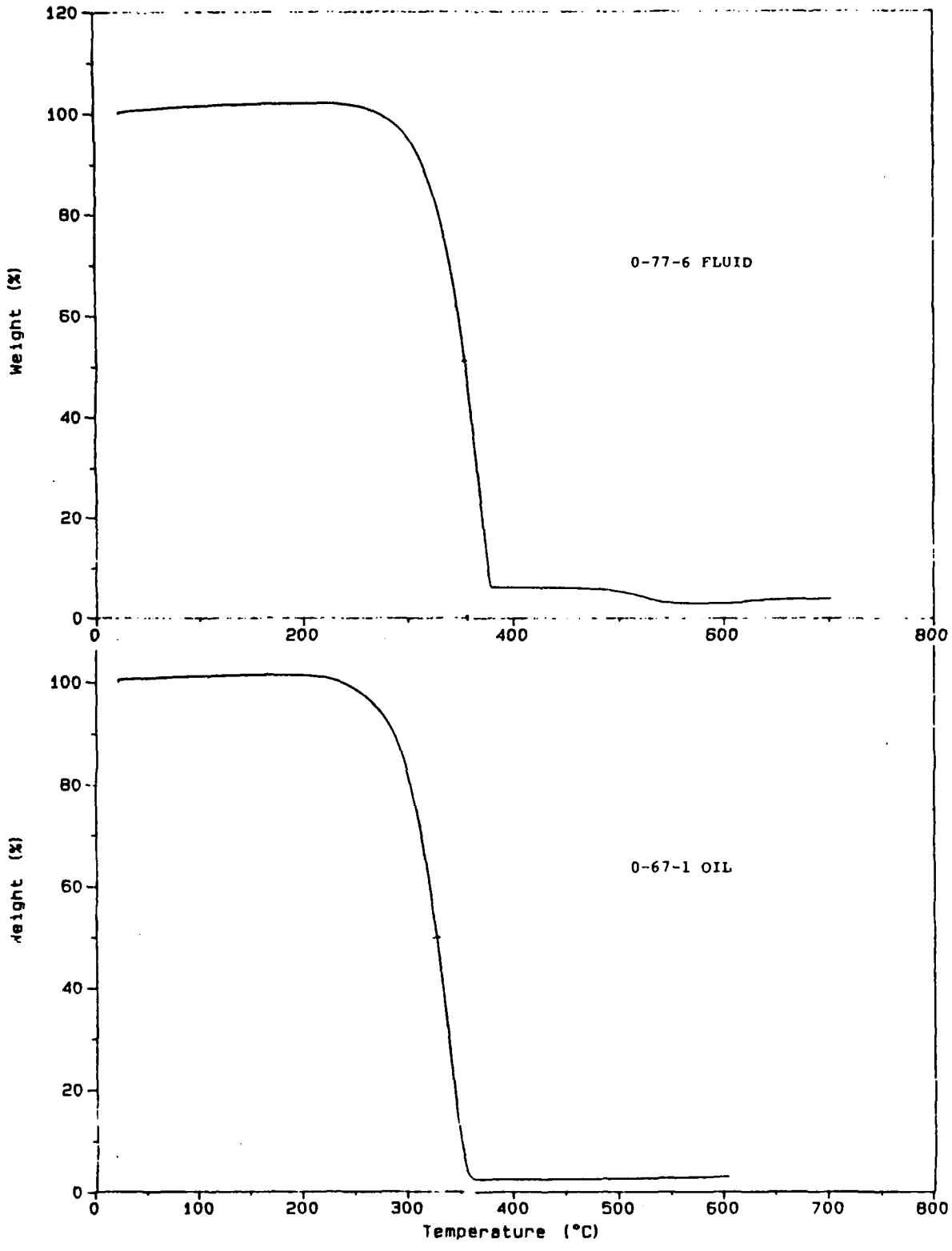

Figure 50. Thermogravimetric Analysis of Fresh 0-77-6 and 0-67-1 Fluids (20^{o}C/min in Nitrogen)

products since the thermograms from these isolated species do not experience weight loss (in nitrogen) below 400°C and the two fluids undergo rapid evaporation between 300 and 400°C.

(4) Infrared Spectroscopic Analyses

The Sn species were then analyzed (KBr pellets) by infrared spectroscopy to better characterize the organic component of the Sn species. The infrared spectrum (400-2000 cm^{-1}; no peaks detectable above 2000 cm^{-1}) of the Sn species presented in Figure 51 is representative of the spectra produced by the Sn species isolated from the different stressed 0-77-6 fluids. The infrared spectra of 5P4E and SnO_2 are included in Figure 51 for reference. The infrared spectrum of the Sn species contains peaks which are similar to those present in the spectra of SnO_2 and 5P4E.

If the Sn species isolated from the stressed 0-77-6 fluids were washed repeatedly with THF until the THF washings were colorless, the remaining solid produced an infrared spectrum (Figure 52) which was slightly different from the spectrum in Figure 51. In addition to the peaks present in Figure 51, the THF washed Sn species had a broad peak centered at 1730 cm^{-1} which was indicative of a carbonyl group. The infrared spectra of the solids precipitated from the stressed 0-67-1 oils with the RULLER solvent also had a peak centered at 1740 cm^{-1} but did not contain the SnO_2 peak centered at 550 cm^{-1}. The GPC and XPS analyses of the RULLER solvent precipitated solids indicated that the solids were high molecular weight, oxidized polymers (MW = 2000 - 4000) of polyphenyl ether containing less than 1% Sn.

Thus, the infrared spectroscopic analyses indicate that the Sn species contain SnO_2 and organic species similar to 5P4E. The fact that the Sn species produce spectra with and without carbonyl groups indicates that

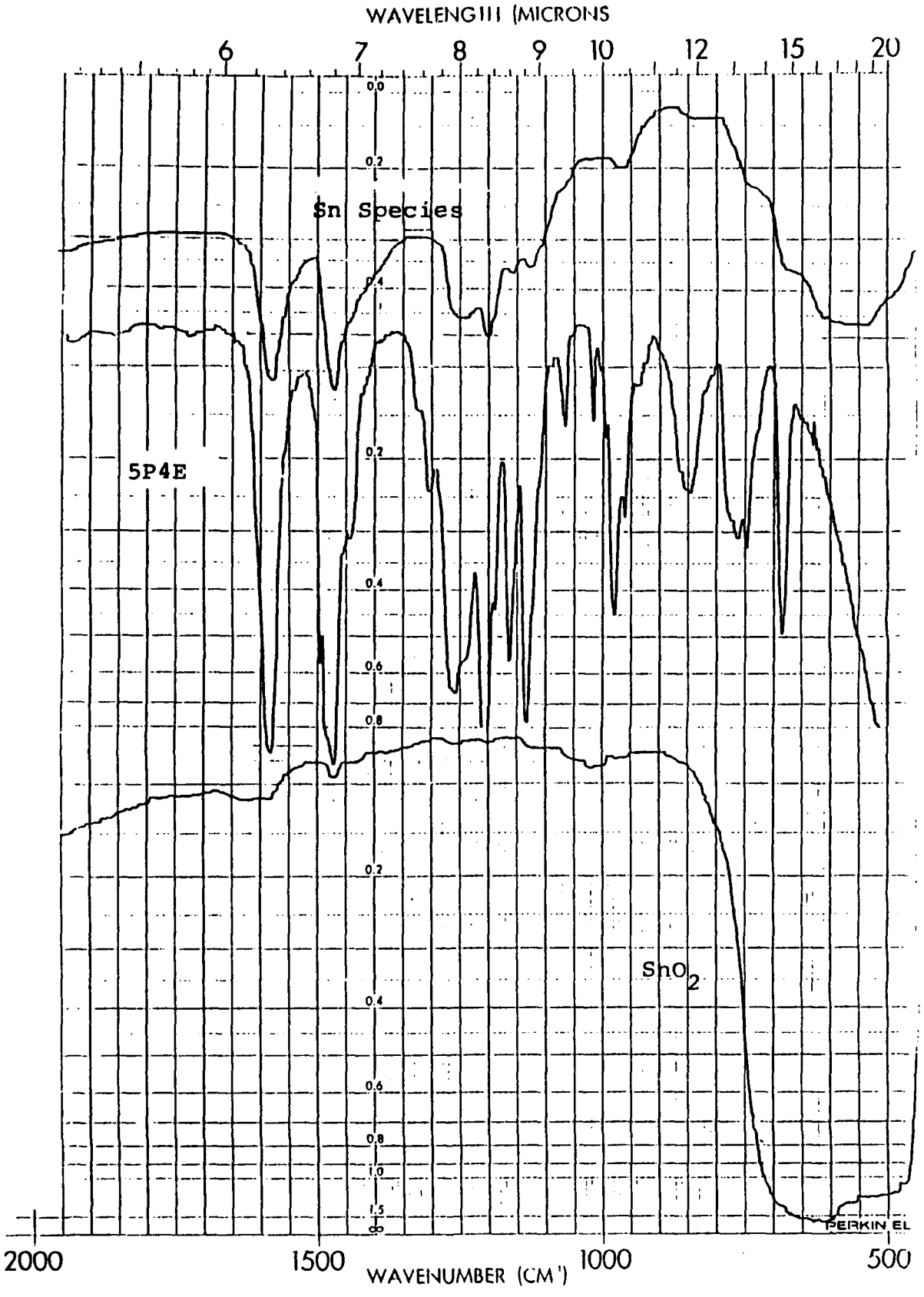

Figure 51. Infrared Spectra of the Isolated Sn Species from 3% Additive A in 0-77-6 Stressed 18 Hours at 320°C in Air, 5P4E Polyphenyl Ether (0-77-6) and SnO_2

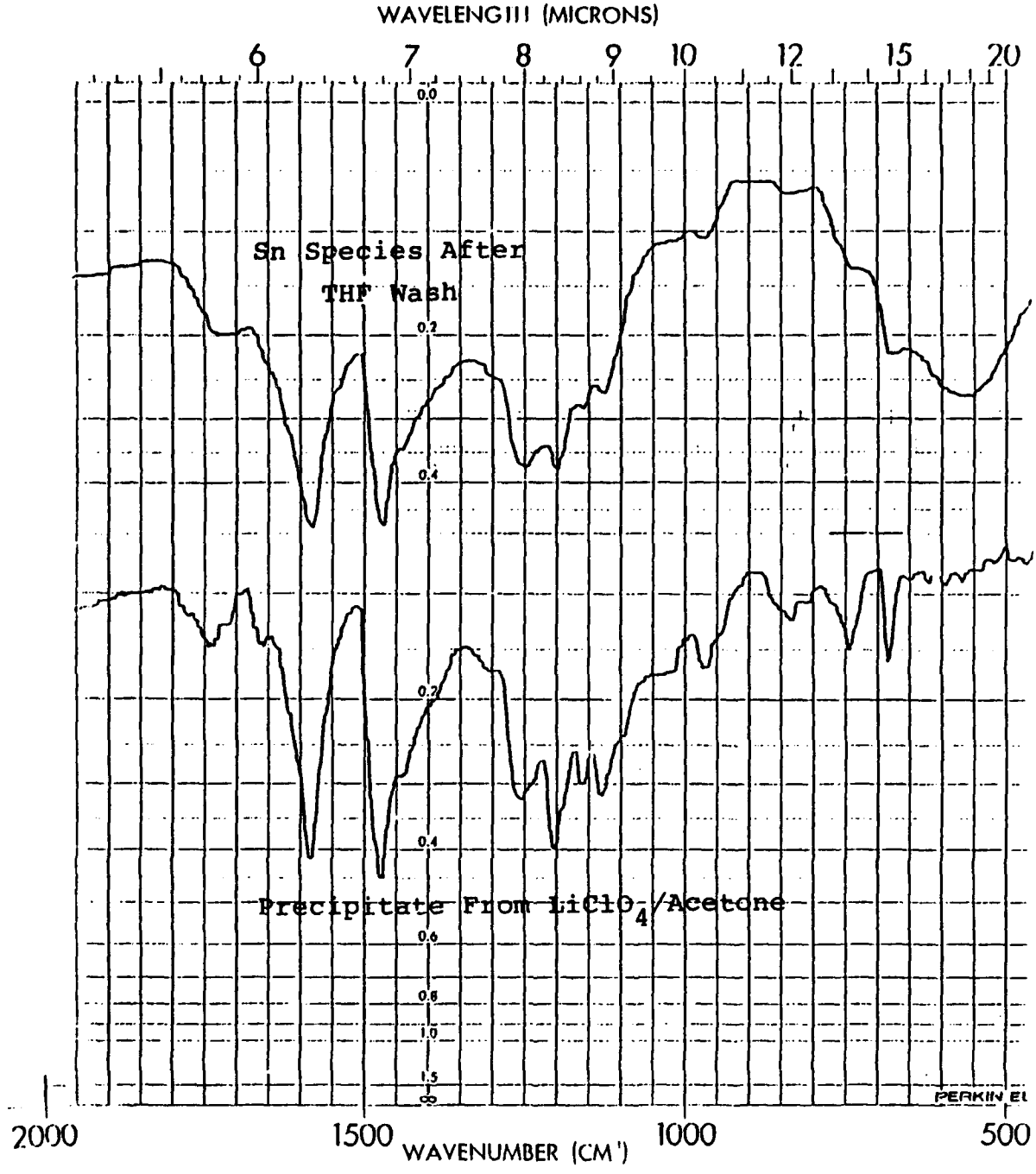

Figure 52. Infrared Spectra of the Isolated Sn Species from 3% Additive A in 0-77-6 Stressed 18 Hours at 320°C in Air After Repeated THF Washings (Top) and the Precipitate Produced by Diluting the 120 Hour Stressed 0-67-1 Oil Sample with the $LiClO_4$/Acetone Solution (Bottom)

the Sn species contain polymers that have been oxidized to differing degrees, i.e., presence of carbonyl group indicative of severe oxidation since phenyl ring opening is required for formation of carbonyl.

(5) X-ray Photoelectron Spectrometric Technique

As a final characterization of the Sn species, the isolated solids were analyzed (evaporated films) by the XPS technique. For reference SnO_2 and additive A were also analyzed (evaporated film and dry powders). Due to conductivity differences among the different compounds analyzed by XPS, the measurements listed in Table 34 were referenced to the C 1s line (literature 285.0 eV) for comparing the additive and Sn species and were referenced to the O 1s (O=) line (literature 531.2 eV) for comparing the SnO_2 and Sn species. The hydrogen content of the Sn species cannot be determined by XPS, and consequently, were not included.

The first compound studied using XPS was additive A. The binding energy of the Sn $3d_{5/2}$ orbital determined by XPS for this material can be dependent upon the sample preparation technique. Techniques involving vapor deposition or recrystallization of the additive A prior to XPS analysis lower the determined binding energies. As seen in Table 35, the binding energy of the Sn $3d_{5/2}$ orbital is lowered by recrystallization of the additive prior to XPS analysis. The atomic formula determined for the additive by XPS analysis indicates that the material as received contains oxygen, most likely in the form of SnO and SnO_2. Evidence for SnO and SnO_2 in additive A is given by XD spectrum in Figure 48 and that the O content of the additive decreases upon recrystallization. In addition to the decrease in O content upon recrystallization, the carbon content of the additive as determined by XPS is increased dramatically by recrystallization.

The XPS results (20 A depth), in Table 35 indicate that the

TABLE 35

CORRECTED SN $3d_{5/2}$ BINDING ENERGIES AND ATOMIC FORMULA DERIVED FROM XPS ANALYSES OF SN CONTAINING COMPOUNDS

Compound	Sn $3d_{5/2}$ Binding Energy (eV)	Atomic Formula	
Additive A			
Powder (as received)	486.1[a]	$SnC_{18.9}O_{2.3}$	
Recrystallized and Mounted in Dry Box	485.7	$SnC_{44}O_{0.4}$	
SnO_2			
Powder (as received)	486.9[b]	$SnO_{1.74} \cdot C_{0.7}O_{1.0}$	
Dried Film[c]	486.9	$SnO_{2.0} \cdot C_{1.2}O_{0.8}$	
Dried Film[d]	486.8	$SnO_{2.0} \cdot C_{2.0}O_{1.1}$	
		($SnO_2 \cdot H_2O$: Theoretical)	
Sn Species			
0-77-6 Plus Additive A Stressed in Air			
1 h[c]	486.9[b]	$SnO_{2.0} \cdot C_{7.1}O_{1.0}$	$(SnO_{2.0})_{4.2} \cdot O_{0.2}$ 5P4E[e]
18 h[c]	486.7	$SnO_{2.1} \cdot C_{13.3}O_{2.1}$	$(SnO_{2.1})_{2.3}O_{0.7}$ 5P4E
18 h[e]	486.8	$SnO_{2.4} \cdot C_{23.1}O_{3.8}$	$(SnO_{2.4})_{1.3}O_{0.9}$ 5P4E

TABLE 35 (CONCLUDED)

CORRECTED SN $3d_{5/2}$ BINDING ENERGIES AND ATOMIC FORMULA DERIVED FROM XPS ANALYSES OF SN CONTAINING COMPOUNDS

Compound	Sn $3d_{5/2}$ Binding Energy (eV)	Atomic Formula	
O-77-6 Pluss Additive A Stressed in Argon			
8 h[c]	487.2[b]	$SnO_{1.7} \cdot C_{8.7}O_{1.4}$	$(SnO_{1.7})_{3.4}O_{0.8}$ 5P4E
8 h[d]	487.0	$SnO_{1.9} \cdot C_{9.0}O_{1.4}$	$(SnO_{1.9})_{3.3}O_{0.6}$ 5P4E
Filtered from O-67-1 Oil Stressed 120 h	486.7	$SnC_{87.7}O_{22.4}$	$Sn_{0.34}O_{3.7}$ 5P4E

[a]Corrected based on C 1s line = 285.0 eV

[b]Corrected based on O 1s (O =) line = 531.2 eV

[c]From toluene

[d]From THF

[e]Assumption: Organic Component Based on 5P4E

surface of the additive particles are coated with a thin layer of Sn oxides. The XD spectrum indicates that the additive as received contains a small amount of Sn oxides. Recrystallization removes the Sn oxide coating of the particles decreasing the O and increasing the C determination of the XPS analyses. Thus, the binding energy of 485.7 eV is assigned to the $3d_{5/2}$ orbital which was assigned to additive A. The fact that the XPS carbon determination is high for additive A cannot be explained at this time. No elemental analyses of additive A performed by XPS have been reported to date.

To determine if the XPS analyses could detect differences in the Sn $3d_{5/2}$ binding energies of additive A and SnO_2, SnO_2 powder was analyzed by XPS. In contrast to the 485.7 eV binding energy assigned to additive A, the binding energy of the SnO_2 was determined to be 486.9 eV by XPS. With the exception of the detected C, the elemental analyses of the SnO_2 performed by XPS are in full agreement with the theoretical values for SnO_2. If the SnO_2 was suspended in toluene or THF prior to the XPS analysis, the binding energies and elemental analyses remained unchanged but the carbon content determined by XPS increased in respect to the untreated SnO_2 powder. These results indicate that organic compounds are being extracted from the solvents onto the surfaces of the SnO_2 particles, especially for the strong solvent THF.

The results in Table 35 indicate that XPS analyses are able to distinguish additive A and SnO_2 compounds by Sn $3d_{5/2}$ binding energy differences and by elemental analysis differences. The Sn species isolated from the 1 and 18 hour stressed (air) samples of O-77-6 fluid (plus Additive A) were analyzed by XPS as films dried from toluene (Figure 53) for determining its chemical nature.

The Sn $3d_{5/2}$ binding energies listed in Table 35 for the 1 and

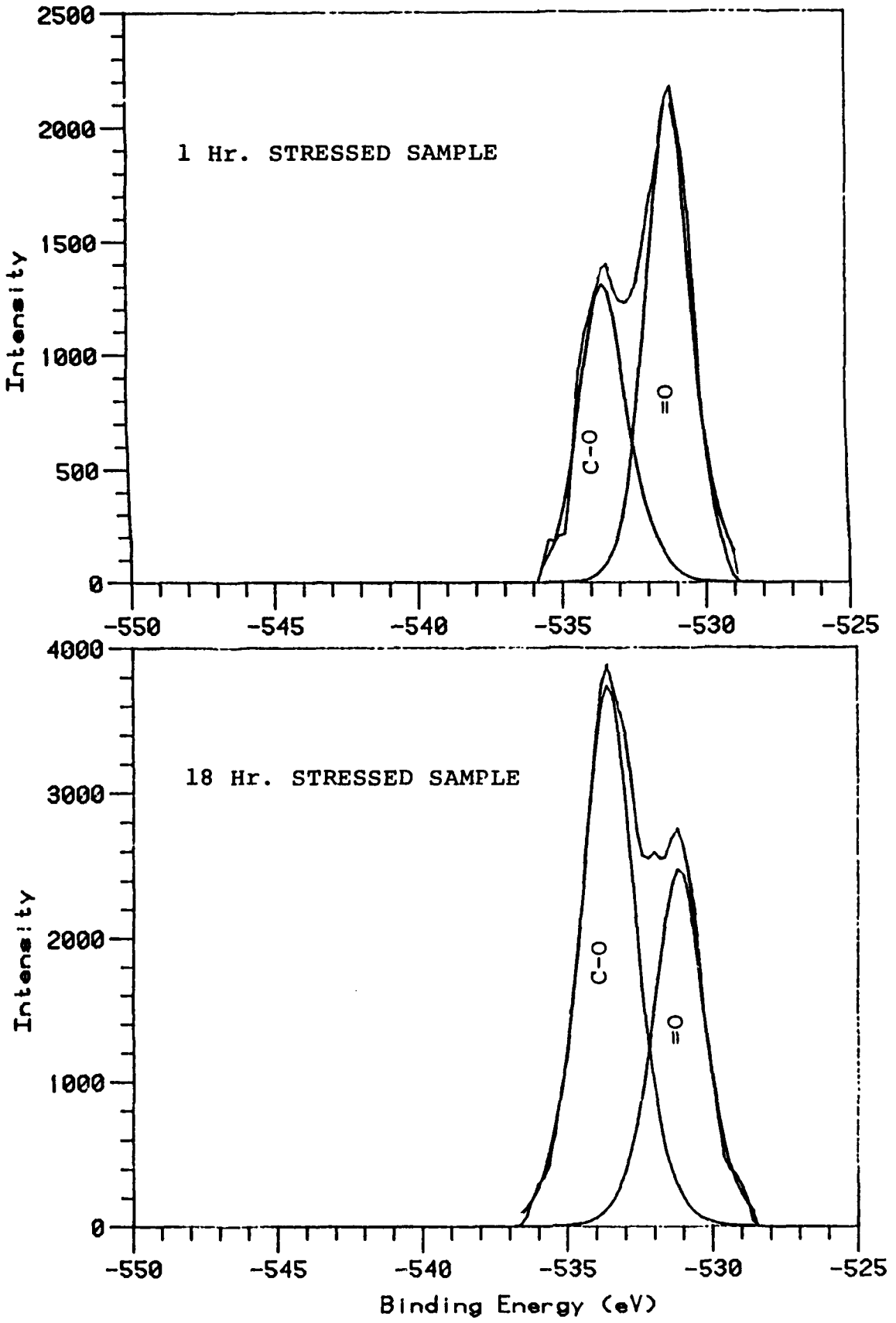

Figure 53. Oxygen 1s XPS Spectra of the Isolated Sn Species from Additive A in O-77-6 Stressed for 1 and 18 Hours in Air at 320°C

18 hour stressed O-77-6 samples are 486.9 and 486.7 eV, respectively, and are in agreement with the binding energy assigned to SnO_2. The XPS analyses detected two types of O in the Sn species. The O binding energy of 533.5 eV is assigned to a single bonded oxygen (-O, ether linkage) and the binding energy of 531.2 eV is assigned to a double bonded oxygen (=O, SnO_2). The data in Table 35 for the 1 and 18 hour stressed O-77-6 samples shows that the ratio of Sn to O is 1:2 also indicating the Sn in the isolated solid is SnO_2. Thus, the stressing time does not appear to have an effect on the chemical nature of the Sn present in the isolated solids.

In contrast to the chemical nature of the Sn, the elemental analyses and the ratio of =O to -O for the solids isolated from the 1 and 18 hour stressed O-77-6 plus additive A samples change dramatically with stressing time. As the stressing time increases from 1 to 18 hours the amount of carbon and -O in the isolated solid increase in respect to the amount of SnO_2 in the isolated solid. Assuming that the carbon and -O are from 5P4E segments, the ratio of SnO_2 to 5P4E decreases from 4.2 to 2.3 with increasing stressing time. Also, the amount of extra oxygen (extra oxygen = total single bonded oxygen - single bonded oxygen associated with 5P4E) increases from 0.2 to 0.7 per 5P4E segment as the stress time increases from 1 to 18 hours.

Since THF washings affected the infrared spectra of the isolated Sn species, XPS analysis of the solid remaining after repeated THF washings of the Sn species isolated from the 18 hour stressed O-77-6 plus additive A samples was performed. Although the Sn $3d_{5/2}$ binding energy of the Sn species was not affected by the THF washings, the ratio of SnO_2 to 5P4E was decreased from 2.3 to 1.3 and the amount of extra oxygen per 5P4E segment was increased slightly from 0.7 to 0.9 by the THF washings. The THF washings

also increased the =O to Sn ratio from 2.1 to 2.4 for the Sn species.

Thus, these results indicate that the Sn in the solids isolated from the stressed O-77-6 fluids is present as SnO_2 and that the amount of oxidized (extra oxygen) 5P4E associated with the SnO_2 increases with stressing time. The THF washings demonstrated that the Sn species isolated from the 18 hour O-77-6 fluid contains 5P4E polymers that have been oxidized to differing degrees (in agreement with infrared spectroscopy results). The increase in the =O to Sn is most likely the result of inaccurate peak stripping of the O 1s peaks causing oxygen not associated with the Sn to be assigned to the Sn by the XPS analysis.

The isolated solid from the 8 hour stressed sample was analyzed by XPS as a film dried from toluene for determining the chemical nature of the Sn species produced by stressing the O-77-6 fluid containing additive A in the absence of air (argon atmosphere). The Sn $3d_{5/2}$ binding energy is 487.2 eV which is 0.3 eV higher than the binding energy assigned to SnO_2 (Table 35). Also the ratio of Sn to =O is 1 to 1.7 which is below the 1 to 2 ratio expected for SnO_2. Thus, these results indicate that the Sn in the solid isolated from the argon stressed O-77-6 fluid is a mixture of SnO_2 and another O containing Sn species, most likely SnO (XD spectrum indicated presence of SnO_2 and SnO).

One surprising result for the Sn species isolated from the O-77-6 fluid stressed in argon is the high amount of extra oxygen per 5P4E segment. Since the O-77-6 fluid was stressed in the absence of air, the presence of oxygenated polymers of 5P4E is unlikely. Also, when the extra oxygen is added to the oxygen associated with Sn, the Sn to =O ratio becomes 1 to 2 as expected for SnO_2. Further, when the isolated solid of the 8 hour O-77-6 sample in argon was washed with THF, the Sn $3d_{5/2}$ binding energy

decreased slightly but the SnO_x to 5P4E ratio remained constant. The washing with THF also increased the =O associated with the Sn [same as 18 hour in air sample (Table 35)] and decreased the extra oxygen per 5P4E segment.

Thus, these results indicate that the Sn in the solid isolated from the O-77-6 fluid stressed in argon is present as a mixture of SnO_2, SnO, and possibly, other O containing Sn compounds. The THF washings demonstrated that the isolated solid is one main composition (compound or mixture) with a ratio of Sn to 5P4E of 3.3 to 1. The extra oxygen in the elemental analysis in Table 35 is most likely associated with the Sn and not the 5P4E. The XD spectrum of the Sn species from the argon stressed O-77-6 fluid also indicated the presence of SnO_2 and another compound tentatively identified as SnO.

The Sn species filtered from the 120 hour sample was analyzed by XPS for determining if the Sn species filtered from the stressed O-67-1 oil were similar to those isolated from the stressed 1-6% additive A/O-77-6 fluids. The Sn $3d_{5/2}$ binding energy determined for the filtered Sn species is the same as the binding energy of the Sn species isolated from the 18 hour stressed O-77-6 fluid. Due to the high carbon to Sn ratio, 87 to 1, and oxygen to Sn ratio, 22 to 1, the double bonded oxygen associated with the Sn could not be stripped from the O 1s peaks shown in Figure 54. However, if the Sn is assumed to be SnO_2 from its Sn $3d_{5/2}$ binding energy, the number of extra oxygen atoms per 5P4E segment is 3 indicative of highly oxidized 5P4E polymers. Due to the small amount of solid isolated on the filter, THF washings of the solid could not be performed. The RULLER solvent produced precipitate isolated from the 120 hour O-67-1 sample gave a Sn to 5P4E ratio of 0.3 to 1, an extra oxygen to 5P4E ratio of 2.5 to 1, and a Sn $3d_{5/2}$ binding energy of 486.6 eV all in agreement with the filtered sample.

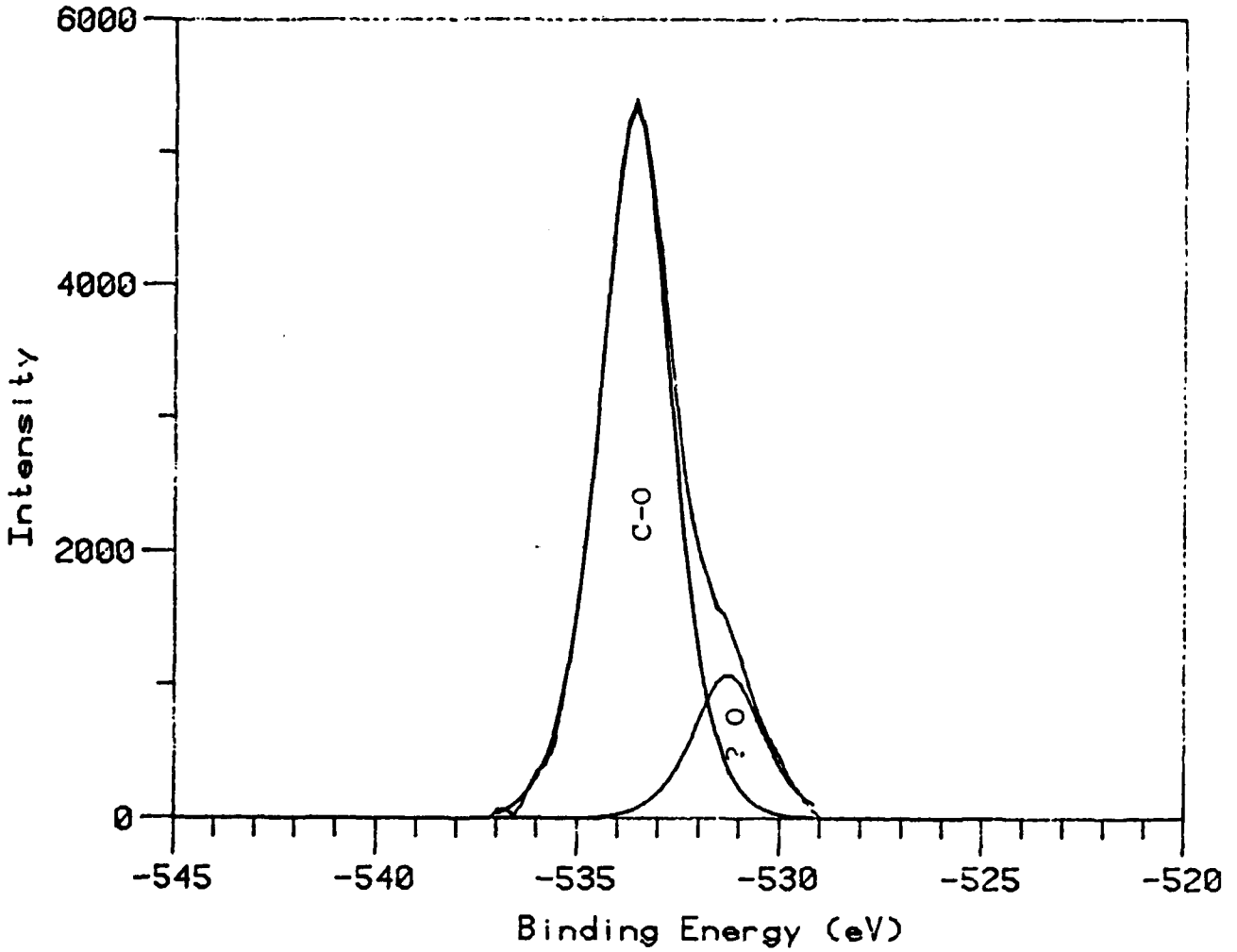

Figure 54. Oxygen 1s XPS Spectrum of Solid Filtered from O-67-1 Stressed 120 Hours in the Corrosion and Oxidation Test at 320°C

Thus, these results indicate the Sn is present as SnO_2 in the stressed O-67-1 oils and that the amount of oxidized 5P4E polymers associated with the SnO_2 is much higher than for the stressed O-77-6 fluids. The higher 5P4E to SnO_2 ratio in the stressed O-67-1 oils than in the stressed O-77-6 plus additive A fluids was expected since the additive is present in a lower concentration in the O-67-1 oil.

(6) Mossbauer Analysis

Since Mossbauer Spectroscopy is an analytical technique capable of determining the valence state and bonding ligands on tin (as well as other metals), an oxidized polyphenyl ether (O-67-1, corrosion and oxidation test at 320°C, 24 hours) was sent to the University of North Carolina at Asheville (UNCA) for such an analysis. Because of the great sensitivity of this technique, it is possible to analyze the active tin containing compound(s) in the lubricant without the need for isolation or preconcentration. As shown in Figure 55, an adequate spectrum could be obtained on this sample despite the small amount of tin present in the lubricant. Because the Mossbauer spectra showed no change in the absorption maxima relative to that of the $BaSnO_3$ source (i.e. doppler shift = 0), this was interpreted to mean that all of the tin in the stressed PPE existed as SnO_2. The fact that tin oxide would eventually form from additive A is not surprising since it is the most oxidatively stable form of tin. But the results here indicate that the oxide forms very quickly and would appear to be the only tin species in the lubricant capable of acting as an inhibitor. Analysis of a series of oxidatively stressed samples would be needed to determine if this remains true throughout the life of the lubricant.

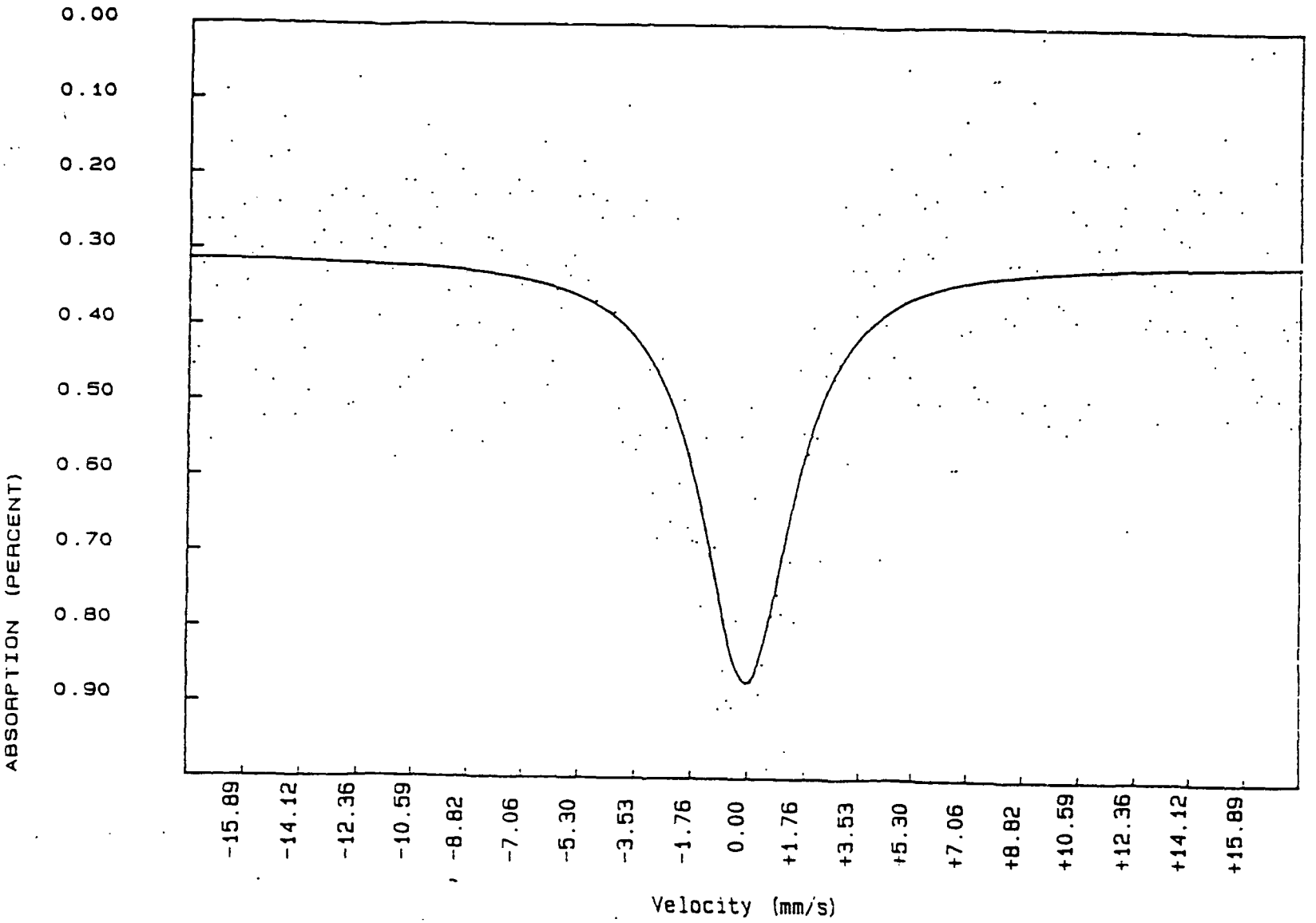

Figure 55. Mossbauer Spectra of O-67-1 Stressed in the Corrosion and Oxidation Test at 320°C for 24 Hours

(7) Summary

All of the analytical techniques used in this study indicate that the thermal-oxidation product of additive A in polyphenyl ether lubricant O-67-1 is SnO_2. The tin species isolated from oxidatively stressed PPEs formulated with various concentrations of additive A was shown to be SnO_2 in particle sizes below 1000 angstroms along with high molecular weight oxidation products of the polyphenyl ether. The XD spectra show that in the early stages of oxidation the crystal structure of the SnO_2 particles is unaffected by the presence of the polyphenyl ether oxygenated polymers. Due to the broadness of the peaks and the high noise level of the background, the XD spectra gave inconclusive results on the crystal structure of the SnO_2 in the later stages of thermal-oxidation.

The thermogravimetric analyses of the SnO_2 particles showed that the polymers associated with the particles were thermally stable up to 400°C and were only oxidatively stable up to 200°C undergoing rapid oxidation at 400°C. Finally, Mossbauer spectroscopy analysis for tin in O-67-1 PPE lubricant stressed 24 hours in the corrosion and oxidation test at 320°C confirmed that SnO_2 was the only Sn species present in the sample.

5. LUBRICANT DEPOSITION STUDIES

a. AFAPL Static Coker Study

(1) Introduction

Many requirements must be met by a lubricant for satisfactory performance in turbine engines. This performance has generally been obtained through upgrading of specification requirements which resulted in lubricant formulations with improved performance characteristics and through engine designs which have reduced the severity of lubricant stressing. However, with increased emphasis on higher engine performance resulting in smaller oil

capacities and higher operating temperatures, the need for defining and measuring lubricant properties continues. Lubricant deposition has been and is continuing to be an extremely important lubricant property. A variety of tests have been developed for measuring and describing lubricant deposition.[1] These tests have provided information relative to deposit formation and have been used for measuring deposition characteristics of ester type lubricants. Since test parameters are quite varied, correlation among tests and with actual engine performance is marginal. Most of these tests require large sample volumes and are time consuming and expensive.

The initial effort involving the static coker[11] was directed toward developing a small volume, short time test which would permit good control over test variables and provide for determining weight of deposits along with deposit description. The effort of Phase 1 of this study describes further development of the static coker and its use for investigating the effects of test specimen material, test temperatures, lubricant prestressing, ester volatility, antioxidants and wear debris on lubricant deposition.[1]

The effort of Phase 2 described herein continued with the investigation of the effects of test specimen material, lubricant prestressing and the effects of wear debris on various type lubricants. Investigations relative to coking deposits as a function of test time and temperature along with deposit solubility were conducted. Limited testing of new and stressed polyphenyl ether fluids was conducted using the normal and a modified design of the AFAPL Static Coker.

(2) Apparatus and Procedure

The apparatus and procedure used for the major portion of the Phase 2 study involving ester base lubricants and test temperatures of 315°C

and below has been previously described.[1] Some of the testing conducted on the high temperature polyphenyl ether (5P4E) involved using a stainless steel seal in place of the polytetrafluoroethylene (PTFE) seal and modified measurements described under Section (4).

(3) Test Lubricants

Lubricants and fluids used in Phase 2 of this study are described in Table 36.

(4) Results and Discussion

(a) Coking Study of Correlation Lubricant OP-369

Coking tests were conducted on correlation test lubricant POSL coded OP-369 which is being studied using static cokers of similar design by the German Aerospace Research Establishment (GARE). Testing was conducted at five temperatures with four tests being conducted at each temperature. The test data along with all static coker data is given in Table A-3. A summary of the data for OP-369 is given in Table 37 and 38 and shown graphically in Figure 56. This data shows good test repeatability especially at test temperatures of 280°C and above. This lubricant is unusual in that the deposits were hard at all test temperatures. Most 5 cSt lubricants have oily and tacky deposits at test temperatures below 300°C and a test time of 3 hours.

(b) Effect of Brass Test Specimens on Deposits

Static coking tests were conducted at 315°C using brass (QQ-B-613 Specification) metal test specimens on four MIL-L-7808 lubricants with the test results being given in Table 39.

TABLE 36

DESCRIPTION OF TEST FLUIDS USED IN COKING STUDY

Test Fluid	Description
O-67-1	Formulated Polyphenyl Ether
O-71-6	MIL-L-23699 Lubricant
O-77-15	MIL-L-23699 Lubricant
O-79-16	MIL-L-7808 Lubricant
O-79-17	MIL-L-7808 Lubricant
O-79-18	MIL-L-23699 Lubricant
O-79-20	MIL-L-7808 Lubricant
O-82-2	MIL-L-7808 Lubricant
O-82-3	MIL-L-7808 Lubricant
O-82-14	MIL-L-7808 Type Lubricant
O-85-1	4 cSt Candidate Lubricant
O-86-2	Different Lot O-85-1
O-87-3	4 cSt Candidate Lubricant
TEL-6031	7.5 cSt Lubricant
TEL-6032	7.5 cSt Lubricant
TEL-7042	MIL-L-23699 Lubricant
TEL-7043	MIL-L-23699 Lubricant
OP-369	Commercial 5 cSt Lubricant
RR-A	5 cSt Lubricant
RR-B	7.5 Lubricant
RR-C	5 cSt Lubricant
RR-D	3 cSt Lubricant
RR-E	3 cSt Lubricant
RR-F	5 cSt Lubricant
RR-G	7.5 cSt Lubricant
RR-H	7.5 cSt Lubricant

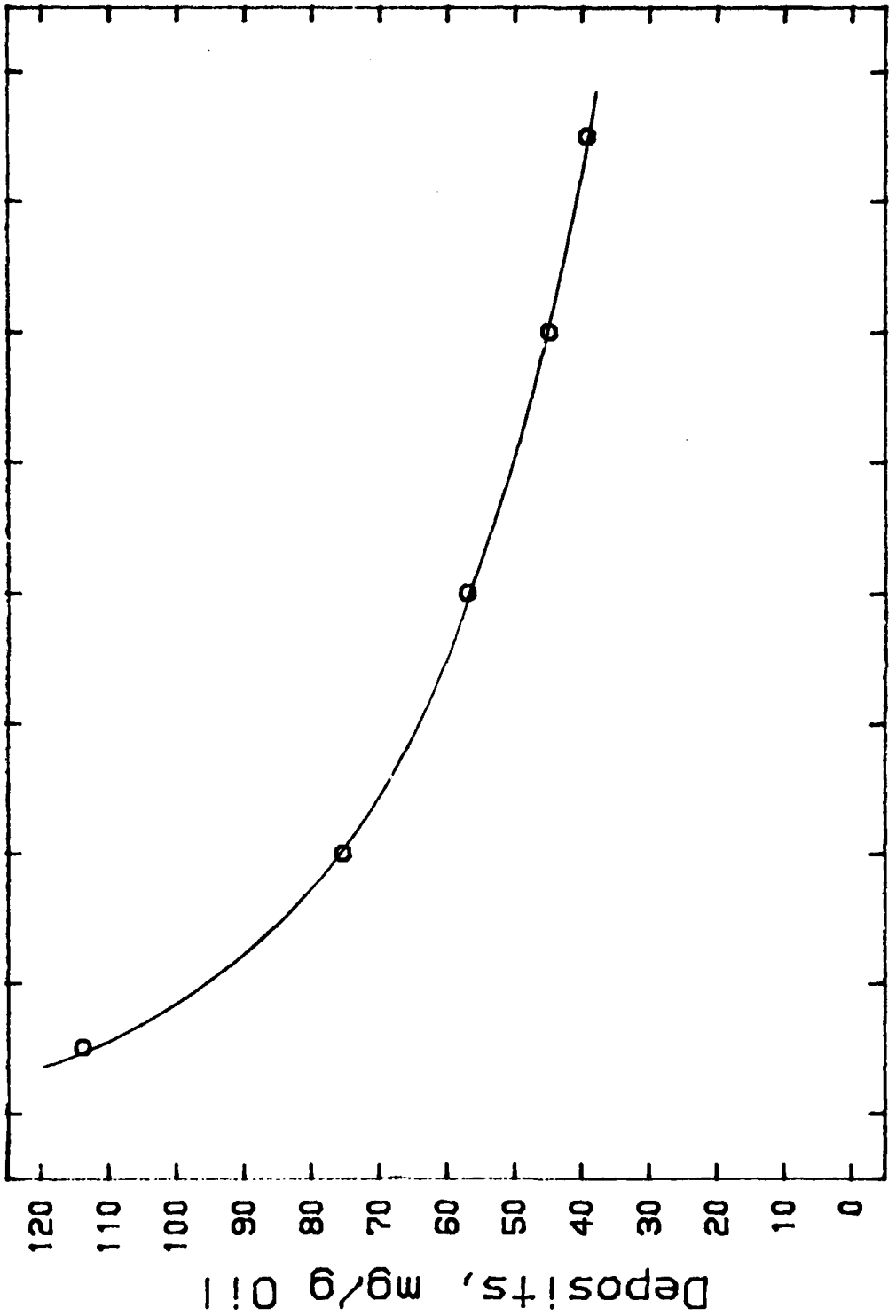

Figure 56. AFAPL Static Coker Deposits for Lubricant OP-369 (180 min Test Time)

TABLE 37

AFAPL STATIC COKER TEST DATA FOR LUBRICANT OP-369
(180 MIN TEST TIME)

Test Temperature, °C	Coker No.	Deposits mg/g oil	Deposit % Wt
245	1	114.1	11.41
	2	119.9	11.99
	3	109.4	10.94
	4	111.3	11.13
	Mean	113.7	11.37
	Std Dev	4.6	0.46
260	1	83.5	8.35
	2	74.6	7.46
	3	67.6	6.76
	4	75.0	7.50
	Mean	75.2	7.52
	Std Dev	6.5	0.65
280	1	58.5	5.85
	2	56.0	5.60
	3	57.5	5.75
	4	55.5	5.55
	Mean	56.9	5.69
	Std Dev	1.4	0.14
300	1	47.8	4.78
	2	43.2	4.32
	3	43.6	4.36
	4	45.1	4.51
	Mean	44.9	4.49
	Std Dev	2.1	0.21
315	1	39.6	3.96
	2	41.1	4.11
	3	37.2	3.72
	4	39.3	3.93
	Mean	39.3	3.93
	Std Dev	1.6	0.16

TABLE 38

DESCRIPTION OF AFAPL STATIC COKER DEPOSITS
FOR LUBRICANT OP-369 (180 MIN TEST TIME)

Test Temperature	Description of Deposits
245°C	Hard brown to black shiny wavy deposit.
260°C	Hard brown to black shiny wavy deposit.
280°C	Hard black shiny wavy deposit.
300°C	Hard black shiny wavy deposit.
315°C	Hard black shiny wavy deposit.

TABLE 39
COMPARISON OF AFAPL STATIC COKER TEST DEPOSITS
USING BRASS AND SHIM STOCK TEST SPECIMENS
AT 315°C AND 180 MIN TEST TIME

	Deposit, mg/g Oil	
	Brass	Shim Stock
O-79-16	12.8	14.1
O-79-20	14.3	14.7
O-82-2	12.1	14.6
O-82-14	17.4	16.7

The above data shows that for three of the lubricants, the brass gave slightly lower deposit levels and slightly higher deposit levels for lubricant O-82-14. For any of the oils, the difference in deposits between the brass and shim stock test specimens is small and not as great as was found with aluminum or stainless steel test specimens.[1]

(c) Effect of Wear Debris on Lubricant Coking

Coking tests were conducted on lubricant O-86-2 after pin-on-disk wear testing containing 560 ppm iron. A deposit value of 30.5 mg/g oil was obtained which is a little higher than the deposit value of 27.1 mg/g oil for new O-86-2. This difference is greater than the effect of wear debris on deposits previously reported[1] but still shows that wear debris does not have a large effect on static coker deposits for the ester base lubricants studied.

(d) Solubility Study of Deposits

Solubility studies were conducted on static coking deposits obtained for lubricant O-85-1 at test temperatures of 215°C, 230°C, 245°C, 260°C, 300°C and 315°C (180 minutes coking time) using pentane and toluene as

the solvents. One shim stock test specimen used for each of the coking test temperatures was weighed and placed in a jar containing 50 mL of pentane which was then sealed. After 24 hours of soaking the pentane was decanted and filtered through a preweighed 5 micron filter. The shim stock specimen was dried at 50°C for one hour, cooled to room temperature and reweighed. The pentane soluble portion of the coking deposits were calculated from the loss of specimen weight and the amount of deposits obtained from filtering the pentane. The same specimen was then placed in a jar containing 50 mL of toluene which was then sealed. After 24 hours of soaking the toluene was decanted and filtered through a preweighed 5 micron filter. The specimen was dried at 50°C for one hour, cooled to room temperature and reweighed. The toluene soluble portion of the coking deposits was calculated from the specimen weight loss (weight before pentane soak and weight after toluene soak) and the amount of deposits obtained from filtering the pentane and toluene. Figure 57 compares the AFAPL static coker deposits for lubricant 0-85-1 before and after the pentane solubility test and shows great deposit solubility at temperatures of 230°C and below with the deposit being mostly heavier esters of the test oil. A mixture of esters and residues make up the deposits between 230°C and 260°C. The coking deposits above 260°C show very little pentane solubility and only minor decreases in coking deposit levels with increasing coking temperatures. The deposit at 245°C was slightly tacky but the deposits were hard at test temperatures of 260°C and above. Figure 58 shows the comparison of pentane and toluene solubility of the deposits obtained at the various test temperatures. Significant differences exist between pentane and toluene solubility only between coking temperatures of about 245°C to 290°C. No difference in pentane or toluene solubility was observed at test temperatures of 300°C or 315°C.

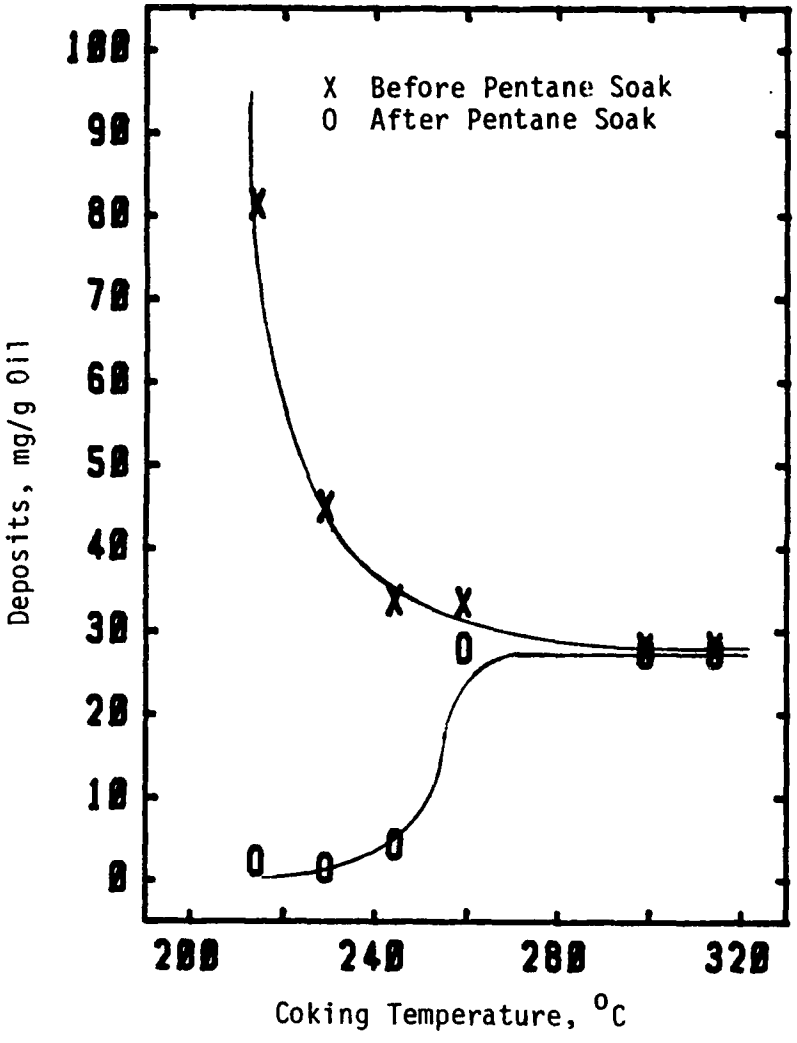

Figure 57. AFAPL Static Coker Deposits for Lubricant O-85-1 Before and After Pentane Solubility Test

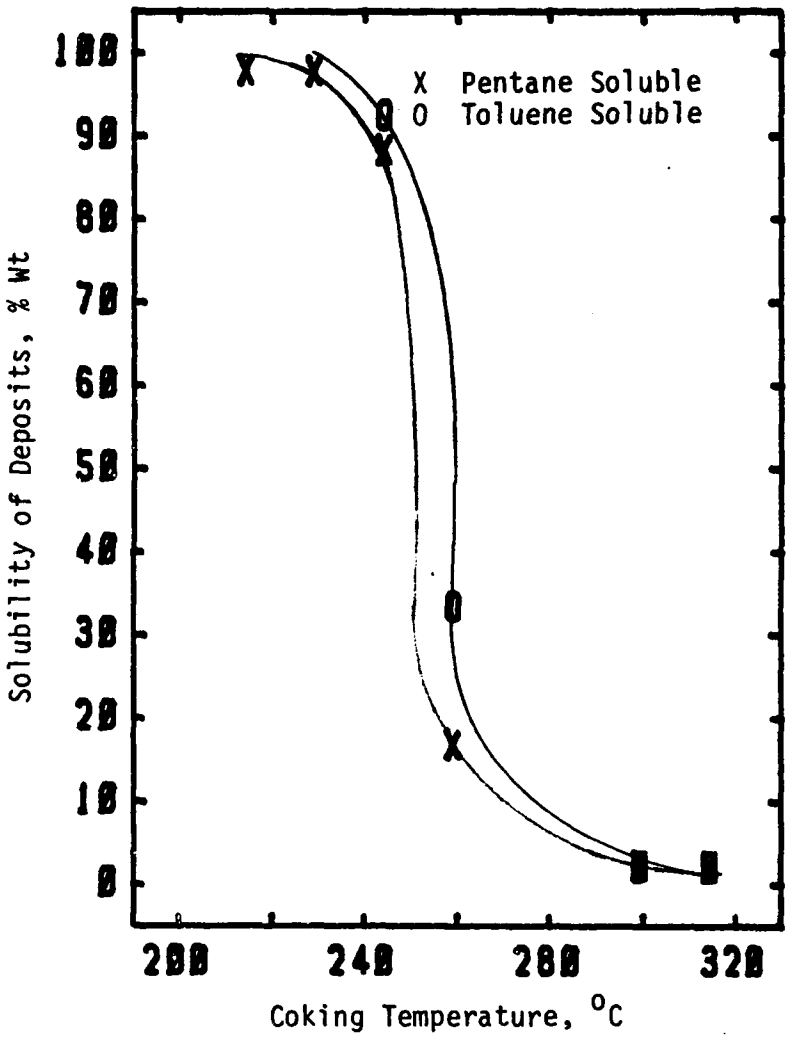

Figure 58. Solubility of AFAPL Static Coker Deposits for Lubricant O-85-1

(e) Effect of Confined Heat and Oxidative Stressing on AFAPL Static Coker Deposits

The effects of prior confined heat and oxidative stressing of the lubricant on coking deposits for 9 lubricants are shown in Table 40. Stressing conditions and degree of stressing as measured by changes in TAN and viscosity are also shown. The data in this table shows that confined heat stressing has less effect on coking than oxidative stressing even for some confined heat stressed samples showing much higher TAN. The increase in coking deposits of the oxidatively stressed lubricants is somewhat related to change in viscosity (as would be expected) but not in a quantitative way. The increase is highly lubricant formulation dependent. Although limited testing using oxidative stressing with condensate return was conducted the data does show that the use of condensate return can either increase or decrease the static coking characteristics of the lubricant.

(f) Static Coker Deposits as a Function of Test Time and Temperature

The effects of test temperature and test time on AFAPL Static Coker deposits for lubricant O-85-1 are given in Table 41.

TABLE 40

EFFECTS OF CONFINED HEAT AND OXIDATIVE STRESSING ON AFAPL STATIC COKER DEPOSITS

Test Lubricant	Stressing Conditions	TAN Increase	% Viscosity Increase, 100°C	Static Coker Deposits, % Wt (3 h, 315°C)	% Increase
0-85-1	New	-	-	2.77	-
	48 h, OX[1] @ 205°C	0.31	4.7	3.28	18.4
	168 h, OX @ 205°C	0.94	24.5	4.68	68.9
	48 h, CH[2] @ 205°C	0.88	-4.2	2.84	2.5
	96 h, CH @ 205°C	2.39	0.0	2.95	6.5
	72 h, OX @ 215°C	1.84	17.0	3.82	37.9
	72 h, OX @ 215°C W/CR[3]	3.82	14.4	2.27	-18.0
0-79-18	New	-	-	3.99	-
	24 h, OX @ 205°C	0.30	2.8	4.42	10.8
	24 h, OX @ 215°C W/CR[3]	1.78	6.2	4.59	15.0
	48 h, OX @ 205°C	0.83	5.3	4.43	11.0
	168 h, OX @ 205°C	0.59	14.1	5.90	47.9
	24 h, CH @ 205°C	0.31	-0.2	4.18	4.8
	48 h, CH @ 205°C	0.76	0.9	3.75	-6.0
	72 h, CH @ 205°C	2.18	0.7	4.35	9.0
0-77-15	New	-	-	3.34	-
	24 h, OX @ 205°C	0.31	7.5	4.30	28.7
	24 h, CH @ 205°C	1.20	5.4	3.80	13.8
	48 h, CH @ 205°C	2.99	4.0	3.89	16.5

TABLE 40 (CONCLUDED)

EFFECTS OF CONFINED HEAT AND OXIDATIVE STRESSING ON AFAPL STATIC COKER DEPOSITS

Test Lubricant	Stressing Conditions	TAN Increase	% Viscosity Increase, 100°C	Static Coker Deposits, % Wt (3 H, 315°C)	% Increase
O-79-16	New	-	-	1.41	-
	24 h, OX @ 205°C	0.31	8.5	2.21	56.7
	48 h, CH @ 205°C	2.49	2.2	1.82	29.1
O-79-17	New	-	-	1.32	
	48 h, OX @ 205°C	0.44	13.1	2.34	77.3
	48 h, CH @ 201°C	2.66	2.4	1.92	45.4
O-79-20	New	-	-	1.47	-
	48 h, OX @ 205°C	0.35	7.5	2.89	96.6
	48 h, CH @ 205°C	1.38	4.0	2.46	67.4
O-82-2	New	-	-	1.46	-
	48 h, OX @ 205°C	3.12	14.7	2.62	79.4
	48 h, CH @ 205°C	3.45	2.7	1.83	25.3
O-82-3	New	-	-	1.47	
	48 h, OX @ 205°C	1.18	26.1	3.34	127.2
	48 h, CH @ 205°C	1.11	3.5	1.79	21.8
	New	-	-	1.69	-
O-82-14	24 h, OX @ 205°C	1.43	11.5	3.05	80.5
	48 h, CH @ 205°C	6.05	6.5	2.64	56.2

[1]OX Oxidative Stressing

[2]CH Confined Heat Stressing

[3]W/CR With Condensate Return

TABLE 41
EFFECT OF TEST TEMPERATURE AND
TEST TIME ON AFAPL STATIC COKER DEPOSITS
FOR LUBRICANT O-85-1

Test Temperature °C	Test Time 3 h	5 h	8 h	16 h
		(Deposits, mg/g)		
215	81.1	45.4	36.1	39.8
230	44.6	31.5	32.4	23.1
245	33.5	30.7	24.6	18.3
260	38.9	32.6	27.6	23.0
300	27.6	25.3	25.6	19.2
315	27.7	25.0	22.3	17.4

The deposits at 215°C were oily and tacky for all test periods with a poor repeatability (approximate standard deviation of 3mg/g) which would be expected. At 230°C the deposits were tacky up to 8 hours but were hard at 16 hours. At 245°C the deposits were hard after 5 hours and for all temperatures above 245°C, the deposits were hard for all test periods. The data in Table 41 is as expected except for the increase in deposits at 260°C for all test periods and then a decrease for all test temperatures and time periods above 260°C. The increase and decrease in deposits between the temperatures of 250°C, 260°C and 300°C cannot be explained by test repeatability since several tests were conducted at each test temperature and the increase at 260°C occurring at all test times. The test repeatability was also worse at 260°C than at 245°C or 300°C. This increase/decrease in deposits indicates that an optimum temperature exists where maximum volatility occurs with minimum degradation and subsequent deposition. This variation in deposits occurs in the same temperature range where significant

difference in pentane and toluene solubility of the deposits occur (Figure 58). Table 42 shows the rate of change in the deposits with respect to test time. The data in Table 42 shows the expected decrease with time and is fairly constant for all test temperatures except the low test temperature of 215°C. The percent change per hour for the time period between 8 and 16 test hours (excluding 215°C test data) is 2.9% with a standard deviation of 0.51. The data does show that, overall, deposit levels do change a small percent with increasing test time.

TABLE 42
RATE OF CHANGE IN AFAPL STATIC COKER
DEPOSITS WITH TIME FOR LUBRICANT O-85-1

	% Change /h		
Test Temp, °C	3 to 5 h Time Period	5 to 8 h Time Period	8 to 16 h Time Period
215	22.0	6.8	1.2 (Increase)
230	14.7	0.9 (Increase)	3.4
245	4.2	6.6	3.2
260	8.1	5.1	2.1
300	4.2	0.4 (Increase)	3.1
315	4.9	3.6	2.7

The effects of test temperature and test time on AFAPL Static Coker deposits for the 4 cSt fluid O-87-3 has also been completed at various test temperatures for 3, 5 and 8 hour test periods with a summary of the test data being given in Table 43.

TABLE 43

EFFECT OF TEST TEMPERATURE AND
TEST TIME ON AFAPL STATIC COKER DEPOSITS
FOR LUBRICANT O-87-3

Test Temperature	Test Time		
	3h	5 h	8 h
(°C)		(Deposits, mg/g)	
215	245.1[a]	6.8	6.1
230	91.1[a]	8.7	4.8
245	9.2	6.8	-
260	24.7	19.4	17.0
285	17.8	17.8	16.6
300	17.6	17.0	10.4
315	17.8	13.7	8.2

[a]Oil

The test data given in Table 43 also shows a decrease/increase/decrease trend in deposits for all test times as the test temperature is increased from 215°C to 315°C with the deposit level being much higher at the 260°C test temperature than at either 245°C or 285°C. This apparent or near optimum temperature where maximum volatility and minimum deposits occur is near the same temperature as the 4 cSt lubricant O-85-1. The deposits after 5 and 8 hour test periods at test temperatures of 245°C and below were still slightly oily and tacky although very little deposits existed.

Lubricant O-87-3 volatility characteristics during the static coking test were very sensitive to hood airflow which varied during the last few tests conducted at test temperatures of 245°C and below which caused poor repeatability. These changes in airflow were detected by changes in the hood's Dwyer Gage readings.

Although small changes in hood airflow most likely have had

some small effect on test repeatability of other lubricants no other lubricant studied showed this degree of sensitivity to changes in hood conditions. The changes in hood conditions did not show such effects at test temperatures above 245°C.

Static coker testing of some lubricants for test periods longer than 3 hours can cause severe flaking which affects deposit weights. For example, static coking testing of the 7.5 cSt lubricant TEL-6031 was conducted at 315°C using shim stock test specimens for a test duration of 6 hours instead of the normal 3 hour test period. A deposit value of 12.6 mg/g of oil was obtained which is much lower than the deposit value of 30.5 mg/g oil obtained using the 3 hour test period. During the last part of the test prior to removing the test specimens from the brass base section the deposits started to flake with many coke particles being removed by the hood draft. This continued after removing the test specimen from the base. The amount of flaking and subsequent loss of deposits accounted for much of the reduced deposit value for the 6 hour test.

(g) AFAPL Static Coker Testing of High Temperature Lubricant O-67-1

Testing of the PTFE seals was conducted at various temperatures for determining maximum temperature capability prior to testing the high temperature lubricant O-67-1. Measurements of the PTFE seals were made before and after testing for determining the temperature where plastic flow started. When the shim stock surface was 356°C (673°F) no change in the seal appearance or measurements occurred after approximately 4 test hours with a loading of 2.7 kg. The seal showed a slight change in both visual appearance and measurements at a shim stock test temperature of 360°C (680°F). Since this data indicates the maximum testing temperature using the

PTFE seals is about 355°C, stainless steel seals were made with the same dimensions as the PTFE seals.[1]

Testing of new and stressed O-67-1 (5P4E) lubricant was conducted at 355°C, shim stock surface and using both PTFE and stainless steel seals. A surface temperature of 355°C was used since previous testing showed that this was the maximum operating temperature of the PTFE. A summary of the test data is given in Table 44.

TABLE 44
AFAPL STATIC COKER DEPOSITS FOR NEW AND STRESSED
O-67-1 (5P4E) LUBRICANT AT 355°C

Lubricant	Test Sample Size, mL	Hours 320°C C&O Stressing	Deposits, mg/g PTFE Seal	Deposits, mg/g Stainless Steel Seal
O-67-1[a]	0.25	0	11.2 (= 0.5)	8.4 (= 2.8)
O-67-1[b]	0.25	0	7.1 (= 3.0)	8.4 (= 2.8)
O-67-1[a]	0.25	168	14.9 (= 0.9)	9.2 (= 2.5)
O-67-1[b]	0.25	168	13.4 (= 2.3)	10.8 (= 0.2)
O-67-1[a]	0.25	240	28.7 (= 1.8)	11.6 (= 0.6)
O-67-1[b]	0.25	240	25.8 (= 5.9)	22.7 (= 2.8)
O-67-1[a]	0.50	0	3.6 (= 0.1)	3.1 (= 0.1)
O-67-1[b]	0.50	0	3.4 (= 0.5)	3.7 (= 0.1)

[a]Deposits not considering weight loss of PTFE seals or deposits on stainless steel seals

[b]Deposits considering weight loss of PTFE seals and deposits on stainless steel seals

The PTFE seals stick to the shim stock test specimen at the test temperature of 355°C and leave a small amount of PTFE on the test specimens. This results in slightly higher deposit values. Due to the much higher thermal conductivity of the stainless steel seals which causes a higher seal temperature and the higher interfacial surface tension of the steel seals and the 5P4E fluid, the stainless steel seals can contain significant amounts of deposits. The data in Table 44 does show that

stressing of 5P4E fluids increases the deposits obtained using the AFAPL Static Coker. Preliminary results indicate sample size has a great effect on coking deposits as shown by the 0.25 mL and the 0.50 mL sample size data shown in Table 44.

(5) Summary

This study has shown the static coker deposition tester to be a good low cost, short time laboratory test for studying the coking characteristics of lubricants under high temperature static oil conditions. In addition to the findings of Phase 1 of this study,[1] Phase 2 efforts have shown the following:

(a) Shim Stock coking surface gives the highest deposit values compared to aluminum, stainless steel, brass or quartz.

(b) Nascent wear debris has a very small effect on AFAPL Static Coker measurements.

(c) Solubility studies showed that significant difference in pentane and toluene solubility of O-85-1 lubricant deposits occurred only between 245°C and 290°C. No difference was observed in deposit solubility above or below these temperatures.

(d) For some lubricants an optimum test temperature exists where maximum volatility and low rates of degradation occur which provides for lower deposit values than obtained at temperatures above or below this temperature. This critical temperature was approximately 245°C for the two 4 cSt lubricants studied.

(e) Although hard coking deposits are obtained after 3 hours at the higher test temperatures, the deposits continue to decrease slightly with test time.

(f) Thermal and oxidative stressing were found to influence the

quantity of coking deposits produced with the Static Coker. The oxidative stressing had a much greater effect on changes in coking values. These increases are only partially due to lowering of volatility during the oxidation stressing but are also due to degradation.

(g) The use of condensate return during oxidative stressing of lubricants prior to static coking testing can either increase or decrease the deposit level depending upon the lubricant formulation.

(h) Limited testing has shown that the AFAPL Static Coker can be used for investigating the coking characteristics of high temperature fluids at test temperatures above 350°C by using stainless steel seals in place of PTFE.

(i) The deposit values obtained for the high temperature lubricant O-67-1 (5P4E fluid) is very sample size dependent at a test temperature of 355°C. Additional studies are required with high temperature lubricants with respect to test time, test temperature and sample volume for developing a high temperature coking test.

b. Micro Carbon Residue Tester (MCRT)

(1) Introduction

Lubricant coking studies were conducted using the Micro Carbon Residue Tester (MCRT)[12] for participating in establishing the repeatability and reproducibility of the MCRT and for determining the correlation between the MCRT and the AFAPL Static Coker using new and stressed lubricants. This test, like the Static Coker, measures the deposits formed by a lubricant under conditions where lubricant volatility is an important factor. These conditions exist in areas of turbine engines where there is low or no oil flow and trapped pockets of lubricants are present due to fog or mist lubrication. Temperature rise due to heat soak-back on engine shut-down also

contributes to coking under these conditions.

(2) Test Apparatus and Procedure

The MCRT contains a small programmable controlled oven which allows for time/temperature sample heating operations. The unit is designed such that a series of glass vials with weighed amounts of sample are positioned in the oven using an aluminum basket. The appropriate heating program is then selected and the test is initiated. At the end of the test the vials are reweighed and the percent weight of coke is determined for each vial. The average of all vials (12 using 12 X 35 mm vials were used in this study) is reported as the coking value. During the test period, air is flowed through the oven which removes the volatile material. All testing conducted using the MCRT was performed in accordance with the procedure described by Reference 13 (presoak of 1 hour at 150°C, 30 hour test period at 275°C).

(3) Test Lubricants

Lubricants and fluids used in the MCRT coking studies are described in Table 36, Description of Lubricants Used in Coking Study.

(4) Results and Discussion

All MCRT coking test data generated under this research program are given in Table A-4.

A summary of the MCRT coking test data for ester type lubricants is given in Table 45 along with the corresponding AFAPL Static Coker data. The viscosity at 100°C is given which describes the "type" of the lubricant. The data in Table 45 shows the AFAPL Static Coker gives approximately 10 % less deposits than the MCRT and in most cases similar standard deviation. The standard deviation for the MCRT is based on 12 tests and usually 2 to 4 tests for the AFAPL Static Coker.

TABLE 45

AFAPL STATIC COKER DATA AND MCRT
COKING DATA FOR VARIOUS LUBRICANTS

Lubricant	Viscosity (100°C) cSt	MCRT Residue (275°C, 30 h) % wt	AFAPL Static Coker Deposits (315°C, 3 h) % wt
RR-A	5.10	27.37 ± 0.19	3.67 ± 0.27
RR-B	7.49	13.70 ± 0.35	1.61 ± 0.06
RR-C	5.15	25.69 ± 0.23	2.95 ± 0.36
RR-D	3.18	12.08 ± 0.39	1.39 ± 0.18
RR-E	3.59	9.68 ± 0.19	0.84 ± 0.06
RR-F	4.59	22.16 ± 0.29	3.32 ± 0.21
RR-G	7.37	11.98 ± 0.20	0.81 ± 0.09
RR-H	4.95	24.56 ± 0.36	3.49 ± 0.22
TEL-6031	7.53	18.42 ± 0.41	3.05 ± 0.31
TEL-6032	7.50	12.16 ± 0.24	1.04 ± 0.01
O-71-6	4.95	21.67 ± 0.35	3.20 ± 0.29
O-77-15	4.95	24.20 ± 0.58	3.34 ± 0.04
O-79-18	5.29	24.06 ± 0.54	3.99 ± 0.27
TEL-7042	5.02	21.92 ± 0.40	3.43 ± 0.28
O-79-16	3.16	12.51 ± 0.29	1.41 ± 0.11
OP-369	5.02	26.95 ± 0.36	3.93 ± 0.16
O-85-1	4.04	14.81 ± 0.48	2.77 ± 0.23
O-79-17	3.35	10.11 ± 0.23	1.32 ± 0.17
TEL-7043	5.06	22.05 ± 0.41	3.56 ± 0.19
O-79-20	3.47	11.44 ± 0.46	1.47 ± 0.15
O-82-3	3.45	7.37 ± 0.35	1.47 ± 0.20
O-82-2	3.33	17.28 ± 0.33	1.46 ± 0.13
O-82-14	3.40	18.51 ± 0.47	1.69 ± 0.09
O-87-3	4.01	16.73 ± 0.94	1.78 ± 0.18
O-86-2	4.01	15.25 ± 0.50	2.71 ± 0.23

The correlation between the two tests is shown in Figure 59. The 5 cSt lubricants give greater deposits levels than the 3 cSt lubricants as expected due to lower volatility of these higher viscosity fluids. However, three of the four 7.5 cSt oils give deposits levels more closely to the 3 cSt lubricants while the fourth 7.5 cSt lubricant gave coking values between the 4 cSt and 5 cSt fluid. Although a general correlation exists between the two tests, some lubricants show less deposits than expected using the MCRT and some show greater deposits than expected.

The effects of prior confined heat and oxidative stressing of the lubricant on MCRT deposit values are shown in Table 46. Stressing conditions and degree of stressing as measured by changes in TAN and viscosity are also shown. The data in Table 46 shows that changes in MCRT deposits due to stressing are similar to the changes shown by the AFAPL Static Coker in that confined heat stressing has less effect than oxidative stressing. However, the changes in deposits for oxidatively stressed lubricants are very formulation dependent with some stressed lubricants showing larger deposit increases with the MCRT while other stressed lubricants give larger deposit increases with the AFAPL Static Coker. The correlation between the MCRT and the Static Coker for stressed lubricants is shown by Figure 60. Comparison of Figures 59 and 60 show that stressed lubricants give a poorer correlation between the two tests than new lubricants.

Limited MCRT evaluation of new and stressed polyphenyl ether lubricant O-67-1 was conducted using the same parameters used for the ester base lubricants expect that the 30 hour coking temperature was 350°C. Results of this testing are given in Table 47.

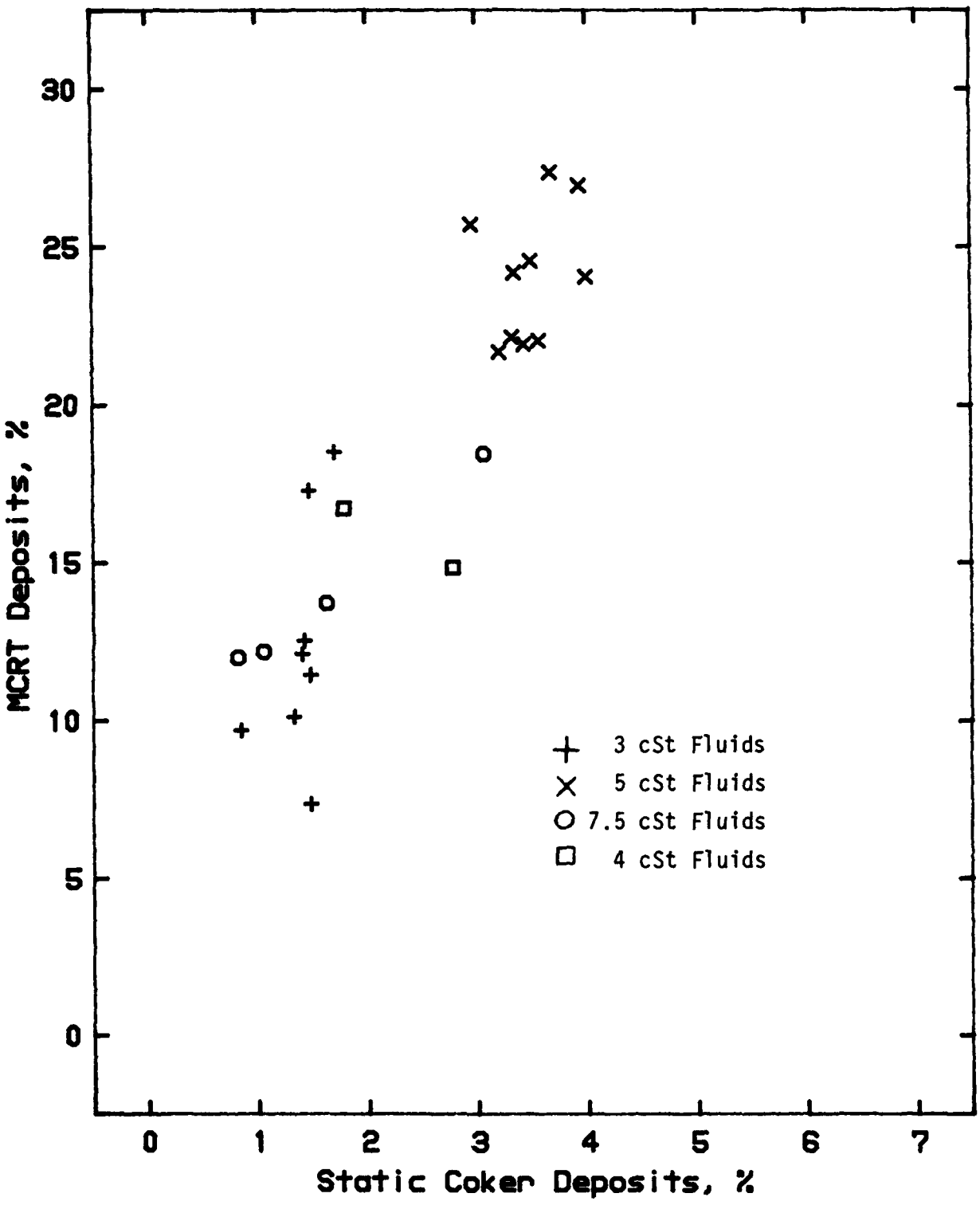

Figure 59. Correlation of AFAPL Static Coker Deposits with MCRT Deposits (New Oil)

TABLE 46

EFFECTS OF CONFINED HEAT AND OXIDATIVE STRESSING ON MCRT DEPOSITS

Test Lubricant	Stressing Conditions	TAN Increase	% Viscosity Increase, 100°C	MCRT Deposits, % Wt (3 h, 315°C)	% Increase
O-85-1	New	-	-	14.81	-
	48 h, OX @ 205°C	0.31	4.7	16.09	8.6
	168 h, OX @ 205°C	0.94	24.5	19.04	28.6
	48 h, CH @ 205°C	0.88	-4.2	15.22	2.8
	96 h, CH @ 205°C	2.39	0.0	15.48	4.5
	72 h, OX @ 215°C	1.84	17.0	18.51	25.0
	72 h, OX @ 215°C W/CR	3.82	14.4	13.58	-8.3
O-79-18	New	-	-	24.06	-
	24 h, OX @ 205°C	0.30	2.8	27.84	15.7
	24 h, OX @ 215°C W/CR	1.78	6.2	25.05	4.1
	48 h, OX @ 205°C	0.83	5.3	27.41	13.9
	168 h, OX @ 205°C	0.59	14.1	27.56	14.5
	24 h, CH @ 205°C	0.31	-0.2	28.82	19.8
	48 h, CH @ 205°C	0.76	0.9	28.42	18.1
	72 h, CH @ 205°C	2.18	0.7	26.75	11.2
O-77-15	New	-	-	24.20	-
	24 h, OX @ 205°C	0.31	7.5	26.96	11.4
	24 h, CH @ 205°C	1.20	5.4	25.13	3.8
	48 h, CH @ 205°C	2.99	4.0	25.43	5.1
O-79-16	New	-	-	12.51	-
	24 h, OX @ 205°C	0.31	8.5	15.20	21.5
	48 h, CH @ 205°C	2.49	2.2	12.76	2.0

TABE 46 (CONCLUDED)

EFFECTS OF CONFINED HEAT AND OXIDATIVE STRESSING ON MCRT DEPOSITS

Test Lubricant	Stressing Conditions	TAN Increase	% Viscosity Increase, 100°C	MCRT Deposits, % Wt (3 h, 315°C)	% Increase
0-79-17	New	-	-	10.11	-
	48 h, OX @ 205°C	0.44	13.1	14.69	45.3
	48 h, CH @ 201°C	2.66	2.4	11.73	16.0
0-79-20	New	-	-	11.44	-
	48 h, OX @ 205°C	0.35	7.5	15.71	37.3
	48 h, CH @ 205°C	1.38	4.0	13.86	21.1
0-82-2	New	-	-	17.25	-
	48 h, OX @ 205°C	3.12	14.7	22.89	32.5
	48 h, CH @ 205°C	3.45	2.7	19.83	14.8
0-82-3	New	-	-	7.37	-
	48 h, OX @ 205°C	1.18	26.2	15.81	114.5
	48 h, CH @ 205°C	1.11	3.5	9.24	25.4
0-82-14	New	-	-	18.51	-
	24 h, OX @ 205°C	1.43	11.5	20.41	10.3
	48 h, CH @ 205°C	6.05	6.5	20.74	12.0

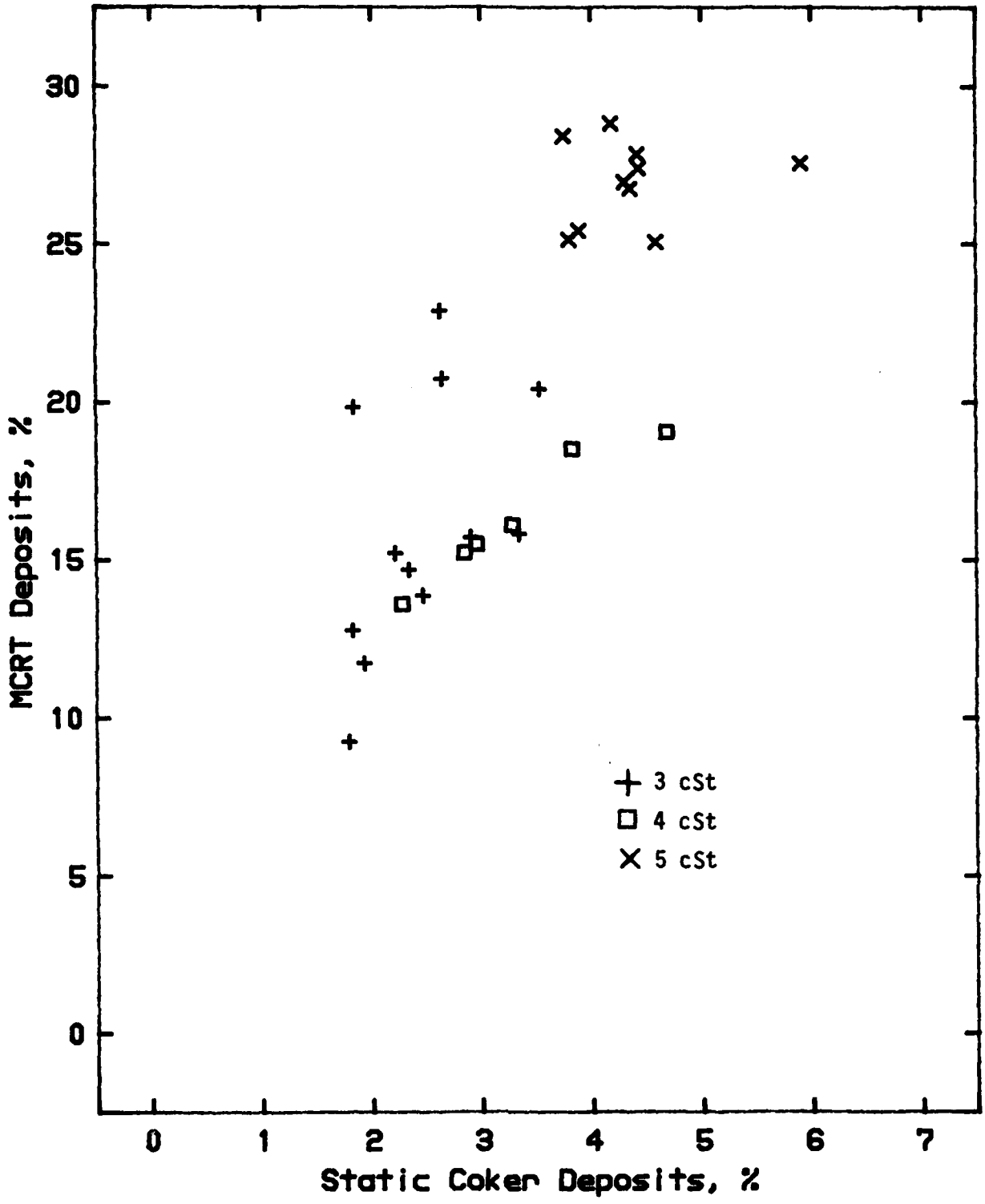

Figure 60. Correlation of AFAPL Static Coker Deposits with MCRT Deposits (Stressed Oil)

TABLE 47

MCRT AND AFAPL STATIC COKER DEPOSITS
FOR NEW AND STRESSED O-67-1 LUBRICANT

Lubricant	40°C Viscosity Change, %	MCRT Deposits 350°C % wt	Static Coker Deposits 355°C % wt
O-67-1	-	2.39 ± 0.52	1.12 ± 0.05
O-67-1 after 168 h, 320°C C&O Testing	38.2	4.32 + 0.29 (80.7% Increase)	1.49 + 0.09 (33.0% Increase)
O-67-1 after 240 h, 320°C C&O Testing	81.9	8.69 ± 1.44 (263.6% Increase)	2.87 ± 0.18 (156.2% Increase)

The data in Table 47 shows very good correlation in the coking values between the two tests. The data in both tests also correlates well with the viscosity increase which would contribute to the good correlation between the two coking tests.

The deposits produced by the MCRT were hard brown to black lacquer type deposits. The 240 hour stressed sample had deposits on the outside and bottom of the glass vials indicating a problem with using the small vials and the normal 0.5 gram sample. The 168 hour sample had deposits near the top of the vials but not outside of the vials which gave better repeatability.

Throughout all MCRT testing, a trend was noticed in which specific vial positions gave the lowest of the 12 results and others which gave the highest results. This would indicate that either a small temperature difference exists within the oven or that a nonuniform airflow exists within the oven. The extent of this effect on deposits varied from one lubricant to another.

(5) Summary

The MCRT showed good correlation with the AFAPL Static Coker considering the differences between the two tests although both give deposit values which are somewhat dependent upon volatility. The correlation between the two tests was not as good for prestressed (thermal or oxidative) lubricants. Some lubricants showed greater increase in deposits with the Static Coker while other lubricants gave greater increases in deposits with the MCRT. The changes in deposit levels due to prestressing using either test are very lubricant formulation dependent.

The 0.5 gram sample normally used produced deposits on the outside of the glass vials for the stressed high temperature fluids and indicates further studies are required for developing a MCRT test for high temperature lubricants.

Slight variations were found in deposit values for various vial positions of the MCRT. However good test repeatability was obtained when the average of all 12 vials were used for the final coking value.

c. Coking Propensity Test

(1) Introduction

The coking propensity test developed by Rolls-Royce Ltd. measures the deposits formed by a lubricant under static conditions where lubricant volatility is an important factor. Thus, this test gives deposits measurements similar to the AFAPL Static Coker or the MCRT.

(2) Test Apparatus

The test apparatus consists of cylindrical metal dishes with the procedure requiring sandblasted aluminum dishes. Stainless steel (302) and polished aluminum test dishes were also used in this study for investigating the effect of metal and surface type on deposit levels. Coking of the test

lubricants was conducted using a Blue M, Class A, Batch oven, Model No. PDM-106A-GHP having horizontal forced air circulation. A baffle was used to prevent the air flowing directly over the test dishes. Coking propensity dishes are described in Reference 1.

(3) Test Procedure

The test procedure has been previously described in Phase 1 of this study and given in Reference 1.

(4) Test Lubricants

Lubricants studied during Phase 2 of the Coking Propensity Study are listed in Table 48.

TABLE 48

LUBRICANTS USED IN COKING PROPENSITY STUDY

Lubricant	Description
O-71-6	MIL-L-23699 Type
O-77-15	MIL-L-23699 Type
O-79-18	MIL-L-23699 Type
O-85-1	4 cSt Candidate Lubricant
O-86-2	4 cSt Candidate Lubricant
TEL-6031	7.5 cSt Lubricant
TEL-6032	7.5 cSt Lubricant

(5) Results and Discussion

Coking propensity testing of MIL-L-23699 lubricants O-71-6, O-77-15 and O-79-18, the 4 cSt candidate lubricant O-85-1 and two 7.5 cSt lubricants TEL-6031 and TEL-6032 were conducted using stainless steel dishes at a test temperature of 235°C. Test data is given in Table 49. As expected from AFAPL Static Coking testing, the MIL-L-23699 fluids gave the highest deposit levels. Lubricant O-85-1 (4 cSt fluid) gave a deposit level close to the MIL-L-23699 oils while the two 7.5 cSt viscosity lubricants had much lower deposit levels. The three MIL-L-23699 lubricants and lubricant O-85-1 gave similar types of deposits. These deposits were hard, dark brown to black, and flaky. The two 7.5 cSt fluids gave deposits similar to the other fluids but slightly less flaky. The coking propensity testing gave the same relative ranking of the various types of lubricants as the AFAPL Static Coker and the Microcarbon Carbon Residue Tester.

Coking propensity testing of lubricant O-86-2 at a test temperature of 260°C was conducted for comparison of coking propensity test data with that obtained with O-85-1 (O-86-2 being a different lot of laboratory formulated O-85-1). No significant difference in the coking propensity deposits were found with O-85-1 having a deposit value of 8.6 mg/g oil compared with 7.3 mg/g oil for lubricant O-86-2 when using stainless steel test dishes. Table 50 shows the lubricant coking propensity test data at 260°C using stainless steel, aluminum and sandblasted aluminum test dishes. Sandblasted aluminum dishes gave a slightly lower deposit level which is consistent with all coking propensity testing using sandblasted dishes.

TABLE 49

LUBRICANT COKING PROPENSITY TEST DATA
235°C TEST TEMPERATURE

Lubricant	Type Test Dish	Avg Test Cycle (mg)	DEPOSIT MEASUREMENTS Total/10[a] Cycles (mg)	Total/10[b] Cycles (mg)	Total/20[c] Cycles (mg)	Total/20[d] Cycles (mg)	Residue[c] (mg/g oil)	Residue[d] (mg/g oil)
0-71-6	Stainless Steel	7.2	72.2	72.2	144.4	144.4	15.6	15.6
0-77-15	"	5.7	56.6	56.6	113.2	113.2	12.2	12.2
0-79-18	"	8.1	80.6	80.6	161.2	161.2	16.7	16.7
0-85-1	"	5.8	58.5	58.5	117.0	117.0	12.6	12.6
TEL 6031	"	4.7	47.0	47.0	94.0	94.0	9.4	9.4
TEL 6032	"	1.7	16.6	16.5	33.2	33.0	3.5	3.4

[a] *Mean Value*

[b] Final test dish weight minus initial weight for 10 cycles

[c] Calculated from the mean for 10 cycles

[d] Calculated from final & initial weight for 10 cycles

TABLE 50

LUBRICANT COKING PROPENSITY TEST DATA
260°C TEST TEMPERATURE

Test Lubricant	Type Test Dish	DEPOSIT MEASUREMENTS Avg/Test Cycle (mg)	Total/10[a] Cycles (mg)	Total/10[b] Cycles (mg)	Total/20[c] Cycles (mg)	Total/20[d] Cycles (mg)	Residue[c] mg/gm oil	Residue[d] mg/gm oil
0-86-2	Stainless Steel	3.4	34.4	34.4	68.8	68.8	7.3	7.3
0-86-2	Aluminum	3.6	35.8	35.8	71.6	71.6	7.5	7.5
0-86-2	Sandblasted Aluminum	3.0	30.0	30.0	60.0	60.0	6.3	6.3
0-85-1	Stainless Steel	4.1	40.8	40.8	81.6	81.6	8.6	8.7

[a]Mean Value

[b]Final test cup weight minus initial weight for 10 cycles

[c]Calculated from the mean for 10 cycles

[d]Calculated from final & initial weight for 10 cycles

(6) Summary

Coking propensity testing conducted on the various lubricants gave the same relative ranking of the various lubricants as the AFAPL Static Coker and the Microcarbon Residue Tester (MCRT).

Good test reproducibility was obtained for two different lots of a 4 cSt candidate lubricant.

Sandblasted aluminum dishes gave slightly lower deposit levels which is consistent with all coking propensity testing using sandblasted dishes.

6. LUBRICANT FOAMING STUDY

a. Introduction

The foaming characteristics of turbine lubricants are normally determined using both static and dynamic testing described in AFAPL-TR-75-91, ASTM Method D892 and Federal Test Method Standard 791, Methods 3213 and 3214. A limitation of these foam tests is the large quantity of sample required which prevents determining the foaming characteristics of small samples of used lubricating fluids. The objective of this study was the development of a static foaming test requiring 25 mL or less sample and which correlates with Federal Test Method Standard 791, Method 3213.

During Phase I of this effort, many physical properties of foam test equipment, test conditions and synergistic effects of some lubricants and test equipment were shown to affect foaming values obtained during testing. Considering all these factors the best correlation between Test Method 3213 and a small sample volume test was obtained using a 25 mL sample, 13/16 inch diameter 5 micron rated pore size metal sparger, 1000 cc/min airflow and a 250 cc graduated cylinder.

The second phase of this study was directed towards improving the correlation between the two tests. Testing of selected lubricants were

scheduled such that all testing on each lubricant would be conducted within a minimum time period usually one or two days. This would eliminate or reduce the effects of changes occurring in foaming characteristics of some lubricants with storage time which has been shown to exist.[1]

b. Test Apparatus

The test apparatus for conducting the standard foam test and the various test apparatus used for the small volume foam testing has been previously described.[1]

c. Test Procedure

The test procedure for Method 3213 and for the developed small volume test has been described.[1] A modification to the small volume test procedure was made during Phase 2 of this study for those tests being conducted for investigating the effects of airflow on non-foaming oils and having different aeration characteristics. This change in procedure required a 15 minute aeration period at 1000 cc/min airflow or until a constant foam and/or aeration value was obtained. The airflow was then reduced to various levels with a 10 minute aeration period at each airflow or until constant foam/aeration values were obtained.

d. Test Lubricants

Thirteen fluids having different foaming and aeration characteristics were investigated during Phase 2 of this study and are described in Table 51.

The fluids containing the DC-200 methyl silicone were prepared by blending the required amount of a 1.00% silicone concentration in toluene with the base fluid using mechanical agitation.

TABLE 51

LUBRICANTS AND FLUIDS USED FOR FOAMING AND AERATION STUDY

Lubricant or Fluid	Description
O-76-1 plus 6 ppm DC-200-20 cSt*	MIL-L-7808 Lubricant with Silicone
5K3L6	MIL-7808 Lubricant
O-76-5 plus 2.0% TCP and 2.0% PANA	TMPH Ester with Additives
O-79-17 plus 3 ppm DC-200-500 cSt**	MIL-L-7808 Lubricant with Silicone
O-79-16	MIL-L-7808 Lubricant
O-82-3	MIL-L-7808 Lubricant
O-79-17	MIL-L-7808 Lubricant
O-76-1 plus 3 ppm DC-200-20 cSt	MIL-L-7808 Lubricant with Silicone
O-82-2	MIL-L-7808 Lubricant
O-79-20	MIL-L-7808 Lubricant
O-82-14	MIL-L-7808 Type Lubricant
O-76-5 plus 1.5% TCP and 1.5% PANA	TMPH Ester with Additives
O-67-21 (75%) and O-79-17 (25%)	Mixture of MIL-L-7808 Lubricants

*Dow Corning Methyl Silicone DC-200 with 20 cSt Viscosity at 25°C

**Dow Corning Methyl Silicone DC-200 with 500 cSt Viscosity at 25°C

e. Results and Discussion

(1) Repeatability of Test Data Between Phase 1 and Phase 2 for Lubricants having Distinct Foaming Characteristics

Improving the correlation between Fed. Test Method 3213 and the small volume test was attempted by conducting all testing within a short time period, usually 1 or 2 days, instead of testing over a long time period (12 months or more as occurred in Phase 1). The test data, along with all foaming test data obtained using Method 3213 and the small volume test obtained during Phase 2 is given in Tables A-5 and A-6 which details each test as to conditions of testing and various recorded values such as oil volume at maximum foam height, foam volume, collapse time, airflow rates, etc.

Two fluids (O-79-17 containing 3 ppm DC-200-500 cSt) and O-76-1 containing 3 ppm DC-200-20 cSt) were retested during Phase 2 with a summary of all testing for these two fluids being given in Table 52. The data in Table 52 showed no improvement in conducting all foam testing of these two fluids within a short time period. Therefore repeat testing of previously tested lubricants having various foaming characteristics was discontinued.

(2) Correlation of Test Method 3213 Foam Test Data with 25 mL Volume Foam Test Data

Test data used for determining the correlation between the Test Method 3213 foam data and the 25 mL volume foam test data consists of all data developed during both phases of the study with an average of 3 or more individual foam tests being conducted on the same fluid with the same test and air dispenser. Table 53 gives a comparison of the foam test data obtained using the two tests including foam values, existence of an oil/foam interface and degree of aeration.

Lubricants having a distinct oil/foam interface in both tests

TABLE 52

REPEATABILITY OF FOAM TESTING

Lubricant	ASTM Test With Diffuser Stone 200 mL[a]	ASTM Test With Diffuser Stone 25mL[a]	13/16" 5 Sparger 25 mL[a]	11/16" 5 Sparger 25 mL[a]
O-79-17 Plus 3 ppm DC-200				
Phase 2 Testing	180	102	88	20
	210	68	102	18
	185	74	88	22
	195	-	-	-
Phase 2 Mean	193	81	93	20
Std. Dev.	12	18	8	2
Phase 1 Testing	230	74	94	22
	225	54	78	18
	215	80	-	-
	195	-	-	-
	225	-	-	-
Phase 1 Mean	218	69	86	20
Std. Dev.	14	14	11	2
Mean of all Testing	205	75	90	20
Std. Dev.	18	16	9	2
O-76-1 Plus 3 ppm DC-200				
Phase 2 Testing	150	22	28	10
	150	20	28	18
	-	56	22	16
Phase 2 Mean	150	33	26	15
Std. Dev.	-	20	3	4
Phase 1 Testing	160	14	31	14
	135	14	26	-
Phase 1 Mean	148	14	29	14
Std. Dev.	18	-	4	-
Mean of all Testing	149	26	27	15
	10	18	3	3

[a]1000 cc/min airflow

TABLE 53

COMPARISON OF FOAM TEST DATA USING FED. METHOD 3213 AND 25 ML VOLUME TEST FOR VARIOUS AIR DISPERSERS AND 1000 CC/MIN AIRFLOW

Test Method, Foam Volume and Degree of Aeration

	Fed. Method 3213, 200 mL Sample		25 mL Volume Test		
Lubricant	ASTM Stone	13/16" 5 micron Sparger	13/16" 5 micron Sparger	11/16" 5 micron Sparger	ASTM Stone
O-76-1 plus 6 ppm DC-200-20 cSt	290 oil/foam interface	305 oil/foam interface	72 oil/foam interface	15 oil/foam interface	52 oil/foam interface
5K-3L6	415 oil/foam interface	455 oil/foam interface	150 oil/foam interface	133 oil/foam interface	104 oil/foam interface
O-76-5 plus 2% TCP and 2% PANA	480 oil/foam interface	500 oil/foam interface	175 oil/foam interface	110 oil/foam interface	123 oil/foam interface
O-79-17 + 3 ppm DC-200-500 cSt	205 oil/foam interface	240 oil/foam interface	90 oil/foam interface	20 oil/foam interface	75 oil/foam interface
O-79-16	48 oil/foam interface	58 oil/foam interface	108 no oil/foam interface (milkshaking)	94 no oil/foam interface (milkshaking)	88 no oil/foam interface (milkshaking)
O-82-3	12 oil/foam interface	15 oil/foam interface	12 oil/foam interface	11 oil/foam interface	-
O-67-21 (75%) and O-79-17 (25%)	465 oil/foam interface	-	176 oil/foam interface	144 oil/foam interface	-

TABLE 5 3 (CONCLUDED)

COMPARISON OF FOAM TEST DATA USING FED. METHOD 3213 AND 25 ML VOLUME TEST FOR VARIOUS AIR DISPERSERS AND 1000 CC/MIN AIRFLOW

	Test Method, Foam Volume and Degree of Aeration				
	Fed. Method 3213, 200 mL Sample		25 mL Volume Test		
Lubricant	ASTM Stone	13/16" 5 micron Sparger	13/16" 5 micron Sparger	11/16" 5 micron Sparger	ASTM Stone
0-79-17	12 oil/foam interface	-	63 no oil/foam interface severe aeration	8 oil/foam interface	10 oil/foam interface
0-76-1 plus 3 ppm DC-200-20 cSt	148 oil/foam interface	18 oil/foam interface	26 oil/foam interface	15 oil/foam interface	26 oil/foam interface
0-82-2	10 oil/foam interface	15 oil/foam interface	49 no oil/foam interface severe aeration	24 oil/foam interface	42 oil/foam faint oil/foam interface
0-79-20	18 oil/foam interface	16 oil/foam interface	56 no oil/foam interface severe aeration	14 oil/foam interface	-
0-82-14	93 oil/foam interface	120 oil/foam interface	128 no oil/foam interface (foam & aeration)	114 no oil/foam interface (foam & aeration)	-
0-76-5 plus 1.5% PANA and 1.5% TCP	311 oil/foam interface	325 oil/foam interface	123 oil/foam interface	58 oil/foam interface	113 oil/foam interface

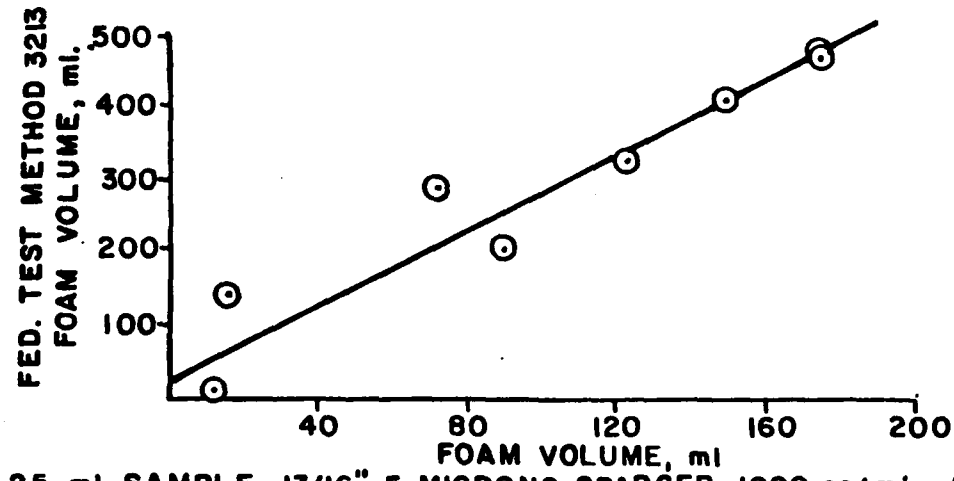

LUBRICANTS HAVING DISTINCT
OIL FOAM INTERFACE

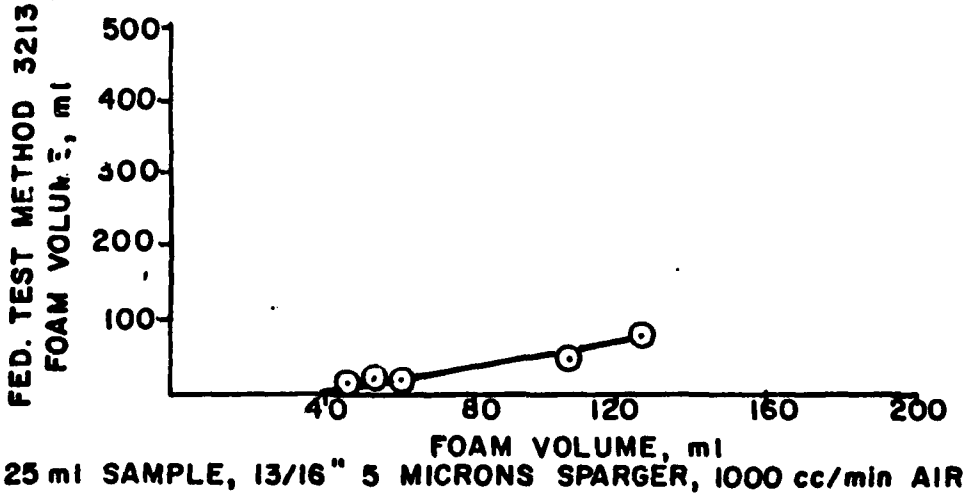

LUBRICANTS HAVING NO OIL / FOAM
INTERFACE AND SEVERE AERATION

Figure 61. Correlation Between Fed. Test Method 3213 and 25 mL Volume Foam Test for Lubricants with Oil/Foam Interface and Lubricants Having Severe Aeration and No Oil/Foam Interface

gave relatively good correlation between the foam values obtained using the two tests and is shown graphically in Figure 61.

Five lubricants gave very poor correlation between the two tests which is also shown in Figure 61. Three of these lubricants (O-79-17, O-79-20 and O-82-2) had low foaming values (20 or below) using Method 3213 but gave severe aeration and no oil/foam interface which resulted in the aeration being measured as foam using the small volume test. The effects of changing airflow rates for these lubricants are shown in Figures 62 and 63. These figures show that for airflows above 750 cc/min oil aeration becomes very severe for these three lubricants using the small volume test. Lubricant O-82-14 also shown in Figure 63 was very sensitive to airflow rates above 500 cc/min in either test and produced an aeration/foam mixture which gave difficulty in determining exactly what was aeration and what was foam when using the small volume test. Lubricant O-79-16 produced a "milkshaking" appearance using the small volume test with a questionable oil/foam interface at an airflow of 800 cc/min. This lubricant also gives "milkshaking" using Method 3213 at airflow rates just above 1000 cc/min as shown by Figure 64. This does not increase the height of foam but increased the reported foam volume greatly and abruptly due to the disappearance of an aeration/foam interface at which time all aerated lubricant is reported as foam.

f. Summary

This study has shown that many physical properties of foam test equipment, test conditions, synergistic effects of some lubricants and test equipment and the different degrees of lubricant aeration characteristics affect measured foam values. Specifically, this study has shown the following in addition to the conclusions of Phase 1 effort.[1]

(1) The correlation was good between Method 3213 and the small

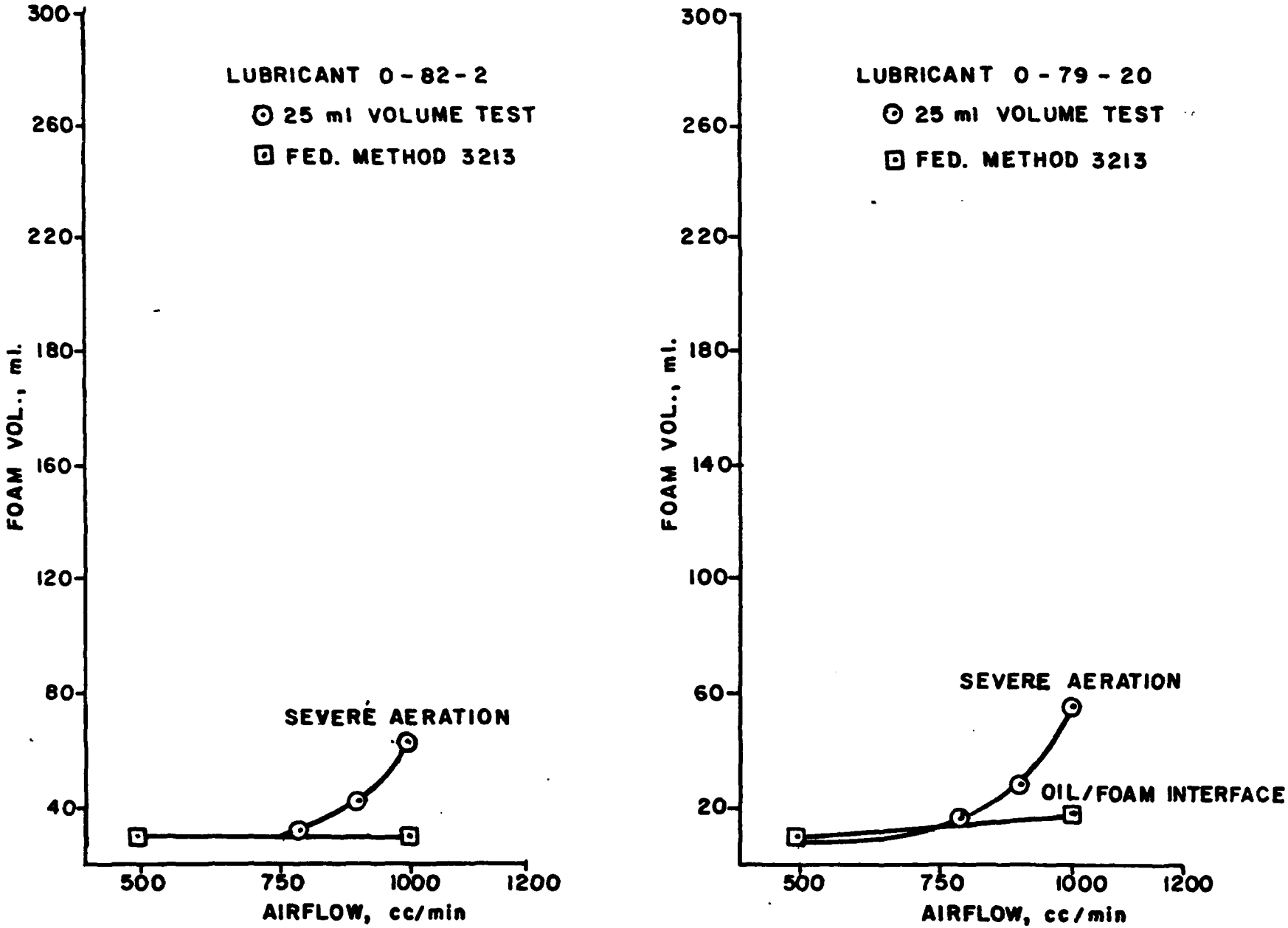

Figure 62. Effect of Airflow on Degree of Aeration and Foaming for Lubricants 0-82-2 and 0-79-20 (13/16" Diameter 5 Micron Sparger used for 25 mL Test)

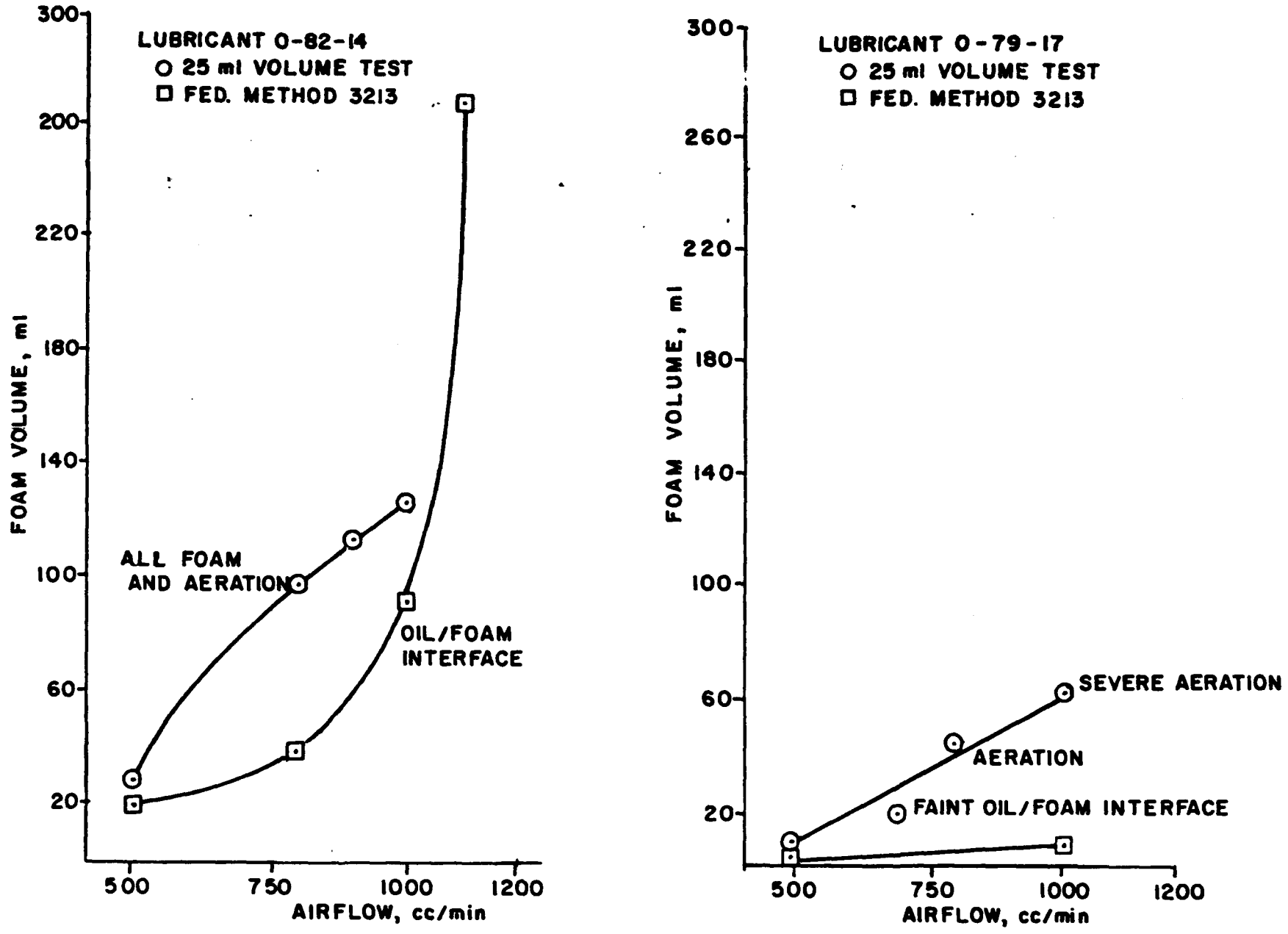

Figure 63. Effect of Airflow on Degree of Aeration and Foaming for Lubricants O-82-14 and O-79-17 (13/16" Diameter 5 Micron Sparger used for 25 mL Test)

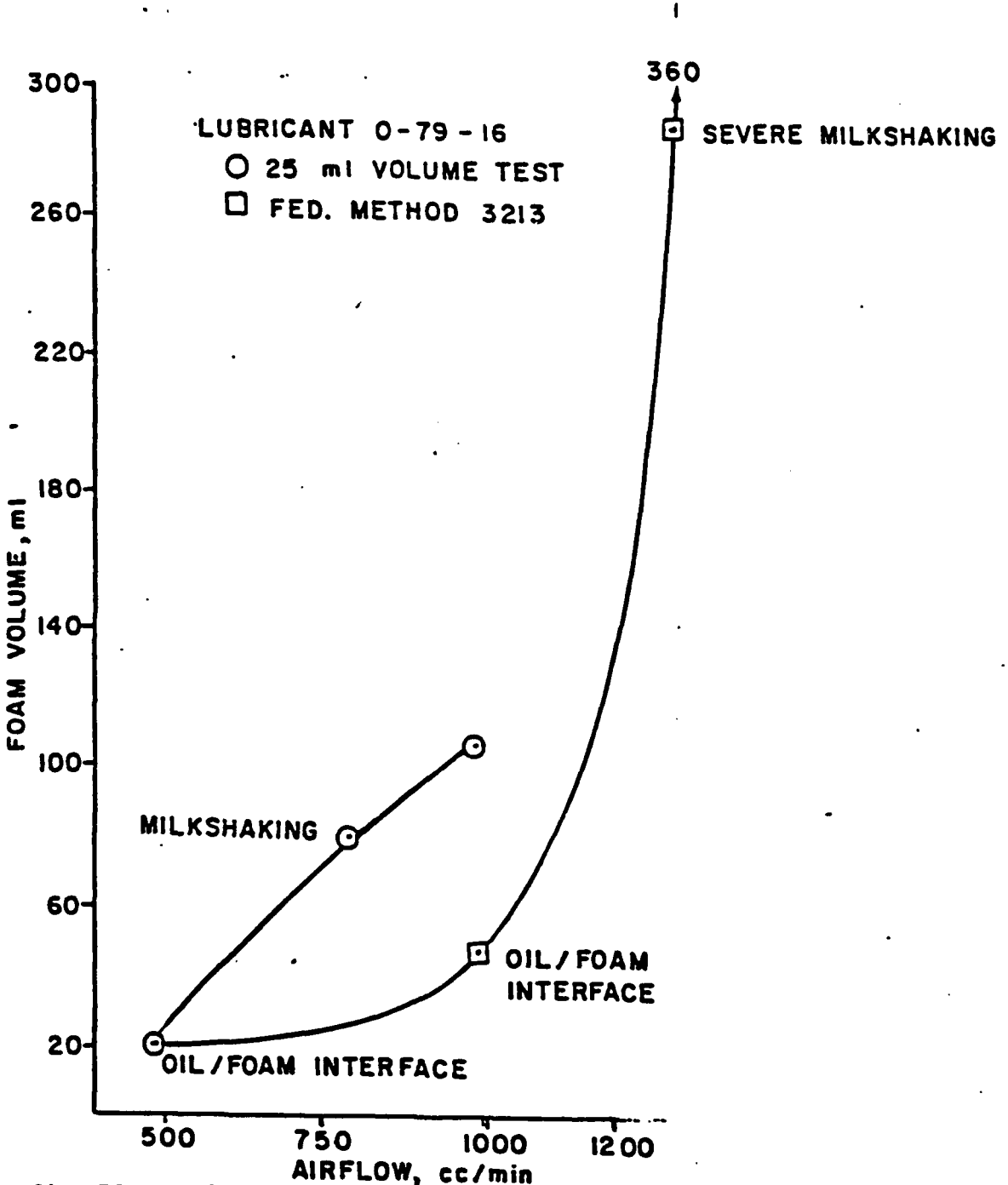

Figure 64. Effect of Airflow on Degree of Aeration and Foaming for Lubricant 0-79-16 (13/16" Diameter 5 Micron Sparger used for 25 mL Test)

volume method using the 13/16" diameter 5 micron pore size sparger and 1000 cc/min airflow for lubricants having distinct oil/foam interfaces.

(2) No correlation existed between the two tests for non-foaming lubricants (20 mL foam) having differences in aeration characteristics.

(3) Changing airflow rates, sparger diameter or rated pore size does not improve the correlation between the two tests.

(4) The small volume test showed large differences in the aeration characteristics of low foaming oils not shown or considered in Method 3213.

(5) Lubricants having severe aeration characteristics but low foaming values could cause problems such as pump cavitation. The degree of aeration should be considered during foam testing.

SECTION III

DEVELOPMENT OF IMPROVED LUBRICATION SYSTEM HEALTH MONITORING TECHNIQUES

1. INTRODUCTION

Diagnostic methods for determining the health of gas turbine engines include the use of oil contamination monitors as important indicators of the condition of lubricant-wetted components. The primary engine health monitoring technique used extensively by the United States Air Force is the Spectrometric Oil Analysis Program (SOAP). Health monitoring devices used by SOAP are specifically designed to monitor the change in specific wear metal concentration with time. Atomic emission (AE) and atomic absorption (AA) spectrometric analysis involves the measuring and trending of contamination levels while in-line magnetic plugs and chip detectors are used to detect a rapidly progressing component failure before it becomes catastrophic.

Emission and absorption spectrometers have been shown to be effective in detecting wear particles smaller than 3-10 microns.[14] Chip detectors generally monitor particles larger than 100 microns. Wear particles with sizes above the SOAP spectrometers' and below the chip detectors' detection limits can be determined using Ferrographic techniques.[15] The Ferrograph has been developed to magnetically precipitate wear particles according to their sizes onto a glass slide. Individual particles may be observed and studied by using a bichromatic microscope or a scanning electron microscope.

Since all currently used monitoring techniques are particle size dependent, costly, and not specific for all wear mechanisms, the particle detection capability of engine health monitoring techniques was investigated. During the evaluation period, techniques that can improve particle detection and improve the diagnostic capabilities of wear metal analysis methods were

also considered. The impact of using 3 micron absolute filters in the engine lubrication system was evaluated with regard to continued use of present Air Force engine health monitoring techniques. A microfiltration test rig was built to simulate fine filtration in lubrication systems, to determine the effect of fine filtration on engine wear debris and determine the impact of fine filtration on SOAP.

2. BACKGROUND

During the past 15 years, increasing costs of materials and labor have focused attention on the problems generated from the wear of oil-wetted components. The detection and identification of wear particles is of critical importance since their presence is indicative of component wear. Another critical factor is that these particles can often accelerate more complex wear mechanisms which further degrade component surfaces. Several cases have been documented where large metallic wear particles produced by severe wear mechanisms are not being quantitatively analyzed. The inability to detect large wear particles has led to engine component failure without prior indication of wear as determined by spectrometric analysis techniques.[16] The failure of SOAP to predict impending engine failure is directly related to the particle detection limitations of currently used SOAP wear monitors.

Corrosion, fluid breakdown, fatigue, adhesion, and abrasion are primary wear mechanisms which produce wear metal particles of different types and morphology. Normal rubbing wear produces small particles which are readily detected by SOAP spectrometers while the large particles produced by abrasion and erosion are not readily detected and their presence can rapidly degrade component surfaces in the oil-wetted system.

Filtration constantly removes the large particles of wear and other

debris suspended in the fluid. This process should maintain a relatively clean lubricant within the system. If wear particles are not removed, they can generate secondary wear modes which may further degrade component surfaces. However, if wear debris is removed by filtration, valuable information about the health of the engine can be lost. Because wear particles carry within them important information about the mechanisms of wear, and because their size can be directly related to severity of wear, it may be important that these particles be captured and analyzed.

The analysis of wear particles is an important tool for diagnosing wear regimes and predicting life expectancy of oil-wetted components. The study of particle morphology can reveal a wealth of detailed and important information about the health of an engine. Information which can be determined by analyzing wear debris includes particle shapes, composition, size distribution, concentration, and rate of wear. If obtained, this information can be used to identify engine components experiencing wear so that appropriate maintenance action can be taken to replace abnormally wearing engine components.

The effectiveness of two rotating disk emission spectrometers and two plasma emission spectrometers and one atomic absorption spectrometer were previously evaluated for analyzing metallic particles. None of these instruments quantitatively analyzed particles larger than 3-10 microns. The rotating disk electrode (RDE) emission spectrometer utilized by SOAP can detect up to 10 micron in size particles but cannot quantitatively analyze particles larger than 1-3 microns.[15,17]

The poor particle detection capability of the various spectrometric methods is primarily the result of the limitations inherent in their sample introduction systems and source energy. Although the present sample

introduction systems are designed to transport homogeneous solutions, these systems can be improved to transport nonhomogeneous samples and thereby improve the particle detection capabilities of the spectrometer.[17]

Complete characterization of wear particles as to their size, shape, and chemical nature is not possible by SOAP. Clearly, supplementary methods of independently measuring the size, shape, and chemistry of particles are required.

3. ATOMIC EMISSION SPECTROMETER

a. Rotating Disk Electrode Ashing Study

(1) Introduction

The goal of this effort was to improve the particle detection capability of the atomic emission spectrometer. Direct application of the oil sample to the rotating disk electrode (RDE) was studied using 75 µL sample volumes and two exposure times. Once the optimum exposure time was determined, higher density carbon disks and gold coated disks were used.

(2) Procedure

An oil sample volume of 75 µL was placed on a disk of the RDE (Thermo-Jarrell Ash Model 750) while slowly rotating the disks on a glass rod. The glass rod was placed on a grooved edge petri dish so that the disks would not touch the dish. The disk was ashed in a muffle furnace at 500°C for 10-12 minutes and was cooled in a desiccator for 10 minutes. Duplicates were run on most of the samples to determine the repeatability of analysis.

(3) Effect of Exposure Time and Spark Intensity

The emission spectrometer exposure time as well as the spark intensity were varied and the results are reported in Tables 54 and 55. These parameters were studied using 75 µL sample volumes. The data shows that repeatability is poor in all cases; however, the 10 second exposure time

TABLE 54
EFFECT OF SPARK INTENSITY ON EMISSION SIGNAL OF FE PARTICLES
USING 10 SEC EXPOSURE TIME AND 75 µL SAMPLE VOLUME

	Spark Intensity			
Sample	80 Conc (ppm)	85 Conc (ppm)	90 Conc (ppm)	95 Conc (ppm)
5-10 micron	378	873	399	707
44.2 ppm	156	511	387	602
10-20 micron	158	484	179	490
45 ppm	99	292	129	271
20-30 micron	184	69	118	144
40.3 ppm	31	56	97	21
Blank	0	2	1	2
	0	0	0	2
100 ppm Fe Std	145	205	150	143
200 ppm Fe Std	293	324	357	273
	219	266	189	266

TABLE 55
EFFECT OF SPARK INTENSITY ON EMISSION SIGNAL OF FE PARTICLES
USING 20 SEC EXPOSURE TIME AND 75 µL SAMPLE VOLUME

	Spark Intensity			
	80	85	90	95
Sample	Conc (ppm)	Conc (ppm)	Conc (ppm)	Conc (ppm)
5-10 micron	79	58	92	67
44.2 ppm	40	47	56	39
10-20 micron	12	49	52	57
45 ppm	6	23	27	-
20-30 micron	12	33	26	20
40.3 ppm	9	13	19	-
Blank	0	0	1	2
	0	0	-	-
50 ppm Fe Std	35	48	71	-
	29	34	-	-
100 ppm Fe Std	82	118	103	132
	69	118	88	111
200 ppm Fe Std	-	198	232	232
		163	226	213

gave higher emission signals than the 20 second exposure. A spark intensity of 85 or greater was optimum for the analysis of dissolved Fe (Conostan Standard) and iron particles. The results also show that the spark source analyzed smaller size particles (5-10 microns) more effectively than the larger ones.

(4) Effect of Surface Density on Emission Signal

Rotating disks were coated first with germanium and then with gold by vaporizing and condensing metal on the surface of the disk. The coating process was performed using Evaporator Model 12500 (Ernest F. Fullam Incorp., Schenectady, NY). High and low apparent density disks, 1.8 and 1.6 g/cm^3, respectively, obtained from Ultra Carbon were also used in the study. Twenty-five microliter samples were applied on the surface of the disks. The disks were ashed and analyzed by emission spectroscopy using a 10 sec exposure time and a spark intensity of 90. The comparative results reported in Table 56 show that the higher density disks were the best for dissolved Fe (Conostan Standard). The high density surface provided less permeability for the dissolved Fe and therefore Fe remained on the surface and was evidently analyzed more efficiently than Fe on the lower density disks. However, lower density disks gave higher results for Fe particles larger than 10 microns than the higher density disks. Larger particles may tend to be trapped in the craters of the more porous surface and provide a better target for the spark than the loosely seated particles on the higher density disk surface. Gold plated disks gave the best signal for particles less than 10 microns.

b. Electronic Spark Source with Reversible Polarity Pin Stand

(1) Introduction

Different bottom electrode geometries were studied in order to determine which shape gave a maximum, repeatable signal. Four different

TABLE 56
EFFECT OF DISK ELECTRODE SURFACE DENSITY ON THE
FE EMISSION ANALYTICAL SIGNAL

	Au Coated Disks	Ultra Carbon	Old Disks
Sample[a]	Conc (ppm)	Conc (ppm)	Conc (ppm)
Blank	1	3	1
		2	
100 ppm Std	140	297	49
	129	294	37
200 ppm Std	285	704	116
	277	702	96
0-5 um	58	25	37
# 2	50	19	35
5-10 um	298	163	105
44.2 ppm[b]	283	97	90
10-20 um	44	12	71
45 ppm[b]	32	6	52
20-30 um	30	13	54
40.3 ppm[b]	28	3	48

[a] 25 uL Sample Volume Was Used
[b] Gravimetric Concentration

techniques were used with the last two yielding the best results.

(a) A commercially available bottom cup electrode used with a graphite powder oil mixture.

(b) The same electrode but only oil was used in the cup.

(c) A shallow concave electrode which was manufactured in-house.

(d) A cup-tip electrode which was manufactured in-house

(2) Procedure

(a) Electrodes

Approximately 20 mg of graphite was placed in the cup electrode. This amount was sufficient to fill approximately half the cup. Ten µL of oil sample was pipetted onto the graphite which absorbed it. The electrodes were then placed in a muffle furnace at 500°C for 5 to 6 minutes in order to ash the sample. The electrodes were removed from the furnace and were allowed to cool in a desiccator for about ten minutes. No ashing was performed on the second set of electrodes which utilized the same bottom cup, the same sample size but no graphite powder was added. For the third set two modified forms of the cup electrode were used (Figure 65). The cups of the electrodes were snapped off leaving a flat surface. A concave tip electrode with a rise in the center and a small lip on the edge was made using a lathe (Figure 65a). One other lathe cut tip was used which differs from the previous electrode in that it was completely concave and had no rise in the center (Figure 65b). Ten µL sample size was used with these lathe cut electrodes along with a 5 minute ashing period.

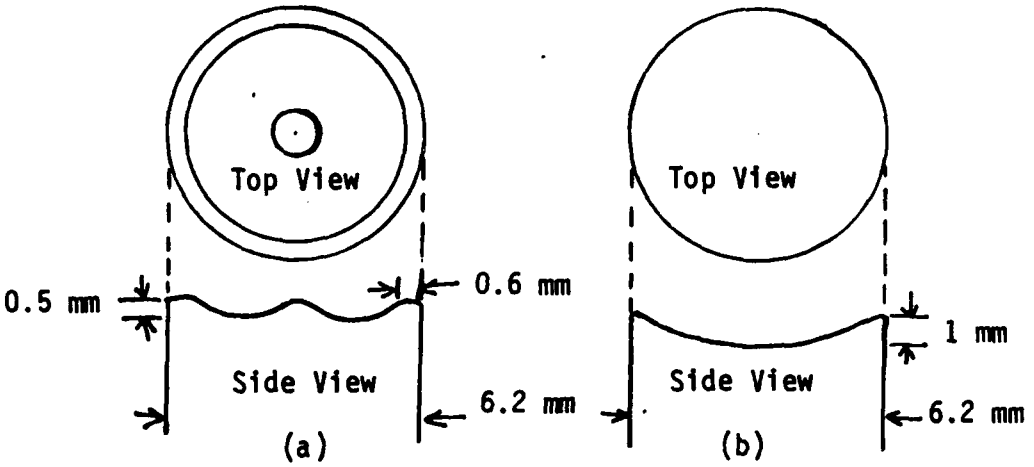

Figure 65. Top View and Side View of DC Arc Bottom Electrodes' Configurations Having (a) Concave Dip with a Rise in Center and (b) Concave Dip

The fourth set of electrodes were made from the top (pin) electrode having the tip modified to look like a cup with a rise in the center (Figure 66). A sharpener (Figure 67) was designed and mounted on a motor similar to the atomic emission top electrode sharpener. It is capable of creating a cup-tip on the AE pin electrode. The cup-tip has approximately a 10 μL capacity.

(b) Emission Spectrometer Parameters

On each type of the above samples the parameters such as preburn time, exposure time, electrode gap setting, spark intensity and the

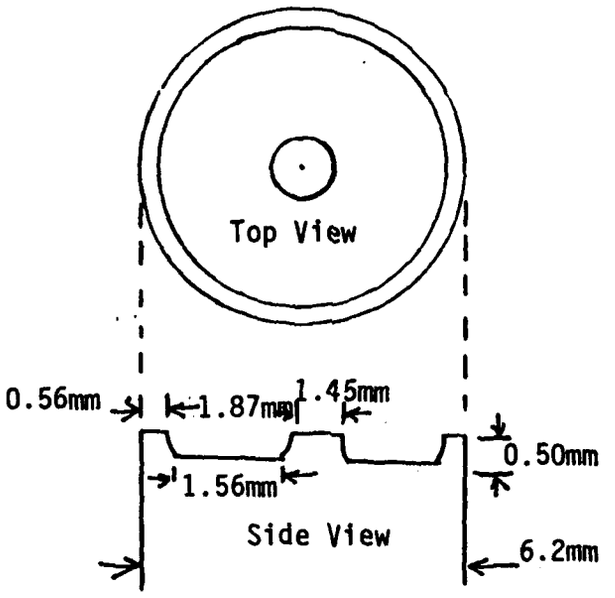

Figure 66. Cup-Tip Electrode

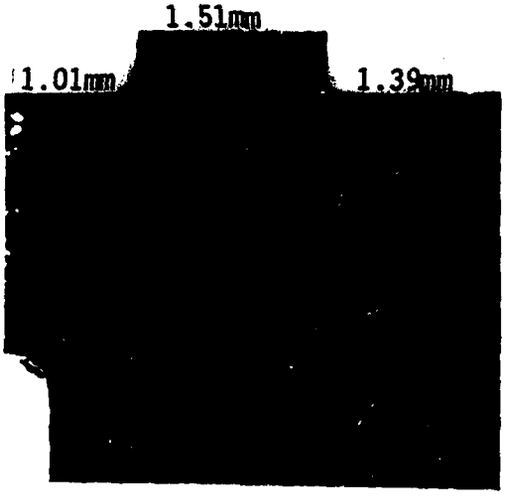

Figure 67. Side View of Cup-Tip Electrode Sharpener

gas flow were held constant. Below is a summary of the instrument settings used for this study.

Preburn	0 Seconds
Exposure	15 Seconds
Electrode Gap	3.0 mm
Spark Intensity (SI)	80%
Gas Flow (Air)	4 L/min

(3) Results and Discussion

Poor results of Fe concentrations were obtained (Table 57) with the graphite oil mixture in the bottom cup electrode. After several runs it was determined that the spark was expelling the majority of the oil/graphite mixture. In an attempt to minimize this problem the oil sample was pipetted directly into the cup electrode. Very little improvement was noted except in the 100 ppm Fe Conostan Standard. Upon inspection of the lower cup electrode it was noted that most of the spark discharge was occurring on the rim of the cup. A shallow cup was used and as can be seen in Table 58 the concentrations and intensities were improved considerably.

The intensities were increased again by using a lathe to cut the electrodes to a very shallow concave tip. The blank Fe value increased possibly due to the cutting tool contamination. Two other analyses were made using a deeper lathe cut tip as shown in Figure 65b. A decrease in intensity was noted and no further electrodes were made in that configuration.

A different lower electrode configuration was used in order to improve the AE spectrometer's sensitivity. A cup electrode sharpener was designed and mounted on a motor similar to that of the top electrode sharpener. A silver coating was applied to some of the cup electrodes in order to reduce the porosity of the graphite surface. An aliquot of 10 µL of the oil sample was deposited on the cup electrode and ashed for 20 minutes in the muffle furnace at 500°C. The electrode was allowed to cool to room

TABLE 57
EFFECT OF CUP GEOMETRY OF THE DC ARC STAND ON FE EMISSION SIGNAL

Mode / Sample	Ashed Graphite/ Oil Mixture in Cup Electrode Conc (ppm)	No Ashing Oil in Cup Electrode Conc (ppm)	Ashed Hand Concave Electrode Conc (ppm)	Ashed Lathe Cut Electrode Conc (ppm)	Direct Reading Normal Conc (ppm)
Blank	0	0	3	14	0
100 ppm Fe Std	8	38	30	86	196
	2	37	30	53	177
5-10 µm 44.1 ppm Fe	0	0	64	80	-
	0	0	54	76	-
5-10 µm 201 ppm Fe	22	3	423	900	-
	9	0	244	900	-
10-20 µm 7.5 ppm Fe	0	-	-	23	0
	0	-	-	15	-
10-20 µm 45 ppm Fe	0	-	-	98	-
	0	-	-	63	-
10-20 µm 90 ppm Fe	13	0	33	109	1
	0	0	16	92	0
20-30 µm 7.5 ppm Fe	0	10	-	45	0
	0	-	-	29	0
20-30 µm 15.3 ppm Fe	0	-	-	114	0
	0	-	-	49	0
20-30 µm 40.3 ppm Fe	0	-	-	69	-
	0	-	-	45	-
20-30 µm 95 ppm Fe	4	0	28	75	4
	3	0	13	70	0
POD #1 140 ppm Fe	17	59	-	766	478
	15	7	-	753	449
TF39 97 ppm Fe	0	38	-	114	182
	-	33	-	98	181
325 mesh 85 ppm Fe	4	14	-	808	38
	1	8	-	421	37

temperature in a desiccator prior to AE analysis. Figure 68 shows the analytical curves for Fe Conostan standards using the cup electrode, silver coated cup electrode, and the regular rotating disk electrode. The silver coated cup electrode produced higher emission signals than the uncoated cup electrode. It seems that the Fe in Conostan standard (containing oil soluble organometallic Fe) was absorbed beyond the uncoated graphite surface and thus produced lower Fe emission signals. However, coating the cup electrode surface with silver minimized the "soaking" effect. Apparently, the silver layer was not thick enough to totally eliminate soaking of the oil since the values obtained from the rotating disk electrode were higher for Fe Conostan for concentrations of less than 50 ppm.

Conostan standards of 0, 10, 50 and 100 ppm of Fe prepared in MIL-L-7808 were studied using the cup-tip electrode comparing uncoated, silver coated cup type electrodes (evaporative coating), double coated silver electrodes and single coated gold electrodes. For each analysis an aliquot of 10 microliters of the oil sample was deposited on the cup electrode and ashed for 20 minutes in a muffle furnace at 500^{o}C. The electrode was then allowed to cool to room temperature in a desiccator prior to AE analysis. The ashed electrodes containing the sample were analyzed using a 0 second preburn and a 10 second exposure.

The coated electrodes gave a much better linear relationship between emission intensity and concentration (Figure 69). More specifically the double coated silver electrodes gave the highest intensities, with the 100 ppm iron standard giving intensity values approximately 4 times greater than the uncoated electrodes. The gold coated electrodes gave intensity values close to those of the double coated silver electrodes. the single coated silver electrodes gave intensities approximately 25% lower than the

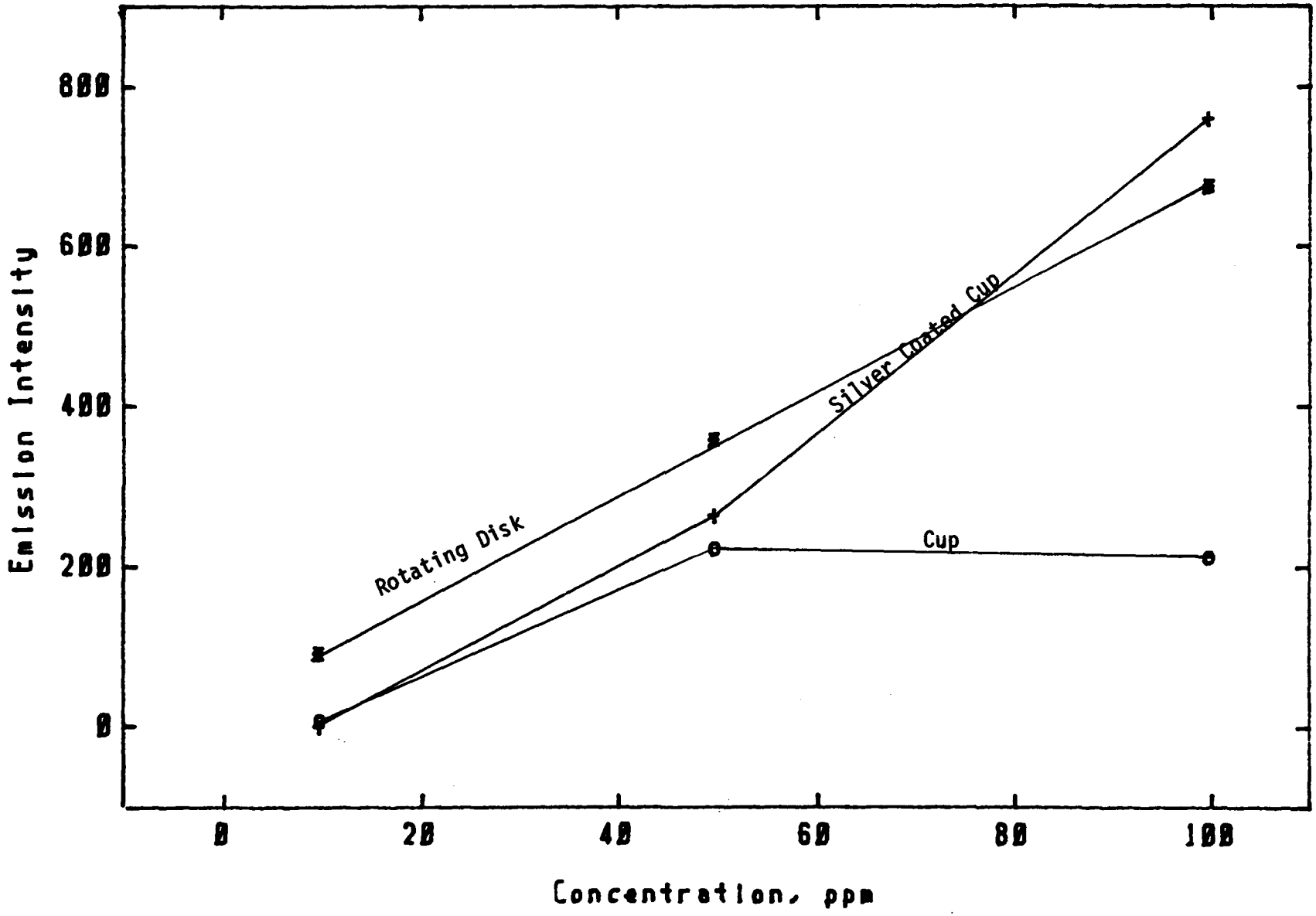

Figure 68. Atomic Emission Intensities Using Fe Conostan Standards and Three Types of Lower Electrodes

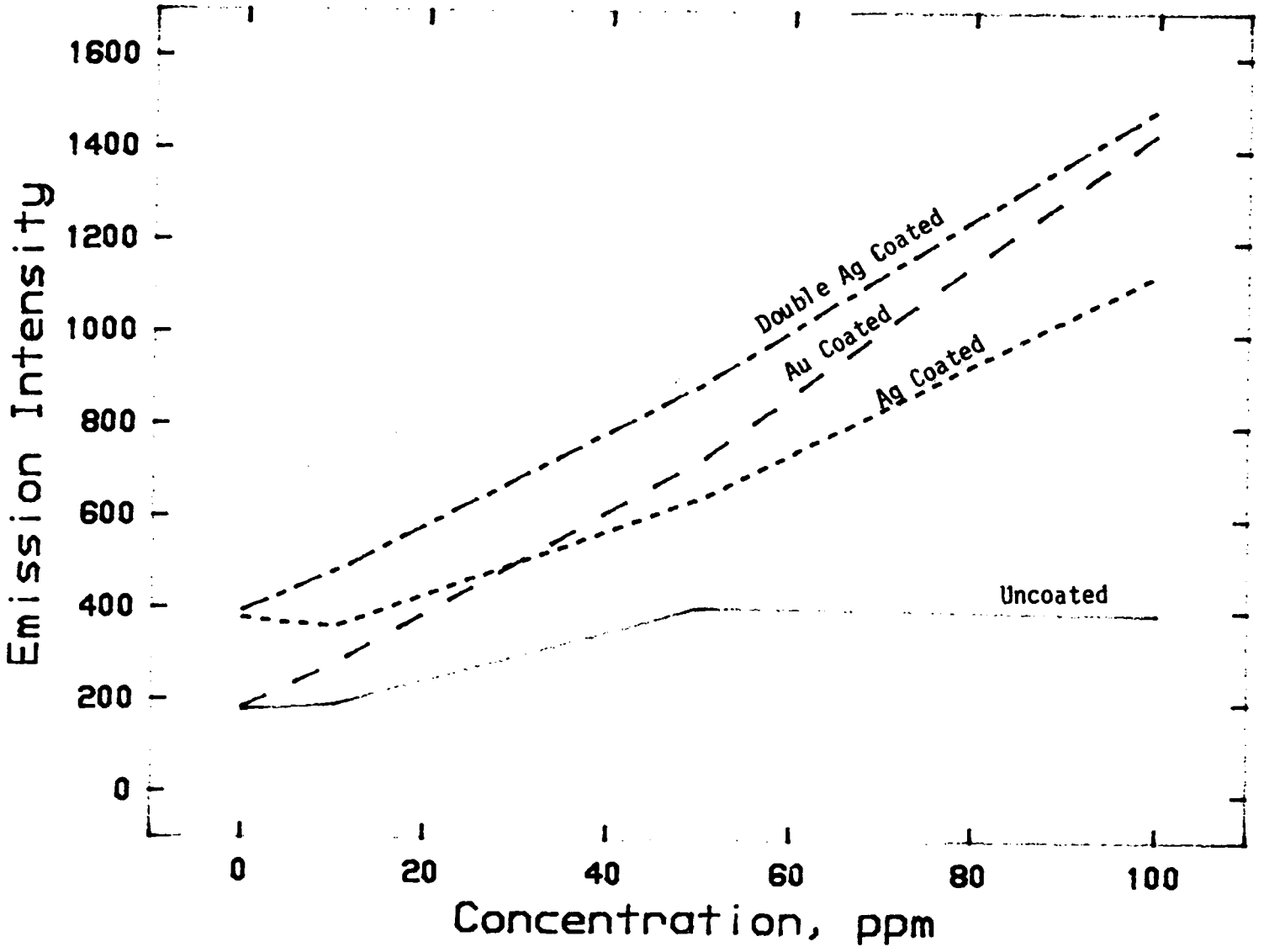

Figure 69. Emission Intensities for Fe Standards Using Coated and Uncoated Cup-Tip Electrodes

double coated silver electrodes but still approximately 3 times greater than the intensities of the uncoated electrodes. The coated electrodes also gave higher intensity readings for the 10 and 50 ppm standards. Since the coating thickness was not determined for the coated electrodes, the difference in the analytical results between the different coated electrodes could be due to differences in the coatings. However, the data does show that soaking of the oil soluble organometallic iron (Conostan Standards) beyond the graphite surface produces lower Fe emission signals, while for undissolved Fe, the particles tend to stay at the surface of the electrode and the analysis is more quantitative. Therefore, if the Fe standard is absorbed beyond the surface and the Fe particulate in the sample is not, the result would be exaggerated.

A pin-on-disk wear test oil sample (POD # 1) containing Fe wear debris from 1018 steel specimen was analyzed using the above coated and uncoated electrodes. The results (Table 58) show the gold coated electrode yielded the lowest value (least exaggerated).

TABLE 58

ATOMIC EMISSION INTENSITIES FOR UNCOATED AND COATED CUP-TIP ELECTRODES

Fe Concentration (ppm)	Uncoated	Double Ag	Ag	Au
0	179 ± 11	394 ± 98	378 ± 136	184 ± 28
10	190 ± 4	479 ± 58	359 ± 97	277 ± 28
50	404 ± 113	887 ± 204	642 ± 38	724 ± 116
100	393 ± 12	1491 ± 179	1131 ± 159	1438 ± 417
POD # 1 (ADM =24-28 ppm)	471 ± 146	1154 ± 173	829 ± 257	655 ± 39
Fe ppm in POD # 1 Using linear regression	97.7 ± 12.1	70.9 ± 12.1	64.7 ± 14.9	39.9 ± 6.0

(4) Conclusions

The ashing technique used in this work offers several advantages relative to the conventional rotating disk technique. Ashing minimizes the matrix interference, increases the sensitivity of the spectrometer by preconcentrating the sample on the surface of the electrode and reduces sample analysis time. These studies have also shown that a correlation exists between the intensity of the analytical signal obtained and the geometry of the electrode's surface exposed to the spark. An optimum tip geometry was found by taking the following configurations into consideration. If the electrode tip is cut too deep the spark discharge was mainly on the rim missing a good portion of the sample. A shallow cup accommodates only a small volume of sample which produces a reduced emission signal. The shallow concave electrode with a raised center appears to optimize the two extreme configurations and higher density carbon would help prevent the oil sample from soaking into the electrode. The coated cup-tip electrode, which is similar to a shallow concave electrode with a raised center, gave the most promising results for standards and oil samples containing wear debris. Several coating techniques are still under investigation.

4. MICROFILTRATION

a. Introduction

Introducing fine filtration in lubrication systems may be beneficial in reducing the amount and size of wear debris, minimizing three-body wear and increasing the time between oil changes. However, the impact of using fine filtration (3-10 micron) in aircraft lubrication systems is of primary concern here because it removes larger size wear particles from the main stream of lubrication systems. Since wear particles carry within them important information about the health of oil-wetted parts, their removal through filtration may result in losing valuable information about engine

wear. Another factor of concern is the effect of fine filtration on the threshold values already established in SOAP. The Air Force relies on these guidelines to determine the health of their operating engines. Any change within the lubrication system such as filtration could have an impact on the analytical results and the present threshold values and guidelines may have to be revised.

In this work, a microfiltration test rig was designed and built during the first phase of this program.[1] Six different oil samples were filtered through the 3 micron filter. The wear debris was characterized in the pre-filtered and post-filtered samples and the particle size distribution was determined. Spectrometric Oil Analysis was also performed to evaluate the impact of microfiltration on SOAP.

b. Background

Within the last decade ultrafine filtration has been introduced into several new engines by retrofitting micron size filters into these engines. The primary objective is to extend component life by reducing the amount and size of wear debris in the lubrication system. The development of the first known 3 micron absolute oil filter for the development of the T53 gas turbine lubrication system is described by Lynch and Cooper.[18] The filter ran for approximately 300 hours without clogging. Its use provided a cleaner lubrication environment and decreased the frequency of filter inspection and oil drains. As a result one of the major benefits immediately realized was the prevention of abrasive wear caused by 1-5 micron particles. The result of this project provided the background data for the more extensive testing program at Fort Rucker which was established in 1978.[19] The Army established a research and development effort to develop an advanced oil debris discrimination and filtration system for the Bell UH-1/AH-1 helicopters.

Thirty-eight UH-1's were fitted with 3 micron (β_3>200) filters on the engine and transmission lubrication systems in conjunction with full-flow debris monitoring chip detectors. A flight test program was run with more than 70,000 flight hours logged. The major results claimed in this program were as follows:

(1) Engine oil and transmission oil change intervals increased by tenfold and threefold, respectively.

(2) The average filter life was over 1000 hours.

(3) Reduced seal wear and very clean oil wetted component conditions were realized.

(4) "Nuisance" chip lights were greatly reduced.

Wansong[20] deals with the maintainability benefits of 3 micron filtration on the General Electric T700 engine which powers the H-60 series and AH-64 Helicopters. This is the first production engine that incorporates 3 micron lube oil filters from its inception.

Since analysis for wear debris has proven to be a valuable diagnostic tool for determining the health of an engine, the use of fine filtration would raise an important question as to the effectiveness of spectrometric oil analysis due to the filter's "removal" of debris detectable by the spectrometer. Therefore, one of the main objectives of this task was to determine the impact of microfiltration on Spectrometric Oil Analysis Program (SOAP). For this effort a microfiltration test rig was developed in order to simulate wear debris generation and the engine filtration system.

c. Apparatus

Test rig assembly, filter element, filter housing and schematic were reported in the Interim Report[1] of the first phase of this program.

d. Test Lubricants

Table 59 describes the six oils used in the microfiltration test rig.

Used engine oils as well as fresh MIL-L-7808 oil were doped with wear metals generated from a pin-on-disk wear test. Unless otherwise mentioned, each sample was filtered four times and the nomenclature of the pre-filtered and post-filtered samples for each pass are described in Table 60.

TABLE 59

DESCRIPTION OF MICROFILTRATION TEST FLUIDS

Test No.	Description of Test Fluid
1	Qualification No. 11E (MIL-L-7808), containing pin-on-disk wear metal generated from Falex wear test of O-86-2.
2	Oil from Test No. 1, with additional pin-on-disk wear metal.
3	Used MIL-L-7808 lubricant from a test stand J57 aircraft engine.
4	Qualification No. 05A (MIL-L-23699), with wear debris taken from engine simulator.
5	Used 10W30 weight automotive lubricant, containing visibly large amount of debris.
6	Used MIL-L-23699 lubricant from T56 aircraft engine gearboxes.

TABLE 60

DESCRIPTION OF NOMENCLATURE OF MICROFILTRATION TEST SAMPLES

Test Sample	Description
A-1	Pre-filter, first pass
A-2	Post-filter, first pass
B-1	Pre-filter, second pass
B-2	Post-filter, second pass
C-1	Pre-filter, third pass
C-2	Post-filter, third pass
D-1	Pre-filter, fourth pass
D-2	Post-filter, fourth pass

e. Results and Discussion

(1) Wear Debris Generated Within Filtration Test Rig

The amount of wear debris generated by the two gear pumps used in the microfiltration test rig was investigated using iron analyses (AE and ADM) and ferrography.

The main gear pump (Brown and Sharp Model 53) is used for circulating and filtering the test fluid and was evaluated for wear by adding 24 liters of test lubricant to the rig and circulating the fluid for 30 minutes using a 3 micron filter. Samples were then taken at the 1/2 inch and 1/4 inch sampling ports. The filter element was removed and the test lubricant was then circulated for one hour. Samples were again taken from the 1/2 inch and 1/4 inch sampling parts. Coding of the samples are as follows:

Sample Code	Identification
# 1	Sample from 1/2" port. Filter in system, 30 min run.
# 2	Sample from 1/4" port. Filter in system, 30 min run.
# 3	Sample from 1/2" port. No filter in system, one hour run.
# 4	Sample from 1/4" port. No filter in system, one hour run.

Emission Spectrometric analysis of the four samples showed zero ppm iron for samples # 1, # 2 and # 4. Sample # 3 gave a value of 1 ppm iron. The iron content of each sample was also determined using the ADM (acid dissolution/atomic absorption) procedure. The iron content using this technique was 2.3 ppm for samples # 1 and # 2, 2.4 ppm for sample # 3 and 2.6 ppm for sample # 4.

Ferrographic analysis of the samples including percent area covered measurements are give in Table 61.

TABLE 61

FERROGRAPHIC ANALYSIS OF MFR GEAR PUMP TEST SAMPLES

Sample	# 1	# 2	# 3	# 4
Ferrogram Reading (% area covered)				
Entry position	2.9	3.3	16.4	12.8
50 mm position	0.0	0.0	1.7	1.5
10 mm position	0.0	0.0	0.0	0.0
Microscopic Analysis (Type particle)				
Normal Rubbing Wear	Very Few	Very Few	Moderate	Moderate
Severe Wear	Couple	Couple	Few	Few
Cutting Wear	None	None	Few	Few
Dark Metallo-Oxides	None	None	Few	Few
Non-Metallic, Amorphous	Few	Few	Few	Few
Direct Ferrograph Reading				
L (1 mL)	0.5	1.6	1.1	1.1
S (1 mL)	0.6	0.6	1.3	1.9

The second gear pump used in the filtration rig (Viking Model 32) is used for transferring the microfiltration test rig filtered lubricant from Tank B (7 gallon stainless steel seamless container) back into Tank A (microfiltration test rig tank) and for circulating test lubricant from the Falex Wear Tester back into the microfiltration test rig. The small gear pump (1/2 GPM) was disconnected from the test rig and "Poly-Flo" tubing was connected to the inlet and outlet of the pump. The pump was cleaned by circulating 1500 mL of clean lubricant (Qual 11E) through the pump. A 4 liter beaker containing 1500 mL of new oil was used as an oil reservoir. The oil was circulated through the pump for 1 minute and a "before" test sample was taken. The oil was then circulated for 30 minutes and an "after" test sample was taken. Analyses conducted on these two samples are given in

Table 62.

TABLE 62

ANALYSIS OF WEAR DEBRIS FROM SMALL GEAR PUMP

Sample	"Before" Test	"After" Test
Ferrogram Reading (% area covered)		
Entry Position	0.8	0.9
50 mm Position	0.2	0.5
10 mm Position	0.0	0.0
DR Ferrograph Readings		
L Value	1.5	1.2
S Value	1.1	0.9
L/S	1.36	1.33
Iron Analysis		
AE (ppm)	0.9	1.0
ADM (ppm)	0.7	1.6

The data for both gear pumps show that a very small amount of wear debris can be generated by the pumps but is of such a small quantity that this debris would not interfere with subsequent filtration studies.

(2) Wear Metal Generator

It was reported earlier[1] that the pin-on-disk wear configuration produced desirable particle size distribution (0-20 microns) suitable for the microfiltration test rig tests. Several tests under different loads and speeds were performed using 1018 steel disks and 8620 steel pins for determining optimum conditions for generating a high wear rate. In 2-hour tests, the highest wear produced was 186.0 mg from a 65 lb load and 100 fpm speed.

Wear metal generated from the pin-on-disk wear tests under different loads and speeds was analyzed for particle size distribution using a Direct Reading (DR) Ferrograph. The DR Ferrograph provides a good assessment of the ratio of the large particles (>5 microns) to the small ferromagnetic particles (1 to 2 microns) in oils. The results from the DR ferrographic analysis as well as the speeds, loads and weight losses from the wear tests are shown in Table 63.

TABLE 63

DIRECT READING FERROGRAPH RESULTS FOR THE PIN-ON-DISK WEAR TEST SAMPLES

P.O.D.[a] Sample #	Large Particles >5 microns	Small Particles 1-2 microns	Large/Small Ratio	Wt. Loss mg	Load lbs.	Speed ft/min
34	10.9	3.3	3.3	45.1	50	197
35	20.6	8.4	2.4	48.4	50	49
36	42.7	20.8	2.0	9.8	20	49
37	29.6	7.6	3.9	106.2	50	98
39	35.1	14.4	2.4	6.7	20	142
40	71.2	37.9	1.9	3.1	35	49
41	47.6	18.6	2.6	42.9	35	49
42	26.0	5.3	4.9	114.4	65	49
43	21.6	8.1	2.7	21.9	50	150
44	40.1	12.7	3.2	149.4	65	98
45	39.5	17.8	2.2	34.7	100	24
46	16.9	4.7	3.6	186.0	100	74
47	12.2	4.3	2.8	16.3	100	122
48	25.2	10.8	2.3	9.4	20	197
49	48.7	22.1	2.2	4.7	35	197
50	20.6	10.2	2.0	8.0	50	197
51	25.8	10.8	2.4	112.2	80	49

[a]All Samples were diluted to 3 ppm in O-86-2 for Ferrographic analyses

This data shows that high wear is produced, as would be expected, under high load and low speeds. Test #46 and #51 produced 186.0 and 112.2 mg of wear under high loads and relatively low speeds. However, for the particles produced under these conditions the ratio L/S tends to be higher than those particles produced under high speeds and low loads. Figure 70 illustrates the variation of the ratio L/S of the large particles (>5 microns) to the small particles (1 to 2 microns) with respect to the product of load and speed. The data shows that for all loads and speeds used most of the L/S ratios are less than 3. These ratios of wear particles should provide an adequate particle size distribution for the microfiltration test rig study.

(3) Operating and Test Parameters for the Filtration Test Rig

A 100 psi relief valve having a flow coefficient (C_v of 1.8) was installed in order to accommodate a flow of 20 gallons per minute (GPM). The upstream pressure (P_1), downstream pressure (P_2) and the flow in GPM were monitored during the initial operation of the test rig. Table 64 reports P_1, P_2 and ΔP in psi as well as the flow in GPM for the filtration system with and without the filter element. As the flow was varied from 6.1 GPM (filter valve and bypass valves opened) to 21.2 GPM (filter valve opened and bypass valve closed) P increased from 4.9 to 28.8 psi when the system ran with the filter element in the filter housing. However, when the filter element was removed and the rig was operated under similar flow conditions, P was significantly lower and ranged from 2.8 to 19.1 psi. Examining the filter housing revealed the presence of a relief valve which according to specification has a cracking pressure of 14 psi and a full flow at 18 psi. It can be seen from Table 64 that the filter housing relief valve cracked

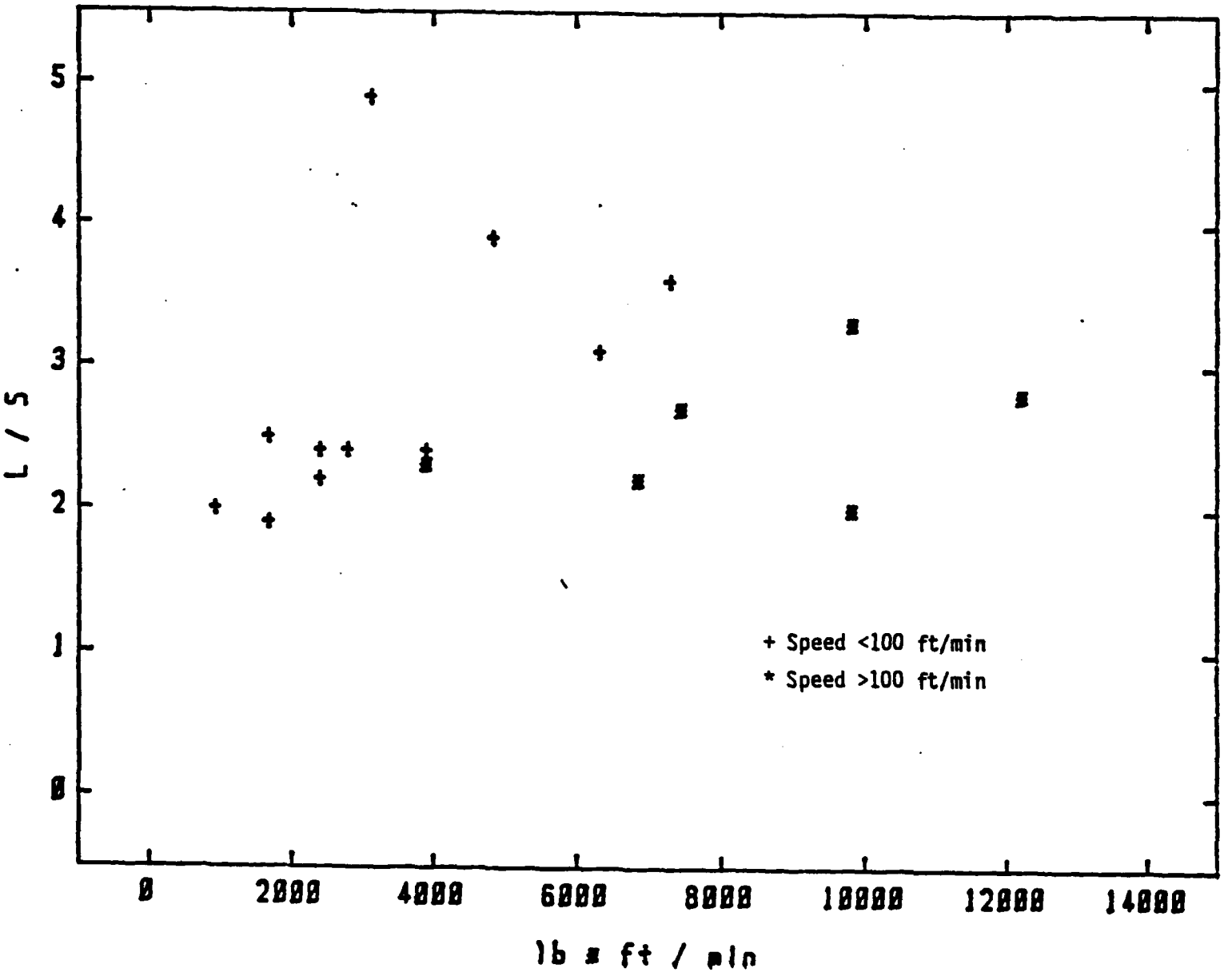

Figure 70. Variation of the Ratio L/S (Large Particle/Small Particle) with the Product of Load and Speed for Wear Debris Generated from Pin-On-Disk Wear Tests

open at about 14 GPM with the filter element in the housing and at less than 19 GPM without the filter element. The filter housing relief valve was permanently disabled for this work due to the 100 psi safety check valve within the filtration system.

TABLE 64

VARIATION OF OIL FLOW AND PRESSURE IN FILTER HOUSING WITH AND WITHOUT THE FILTER ELEMENT

No Filter				With Filter			
P1 psi	P2 psi	ΔP psi	Flow GPM	P1 psi	P2 psi	ΔP psi	Flow GPM
3.7	0.9	2.8	7.4	5.2	0.3	4.9	6.1
5.9	1.8	4.1	9.2	6.0	0.5	5.5	6.5
10.3	3.6	6.7	12.1	9.9	1.6	8.3	9.0
15.2	5.6	9.6	14.7	15.2	3.3	11.9	11.8
20.1	7.5	12.6	17.0	20.0	4.8	15.2	14.0
25.8	9.8	16.0	19.4	25.5	6.5	19.0	16.2
30.5	11.4	19.1	21.1	30.2	8.1	22.1	18.0
30.6	11.5	19.1	21.2	40.0	11.2	28.8	21.2

Table 65 reports the parameters monitored for each test during the microfiltration test rig operation.

TABLE 65

PARAMETERS MONITORED DURING THE MICROFILTRATION TEST RIG OPERATION

Test No. 1

	1st Pass	2nd Pass	3rd Pass	4th Pass
Flow rate (GPM)	18.5	18.5	18.4	18.5
P_1(psi)[a]	26.3	26.2	26.7	26.5
P_2(psi)[b]	10.4	10.7	10.7	10.9
Tank Temp (°C)	102	102	101	100
Line Temp at Filter (°C)	101	102	101	100

[a] P_1 = Pressure upstream of filter
[b] P_2 = Pressure downstream of filter

Test No. 2

	1st Pass	2nd Pass	3rd Pass
Flow rate (GPM)	18.7	18.4	18.9
P_1(psi)	26.4	26.8	27.1
P_2(psi)	11.5	10.7	10.9
Tank Temp (°C)	100	100	99
Line Temp at Filter (°C)	100	100	99

Test No. 3

	1st Pass	2nd Pass	3rd Pass
Flow rate (GPM)	10.7	12.6	17.7
P_1(psi)	24.2	24.9	25.0
P_2(psi)	9.6	9.7	10.0
Tank Temp (°C)	105	100	100
Line Temp at filter (°C)		99	99

Test No. 4

	1st Pass	2nd Pass	3rd Pass
Flow Rate (GPM)	18.1	18.0	19.3
P_1(psi)	30.0	30.0	31.0
P_2(psi)	13.0	13.0	13.0
Tank Temp (°C)	104	100	100
Line Temp at Filter(°C)	103	99	99

TABLE 65 (Continued)

Test No. 4 After 3rd Pass

	Test Time			
	Initial	10 min	40 min	60 min
Flow Rate (GPM)	20.8	20.7	20.5	20.6
P_1(psi)	30.0	29.0	28.6	28.6
P_2(psi)	9.2	11.0	8.7	8.7
Tank Temp (^oC)	96	101	102	102
Line Temp at Filter(^oC)	96	101	102	103

Test No. 5

	1st Pass	2nd Pass[c]	3rd Pass	4th Pass
Flow Rate (GPM)	11.1	18.1	18.4	18.4
P_1(psi)	148	30.9	33.3	34.0
P_2(psi)	11.2	11.6	12.1	12.1
Tank Temp (^oC)	102	100	100	100
Line Temp at Filter(^oC)	101	99	99	99

[c]Second Filter. First filter plugged opening bypass valve on first pass

Test No. 6

	1st Pass	2nd Pass	3rd Pass	4th Pass
Flow Rate (GPM)	18.2	18.5	18.7	18.7
P_1(psi)	28.3	29.1	29.3	28.9
P_2(psi)	11.8	11.7	11.9	11.9
Tank Temp (^oC)	102	100	100	100
Line Temp at Filter (^oC)	101	99	99	99

(4) Microfiltration Testing

(a) Test No. 1

Test Rig

The microfiltration test rig was run after a new filter was installed. The 6.5 gallons of Qual-11E (MIL-L-7808) was doped with 519 gm of O-86-2 containing approximately 1200 ppm Fe wear debris. The Fe wear debris was obtained from several pin-on-disk wear tests as previously described. The sample containing the iron wear was sonically agitated prior to addition

to the rig's oil tank (A). The oil in the rig was allowed to circulate in the bypass mode for 30 minutes. Approximately 300 mL aliquot (A-1a) was sampled before filtering from Tank A and another 300 mL aliquot (A-1) was sampled before filtering at the sampling valve. The oil was allowed to pass through the 3 micron filter and was collected in a 7-gallon container (Tank B). The main pump was turned off soon after the oil was emptied from Tank A. The process of filtering took approximately 15 seconds. During this time, the temperature of the oil in Tank A and in the lines, the pressures of the oil before and after the filter assembly and the oil flow rate were recorded and the results are shown in Table 65. A third 300 mL aliquot (A-2) was taken from Tank B immediately after the oil was filtered for analysis. Similar size aliquots were taken before and after filtering for the second, third and fourth passes with the exception of no A-1a samples being taken. The temperature, pressure and flow rate of these runs were also monitored and recorded in Table 65. Table 65 reveals very little changes in the parameters of the four passes and that these conditions were reproducible in the four runs.

Spectrometric Analysis

Wear debris before and after filtering through the 3 micron filter was analyzed by atomic absorption (AA), atomic emission (AE) and acid dissolution method (ADM). The analytical results are reported in Appendix B and illustrated in Figure 71. The acid dissolution method data shows a significant decrease in the amount of debris captured by the filter after the first pass (62%). However, very little amount of debris was captured for the subsequent passes. In the direct analysis of these samples by AA and AE, a much smaller amount of wear debris was shown to be captured by the filter after the first pass. AA shows less than 7% was captured after the second

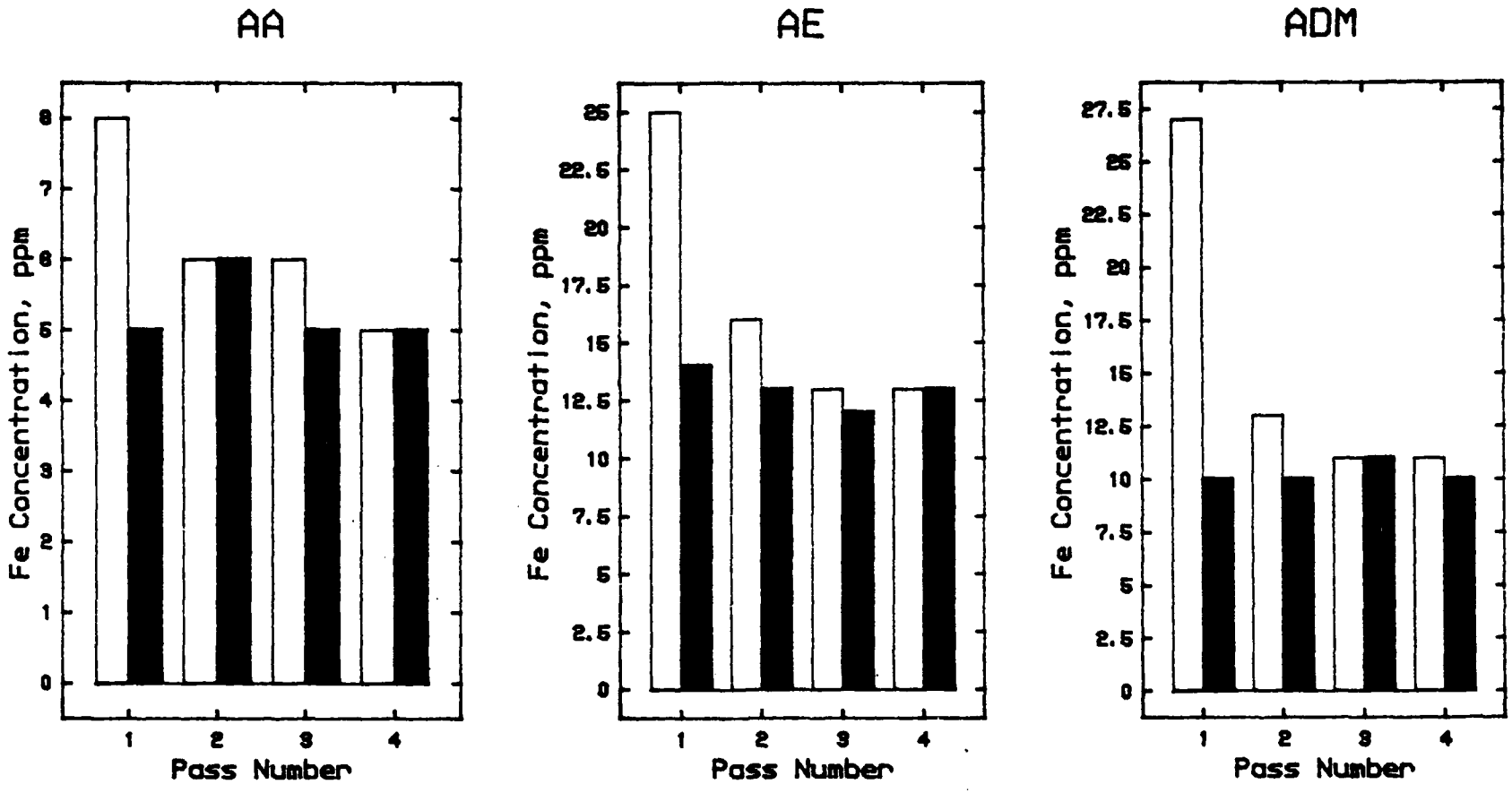

Figure 71. Iron Concentration of Pre- and Post-filter Samples for the First, Second, Third and Fourth Passes of Microfiltration Test No. 1 Using AA, AE and ADM; □ = Pre-filter ■ = Post-filter (MIL-L-7808 Lubricant Containing Pin-On-Disk Wear Debris)

and third passes and practically no debris was shown to be held after the fourth pass. AE revealed that 29% was held on the filter for the second pass and less than 3% for the third and fourth passes.

It is well known that both AA and AE spectroscopy are particle size dependent and do not completely analyze Fe particles greater than 3 microns. Furthermore, the AE results are enhanced by approximately 2 to 3 times the actual values because the ester based lubricants enhance the Fe emission signal relative to hydrocarbon oils. It is for the above reasons that AA and AE values are lower than the ADM. After the second pass neither spectrometer shows significant decrease in the amount of Fe in the filtrate. However, the amount of Fe in the B-1 sample prior to the second pass has increased. No definite explanation can be offered for this increase except that cross contamination from the residual wear particles of the first pass in the bypass lines and pump could be responsible for the increase.

Particle Size Distribution (PSD)

Nuclepore filters were used to determine the PSD of the pre-filtered and post-filtered samples. ADM, Portable Wear Metal Analyzer (PWMA) and AE were used to analyze for Fe in the unfiltered sample and in the filtrates having maximum sizes of 0.4, 1, 2, 3, 5, 8, 10 and 12 microns and the results are shown in Figure 72. The PWMA used in this work was a preproduction prototype, graphite furnace atomic absorption spectrometer. The data from the above three analytical methods shows that the rig's 3 micron filter is effective in capturing the larger particles and allows particles with sizes less than 3 microns to pass through the filter.

Based on the spectrometric analysis and PSD data, microfiltration did influence the AE and AA results. AE and AA were sensitive to the pre-filtered sample. Their results of the pre- and

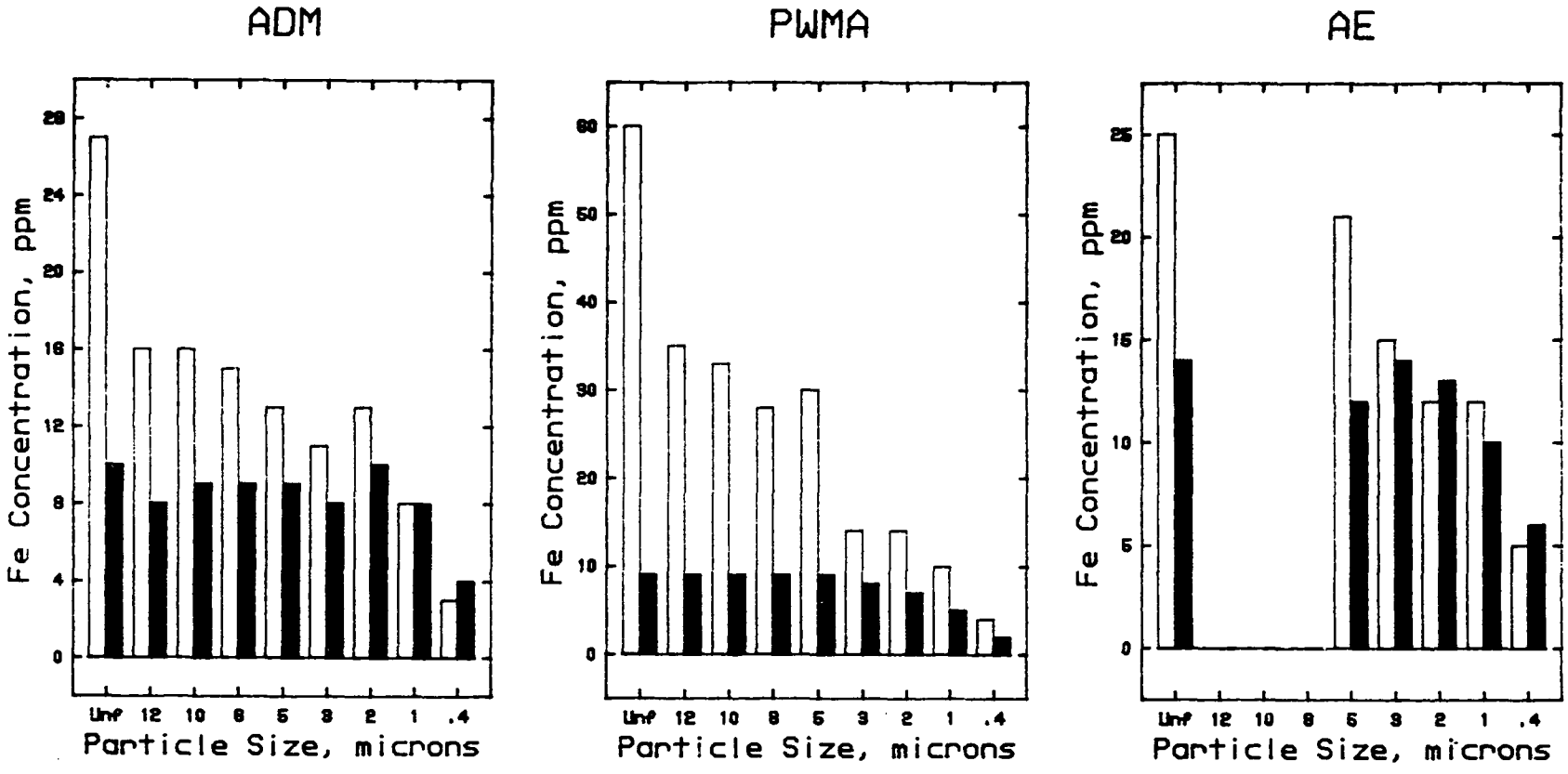

Figure 72. Particle Size Distribution of Iron Wear Debris in Pre- and Post-filter Samples from Microfiltration Test No. 1 Using ADM, PWMA and AE; □ = Pre-filter, ■ = Post-filter

post-filtered samples correlated with the ADM values. These experiments also reveal that AA and AE respond to changes in particle size in spite of the fact that AA and AE do not quantitatively analyze iron particles larger than 1-3 microns.

Ferrographic Analyses

Analytical ferrographic analyses conducted on the samples obtained from microfiltration Test No. 1 using the normal 3 mL sample and diluted samples are given in Tables 66 and 67. Dilutions with clean oil were necessary due to the large amount of wear particles present. Microscopic examination of the ferrograms prepared from the unfiltered sample showed the debris to consist of normal wear, severe wear and cutting wear particles and some nonmetallic debris. As expected, after the first pass through the 3 micron filter, the debris present in all subsequent samples consisted primarily of small normal wear and non-wear particles and a few fibers. Table 66 shows optical density readings of the analytical ferrograms prepared from samples taken from microfiltration Test No. 1 using the standard 3 mL sample size. The data in Table 66 shows the ferrograms contain too much debris for obtaining meaningful optical density readings. This is shown by all L/S values (ratio of large particles to small particles) being close to 1. The high optical density readings (40 and above) obtained at the 10 mm ferrogram position also show excessive debris concentrations for all the samples and that many small particles are not captured on the ferrograms. Table 67 shows optical density readings of analytical ferrograms prepared from the samples obtained from the microfiltration test after dilution to reduce the optical density readings. Data in Table 67 shows that debris concentration has a great effect on L/S ratios. For example Sample A-1 has a L/S value of 1.39 undiluted and 2.45 L/S value when diluted 1 to 9. Sample

TABLE 66

OPTICAL DENSITY READINGS OF ANALYTICAL FERROGRAMS
FOR MICROFILTRATION TEST NO. 1
(Standard 3 mL Sample)

Sample Identification	% Area Covered - Incident Light Ferrogram Position						
	Entry	50 mm	40 mm	30 mm	20 mm	10 mm	L/S[a]
A-1 (Pass 1 Before Filter, Tank)	83.4	79.1	55.9	46.6	45.9	48.0	1.05
A-2 (Pass 1 Before Filter, ¼" Port)	84.3	83.7	75.4	60.2	51.9	43.3	1.01
A-3 (Pass 1 After Filter)	52.4	52.0	49.0	42.9	42.3	42.3	1.01
B-1 (Pass 2 Before Filter)	67.8	62.2	47.1	44.2	43.0	44.6	1.09
B-2 (Pass 2 After Filter)	55.2	55.7	52.4	43.8	38.0	39.7	0.99
C-1 (Pass 3 Before Filter)	56.9	59.5	53.0	44.8	41.6	47.3	0.96
C-2 (Pass 3 After Filter)	52.6	55.8	50.0	46.1	44.2	46.6	0.94
D-1 (Pass 4 Before Filter)	50.7	50.7	54.2	44.1	42.1	43.8	1.00
D-2 (Pass 4 After Filter)	50.5	53.1	47.0	44.5	44.0	47.8	0.95

[a]L/S-Ratio of large particles (entry position) to small particles (50 mm position)

TABLE 67

OPTICAL DENSITY READINGS OF ANALYTICAL FERROGRAMS
FOR MICROFILTRATION TEST NO. 1
(1 mL and Diluted Samples)

Sample	% Area Covered - Incident Light Ferrogram Position						
	Entry	50 mm	40 mm	30 mm	20 mm	10 mm	L/S[a]
A-1 (Pass 1 Before Filter, Tank)	73.6	52.8	24.0	16.6	13.9	20.5	1.39
A-1 (Pass 1 Diluted 1:9)	25.7	10.5	4.3	3.3	2.0	0.8	2.45
A-2 (Pass 1 Before Filter, ¼" Port)	71.4	42.2	30.3	21.6	20.5	21.5	1.69
A-3 (Pass 1 After Filter)	48.6	42.0	39.0	20.1	19.1	20.0	1.16
B-1 (Pass 2 Before Filter)	63.1	48.3	35.7	21.6	16.9	21.4	1.31
B-1 (Pass 2 Diluted 1:9)	17.7	13.5	4.8	3.4	4.2	5.8	1.31
B-2 (Pass 2 After Filter)	45.7[b]	44.7	28.5	17.3	14.2	14.8	1.02
C-1 (Pass 3 Before Filter)	34.8	32.0	34.5	21.6	14.1	13.2	1.09
C-2 (Pass 3 After Filter)	49.8[c]	43.7	31.5	18.6	12.3	13.2	1.14
D-1 (Pass 4 Before Filter)	26.3	35.7	29.2	21.3	15.4	13.6	0.74
D-2 (Pass 4 After Filter)	35.1[c]	42.6	30.4	25.4	19.0	15.0	0.82

[a]L/S-Ratio of large particles (entry position) to small particles (50 mm position)

[b]No true entry deposit. Start of small wear debris

[c]Entry consisting of small wear particles and nonmetallic debris

B-1 had high optical density readings for the entry and 50 mm positions but the same L/S value as the B-1 sample after diluted 1 to 9. This is due to the efficiency of the 3 micron filter retaining the large particles.

Samples obtained from the microfiltration Test No. 1 were evaluated using the Direct Reading (DR) Ferrograph with the test data being given in Table 68.

TABLE 68

DR FERROGRAPH DATA FOR MICROFILTRATION TEST NO. 1

Sample Identification	L Reading	S Reading	L/S Ratio
A-1 (Pass 1 Before Filter)	66.2	25.4	2.61
A-1 (Pass 1 Diluted 1:9)	9.1	3.3	2.75
A-2 (Pass 1 After Filter)	33.7	24.4	1.38
B-1 (Pass 2 Before Filter)	49.9	27.0	1.85
B-2 (Pass 2 After Filter)	41.3	27.7	1.49
C-1 (Pass 3 Before Filter)	40.2	26.5	1.52
C-2 (Pass 3 After Filter)	41.2	27.5	1.50
D-1 (Pass 4 Before Filter)	35.5	24.1	1.47
D-2 (Pass 4 After Filter)	32.0	21.4	1.50

Data shows the L/S ratio remains nearly constant after the first pass through the 3 micron filter. The slightly higher L/S value for the B-1 sample than the A-2 sample is probably due to the small amount of oil remaining in the lube system after the first pass which had not gone through the 3 micron filter. Both the analytical and DR ferrograph data supports the particle size distribution data. The ferrographic data shows that the 3 micron absolute filter is effective in capturing the larger particles and allows particles with sizes less than 3 microns to pass through the filter.

(b) Test No. 2

Test Rig

The microfiltration test rig was run for the second time using a new filter. The Qual-11E (MIL-L-7808) oil used in Test No. 1 contained very fine wear particles which remained in the oil after passing four times through the 3 micron filter during Test No. 1. This oil was doped again with approximately 1.2 g of Fe wear debris prior to use in Test No. 2. The Fe wear was collected from several pin-on-disk wear tests using 1018 steel specimens. The pin-on-disk wear sample was sonically agitated and vigorously handshaken prior to addition to the rig's oil tank (A). The oil in the rig was allowed to circulate in the bypass mode for 30 minutes at 100°C. Approximately 300 mL (Sample A-1) was obtained before filtering at the sampling valve. The oil was allowed to pass through the rig's 3 micron filter and was collected in a 7-gallon container (Tank B). The main gear pump was turned off as soon as the oil was emptied from Tank A. As in Test No. 1, it took approximately 15 seconds to filter 6.5 gallons of oil at 18.7 GPM. During the filtering process, the temperature in Tank A and in the lines, the pressures in the lines before and after the filter assembly and the oil flow rate were recorded and found to be identical to the conditions of Test No. 1. A 300-ml aliquot (A-2) was taken from the container (Tank B) immediately after filtration. Similar size aliquots were taken before and after filtering for the second and third passes. These samples were analyzed to determine the capturing efficiency of the rig's 3 micron filter and the particle size distribution of the wear particles.

Spectrometric Analysis

Samples taken before and after microfiltration were

analyzed for iron wear debris using atomic absorption (AA), atomic emission (AE) and acid dissolution method (ADM). Analytical results are reported in Appendix B and illustrated in Figure 73. The acid dissolution method data shows a significant amount of debris was captured by the filter after the first pass (55%). However, a smaller amount of wear debris was captured in the second (22%) and third pass (5%). Similar trending in direct AA and AE analytical results were obtained for the filtered and unfiltered samples of the three passes but with lower values than the ADM. However, it is clearly shown that the 3 micron filter removes the large particles of wear debris after the first pass and that the amount of Fe in the filtrate remains constant except for B-1. As in Test No. 1 possible cross contamination from the lines and pump could have contributed to this increase in Fe.

Particle Size Distribution

The particle size distribution (PSD) was determined for the unfiltered and filtered samples in order to determine the effective particle size of the filter. The effective particle size of the filter is the particle size that is larger than the pore size of the filter. Therefore, wear particles with sizes larger than the effective size of the filter will be captured by the filter. Figure 74 shows the PSD for the pre- and post-filtered samples of Test No. 2. Again it is seen that the microfiltration test rig filter is effective in retaining particles larger than 3 micron.

The PSD as shown by the ADM curves indicate that this sample has smaller particles than Test No. 1 sample. For this reason microfiltration did not impact the AA results (Figure 73) but differences are still seen by the AE and ADM.

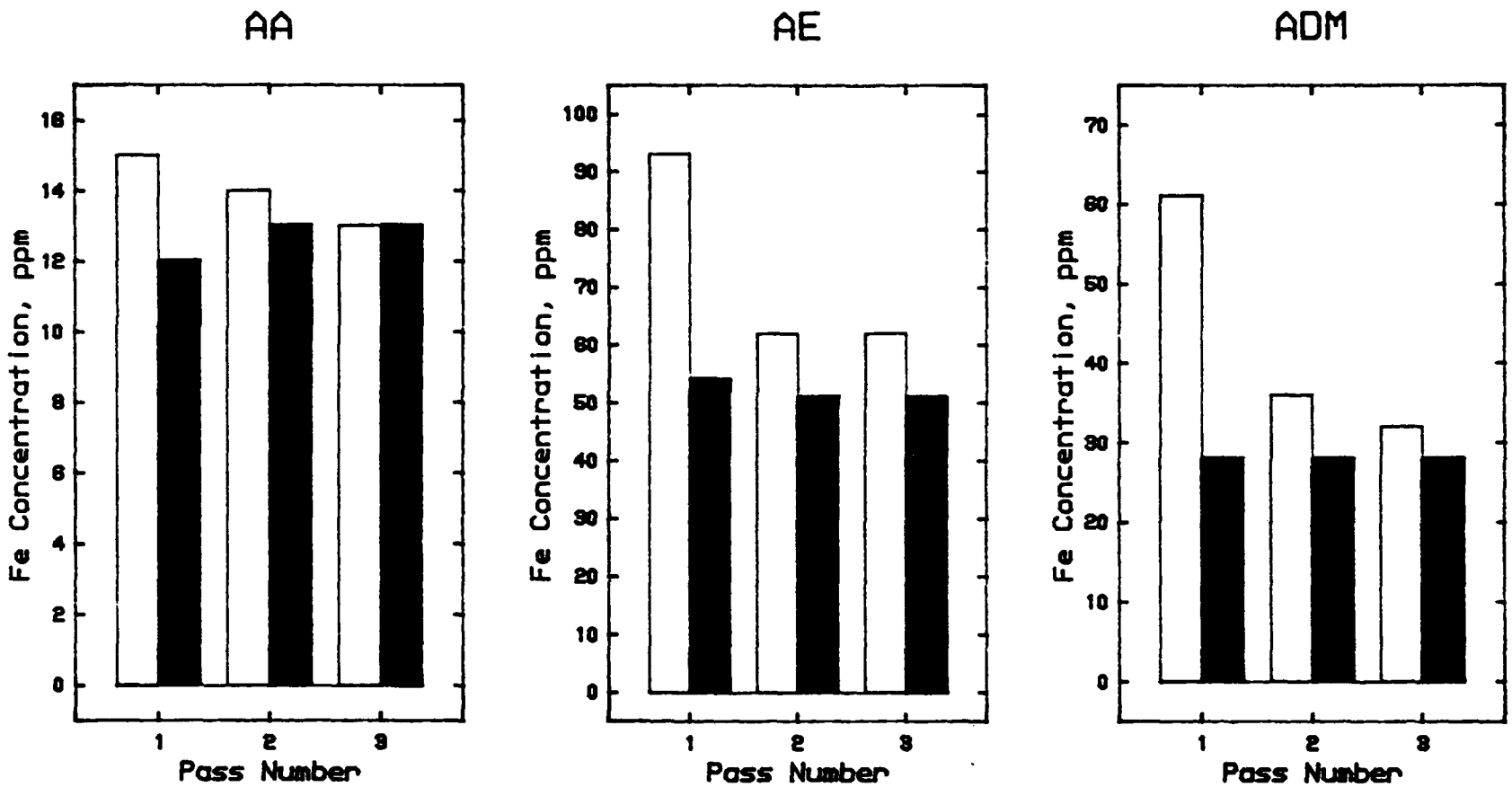

Figure 73. Iron Concentration of Pre- and Post-filter Samples for the First, Second and Third Passes of Microfiltration Test No. 2 Using AA, AE and ADM; □ = Pre-filter, ■ = Post-filter (MIL-L-7808 Oil from Test No. 1 with Additional Pin-On-Disk Wear Debris)

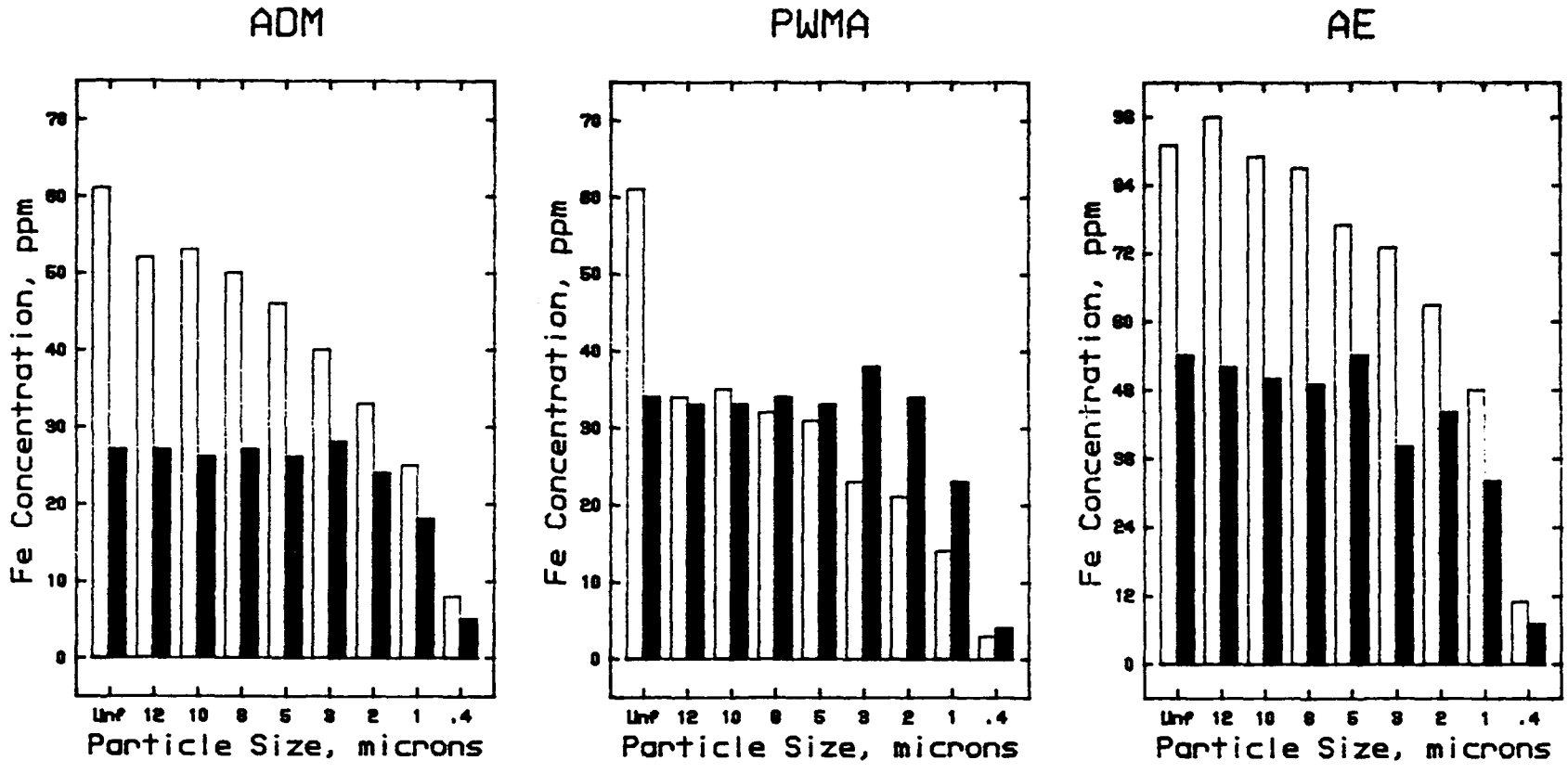

Figure 74. Particle Size Distribution of Iron Wear Debris in Pre- and Post-filter Samples from Microfiltration Test No. 2 Using ADM, PWMA and AE; □ = Pre-filter, ■ = Post-filter

TABLE 69

OPTICAL DENSITY READINGS OF ANALYTICAL FERROGRAMS
FOR MICROFILTRATION TEST NO. 2
(1 mL and Diluted Samples)

Sample	% Area Covered - Incident Light Ferrogram Position						
	Entry	50 mm	40 mm	30 mm	20 mm	10 mm	L/S[a]
A-1 (Pass 1 Before Filter, 0.1 mL Sample)	46.9	27.0	14.0	10.3	9.3	7.6	1.74
A-1 (Pass 1 Before Filter, 0.05 mL Sample)	31.4	21.2	8.7	7.1	6.7	9.3	1.48
A-2 (Pass 1 After Filter, 1 mL Sample)	55.1	53.8	48.9	39.2	34.3	34.0	1.02
A-2 (Pass 1 After Filter, 0.1 mL Sample)	17.0	14.5	9.5	7.4	7.0	9.1	1.17
B-1 (Pass 2 Before Filter, 0.1 mL Sample)	28.2	21.2	17.5	13.6	15.8	15.4	1.37
B-2 (Pass 2 After Filter, 0.1 mL Sample)	11.6	17.6	11.4	12.0	5.7	7.6	0.66
C-1 (Pass 3 Before Filter, 0.1 mL Sample)	16.0	14.2	9.2	6.3	6.8	13.6	1.13
C-2 (Pass 3 After Filter, 0.1 mL Sample)	8.7	10.1	7.2	9.1	8.2	14.9	0.86

[a]L/S-Ratio of large particles (entry position) to small particles (50 mm position)

Ferrographic Analyses

Analytical ferrographic analyses conducted on the samples obtained from microfiltration Test No. 2 showed the debris to contain a major quantity of small normal wear particles and minor quantities of larger severe wear and nonmetallic particles and fibers. After the first pass through the 3 micron filter, the debris in all subsequent samples consisted of small normal wear and some nonmetallic debris. Optical density readings and L/S values are given in Table 69. The L/S values are similar to those obtained from microfiltration Test No. 1 except that the values for the unfiltered sample and filtered samples are slightly lower compared to their respective values obtained from Test No. 1. This is due to the much higher level of small (less than 3 micron) wear particles. The ferrographic data for Test No. 2 (Table 70) also shows the 3 micron absolute filter to be effective in capturing particles above 3 microns.

TABLE 70

DR FERROGRAPH DATA FOR
MICROFILTRATION TEST NO. 2

Sample Identification	L Reading	S Reading	L/S Ratio
A-1 (Pass 1 Before Filter, 20X Dil.)	36.0	17.8	2.02
A-2 (Pass 1 After Filter, 10X Dil.)	29.1	22.0	1.27
B-1 (Pass 2 Before Filter, 10X Dil.)	43.1	27.9	1.54
B-2 (Pass 2 After Filter, 10X Dil.)	30.1	24.9	1.21
C-1 (Pass 3 Before Filter, 10X Dil.)	33.3	25.0	1.33
C-2 (Pass 3 After Filter, 10X Dil.)	27.1	21.8	1.24

The DR Ferrograph data is similar to the Analytical Ferrograph data and shows very little change in the L/S values after the first pass.

Figure 75 shows the relationship between DR Ferrograph L/S values and L/S values obtained from the analytical ferrograph for both microfiltration tests. Data plotted consists of the values for the unfiltered oil and values obtained on the samples after successive passes through the 3 micron filter. Similar curves occur for both tests with the L/S value remaining constant after the first pass through the filter using the DR Ferrograph. However, the L/S values obtained using the analytical ferrograph show a large decrease after the first pass and continue to slowly decrease after each subsequent pass through the filter. This difference could be due to the different way in which the L/S values are measured.

L/S values can be calculated from the iron concentration by defining a small wear particle as being below a fixed size. Table 71 gives the L/S values based on 5 micron Nuclepore filtration and subsequent iron analysis by the ADM method.

TABLE 71

L/S VALUES FOR MICROFILTRATION TESTS NO. 1 AND NO. 2
BASED ON 5 MICRON FILTRATION AND ADM IRON ANALYSIS

	L/S Value	
	Test No. 1	Test No. 2
Before First Pass Through Filtration Rig	1.13	0.16
After First Pass Through Filtration Rig	0.32	0.07

L/S values determined by this technique are much lower than those based on ferrography which is probably due to no interference of nonmetallic debris, the definition of "small" particles and the difference in weight versus optical density measurement for determining particle size ratios. The much lower L/S value for Test No. 2 is due to the high

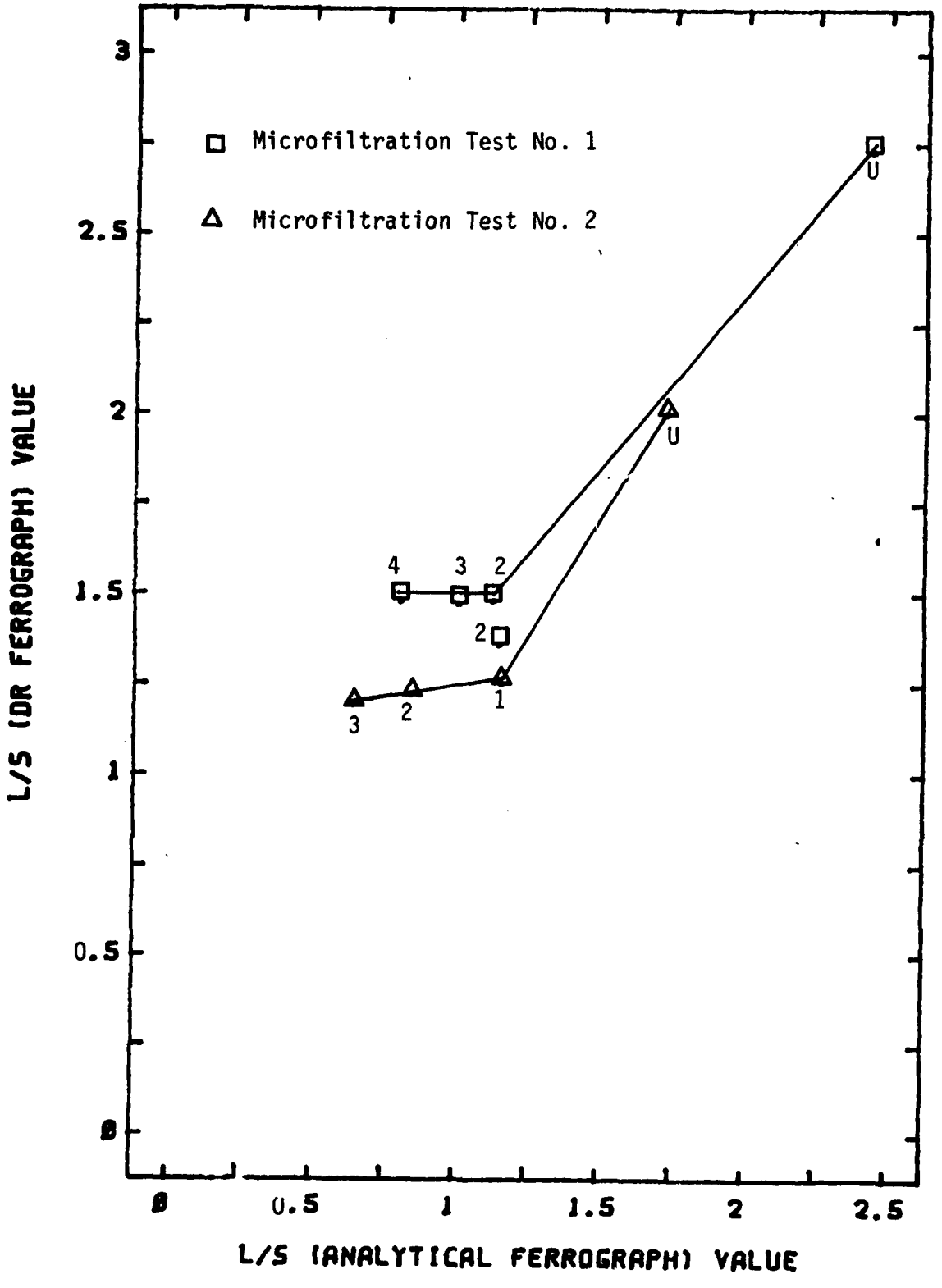

Figure 75. Comparison of L/S Values for the Analytical and DR Ferrograph. U-Unfiltered, 1-First Pass, 2-Second Pass, 3-Third Pass and 4-Fourth Pass Through 3 Micron Filter

concentration of small (less than 3 micron) wear particles in the second test fluid.

(c) Test No. 3

Test Rig

The microfiltration test rig was run for the third time using a new filter. Lubricant used for the test consisted of 3.5 gal of used MIL-L-7808 lubricant obtained from an operational aircraft engine which showed a high iron content of 35 ppm measured by the Air Force Spectrometric Oil Analysis Program. Prior to the third test, the microfiltration rig was cleaned as follows:

Step 1. Filtration rig was operated in bypass mode for 5 minutes containing 3 gal of clean oil. The oil was then pumped through the clean up filter and into a container for disposal. The tank drain valve was then opened for drainage of oil in the lines. The filter housing was removed and cleaned. All oil in the system was drained by rotating the large gear pump by hand.

Step 2. Filter housing was installed, tank drain valve closed and 3 gal of clean oil was added to the filtration rig. The filtration rig was then cleaned as in Step 1.

Step 3. Same as Step one but using 2.5 gal of new MIL-L-7808 oil.

Step 4. Same as Step 3.

The test oil was then added to the rig and allowed to circulate in the bypass mode for 30 minutes at 100°C. Approximately 300 mL (Sample A-1) was obtained at the sampling valve before filtering. The oil was allowed to pass through the rig's new 3 micron filter and was collected in a 7-gallon container (Tank B). The main gear pump was turned off as soon

as the oil was emptied from Tank A. During the filtering process which took approximately six to nine seconds, the temperature in Tank A and in the lines, the pressure in the lines before and after the filter assembly and the oil flow rate were recorded and found to be very similar to the conditions for Test No. 1. A 300-ml aliquot (A-2) was taken from the container (Tank B) immediately after filtration. The oil was transferred from Tank B back into Tank A (rig tank) and again circulated. Similar size aliquots were taken before and after filtering for the second and third passes.

Spectrometric Analysis

Samples taken before and after microfiltration of oil sample used in Test No. 3 were analyzed by atomic absorption (AA), atomic emission (AE) and acid dissolution method (ADM). Figure 76 compares the results of the pre- and post-filtered samples for all passes through the rig's 3 micron filter. It is clearly shown that the concentration detected by AA and AE for the stock sample prior to the first pass is slightly higher than the post-filter sample. Little change in concentration is seen for samples of the second and third passes. ADM gave similar results. It seems, for this particular used oil sample, that the particle size of iron containing wear species was small (less than 3 micron) and generally the particles passed through the microfiltration rig test filter. Therefore, the effect of microfiltration on the spectrometric analysis of this used oil sample is practically nil.

Particle Size Distribution

The particle size distribution (PSD) was determined for the pre- and post-filtered samples of the first pass in order to determine the effective particle size of the filter. The effective particle size of the filter is the particle size that is larger than the pore size of the

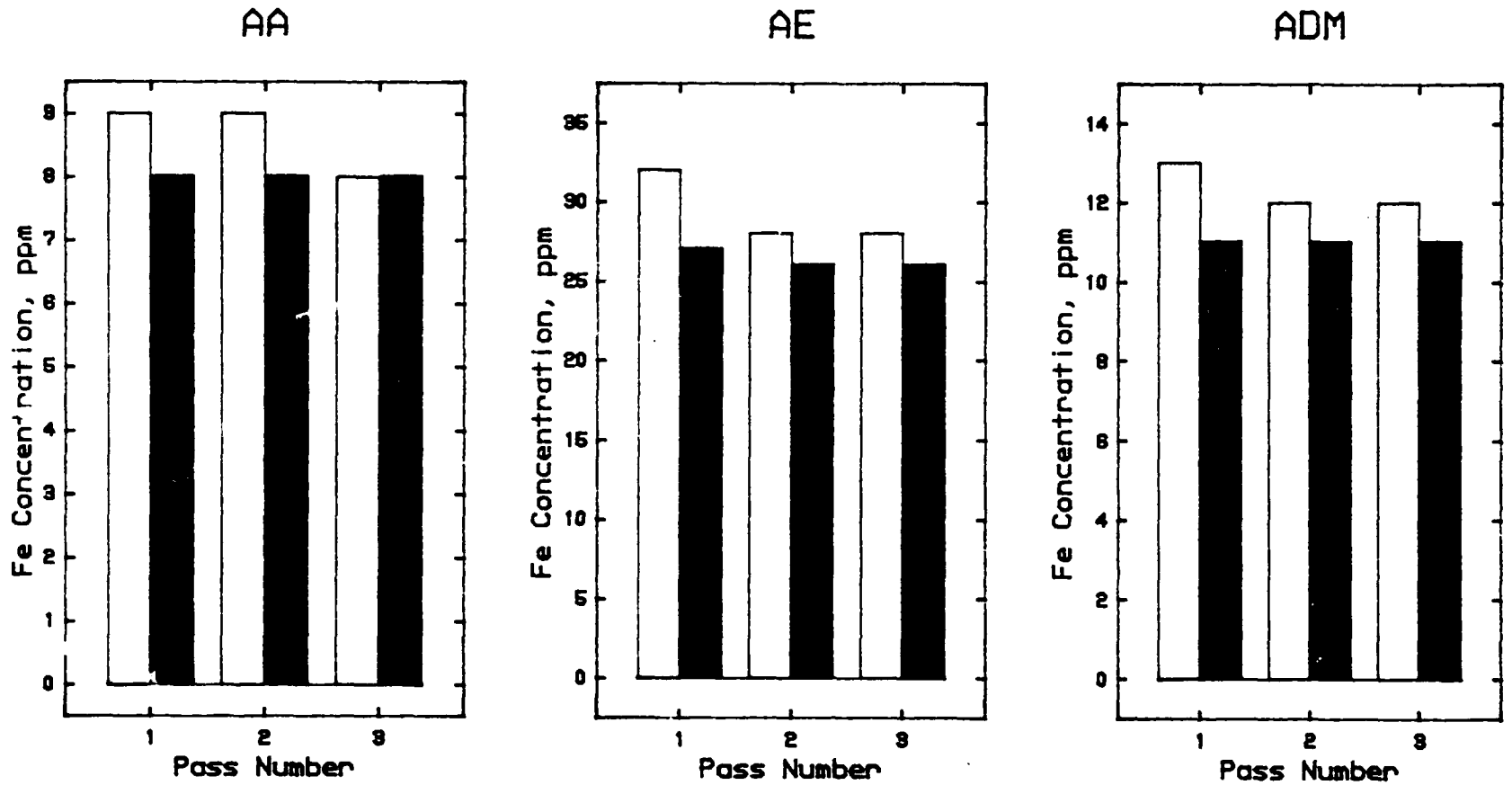

Figure 76. Iron Concentration of Pre- and Post-filter Samples for the First, Second and Third Passes of Microfiltration Test No. 3, Using AA, AE and ADM; □ = Pre-filter, ■ = Post-filter (Used MIL-L-7808 Lubricant from Test Stand J57 Engine)

microfiltration rig test filter. Therefore, wear particles with sizes larger than the effective size of the filter will be captured by the filter. Figure 77 shows the PSD for the pre- and post-filtered samples (A-1 and A-2). It is shown that practically all the particles in this used oil sample are smaller than the effective particle size of the test rig filter. Similar results were obtained using AE and PWMA (Figure 77). The data in Figure 77 shows that the majority of particles in this sample were less than one micron.

Ferrographic Analyses

Microscopic examination of an analytical ferrogram prepared from the unfiltered sample showed the debris to contain a major quantity of small normal wear particles and minor quantities of larger severe wear, cutting wear, carbon, nonmetallic particles and fibers. After the first pass through the 3 micron filter, the debris present in all subsequent samples consisted of small normal wear particles, some nonmetallic debris and very few large wear particles. Table 72 gives the optical density readings obtained on the samples and shows that very few large particles existed prior to filtration and that much of the debris was very small which is evident by the high optical density readings at the 20 mm and 10 mm positions (exit end of ferrograms).

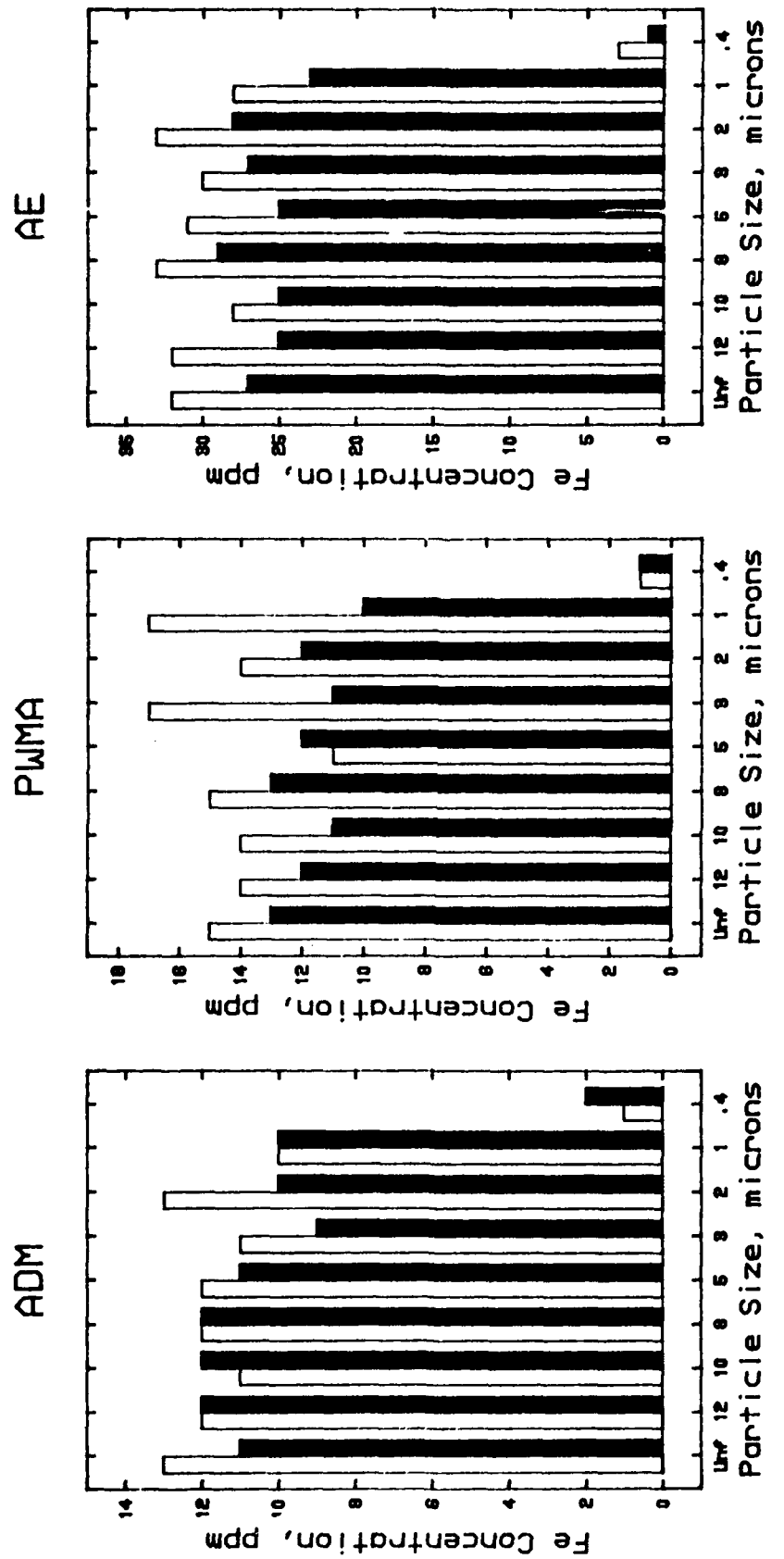

Figure 77. Particle Size Distribution of Iron Wear Debris in Pre- and Post-filter Samples from Microfiltration Test No. 3 Using ADM, PWMA and AE; □ = Pre-filter, ■ = Post-filter

TABLE 72

OPTICAL DENSITY READINGS OF ANALYTICAL FERROGRAMS
FOR MICROFILTRATION TEST NO. 3

Sample (3 mL)	Entry	% Area, Covered - Incident Light Ferrograph Position					
		50 mm	40 mm	30 mm	20 mm	10 mm	L/S[a]
A-1 (Pass 1 Before Filter)	25.9	36.8	44.6	48.0	51.7	60.2	0.70
A-2 (Pass 1 After Filter)	36.5b	41.3	47.0	50.5	55.5	45.6	0.88
B-1 (Pass 2 Before Filter)	29.1	33.3	38.9	45.3	50.5	57.2	0.87
B-2 (Pass 2 After Filter)	38.9b	36.9	45.8	47.1	50.4	57.9	1.05
C-1 (Pass 3 Before Filter)	23.2	26.3	35.0	39.3	44.7	51.3	0.88
C-2 (Pass 3 After Filter)	33.1b	36.0	44.2	47.7	50.2	59.2	0.92

[a]L/S-Ratio of large particles (entry position) to small particles (50 mm position)

[b]Entry consisting of small wear particles and nonmetallic debris

The samples were also evaluated using the DR Ferrograph with the data being given in Table 73. The data obtained from the DR Ferrographic analysis is very similar to the data obtained from the analytical ferrograph and shows a very small amount of large debris present in the unfiltered sample.

TABLE 73

DR FERROGRAPH DATA FOR MICROFILTRATION TEST NO. 3

Sample Identification	L Reading	S Reading	L/S Ratio
A-1 (Pass 1 Before Filter)	44.2	40.8	1.08
A-2 (Pass 1 After Filter)	34.4	32.9	1.04
B-1 (Pass 2 Before Filter)	39.9	36.8	1.08
B-2 (Pass 2 After Filter)	37.2	34.7	1.07
C-1 (Pass 3 Before Filter)	39.6	37.5	1.06
C-2 (Pass 3 After Filter)	36.8	34.2	1.08

(d) Test No. 4

Test Rig

The microfiltration system was flushed with 3 gal of new MIL-L-23699 oil (Qual. No. 01F) by circulating the oil for 5 minutes and then draining. The system was flushed the second time with 3 gal of MIL-L-23699 (Qual. No. 01F) and again circulating the oil for 5 minutes and draining.. Due to the very bad odor of the Qual. No. 01F oil, the test rig was flushed with 3 gal of new MIL-L-23699 oil (Qual No. 05A). Debris taken from engine simulator (oil tank) test number 0873 was washed with pentane, dried and weighed giving a total weight of deposits of 1.1 grams. Ferrographic analysis of a 200 ppm mixture of this debris in MIL-L-7808 showed a moderate amount of normal rubbing wear, heavy amount of severe wear and heavy amounts of carbon and glass fibers. The analysis of the 200 ppm sample gave 28 ppm iron (14% wt) by AE and 69 ppm (35% wt) ay ADM analysis.

The remaining debris (approximately 1 gram) was mixed with 2 quarts of new MIL-L-23699 oil (Qual. No. 05A) and then placed in the filtration rig's oil tank. Additional new oil was added giving a total of 4 gallons of oil in the test rig's tank. A new 3 micron filter was installed prior to testing. Circulation of the oil and debris was initiated in the "bypass mode." Oil circulation was continued for 40 minutes until the oil temperature reached 100°C. Sampling was then conducted before and after successive passes through the 3 micron filter.

The oil was circulated continuously through the filter and back to the microfiltration test rig's tank for 1 hour after the third pass to determine if multiple passes through the filter reduced the iron content of the 3rd pass. Test parameters with respect to filtration time after the third pass were monitored. Samples were taken before and after the filter

upon completion of the 1 hour test (samples D-1 and D-2).

Spectrometric Analysis

ADM results shown in Figure 78 of MFR Test No. 4 samples indicate that most all of the Fe in the Sample A-1 was retained on the rig's 3 micron filter. However, Sample B-1 taken prior to the second pass contained about a third of the original Fe. This Fe contamination could not have been generated from the gear pump because a subsequent sample, D-1 taken prior to the fourth pass did not show an appreciable amount of Fe. Therefore, it is concluded that this contamination is due to the Fe remaining in the residual oil within the system after the first pass. Spectrometric analysis using AA, AE and PWMA (Figure 78) of samples from Test No. 4 was instrument dependent with PWMA showing the best agreement with the ADM. However, AE and AA showed much lower values of Fe for A-1 due to the presence of an appreciable amount of large particles of Fe wear debris.

Particle Size Distribution

The particle size distribution (PSD) of iron wear debris was determined for samples taken from Microfiltration Rig (MFR) Test No. 4 before (A-1) and after (A-2) the first pass. Nuclepore membrane filtrations coupled with ADM and AE were conducted on A-1 and A-2 and the results are shown in Figure 79. The plot shows that 50% of the particles are $\geq$10 microns in the A-1 sample. However, after the first pass through the MFR test filter, very small amount of iron is shown to have passed through and that in A-2 most all of the iron wear debris was retained on the MFR filter. Similar results are shown using the AE technique except that AE results for the unfiltered sample (A-1) were approximately half of the ADM results shown in Figure 78.

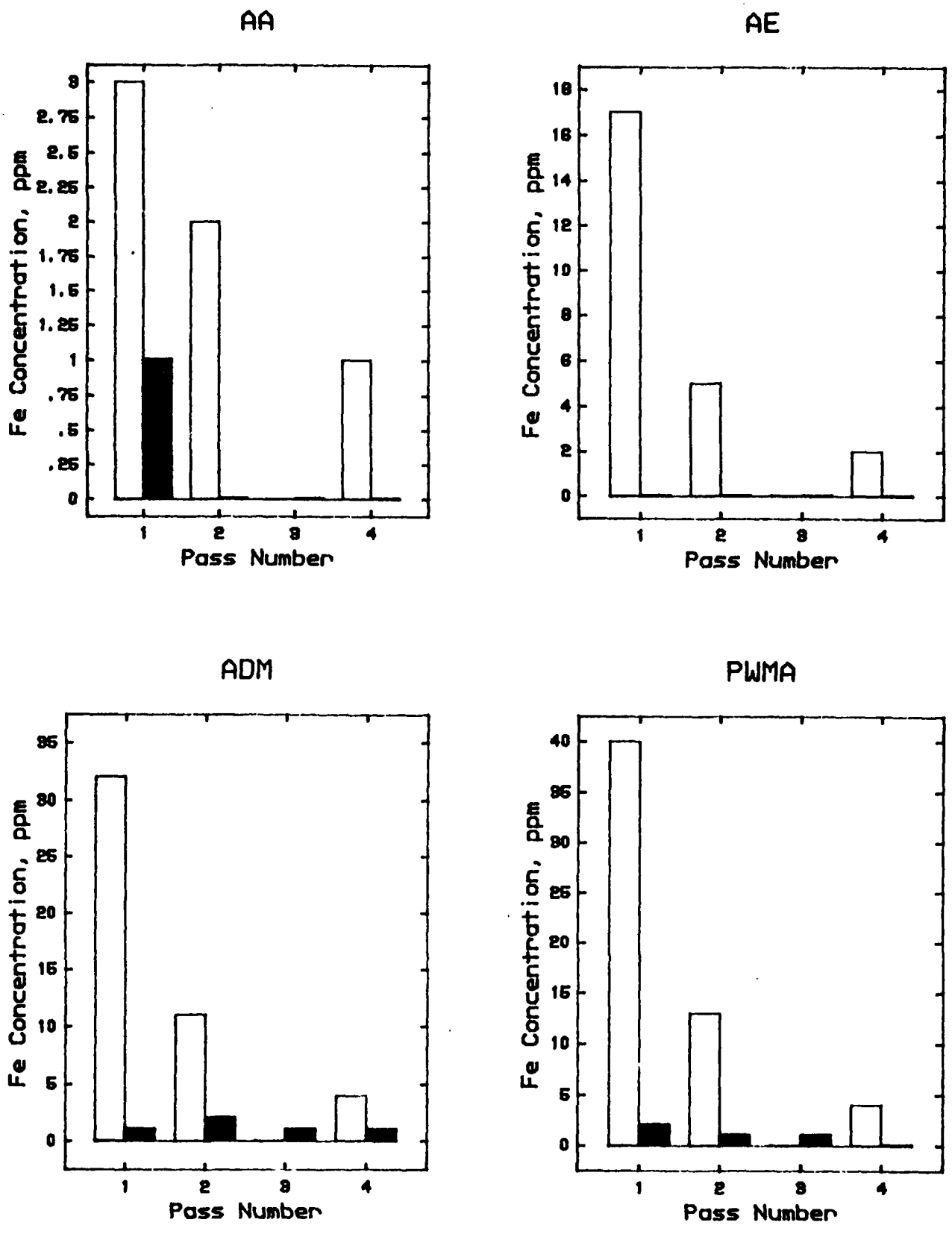

Figure 78. Iron Concentration of Pre- and Post-filter Samples for the First, Second, Third and Fourth Passes of Microfiltration Test No. 4 Using AA, AE, ADM and PWMA; □ = Pre-filter, ■ = Post-filter (MIL-L-23699 Lubricant with Wear Debris from Engine Simulator)

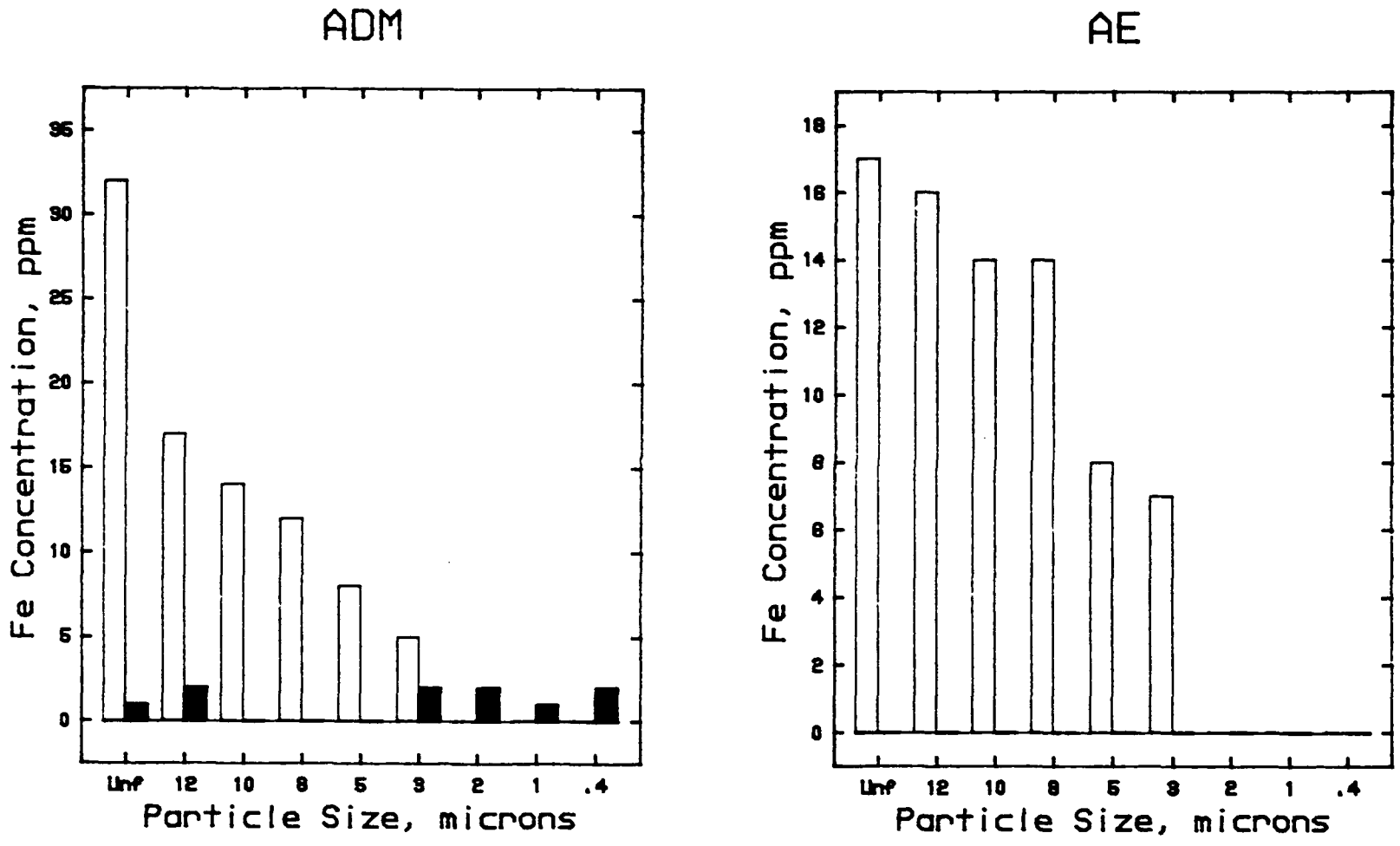

Figure 79. Particle Size Distribution of Iron Wear Debris in Pre- and Post-filter Samples from Microfiltration Test No. 4 Using ADM and AE; □ = Pre-filter, ■ = Post-filter

Ferrographic Analyses

Microscopic examination of the analytical ferrograms prepared from the unfiltered sample showed the debris to contain a major quantity of severe and cutting wear particles, black oxide particles and nonmetallic debris including a large amount glass fibers. Low levels of normal rubbing wear, cellulose fibers and carbon particles were also present. The glass fibers were from removing the insulation material during teardown of the engine simulator from which the wear debris was obtained. After the first pass through the 3 micron MFR filter, the debris present in all subsequent samples consisted of a few small normal wear particles and some nonmetallic debris. Table 74 shows the optical density readings of the analytical ferrograms prepared from the samples A-1 (before first pass thru filter) and A-2 (after first pass thru filter) along with L/S values obtained with the DR Ferrograph. Ferrograms were not prepared for samples taken before and after subsequent filter passes due to the high efficiency of the 3 micron filter and the low iron values of the samples.

The data in Table 74 shows that Sample A-1 (before first pass through the filter) contained a large ratio of large to small particles. The data also shows that the entry deposit does not always give the maximum density reading which can be 0.5 to 1.0 mm lower on the ferrogram than the entry deposit position which can give low L/S values. The L/S values calculated from either the entry position or tne position of maximum percent coverage is very highly sample size dependent. The L/S values obtained using the DR Ferrograph correlated with the L/S values obtained with the Analytical Ferrograph when using a 1 mL sample.

The complete data obtained using the DR Ferrograph is given in Table 75.

TABLE 74

OPTICAL DENSITY READINGS OF ANALYTICAL FERROGRAMS AND L/S VALUES FOR SAMPLES OBTAINED FROM MICROFILTRATION TEST NO. 4

% Area Covered (Incident Light)

Ferrograph Position, mm

Sample	Sample[1] Size, mL	Entry	Max. % Covered	50	48	40	30	20	10	L/S[2]	L/S[3]	L/S[4]
A-1[5]	3.0	77.8 (54.0 mm)	-	50.3	-	-	-	-	31.0	1.55	-	-
A-1	1.0	68.9 (55.0 mm)	82.7 (54.5 mm)	28.1	-	30.2	17.9	18.2	15.1	2.45	2.94	2.6
A-1	0.5	60.0 (54.0 mm)	76.4 (53.1 mm)	17.3	27.7	16.8	19.2	18.1	11.6	3.47	4.42	
A-1	0.25	52.9 (54.5 mm)	67.5 (54.0 mm)	14.0	-	8.7	8.6	7.6	3.5	3.78	4.82	
A-1	0.10	23.9 (54.1 mm)	26.3 (53.7 mm)	3.9	-	2.8	3.6	4.2	5.7	6.13	6.74	
A-2[6]	3	9.0 (54.1 mm)	9.0 (54.1 mm)	6.7	-	7.4	5.4	7.9	4.0	1.34	1.34	1.5

[1]Sample sizes other than 3 mL were diluted to 3 mL with new MIL-L-7808 lubricant

[2]L/S: Ratio of large particles (entry position) to small particles (50 mm position) of analytical ferrograms

[3]L/S: Ratio of large to small particles obtained from large particles (maximum area covered above 50 mm) to small particles (50 mm position) of analytical ferrograms

[4]L/S: Ratio of large to small particles obtained from DR Ferrograph

[5]A-1: Pass number 1, before filter

[6]A-2: Pass number 1, after filter

TABLE 75

DIRECT READING FERROGRAPH DATA FOR
MICROFILTRATION TEST NO. 4

Sample	Sample Size mL	L Value	S Value	L/S Value
A-1	1.00	81.6	31.2	2.6
A-1	0.03[a]	3.1	1.4	2.2
A-2	1.00	7.0	4.8	1.5

[a]Sample mixed with new MIL-L-23699 oil to provide 1 mL of oil for test

The data in Table 75 indicates that the L/S values obtained using the DR Ferrograph is not as sample size sensitive as the Analytical Ferrograph although they may be low compared to the actual L/S values.

(e) Test No. 5

Test Rig

The test rig was flushed two times with mineral oil, Grade 1005, MIL-L-6081. A new 3 micron filter was installed and the test rig was charged with 5 gallons of used 10W30 weight automotive oil containing a large (visible) amount of debris. The oil was circulated in the "bypass" mode until the tank oil temperature reached 100°C. A sample was then taken prior to the first pass through the filter. During the first pass through the filter, the flow rate was 11.1 GPM, tank temperature 102°C, filter inlet temperature 101°C, pressure upstream of filter reached 148 psi (relief valve became partly opened) and the down stream filter pressure was 11.2 psi. A new filter was installed prior to subsequent passes through the 3 micron filter. The parameters monitored during microfiltration Test No. 5 were given previously (Table 65)

Spectrometric Analysis

Total Fe (ADM) content in aliquots A-1 thru D-2 of MFR Test

No. 5 showed no appreciable difference (Figure 80). Similar trends were observed in AA, AE and PWMA results. Since the Fe content did not change after any pass through the rig's 3 micron filter, the particles of wear debris were smaller than 3 micron. AE results were comparable to ADM but AA was 25% lower than ADM and seems to be particle size dependent even at this level of particle size (<3 micron). However, the PWMA gave the lowest values with less than 50% of the ADM. This anomaly cannot be explained based on the nature of matrix (heavy hydrocarbon oil) since the graphite furnace has an ashing cycle that destroys the matrix prior to atomization. The delivery volume of the 10 µL for this viscous oil was 90% of the standard in MIl-L-7808 and therefore, this difference cannot be responsible for the low results. The wavelength chosen for Fe analysis in the PWMA is the 385.99 nm. The graphite furnace Model 500 on the Perkin-Elmer AA Model 3030 was used to analyze samples from MFR Test No. 5 using the 385.99 and 248.3 lines. The results were similar and agreed with the ADM values. Verification of the PWMA anomalous results is still being pursued. However, Quinn's work provides some understanding concerning the capability of the PWMA in detecting various sizes and concentrations of metal powders in oils.[21]

Particle Size Distribution (PSD)

Difficulty was experienced in filtering MFR Test No. 5 samples thru the Nuclepore filters of 2 micron or less due to the heavy nonmetallic debris present in the used motor oil. Therefore, PSD of less than 2 micron was not determined on this sample.

Nuclepore membrane filtrations coupled with ADM and AE were also conducted on A-1 and A-2 and the results are shown in Figure 81. The ADM graph shows that nearly all the particles in the A-1 sample are very small and below 2 microns. Also, the A-2 results are approximately the same

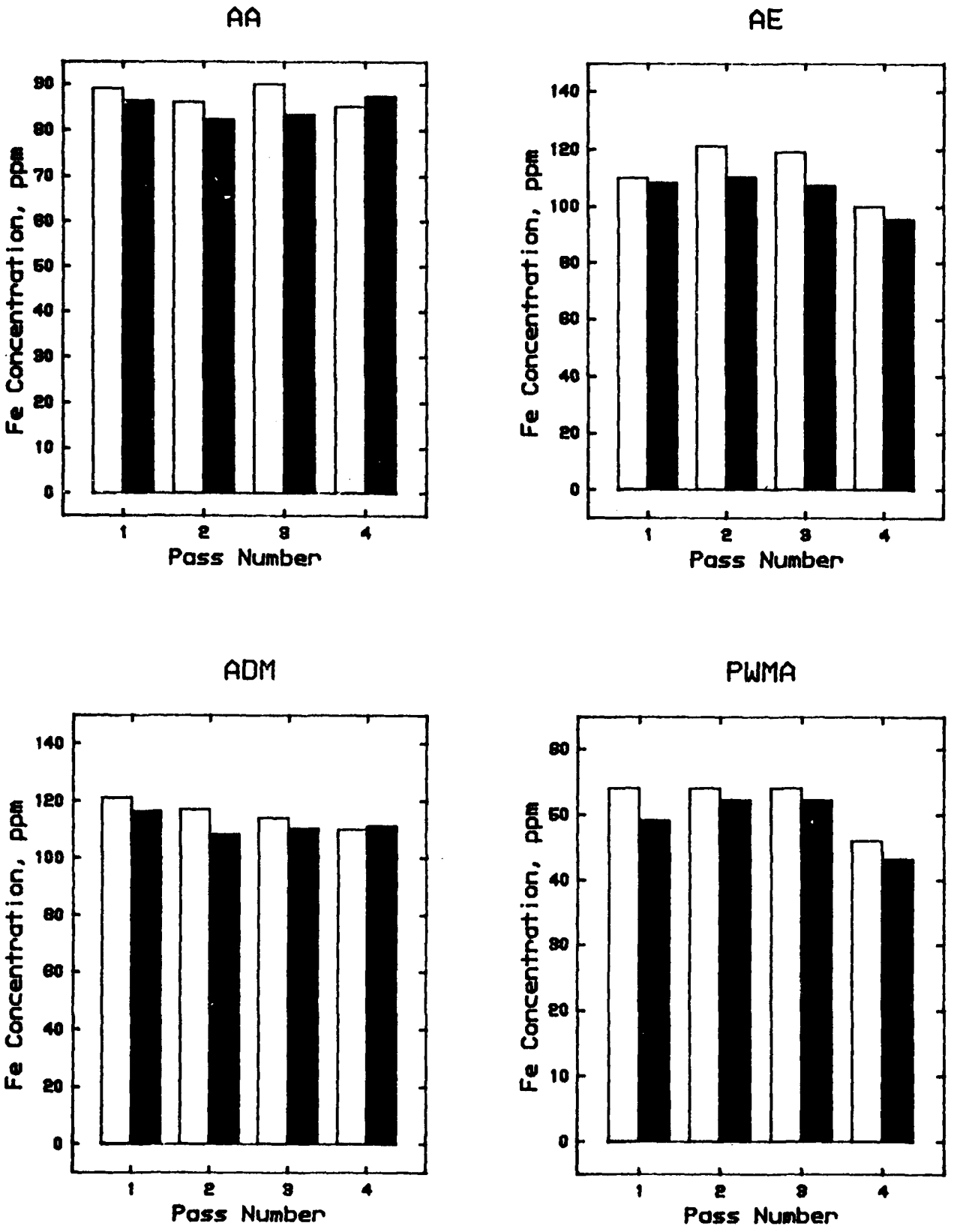

Figure 80. Iron Concentration of Pre- and Post-filter Samples for the First, Second, Third and Fourth Passes of Microfiltration Test No. 5 Using AA, AE, ADM and PWMA; □ = Pre-filter, ■ = Post-filter (Used 10W30 Automotive Oil)

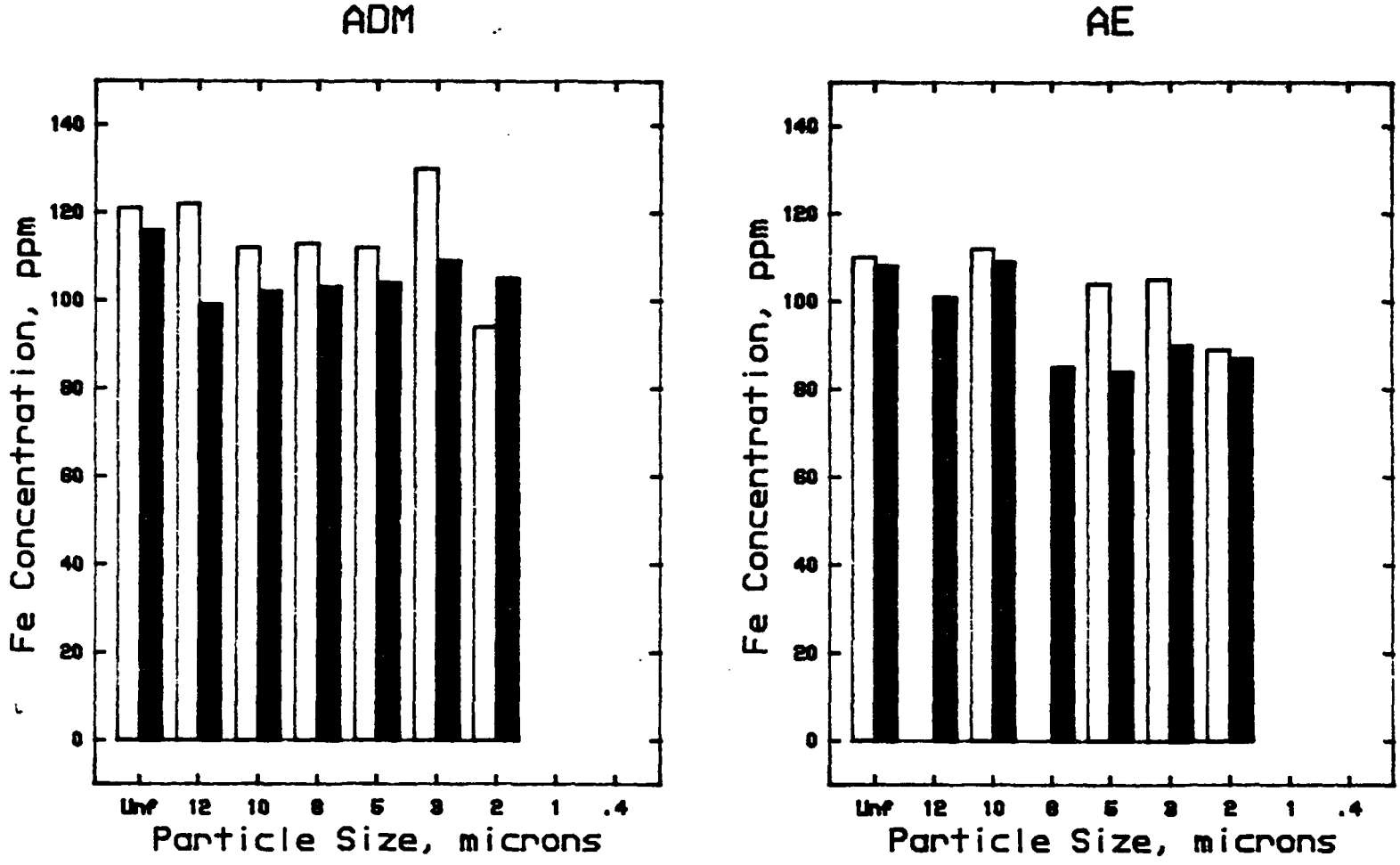

Figure 81. Particle Size Distribution of Iron Wear Debris in Pre- and Post-filter Samples from Microfiltration Test No. 5 Using ADM and AE; □ = Pre-filter, ■ = Post-filter

TABLE 76

OPTICAL DENSITY READINGS OF ANALYTICAL FERROGRAMS AND L/S VALUES FOR SAMPLES OBTAINED FROM MICROFILTRATION TEST NO. 5

% Area Covered (Incident Light)

Ferrograph Position, mm

Sample	Sample[1] Size, mL	Entry	Max. % Covered	50	40	30	20	10	L/S[2]	L/S[3]	L/S[4]
A-1[5]	1	67.3 (54.1 mm)	74.5 (53.7 mm)	61.5	46.3	38.7	37.4	34.9	1.09	1.21	-
A-1	0.5	52.0 (55.0 mm)	56.2 (53.7 mm)	43.5	33.6	23.7	22.7	23.0	1.20	1.29	-
A-1	0.25	37.0 (53.2 mm)	44.0 (52.3 mm)	34.3	13.6	9.4	8.4	5.3	1.08	1.28	2.4
A-2[6]	1	68.4 (54.1 mm)	68.4 (54.1 mm)	63.2	46.6	32.7	31.4	25.6	1.08	1.08	
A-2	0.5	37.2 (54.5 mm)	37.2 (54.5 mm)	36.2	29.0	22.7	19.3	15.8	1.03	1.03	1.9

[1] Samples diluted to 3 mL with new MIL-L-6081 lubricant

[2] L/S: Ratio of large particles (entry position) to small particles (50 mm position) of analytical ferrograms

[3] L/S: Ratio of large to small particles obtained from large particles (maximum area covered above 50 mm) to small particles (50 mm position) of analytical ferrograms

[4] L/S: Ratio of large to small particles obtained from DR Ferrograph

[5] A-1: Pass number 1, before filter

[6] A-2: Pass number 1, after filter

as those of A-1 indicating the particles are too small to be retained on the MFR test filter. Figure 81 also shows the AE results to be similar to those of the ADM. The reason for this similarity is the fact that the particles in this sample are very small (<2 microns) and that they are efficiently analyzed by AE and therefore yielding results comparable to ADM.

Ferrographic Analysis

Microscopic examination of the ferrograms prepared from the unfiltered and filtered samples showed a very heavy concentration of small highly magnetic wear particles, a moderate amount of carbon and a minor amount of non-wear debris. Table 76 shows the optical density readings of the samples A-1 (before filtering) and A-2 (after first pass thru the 3 micron filter. This data shows that only a very few large particles existed in the unfiltered sample and that sample size did not have as large effect on L/S values as that shown for Test No.4.

The DR Ferrograph data is given in Table 77.

TABLE 77

DIRECT READING FERROGRAPH DATA FOR MICROFILTRATION TEST NO. 5

Sample	Sample Size mL	L Value	S Value	L/S Value
A-1 (Before Filter)	0.25a	78.6	32.3	2.4
A-2 (After Filter)	0.25	57.7	31.0	1.9

[a]Sample mixed with new MIL-L-6081 oil to provide 1 mL of oil for test

Sample A-1 of Test No. 5 contains a much smaller ratio of large to small particles than that obtained for the A-1 sample of Test No. 4 although the calculated L/S values for either the Analytical or DR Ferrograph data do not show this difference. Microscopic evaluation of the analytical

ferrograms and wear metal analyses does show a smaller L/S ratio for Test No. 5.

For Test No. 5, the entry deposit does not give the maximum density reading but the difference in density readings between the entry position and position of maximum density is not as large as was observed for the ferrographic data for MFR Test No. 4. The L/S values obtained using the DR Ferrograph are about the same as those obtained for Test No. 4 and are larger than those calculated from the analytical ferrograms for Test No. 5.

(f) Test No. 6

Test Rig

A 5 gallon sample of used MIL-L-23699 lubricant obtained from T56 engine gearboxes was received from the 317th FMS, Pope AFB, NC for use in the microfiltration studies. Preliminary analysis of the lubricant prior to transferring to the microfiltration rig (MFR) showed a 15 ppm iron content determined using the Portable Wear Metal Analyzer (PWMA). Analytical ferrographic analysis of the sample showed a moderate to heavy amount of severe wear, dark oxides and nonmetallic debris, a moderate amount of normal wear and carbon particles and a few cutting wear and chunk type particles.

Prior to testing the MFR was flushed with four gallons of new MIL-L-23699 lubricant three times. A post sample of the third flushing oil showed a zero ppm iron content using the PWMA and ferrographic analysis showed very few particles of any type. The 5 gallon test sample was added to the MFR and circulated in the "filter by-pass" mode until the test temperature was reached. A new 3 micron absolute filter was installed and four passes were made thru the filter. During each pass the filtered fluid was collected in a precleaned stainless steel seamless container. Samples were taken immediately before and after each pass. The parameters monitored

during the microfiltration test were given in Table 65.

Spectrometric Analysis

The used oil from a T56 gas turbine engine was filtered four times. Samples collected from the four passes were analyzed by AA, AE, PWMA and ADM and the results are graphically illustrated in Figure 82.

The atomic emission results for Fe in ester base lubricants were higher than the AA results. This was expected since the AE spectrometer is calibrated with Conostan standards in hydrocarbon oils and the results for Fe are always 2 to 3 times higher due to the enhancement of the matrix of the ester base lubricants. In AA, matrix effect is usually minimized since both standard and sample are diluted with some organic solvent prior to analysis. If AE values were adjusted for matrix enhancement they would be comparable to the AA values. Except for A-1 sample, AA and PWMA values for all samples are about the same. A-1 apparently contained large metallic particulates which were more effectively analyzed by the PWMA. As expected ADM gave the highest values. However, the ADM values for A-1 seem to be lower than the PWMA value. If one considers the 10% repeatability of the PWMA obtained for the result of this sample, the PWMA and ADM values would be comparable. Except for the A-1 sample, the PWMA values for the B, C and D samples were low and comparable to A-2. In summary, AA and AE did not appreciably differentiate between A-1 and the rest of the samples. However, the PWMA and ADM showed appreciable decrease in the Fe after the first pass.

Particle Size Distribution

Determination of the particle size distribution (PSD) was performed only on the first pass samples, A-1 and A-2. The samples were filtered through 5.0, 3.0, 2.0, 1.0 and 0.4 micron Nuclepore membranes and the filtrates were analyzed using ADM, PWMA and AE (Figure 83). These

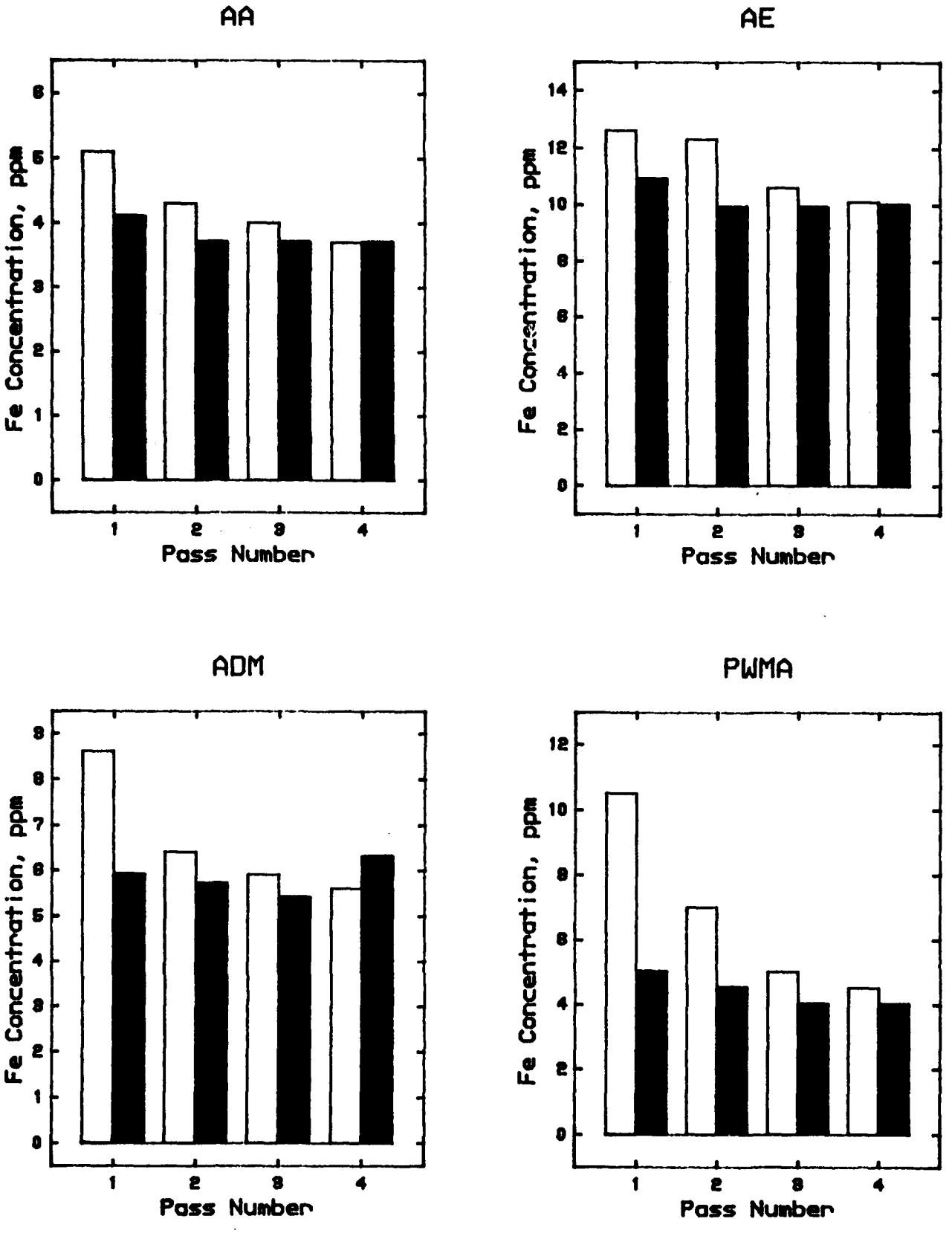

Figure 82. Iron Concentration of Pre- and Post-filter Samples for the First, Second, Third and Fourth Pass of Microfiltration Test No. 6 Using AA, AE, ADM and PWMA; □ = Pre-filter, ■ = Post-filter (Used MIL-L-23699 Lubricant from T56 Engine Gearboxes)

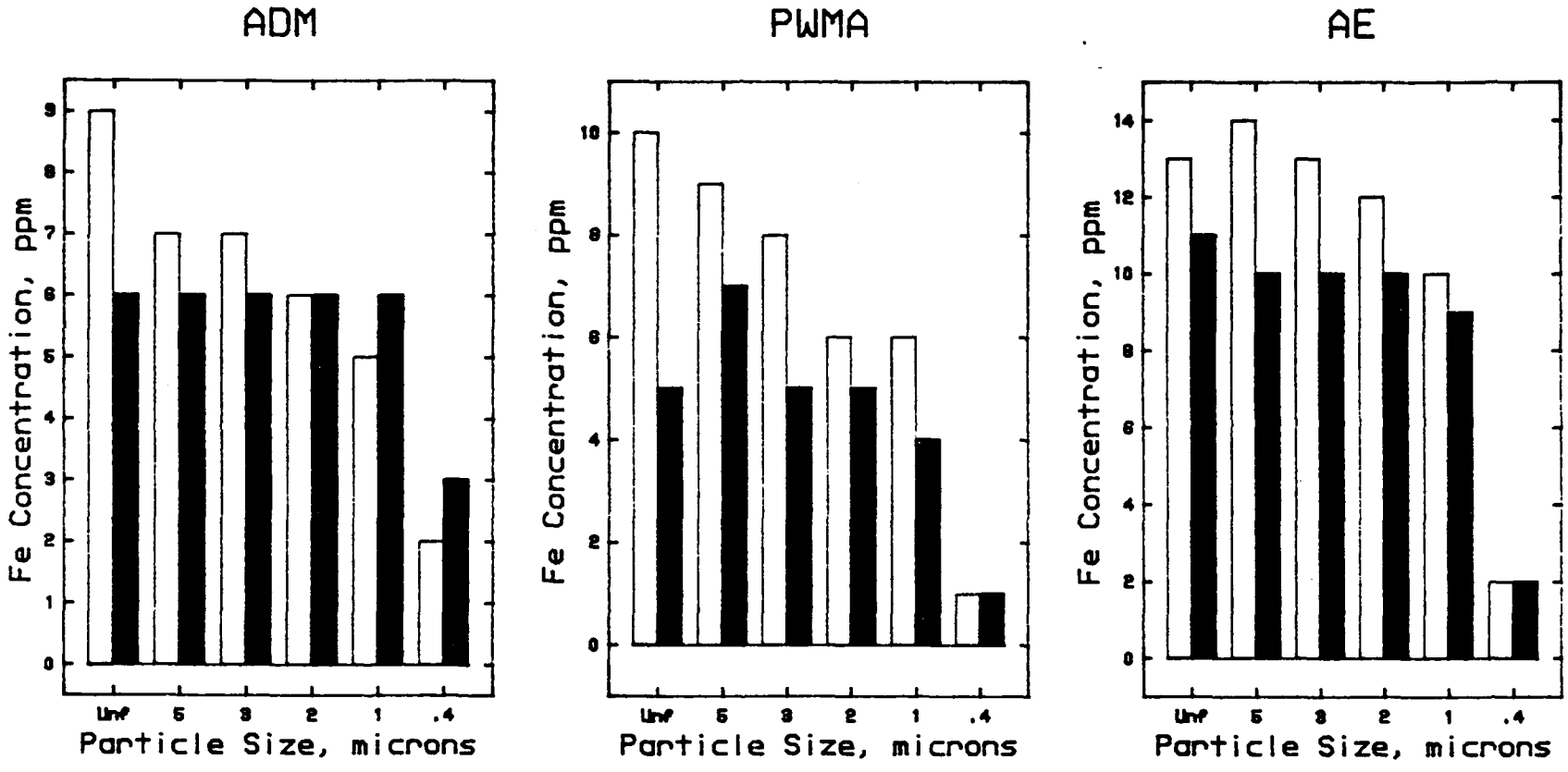

Figure 83. Particle Size Distribution of Iron Wear Debris in Pre- and Post-filter Samples from Microfiltration Test No. 6 Using ADM, PWMA and AE; □ = Pre-filter, ■ = Post-filter

analytical techniques reveal that the size of the Fe wear debris is mostly less than one micron. Other significant wear metals were also found in this sample (Tables 78 and 79). AE analyses of the filtrates showed lower concentrations for only Fe and Mg of the filtrates below 1 micron (Table 78). All other metal concentrations remained fairly constant. Even though the PWMA concentrations of Cu, Mg and Si were low and below 3 ppm, the data showed that these metals exist mostly in particulate form (<0.4 microns, Table 79).

Ferrographic Analyses

Analytical ferrographic analyses were conducted on samples taken before and after the first filter pass of the 6th microfiltration test. Microscopic examination of the ferrogram prepared from the unfiltered sample A-1 showed the debris to consist of a moderate to heavy amount of severe wear particles, moderate amounts of normal rubbing wear, cutting wear, dark metallic oxides and non-wear debris, and a few chunk and red oxide type particles. After the first pass thru the 3 micron absolute filter the debris present in Sample A-2 consisted of few to moderate amounts of small normal wear particles and a few non-wear particles. Table 80 shows the optical density readings of the analytical ferrograms prepared from the Samples A-1 (before first pass thru filter) and A-2 (after first pass thru filter) along with L/S values obtained with the DR Ferrograph. Ferrograms were not prepared for samples taken before and after subsequent filter passes due to the high efficiency of the 3 micron filter. The data in Table 80 does not show high L/S values which might be expected from a gearbox sample. This is supported by the analytical (AE, ADM, etc.) data and particle size distribution data. The data in Table 80 also shows that visual evaluations of ferrograms may not agree with L/S values or with AE, AA, ADM or PWMA

TABLE 78

PARTICLE SIZE DISTRIBUTION OF FE, CU, MG, SI AND ZN IN MICROFILTRATION TEST NO. 6 SAMPLES USING AE

Sample	Concentration (ppm) Fe	Cu	Mg	Si	Zn
A-1, Unfiltered	12.6	2.1	5.0	4.0	4.2
<5.0 µm	14.4	3.5	6.4	6.7	6.8
<3.0 µm	13.4	3.6	5.8	6.5	6.6
<2.0 µm	12.2	3.1	5.8	6.7	6.2
<1.0 µm	10.0	3.1	5.1	5.2	6.6
<0.4 µm	1.9	2.2	2.6	4.5	4.0
A-2, Unfiltered	10.9	2.5	4.8	4.0	5.1
<5.0 µm	9.7	2.0	5.0	5.2	5.0
<3.0 µm	10.0	3.0	5.1	5.4	5.4
<2.0 µm	10.4	3.1	5.3	6.3	6.1
<1.0 µm	9.4	3.0	5.0	6.2	5.8
<0.4 µm	1.9	2.8	2.4	4.3	4.3

TABLE 79

PARTICLE SIZE DISTRIBUTION OF FE, CU, MG AND SI IN MICROFILTRATION TEST NO. 6 SAMPLES USING PWMA

Sample	Concentration (ppm) Fe	Cu	Mg	Si
A-1, Unfiltered	10	2	3	3
<5.0 µm	9	2	3	1
<3.0 µm	8	1	2	1
<2.0 µm	6	0	2	0
<1.0 µm	6	1	2	1
<0.4 µm	1	0	1	1
A-2, Unfiltered	5	1	2	2
<5.0 µm	7	1	2	1
<3.0 µm	5	1	2	1
<2.0 µm	5	1	2	1
<1.0 µm	4	1	2	1
<0.4 µm	1	0	1	1

TABLE 80

OPTICAL DENSITY READINGS OF ANALYTICAL FERROGRAMS AND L/S VALUES FOR SAMPLES OBTAINED FROM MICROFILTRATION TEST NO. 6

% Area Covered (Incident Light)

Ferrograph Position, mm

Sample	Sample Size, mL	Entry	Max. % Covered	50	40	30	20	10	L/S[1]	L/S[2]	L/S[3]
A-1[4]	3	40.2 (53.5 mm)	46.2 (52.5 mm)	36.4	29.7	24.1	27.2	32.2	1.10	1.26	1.59
A-2[5]	3	8.1 (54.9 mm)	8.1 (54.9 mm)	10.1	11.5	9.4	18.6	16.9	0.80	0.80	1.26

[1]L/S: Ratio of large particles (entry position) to small particles (50 mm position) of analytical ferrograms

[2]L/S: Ratio of large to small particles obtained from large particles (maximum area covered above 50 mm) to small particles (50 mm position) of analytical ferrograms

[3]L/S: Ratio of large to small particles obtained from the DR Ferrograph

[4]A-1: Pass Number 1, before filter

[5]A-2: Pass number 1, after filter

analyses. This could be partially due to visual bias towards large particles in the visual evaluation of the ferrograms, the relatively low total iron content of the sample and the fact that all small or dissolved particles are not captured by the ferrograph.

The complete DR Ferrograph data for Samples A-1 and A-2 are given in Table 81.

TABLE 81

DIRECT READING FERROGRAPH DATA FOR MICROFILTRATION TEST NO. 6

Sample	Sample Size mL	L Value	S Value	L/S Value
A-1 (Before Filter)	1	49.1	30.9	1.6
A-2 (After Filter)	1	21.3	16.9	1.3

The DR Ferrograph data shows lower L/S values as well as lower L and lower S values compared to Test No. 5 and a lower L value but a larger S value compared to Test No. 4. This agrees with other analytical data showing Test No. 4 to have larger size particles.

(5) Correlation of Microfiltration Testing

The correlation of all the microfiltration test data is shown in Figures 84 thru 86. Data used for developing these figures is given in Appendix B.

Figure 84 shows the correlation of percent iron having particle size greater than 3 microns with percent of iron captured by the MFR 3 micron filter, the percent decrease in L/S values using the Analytical Ferrograph and percent decrease in L/S values using the DR Ferrograph with the iron analyses being made by ADM for the six filtration tests. Very good correlation is shown between the percent iron removed by the 3 micron filter

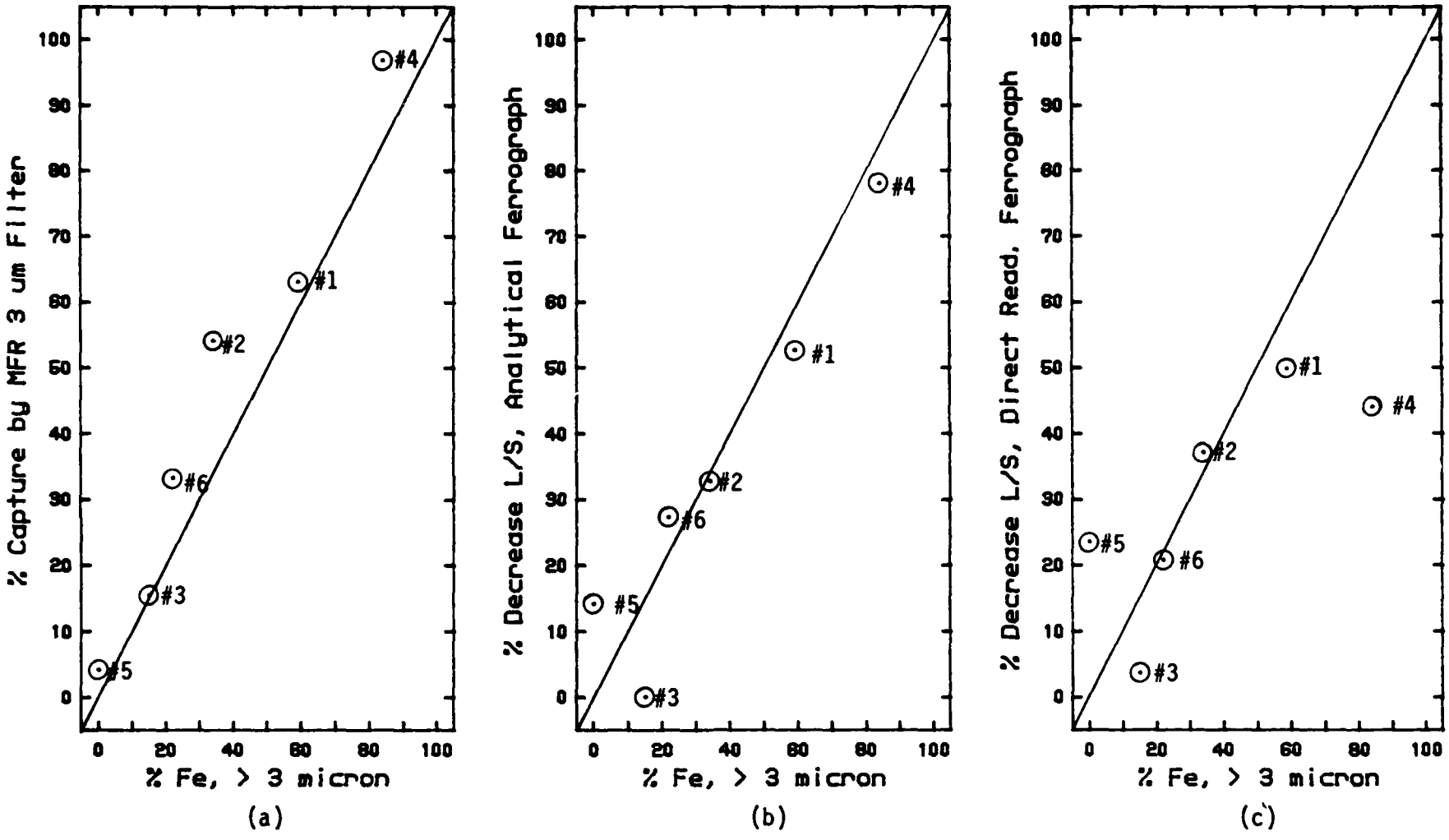

Figure 84. Correlation of % Iron Greater than 3 Microns with % Iron Captured by the MFR 3 Micron Filter and % Decrease in L/S Values Using the Analytical and DR Ferrographs with % Iron Being Determined by ADM (# 1, #2, ... Indicate MFR Test No.)

and the theoretical value which should have been removed based on ADM/particle size analyses. The L/S values obtained using the Analytical Ferrograph gave good correlation between the percent change of L/S values with percent iron above 3 microns but showed a small reversal for Tests No. 3 and No. 5 which contained very few large particles. No correlation is shown for the percent iron above 3 microns and percent change in L/S values using the DR Ferrograph.

Figure 85 shows the correlation of percent iron having particle size greater than 3 microns with percent of iron captured by the MFR filter and percent change in Analytical and DR Ferrograph L/S values when the iron analyses were conducted using AE. This data shows that correlation still exists between the percent iron removed by the MFR filter versus percent iron above 3 microns. However, when using AE analyses, a shift is shown as the percent particles above 3 microns is increased. This is due to the decrease in AE sensitivity (detector response) for large particles. The L/S values obtained using the Analytical Ferrograph showed correlation between the percent change of L/S values with percent iron above 3 microns except for the samples having very few large particles. The data shown for the DR ferrograph using AE iron analyses is very similar to that obtained when using ADM with no correlation in DR L/S values with percent iron particles above 3 microns.

Figure 86 shows the correlation of iron having particle size greater than 3 microns with the percent of iron captured by the MFR filter and percent change in Analytical and DR Ferrograph L/S values when the iron analyses were conducted using the PWMA. Samples from Tests No. 4 and No. 5 were not investigated using the PWMA. The data in Figure 86 shows similar trending for the all three parameters (% iron captured by MFR filter and the

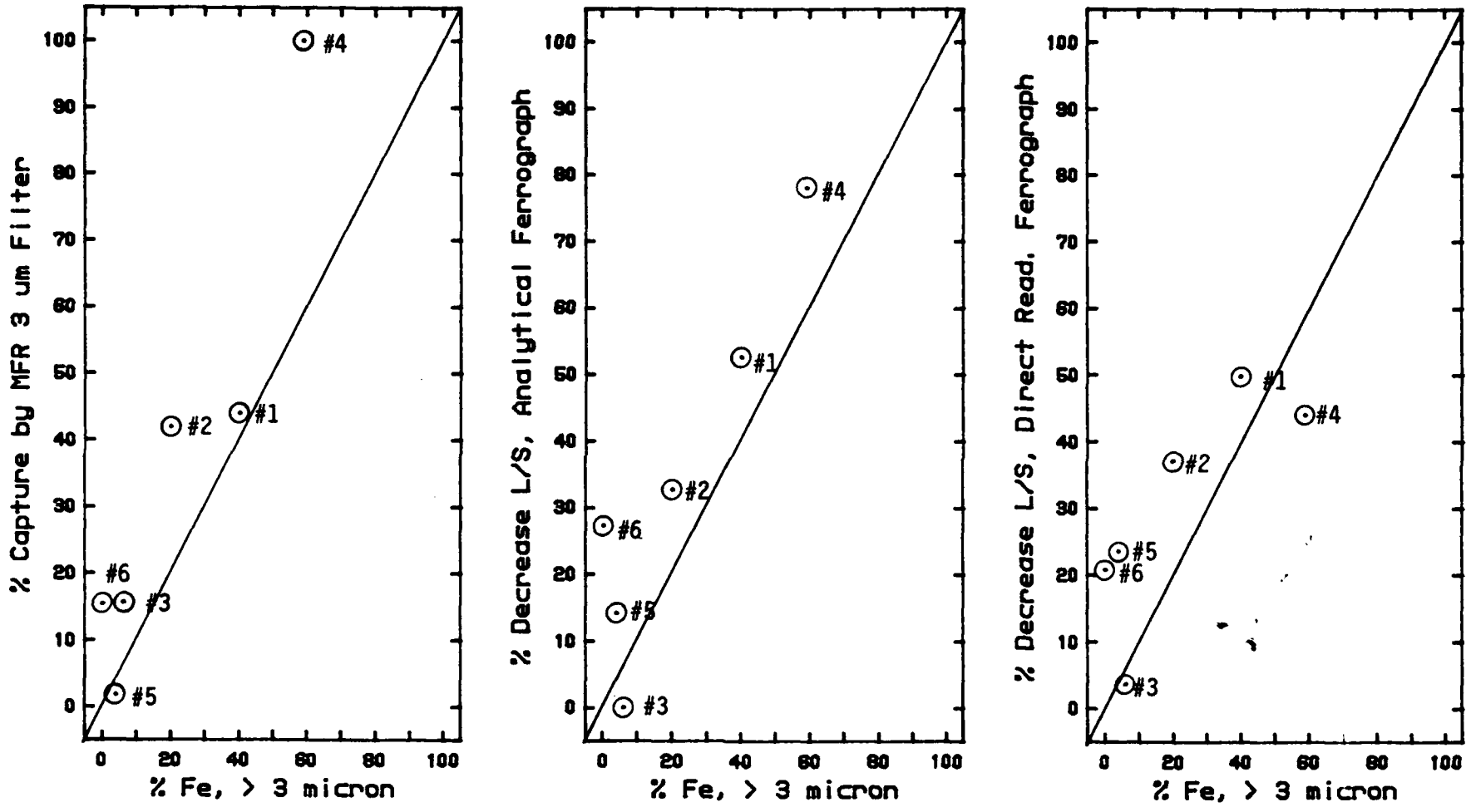

Figure 85. Correlation of % Iron Greater than 3 Microns with % Iron Captured by the MFR 3 Micron Filter and % Decrease in L/S Values Using the Analytical and DR Ferrographs with % Iron Being Determined by AE (#1, #2, ... Indicate MFR Test No.)

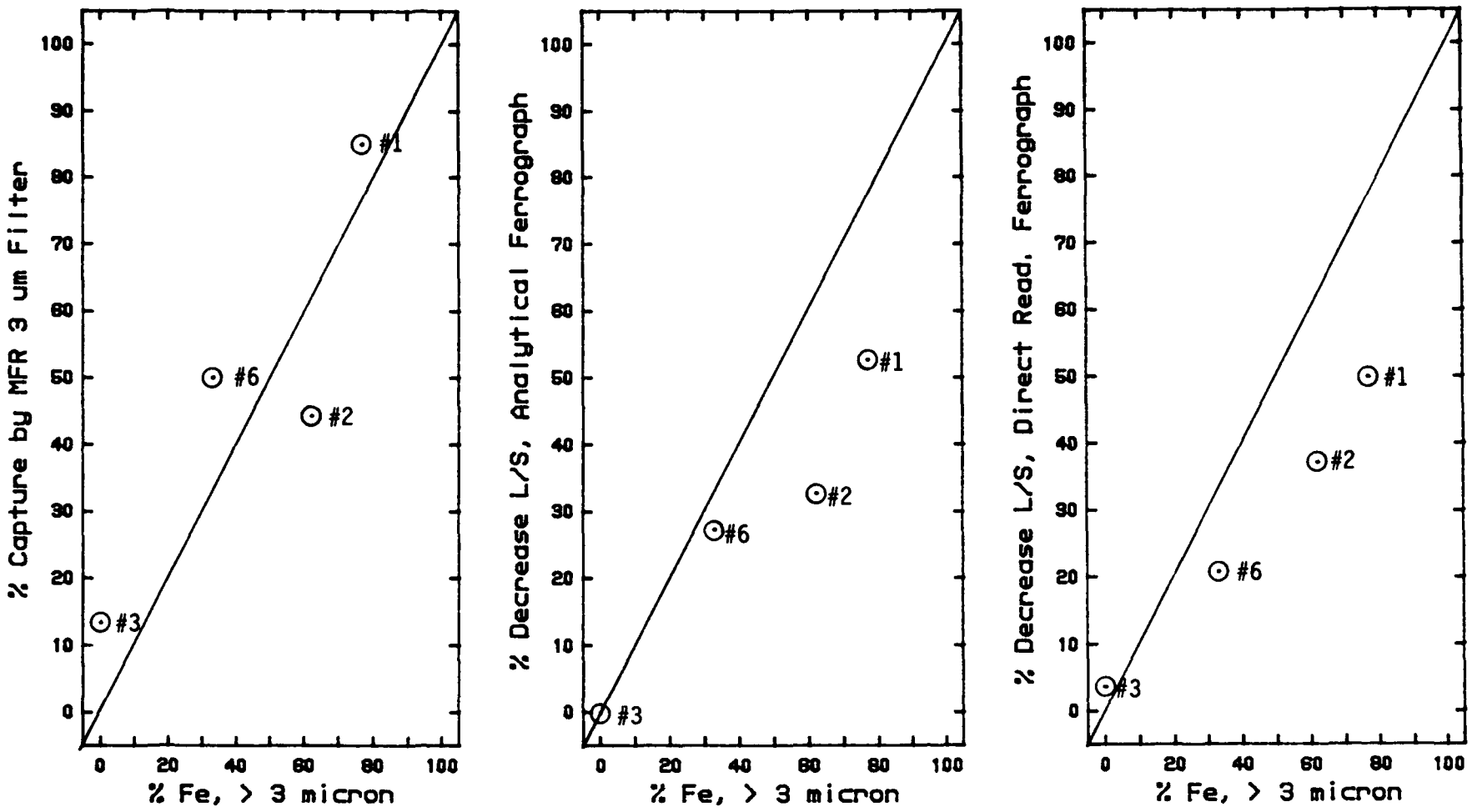

Figure 86. Correlation of % Iron Greater than 3 Microns with % Iron Captured by the MFR 3 Micron Filter and % Decrease in L/S Values Using the Analytical and DR Ferrographs with % Iron Being Determined by the PWMA (#1, #2, ... Indicate MFR Test No.)

change in L/S values for the Analytical and DR Ferrographs) when the percent iron is determined using the PWMA. However, samples from Tests No. 2 and No. 6 show a small reversal in ranking relative to the percent of iron captured by the MFR filter based on ADM analyses.

Figure 87 shows the correlation of percent iron greater than 3 microns determined by ADM with percent captured by the MFR as determined by AE, PWMA and AA analyses. Data for the AE analyses is very similar to Figure 84(a) except for a small decrease in percent particles captured by the MFR which is due to decrease in sensitivity of AE to increasing particle size for the samples containing large particles. The data for the PWMA analyses show similar data as that for AE except for a reversal for Test No. 6. Data for AA analyses (right hand graph) shows distinct bias against large particles which has previously been reported (Figure 84).

(6) Conclusions

(a) Preliminary investigation of microfiltration of limited number and type of samples used indicates that the 3 micron filter operating parameters are compatible with the present operating parameters of operational engines and can be used without serious adverse effect.

(b) Operating parameters monitored during the six tests indicate that microfiltration can be used in lubrication systems where different types of oils are used. The six tests demonstrated the capability of using MIL-L-7808, MIL-L-23699. However, large pressure differential across the filter was obtained after the first pass when used mineral oil was used.

(c) Impact of microfiltration on SOAP cannot be fully identified based on microfiltration of limited number and type of samples used. However, the results of this study showed that SOAP threshold values

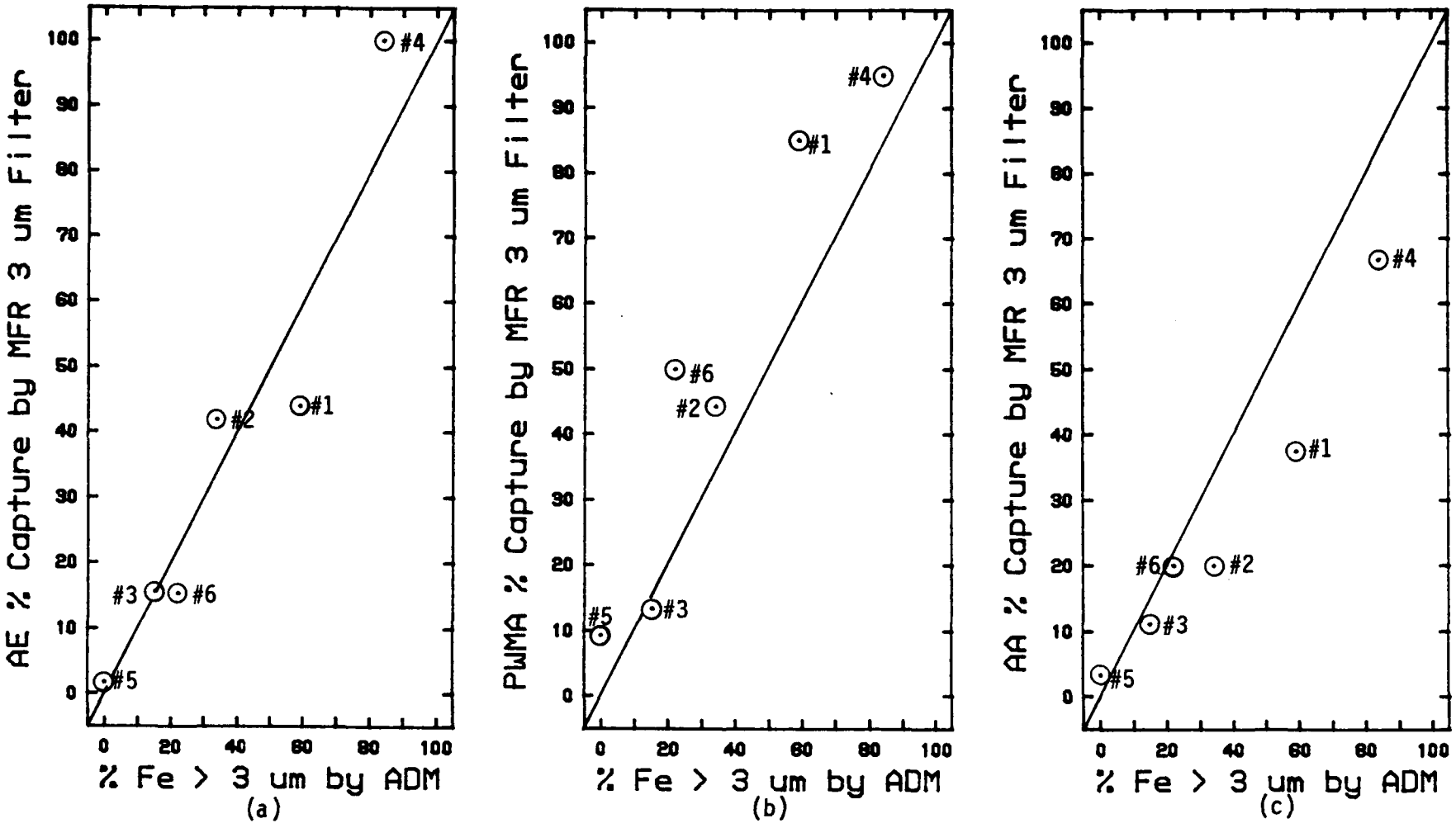

Figure 87. Correlation of % Iron Greater than 3 Microns Determined by ADM with % Iron Captured by the MFR as Determined by AE, PWMA and AA Analyses (#1, #2, ... Indicate MFR Test No.)

may be influenced by the use of microfiltration, especially in samples with particle size >3 micron.

(d) Spectrometric methods also revealed that the level of contaminants after the first pass (even after one hour of recycling the oil at about 18 GPM, Test No. 4) remained constant.

(e) Spectrometric methods showed that the efficiency of 3 micron absolute filtration is almost 100% in removing iron wear debris larger than 3 micron. Efficiency for non-wear debris was not determined.

(f) Comparative analytical techniques showed that SOAP instruments (AA and AE) were able to detect the significant changes in the concentration of wear debris after the first pass through the 3 micron absolute filter for samples containing significant amount of Fe debris greater than 3 micron. However, analytical methods including AA and AE showed no change in concentration for the first and subsequent passes for samples containing Fe wear debris less than 3 micron.

(7) Recommendations

(a) Use of doped samples in this study are not typical of SOAP samples even for those samples from engines having particles greater than 3 micron. Additional studies need to be conducted on samples taken from normally and abnormally operating engines in order to identify fully the impact of microfiltration on SOAP. These samples must include complete drain samples and the SOAP samples, which indicated abnormal operation and the need for TDR or engine repair. These SOAP samples are required for identifying the particle size of wear which indicates normal and/or abnormal wear.

(b) Proper sampling procedures in field operation must be followed in obtaining representative samples for SOAP and microfiltration study so that correlation between true SOAP readings and microfiltration results can be made.

(c) Modification of the microfiltration test rig is recommended to include a variable speed motor to vary GPM for future studies to simulate different operational flow conditions and to determine filter efficiency as a function of flow rate.

(d) Determine the impact of microfiltration on SOAP using oil samples from the fleet of UH-1/AH-1 helicopters equipped with microfiltration systems.

(e) Multi-pass test is recommended for continuously doping the microfiltration system with wear debris from a wear debris generator. Sampling should be done upstream and downstream to determine the efficiency of the microfiltration filter with time.

(f) Wear debris capacity of the test filter should be determined by continuously adding wear and non-wear debris and monitoring the pressure drop across the filter until the filter element collapses or the bypass safety valve opens (100 psi). A plot of the amount of wear debris versus the differential pressure should reveal the dirt capacity of the filter.

5. DETERMINATION OF METALLIC IRON IN WEAR DEBRIS USING A WEAR PARTICLE ANALYZER

a. Introduction

Depending upon the mechanism of wear occurring within lubrication systems different types of wear debris are expected to be produced in lubricating oils. The wear debris can be metallic (mechanical wear), oxidized and/or metallo-organic (chemical wear) in nature and can range from dissolved species to millimeter sized particles.

The Spectrometric Oil Analysis Program (SOAP) is used primarily by

the USAF to monitor changes in specific wear metal concentrations in lubrication systems using atomic emission and atomic absorption spectroscopy. Magnetic plugs and chip detectors are also used as on-line engine health monitoring techniques. However, the detection capability of these techniques is influenced not only by the nature of wear metal species generated within the oil wetted system but by the type, morphology and size of the wear metal particles. Depending upon the wear metal being analyzed the particle size sensitivity of SOAP spectrometers is limited to 3-10 microns.[21,22] However, the on-line monitoring devices detect only those ferromagnetic particles typically larger than those analyzed by SOAP. Therefore, development of a technique for monitoring wear metal debris having particle size sensitivity above SOAP and below the particles captured by magnetic plugs and chip detectors is of critical importance for predicting engine failure.

One of the techniques being considered is a Wear Particle Analyzer (WPA), a commercially available device which measures the concentration of ferromagnetic particles in used oils. This instrument is capable of detecting the metallic form of iron. Since the metallic form of iron is indicative of severe wear,[22] the evaluation of the WPA as a supplementary oil analysis technique could be beneficial to SOAP. Particle capture efficiency, particle size detection limit, sample flow rate and filter fiber size effects are among the parameters which were evaluated.

b. Instrumentation

(1) WPA

Instrumentation and techniques were described elsewhere.[23,24] The magnetic filter is a compressed bed of steel fibers that are magnetized when inserted into the WPA. The filters are available in different grades to preferentially collect particles larger than a chosen size and handle oils of

different viscosities.

Filter	Fiber Size (microns)	Packing Density
F1	15-25	High
F2	41-58	High
F3	102-152	High
F4	15-25	Low

Filters with larger fibers preferentially collect larger magnetic particles. Fibers with lower compression pass oils with higher viscosities. These two parameters allow some flexibility in choosing the filter for a particular analysis. For this work, the F1 and F4 filters were used for analyzing MIL-L-7808 and higher viscosity oils.

(2) Magnetometer

The magnetometer measures the concentration of ferromagnetic species in the sample, independent of particle size.[25] It was one of the tools used to determine the accuracy and particle capture efficiency of the WPA. Measurements of the magnetic iron content were made on oil samples before and after analysis by the WPA. The difference in these values should equal the WPA readout.

(3) Acid Dissolution Method (ADM)

This method was developed by the University of Dayton and reported elsewhere.[26] ADM measures the total concentration of iron, independent of particle size or chemical form.

(4) Solvent Extraction/Atomic Absorption (SE/AA)

This technique was also developed by the University of Dayton research group.[27] It was used to determine the chemical nature of Fe in the 325 mesh, Fe_3O_4, pin-on-disk and used oil samples. The concentration of metallo-organic iron (Fe_O), iron oxide (Fe_{Ox}) and metallic iron (Fe_M) were

determined. Nitric acid was used to extract metallo-organic and metallic iron while piperidine was used to extract metallo-organic iron. Using Fe concentrations obtained from the above extractions and from the acid dissolution method (Fe_{Total}), the concentrations of Fe_O, Fe_{Ox} and Fe_M were calculated. Assuming that ferromagnetic iron in used oils is mostly metallic iron, only the results of SE/AA total Fe and metallic iron concentrations are considered for the purpose of determining the accuracy of the WPA readout.

c. Samples

(1) 325 Mesh Fe Powder

An iron powder sample was prepared from a commercially available 325 mesh Fe powder. One gram of Fe powder was mixed with about a liter of fresh ester base lubricant (MIL-L-7808) in a one-liter flask. The flask was handshaken for a few minutes, agitated in an ultrasonic bath for approximately one hour, handshaken and then allowed to sit undisturbed for four hours, after which the oil was decanted. The Fe concentration in the decanted oil was determined by the acid dissolution method. A portion of the well agitated oil sample was diluted with fresh MIL-L-7808 lubricant to 85 ppm Fe. All samples containing suspended metal particles were handshaken, ultrasonically agitated and vigorously handshaken prior to dilution and analysis.

(2) Sieved Fe Powder

Fe powder was sieved using a sonic sifter equipped with 5-, 10- and 20 micron Ni mesh screens. The 0-5 micron particles are those that passed through the 5 micron sieve, while the 5-10 and 10-20 micron fractions are those that passed through their respective larger size sieves and were captured on the smaller size sieve. Oil samples containing the 0-5, 5-10 and 10-20 micron Fe powder were prepared gravimetrically by weighing a known

amount of the sieved powder and mixing with the proper amount of oil to prepare a desired Fe concentration.

(3) Fe_3O_4 Powder

Commercially available Fe_3O_4 was mixed with the proper amount of ester based oil MIL-L-7808 to the desired concentration.

(4) Pin-On-Disk Samples

The pin-on-disk (POD) samples were generated by a wear test machine using the pin-on-disk wear test configuration. The wear debris generated from the 1018 steel specimen in MIL-L-7808 ester based lubricants was tested without dilution.

(5) Used Engine Oil Samples

The used engine oil samples were obtained from operational turbine jet engines and run without dilution. Some oils were diluted with hexane or kerosene to study the dilution effect on the WPA readout and to minimize their viscosity effect on the flow rate through the WPA filter.

d. Analytical Procedures

(1) WPA Calibration

A 15 minute warm up period allowed ample time for the meter to stabilize before calibration. The meter was adjusted to zero using the zero control with range knob at 100. A 50-ppm or a 66-ppm standard which was provided by the manufacturer was used to calibrate the instrument. The standard was inserted in place of the magnetic filter. The zero reading was again checked with the standard removed.

(2) Typical Sample Analysis on the WPA

A filter was inserted in the funnel assembly and finger tightened. The plastic funnel-filter assembly was inserted into the WPA filter holder. The instrument was then adjusted to zero with range knob at

100, then it was zeroed on the most sensitive scale (range 1). Samples were agitated in an ultrasonic bath for at least 5 minutes prior to the removal of an aliquot. One to two milliliters of the sample was withdrawn by a disposable tip pipet and the sample was injected into the funnel-filter assembly. Vacuum was applied to draw the sample through the filter at a flow rate of approximately two drops per second. Once the sample was drawn through, 5-6 mL of pentane was used to wash down the funnel-filter assembly. Vacuum was again applied giving a flow rate of 2 drops per second through the filter. The needle on the meter was allowed to stabilize a few seconds after the last drop of the solvent had passed through the filter before a reading was taken. In order to convert the WPA reading to ppm, the WPA reading was divided by the ounces used and by the specific gravity of the fluid analyzed.

(3) Quantitative Collection of the Filtrate

A 30 mL sample vial was placed in the vacuum trap for filtrate collection. A vinyl tube extended into the sample vial from the end of the filter tube. An additional 5 mL of pentane was passed through the filter to wash any particles from the tube into the sample vial. The sample vial was removed and placed in a fume hood overnight to allow the pentane to evaporate. Between each different sample the filter was changed and a new piece of vinyl tubing was used. The vacuum trap was washed thoroughly with pentane when new samples were analyzed.

(4) Particle Size Distribution

A two to three milliliter aliquot of the sample was filtered through 0.4-, 1.0-, 2.0-, 3.0-, 5.0-, 8.0-, 10.0- and 12.0 micron polycarbonate membrane filters. Once the sample had passed through the filter, 6-8 mL of pentane was used to wash the filter and filter housing. For each 2-3 mL aliquot filtered a new filter was used and the above

procedure was repeated 10-12 times in order to collect enough of one filter size sample fraction. The sample bottles of each fraction were placed in a fume hood overnight to allow the pentane to evaporate.

(5) Modified Sample Introduction Technique

A 13 mm diameter filter syringe assembly was used to hold a 0.22 micron filter. The syringe assembly was held vertically in a ring stand clamp and a vacuum hose was attached to the bottom of the syringe assembly. The vacuum was applied after 1.0 mL of sample was deposited evenly on the filter. Three to four milliliters of pentane was used to wash down the filter while the vacuum was still applied. The filter was carefully removed from the syringe housing, was folded into eighths and then pushed into a previously cleaned brass tube similar to the ferromagnetic filter tube. Two wooden dowels were used to compress the filter into the tube. The dowels were marked on the edges to allow the proper depth for compression. The tube containing the filter was inserted into a funnel and the filter funnel assembly was inserted into the detection zone of the previously zeroed WPA. After the filter was inserted in the filter holder the needle was brought on scale by adjusting the range knob. The reading was maximized by slowly rotating the filter assembly while observing the meter.

e. Results and Discussion

(1) Effect of Particle Size and Filter Fiber Size

The efficiency of filters using various particle sizes of Fe powders and pin-on-disk used oil samples were studied and the results are shown in Table 82. This table shows the filter type used, the stock concentration of the sample, the WPA results and the concentration of Fe in the filtrate as determined by ADM. Except for the pin-on-disk sample (POD #1), the filtrates of all samples contained less than 2% of the Fe original

TABLE 82

EFFICIENCY OF FILTERS USING VARIOUS PARTICLE SIZES OF FE POWDERS AND PIN-ON-DISK #1 SAMPLE

Sample	Fe Conc. (ppm)	Filter	WPA[b] (ppm)	Filtrate Fe[c] (ppm)
0-5 um	39	F1	8 ± 1	0.5 ± 0.1
0-5 um	39	F2	11 ± 1	0.4 ± 0.0
0-5 um	39	F3	18 ± 2	0.5 ± 0.1
0-5 um	39	F4	17 ± 0	0.4 ± 0.1
5-10 um	44	F1	12 ± 1	0.6 ± 0.2
5-10 um	44	F2	17 ± 0	0.5 ± 0.1
5-10 um	44	F3	20 ± 2	0.3 ± 0.1
5-10 um	44	F4	25 ± 1	0.5 ± 0.1
10-20 um	45	F1	8 ± 1	0.5 ± 0
10-20 um	45	F2	11 ± 1	0.9 ± 0
10-20 um	45	F3	20 ± 2	0.6 ± 0
10-20 um	45	F4	31 ± 6	0.6 ± 0
325 mesh	85	F1	39 ± 5	1.3 ± 0.1
325 mesh	85	F2	43 ± 3	1.3 ± 0
325 mesh	85	F3	46 ± 3	1.4 ± 0.1
325 mesh	85	F4	48 ± 6	1.6 ± 0.1
POD #1[a]	140	F1	77 ± 2	52.8 ± 0.3
POD #1	140	F2	55 ± 8	54.4 ± 0
POD #1	140	F3	40 ± 1	88.4 ± 0.8
POD #1	140	F4	62 ± 4	52.3 ± 0.7

[a]POD Wear metal generated from pin-on-disk wear test
[b]WPA Concentration is the average of two runs
[c]ADM concentrations

concentration. The low Fe concentration in the filtrates indicates that the filters' capturing efficiency of ferromagnetic debris is better than 98%. However, the same filters exhibited much lower efficiency for the POD sample with less than 63% of Fe being captured. The data also indicate that the WPA readouts are less than 46%, 57% 67% and 56% of the original concentration for the 0-5, 5-10, 10-20 and 325 mesh, respectively. Similarly, the POD #1 Fe sample also exhibited WPA results of less than 55%.

The preliminary results shown in Table 82 indicate that for metal powder samples, as the particle size increases from 0-5 to 10-20 microns, the WPA readout does not significantly change for any filter. Also, for any particle size e.g. 0-5 microns, the WPA readout does not appreciably increase with a decrease in the fiber size of the filter. However, for the pin-on-disk wear test sample, the WPA readout increased in the order of decreasing filter fiber size as follows:

$$F3 < F2 < F4 < F1$$

with F1 (finest fiber size) giving the highest WPA reading. Similar results were obtained for the TF39 used oil sample when volumes of less than 2 mL were analyzed (Table 83). For this reason F1 filters were chosen for the analysis of magnetic wear debris in used gas turbine engine lubricants.

(2) Effect of Sample Volume

Sample volume effect on the WPA readout was also studied using two oil samples containing Fe wear debris. Table 83 shows the WPA results for various sample volumes and different WPA filters for POD #2 and used jet engine oil TF39. The results reveal that the WPA gave proportionally higher readings for smaller sample volumes (less than 2.5 mL). In addition, a

TABLE 83

EFFECT OF SAMPLE VOLUME ON WPA READOUT USING PIN-ON-DISK #2 AND USED ENGINE OIL SAMPLES WITH VARIOUS SIZE WPA FILTERS

Sample	Filter	Sample Volume (ml)	WPA (ppm)
POD #2[a]	F1	5.7	15.0
POD #2	F1	2.5	21.0
POD #2	F1	1.7	23.2
POD #2	F2	6.2	15.4
POD #2	F2	2.4	19.0
POD #2	F2	1.5	15.0
POD #2	F3	5.8	16.9
POD #2	F3	2.4	21.8
POD #2	F3	1.4	23.3
TF 39[b]	F1	40.5	2.4
TF 39	F1	8.0	2.4
TF 39	F1	4.9	2.9
TF 39	F1	1.5	6.6
TF 39	F2	47.4	1.7
TF 39	F2	8.8	2.4
TF 39	F2	4.8	1.8
TF 39	F2	1.5	3.9
TF 39	F3	45.2	1.1
TF 39	F3	8.7	1.4
TF 39	F3	6.3	1.6
TF 39	F3	1.6	3.2

[a] 47 ppm Fe POD (pin-on-disk) diluted 1:1 with kerosene
[b] TF 39 used turbine engine oil, diluted 1:1 with hexane

pin-on-disk sample (POD #3) was analyzed without dilution. Results in Table 84 indicate that the F1 filter gave the highest readout and the best repeatability for a 2.0 mL sample volume. The above results further indicate that diluting the sample with a solvent has no apparent effect on the WPA readout and the WPA results for the different magnetic filters are in the expected order.

(3) Particle Size Limitation

In order to determine the particle size limitation of the WPA, several oil samples containing different sizes of Fe wear debris were analyzed using F1 filters. Wear particles generated from pin-on-disk wear test experiments using steel specimens were filtered through 12.0, 10.0, 8.0, 5.0, 3.0, 2.0, 1.0 and 0.4 micron polycarbonate membrane filters and an aliquot from each filtrate was analyzed by the WPA using F1 filter and by the ADM. The ADM gives an accurate assessment of the total concentration of metal species in lubricating oils. Figure 88 shows the particle size distribution and the WPA results of the pin-on-disk samples POD #4 and POD #5. Since the WPA detects only the magnetic species its results are expected to be lower than the ADM because these samples may contain both magnetic (metallic) and nonmagnetic (oxidized, metallo-organic, etc.) forms of iron. Even though the WPA results are much lower than the ADM, they generally trend with those of the ADM curves. They also show no loss of sensitivity due to smaller particle sizes especially in the range of less than 3 microns.

Similarly, Figure 89 shows the particle size distribution (ADM Curve) and the WPA results of another pin-on-disk sample (POD #6) and a used oil sample TF39. These samples contained much smaller particles and were only filtered through 5.0, 3.0, 2.0, 1.0 and 0.4 micron polycarbonate membrane filters for determining their particle size distributions. The

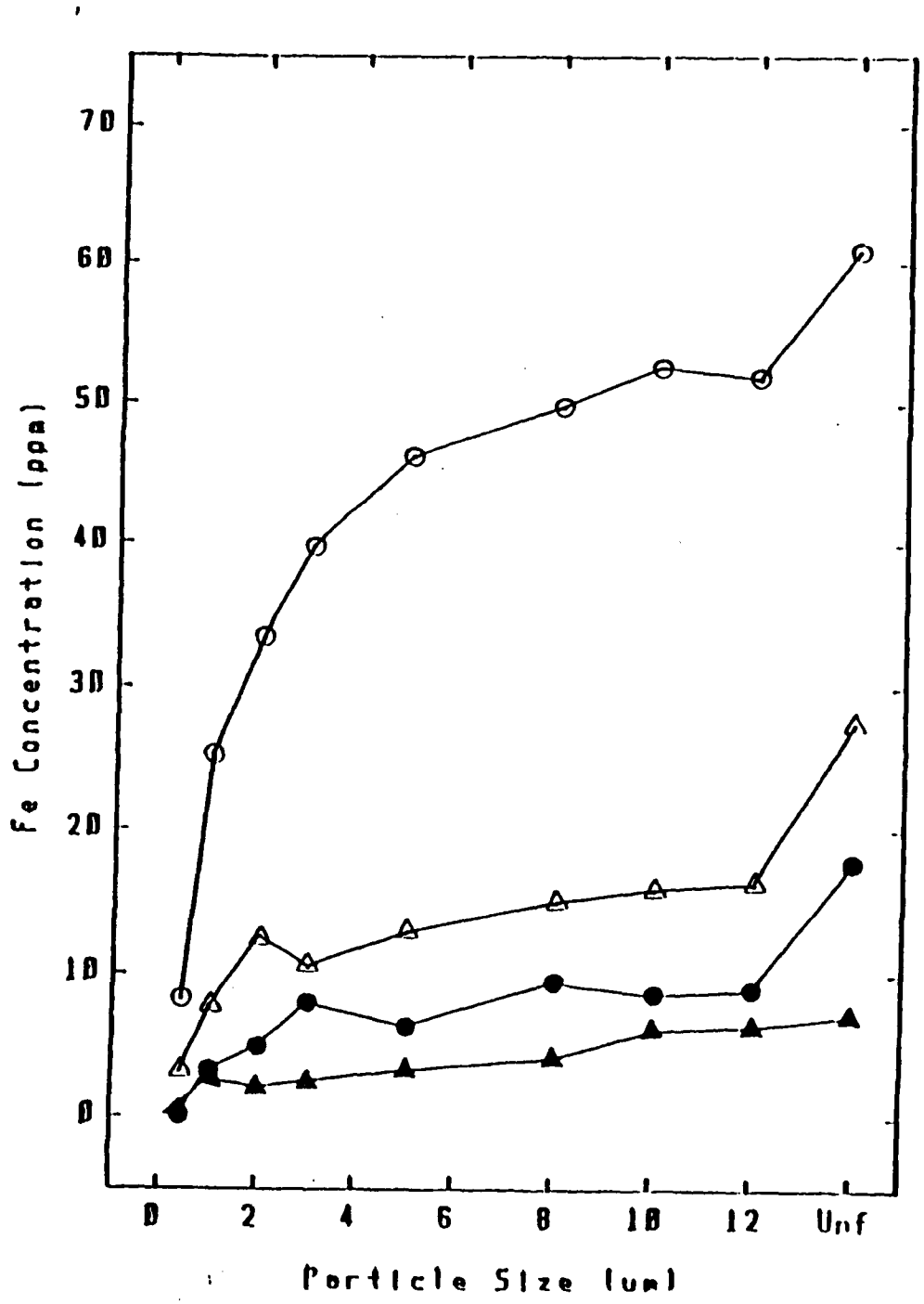

Figure 88. ADM and WPA Analyses of Two Pin-On-Disk Samples

○ ADM of POD #4; ● WPA of POD #4 Using F1 Filter;

△ ADM of POD #5; ▲ WPA of POD #5 Using F1 Filter

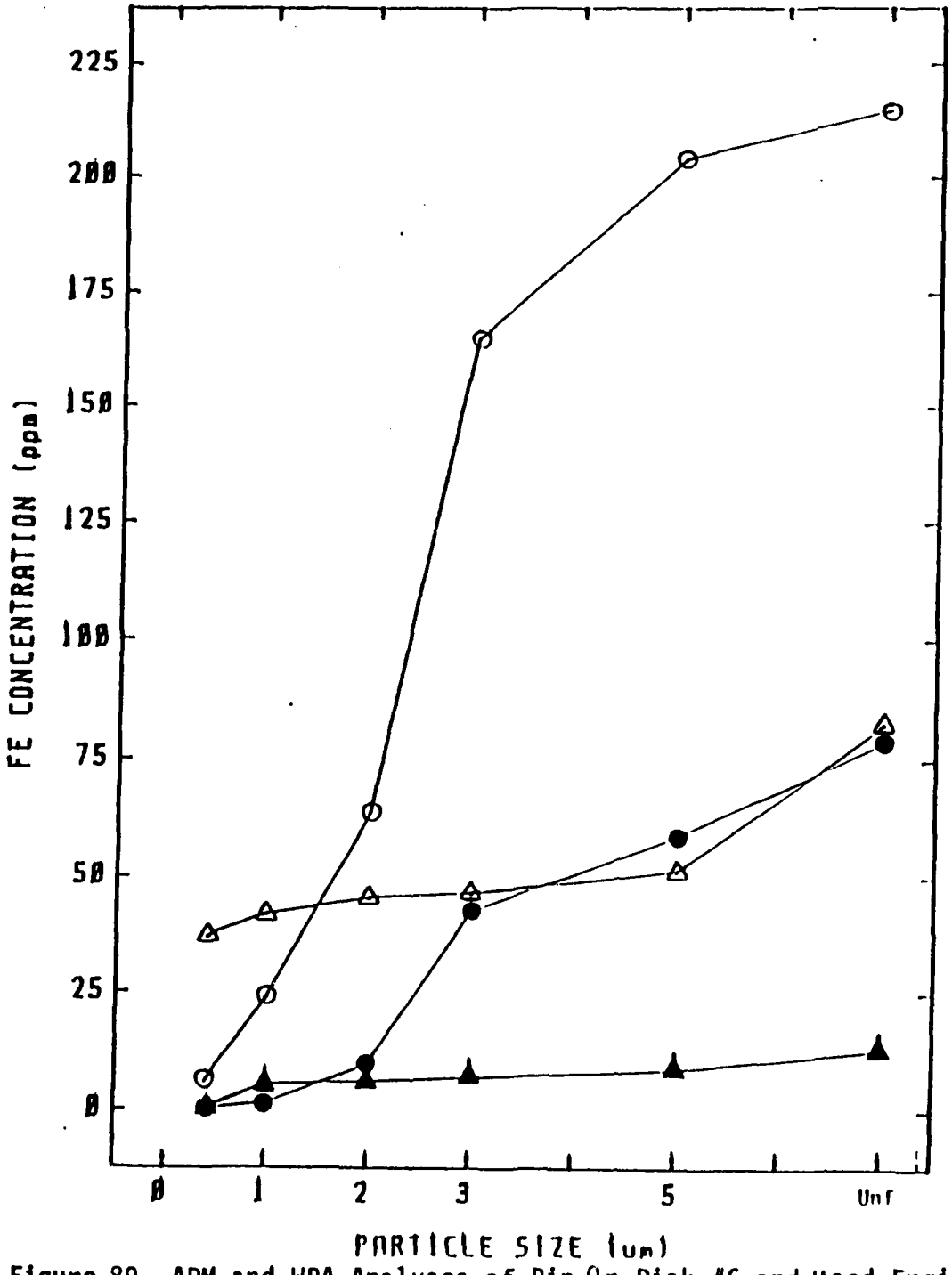

Figure 89. ADM and WPA Analyses of Pin-On-Disk #6 and Used Engine Oil

○ ADM of POD #6; ● WPA of POD # 6 Using F1 Filters;

△ ADM of TF 39 Used Oil Sample; ▲ WPA of TF39 Using F1 Filter.

results for the above two samples also showed that the WPA results were less than but parallel the ADM results.

The acid dissolution method, solvent extraction/atomic absorption, magnetometer and WPA values were obtained for POD #4 sample filtered through 5.0-, 3.0-, 1.0-, 0.4 micron polycarbonate membrane filters. Table 85 shows Fe concentrations obtained from these various techniques versus particle size. The ADM yielded the highest values for Fe followed by SE/AA (only one data point is available), magnetometer and WPA. The ADM is expected to yield the highest value because it measures the concentration of all chemical forms of Fe. The SE/AA value was only the metallic Fe content in the sample. The magnetometer and WPA are expected to measure only the magnetic form of Fe. The difference in the magnetometer values before and after passage through the WPA should approximate the WPA value for that sample. Furthermore, the magnetic Fe values determined by the magnetometer should approximate those of the SE/AA total metallic Fe. Unfortunately, only one data point (unfiltered) of SE/AA is available and it is 30 and 50% higher than the magnetometer and WPA, respectively. The WPA values seem to be close to the magnetometer for particles between 1 and 3 microns but the values were lower for particles above 5 and below 0.4 microns.

An analytical ferrograph[28] was used to substantiate the particle size limitation of the WPA. The filtrate from POD #4 sample after analysis by WPA using F1 filter was analyzed by analytical ferrography. Examination of the ferrogram by optical microscopy revealed that most of the particles were less than 3 micron.

(4) Modified Sample Introduction System

The sample introduction system of the WPA was modified in order to improve the WPA readout capability. Samples were filtered through a 13 mm

TABLE 84

REPEATABILITY OF THE WEAR PARTICLE ANALYZER FOR DIFFERENT SAMPLE VOLUMES AND FILTERS USING PIN-ON-DISK #3 OIL SAMPLE

Sample Size[a] (mL)	F1 (ppm)	F2 (ppm)	F3 (ppm)	F4 (ppm)
2.0	22.7 ± 0.7[b]	9.9 ± 1.3	9.8 ± 0.6	20.7 ± 0.9
1.5	20.5 ± 1.2	10.6 ± 0.3	8.8 ± 0.7	16.5 ± 1.3
1.0	20.3 ± 4.1	12.4 ± 2.0	8.4 ± 1.3	18.8 ± 1.1

[a]Pin-on-disk sample contained 53 ppm Fe
[b]All samples were run 3 times

TABLE 85

PARTICLE SIZE DISTRIBUTION OF FE IN PIN-ON-DISK SAMPLE #4 USING ACID DISSOLUTION METHOD (ADM), SOLVENT EXTRACTION/ ATOMIC ABSORPTION (SE/AA),MAGNETOMETER AND WEAR PARTICLE ANALYZER (WPA)

	Fe Concentration (ppm)					
Sample	WPA	Magnetometer Before WPA	First Pass After WPA[a]	Δ[c]	SE/AA	ADM
Unfiltered	24.8	35.0	3.0	32.0	50	61
<5 um	6.4	10.5	2.2	8.3	ND[b]	46.2
<3 um	8.0	8.0	2.3	5.7	ND	39.8
<1 um	3.3	3.4	2.2	1.2	ND	25.2
<0.4 um	0	0.6	0.8	0	ND	8.2

[a]First Pass = Magnetometer readout after sample passed through WPA filter
[b]ND = Not Determined
[c]Δ = Difference in magnetometer readout before and after passage through the WPA

diameter, 0.22 micron pore size filter. The filter containing the captured debris was then compressed and inserted into a brass tube similar to the ferromagnetic filter tube. The brass tube was then inserted into the WPA filter assembly for analysis.

The results of the WPA readouts for the modified filter and the F1 filter are reported in Table 86. Two different aliquots of each sample were analyzed using each filter. In general, the results showed some improvement due to an increase in sample volume except for POD #4. Using the 0.22 micron filter, the results significantly improved only for the 325 mesh Fe sample. There was a decrease in the Fe_3O_4 and the TF39 samples and no significant change for the POD samples. Difficulty was experienced in filtering the POD and TF39 samples through the 0.22 micron filter due to the presence of higher amounts of nonmetallic debris which plugged the filter. Filtering smaller volumes of these samples did not clog the filter but decreased the WPA sensitivity. The modified filter method has proven to be efficient provided that a different method of filtration is found which will allow all types of oil samples to be filtered without difficulty. It has indicated at least in the case of the 325 mesh sample that metallic particles are somehow prevented from reaching the sensitive zone and if captured on a filter and introduced to the sensitive zone the WPA results will improve.

(5) Effect of Flow Rate

Several used oil samples were analyzed for Fe using the regular (3 mL per min) and the fast flow rate (25 mL per min). For most samples, the faster flow rate enhanced the results with the iron powder (325 mesh) sample showing the most significant improvement (Table 87). However, POD #4 sample showed no change while H48 showed a decrease. H48 contains a heavy amount of metallic iron (325 ppm) and nonmetallic debris which seemed to lower the flow

TABLE 86

RESULTS OF MODIFIED SAMPLE INTRODUCTION SYSTEM IN THE WPA

Fe Sample	ADM Conc. (ppm)	Sample Size (mL)	0.22 μm Filter (ppm)	F1 Filter (ppm)
325 mesh	340	4.0	202 ± 14[a]	91 ± 28
325 mesh	340	1.0	180	157 ± 11
325 mesh	85	1.0	52 ± 7[b]	39 ± 5
POD #4	62	1.0	21	23
POD #4	62	2.0	-	26
POD #5	24	1.0	10	10
POD #5	24	2.0	6	12
POD #6	35	1.0	18	20
Fe_3O_4	209	1.0	68	108
Fe_3O_4	209	2.0	87	117
TF 39	97	0.5	9	15
TF 39	97	2.0	-	17

[a]Result of 4 runs
[b]Result of 9 runs

TABLE 87

EFFECT OF FLOW RATE ON WPA RESPONSE

Sample	3 mL per min (ppm)	25 mL per min (ppm)
F19	5	7
F22	9	11
F39	-	17
F45	1	3
H48	88, 181[a], 64[b]	65[c]
POD #4	30	29 ± 2[d]
325 Mesh	39	59 ± 5[d]

[a]F2; [b]F3; [c]F4; [d]Average of 5 runs, all others one run. 2 g aliquot was used for each run.

through the F1 filter. Therefore, larger fiber size filter (F2) improved the flow and significantly increased the results.

(6) Comparative Analyses

Several samples including iron powder, iron oxide, steel wear debris and engine wear debris were analyzed using ADM, SE/AA, magnetometer and the WPA techniques. Table 88 shows that ADM gave the highest values for Fe as expected. WPA #1 values were consistently higher than WPA #2 which could be due to sampling techniques by different operators and/or the use of different filters. F1 filters were used with WPA #1 and F4 with WPA #2. The WPA #2 results were consistently lower than the magnetometer. This discrepancy is attributed to the fact that some magnetic iron passed through the WPA filter and was not analyzed and some was retained in the tube above the analytical zone. The latter was minimized by allowing the sample to flow at a faster flow rate which resulted in doubling the WPA results of magnetic iron in the 325 mesh sample. Table 88 also shows that the SE/AA technique yielded higher results (16-30% greater) than the magnetometer in the case of 325 mesh and POD samples. These samples contain mainly metallic iron. However, the magnetometer reading for Fe_3O_4 was much higher than the SE/AA mainly because Fe_3O_4 is magnetic. In the case of TF39 sample, a higher magnetometer reading is also produced. This could be due to the possibility that in the piperidine extraction higher values were obtained because the piperidine layer (lower layer) was contaminated with finely suspended (<1 micron) metallic iron particles. If higher Fe_0 values are subtracted from the nitric acid extraction values ($Fe_0 + Fe_M$), it will produce lower metallic iron content.

Filtrates of samples analyzed by the WPA #2 using F4 filters were analyzed by the magnetometer. The results are reported in Table 88.

TABLE 88

IRON CONCENTRATIONS OBTAINED FROM USING ADM, WPA AND MAGNETOMETER

Fe Sample	ADM Tot. Fe (ppm)	SE/AA Met. Fe (ppm)	WPA #1[c] (ppm)	Magnetometer Before WPA[e] (ppm)	Magnetometer After WPA[f] (ppm)	Δ[g] (ppm)	WPA #2[e] (ppm)
5-10 um	82.8	ND[a]	ND	64.4	3	61.4	43.2
10-20 um	16.5	ND	ND	6.7	ND	6.7	1.2
20-30 um	40.3	ND	21.7	35.9	ND	35.9	19.8
325 mesh	85	87	39 (59)[d]	72.8 $\pm$ 4.0	0	72.8	26.2 $\pm$ 4.2
Fe_3O_4	209	16 (186)[b]	117	102.6 $\pm$ 0.2	12.3	90.3	91.8 $\pm$ 9.5[h]
POD #4	62	50	30 (29)[d]	35.0 $\pm$ 0.8	3.0	32.0	24.8 $\pm$ 0.8
POD #5	24	21	12	14.6 $\pm$ 0.1	1.6	13.0	9.6 $\pm$ 0.1
POD #6	35	ND	20	18.5	3.3	15.2	14.8
TF 39	97	4	17	13.4 $\pm$ 0.4	5.9	7.5	10.3 $\pm$ 0.8

[a] ND = Not Determined
[b] Value of iron in iron oxide using SE/AA
[c] F1 filter was used
[d] F4 filter at fast flow rate
[e] Average of 2 runs using F4 filter, analyses by R.T. Lewis
[f] Magnetometer reading after passage through WPA #1 using F1
[g] Δ = Difference im magnetometer readout before and after passage through the WPA #2
[h] Average of 4 runs

Magnetometer reading of the sample after passage through the WPA filter for the oxide, POD and used oil samples indicated that 11 to 36% of the magnetic particles were not captured by the WPA #2 F4 filter. However, the magnetometer did not show any magnetic particles in the filtrate of the 325 mesh after the first pass and small amounts (4%) for the 5-10 micron sample. The sum of the magnetometer reading of the first pass and the WPA #2 should agree with the magnetometer reading of the total sample. In that regard, only the iron oxide and TF39 agreed. All others were lower than expected.

(7) Analysis of Used Oils

Fifteen samples from different operational engines, previously analyzed for metallic iron using SE/AA[27,29] were analyzed by the WPA. The results of these two techniques are reported in Table 89. In general, a fair agreement was found between SE/AA metallic Fe results and the WPA results for the H and P samples. This was true even if the sample contained a fair amount of particles less than 0.6 microns. However, some discrepancies are noted between the two techniques for the R and F samples. Further work is needed to explain the poor correlation.

The results of the ADM and WPA analyses for Fe in Engine Simulator test samples are shown in Figure 90 along with the ratio of WPA/ADM values. The ADM curve has a much higher slope than the WPA test data curve. This could attest to the fact that most of the Fe species in the used oil is in the form of very small particles and nonferromagnetic corrosion product which could not be detected by the WPA. Even though the slope of the WPA results is relatively small, there appears to be a definite increase in the iron concentration in the test period from 0 to 100 hours. The ratio of the WPA/ADM values is variable and relatively high during the first 35 hours of sampling. However, it levels off to about 20% after 45 hours.

TABLE 89

COMPARATIVE RESULTS USING THE WEAR PARTICLE ANALYZER AND A SOLVENT EXTRACTION METHOD FOR IRON IN USED TURBINE ENGINE OILS

Sample[a]	WPA Fe Conc.[b] (ppm)	Total Fe[d] (ppm)	SE/AA Metallic Fe (ppm)	SE/AA <0.6 µm (ppm)	SE/AA >0.6 µm (ppm)
H-1	2.4 ± 0.2	5.4	2.3	1.3	1.0
H-23	23.8 ± 0.8	75.4	28.8	13.1	15.7
H-47	3.4 ± 0.2	14.4	3.7	2.8	0.9
H-49	5.5 ± 0.2	33.4	7.9	2.1	5.8
P-7	3.0 ± 0.6	5.7	1.1	-	-
P-48	2.7 ± 0.5	14.5	4.5	-	-
P-58	20.3 ± 1.2	57.4	19.0	11.0	8.0
P-61	3.7 ± 0.4	16.0	7.2	-	-
P-83	2.7 ± 0.3	17.3	5.7	-	-
P-97	4.3 ± 0.7	28.0	7.7	-	-
R-5	4.3 ± 0.5[c]	7.2	1.4	-	-
R-445	5.5 ± 0.5	4.1	1.3	-	-
F-19	6.5 ± 0.7	24.7	19.0	7.0	12.0
F-22	4.9 ± 0.2[c]	25.2	14.1	7.6	6.5
F-39	17.7 ± 0.6[c]	30.4	22.5	2.5	20.0

[a] Sample size used was 2.0 mL through F1 filter type
[b] Each sample was run 3 times
[c] Sample was run 2 times
[d] Fe concentration was determined by ADM

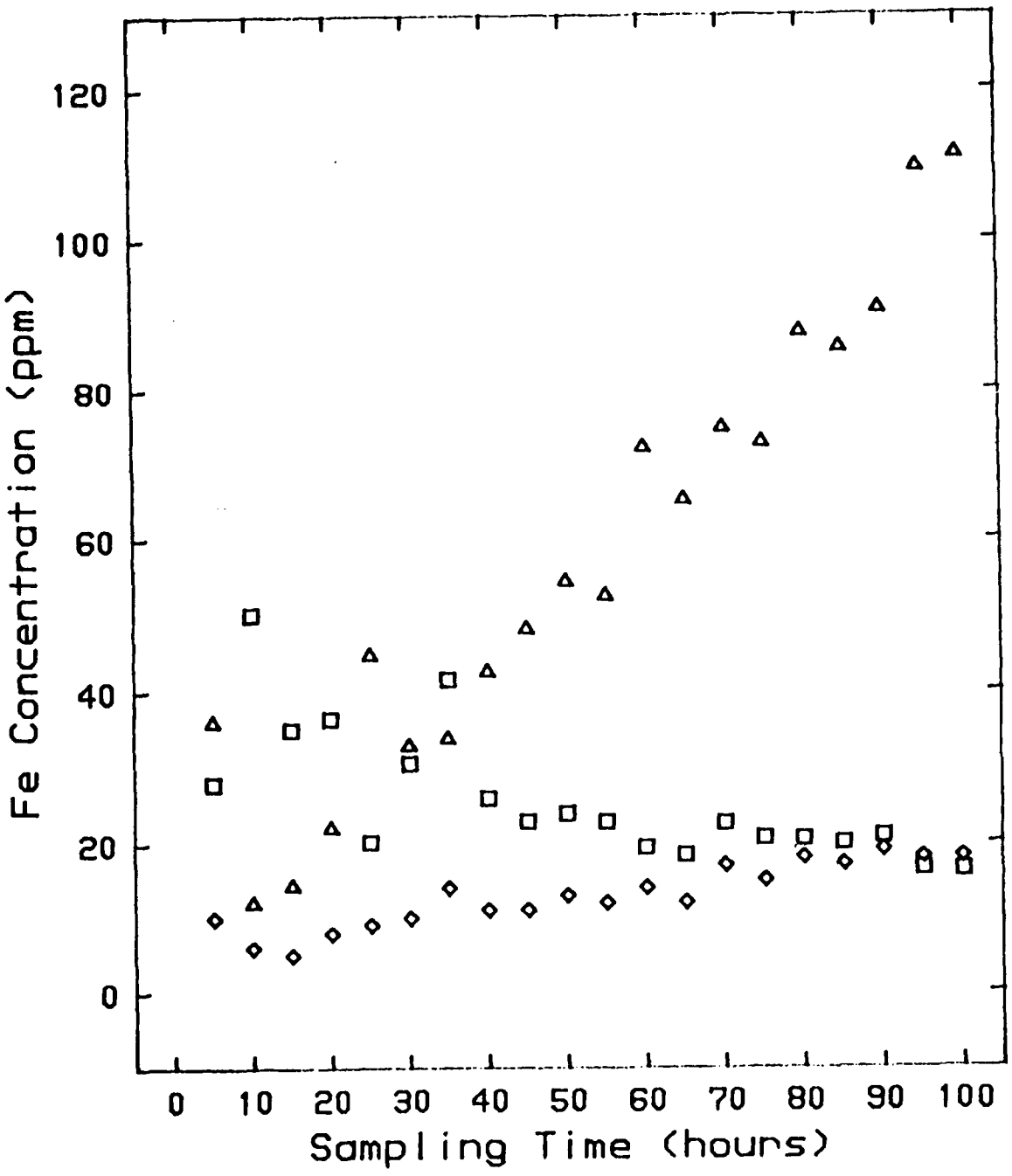

Figure 90. Iron Results of Engine Simulator Test Samples Using ADM and WPA Techniques

△ ADM ; ◇ WPA ; □ WPA/ADM

f. Summary

A study was conducted to investigate the capability of a Wear Particle Analyzer (WPA) in quantitatively determining the concentration of ferromagnetic particles in used lubricants. The effects of sample volume, particle size, particle type, sample flow rate and type of magnetic filter on the WPA reading have been determined using iron powders and an iron oxide suspended in oils, wear metals generated from a wear test machine and used oils from operational aircraft jet engines. Acid dissolution, solvent extraction and magnetometer techniques were used to examine the accuracy of the WPA. Filters made from micron size steel fiber and compressed with a high force gave the highest WPA readout. The optimum sample volume was approximately 2 mL and the effective particle size captured by the WPA filter was less than 3 microns. Higher flow rates improved the results for iron powders. The study reveals that the WPA is an adequate analytical tool for analyzing used oils for metallic iron particles and can be used to supplement other oil analysis techniques.

g. Conclusions

The Wear Particle Analyzer is a technique sensitive to metallic iron, the form of iron most often associated with abnormal wear in lubrication systems. The instrument appears to suffer from a lack of accuracy in the analysis of metal powders and used oil samples, but it responds to changes in the concentration of ferromagnetic wear debris. The accuracy of analyzing metal powders in oil was much lower than the magnetometer and AE/AA. Several attempts were made to improve its accuracy. Only the modified filtration system and higher flow rates improved the results. The modified filter method would be a potential solution to the accuracy problem provided that a better filtration system is found that will allow all types of oils to be

filtered without difficulty. The F4 filter operating at much higher flow rates offered the best method in improving the accuracy of the results.

The above findings reveal that the WPA is not entirely quantitative for analyzing magnetic particles but it is an adequate analytical tool that can be used to supplement oil analysis techniques since oil samples from engines experiencing severe wear contain particles greater than 1-3 microns. Magnetic particles above this range can be readily detected by the WPA and trending techniques can be established for early detection of engines experiencing severe wear. This advantage coupled with its portability and simplicity of use warrant its field testing as a screening device to identify those engines experiencing severe wear.

SECTION IV

INVESTIGATION OF LUBRICANT MONITORING TECHNIQUES

1. INTRODUCTION

The main goal of this study was to investigate the electrochemical properties of degraded synthetic turbine lubricants and to relate these properties to specific chemical changes in the lubricant. Specific properties investigated include dielectric constant, dielectric breakdown strength and that which is measured by the COBRA (Complete Oil Breakdown Rate Analyzer).

2. MONITORING OF LUBRICANTS BY DIELECTRIC CONSTANT

A model NI-2C Lubri Sensor (Northern Instruments Corp.), an oil monitoring device, was used for the analysis of laboratory stressed turbine engine lubricants.

a. Theory and Design of Instrument

The Lubri Sensor measures changes in the dielectric constant of a lubricating oil relative to a fresh oil. Dielectric constant (DC) is defined as "the ratio of the capacity of a condenser with that substance as dielectric to the capacity of the same condenser with a vacuum for dielectric"[30] and as such is a measure of a materials' ability to resist an electric field. This resistance or dampening of the field is due to a buildup of opposing charges on the electrode (capacitor) surface due to orientation of both the permanent and induced dipoles of the molecules of the dielectric.

The Lubri Sensor consists of a bridge with two resonating circuits. One circuit uses a 5 MHz signal and contains the electrode sensor (i.e capacitor) in which the oil sample is placed. The instrument is calibrated

for a particular lubricant by placing the fresh oil in the sensor and tuning the second oscillating circuit by means of a calibration knob until the two circuits are in resonance as indicated by a zero (null) reading on the front panel meter. Placing a degraded lubricant in the sensor causes a change in the oscillator current of the sample circuit due to changes in the dielectric constant of the degraded lubricant relative to the fresh oil. Readings then can be made by either directly reading this current off of the front panel meter (-50 to + 50 μA) or by means of a "deviation scale" knob (0-12 units) which is a measure of the amount of rotation of this knob necessary to bring the meter to null. Initial data analysis indicates that these two readings are directly proportional to each other. Since the deviation scale knob can only read positive displacements (increases in dielectric constant) all data from this instrument in this study will be reported as meter readings (μA).

The Lubri Sensor was designed for use as a monitoring device for automotive oils. As the oil degrades during normal use, oxidation products build up which increase the DC of the oil resulting in a positive reading from the Lubri Sensor. The manual recommends a deviation scale rejection threshold of 4 (a meter reading of about 35 μA) for mineral oil lubricants and 7.5 to 8 for synthetic hydrocarbon lubricants. The instrument is also sensitive to various type of contaminants in the oil. Fuel dilution can cause negative readings while the presence of water and antifreeze can cause large positive readings. Wear particles were reported to cause erratic behavior due to their changing the cell constant of the sensor.

b. Lubri Sensor Analysis of Degraded Turbine Engine Lubricants

In order to determine the usefulness of the Lubri Sensor as a monitoring device for degraded turbine engine lubricants, a series of measurements were made on MIL-L-7808 and MIL-L-23699 lubricants stressed in

the Squires oxidative, Squires confined heat and corrosion and oxidation tests. In addition, an oil with various concentrations of added iron powders was measured.

(1) Confined Heat Stability Test Lubricants

The confined heat stability test is a very mild oxidation test because diffusion of air into the lubricant is limited. The TAN typically reaches fairly high values due to relatively greater retention of volatile components and are mainly the result of thermal degradation of the ester. The Lubri Sensor readings for the lubricants from this test at 190°C for six MIL-L-7808 and two MIL-L-23699 lubricants (O-71-6 and O-77-15) show a fairly consistent rise vs. test hours (Figure 91). When these readings are plotted vs TAN changes, a linear relationship is observed that is fairly formulation independent (Figure 92) with correlation coefficients all greater than 0.99. This correlation is not meant to imply that carboxylic acids are solely responsible for the dielectric constant increase but rather that the DC tester readings are sensitive to basestock degradation of which TAN increase is an effect. Other thermal degradation products as well as smaller amounts of oxidation products also contribute to the observed dielectric constant increase. The small volatilization weight losses (<1%) as well as the minimal amount of oxidation in this test produces only very small viscosity increases, generally less than 5 percent. As a result, no correlation was found between DC tester readings and viscosity changes.

(2) Squires Oxidative Test Samples

Lubri Sensor readings were made on all six MIL-L-7808 lubricants and two MIL-L-23699 lubricants stressed in the Squires oxidative test at 190°C and their plots are shown in Figure 93. The six MIL-L-7808 lubricants show no particular trend vs. stressing time as a group. Two of the

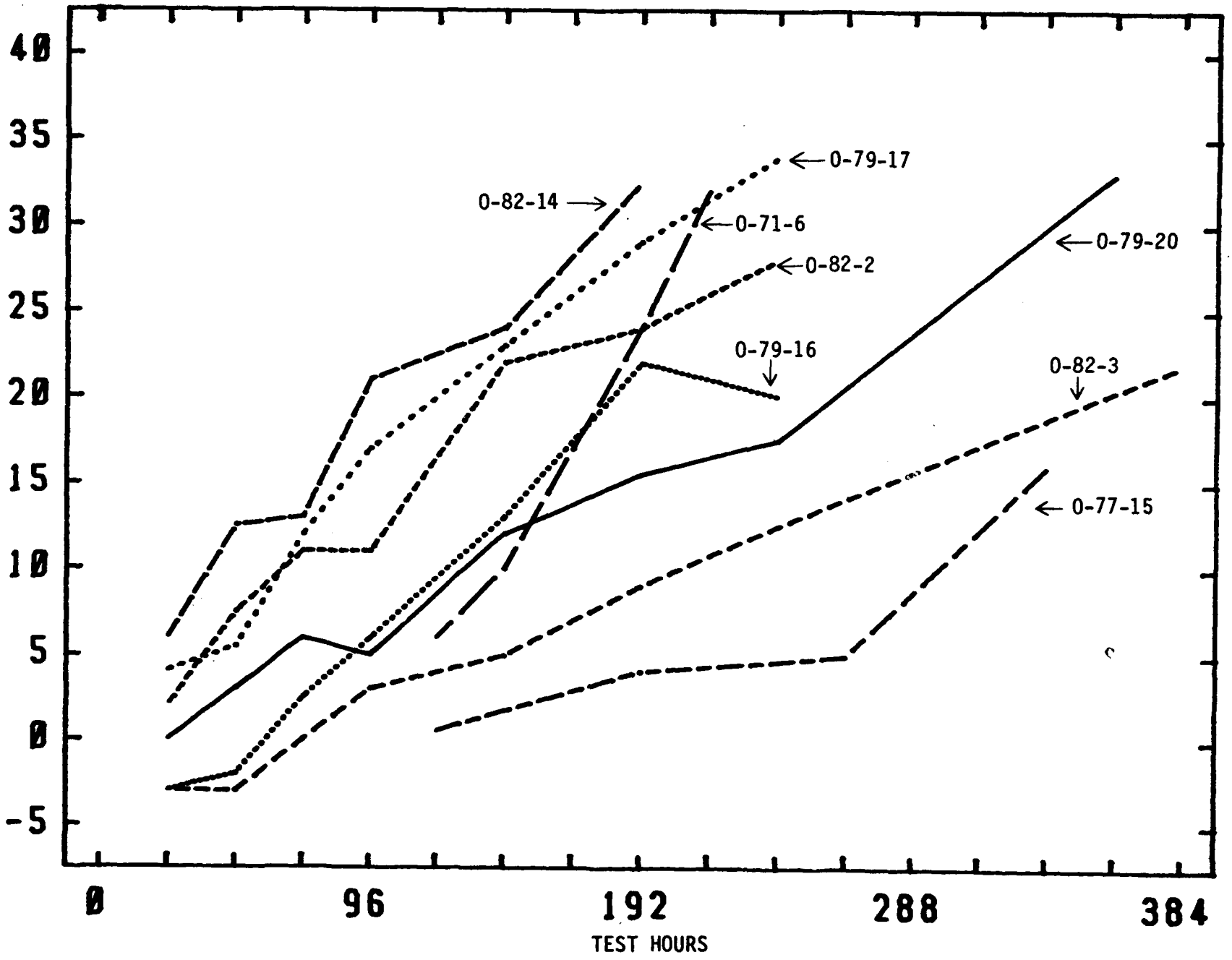

Figure 91. Lubri Sensor Readings for MIL-L-7808 and MIL-L-23699 Lubricants Stressed in the Confined Heat Stability Test

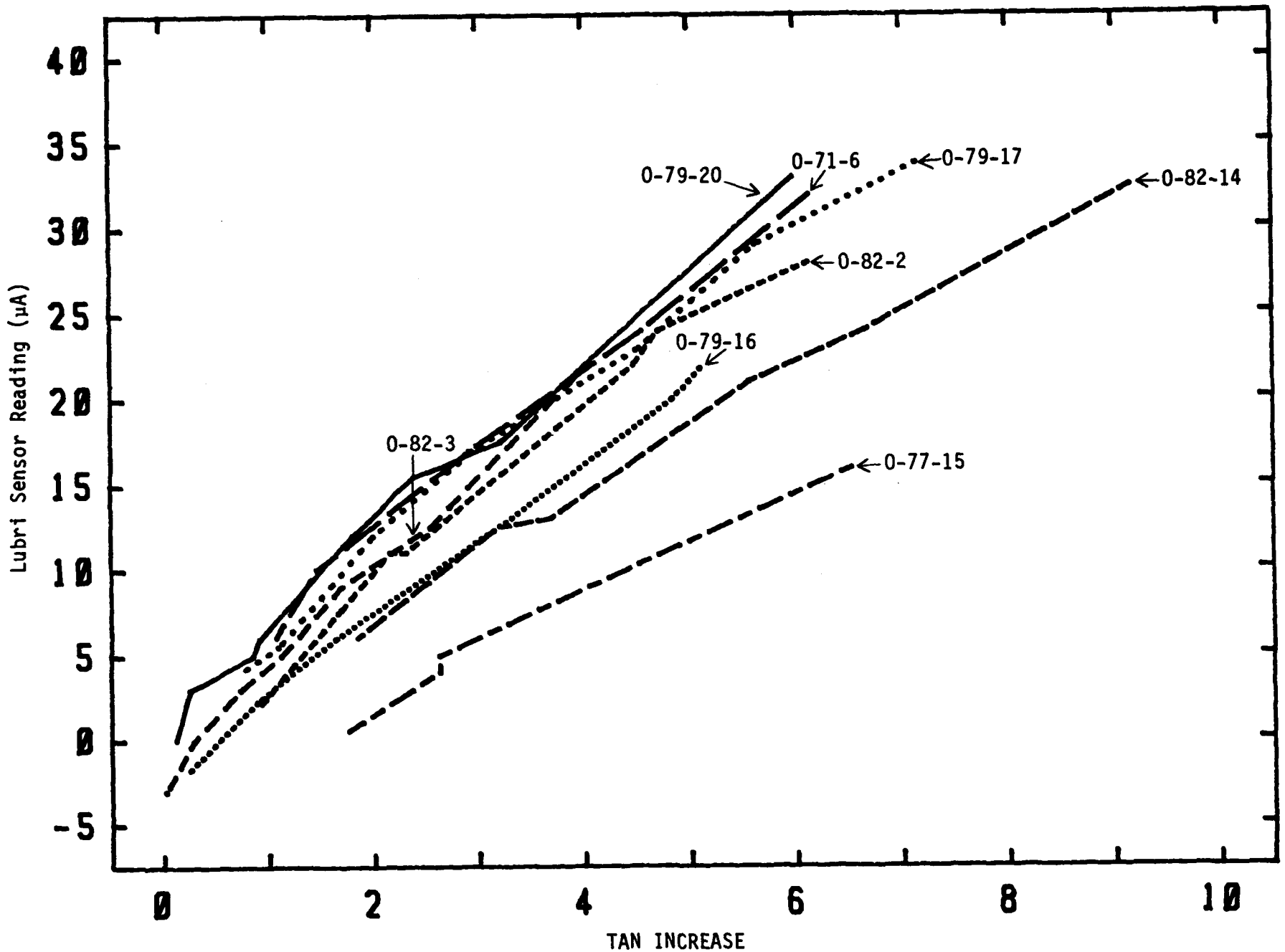

Figure 92. Lubri Sensor Reading vs. TAN Increase for MIL-L-7808 and MIL-L-23699 Lubricants Stressed in the Confined Heat Stability Test

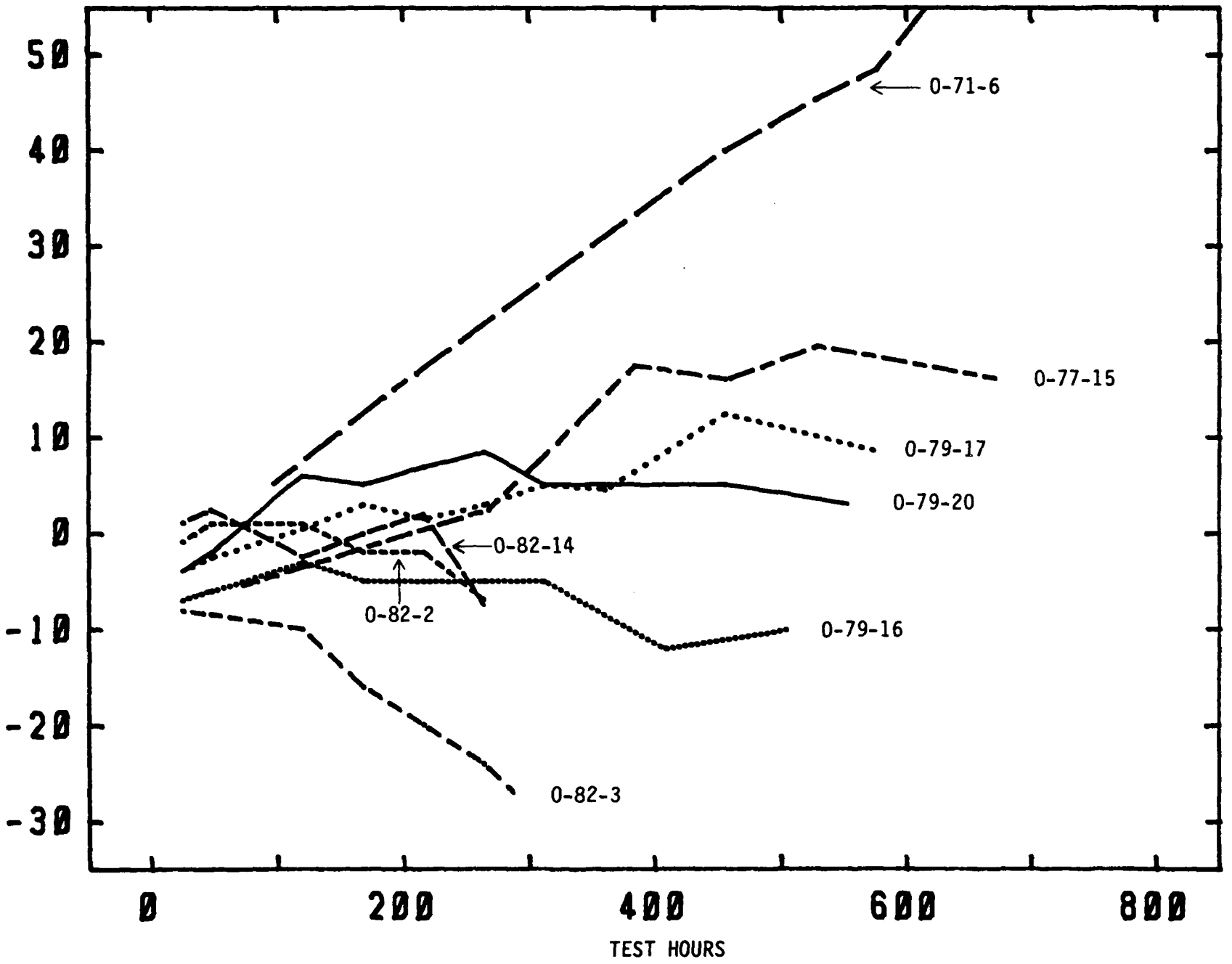

Figure 93. Lubri Sensor Readings for MIL-L-7808 and MIL-L-23699 Lubricants Stressed in the Squires Oxidative Test

lubricants show a modest upward trend (increase in DC), two of the lubricants show no particular trend and the remaining two lubricants show a modest to severe downward trend. This erratic behavior can be explained by the lack of condensate return in this test with the corresponding loss of the more volatile (and higher DC) components including much of the oxidation products. In the case of O-82-14 and O-79-16 it would appear that most of the oxidation products are lost through volatilization along with some of the lighter ends of the ester basestock resulting in a decrease in the DC of these lubricants during the oxidation test. The two MIL-L-23699 oils show positive trends during the oxidation test possibly due to their lower volatility. This behavior can be shown by a plot of volatilization weight loss vs test hours for the eight lubricants (Figure 94). The two MIL-L-23699 lubricants, which exhibit the smallest rate of weight loss, give the highest Lubri Sensor reading increases. Conversely, the two lubricants which display the highest rate of weight loss (O-79-16 and O-82-2) give the lowest Lubri Sensor readings. The data shows that interpretation of Lubri Sensor reading in tests (and engines) that involve considerable amounts of volatilization of the lubricant would be difficult.

The effects of volatilization weight loss on Lubri Sensor readings can be shown by stressing two MIL-L-23699 lubricants in the Squires oxidative test at 215^{o}C with and without condensate return. The results of these analyses are shown in Table 90.

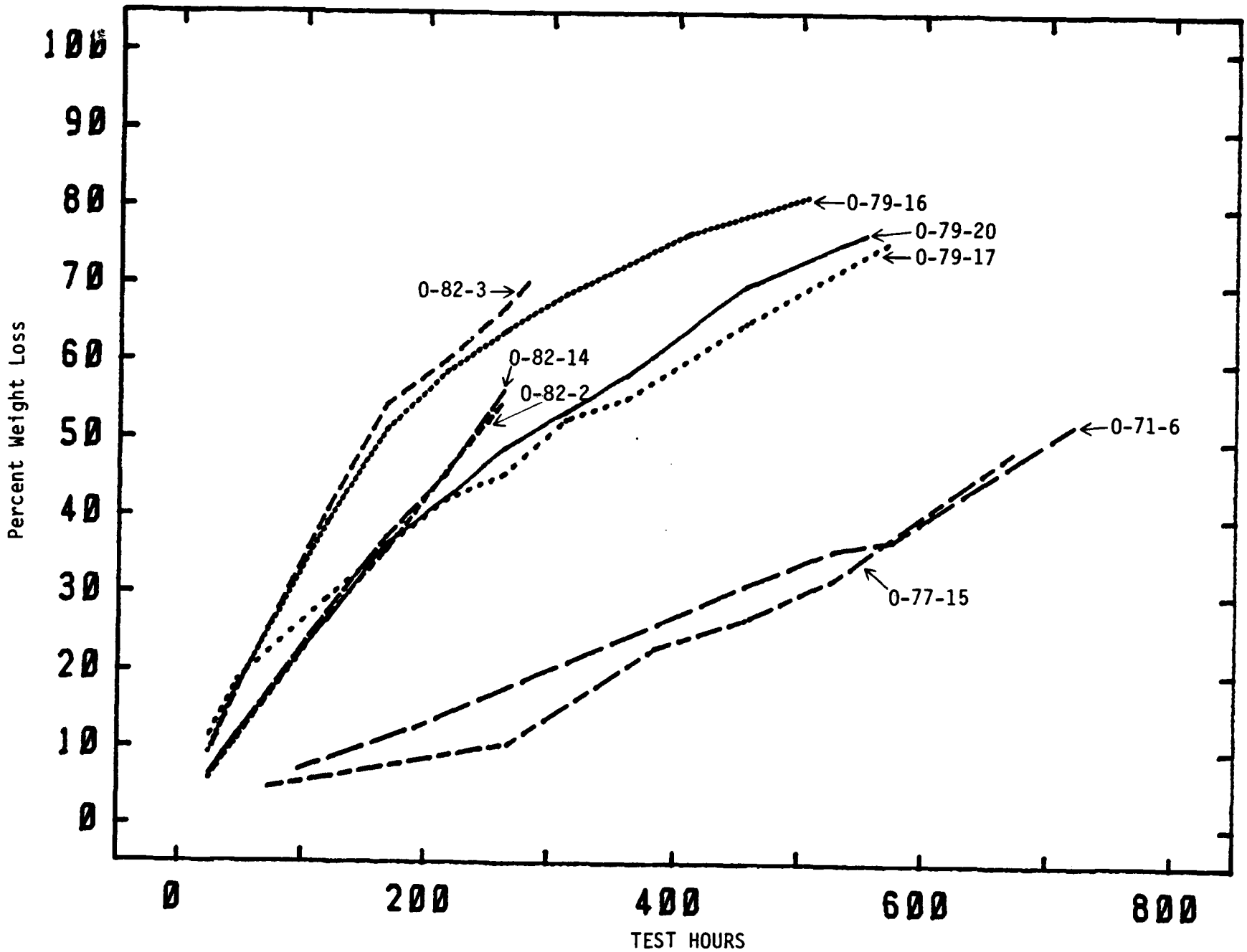

Figure 94. Volatility Weight Loss for MIL-L-7808 and MIL-L-23699 Lubricants Stressed in the Squires Oxidative Test

TABLE 90

EFFECT OF CONDENSATE RETURN ON LUBRI SENSOR READINGS

Lubricant	Test Hours	Lubri Sensor Reading (μA) No Condensate Return	Lubri Sensor Reading (μA) Condensate Return
O-79-18	24	+15	>+50
	48	-	>+50
	72	+33	-
O-85-1	24	+10	+15
	48	+21	>+50
	72	+25	>+50

The data shows that the use of condensate return results in a considerable increase in Lubri Sensor readings. For O-85-1, volatilization weight loss is considerably less for the test with condensate return (Table A-1). Thus the increase in the Lubri Sensor readings for this lubricant is due to greater retention of oxidation products. However, for O-79-18 the use of condensate return accelerated the degradation of the lubricant resulting in relatively greater weight losses, TAN and viscosity increases (Table A-1); therefore the increase in the Lubri Sensor readings for this lubricant is due to the relatively greater degradation of the lubricant induced by the use of condensate return.

(3) Corrosion and Oxidation Test Samples

Lubri Sensor readings were made on four MIL-L-23699 lubricants stressed in the corrosion and oxidation test at 370°F (Figure 95). As

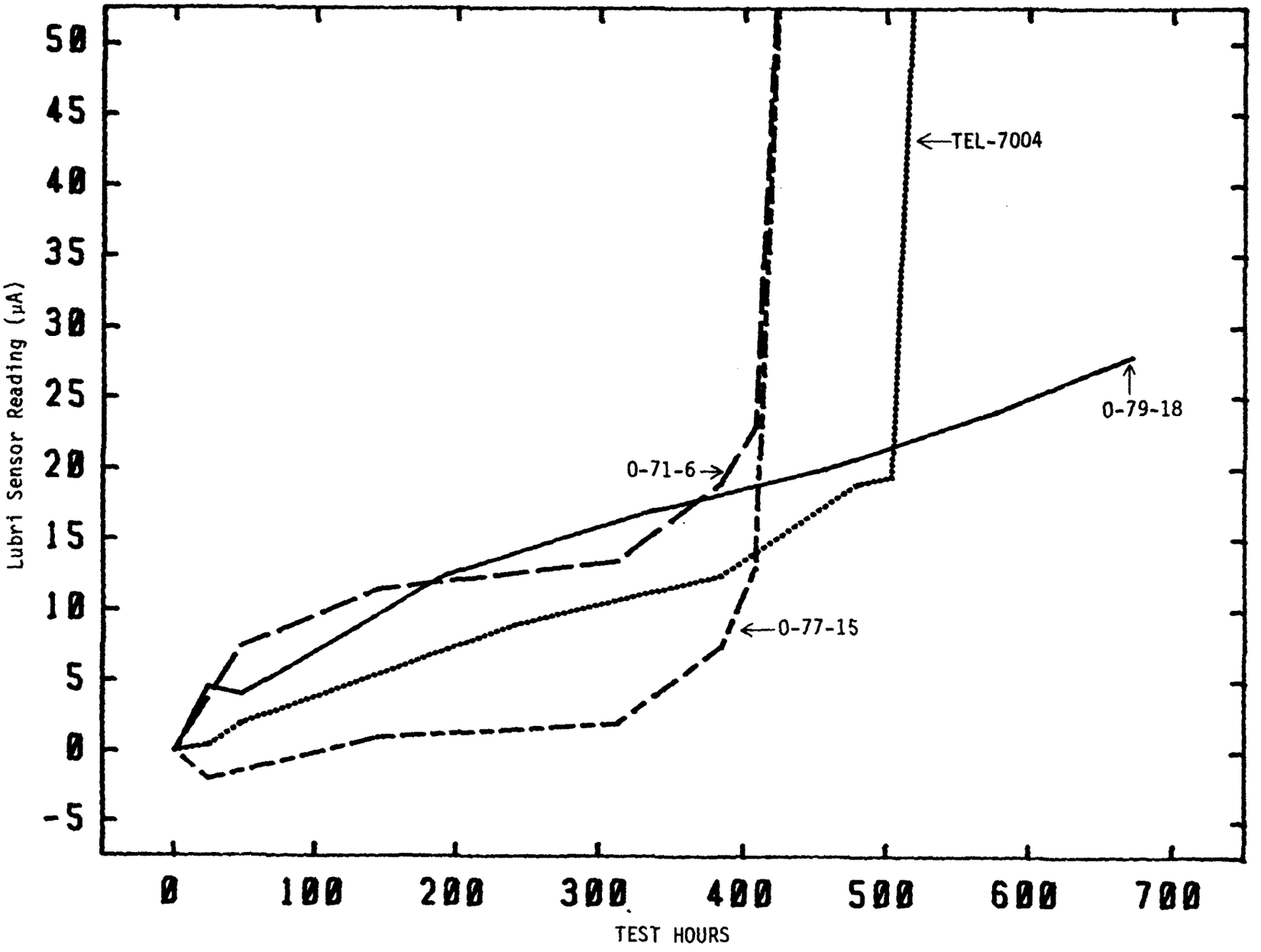

Figure 95. Lubri Sensor Readings for MIL-L-23699 Lubricants Stressed in the Corrosion and Oxidation Test

expected, all lubricants tested showed increases in DC vs. stressing time since this particular test employs condensate return resulting in greater retention of oxidation products in the degraded lubricants. The four MIL-L-23699 lubricants all show a similar rise in DC until the breakpoint of the oil at which time the meter reading went positive offscale (note that the breakpoint sample of O-79-18 was not available for measurement). This behavior is due to the sensitivity of the Lubri Sensor to oxidative consumption of the basestock. As long as the lubricant has sufficient antioxidant capacity, the oxidative consumption of the basestock is minimal and it's DC rises slowly. But at the breakpoint the basestock is rapidly consumed resulting in the production of a large amount of oxidation products with a subsequent large rise in DC.

Figure 96 shows the plots of TAN vs. Lubri Sensor readings for the MIL-L-23699 lubricants. The data shows that TAN and Lubri Sensor readings show an excellent correlation with one another. However, it is not the acids alone that are responsible for the observed DC rise. Carboxylic acids do not have very high DC readings and at the concentrations present in these oils should not contribute significantly to the observed DC rise. For example, addition of butyric acid to O-76-5 (TMPH) basestock sufficient to produce a theoretical TAN of 10.0 produces a Lubri Sensor meter reading change of only +5 μA. But TAN itself is a relative measure of basestock deterioration and it is likely that the other products of ester oxidation (alcohols, ketones, aldehydes, etc.) are responsible for the bulk of the DC increases in these lubricants during oxidative stressing. A similar relationship is observed for viscosity vs. Lubri Sensor readings (Figure 97).

A possible use for the Lubri Sensor in the laboratory would be as an aid for determining sampling intervals and predicting the breakpoint of

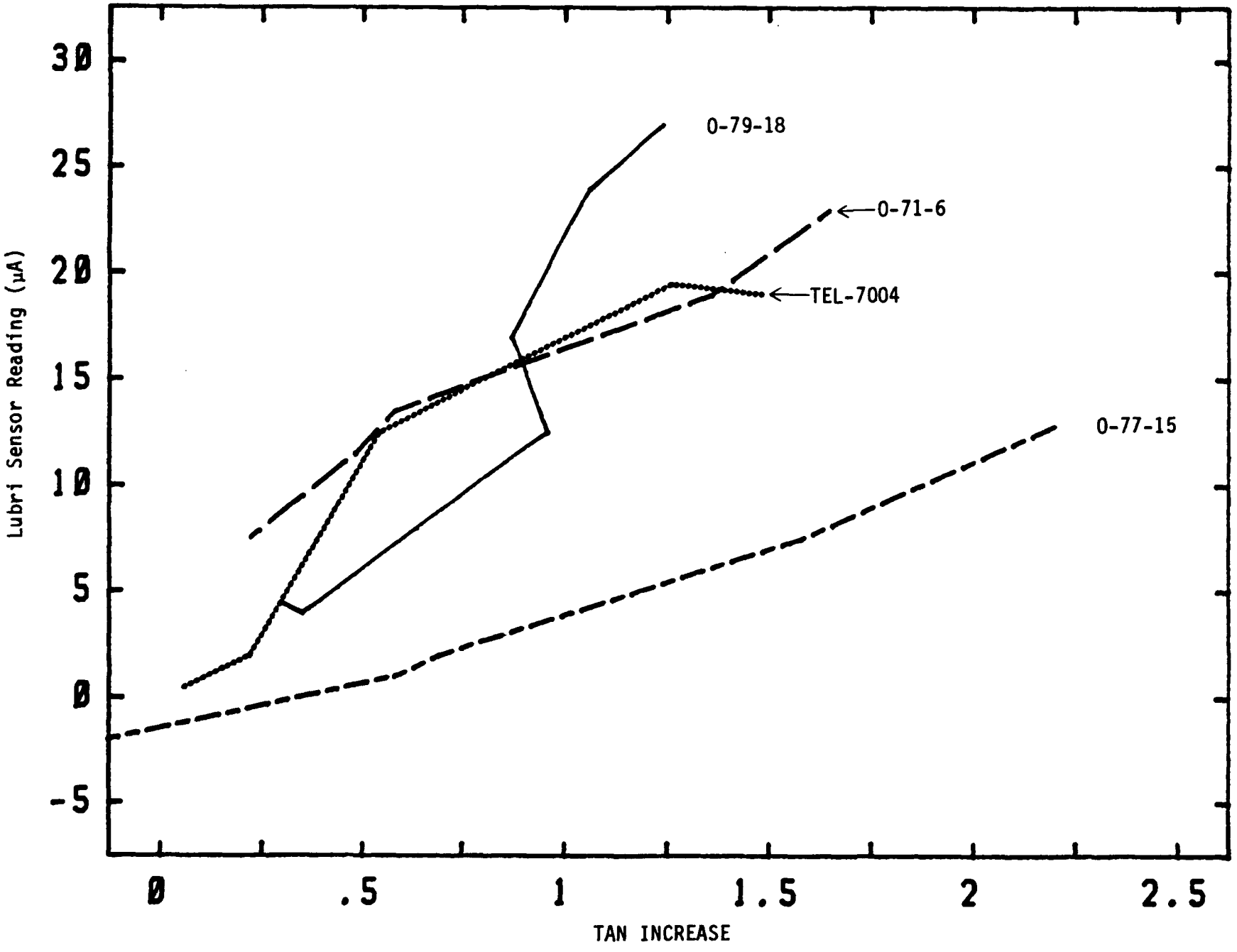

Figure 96. Lubri Sensor vs. TAN Increase for MIL-L-23699 Lubricants Stressed in the Corrosion and Oxidation Test

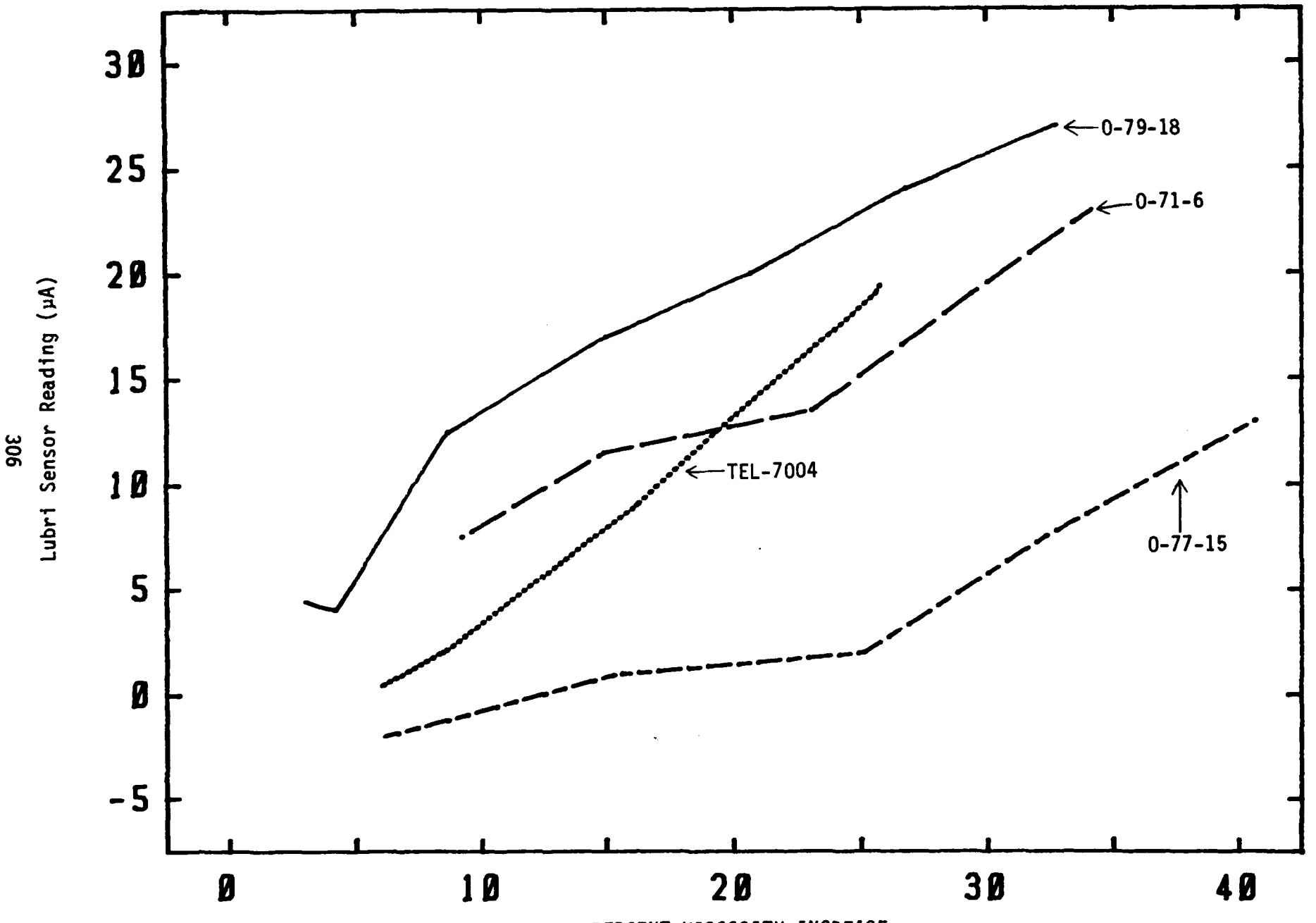

Figure 97. Lubri Sensor Reading vs. Viscosity Increase of MIL-L-23699 Lubricants Stressed in the Corrosion and Oxidation Test

lubricants stressed in the corrosion and oxidation test. It is easy to use and only requires about 0.5 mL of lubricant. It is considerably easier to determine the DC of a lubricant than TAN and viscosity. The Lubri Sensor appears to give ample indication of the breakpoint of the lubricant.

c. Lubri Sensor Analysis of Lubricant with Simulated Wear Particles

The manual for the Lubri Sensor states that the device can be used to detect metal particles in the oil due to their settling out to the bottom of the sensor and causing increases in the meter reading over a period of time. The Lubri Sensor was used to analyze a MIL-L-7808 lubricant (O-79-16) containing 50, 100 and 200 ppm of 5-10, 10-20 and 30-45 micron iron powder. The samples were placed in an ultrasonic bath for 10 minutes and shaken well before analysis. To check the stability of the instrument, readings were taken 1 and 2 minutes after the original readings. The data from these analyses are shown in Table 91.

TABLE 91

LUBRI SENSOR READINGS FOR O-79-16 WITH SUSPENDED IRON POWDER

Particle Size	ppm	Meter Reading (μA) Immediate	after 1 minute	after 2 minutes
5-10 micron	50	-3	-1	0
	100	-3	0	+1
	200	-2	+1	+4
10-20 micron	50	-3	+1	+3
	100	-3	+2	+5
	200	-3	+20	+30
30-45 micron	50	-2	+2	+3
	100	>+50	-	-
	200	>+50	-	-

The readings show a dependency on both concentration and particle size. The major factor here is probably the rate of settling of the particles to the bottom of the sensor which is a function of particle size. While the 200 ppm 5-10 micron particle sample showed little change in its meter reading after two minutes the 100 ppm 30-45 micron particle sample gave an immediate offscale reading. Since this data shows the instrument to be considerably less sensitive to metal particles than traditional SOAP instruments, the Lubri Sensor would not appear to be a completely useful device for this purpose.

d. Calibration Standards

Since there are quite a number of approved MIL-L-7808 and MIL-L-23699 lubricants for use in turbine engines, a problem arises with regard to the use of a common calibration standard. The extent of the problem can be shown by using O-79-20 and O-71-6 as MIL-L-7808 and MIL-L-23699 lubricant calibration standards respectively and measuring the Lubri Sensor readings of the other lubricants. This data is shown in Table 92.

TABLE 92

LUBRI SENSOR READINGS OF FRESH MIL-L-7808 AND MIL-L-23699 LUBRICANTS

	Fresh Lubricant	Meter Reading (μA)
MIL-L-7808	O-79-20	0*
	O-82-3	+11
	O-79-16	+11
	O-79-17	+17.5
	O-82-14	+46
	O-82-2	>+50
MIL-L-23699	O-71-6	0*
	O-77-15	>+50
	O-79-18	-28
	TEL-7004	-2

*Calibration Standard

The latter two MIL-L-7808 oils, which show the greatest deviation, contain large amounts of diesters which have higher DCs than the trimethylolpropane and pentaerithrytol based esters present in the other formulations. Since in an engine any of the approved MIL-L-7808 lubricants could in theory be together in any combination and proportion it is not possible to have a calibration standard for a field tested oil.

e. Lubri Sensor Analysis of Oxidized Polyphenyl Ethers

The Lubri Sensor instrument was used to analyze polyphenyl ether lubricants that had been stressed in the corrosion and oxidation test at 320°C. Initial results of the analyses of these degraded lubricants revealed that they did not give stable Lubri Sensor readings but, upon sitting in the sensor cell, decreased considerably with time. Furthermore, these readings appeared to be not only a function of time but also a function of the thermal history of the lubricant sample.

This behavior can be illustrated by the Lubri Sensor analysis of 0-67-1 that had been stressed in the corrosion/oxidation test at 320°C for 120 hours and is plotted in Figure 98. The lubricant sample, which had been heated mildly and shaken well earlier in the day for the purpose of emission analysis, displays a considerable decay in Lubri Sensor reading, from an initial reading of -10 μA to a reading of -37 μA after two hours. This decay appears to be logarithmic with Lubri Sensor reading vs. log (time) being linear. A repeat analysis of this same sample after three days, in which the sample was not heated or disturbed, gave similar results except that the starting and final Lubri Sensor readings (-29 and -48 μA respectively) were considerably lower. Similar behavior was observed for other degraded polyphenyl ether lubricants.

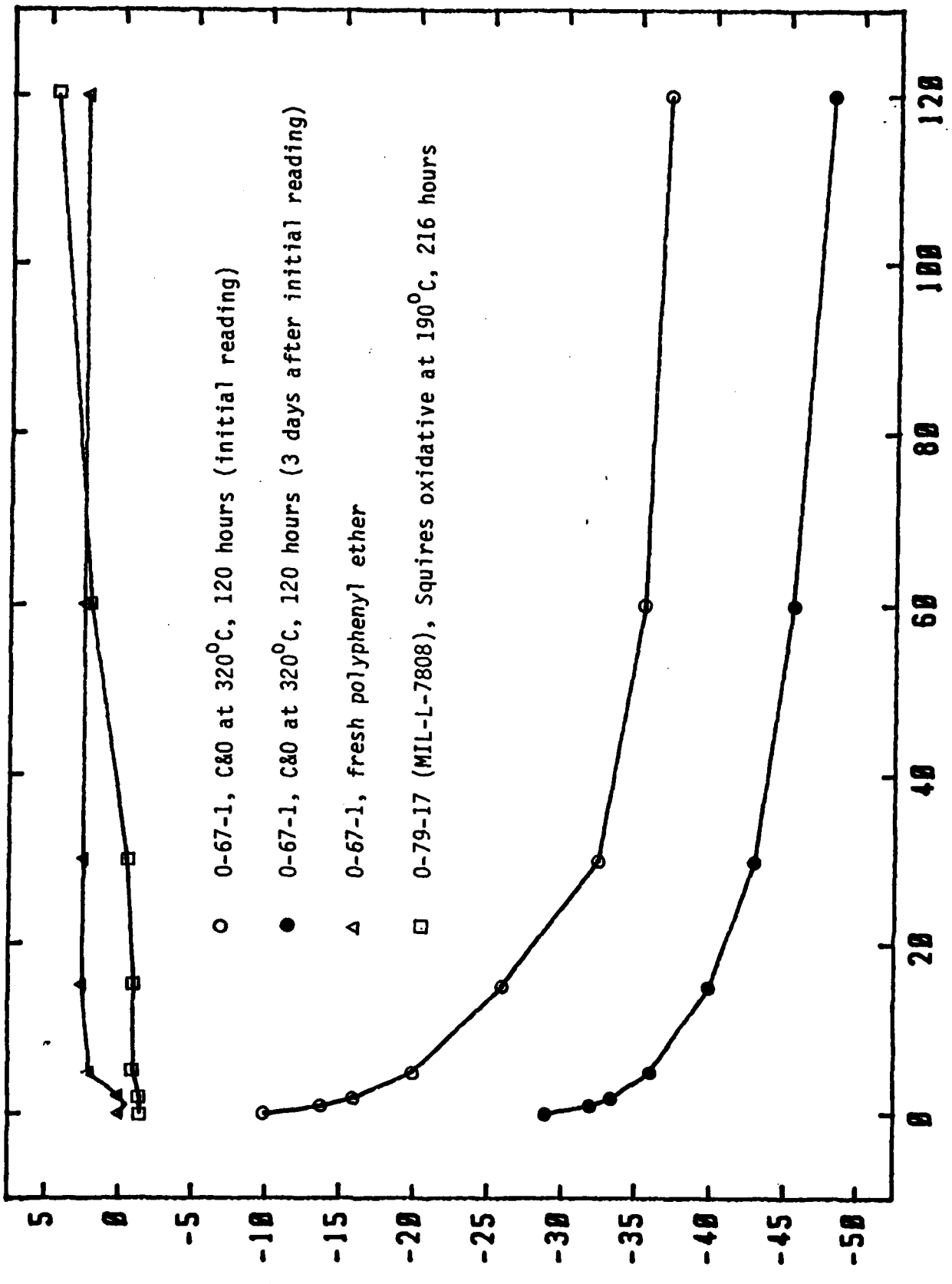

Figure 98. Time Dependency of Lubri Sensor Readings for Polyphenyl Ethers

Although the cause of this behavior is not understood, it may involve some type of phase transition either in the bulk of the lubricant or at the surface. According to the manufacturer of the Lubri Sensor the flat electrode cell of the instrument makes it more sensitive to skin capacitance. Curiously, neither a fresh polyphenyl ether lubricant or a degraded MIL-L-7808 lubricant displayed this decay of dielectric constant behavior as shown by Figure 98. Both of these lubricants showed a slight rise in readings probably due to moisture absorption. Whatever the nature of this behavior, it is obvious that it is not possible to obtain reproducible Lubri Sensor readings from degraded polyphenyl ether lubricants using the present procedure.

f. Summary

The Lubri Sensor, an oil monitoring device that measures changes in the dielectric constant of the oil, was used to analyze laboratory stressed turbine engine lubricants. The results of these analyses show that the most important factor in obtaining meaningful data from this instrument is the total amount of evaporation of volatiles from the test. When loss of oxidation and thermal breakdown products from a test is minimal, as in the Squires confined heat or corrosion and oxidation tests, the presence of these products causes an increase in the dielectric constant of the oil. This increase is proportional to the degree of breakdown of the basestock, particularly the TAN of the oil, and is not very formulation dependent. When there is considerable loss of volatiles, as in the Squires oxidative test, the data appears to be rather meaningless. The instrument was found to be limited in it's capability to detect metal particles in oil, being only sensitive to high concentrations of large particles. Likewise, due to instability of readings, the instrument was not suitable for monitoring

oxidized polyphenyl ethers. The ultimate problem with using the Lubri Sensor as a monitoring device for lubricants in the field is the inability to use a common calibration standard owing to the considerable differences in the dielectric constants of the various approved formulations of MIL-L-7808 and MIL-L-23699 lubricants. However, it could be a useful device for monitoring lubricants in laboratory tests for determining breakpoints and sampling intervals.

3. COMPLETE OIL BREAKDOWN RATE ANALYZER

a. Introduction

The complete oil breakdown rate analyzer (COBRA) is a portable electrochemical instrument that had been studied by the Air Force as a lubricant monitoring device and demonstrated success in identifying abnormally operating engines in aircraft.[31] It had been previously shown by analysis of the instrument's electronic circuitry that COBRA readings were affected by both the resistance and capacitance of the measuring cell.[1] Attempts to relate degradation levels of MIL-L-7808 lubricants to COBRA readings were only partially successful as two lubricants showed unusually large COBRA readings. Preliminary analysis of these two lubricants indicated that the large amount of diesters present in both formulations may be responsible for these high readings. Since the high COBRA readings could not be tied to physical property deterioration, it was assumed that the effect was due to a dielectric increase of the oils causing an increase in the capacitance of the measuring cell. The Lubri Sensor data in Table 92 does indeed reveal a relatively high dielectric constant for the fresh oils (O-82-2 and O-82-14). In order to better understand the factors affecting the COBRA readings of degraded MIL-L-7808 lubricants, the relationship between dielectric changes and COBRA readings was investigated and an attempt

was made to identify charge carriers in the degraded lubricants.

b. Effect of Dielectric Constant Changes on COBRA Response

Since it was speculated that the unusually high COBRA responses of degraded O-82-2 and O-82-14 were due, at least in part, to high diester content (via dielectric constant increase), a more precise determination of this effect was investigated. This effect was studied by dilution of degraded lubricants with ester basestocks of varying dielectric constants. A trimethylolpropane triheptanoate (TMP-777) basestock (O-76-5) with 1% each PANA and DODPA that had been stressed in the Squires oxidative test at 190°C for 120 hours was blended with various levels (by volume) of TMP-777, di-2-ethyl hexyl adipate (D2EHA) and mineral oil (MO). The results (Figure 99) show that dilution with the same basestock (TMP-777) causes a predictable, fairly linear decrease in COBRA readings. However, dilution with D2EHA (possessing a relatively high dielectric constant) actually results in an increase in the COBRA reading until a maxima is reached at about 50% dilution before rapidly falling off at high dilutions. Dilution with MO (possessing a relatively lower dielectric constant) shows a rapid decline at low dilution volumes. It should be noted that the three basestocks used for dilutions had little or no COBRA reading by themselves. A repeat of this experiment using D2EHA with 1 percent each PANA and DODPA stressed in the Squires oxidative test at 190°C for 48 hours gave similar results (Figure 100). This data indicates that while the basestocks, and possibly their oxidative degradation products, do not directly contribute to COBRA readings, they can nevertheless magnify the contribution of the charge carriers in the lubricant via capacitance changes of the measuring cell.

c. Nature of Charge Carrier in COBRA Active Lubricants

Correlation of COBRA activity with the presence of various compounds

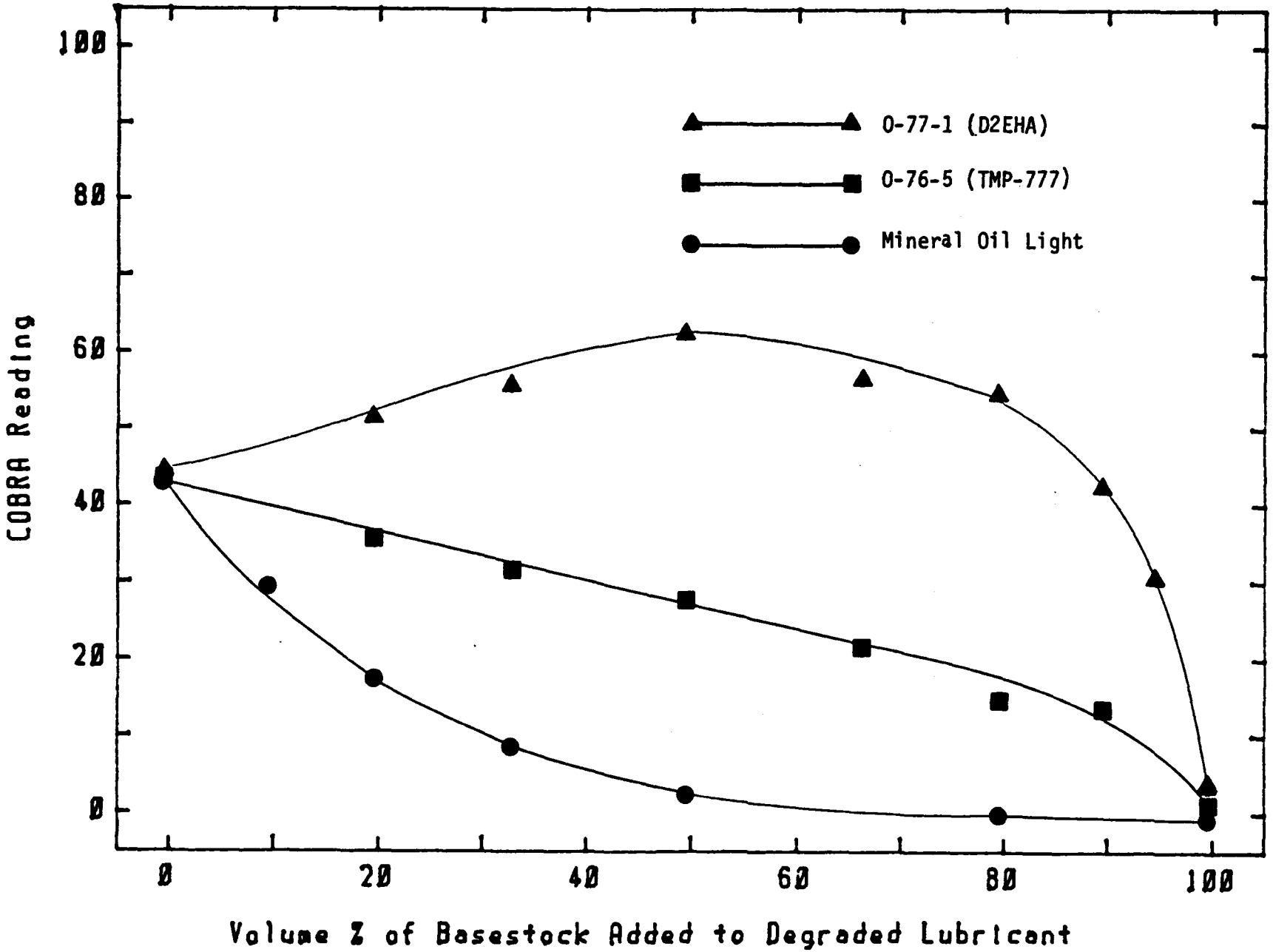

Figure 99. COBRA Reading vs. Volume Percent of Various Basestocks Added to O-76-5 Plus 1% PANA and 1% DODPA from Squires Oxidative Test at 190°C, 120 Hours

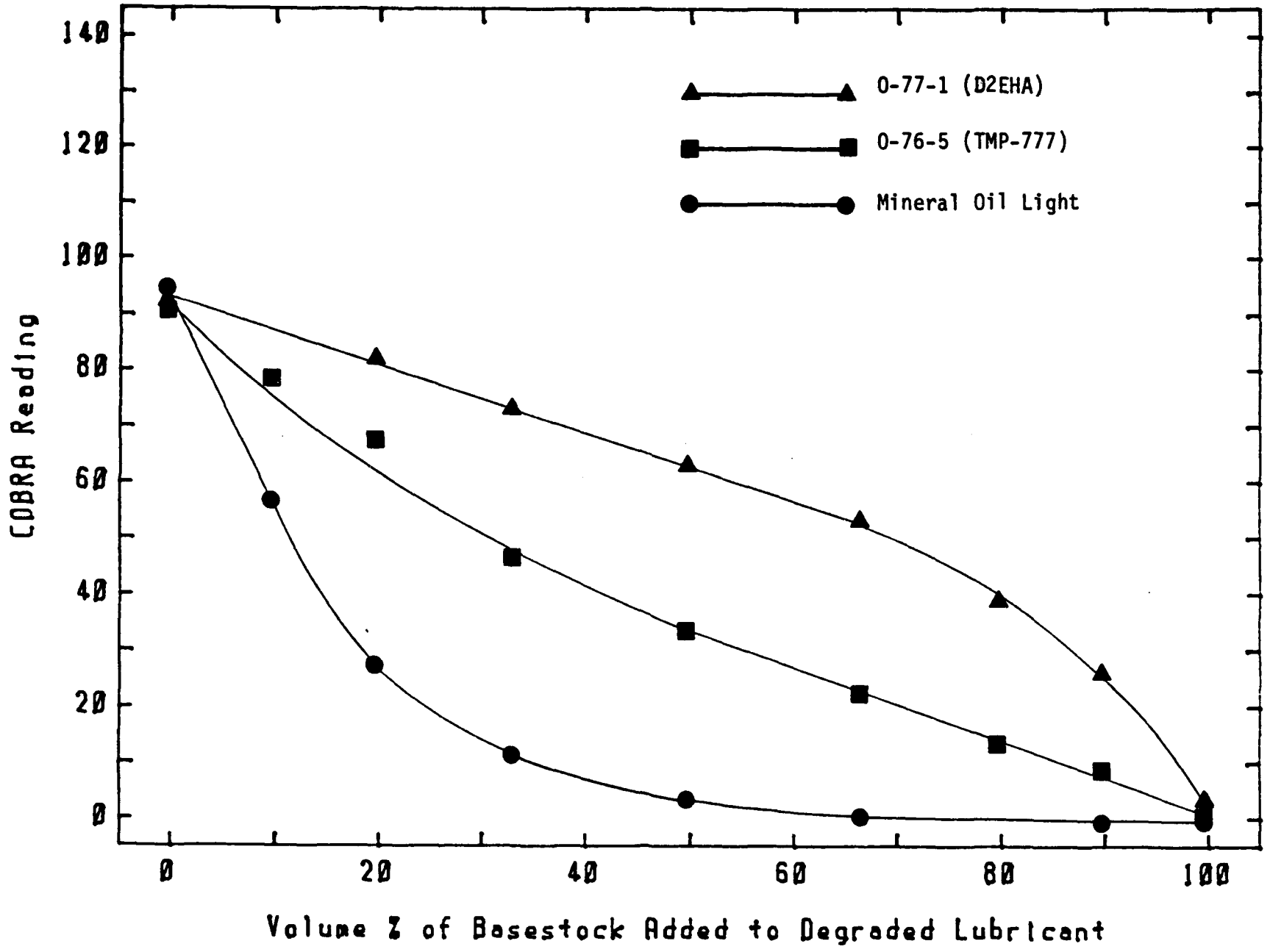

Figure 100. COBRA Reading vs. Volume Percent of Various Basestocks Added to O-77-1 Plus 1% PANA and 1% DODPA from the Squires Oxidation Test at 190°C, 48 Hours

or types of compounds present in a lubricant is hindered by the complex array of oxidation products that exist in such fluids. Furthermore, the nature of the charge carrying species is not known and may be a mixture of mechanisms. Conduction in low dielectric fluids such as lubricants is apparently a complex phenomenon with five different mechanisms identified:[32] 1) Ionic conduction, 2) phoretic type (micellar) 3) a hopping type conduction (electron semiconductor), 4) hopping type of proton conduction and 5) surface conduction. Despite this complexity, attempts were made to identify the nature of charge carrying compounds in oxidized lubricants.

(1) Adsorption Chromatography of Degraded Lubricants

In order to determine more precisely the type and nature of the degradation products in the lubricating oils that are responsible for producing the COBRA readings, chemical fractionation of the lubricant was conducted by open column adsorption chromatography. Adsorption chromatography (using alumina in this case) can fractionate a complicated matrix of compounds into mixtures of similar polarity as controlled by the polarity of the eluting solvent. A non-polar solvent like hexane would allow only the relatively non-polar compounds to elute while a polar solvent like acetone should elute all compounds except those that are very polar or are capable of strong hydrogen bonding (such as carboxylic acids). A short column of alumina (about 5 cm X 0.6 cm ID) was prepared and washed with hexane. Then about 1 mL of a 30% solution of the degraded lubricant in hexane was placed at the head of the column and percolated through. Hexane was added to the column and the effluent collected until it became colorless (about 5 mL). The next fraction was collected by adding acetone to this column and collecting the effluent until it became colorless (about 5 mL). Also, the oil was dissolved in acetone and percolated through the alumina and

the effluent collected (i.e. hexane step was omitted), in order to determine any effects of residual solvent or any lubricant components not eluted from the alumina (acetone only fraction). The solvent from these effluents was evaporated by mild heating under nitrogen. The residual oil was then analyzed by COBRA, reverse phase liquid chromatography (RPLC) and gas chromatography with flame ionization and thermionic specific detectors (GC-FID and GC-TSD). These procedures have been described previously.[1] The two lubricants analyzed were O-77-1 and O-76-5A both with 1% PANA and 1% DODPA from the 48 hour Squires oxidative test at 190°C. The COBRA readings of the fractionated samples are shown in Table 93.

TABLE 93

COBRA READINGS OF DEGRADED LUBRICANTS AFTER ADSORPTION CHROMATOGRAPHY

	COBRA Readings			
Degraded Oil	Orig Oil	Hexane Fraction	Acetone Fraction	Acetone only Fraction
O-77-1 + 1% PANA + 1% DODPA Squires oxidative test at 190°C, 48 hrs.	60	1	101	55
O-76-5A + 1% PANA + 1% DODPA Squires oxidative test at 190°C, 48 hrs.	10	0	40	13

The data from the "acetone only" fraction is nearly identical in COBRA reading to the original degraded oil indicating that all the compounds that are responsible for the COBRA response are recovered. Since carboxylic acids should not be eluted under these conditions this data agrees with previous work that showed that the most common thermal-oxidative products of esters (alcohols and carboxylic acids) did not significantly affect COBRA readings[1]. Also noted in the data is that the CCBRA readings of the oil

recovered from the hexane fraction in both samples have been eliminated while that of the acetone fraction have been greatly enhanced. This indicates that virtually all of the species responsible for the COBRA reading are relatively concentrated in the acetone fraction but absent in the hexane fraction. Analysis by GC-FID surprisingly shows very little difference between the hexane and acetone fractions from the O-77-1 degraded lubricant Figures 101 and 102). In both samples the main ester peak (D2EHA) is about 98% peak area and most of the other peaks can be shown by GC-TSD analysis to be nitrogen containing (antioxidant derived) products. The RPLC analysis (with UV detector) does show some differences between the acetone and hexane fractions (Figure 103). The acetone fraction is more concentrated with the more polar and oxygenated species such as N-phenyl-1,4-naphthoquinoneimine (4.1 minutes RT) and two oxidized DODPA species (at 7.2 and 9.1 minutes RT) in addition to PANA (3.9 minutes RT) and the two PANA dimers (at 5.5 and 6.0 minutes RT). The hexane fraction contains a higher concentration of less polar species such as DODPA (10.1 minutes RT) and the PANA/DODPA dimer (17.0 minutes RT). The chromatographic data of O-76-5A samples are similar to those of O-77-1. Relative to the hexane fraction (Figure 104), the GC-FID trace of the acetone fraction (Figure 105) shows a high concentration of trimethylolpropane diheptanoate (diester alcohol, at 15.7 minutes RT). The RPLC traces of O-76-5A are similar to O-77-1 samples. To what extent antioxidant oxidation products are responsible for the COBRA readings cannot be easily determined without knowing the effect of higher molecular weight oxidation products of the basestock and antioxidants which may not have been detected by these methods. For this reason, infrared spectroscopy was used to analyze the alumina fractions of selected oxidation tested MIL-L-7808 lubricants. The IR spectra of the various fractionated lubricants was obtained on a Perkin-Elmer

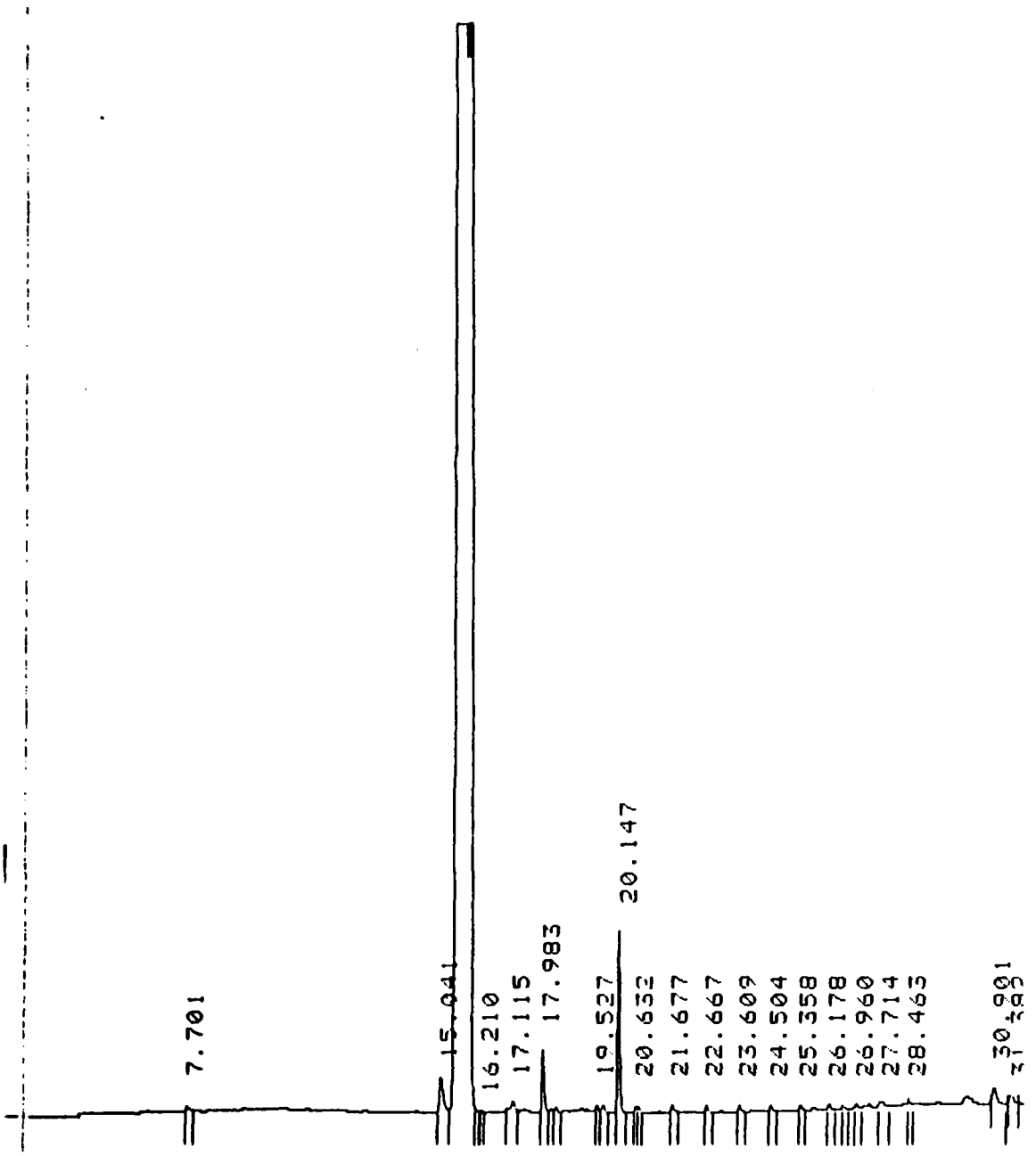

Figure 101. GC-FID Trace of Hexane Fraction of O-77-1 Plus 1% PANA and 1% DODPA from the 48 Hour Squires Oxidation Test

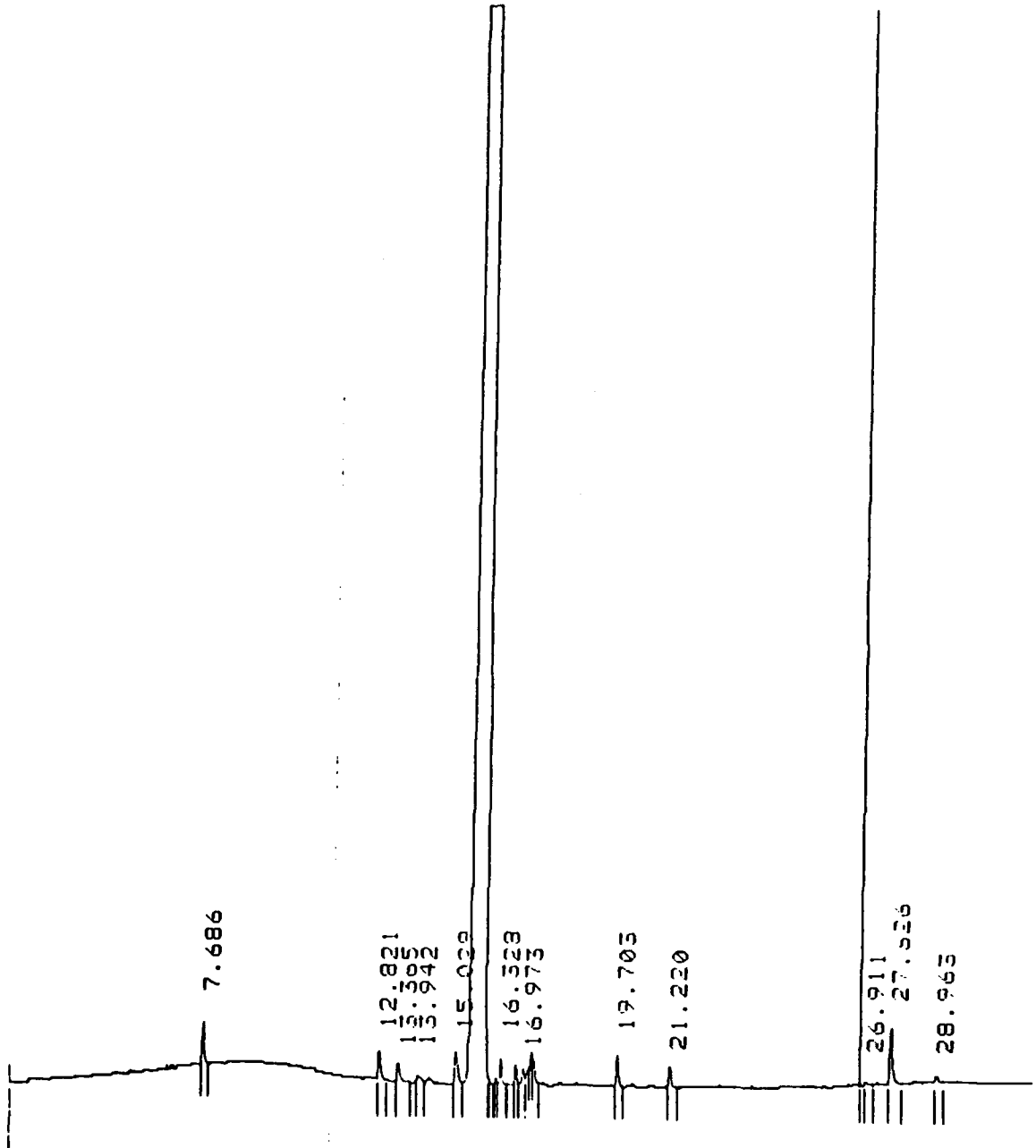

Figure 102. GC-FID Trace of Acetone Fraction of O-77-1 Plus 1% PANA and 1% DODPA from the 48 Hour Squires Oxidation Test at 190°C

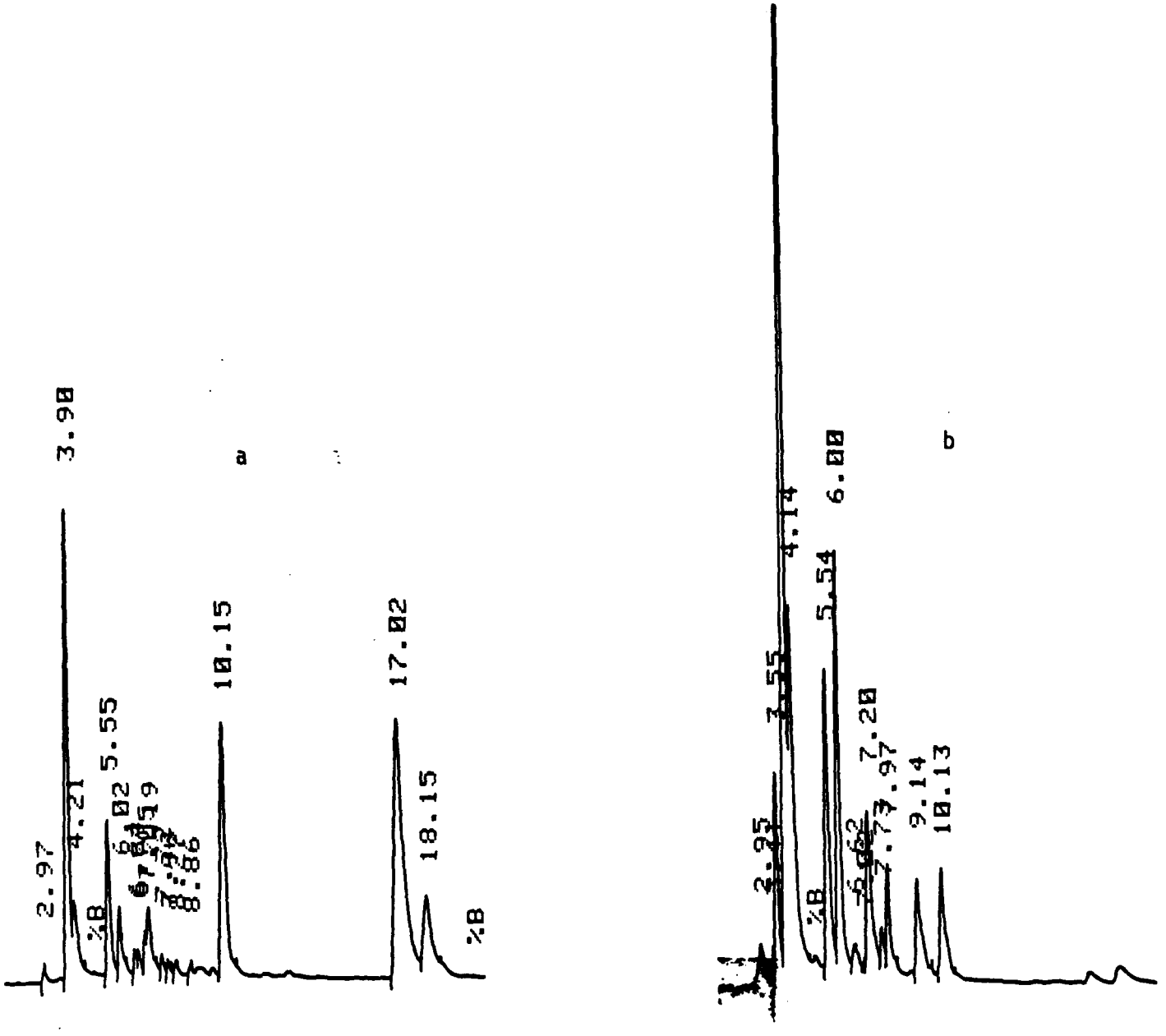

Figure 103. RPLC Traces of a) Hexane Fraction and b) Acetone Fraction of O-77-1 Plus 1% PANA and 1% DODPA from the 48 Hour Squires Oxidation Test at 190°C

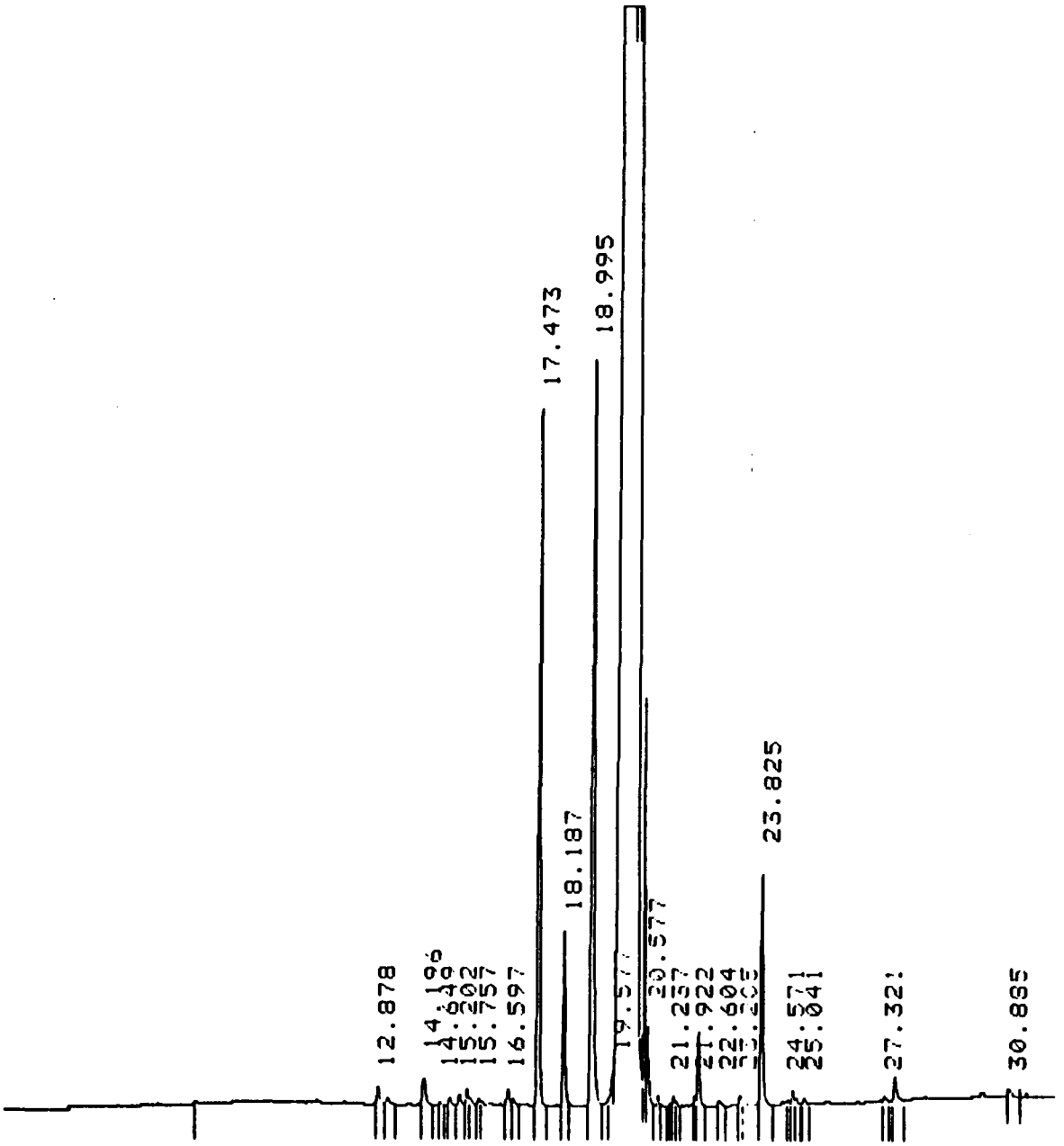

Figure 104. GC-FID Trace of Hexane Fraction of O-76-5A Plus 1% PANA and 1% DODPA from the 48 Hour Squires Oxidation Test at 190°C

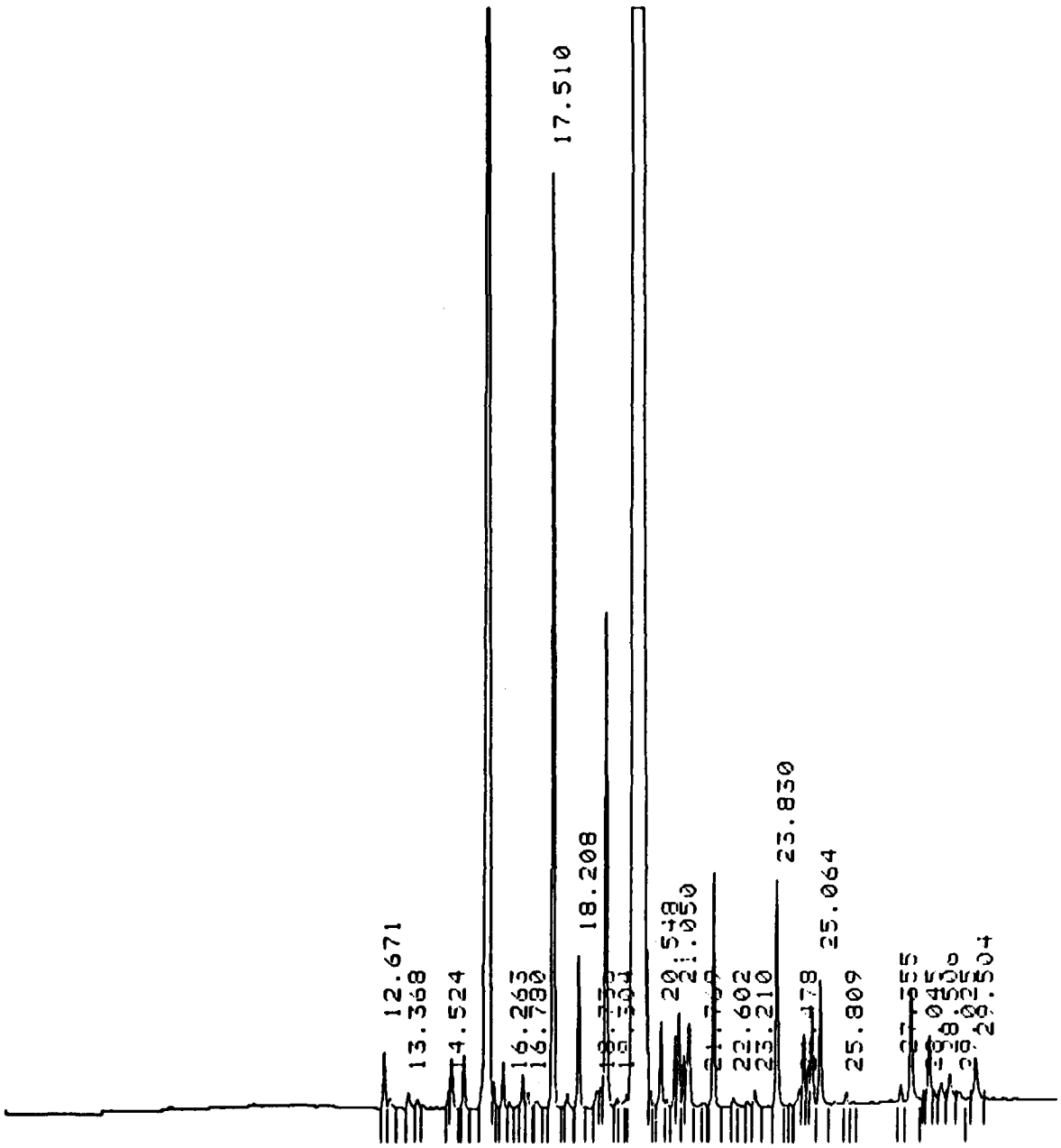

Figure 105. GC-FID Trace of Acetone Fraction of O-76-5A Plus 1% PANA and 1% DODPA from the 48 Hour Squires Oxidation Test at 190°C

521 infrared spectrophotometer as neat films between NaCl plates. Spectra were obtained for both the hexane and acetone fractions as well as the original degraded oils at normal scale expansion (1X) and higher scale expansion (5X). It was found that the spectral differences were mainly limited to two bands, the 3300 to 3600 cm^{-1} region (Band I) and the 1500 to 1650 cm^{-1} region (Band II). In general the absorptions in the fractionated samples could be seen in the original degraded oils, although they were mostly very weak.

Table 94 shows the IR absorptions for the hexane and acetone fractionated oils for Band I and II and their respective COBRA readings. For almost all of the hexane fractions, there was no activity in Band II, and weak activity in Band I centered around 3440 cm^{-1}. Although GC and HPLC analysis of earlier fractionated sample showed the hexane fraction to be relatively rich in the less polar antioxidants such as DODPA and the PANA/DODPA dimer, the N-H stretch absorption of these compounds is very weak. The most acceptable explanation for this absorption is an overtone band of the very intense ester carbonyl absorption band (1735 cm^{-1}).

The acetone fractions of the degraded oils showed much activity in the Band I region of the IR spectra. Most of this activity is due to the alcohols that are present in the degraded lubricant due to hydrolysis of the ester. It had been previously shown that alcohols do not greatly affect COBRA readings at the approximate concentrations seen in degraded lubricants.[1] The Band II region of the acetone fractions also shows considerable activity. Among the possible structural assignments for these absorptions are the C=C in place skeletal vibrations of an aromatic ring and those of various N=O stretches (nitro, nitramine, nitroso, etc.). There does not seem to be any likely source for N=O type compounds. The aromatic C=C absorptions occur at

TABLE 94

IR ABSORPTIONS OF FRACTIONATED MIL-L-7808 LUBRICANTS

Lubricant	Alumina Fraction	IR Absorptions* Band I(cm^{-1})	Band II(cm^{-1})	COBRA
O-82-14D, Squires Oxidative Test at at 190°C, 24 hours	Hexane	3440 (w)	1600 (w)	6
	Acetone	3450 (s,br)	1500 (s,sh) 1580 (s,sh)	>200
O-82-14D, Squires Confined Heat Test at 190°C, 24 hours	Hexane	3360 (m) 3440 (w)	None	5
	Acetone	3500 (s,br)	1600 (s,sh) 1580 (s,sh) 1500 (s,sh)	>200
O-77-1 + 1% PANA + 1% DODPA, Squires Oxidative Test at 215°C, 24 hours	Hexane	3440 (w)	None	1
	Acetone	3500 (s,br) 3430 (s,sh)	1650 (m,sh) 1590 (s,sh) 1500 (m)	>200
O-76-8 + 1% PANA + 1% DODPA, Squires Oxidative Test at 190°C, 24 hours	Hexane	3435 (w)	None	7
	Acetone	3500 (br,m) 3435 (m)	1580 (m,br)	>200
O-82-2, Squires Oxidative Test at 190°C, 24 hours	Hexane	3440 (w)	None	1
	Acetone	3500 (br,s) 3450 (br,s)	1600 (s,sh) 1580 (s,sh) 1500 (s,sh)	100
O-82-3, Squires Oxidative Test at 190°C, 24 hours	Hexane	3440 (w)	None	0
	Acetone	3500 (s,br) 3450 (s,br)	1580 (w) 1500 (w)	67

*(s) = strong, (m) = medium, (w) = weak, (sh) = sharp, (br) = broad

(note - intensities are relative to 5X expansion for full scale deflection)

1600, 1580, 1500 and 1450 cm^{-1} with the 1600 and 1500 cm^{-1} absorptions being quite variable in intensity. Since absorptions at these frequencies are commonly seen in the acetone fractionated samples (except for 1450 cm^{-1} which is hidden by other strong absorptions) it seems likely that various aromatic compounds are responsible for the Band II activity and that their most likely source is from the oxidation of the aromatic amine antioxidants.

Also noted in the IR spectra of three of the acetone fraction samples is an increase in the intensity of an absorption at 760 cm^{-1} relative to that of the hexane fractions. This absorption exists in the IR spectra of most ester basestocks along with a 720 cm^{-1} absorption due to skeletal vibrations of a linear hydrocarbon chain. An increase in the relative intensity of this absorption may be due to overlap of it with an absorption due to an out of plane bending deformation of an aromatic C-H bond. However the inconsistent nature of this behavior among all lubricant test samples makes this interpretation questionable.

(2) Other COBRA Active Compounds

A type of conductive species that may be a charge carrier in oxidized lubricants is the donor-acceptor (D:A) complex.[33,34] These complexes, sometimes known as charge-transfer complexes, form as a result of an electron transfer between molecules or ions without the existance of a formal covalent bond. Some D:A complexes are stable enough to be isolated as solids with melting points but generally their existance is inferred by physical property changes such as solubility, spectrophotometric measurements and conductivity increases. Among the numerous D:A complexes reported, the most interesting are those reported to form between various quinones and aromatic hydrocarbons. Similar type compounds, such as quinoneimines, are known to be oxidation by-products of the aromatic amine antioxidants that are

used in MIL-L-7808 formulations. Since it is not possible to isolate sizeable quantities of antioxidant oxidation products for testing, known D:A complexes similar to these were made up in various ester basestocks and various concentrations to determine the effect of such complexes on COBRA readings. Specifically the following known complexes were tried; Benzoquinone: Hydroquinone, Naphthoquinone: Hydroquinone, Tetrachloroquinone: Stilbene, Anthroquinone: Stilbene. Also studied were Benzoquinone: PANA and Benzoquinone: DODPA. These were made up in various representative concentrations (0.1 to 0.5%) in TMP-777 and D2EHA in a 1:1 ratio. In all cases the COBRA readings of these solutions showed little or no change relative to the ester basestocks. Undoubtedly, the ability of a D:A complex to contribute to the conductivity of a solution would depend on the ionic nature of the complex and it may be that none of those tested here are sufficiently ionic to do so. Nevertheless, there is no evidence here to support a D:A complex charge carrying mechanism in oxidized lubricants.

It has been found that some chemical compounds are capable of producing high COBRA readings in ester basestocks at fairly low concentrations. Most notable among them is p-nitrophenol (PNP) as can be seen by the COBRA readings of it in TMP-777 and D2EHA (Figure 106). As would be expected the higher dielectric constant fluid D2EHA produces a larger effect than that of the TMP-777 solution. Attempts to use these type solutions as COBRA standards were not successful due to long term instability of the fluids.

It has been shown that one additive used in a MIL-L-7808 type lubricant was responsible for unusually high COBRA readings. A proprietary additive of unknown function, A-658, that is present in O-82-14 decomposes during oxidation of the lubricant. This could be shown by formulating a

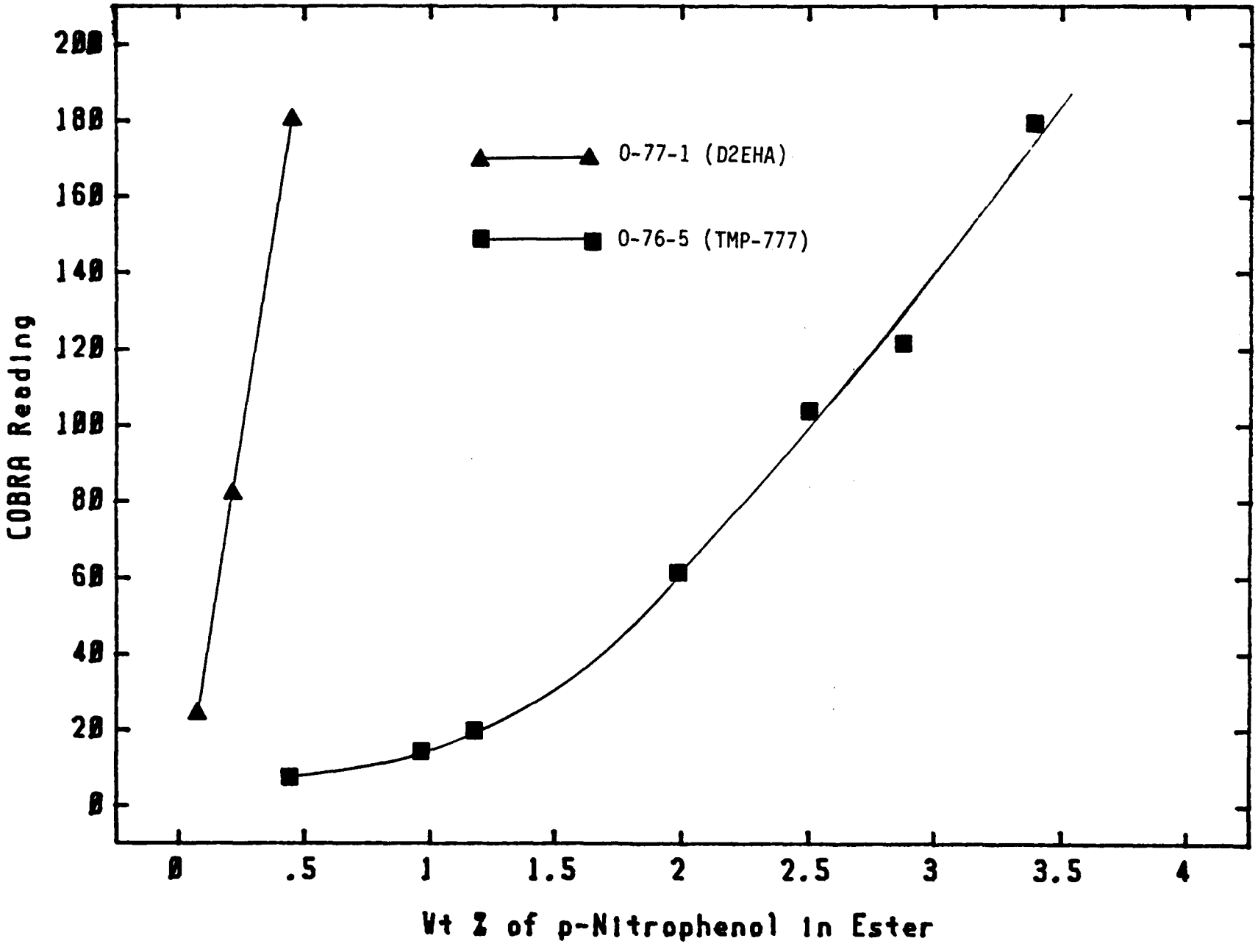

Figure 106. COBRA Reading vs. Weight Percent p-Nitrophenol in O-76-5 and O-77-1

di-2-ethylhexyl adipate basestock containing 1 percent each PANA and DODPA with and without the A-658 additive (in the approximate concentration that it exists in O-82-14) and stressing the lubricants in the Squires oxidative test at 190°C for 24 hours. The COBRA readings of the lubricants are shown in Table 95.

TABLE 95
EFFECT OF ADDITIVE A-658 ON COBRA READINGS OF STRESSED LUBRICANTS

Lubricant	A-658 Present	COBRA Readings Fresh Oil	Stressed 24 H
D2EHA + 1% PANA + 1% DODPA	No	6	20
D2EHA + 1% PANA + 1% DODPA	Yes	6	187
O-82-14	Yes	3	185

The results show A-658 significantly increases the COBRA reading of the lubricant after oxidation.

It would be interesting to conduct similar experiments with the aromatic amine antioxidants that are present in MIL-L-7808 lubricants. Unfortunately, since these additives are responsible for the oxidative stability of the oil, it would be impossible to separate additive effects on COBRA reading from that caused by oxidative degradation of the basestock.

d. Conclusions

The COBRA readings of degraded MIL-L-7808 are influenced by both the nature of the charge carrying species in the lubricant and the dielectric constant of the oil. Although the complexity of lubricant oxidation did not allow identification of specific charge carriers, some general conclusions could be drawn. The most common oxidation products from ester basestocks, such as carboxylic acids and alcohols, do not seem to directly contribute to COBRA readings since adding representative compounds to fresh basestocks have

little or no effect on such readings. Infrared analysis of alumina fractionated degraded lubricants indicated that COBRA activity may be related to the oxidation products of the aromatic amine antioxidants that are present in MIL-L-7808 lubricants. It was shown that some chemical compounds can greatly influence COBRA readings. One particular compound p-nitrophenol proved to be very COBRA active and one additive (A-658) was shown to be responsible for high COBRA readings in an oxidized MIL-L-7808 lubricant. Although it may be that basestock oxidation products do not directly give rise to COBRA readings, their influence on the capacitance of the instruments' measuring cell (via the lubricant's dielectric constant increase) could result in a magnification of the effect of the charge carriers on the COBRA reading.

4. DIELECTRIC BREAKDOWN STRENGTH OF MIL-L-7808 LUBRICANTS

As part of a continuing effort to investigate various electrochemical properties of lubricants, the dielectric breakdown voltage of a number of new and degraded lubricants was measured. The measurements were made using an OC-60A Liquid Dielectric Tester (Hipotronics, Inc.). This instrument complies with ASTM D 877 (Dielectric Breakdown Voltage of Insulating Liquids Using Disk Electrodes). Briefly, the liquid is placed in a cell with disk electrodes placed 2.5 mm apart and a D.C. voltage is applied at a rate of 500 volts/second until the electrodes arc and the voltage at this point is recorded. Because of the large sample requirements of the test cell (90 mL) a limited number of degraded MIL-L-7808 lubricants were measured. The results of these analyses are shown in Table 96.

TABLE 96

DIELECTRIC BREAKDOWN VOLTAGE MEASUREMENTS

	Breakdown Voltage (kV)			
Lubricant/Run #	1	2	3	4
O-77-1 (D2EHA basestock)	31	40	33	-
O-82-2 (MIL-L-7808)	23	19	29	34
O-71-6 (MIL-L-23699)	36	43	38	-
O-71-6, Corrosion/Oxidation test at 370°F, 384 hours	36	35	35	-
O-79-16, Corrosion/Oxidation test at 200°C, 96 hours	29	28	28	-
O-79-16, Squires Oxidative Test at 204°C, 216 hours	40	39	-	-

The data seems to show no correlation with the physical condition of the oil as some degraded oils gave relatively high breakdown voltages. Since it would be expected that conductive species would build up in a degraded oil that would decrease the potential needed to arc the electrodes, the breakdown voltages obtained for the degraded oils are somewhat surprising. Since these results were not encouraging, the potential use of dielectric breakdown strength voltage as a lubricant measuring device was not foreseen and no further investigation into this device was conducted.

SECTION V

LUBRICANT LOAD CARRYING CAPABILITY TEST ASSESSMENT

1. INTRODUCTION

A lubricant's wear performance is currently based upon the lubricant's load carrying capacity (LCC). The LCC of a lubricant is defined as the tooth load, in pounds per inch of tooth face width, at which a predetermined amount of tooth scuffing has been reached. There are several gear test rigs that are used to evaluate lubricants, these being the IAE test used in England, the FZG test used in Germany, and the Ryder Gear Test used in the U.S. The basic operating and evaluation techniques are similar for all the test rigs; that is, the test lubricant is ranked by the load required to cause a specific amount of wear on the test gear teeth for a given operating speed and duration. The LCC of a lubricant, as determined by the Ryder Gear Test, is defined as the load which results in scuffing 22.5% of the face of the test gear teeth. The ASTM D-1947-83 test outlines the Ryder Gear Test for determining a lubricant's LCC. A set of test gears is operated at 10,000 rpm and constant load for ten minutes. The operator then examines each tooth face of the test gear for the percent area scuffed. The load is increased and the test is repeated. This procedure continues until the operator determines that 40% of the tooth surfaces are scuffed. The results of load versus percent area scuffed are plotted and the load per tooth face width corresponding to 22.5% scuffed area is obtained. The Ryder gear test rig has several shortcomings. The test specimens are expensive and the test runs are time consuming and involve a great deal of subjectivity on the part of the operator in determining the percentage of scuffed area of each tooth face.

Also, the tests are sensitive to factors which are difficult to control such as gear tooth geometry, surface finish, and hardness. Other investigators have noted these problems and found that test results are difficult to reproduce between operators and laboratories.[35] Other gear test rigs have similar problems as the Ryder gear test. In addition, there has been little success in correlating lubricant evaluation data between tests. Table 97 lists some of the differences between the Ryder, IAE, and FZG tests. The gear geometries and materials, operating conditions, and failure criterion vary between tests. Numerous studies have concluded that the differences in testing techniques combined with the complexities of wear mechanisms have rendered correlation of test results improbable, if not impossible. Therefore, it is desirable to find an alternative to gear test rigs for determining the LCC of lubricants.

TABLE 97

COMPARISON OF RYDER, IAE AND FZG TEST PARAMETERS

Parameter	Ryder	IAE	FZG
Test Gears			
Diametral Pitch (inches^{-1})	8	4.769	5.64
No. of Teeth (pinion, gear)	28,28	15,16	16,24
Pressure Angle (degrees)	22.5	26.317	22.5
Face Width (inches)	0.25	0.188	0.79
Pinion Speed (rpm)	10,000 max	6000 max	4400 max
Load Time (minutes)	10	5	15
Test Oil Temperature (^{o}C)	74	110	90
Failure Criterion	22.5% Scuff	60% Scuff	Weight loss, Wear rate

2. TEST PROCEDURES

Development of a repeatable, objective, and inexpensive test method to determine the tribological characteristics of oils is desirable due to the problems and costs of the Ryder and other gear tests. Several methods including pin-on-disk, pin-on-ring, disk-on-washer, rotating crossed

cylinders, the Falex gear simulator, the rolling four ball, and the sliding four-ball test can be used for investigating tribological properties. The use of the sliding four-ball test to determine the LCC of oils is currently being considered. The major advantage of this test is that the real area of contact between the balls during sliding can be accurately determined resulting in the calculation of average pressure on the oil film in real time. The development of the four ball test for determining LCC is covered in Section VI along with the development of a specification wear test. Two additional test methods studied under Section V are the four ball extreme pressure and the Falex gear simulator. Both tests are run on a Falex Multi-Specimen Wear Test Machine.

3. RESULTS AND DISCUSSION

a. Extreme Pressure Test

The extreme pressure test (EP) involved a modified Falex Multi-Specimen Wear Machine in the sliding four-ball configuration. Seizure was defined by the onset of chatter within the four-ball setup or welding of the four balls to one another. The initial bulk oil temperature was 75°C; however, the bulk oil temperature increased after the testing began. The upper spindle of the four-ball configuration operated at 1200 rpm. The majority of the EP tests were conducted with the following loading sequence:

392 N for 60 min

667 N for 15 min

890 N for 15 min

1112 N for 15 min

1334 N for 15 min

1446 N for 15 min

Then, increased by 111 N increments for a duration of 15 minutes per increment until seizure occurred

Figures 107 and 108 are the results of an EP test using the previously described loading sequence on lubricant O-79-20. Figure 107 shows the coefficient of friction versus time for this test. Incipient seizure occurred at 75 and 105 minutes of testing; loads of 890 and 1334 N, respectively. Incipient seizure also occurred at 165 and 180 minutes (1779 and 1890 N respectively), but not as severely as the previous two loadings. Total seizure occurred at 190 minutes, or 10 minutes after the application at the 1890 N load. In Figure 108, the bulk oil temperature is plotted against time for the same test. The recorded temperature is that of the surrounding lubricant and the actual temperature of the frictional interface is much higher. The initial temperature of the lubricant was 75°C. This temperature was maintained through the 392 and 667 N load durations. Upon application of the 890 N load the frictional heating of the test specimens was greater than the cooling capacity of the test chamber. At those loads which resulted in incipient seizure the bulk oil temperature increased much more rapidly than during non-seizure loadings. This indicates that the contact zone temperature is much greater during incipient seizure load increments than non-seizure load increments.

Table 98 lists seven additional tests that followed the described loading sequence.

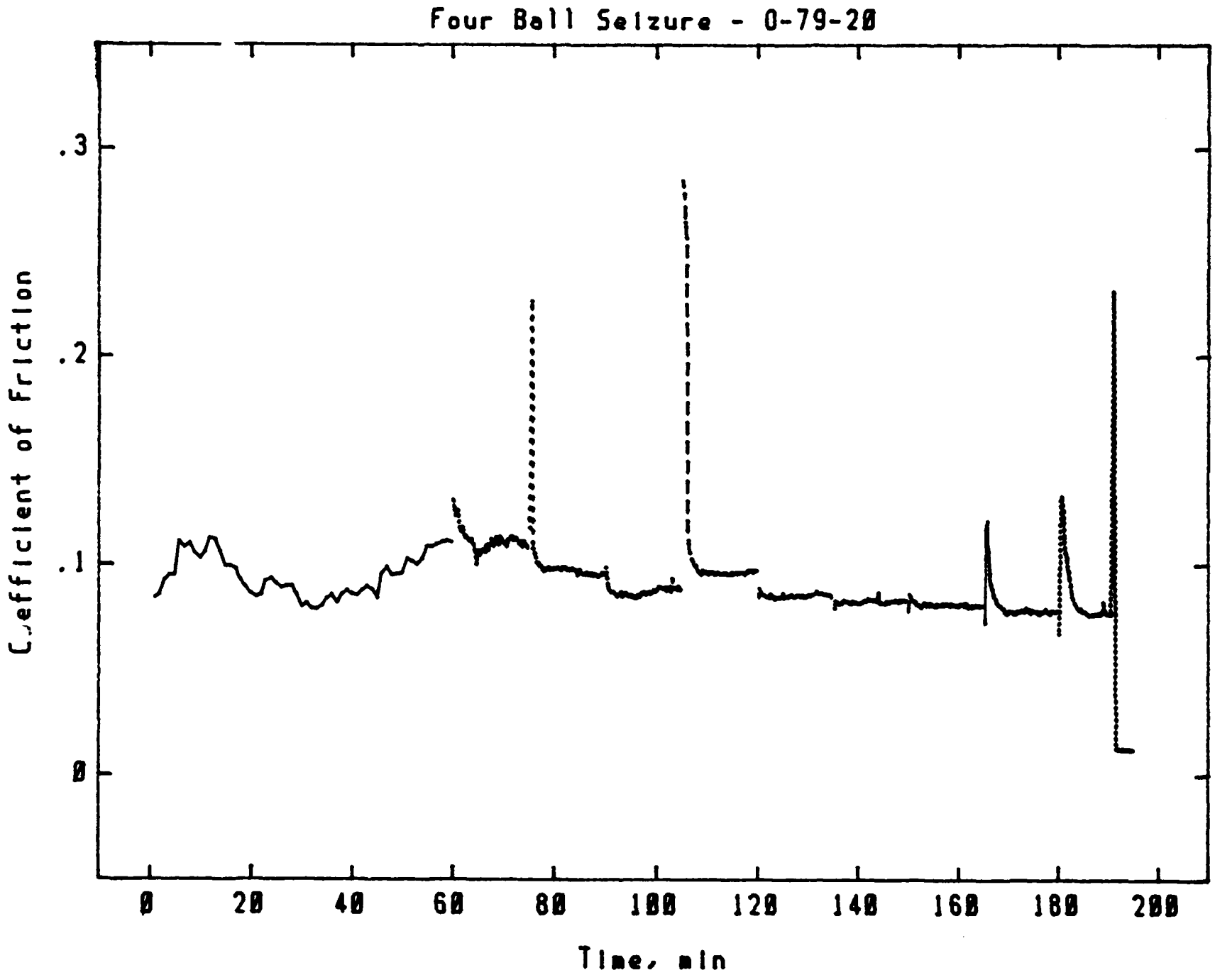

Figure 107. Four-Ball Seizure Test Sequence for 0-79-20 Oil. Seizure Load = 1890 N, Final Scar Diameter = 0.11 Inch

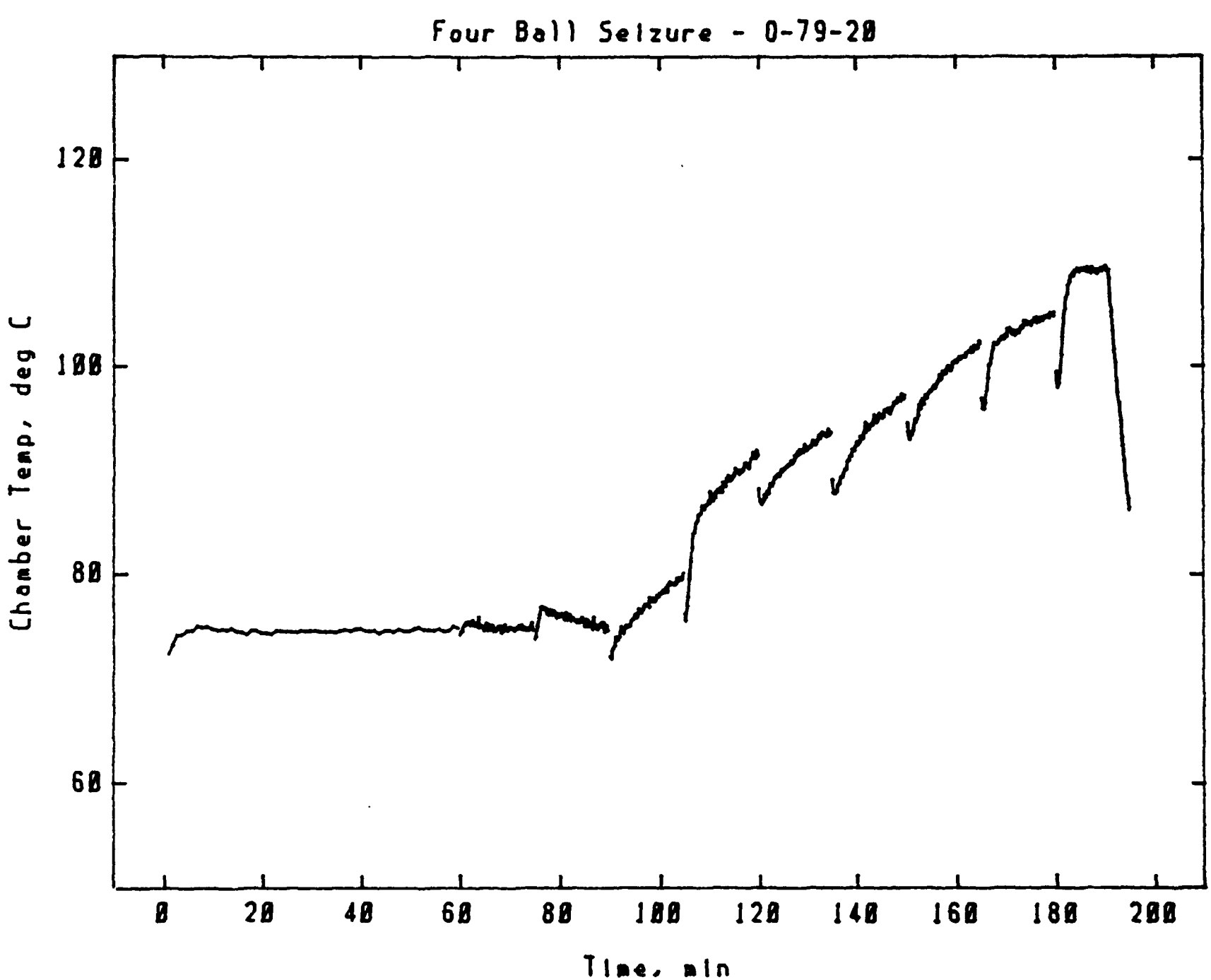

Figure 108. Four-Ball Seizure Test Sequence Showing the Effects of Frictional Heating on Chamber Temperature for Oil 0-79-20

TABLE 98

FOUR-BALL SEIZURE TEST RESULTS FOR MIL-L-7808 TYPE LUBRICANTS

Lubricant	Seizure Load, N
O-72-9	2699+
O-76-1	2699+
O-79-20	1890
O-82-2	1557
O-82-14	1112
O-85-1[a]	1334
O-86-2[a]	1112

[a] 4cSt fluids

Figures 109 through 115 are plots of the coefficient of friction versus time for the above seven tests. Several oils displayed a "recovery" from incipient seizure. The C.O.F. increased significantly for a brief period after the application of a load increment and then returned to a value in the range of the previous load increment. This increasing/decreasing C.O.F. can be clearly seen in Figures 109-112, and 114. Oil O-76-1, Figure 110, shows a particularly jagged C.O.F. plot indicating that the test specimens were on the verge of seizure throughout the latter portion of the test but the oil prevented complete seizure with the maximum load of 2699 N.

Another set of E.P. tests with three different loading sequences were run on oil O-82-2 at 75°C. The first loading sequence was similar to the previously described E.P. tests. The second loading sequence was an attempt to confirm the results of sequence 1 and to narrow the load range in which seizure occurs. For oil O-82-2, Sequence 1 (Table 99) determined that seizure occurred between 1334 and 2224 N. Therefore, the intermediate

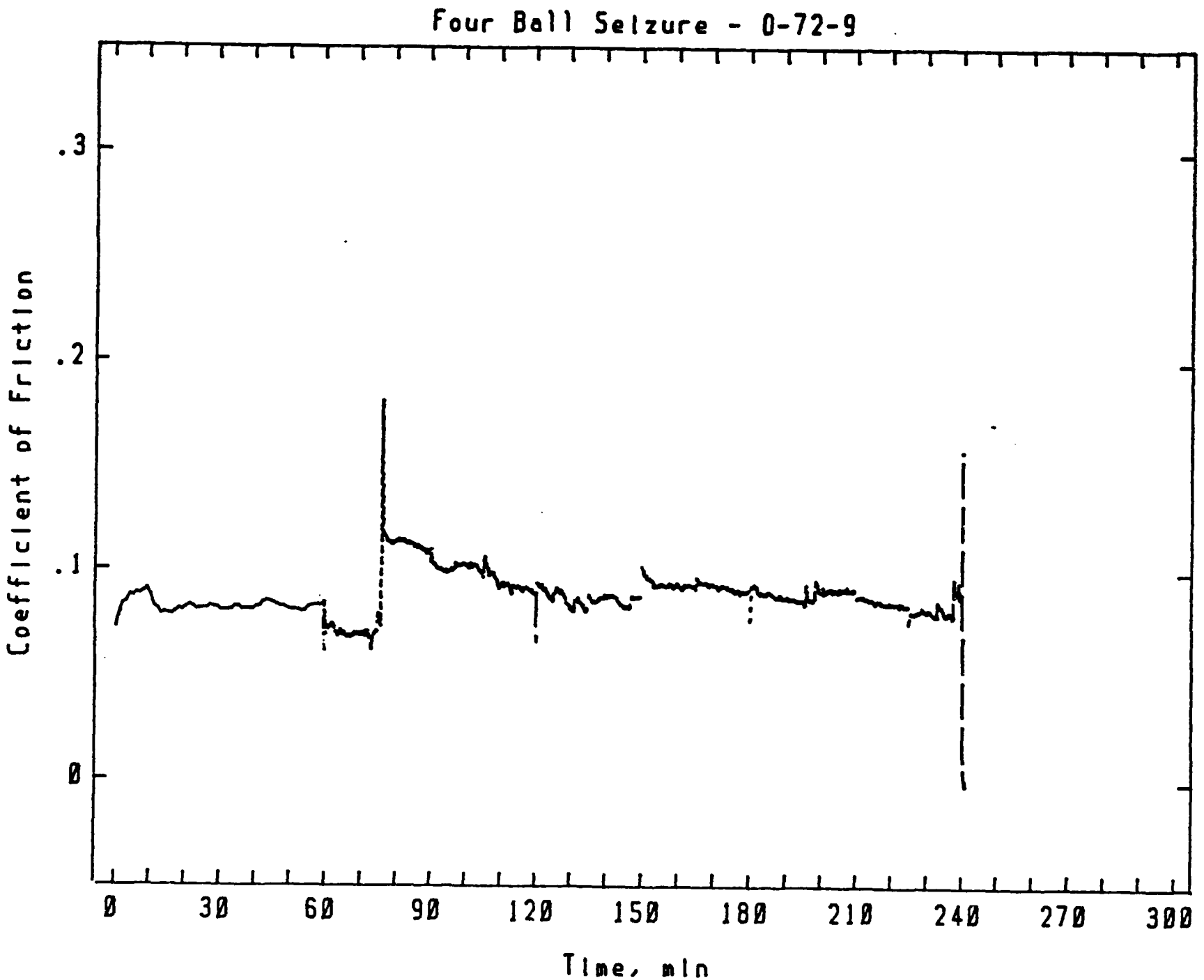

Figure 109. Four-Ball Seizure Test Sequence for 0-72-9 Oil. Seizure Load = 2669+ N, Final Scar Diameter = 0.12 Inch

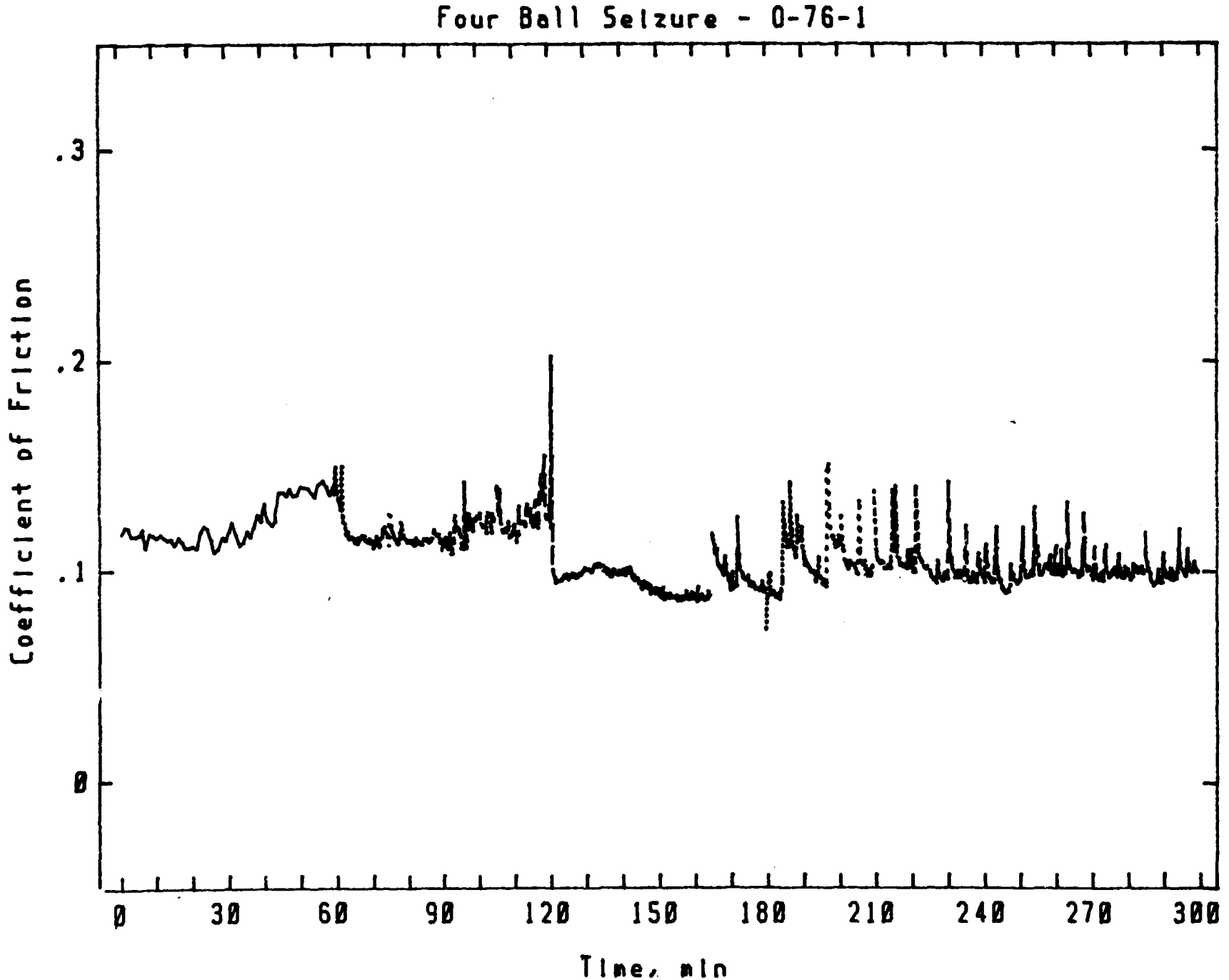

Figure 110. Four-Ball Seizure Test Sequence for 0-76-1 Oil. Seizure Load = 2669+ N, Final Scar Diameter = 0.12 Inch

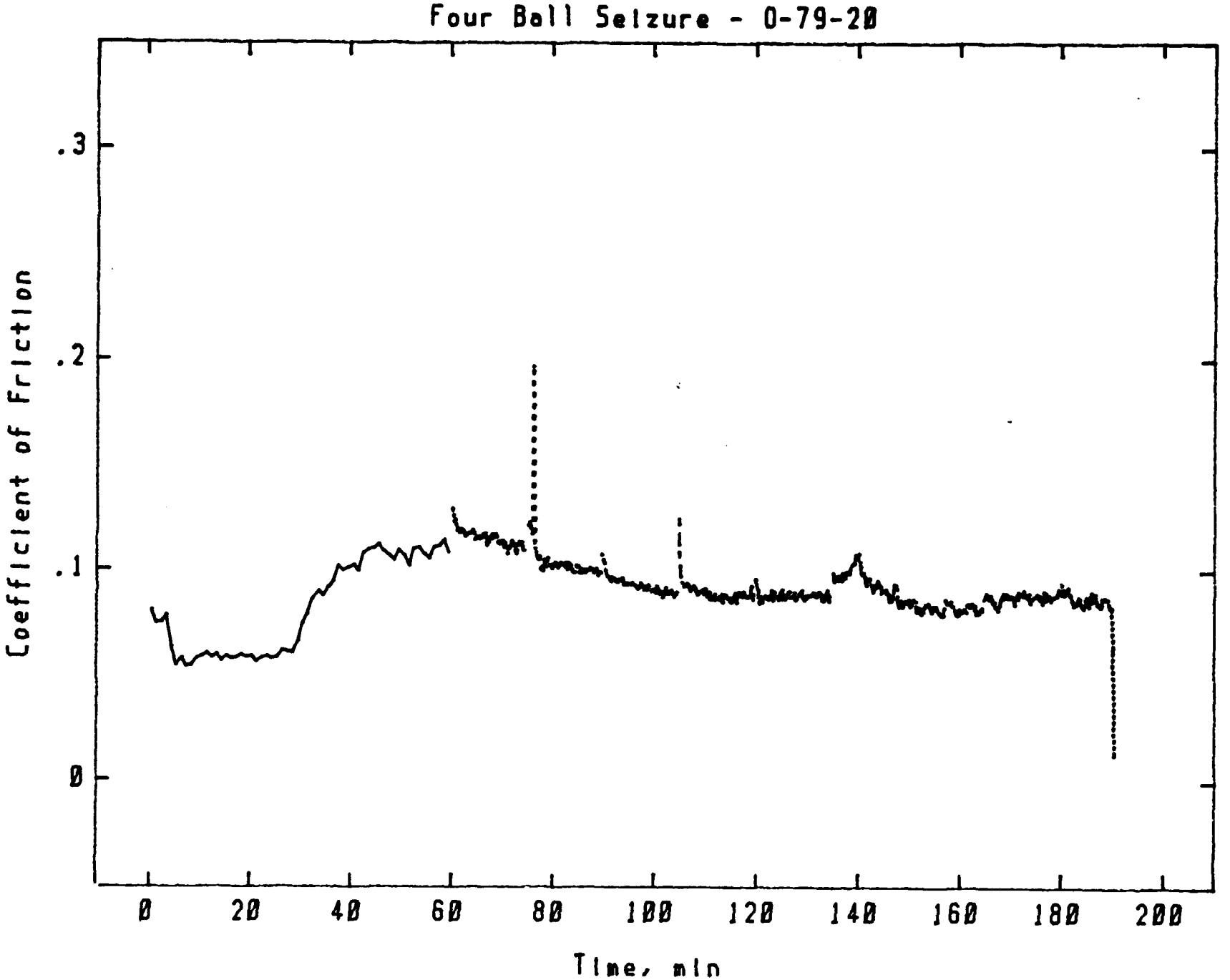

Figure 111. Four-Ball Seizure Test Sequence for 0-79-20 Oil. Seizure Load = 1890 N, Final Scar Diameter = 0.12 Inch

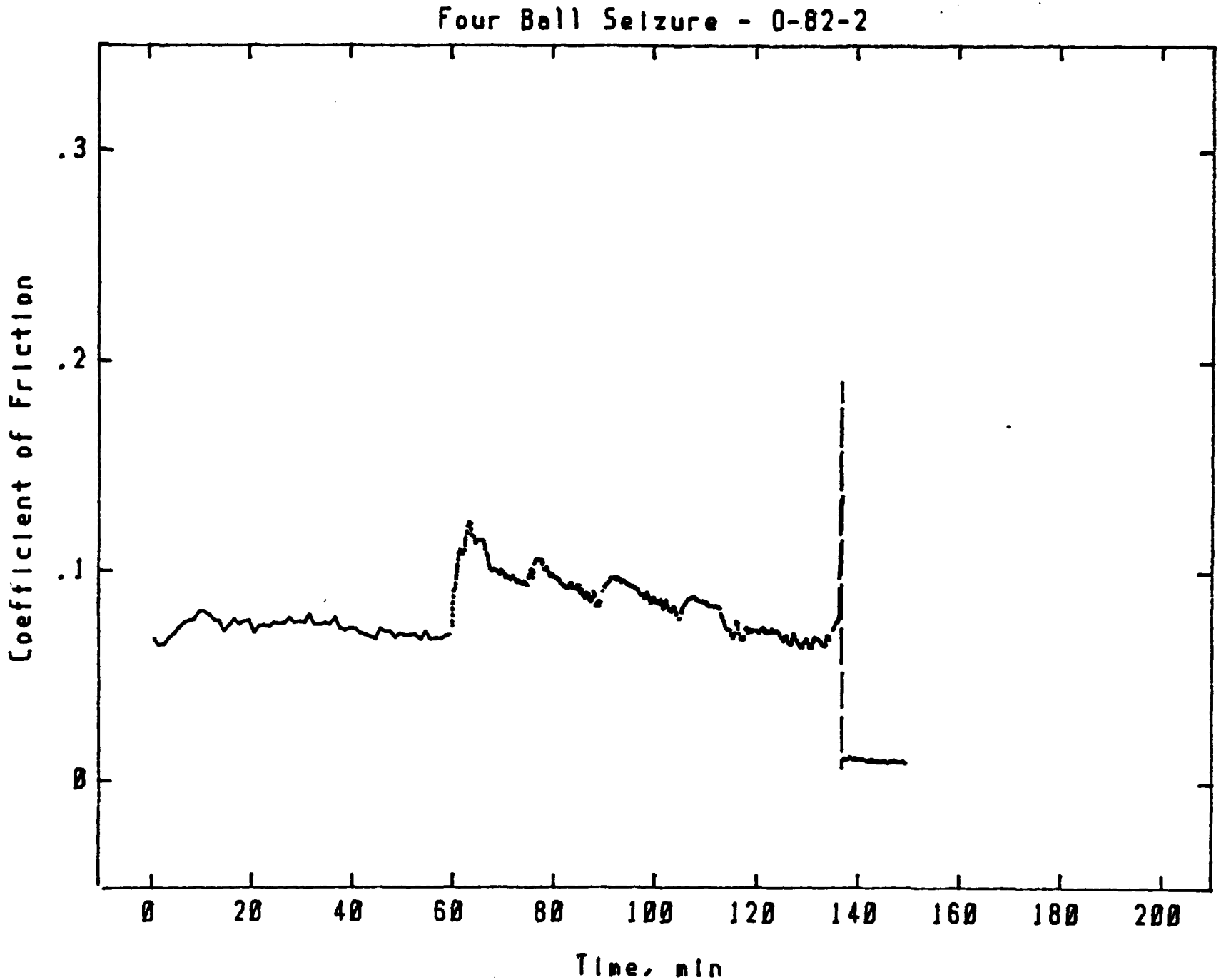

Figure 112. Four-Ball Seizure Test Sequence for 0-82-2 Oil. Seizure Load = 1557 N, Final Scar Diameter = 0.09 Inch

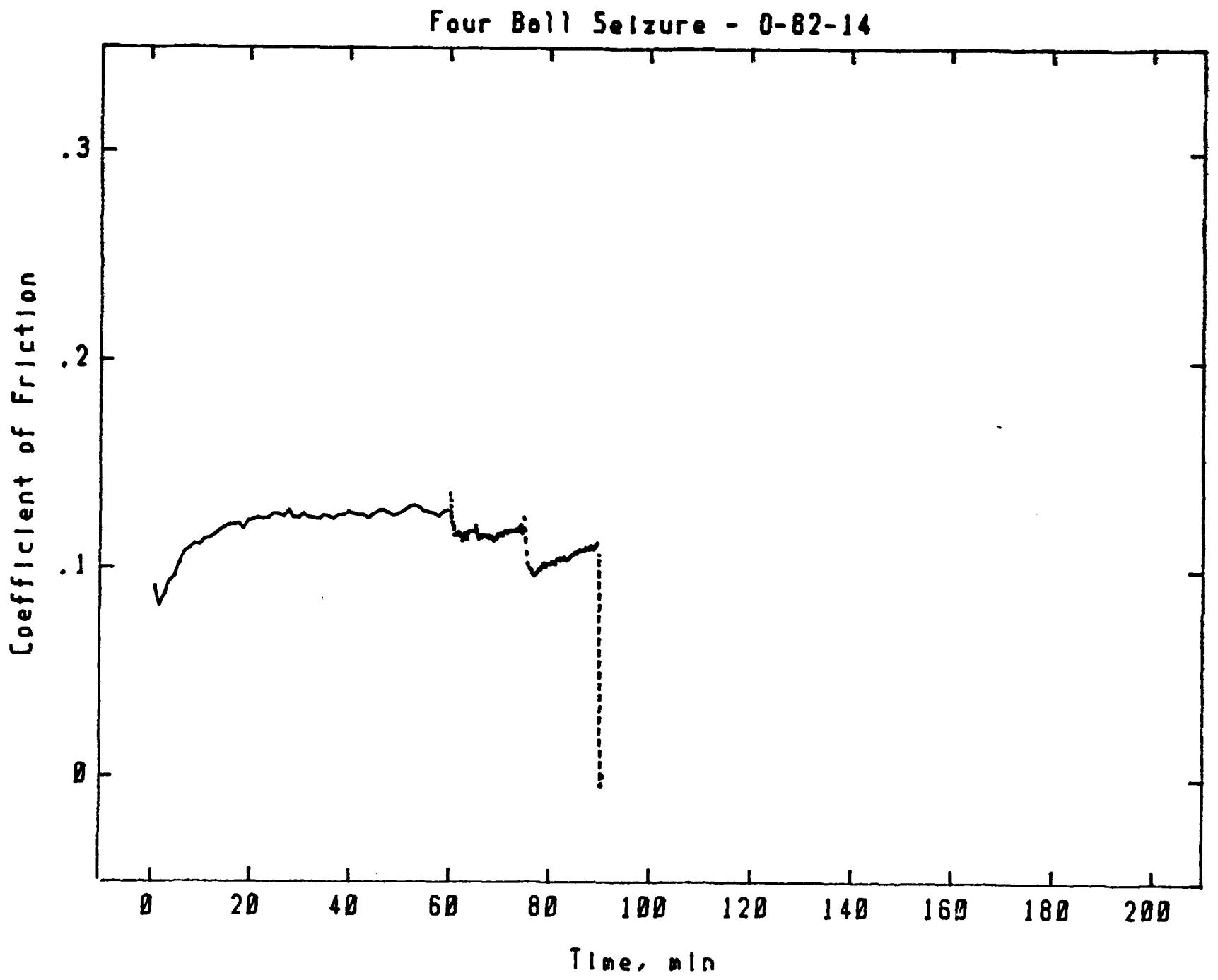

Figure 113. Four-Ball Seizure Test Sequence for 0-82-14 Oil. Seizure Load = 1112 N, Final Scar Diameter = 0.15 Inch

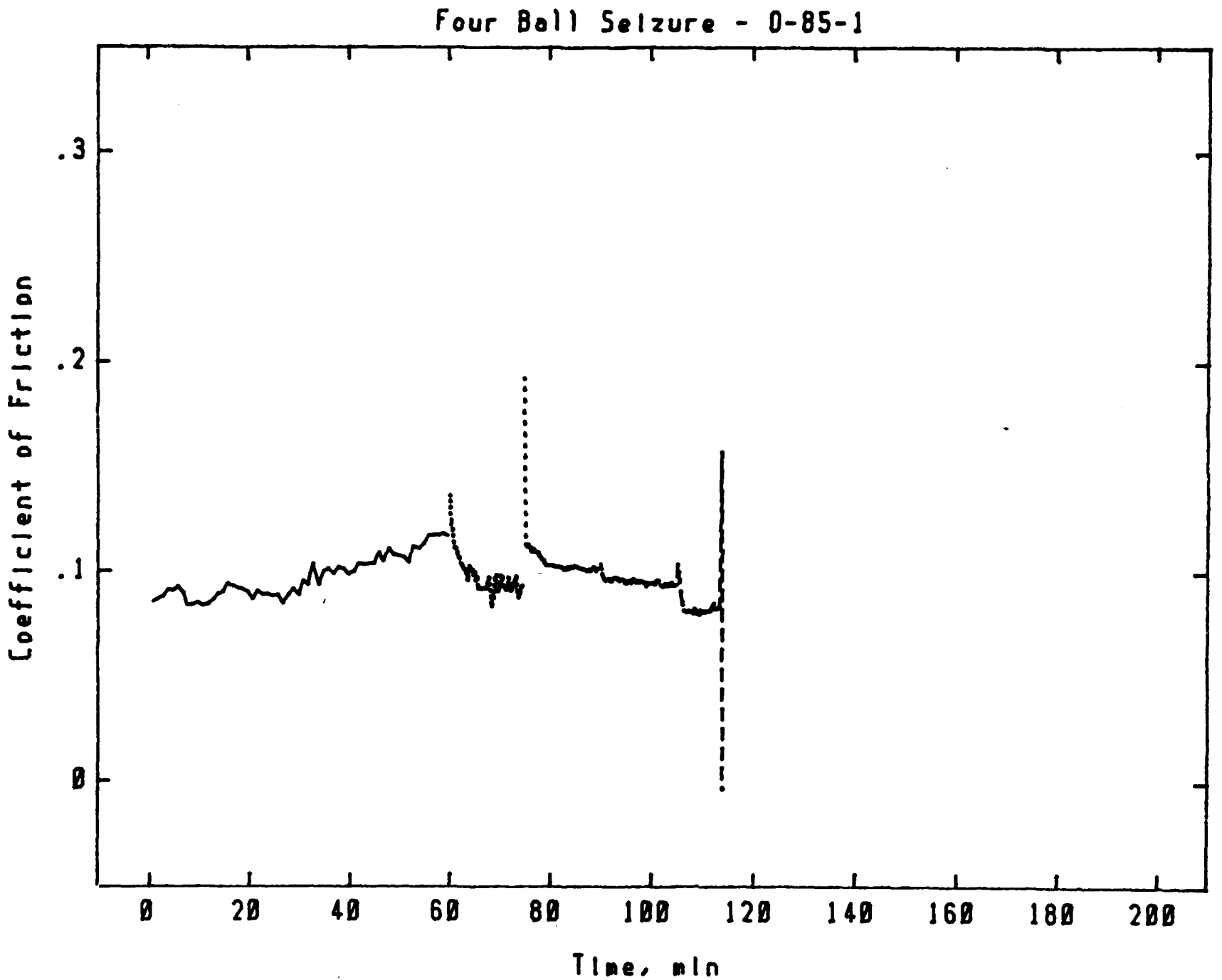

Figure 114. Four-Ball Seizure Test Sequence for O-85-1 Oil. Seizure Load = 1334 N, Final Scar Diameter = 0.11 Inch

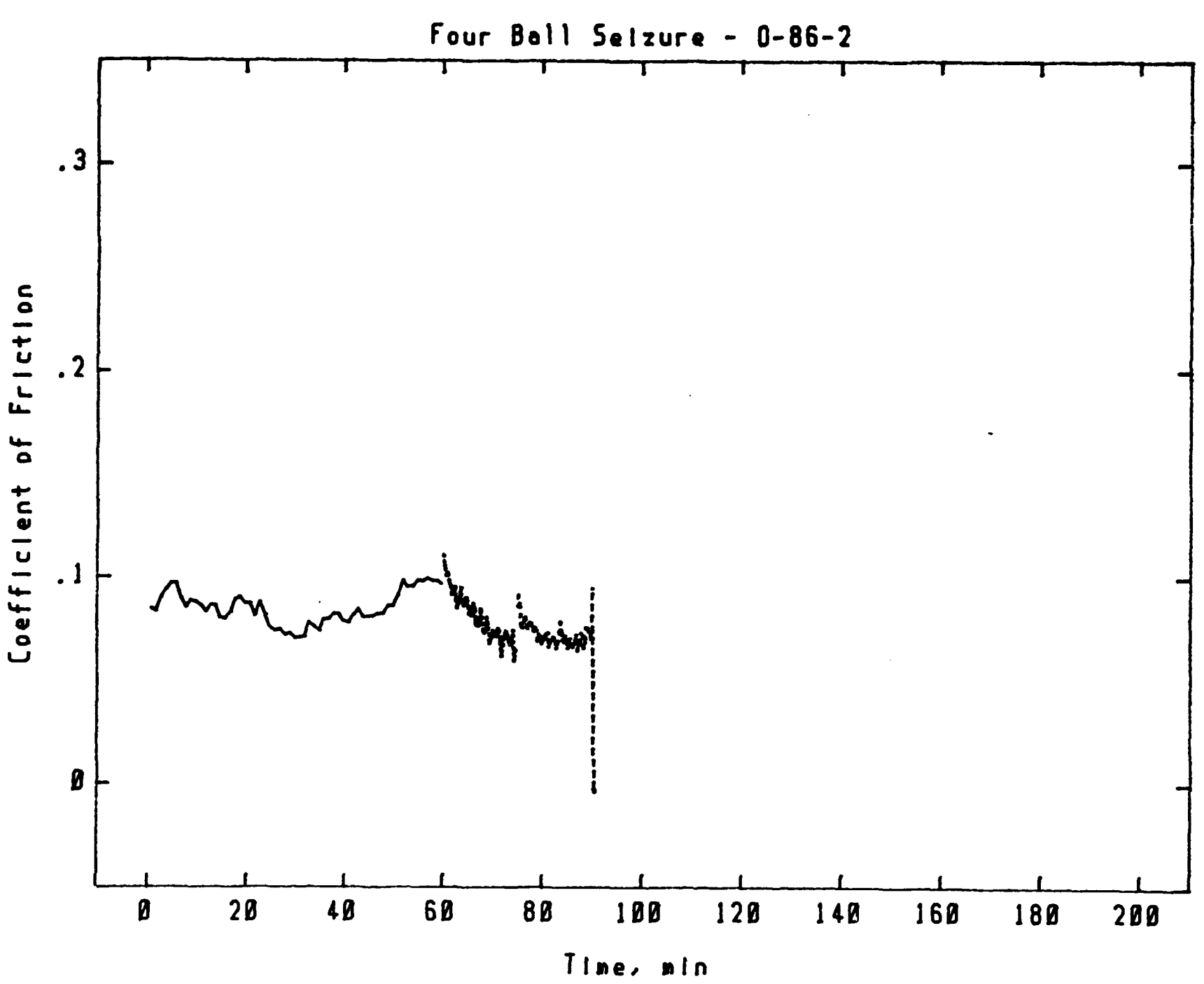

Figure 115. Four-Ball Seizure Test Sequence for 0-86-2 Oil. Seizure Load = 1112 N, Final Scar Diameter = 0.10 Inch

loading steps of 667 and 890 N were omitted in Sequence 2. During Sequence 2 seizure occurred immediately when the 1334 N load was applied. This leads to the conclusion that the seizure load is not independent of the contact area between the four balls.

The results of the third test sequence are shown in Table 100. In this sequence seizure occurred at a load of 1557 N. However, seven minutes elapsed from the time the load was applied until seizure occurred. Since seizure did not occur immediately, there is some time dependent variable responsible for seizure. Among parameters that vary during the test are the scar size, the interface temperature and the formation of/penetration of surface chemical coat. Wear increases the scar size which, in general, leads to less severe operating conditions as shown with Sequences 1 and 2. The contact temperature initially increases with time and this leads to more severe operating conditions.

The LVDT and C.O.F. data from six tests of Sequence 3 are shown in Figures 116 and 117. The LVDT data represents the deflection of the load arm as registered by a linear, variable differential transducer. As wear occurs, the load arm drops. The LVDT data also incorporates the deflection of the test specimens under load (Hertzian stress deflections) and the thermal expansion of the specimens during testing. The deflection of the four balls is shown in Figure 116 by the stepped decrease from 60 to 100 minutes. The slight increase at the onset of each loading is due to thermal expansion of the test specimens.

Figure 117 displays the coefficient of friction versus time. At the beginning of each loading step the C.O.F. is relatively high. This initial increase in C.O.F. is most pronounced at 60 minutes. The C.O.F. trend for oil O-82-2 is similar for two different loading schemes as shown by Figures

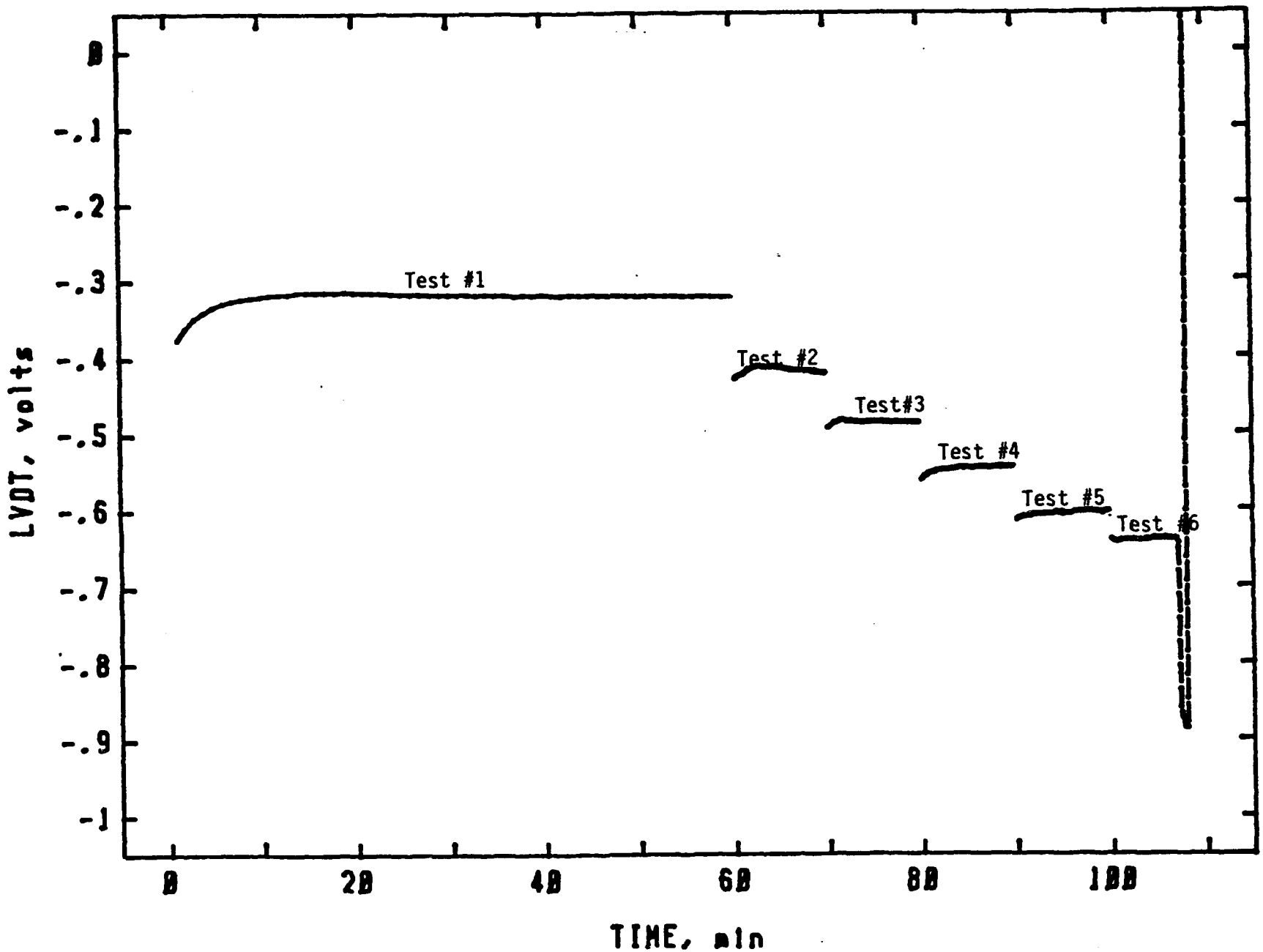

Figure 116. LVDT Versus Time for Six Tests in Four-Ball Seizure Sequence 3. First Test Was 60 Minutes at 400 N Load. Subsequent Tests Were 10 Minutes at 670, 890, 1115, 1335 and 1560 N.

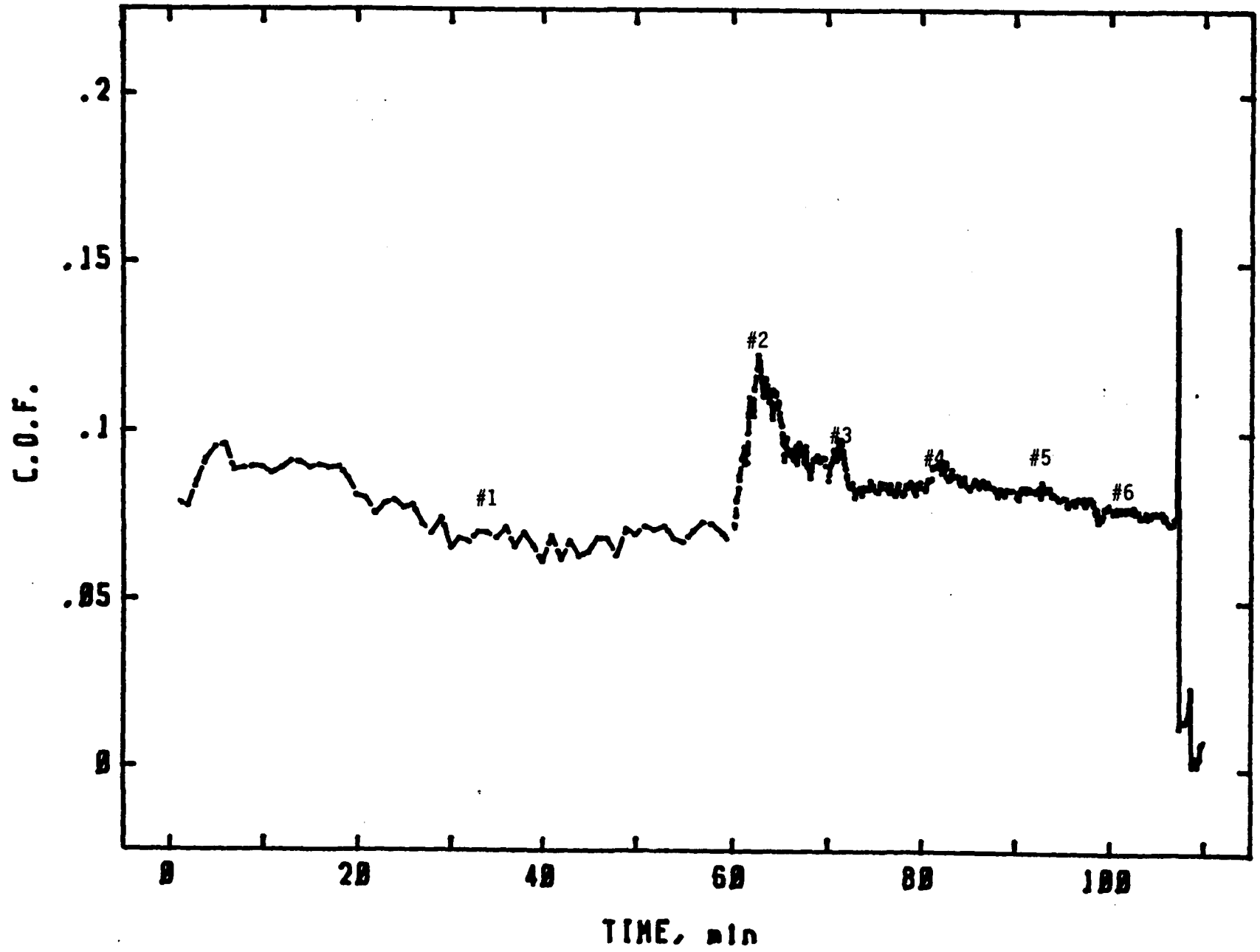

Figure 117. Coefficient of Friction Versus Time for Six Tests in Four-Ball Seizure Sequence 3. First Test Was 60 Minutes. Subsequent Tests were 10 Minutes Each.

112 and 117; however, the time for seizure is different. In the first loading scheme the seizure time was approximately 135 minutes and in the second loading scheme the seizure time was less than 110 minutes.

TABLE 99

CONDITIONS OF FOUR-BALL SEIZURE TEST SEQUENCE 1

Test #	Load, N	Duration, Min
187	400	60
188	667	10
189	890	10
180	1334	10
191	2224	10 seconds

TABLE 100

CONDITIONS OF FOUR-BALL SEIZURE TEST SEQUENCE 3

Test #	Load, N	Duration, Min
203	400	60
204	667	10
205	890	10
206	1112	10
207	1334	10
208	1557	7

b. Gear Simulation Test

The second test method, the Falex gear simulation test, consists of two pins that rotate against two annular rings. A detailed explanation of the test is given by Voitik and Heerdt.[36] Table 101 lists the results of thirteen gear simulation tests with the following operating parameters: 300

rpm, 1557 N load, 80°C bulk oil temperature, and one hour test duration. Although the temperature controller was set to maintain 80°C, the bulk oil temperature rose to approximately 120°C indicating that the frictional heat generated was greater than the cooling capacity of the test chamber, as was the case for the EP tests previously described.

The coefficient of friction (C.O.F.) listed in Table 101 is the average C.O.F. recorded during the last half of the test. During the test there was an initial "break-in" period during each test where the C.O.F. was as high as 0.075. This decreased to approximately 0.05 after 2 to 10 minutes and was relatively constant for the remainder of the test. The average C.O.F. for all the tests was 0.049 with a standard deviation of 0.004. The wear reported in Table 101 is the difference in pin weight measured before and after testing. The wear values ranged from 0.5 mg for 0-82-2 to 15.1 mg for 0-65-26. Two observations can be made about the high wear results of Test 36. The first concerns the C.O.F. recorded during the test. The break-in period as determined from C.O.F. was longer (approximately 22 min.) than for other oils. The second observation pertains to the temperature recorded during the test. Whereas the max temperature reached for other tests was 133°C, with most tests being approximately 120°C, test 36 reached a peak of 140°C after 10 min of testing. This result tends to parallel the results of Ryder gear tests on the same oils. Lubricant 0-65-26 produced a Ryder number of 1900 lbs/in whereas the other oils listed in Table 102 produced much higher LCC numbers.

TABLE 101

WEAR AND COF RESULTS OF GEAR SIMULATION TESTS

Test #	Oil	Wear, mg	Average C.O.F.[a]
37	O-82-2	1.1	0.045
36	O-65-26	15.1	0.047
35	Ref oil C	0.7	0.052
34	O-72-9	1.0	0.044
33	O-76-1	2.4	0.046
32	O-79-16	2.7	0.052
31	O-79-17	1.6	0.051
30	O-79-20	0.7	0.044
21	O-82-2	0.5	0.054
28	O-82-3	0.8	0.052
27	O-82-14	2.0	0.046
26	O-85-1	0.9	0.058
25	O-86-2	0.8	0.050

[a]C.O.F. = Coefficient of Friction

c. Comparison of Different Test Methods

One of the major obstacles in developing a new specification LCC test is that, to insure end-user acceptance, the new test should rank oils in the same order as the established test. This is a very formidable task due to the many variables involved in lubrication wear testing. Some of these variables are surface roughness, material hardness and strength, asperity contact pressure, viscosity-pressure variation, real temperature in the contact zone, type of contact taking place, test duration and wear particle/surface interaction. Nevertheless, it may not be totally impossible to correlate the results of two widely diverse test methods. A paper by Zaskal'ko, et al.[37] describes a procedure to correlate the results of the IAE tester with those of the four-ball tester. Using statistical methods, they correlated the tests in such a way that the maximum error between the two tests was 13% and the average being less than 5%. Correlation of wear testing with Ryder gear testing was studied using three different wear tests

and eight MIL-L-7808 oils. The results and test conditions, along with the previously established Ryder numbers are given in Table 102.

TABLE 102

RESULTS OF VARIOUS TEST METHODS

Oil	Ryder #	Four Ball WSD, mm	Gear Test #1 Wt loss, mg	Gear Test #2 Wt loss, mg
O-86-2	2620	1.28	3.7	0.8
O-85-1	2200	1.26	3.0	0.9
O-82-14	2630	0.46	4.1	2.0
O-82-3	2650	1.12	0.9	0.8
O-82-2	2350	0.34	1.3	0.8
O-79-20	2540	1.48	1.4	0.7
O-79-17	2500	0.43	0.9	1.6
O-79-16	2490	0.36	1.2	2.7

Four ball test. Temp 75°C, Speed 1200 rpm, Load 145 N, Duration 20 hrs.
Gear Sim. test #1. Temp 80°C, Speed 70 rpm, Load 1557 N, Duration 6 hrs.
Gear Sim. test #2. Temp 80°C, Speed 300 rpm, Load 1557 N, Duration 1 hr.

Because of the obvious inappropriateness of comparing the results directly due to the conflicting units (Ryders # is in lb/in, WSD is in mm, Wt loss is in mg) and rating criteria (a larger Ryder number is better, smaller results are better in the other tests) an equation was developed to convert the results to a percentage of the "best" test result. this equation is listed below:

$$\% \text{ of Best} = \left[1 - \frac{|X_{Best} - X|}{X}\right] 100$$

Applying this equation to the results in Table 102 gives the "normalized" results in Table 103. These values are shown in Figures 118 and 119.

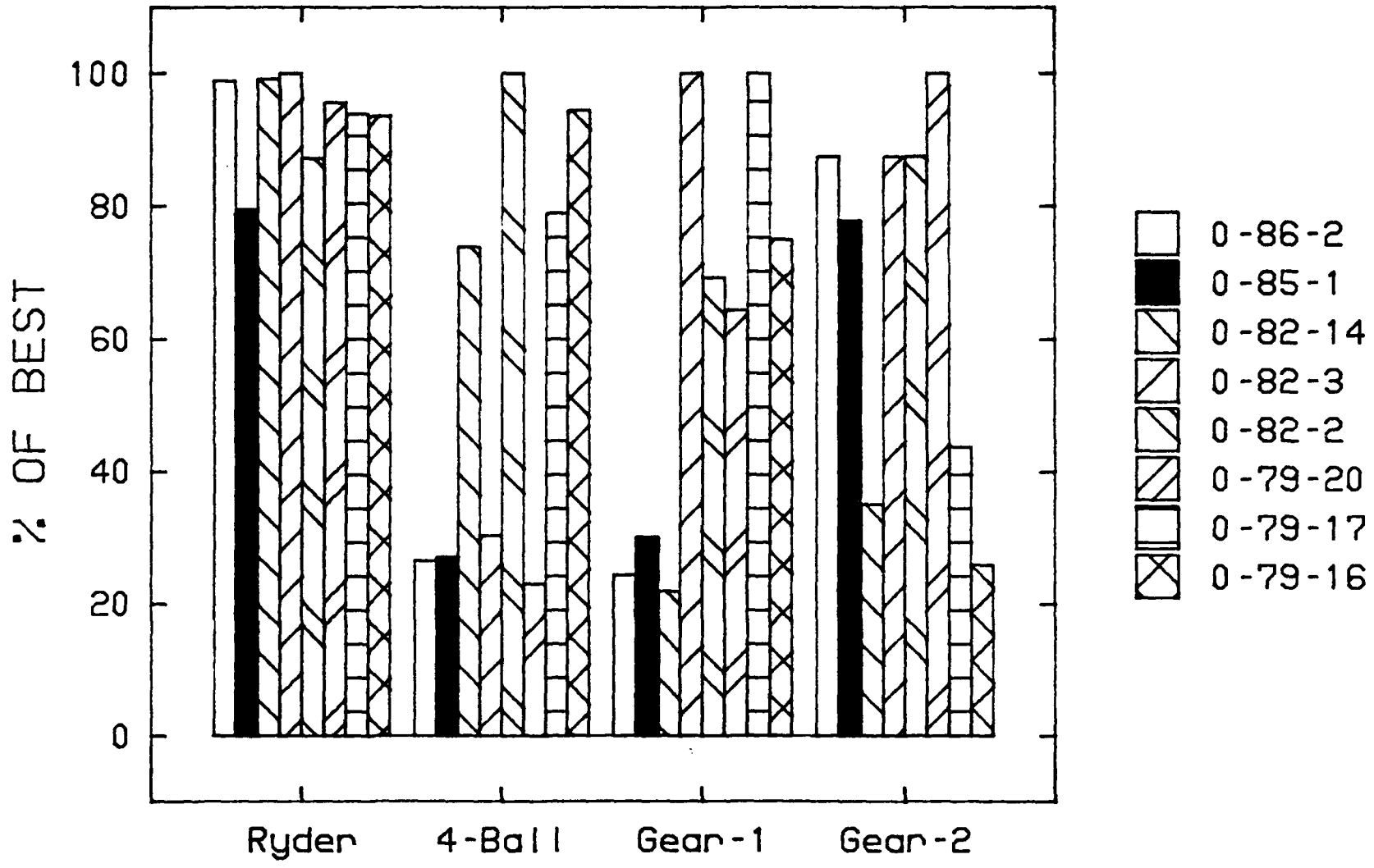

Figure 118. Normalized Results of Four Test Methods on Eight MIL-L-7808 Lubricants, % of Best vs. Test Method

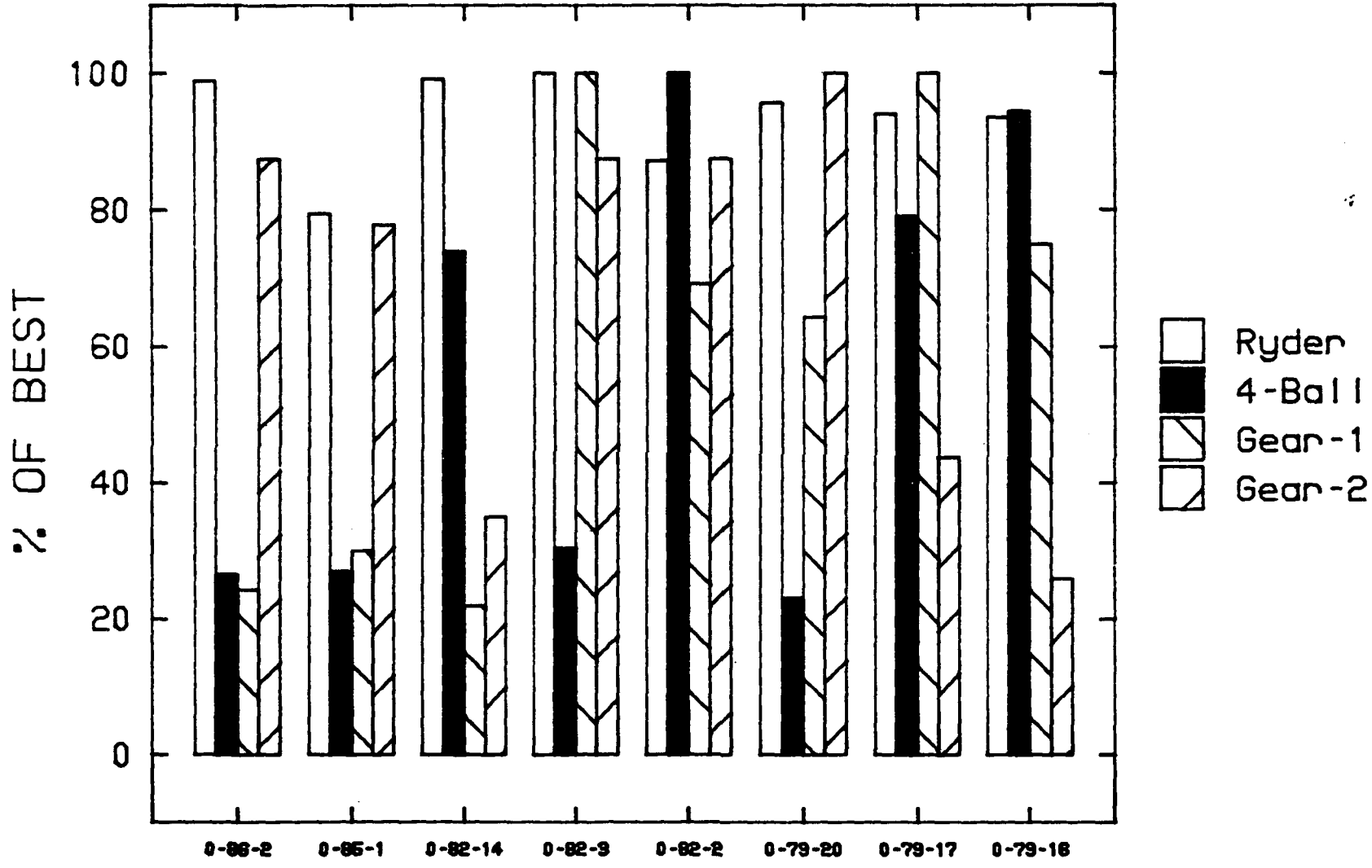

Figure 119. Normalized Results of Four Test Methods on Eight MIL-L-7808 Lubricants, % of Best vs. Oil Type

TABLE 103

NORMALIZED RESULTS OF VARIOUS WEAR TESTS

Oil	Ryder # % of Best	Four-Ball % of Best	Gear Test # 1 % of Best	Gear Test # 2 % of Best
0-86-2	98.9	26.5	24.3	87.5
0-85-1	79.5	27.0	30.0	77.8
0-82-14	99.2	73.9	21.9	35.0
0-82-3	100.0	30.3	100.0	87.5
0-82-2	87.2	100.0	69.2	87.5
0-79-20	95.7	23.0	64.3	100.0
0-79-17	94.0	79.0	100.0	43.7
0-79-16	93.6	94.4	75.0	25.9

Figure 118 shows the test results versus the type of test. The Ryder test appears to yield high percentages with about 20% variation between the high and low oils. The other three tests show large variations between oils. Figure 119 shows the test results plotted against the oil type. This figure shows no clear cut best or worst oil. Table 104 shows how the three tests rank the eight oils.

TABLE 104

RANKING OF OILS BY THE VARIOUS WEAR TESTS

Rank	Ryder	Four-Ball	Gear Test # 1	Gear Test # 2
Best	0-82-3	0-82-2	0-82-3	0-79-20
"	0-82-14	0-79-16	0-79-17	0-82-2
"	0-86-2	0-79-17	0-79-16	0-82-3
"	0-79-20	0-82-14	0-82-2	0-86-2
"	0-79-17	0-82-3	0-79-20	0-85-1
"	0-79-16	0-85-1	0-85-1	0-79-17
"	0-82-2	0-86-2	0-86-2	0-79-16
Worst	0-85-1	0-79-20	0-82-14	0-82-14

Although the Ryder gear numbers ranged from 2200 to 2656 lbs/in for these oils, the difference in their range is within the expected Ryder gear test repeatability (ASTM D 1947). The repeatability of test ASTM D 1947 is

quoted by the test method to be that two determinations ("A and b side of a test gear) in the same apparatus should not differ at the 95% confidence level by more than 787 lbs/in (138 kN/m). Two pairs of tests are considered acceptable by the above criterion, if the averages of these pairs do not differ by more than 557 lbs/in (97.5 kN/m). The reproducibility of test ASTM D 1947 is given as single observations taken at two positions (A and B) at two different installations must agree within 787 lbs/in (138 kN/m) (95% confidence level). The averages from the two installations must agree at the 95% confidence level, within 664 lbs/in (116 kN/m). The Ryder gear numbers of the oils listed in Table 104 represent values obtained on different machines in different laboratories over a long period of time and are averages of Ryder gear test values with the number of test also varying for the various oils. Therefore ranking of these oils according to their Ryder gear values cannot be made with confidence due to their values being essentially equivalent. In order to correlate these test methods more effectively, several oils having significant differences in their wear characteristics as determined by various tests should be investigated.

4. CONCLUSION

Gear test rigs, such as the Ryder, IAE, FZG, are not completely satisfactory test devices for the determination of a lubricant's load carrying capacity. Factors contributing to the problems of gear test rigs include lack of reproducibility due to operator judgement and specimen complexity and the ever increasing cost of gear test specimens. The E.P. four-ball sliding test is very simple and inexpensive to operate. However, the repeatability of the test results provided by the Falex Multi-Specimen Wear Machine needs improvement. Modification of the spindle in the Falex machine to properly retain the upper specimen during E.P. tests and to allow

for a more exact determination of seizure time is expected to improve the E.P. test.

The gear simulation test is another simple and inexpensive wear test method. However, there has not been sufficient data generated to adequately determine repeatability of the test or the ability to correlate test results to the Ryder gear test.

SECTION VI

DEVELOPMENT OF SPECIFICATION WEAR TEST

1. INTRODUCTION

The four-ball wear machine is used to assess the lubricating properties of oils or greases. The traditional method of measuring a lubricant's effectiveness is by running the test for a set period (usually one hour) and measuring the resulting wear scars. In an earlier work[38], investigation of the wear prevention properties of ester base lubricants using a four-ball wear test machine showed that the evaluation of lubricants could be improved by determining the wear scar diameter after the transition period where the scar size levels off. This study is a continuation of that work showing that a single test duration may be inadequate, and that more data can be obtained from the wear rate calculation than simply the average wear scar diameter (WSD).

2. EXPERIMENTAL

a. Apparatus and Procedures

Tests were run using a commercially available multispecimen wear tester configured to run the standard four-ball wear test (ASTM D 4172-82). This test uses four steel balls held in a tetrahedral configuration. The three lower balls are locked in place while the top ball rotates. The applied load is thus supported on three points of contact between the upper and lower balls. Most of the tests were run using ester basestock formulated synthetic lubricants. The test rig had a thermocouple for measuring the bulk lubricant temperature, a load cell for measuring coefficient of friction

(C.O.F.), a magnetic sensor for measuring rpm, and an LVDT for measuring the wear of the test balls.

Preparation of the balls for testing was accomplished according to ASTM D 4172-82. This involved washing the balls with heptane in an ultrasonic bath and air drying. The balls were then clamped into the test cup and 35 ml of oil was added. The temperature was allowed to stabilize and the drive motor was then started. A load was gently applied (no shock loading) and the test was run for 20 hours. During the test, data from the LVDT (and other transducers) was recorded using an A/D converter and microcomputer.

b. Analysis

The geometry of the contacting balls varies continuously during testing in the four ball test due to wear. This makes it somewhat difficult to obtain wear rate values without resorting to running numerous tests of varying durations. In order to calculate the wear rate it is necessary to know how the scar diameter varies with time throughout a test. A mathematical relation is needed to compute the scar size from the LVDT data. An equation was published by Bos[39] that related scar diameter with vertical displacement of the upper ball or the LVDT output in the present study. This equation takes into account not only the effects of wear but also the elastic deformation as the balls touch. This equation is shown below.

$$h = k_1 d^2 + k_2 L/d - k_3 L^{2/3} \qquad (1)$$

where h = vertical displacement, mm
L = load, N
d = scar diameter, mm

for steel balls with diameter = 12.7 mm

$k_1 = 48.22 \times 10^{-3}$ mm^{-1}
$k_2 = 3.55 \times 10^{-6}$ mm^2 N^{-1}
$k_3 = 1.63 \times 10^{-4}$ mm N$^{-2/3}$

This equation cannot be solved directly for d given h because the scar

diameter `d` appears in two terms with different powers. Although a numerical method (such as Newton's method) could be used to solve this equation iteratively, computation time would be increased substantially. For this reason, the middle term was simply deleted from equation 1. Simplifying the resulting equation gives the following relationship between the scar diameter and the vertical displacement.

$$d = [(h + k_3 L^{2/3})/k_1]^{1/2} \qquad (2)$$

Figures 120a thru 120f show the relative accuracy of equations 1 and 2. Also shown in these figures is the relationship between d and h when elasticity effects are ignored (by deleting the term in equation 1) completely (geometrical effects only). Figure 120a, for the no load condition, shows there is no difference in the curves of the three conditions, as expected. As the load is increased (Figures 120b-120f) the error in the simplified Bos equation and the non-elastic equation becomes more pronounced. However, the simplified Bos equation and the full Bos equation show good agreement at scar diameters of greater than 0.8 millimeters and loads of less than 300 Newtons. Since most of our tests were at loads of about 150 N and resulted in scars of equal or greater diameters than this, it was considered acceptable for this study to trade off some accuracy at the smaller scar sizes in order to reduce computation time.

The volume of the scars was calculated from the scar diameter using an equation taken from a paper by Feng[40] and is given below.

$$V = c_1 d^4 - c_2 Wd \qquad (3)$$

where

V = scar volume, mm^3
d = scar diameter, mm
W = load, N
c_1 = constant, 1.55×10^{-2} mm^{-1}
c_2 = constant, 1.09×10^{-6} mm^{-2} N^{-1}

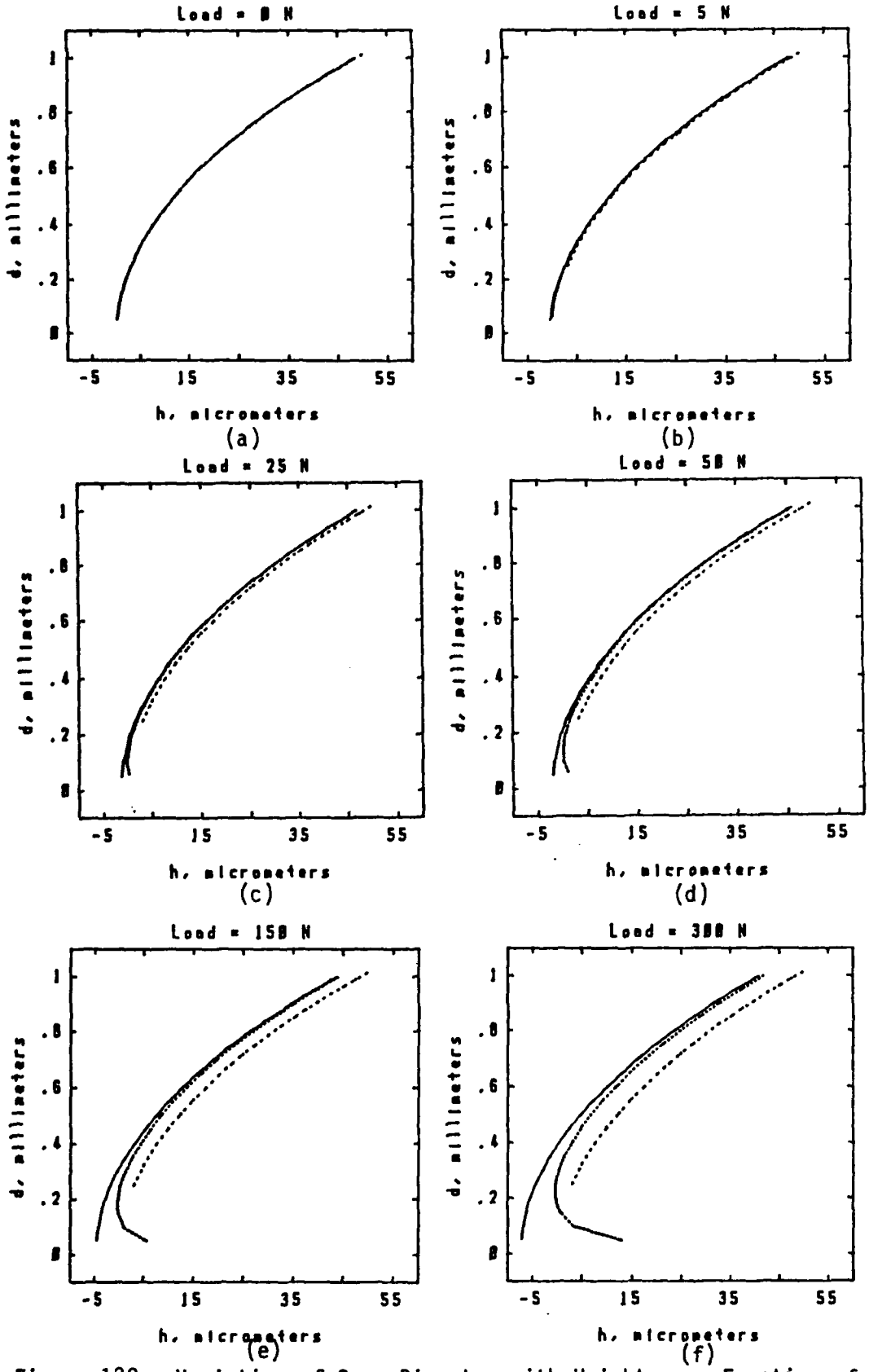

Figure 120. Variation of Scar Diameter with Height as a Function of Load. —— Bos Equation, ___ Modification Bos, ... Geometrical

Calculation of the wear rate of the four-ball wear tests can be made using a microcomputer to apply equations 2 and 3 to the LVDT data taken from wear testing.

It should be noted that the above equations are concerned only with the wear of the lower balls. The derivation of these equations assumed that the upper rotating ball was perfectly spherical, which is not true. Willermet and Kandah[41] made precise measurements of the wear in the four-ball configuration and found that the wear of the rotating ball may vary from one half to more than double the total wear of the three lower balls.

3. RESULTS AND DISCUSSION

a. Accuracy

Figure 121 shows the comparison of WSD calculated from the 20 hour test with the results of eleven discrete tests. All the results illustrated in this figure were run at 1200 rpm, 146 N load, 75°C, using lubricant O-79-20. Discrete tests were run under the same conditions and at various durations ranging from 10 minutes to 20 hours and the scars sizes measured. As the figure shows, the accuracy of the computer program is very good. The program produces the same wear trend information from one test as is obtained from running several tests. This results in a time savings of from 4:1 to 9:1 depending on whether or not operator time is factored in.

b. Load Effects

Tests were conducted on lubricant O-79-20 at various loads, with all other test parameters being constant (temperature, speed, duration). A total of seven tests were analyzed. Of these, six reached a leveling off condition in the twenty hours of testing. The loads in these six tests ranged from 111 to 392 N, but the final scar size showed no dependence on the load applied. The average final scar size was 1.50 ± 0.026 mm. The standard deviation is

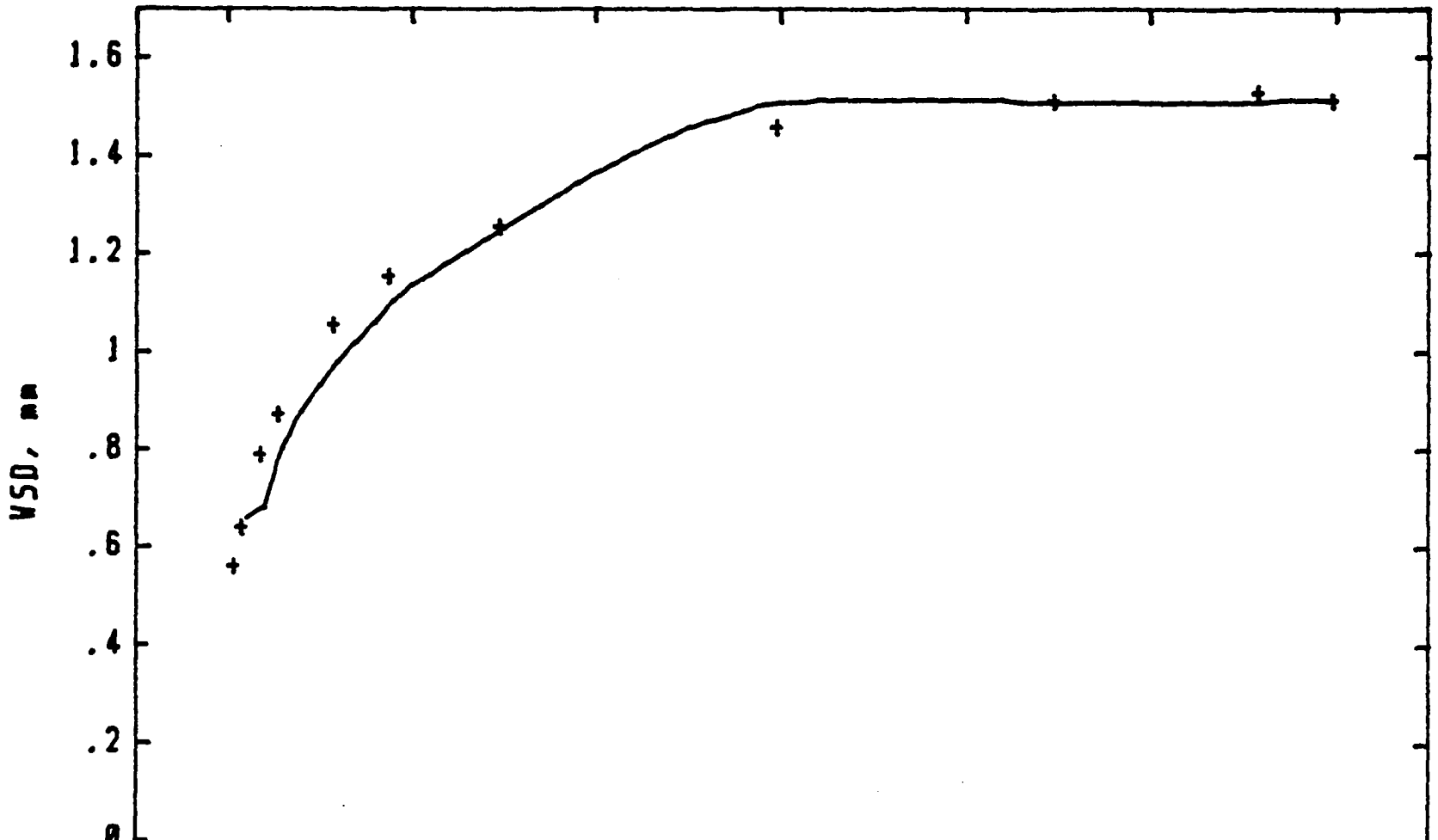

Figure 121. Comparison of WSD Calculated from One 20 Hour Test with the Results of Eleven Discrete Tests

only 1.75% of the average scar size, which is a very small amount of scatter. Although the final scar size showed no significant dependence on the applied load, the volumetric wear rate and time required to reach leveling off were directly influenced by the load. Figure 122 shows the scar volume as a function of time for the seven wear tests using lubricant O-79-20. All the tests exhibit a decidedly linear wear process with time until reaching a scar size of about 1.5 mm whereupon the wear process abruptly decreases by two orders of magnitude.

The high wear rate portion of each wear curve was subjected to a linear least squares curve fit to determine the approximate average wear rate during this portion of the test. The same was done to the low wear rate part of each curve. Table 105 shows the results of this curve fitting. The effect of load on wear and the drastic decrease in wear rate associated with the leveling off phenomenon can be observed. Figure 123 is a plot of the wear rate versus applied load for the portions of the curve before level off occurred. The correlation coefficient for a least squares line through these data points is 0.942 indicating that a straight line provides appropriate representation of the data.

TABLE 105

RESULTS OF FOUR-BALL WEAR TESTS USING O-79-20 LUBRICANT

Load, N	Final WSD, mm	Wear Rate, $mm^3/min \times 10^{-6}$	
		Before Transition	After Transition
67	1.423	55	N/A
111	1.488	90	0.0
156	1.530	121	8.0
245	1.510	141	0.5
289	1.499	167	3.5
334	1.457	143	5.0
392	1.522	196	3.0

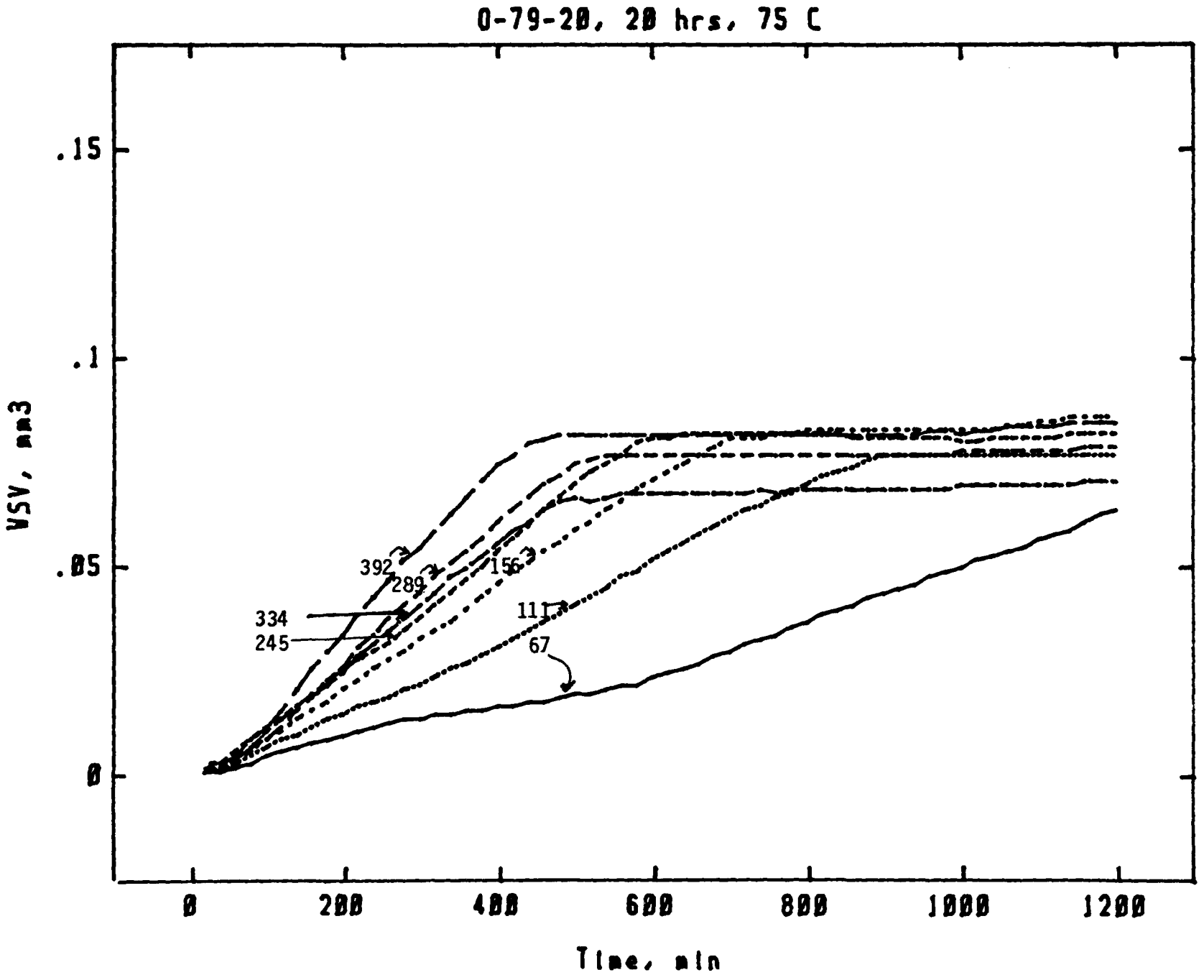

Figure 122. Calculated Wear Scar Volume Versus Time for Seven Four-Ball Tests Using Lubricant 0-79-20 (Loadings in N)

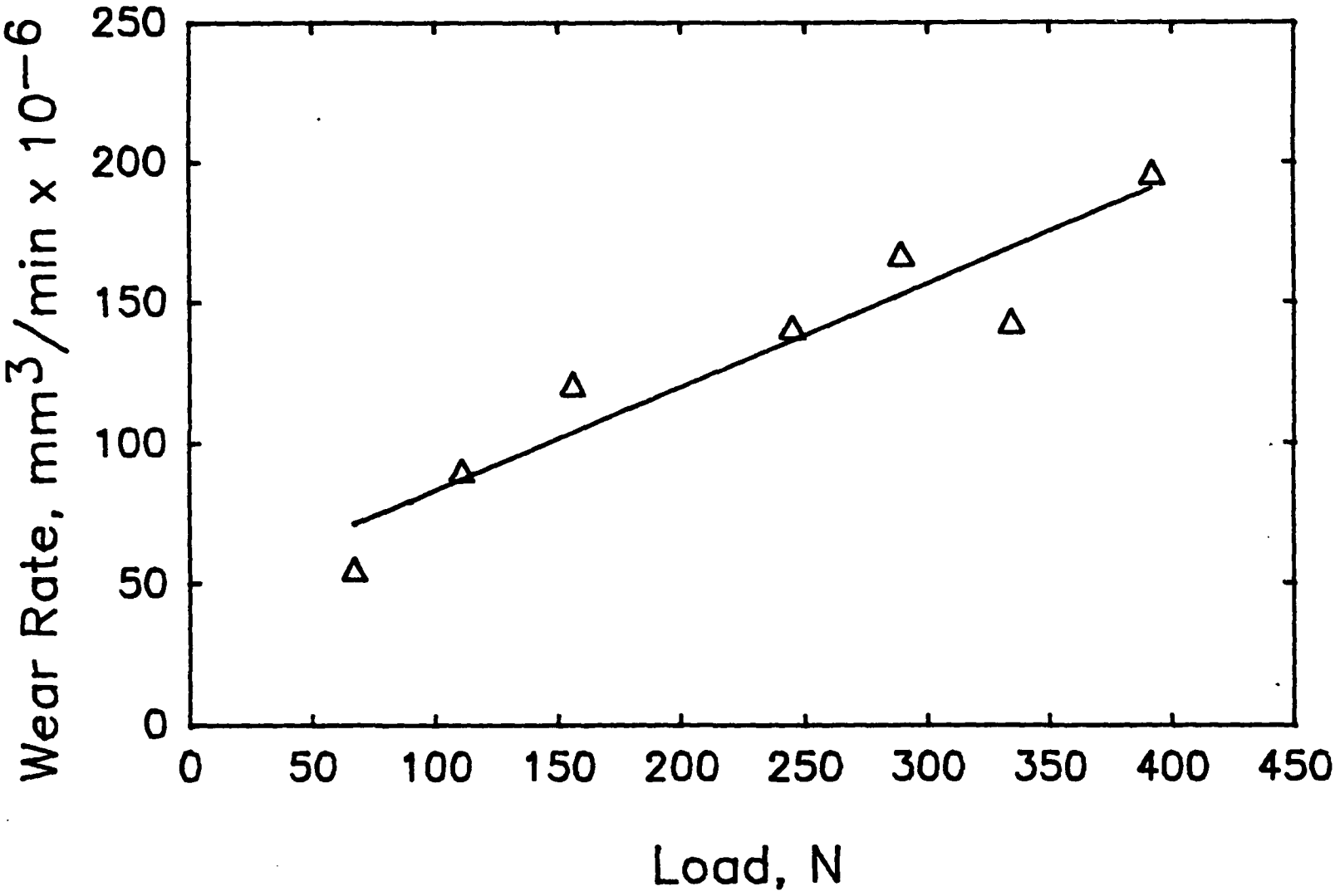

Figure 123. Least Squares Curve Fit to Wear Rate Versus Load Data in the Four-Ball Wear Test Using Oil 0-79-20

c. Speed Effects

Four-ball wear tests were performed at speeds ranging from 200 to 5000 rpm (7.7 to 191.5 cm/s) for determining the relationship between speed and wear rate. However, competing effects in the scar zone cause difficulty in predicting the effect of speed. For example, as speed increases the hydrodynamic effect becomes more pronounced, but at the same time the temperature rises which decreases the viscosity. The net effect of these phenomena is unclear, although the overall trend seems to indicate scar size decreases with increased speed. Figure 124 is the calculated scar volume versus time for tests with oil 0-79-20 (145 N load, temperature 75°C, duration 20 hours). Figure 124 shows the progression of wear scar volume for a speed of 200 rpm (7.7 cm/s) with a relatively slow wear rate indicated. Figure 124 also shows test results at 1200 and 1600 rpm where the wear rate is more rapid but decreases abruptly at some point during the test. Two plots are included for tests at 1200 rpm showing the relative reproducibility under these conditions. Of the remaining plots only 2000 rpm (b) and 3000 rpm show significant trends and a definite change in wear rate part way through the test. Speeds of 2000(a) and (c), 4000 and 4500 rpm resulted in scar sizes of about 0.7 mm diameter. As this figure shows, this is below the threshold of applicability for the wear scar calculation program as it is currently written because the curves show no definite wear trending. Errors are introduced due to the distortion caused by temperature transients, the wear period being too brief, and the fact that the simplifying assumptions used in the development of the program resulted in the largest errors being produced at the smallest scar sizes. A partial solution may be to modify the data acquisition program such that it samples data much more frequently during the initial, high wear stages of a test. Figure 125 shows the final

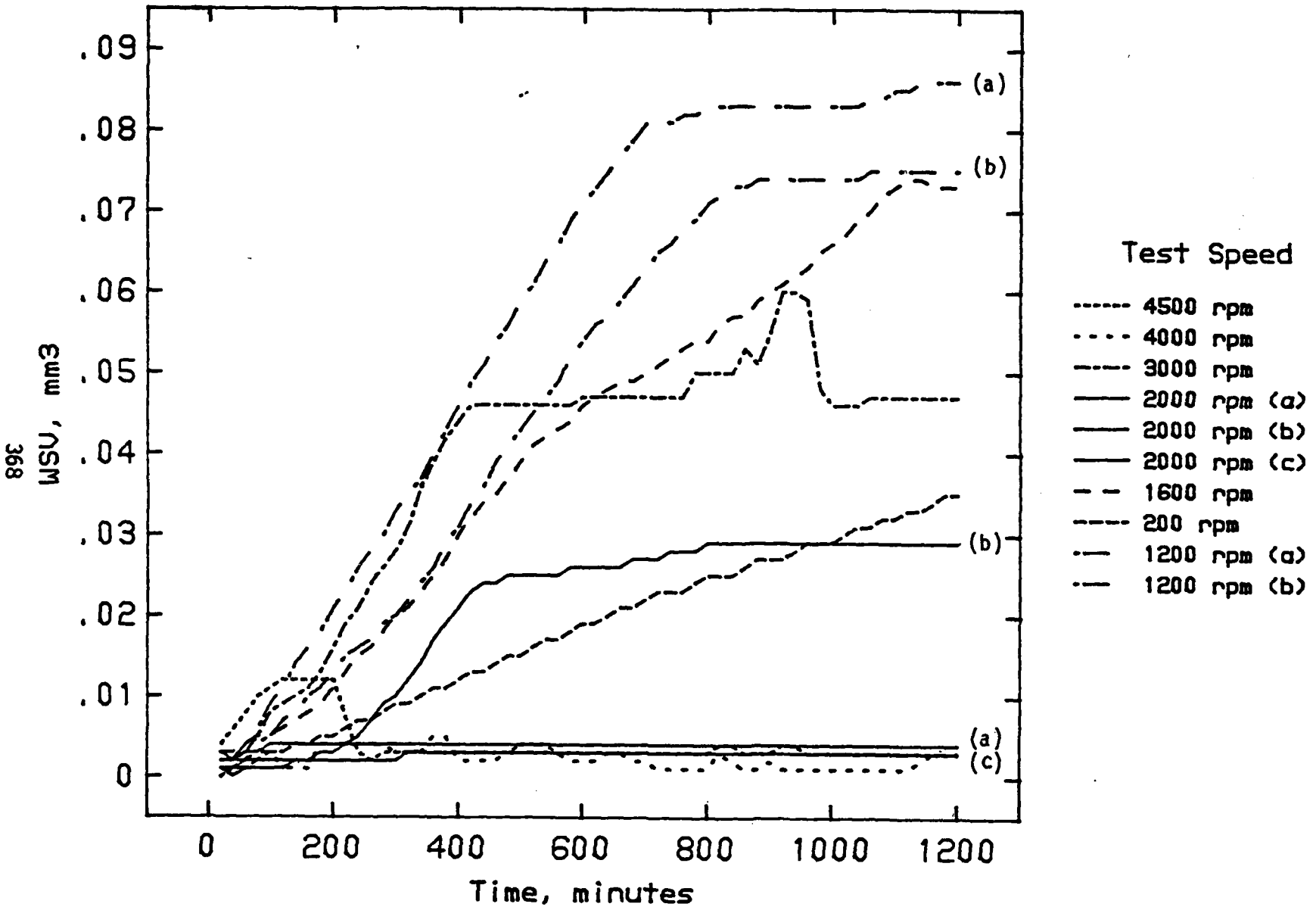

Figure 124. Computed Wear Scar Volume (WSV) Versus Time for Oil 0-79-20

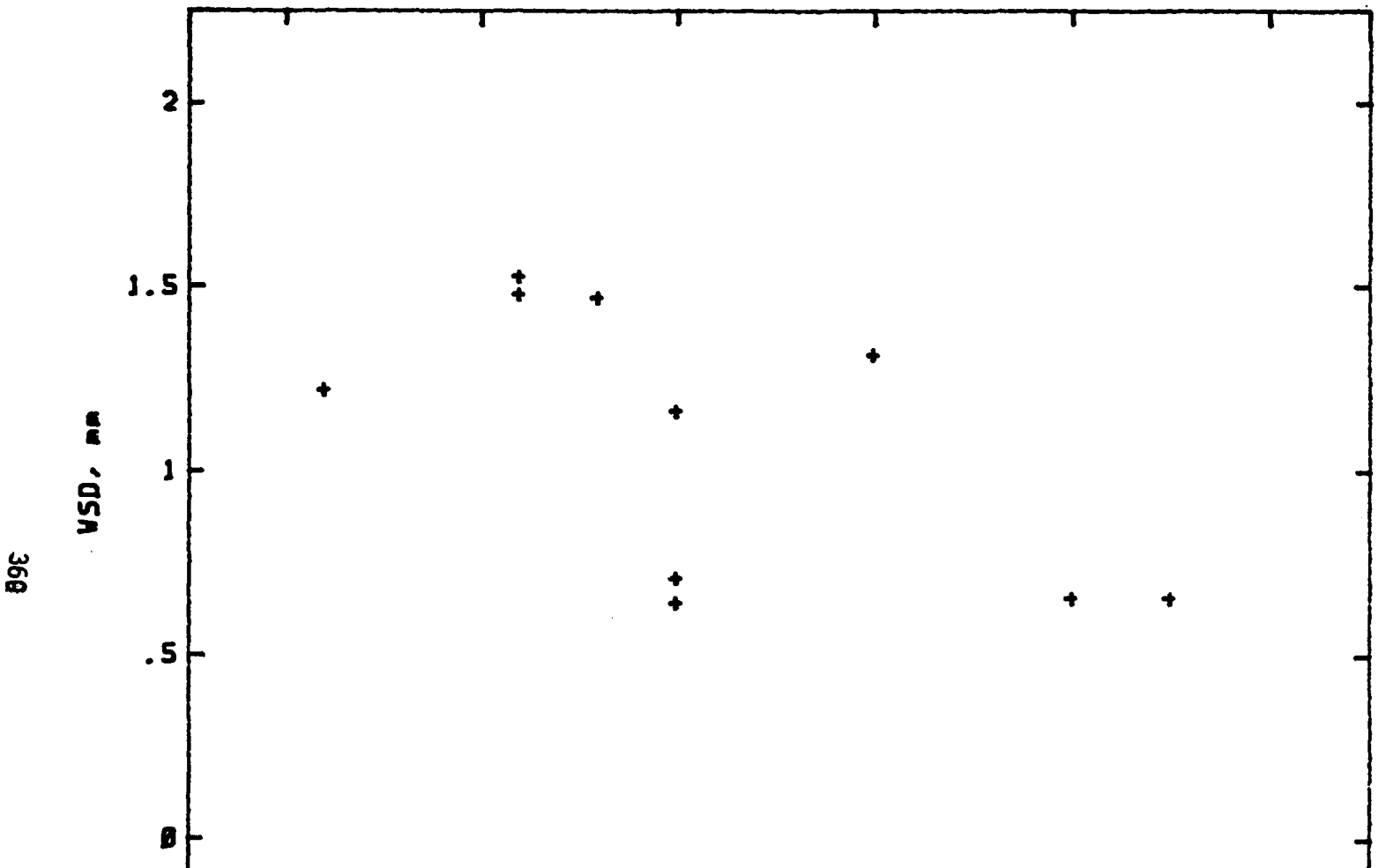

Figure 125. Final Wear Scar Diameter (WSD) Versus Speed in Oil 0-79-20

scar diameter versus speed for tests in O-79-20 and shows the wide scatter associated with the speed tests.

d. Differences in Wear Prevention Properties of Lubricants

Table 106 shows the lubricants tested and the final scar size with test conditions of 1200 rpm, 75°C, 145 N load and 20 hour duration. The test results were arranged into two groups. Tests resulting in scar sizes of 0.9 mm or greater were termed "poor", while those with scar sizes of less than 0.9 mm were "good". Analyses of the good oils using the wear scar volume calculation program was not possible because the scars were too small. The 13 poor oils were analyzed using the wear scar volume (WSV) calculation program to obtain WSV versus time for each lubricant. Table 107 gives the calculated wear rates.

The above results were then used in a linear regression program to arrive at an average wear rate value for the oils. In 11 of 13 tests the linear regression was broken into two parts; one was for 0-10 hours of testing, and the other for 10-20 hours. These tests exhibited varying degrees of linearity in wear, with the extreme cases being those of oil O-79-20 and O-77-10. Testing with oil O-79-20 showed a very sharp decrease in wear rate, going from 97 x 10^{-6} mm^3/min to 6 x 10^{-6} mm^3/min after about twelve hours of testing. However, testing with oil O-77-10 showed a different behavior. The wear rate was nearly constant at 37 x 10^{-6} mm^3/min throughout the entire 20 hours of testing. For some oils the wear rate increased while in others the wear rate decreased with time. Figures 126 and 127 show the calculated WSV versus time for the 13 poor oils.

e. One Hour Versus Twenty Hour Testing

Figures 128 and 129 show the final scar size for several lubricants under two loads (147 and 392 N) and two test durations (1 and 20 hour). The

TABLE 106

CHARACTERIZATION OF VARIOUS LUBRICANTS BASED ON SCAR SIZE PRODUCED FROM 20 HR TEST AT 75°C, 1200 RPM, 145 N LOAD

Lubricant	Scar Dia., mm	Poor	Good
0-66-26	0.508		x
0-67-0	1.152	x	
0-67-1	1.390	x	
0-70-6	1.488	x	
0-72-9	0.861		x
0-76-1	1.498	x	
0-77-10	1.296	x	
0-79-16	0.309		x
0-79-17	0.432		x
0-79-20	1.481	x	
0-82-14	0.463		x
0-82-2	0.338		x
0-82-3	1.121	x	
0-85-1	1.262	x	
0-86-2	1.279	x	
OP-369	0.574		x
Ref Oil C	1.540	x	
Hitec 164	1.478	x	
Hitec 166	1.307	x	
Hitec 168	1.173	x	
Valvoline 10W-40	0.450		x

TABLE 107

CALCULATED WEAR RATES OF OILS WITH SCAR SIZES GREATER THAN 0.9 MM

Lubricant	Wear Rate $\cdot 10^{-6}$ mm^3/min 0-10 Hrs	10-20 Hrs
0-67-0	30.3	12.7
0-67-1	55.9	40.3
0-70-6	40.1	90.2
0-76-1	49.2	79.4
0-77-10	36.7	36.8
0-79-20	96.7	6.2
0-82-3	13.6	26.3
0-85-1	35.6	28.1
0-86-2	82.5	28.1
Ref Oil C	82.1	68.5
Hitec 164	53.3	73.3
Hitec 166	29.8	43.9
Hitec 168	21.8	26.9

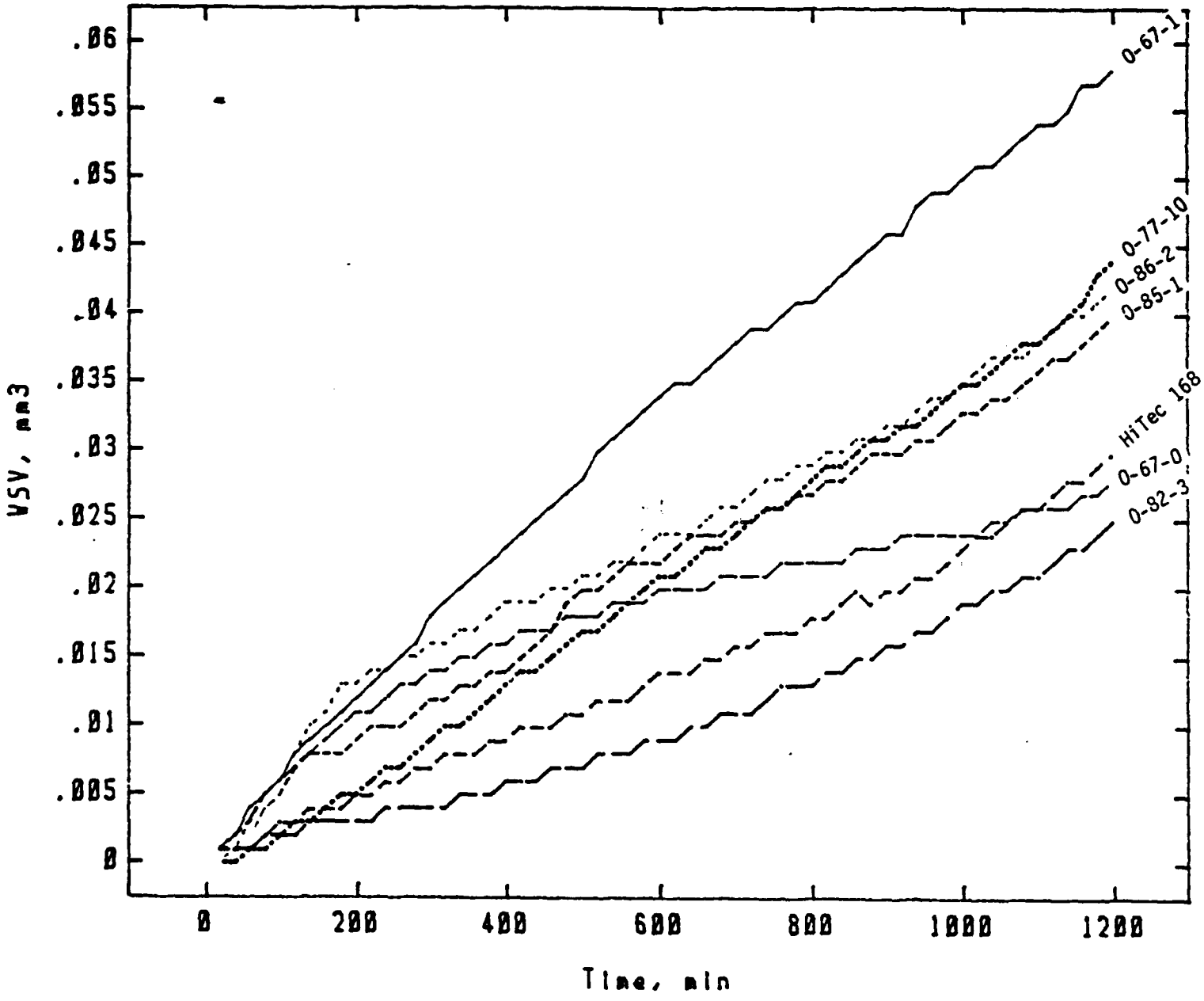

Figure 126. Calculated Wear Scar Volume versus Time for Seven Lubricants Producing Scar Sizes Greater than 0.9 mm

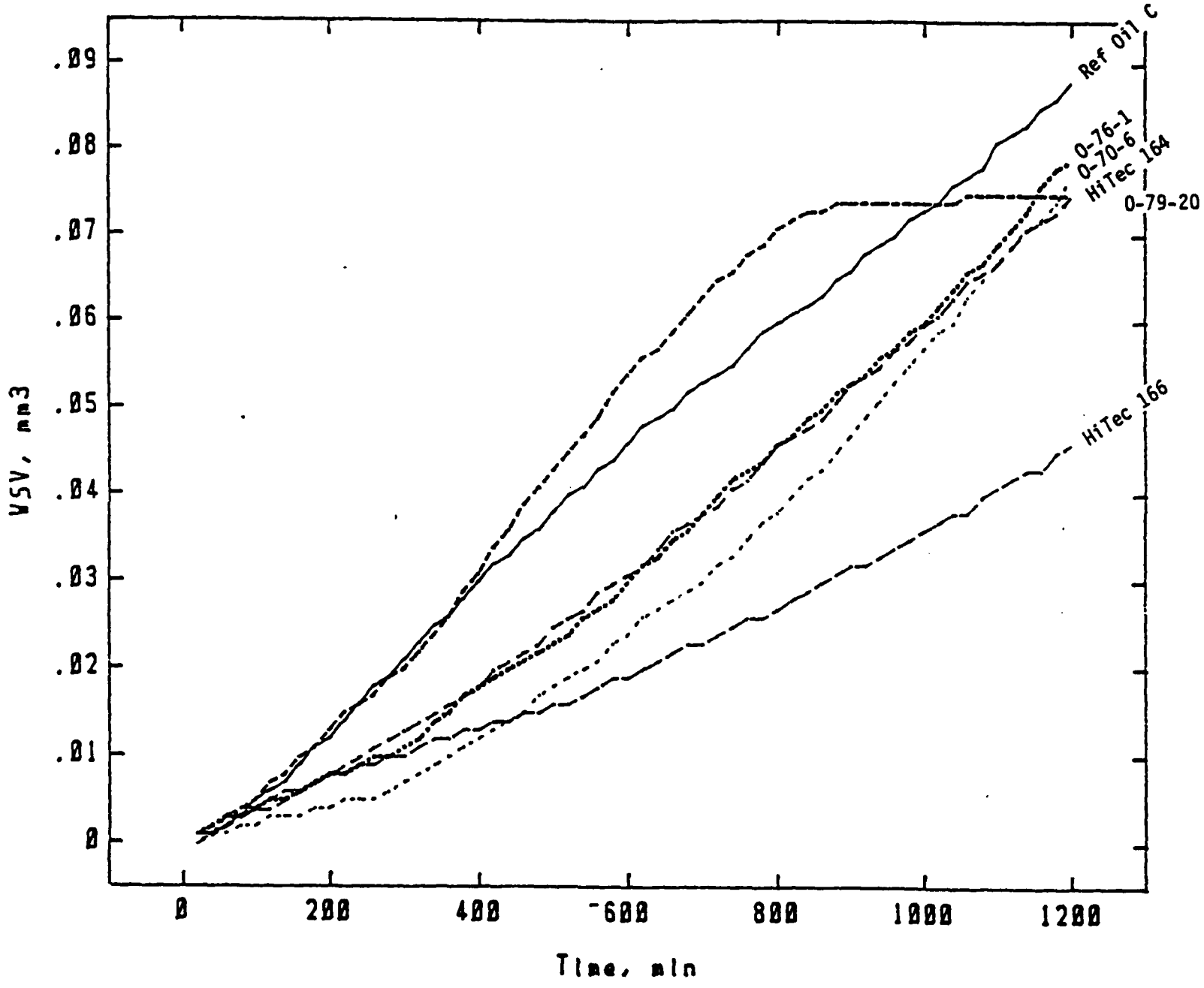

Figure 127. Calculated Wear Scar Volume Versus Time for Six Lubricants Producing Scar Sizes Greater than 0.9 mm

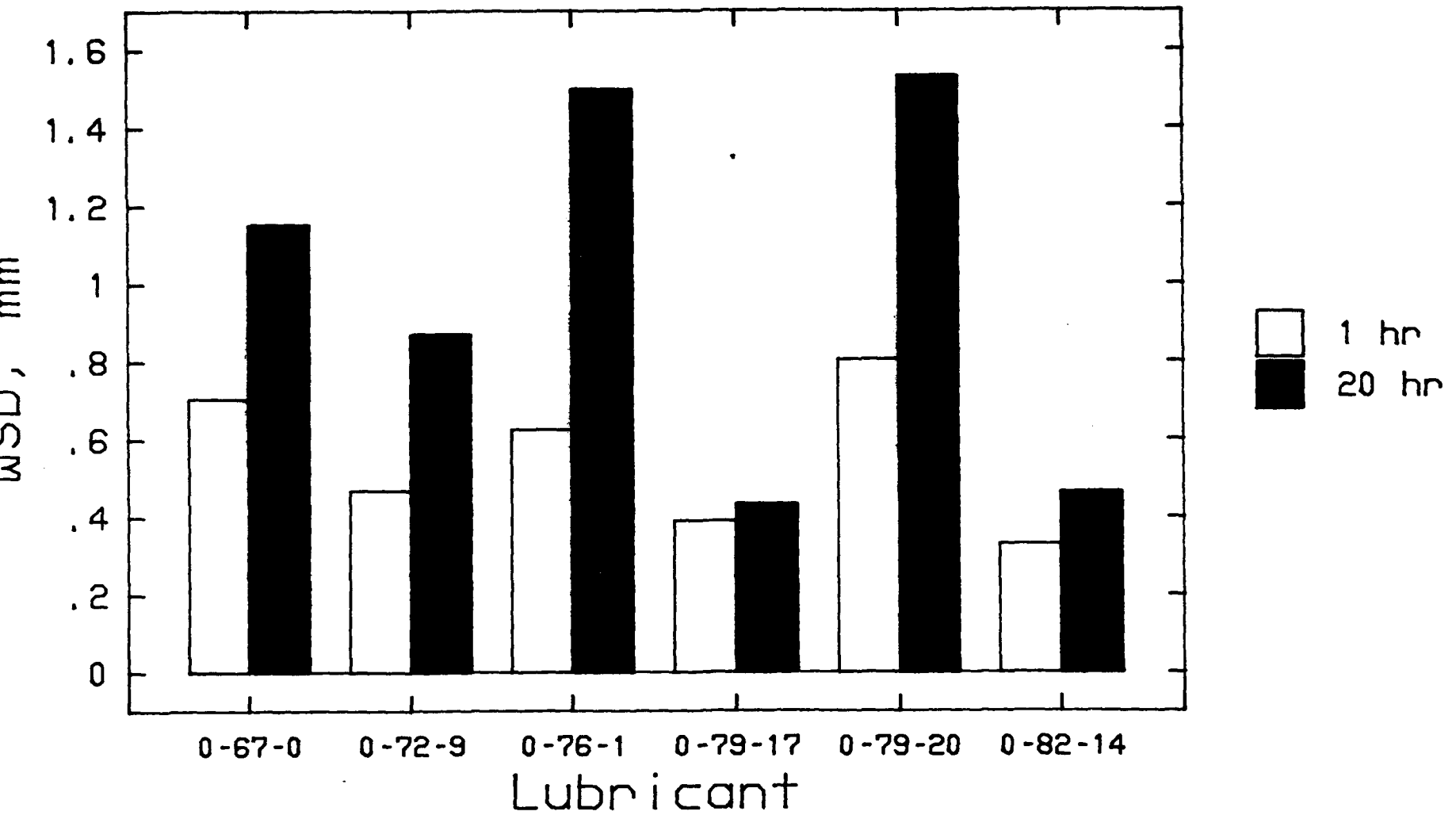

Figure 128. Final Scar Diameters for Various Oils at 1 Hour and 20 Hour Test Durations. Conditions: 145 N Load, 75°C Temp., 1200 rpm

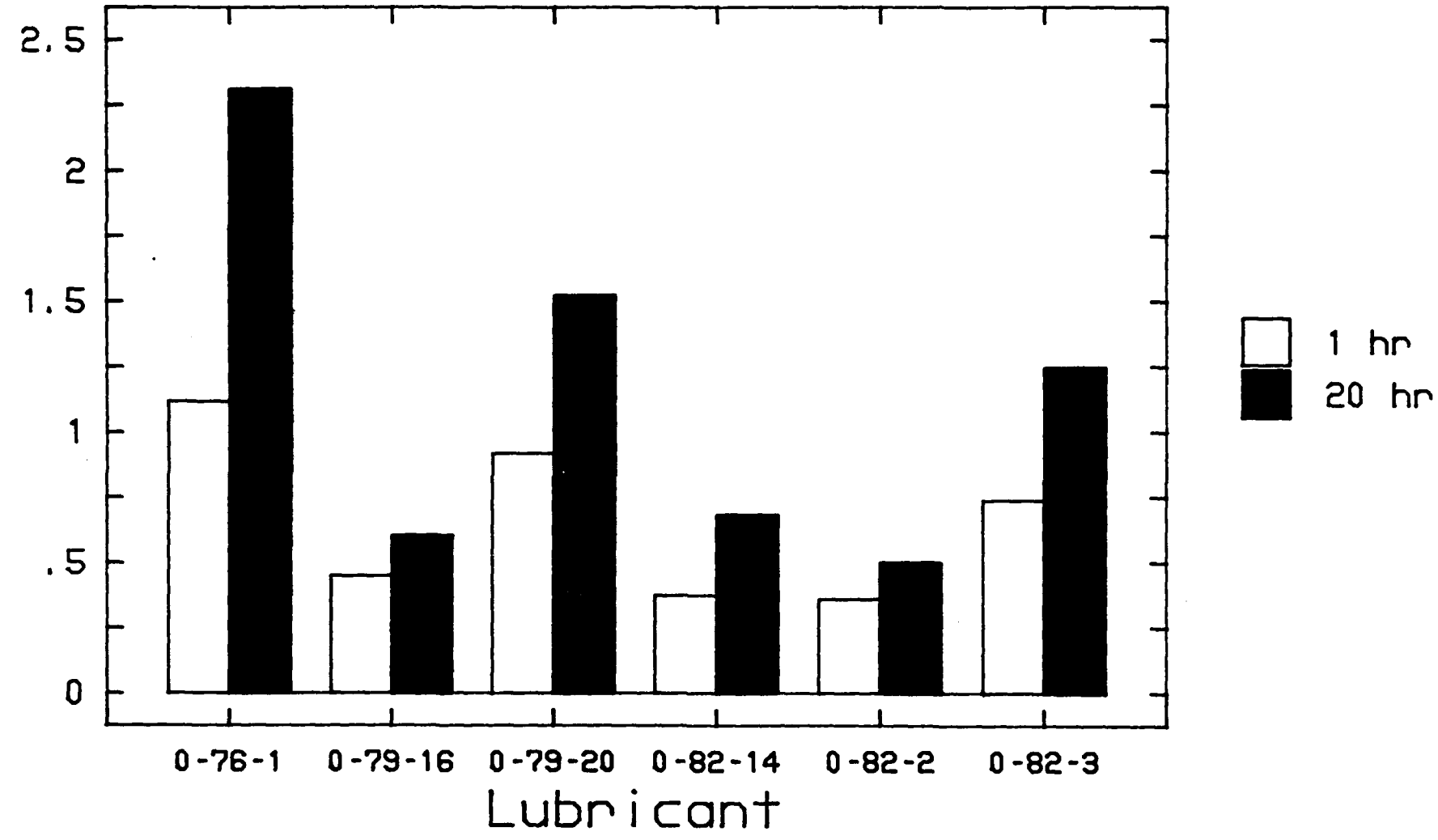

Figure 129. Final Scar Diameters for Various Oils at 1 Hour and 20 Hour Test Durations. Conditions: 392 N Load, 75°C Temp., 1200 rpm

test conditions in Figure 128 for load, temperature and spindle speed were 147 N, 75°C and 1200 rpm, respectively. The conditions in Figure 129 were the same except the load was 392 N. Except for oils O-82-14 and O-79-16, results show the 20 hour test to give bigger scar diameter than the one hour test. The magnitude of the differences among the various oils was also larger for the 20 hour test. For example, in the one hour test, there was no significant difference in scar diameters between O-79-16 and O-79-20 oils, while in the 20 hour test, the scar diameter of the O-79-20 was more than double that of the O-79-16. Therefore, our results showed the 20 hour test to provide greater variation among the various oils.

The initial results indicate that there is an apparent advantage in using a 20 hour four-ball wear test over a one hour wear test. During the first hour of testing the wear scar calculation program does not function correctly. Figures 130 and 131 offer a partial explanation for this point and show that the program operates with the least errors at large scar diameters. In Figure 130 the calculated scar size is shown for a rather poor oil, O-76-1. At small scar diameters the program has errors that result in a larger-than-actual calculated scar size. This is clearly shown in Figure 130. Another cause of the error shown in Figure 130 is the thermal expansion due to frictional heating of the balls and hardware. This heating and expansion appears as a decrease in WSD to the program.

The Hertzian scar size (the scar size after the load is applied but before wear takes place) is 0.33 mm for a 392 N load. This point is shown in Figure 130 with an "estimated wear path" drawn in connecting it to the calculated wear path. From this figure it appears that the first 20 minutes of the calculated wear test data is corrupted from computational and thermal expansion errors. After 20 minutes the scar has grown enough so that the

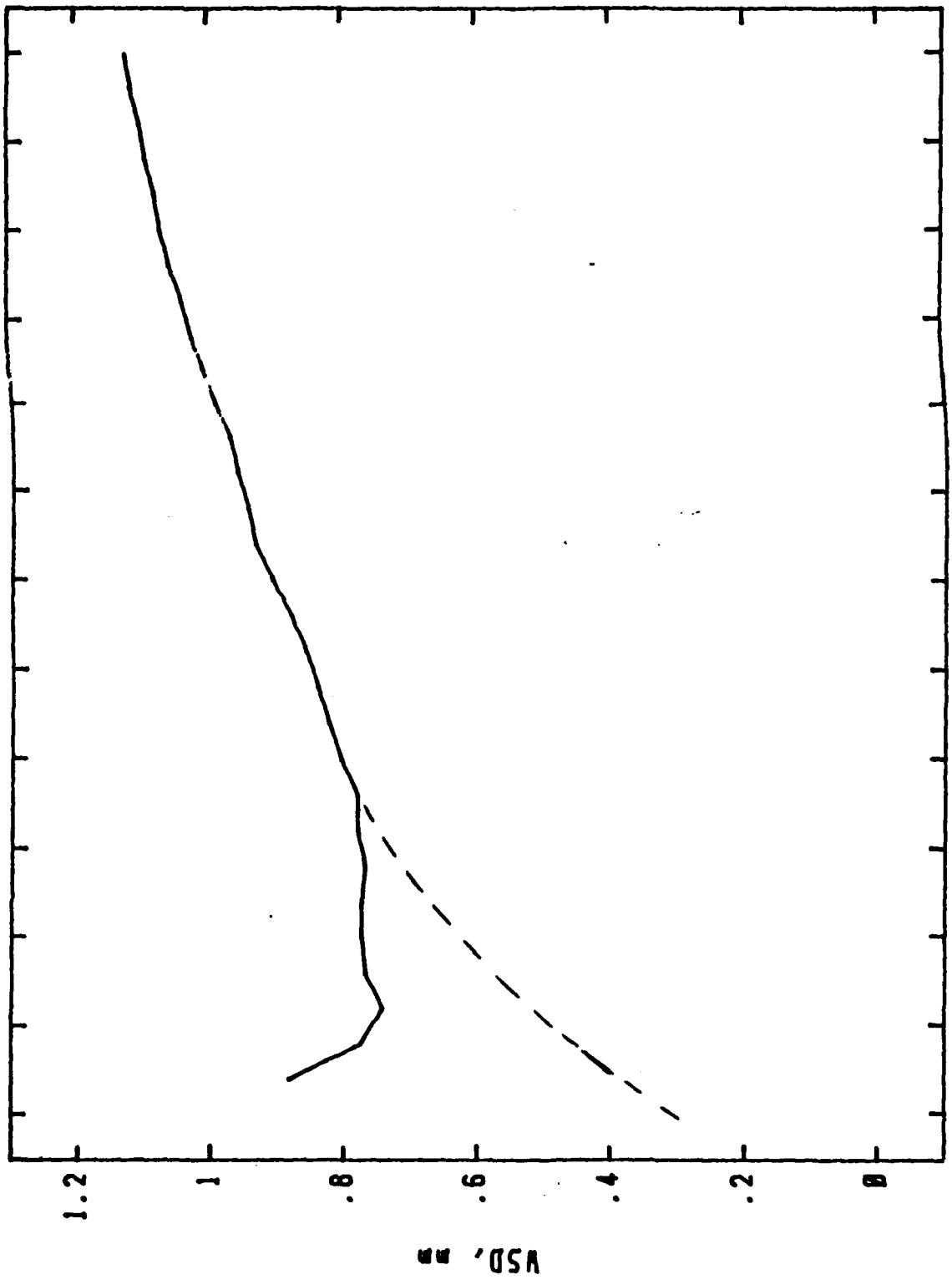

Figure 130. Calculated Scar Diameter from Test of O-76-1. Figure Illustrates Errors Present During Initial Portion of Wear Test. Dashed Line is Estimated Wear Path from Known Diameter at Time Zero

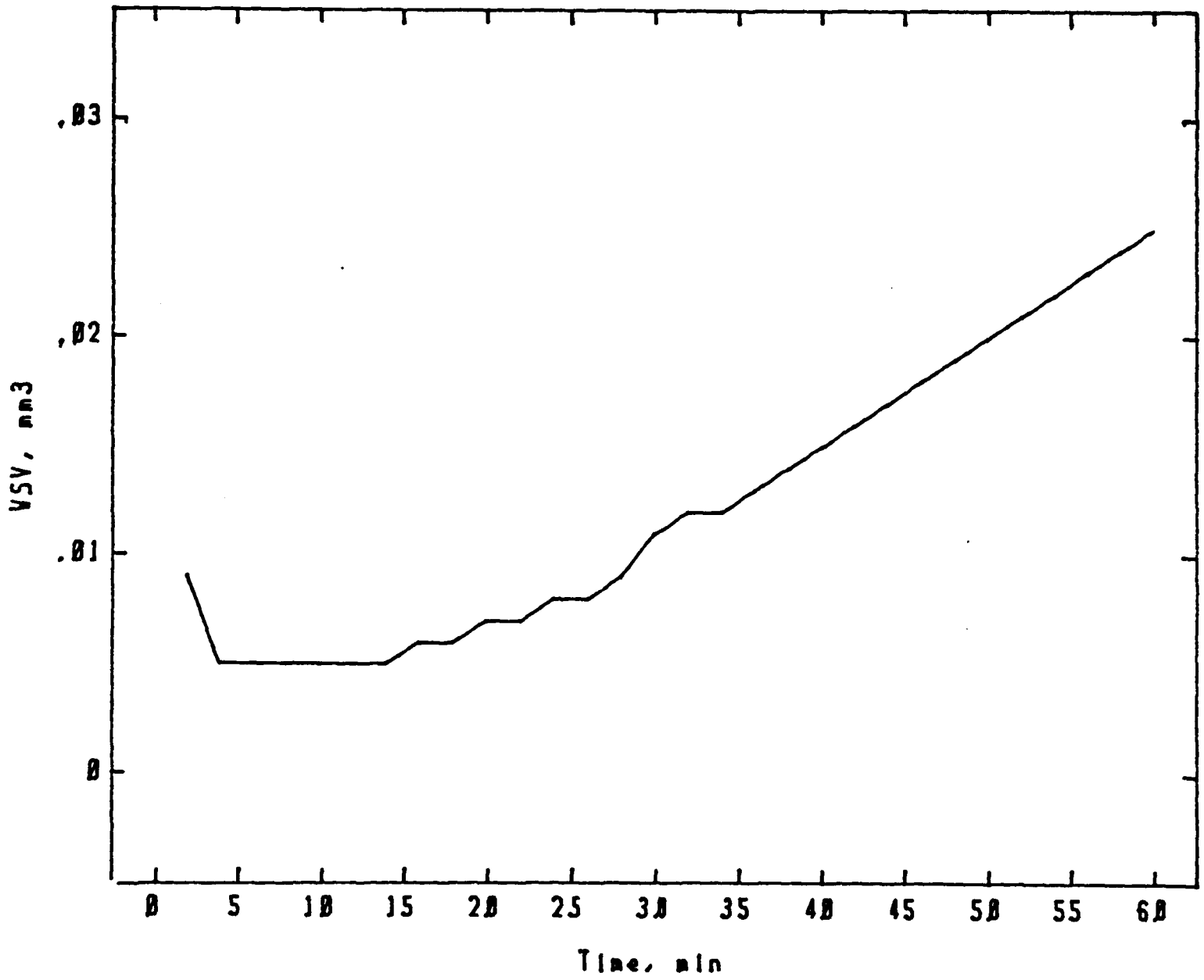

Figure 131. Calculated Scar Volume from Test of O-76-1. Figure Illustrates a Constant Wear Rate During Second Half of Wear Test

computational errors are insignificant, and the transient frictional heating and thermal expansion have reached a steady state and are no longer a factor. Figure 131 shows the calculated wear scar volume from this test. Although the first 20 or 30 minutes of data is corrupt the last 30 minutes are extremely linear and indicate a constant volumetric wear rate of 500 x 10^{-6} mm^3/min. However, Figures 127 and 128 and Table 107 showed changes in the wear rate after the first few hours of testing. For example, during the first 300 minutes (Figure 127) O-76-1 oil had a wear rate of 33 x 10^{-6} mm^3/min but during the last 900 minutes the rate changed to 75 x 10^{-6} mm^3/min. These results also indicate that the variation among the various oils is best seen when the longer test method is applied.

4. SUMMARY

Experiments were conducted to determine the wear rate of lubricated sliding surfaces using a variation of the standard ASTM D 4172-82 four-ball wear test. The relative displacement between the balls was recorded continuously during these tests using a personal computer (PC), an analog to digital (A/D) converter, and a linear variable differential transformer (LVDT). The LVDT output was then used to calculate the variation of wear scar diameter with time. Analysis of this data provided several useful parameters that could be used to characterize lubricants.

5. CONCLUSIONS

By using a microcomputer to collect and analyze data taken from a four-ball wear test machine, it is possible to understand more about how wear progresses during the test. In particular, it was found that the wear proceeds at a fairly constant volumetric rate for various time periods and that rate is dependent on the load and speed. The equations used to calculate the scar diameter are difficult to solve directly, but simplifying

assumptions greatly reduce the computations required while not significantly affecting accuracy in the domain of normal four-ball tests. By using the methods developed in this study, tribologists have another technique at their disposal for evaluating the lubricating properties of fluids.

SECTION VII

DEVELOPMENT OF LUBE DATA STORAGE AND RETRIEVAL SYSTEM

Development and demonstration of the software for the lubricant data storage and retrieval system (LDSR) was completed. A manual for the LDSR system was written and submitted separately fulfilling the requirement of this task.

SECTION VIII

RULLER DEVELOPMENT

1. INTRODUCTION

The objective of this task was to develop an inexpensive, easy to operate, and compact Remaining Useful Life of a Lubricant Evaluation Rig (RULLER). The developed RULLER will be able to perform formulation independent remaining useful life evaluations of used MIL-L-7808 and MIL-L-23699 lubricating oils.

As described in the Interim Technical Report,[1] a single board voltammograph has been developed for performing the reductive-cyclic voltammetric (RCV) techniques. The developed single board voltammograph was incorporated into the hardware of an Apple IIe microcomputer system to produce the first RULLER candidate. The experimental parameters of the single board voltammograph-Apple IIe microcomputer based (SBV-IIe) RULLER candidate were optimized using fresh and laboratory stressed MIL-L-7808J lubricating oils.

During the first phase of this research program reported herein the SBV-IIe RULLER candidate was optimized further by analyzing laboratory stressed MIL-L-23699 oils and by analyzing several series of authentic used MIL-L-7808 and MIL-L-23699 oil samples obtained from normal and abnormal operating aircraft engines.

The second part of the research concentrated on identifying computer systems capable of further miniaturizing the data management system and on producing five RULLER demonstration devices. The third part of the research concentrated on monitoring the results of the field tests performed on the RULLER demonstration devices.

2. EXPERIMENTAL

a. Instrumentation

(1) Universal Single Board Voltammograph

The schematic and parts diagram of the analog portion of the universal single board voltammograph (USBV) used in the RULLER demonstration devices are shown in Appendix C. The initial design of the analog portion of the USBV was based on the CV-1B voltammograph (described in the Interim Technical Report[1]) and on single board voltammographs described in the literature.[42-44]

To enable the USBV to be incorporated into the hardware of any microcomputer with suitable parallel connectors, Model AD565AJD Digital-to-Analog (D/A) and Model AD570JD Analog-to-Digital (A/D) microchips (Analog Devices, Dublin, Ohio) were incorporated into the ramp input and electrode output of the USBV, respectively. The wiring diagrams of the D/A and A/D microchips are shown in Appendix C.

(2) Microcomputer System

The microcomputer system used in the production of each RULLER demonstration device was a Laser 128 microcomputer (Central Point Software, Portland, Oregon) which has 128K of memory and a built-in floppy disk drive.

A Model 7720 parallel interface (Apple Software, Sunnyvale, California) was used to connect the D/A and A/D microchips and the electrode switch of the USBV (SW in Figure C-1) with the Laser 128 microcomputer. The wiring connections of the parallel interface to the D/A and A/D microchips and the electrode switch are shown in Appendix C. The prompting messages and the results of the RULLER analyses were printed on a 3.12 inch wide roll of thermal paper using a Model DPP-400 printer (Acculex, Taunton, Mass).

(3) Atomic Emission Spectrometer - Multichannel Capacitor System

The atomic emission spectrometer used to analyze the wear metal debris present in the used MIL-L-7808 and MIL-L-23699 oil samples was a A/E35U-1 rotating disk electrode-high voltage spark source-atomic emission spectrometer. The A/E35U-1 spectrometer is the predecessor to the A/E35U-3 emission spectrometer currently used by JOAP. Normal JOAP procedures[45] were used for the wear metal analyses.

The multichannel capacitor system connected to the selected photomultipliers of the A/E35U-1 spectrometer has been previously described.[46] An Apple IIe microcomputer system and associated hardware was used to monitor the voltage buildups of the multichannel capacitor system produced by the outputs of the selected photomultiplier tubes. The Apple IIe microcomputer system was also used to calculate and display the difference plots of the voltage buildups of the multichannel capacitor system.

(4) Gas Chromatograph

The gas chromatograph (GC) used in this study was a Hewlett Packard 5890A (Palo Alto, CA) equipped with a J&W Scientific (Folsom, CA) Megabore 15 meter column (DB Wax-1 micron thickness coating) and a flame-ionization detector. The gas chromatograms were printed out on a Hewlett Packard 3393A Integrator.

b. Electrode System

The electrode system used in the production of the RULLER demonstration devices was manufactured from a glassy carbon voltammetry electrode (GCE) (Bioanalytical Systems Inc., West Lafeyette, Indiana) and two 6 cm lengths of 0.5 mm diameter platinum wire (99.95% purity: Aesar, Seabrook, New Hampshire). The GCE was used as the working electrode and the platinum wires were used as the auxiliary and reference electrodes.

The platinum wires were attached to the sides of the GCE (ends of wires level with bottom surface of GCE) with a drop of epoxy adhesive. A heat shrink tube (1/4 inch diameter-black polyolefin material: Newark Electronics, Dayton OH) of 5 cm length was pushed over the three electrode system. The 1/4 inch tube was pushed over the three electrode system until a 1 cm portion of the three electrode system (bottom surface of GCE) extended from the tube. The exposed sides of the three electrode system were coated with 732 RTV silicone rubber (General Electric, Waterford, New York). The 1/4 inch tube was then pushed back toward the bottom surface of the three electrode system until the ends of the tube and the electrode system were level. The encased electrode system was allowed to set undisturbed for 24 hours at room temperature to cure the 732 silicone forming a liquid tight seal between the electrode system and the 1/4 inch shrink tube.

After the 732 silicone rubber was cured, the outer edges of the electrode system's bottom surface were ground with 320 grit silicon carbide paper to remove the excess 732 silicone rubber and shrink tube exposing the ends of the two platinum wires. The entire bottom surface of the electrode system was then polished with an alumina powder suspension (BAS).

The encased electrode system was soldered to a grounded and shielded three-wire cable (diameter of 0.125 inches; Newark Electronics). The opposite end of the cable (1 foot length) was soldered to a five prong connector (Newark Electronics) through which the electrode system was electrically connected to the USBV.

A heat gun was then used to heat shrink the upper (closest to the soldered junction) 1 cm portion of the 1/4 inch heat shrink tube. A 4 cm heat shrink tube (3/8 inch diameter, Newark Electronics) was slid over the soldered junction and the upper portion of the 1/4 inch heat shrink tube.

The 3/8 inch tube was then heated to form an air tight seal over the ends of the electrode system and three wire cable.

c. Laser 128 Microcomputer Software

The computer program used to control the voltage ramp of the USBV and to sample the output of the working electrode was written in machine code due to the speed requirements of the voltammetric technique.

The user prompting and data management program was written in BASIC language to facilitate the changes that were made in the program during the RULLER development.

d. Chemicals

All of the chemicals used during this research were A.C.S. certified and were obtained from either Aldrich Chemical Corp. (Milwaukee, WI) or Fischer Scientific (Cincinnati, OH).

e. Lubricating Oils

(1) Laboratory Stressed MIL-L-23699 Oil Samples

The laboratory stressed MIL-L-23699 oil samples analyzed during this study were prepared from fresh O-71-6, O-77-15, TEL-7004, and O-79-18 MIL-L-23699 lubricating oils at 370°F using Federal Test Method Standard 791B Method 5307.1. The stressed oil samples which were characterized by viscosity (40°C) and total acid number measurements are described in Appendix D.

(2) Used MIL-L-7808 Oils Obtained from Engine Test Stand

The series of used MIL-L-7808 oil samples analyzed during this study were obtained from a normal operating test stand engine. The engine test was performed with a MIL-L-7808J lubricating oil. Physical property measurements and wear metal trending analyses performed on the series of stressed MIL-L-7808J oil samples to confirm the operating conditions of the

T63-A-5A turboshaft engine were normal during the test. The engine test conditions are listed in Table 108.

TABLE 108

ENGINE TEST CONDITIONS

Engine	Allison T63-A-5A Turboshaft
Test:	175 Hours
Bulk Oil Temperature:	250°F
Sampling Intervals:	10 hrs.

(3) Used MIL-L-7808 and MIL-L-23699 Oil Samples Obtained For Evaluating the RULLER Candidate

The series of used MIL-L-7808 and MIL-L-23699 oil samples analyzed during this study were obtained from abnormal operating Air Force gas turbine engines prior to Air Force Oil Analysis Program (OAP) recommended engine removals (Hits) or prior to engine failures (Failures) undetected by the Air Force OAP. Whenever possible, three to five successive samples were obtained from each abnormal operating engine.

Single used gas turbine oil samples were also obtained from Navy J60, F404 and J52 engines (MIL-L-23699 type) and from the transmissions, engines, and gearboxes of Army CH-47D, UH-1H and OV-1 aircraft.

(4) Used Gas Turbine Lubricating Oils Obtained from RULLER Field Test

The gas turbine lubricating oil samples used in the field test were MIL-L-7808 and MIL-L-23699 type oils and were obtained from operating

aircraft located at various Air Force bases.

f. Reductive Cyclic Technique

The RCV technique used by the RULLER is as follows:

Voltammetric Cycles:	10
Voltage Scan Rate:	6 V/sec
Voltage Scan Range:	-0.5 to 1.0 V (Referenced to Platinum Wire)
Sample Size:	100 µL (Positive Displacement Micropipettor)
Voltammetric Solution:	3 mL (750 ppm of Pyridazine)
Electrode System:	Glassy Carbon Working Electrode Platinum Wire Reference Electrode Platinum Wire Auxiliary Electrode
Analysis Container:	3 mL Polyester/Polyethylene Bag
Data Analysis:	Integrate area of reduction peaks

3. RESULTS AND DISCUSSION

a. Development of RULLER Candidate for MIL-L-7808 and MIL-L-23699 Lubricating Oils

(1) Introduction

The research performed to develop the RULLER candidate for used MIL-L-7808 and MIL-L-23699 lubricating oils was performed in two parts. In the first part, the SBV-IIe RULLER candidate was used to analyze laboratory stressed MIL-L-23699 lubricating oil samples. The results of the lubricating oil analyses were then used to ensure that the experimental parameters of the RCV technique were applicable to MIL-L-7808 and MIL-L-23699 oils. Cyclic voltammetric studies were performed on the fresh MIL-L-23699 oils to aid in the interpretation of the SBV-IIe RULLER candidate's results. Four qualified MIL-L-23699 oils were used for this study and are designated O-71-6, O-77-15, TEL-7004 and O-79-18. The MIL-L-23699 oils were stressed at 370°F using Federal Test Method Standard No. 791B Method 5307.1 and characterized by viscosity measurements and TAN measurements as described in Appendix D.

In the second part of the research, authentic used MIL-L-7808 and MIL-L-23699 oil samples were analyzed by the SBV-IIe RULLER candidate to further ensure that the experimental parameters of the RCV technique were applicable to the MIL-L-7808 and MIL-L-23699 formulations being used by the Air Force.

(2) Effects of Lubricating Oil Formulation on the SBV-IIe RULLER Candidate's RUL Evaluations

(a) Introduction

Although previous research[47] has shown that the results of the RCV technique can be used to monitor the RUL of used MIL-L-23699 lubricating oils and that the MIL-L-23699 oils of some T56 engines were being used past the ends of their estimated useful lives, the effects of the various MIL-L-23699 oil formulations on the RUL evaluations of the RCV technique had not been established. Therefore, the mathematical relationships among the RCV results and the RUL of different MIL-L-23699 oils were determined by analyzing fresh and stressed MIL-L-23699 oils with the RCV technique. The stressed MIL-L-23699 oils were stressed and characterized as described in Appendix D. The fresh MIL-L-23699 lubricating oils were also analyzed with cyclic voltammetry to aid in the interpretation of the RCV results for the MIL-L-23699 oils.

The cyclic voltammetric and RCV analyses of the fresh and stressed MIL-L-23699 oils were performed using a 100 µL oil sample diluted with 3 mL of voltammetric solution containing 750 ppm of pyridazine. The cyclic voltammetric analyses of the fresh MIL-L-23699 oils were performed using a 1 V/sec scan rate and a 1.2 to -0.4 V (Platinum wire reference) scan range and were displayed on a X-Y plotter. The RCV analyses of the fresh and

stressed MIL-L-23699 oils were performed using 6-10 V/sec scan rates and a 1.2 to -0.60 V (platinum wire reference) scan range and were displayed on the printer of the Apple IIe microcomputer system.

(b) Cyclic Voltammetric Analyses of the Fresh MIL-L-23699 Lubricating Oils

To initially study the effects of the MIL-L-23699 lubricating oils' formulations on the results of the RCV technique, cyclic voltammetric analyses of the fresh O-71-6, O-77-15, TEL-7004 and O-79-18 MIL-L-23699 lubricating oils were performed. The cyclic voltammograms of the fresh MIL-L-23699 lubricating oils are shown in Figures 132 and 133.

The cyclic voltammograms of the fresh O-71-6, O-77-15 and TEL-7004 oils shown in Figures 132 and 133 are very similar in shape and indicate that a new species (A in Figures 132 and 133) is electrooxidatively generated by successive voltammetric cycles. The reduction waves (B in Figures 132 and 133) produced by the fresh O-71-6, O-77-15 and TEL-7004 oils occur at 0.2 to 0.1 V (platinum reference electrode) and increase with successive voltammetric cycles. Similar cyclic voltammograms are produced by the fresh MIL-L-7808J lubricating oils.[47]

However, the cyclic voltammograms produced by the fresh O-79-18 MIL-L-23699 lubricating oil shown in Figure 133 are very different from the cyclic voltammograms produced by the other fresh MIL-L-23699 oils (Figures 132 and 133) and the fresh MIL-L-7808J lubricating oils.[47] The first voltammetric cycle of the O-79-18 oil produces oxidation waves at lower voltages than the oxidation waves produced by the other MIL-L-23699 oils in Figures 132 and 133. Also, the fresh O-79-18 oil produces several reduction waves of similar size in the 0.4 to -0.4 V range while the other fresh MIL-L-23699 lubricating oils produce one main reduction wave in the 0.2 to

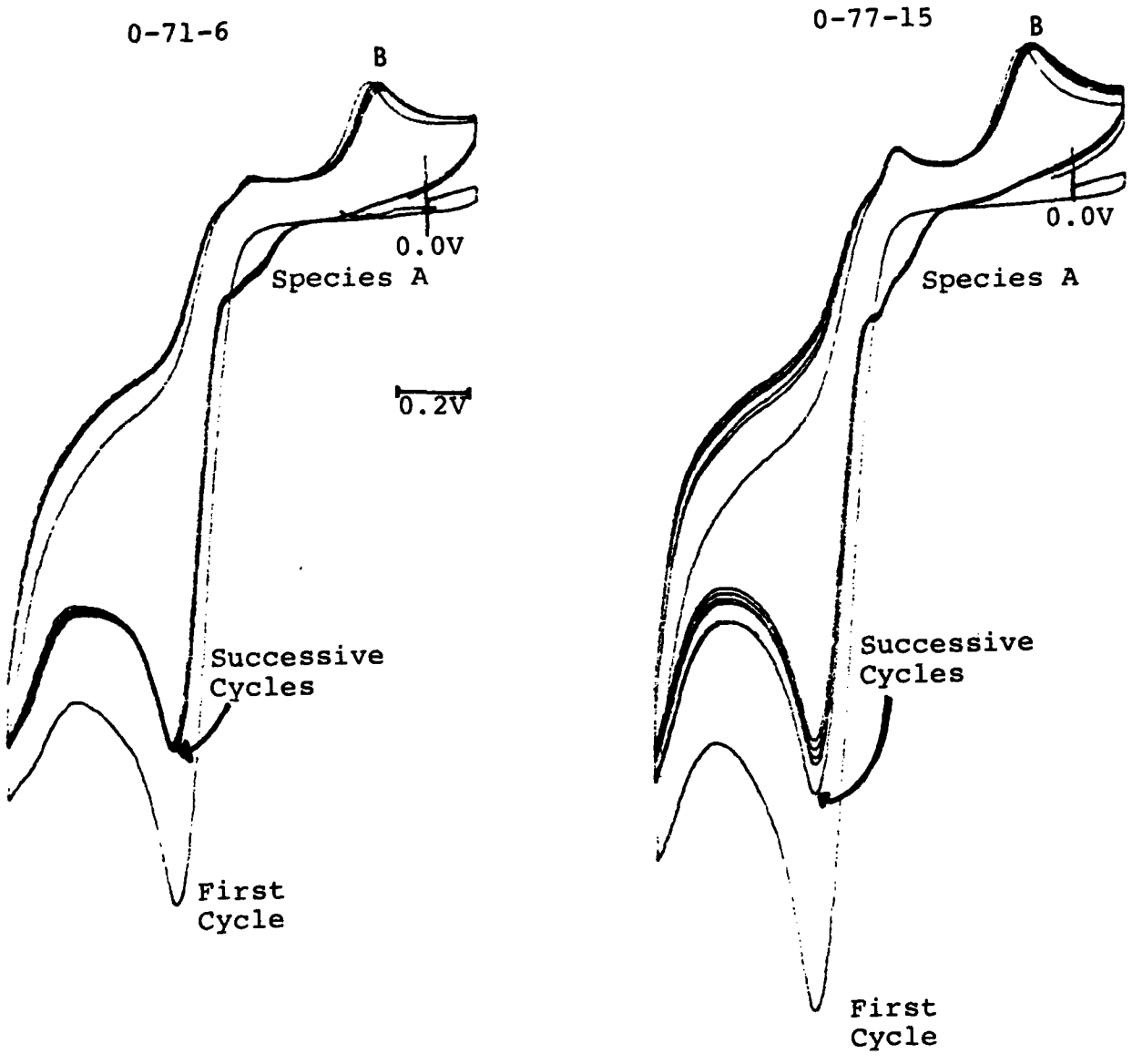

Figure 132. First and Successive Cyclic Voltammograms of the Fresh 0-71-6 and 0-77-15 MIL-L-23699 Lubricating Oils in the -0.4 to 1.2 V Scan Range

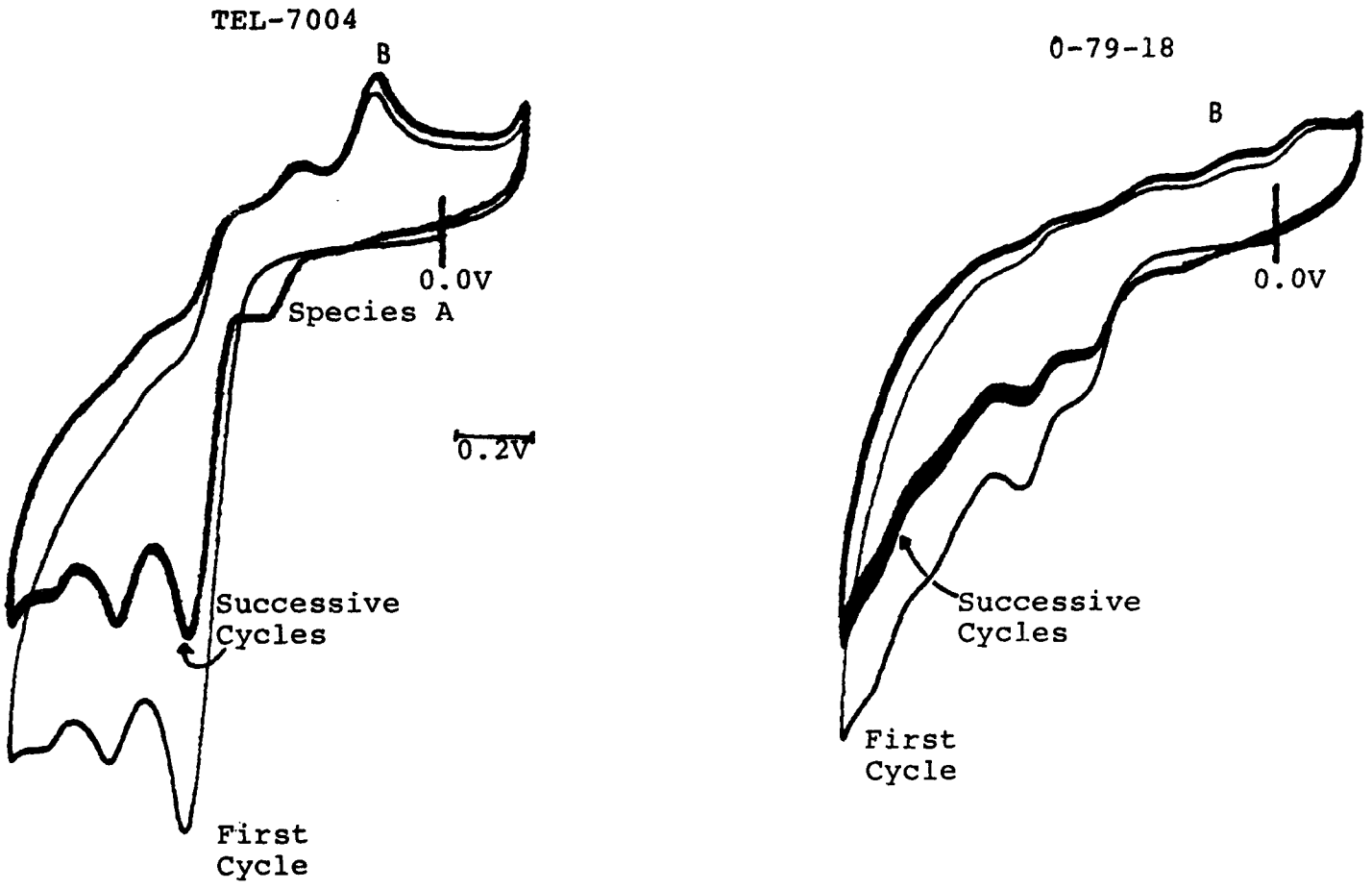

Figure 133. First and Successive Cyclic Voltammograms of the Fresh TEL-7004 and 0-79-18 MIL-L-23699 Lubricating Oils in the -0.4 to 1.2 V Scan Range

0.1 V range. For all of the fresh MIL-L-23699 lubricating oils, the reduction waves increase in height with successive cyclic voltammetric analyses.

(c) Optimization of the RCV Analyses for the MIL-L-23699 Lubricating Oils

Since the cyclic voltammograms demonstrate that the selected MIL-L-23699 lubricating oils contain a wide variety of antioxidant systems and the O-79-18 oil produces reduction waves at voltages different from those produced by the other MIL-L-23699 lubricating oils, the experimental parameters of the SBV-IIe RULLER candidate were modified to make the candidate suitable for use with the MIL-L-7808J and MIL-L-23699 lubricating oils.

An optimization study determined that a voltage scan rate of 6 V/sec and a voltage scan range of 1.0 to -0.5 V (platinum wire reference) would enable the RULLER candidate to determine the reduction wave height of a used oil sample regardless of its oil formulation. In addition to the voltage scan rate and range modifications, modifications were made in the data acquisition system of the RULLER candidate. Since the RULLER candidate used the maximum peak height of the reduction wave to calculate the RUL of the used oil sample, it would not detect the presence of multiple reduction waves. Therefore, for used oil samples which produce multiple reduction waves, the reduction wave height calculated RUL evaluation would be inaccurate. Consequently, the RUL determinations of the RULLER candidate are based on the total area of the reduction wave or waves produced by the used oil sample.

(d) Reduction Voltammograms Produced by the Fresh and Laboratory Stressed O-79-18 Oils

As demonstrated in previous research,[1] the additive package

of the fresh O-79-18 oil is different from the other MIL-L-23699 oils. Additionally, the O-79-18 oil contains high molecular weight compounds of unknown composition which deplete with stressing time, i.e., have antioxidant capacities, and produces a reduction wave at a lower voltage (Figure 133) than the other MIL-L-23699 oils.

To evaluate the effects of stressing time on the reduction waves produced by the O-79-18 oil, the O-79-18 oils stressed for 24, 48, 192, and 480 hours at 370°F were analyzed by the SBV-IIe RULLER candidate. The derivative of the reduction voltammograms were printed for this study to make the different reduction waves produced by the O-79-18 oil distinguishable. The reduction voltammograms for the fresh and the 24, 48, 192, and 480 hours stressed O-79-18 oils are shown in Figure 134.

The reduction voltammograms in Figure 134 show that the fresh O-79-18 oil produces a small broad wave from 0.3 to -0.2 V (platinum wire reference) and a large, sharper wave at -0.4 V. After only 24 hours of stressing at 370°F, the reduction wave at -0.4 V becomes negligible and the small broad wave produced in the 0.3 to -0.2 V region becomes two, large waves. The two large waves in the 0.3 to -0.2 V range then decrease in size with stressing time. The other MIL-L-23699 oils also produce reduction waves in the 0.3 to -0.2 V range (Figures 132 and 133).

These results indicate that upon thermal-oxidative stressing the fresh O-79-18 oil's antioxidant system rapidly produces a new antioxidant system which has a reduction potential similar to the antioxidant systems of the other MIL-L-23699 oils.

(e) Mathematical Relationships Among the SBV-IIe RULLER Candidate's Results and the RUL of the MIL-L-23699 Oils

To determine the mathematical relationships among the

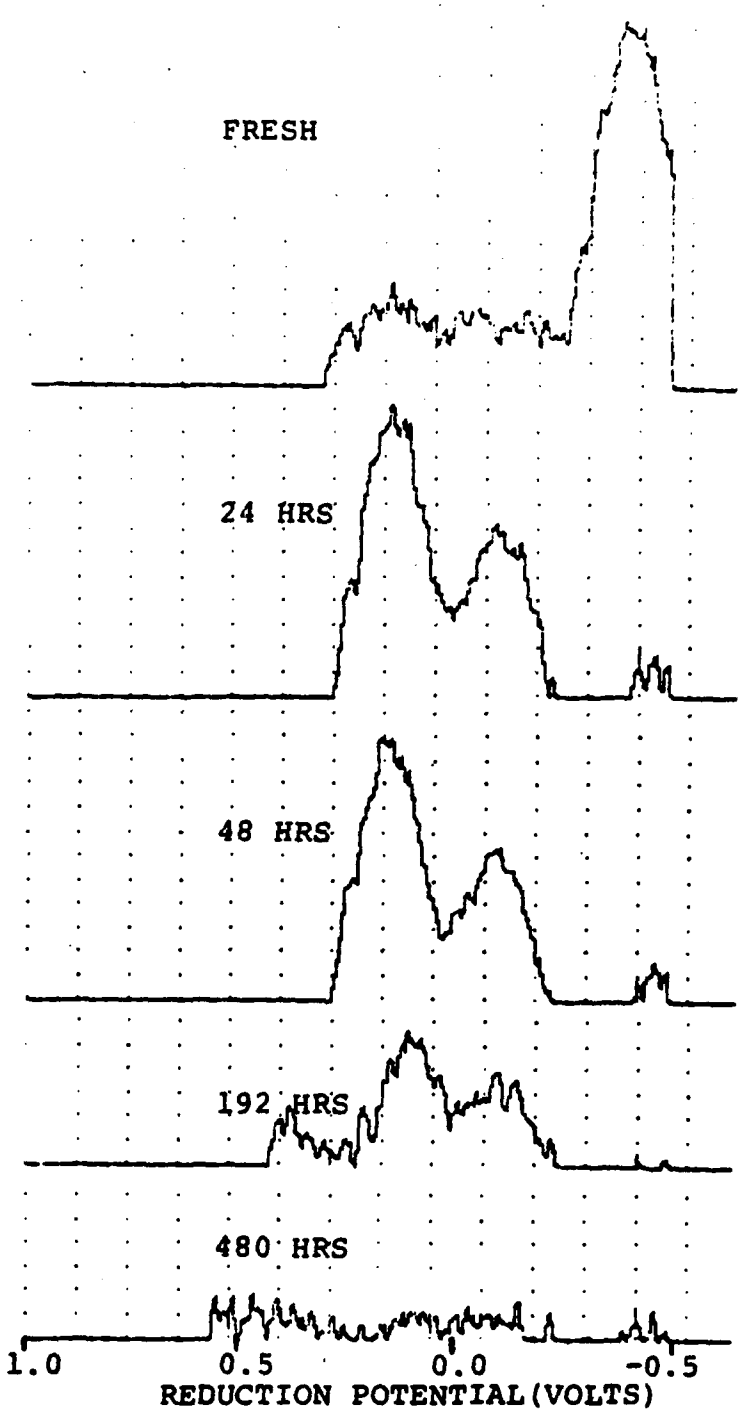

Figure 134. Reduction Voltammograms Produced by the Fresh and the 24, 48, 192 and 480 Hours Laboratory Stressed 0-79-18 011 Samples

SBV-IIe RULLER candidate's results and the RUL of the O-71-6, O-77-15, TEL-7004 and O-79-18 MIL-L-23699 oils, the fresh and stressed oil samples were analyzed by the SBV-IIe RULLER candidate using a -0.5 to 1.0 V scan range (platinum wire reference) and a 6 V/sec scan rate. The ln of the average (seventh to tenth reduction waves) reduction wave area was then plotted versus the hours of RUL at 370°F for each O-71-6, O-77-15, TEL-7004 and O-79-18 oil (useful lives = 336, 336, 456, and greater than 672 hours, respectively). The ln of the reduction wave area versus the hours of RUL at 370°F plots for the O-71-6, O-77-15, TEL-7004 and O-79-18 oils are shown in Figure 135. This figure demonstrates that the SBV-IIe RULLER candidate is capable of evaluating the RUL of used MIL-L-23699 oil samples. The ln plot of the reduction wave areas is linear for the TEL-7004 stressed oil samples with less than 350 hours of RUL and the TEL-7004 oil sample with 0 hours of RUL has a ln value of 0. However, the ln plots for the O-71-6, O-77-15 and O-79-18 oil samples are linear for the entire stressing periods of 336, 336, and 672 hours at 370°F, respectively, and the O-71-6, O-77-15 and O-79-18 oil samples with 0 hours of RUL have a ln value of 0. The assignment of 672 hours of useful life at 370°F to the fresh O-79-18 oil is reasonable since the antioxidant concentrations of the 648 hour stressed O-79-18 oil is below the minimum detection limits of gas chromatography.

To verify the formula independence of the RUL evaluations of the SBV-IIe RULLER candidate, the fresh and stressed TEL-4004 MIL-L-7808J oils were analyzed by the SBV-IIe RULLER candidate using the voltage range of 1.0 to -0.5 V and the scan rate of 6 V/sec. The ln of the average reduction wave area versus hours of RUL at 370°F plot produced by the SBV-IIe RULLER candidate for the TEL-4004 oils is included in Figure 135 and shown to be linear and the TEL-4004 oil with 0 hours of RUL has a ln value of 0, same as

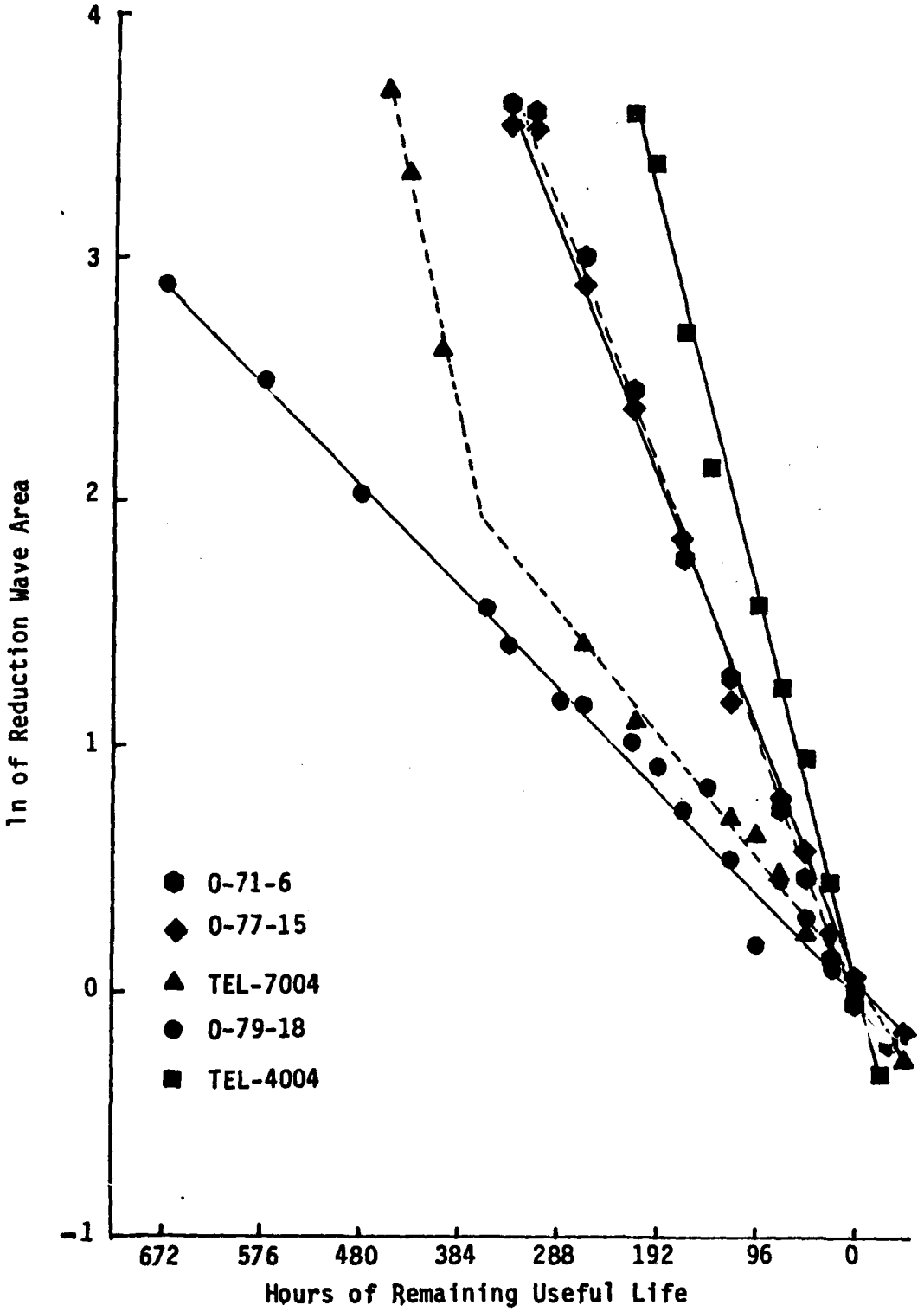

Figure 135. Plots of the ln of the Reduction Wave Area Versus Hours of Remaining Useful Life at 370°F for the Fresh and Laboratory Stressed 0-71-6, 0-77-15, TEL-7004, 0-79-18 (MIL-L-23699) and TEL-4004 (MIL-L-7808) Oils

the MIL-L-23699 oils with 0 hours of RUL.

(f) Summary

These results demonstrate that the SBV-IIe RULLER candidate is capable of evaluating the RUL of different MIL-L-7808 and MIL-L-23699 oils regardless of formulation. The use of area based RUL evaluations improves the accuracy and formula independence of the SBV-IIe RULLER candidate's results in comparison to the height based RUL evaluations. The results of this study also showed that the antioxidant system of O-79-18 MIL-L-23699 oil undergoes dramatic changes during the initial stages of thermal oxidative stressing.

(3) SBV-IIe RULLER Candidate Evaluations of Authentic Used MIL-L-7808 and MIL-L-23699 Oil Samples

(a) Introduction

To evaluate the suitability of the SBV-IIe RULLER candidate for use by the Air Force, series of authentic used MIL-L-7808 and MIL-L-23699 oil samples obtained from normal and abnormal operating engines were analyzed. This exercise was performed to determine if trending analyses of the SBV-IIe RULLER candidate's results could be correlated with the SOAP wear metal results so that predicting incipient engine failures could be improved. Three types of used oil samples were studied:

1) Failures - Used oil samples obtained prior to and after an engine failure which occurred undetected by the Air Force OAP

2) Hits - Used oil samples obtained prior to and after an Air Force OAP recommended engine removal. Abnormal wear confirmed by maintenance inspection

3) Routines - Used oil samples obtained from normal operating engine. Normal wear confirmed by maintenance inspection.

To confirm the presence of normal and abnormal operating

conditions for the studied sample series, particle size distribution and particle composition analyses of the wear debris in the used oil samples were performed using the multichannel capacitor system modified A/E35U-1 atomic emission spectrometer.[46] Except for the time resolution of the spectrometer's photomultiplier outputs, normal OAP operating procedures[45] were followed.

For this study, the fresh TEL-4006 MIL-L-7008J oil and a stressed TEL-4004 MIL-L-7808J oil with 0 hours of RUL were analyzed and their ln of reduction wave areas assigned the values of 100 and 0% RUL, respectively.

(b) Failure Oil Sample Series Analyses

To determine if there is a relationship between the RUL of an oil sample and the severe wear mode which results in engine failure, the F50A-D, F51A-D and F53A-D sample series obtained prior to and after T56 engine failures (MIL-L-23699 oils) were analyzed. The percent RUL versus operating time prior to engine failure plots are shown in Figure 136.

Figure 136 shows that for the F51A-D sample series, the percent RUL of the obtained samples undergoes a rapid decrease prior to the engine failure. In contrast to the F51A-D sample series, the percent RUL values of the F50A-D and F53A-D samples undergo very small changes prior to the engine failures. However, the percent values RUL of the F51A-D and F53A-D series are similar prior to the engine failures. The increases in the percent RUL of the F51A-D and F53A-D series indicate that oil dilutions were performed even though no dilutions were recorded by Air Force OAP personnel.

To determine if the engines were experiencing severe wear modes prior to engine failure, particle size distribution and particle composition analyzes of the wear debris present in the F50A-D, F51A-D and

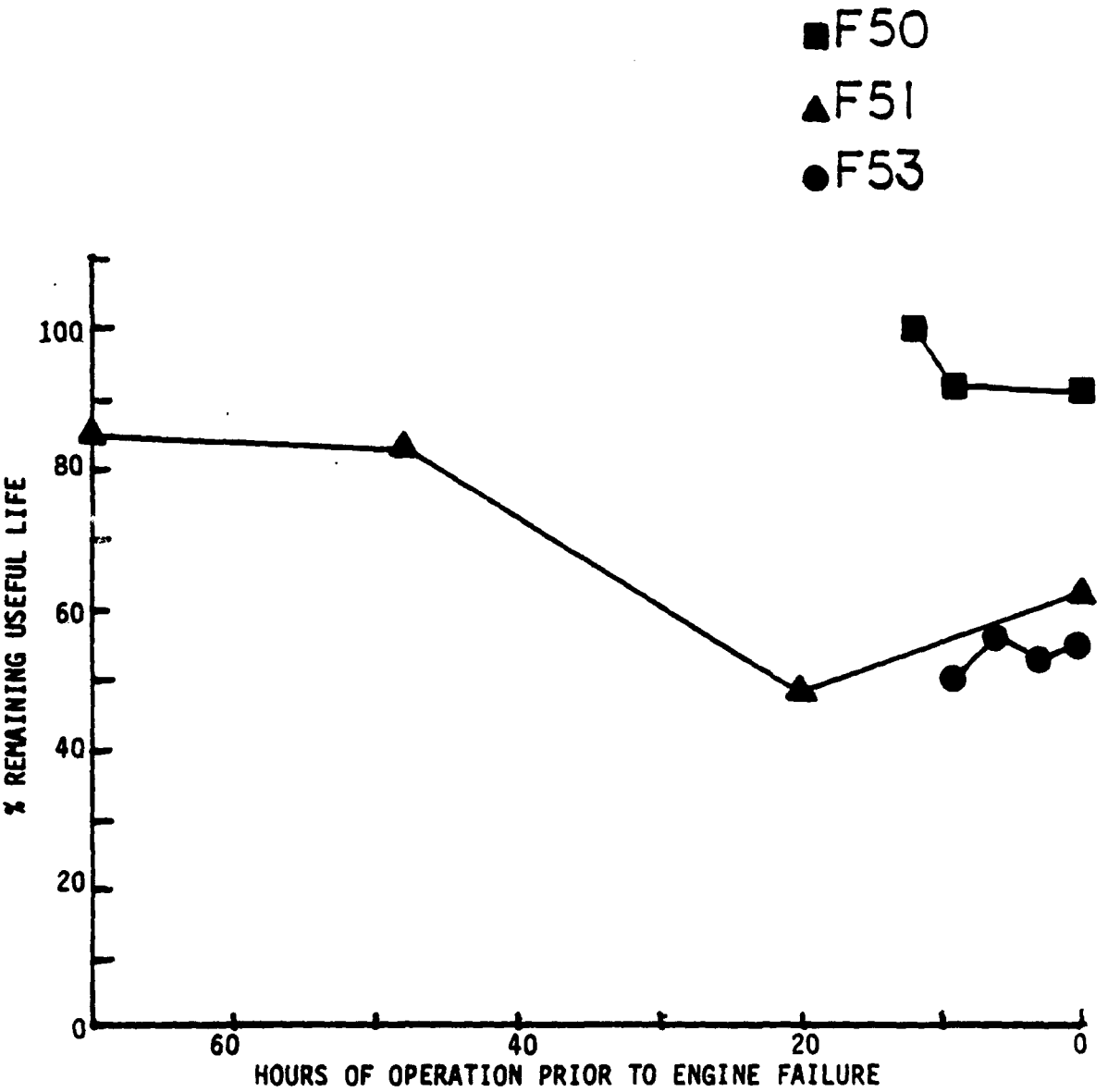

Figure 136. Plots of the % Remaining Useful Life Versus Hours of Operation Prior to Engine Failure for the Used MIL-L-23699 (F50, F51 and F53) Oil Sample Series

F53A-D sample series were determined using the multichannel capacitor system modified A/E35U-1 spectrometer. The difference plots of the voltage buildups produced by the photomultiplier outputs for the monitored channels (Fe, Cu, Ag, Ni) are shown in Figures 137-139 for the F50A-D, F51A-D and F53A-D series, respectively. The difference plots of the voltage buildups produced by the photomultiplier outputs for the Fe, Ag, Ni, and Cu channels are shown in Figure 140 for a C12-10 Conostan standard prepared in MIL-L-23699 oil.

For every Failure sample series, the difference plots of the monitored channels contain numerous peaks which are much larger than those in the difference plots produced by the C12-10 standard. Through calibration with different metal powder suspensions, it was determined that the wear debris in the Failure samples were in the -8 micron particle size range. The corresponding peaks in the Fe, Ag, Ni, and Cu difference plots for the F50A-D and F53A-D sample series (P in Figure 137 and 139 respectively) and in the Fe, Ni, and Cu difference plots for the F51A-D sample series (P in Figure 138) indicate that multicomponent wear debris particles (Fe, Ag, Ni, Cu; Fe, Ni, Cu; Fe Cu; etc.) are present in the oil samples.

The difference plots of the F50, F51, and F53 sample series indicate that the engines may have been experiencing severe wear modes several samples prior to the engine failures.

The percent RUL evaluations presented in Figure 136 and the particle size distribution and particle composition analyses shown in Figure 138 are in good agreement for the F51A-D and F53A-D sample series since both techniques may be indicating abnormal operating conditions are occurring prior to engine failure. For the F50A-D sample series, the particle size distribution and particle composition analyses may be indicating that severe

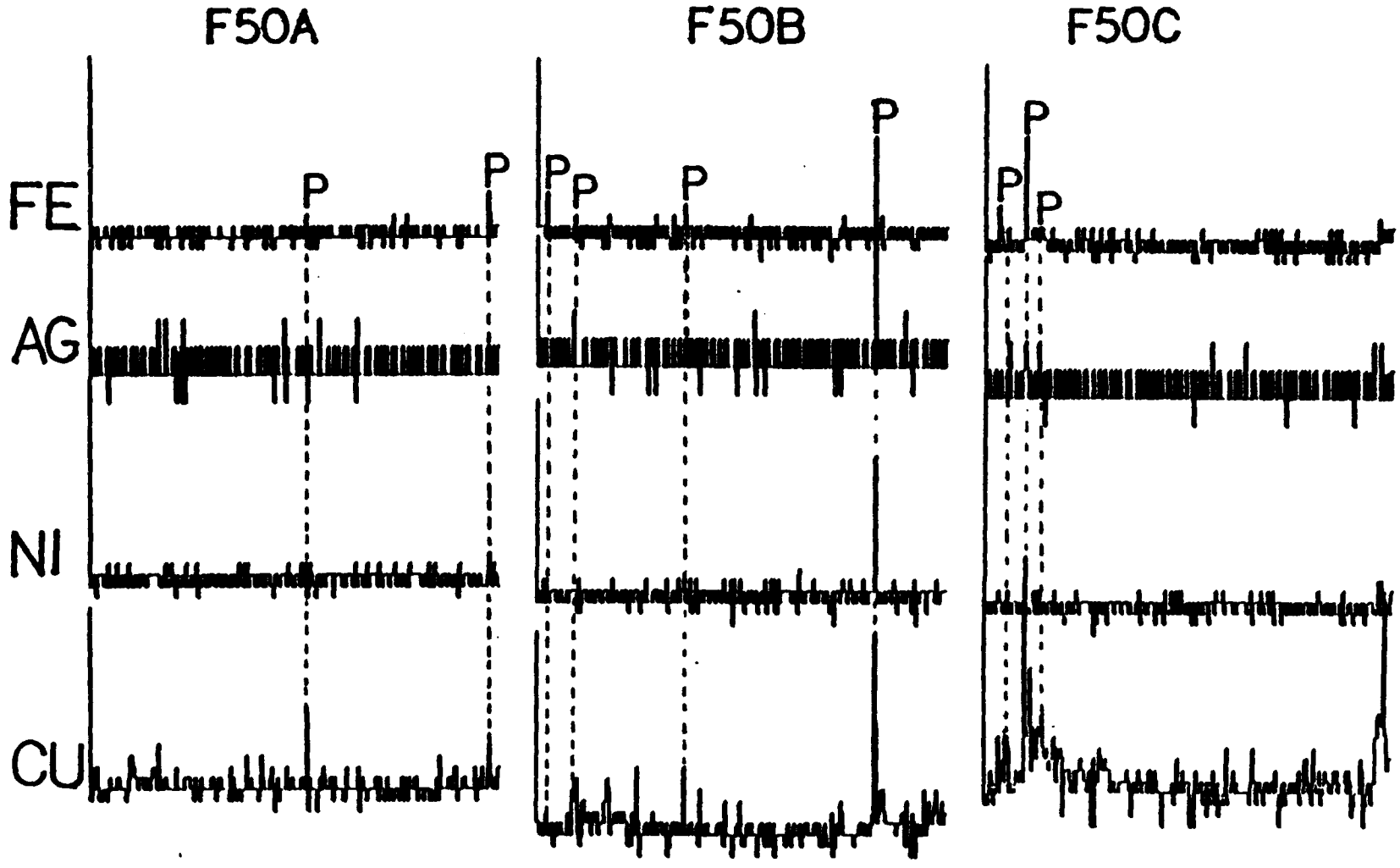

Figure 137. Example Difference Plots (2 Sec) of the Multichannel Capacitor System Connected to the Fe, Ag, Ni and Cu Channels for the F50A-C Used MIL-L-23699 Oil Samples Produced by the Direct Analysis Method on the A/E35U-1 Spectrometer

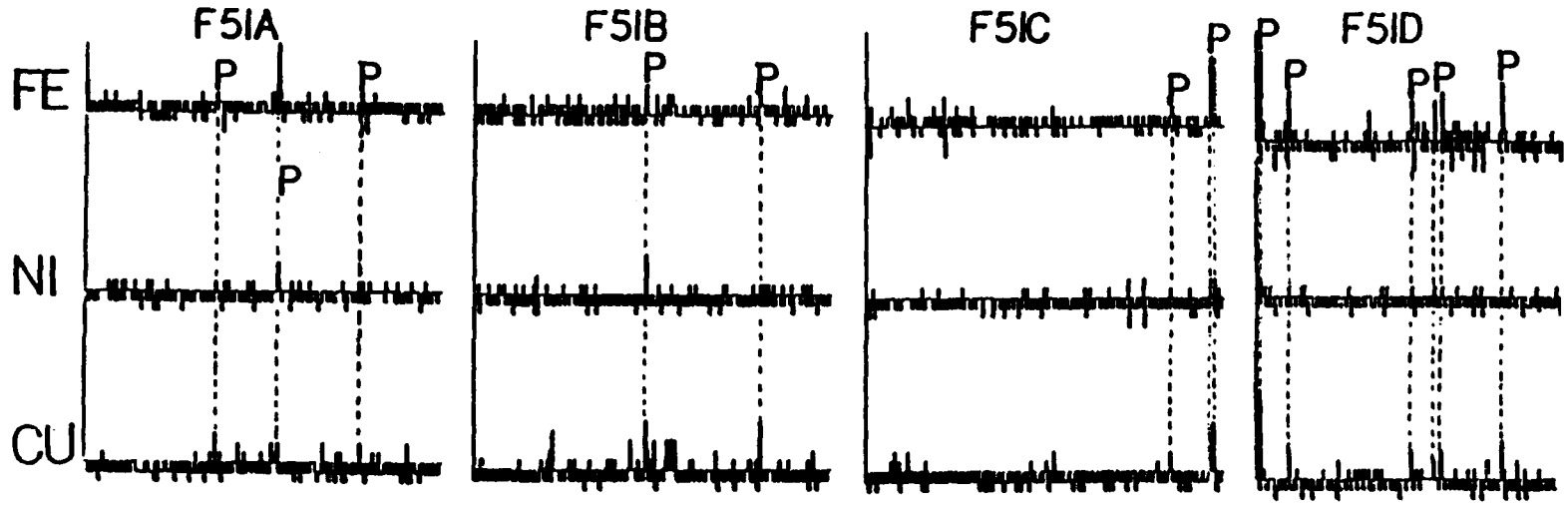

Figure 138. Example Difference Plots (2 Sec) of the Multichannel Capacitor System Connected to the Fe, Ni and Cu Channels for the F51A-D Used MIL-L-23699 Oil Samples Produced by the Direct Analysis Method on the A/E35U-1 Spectrometer

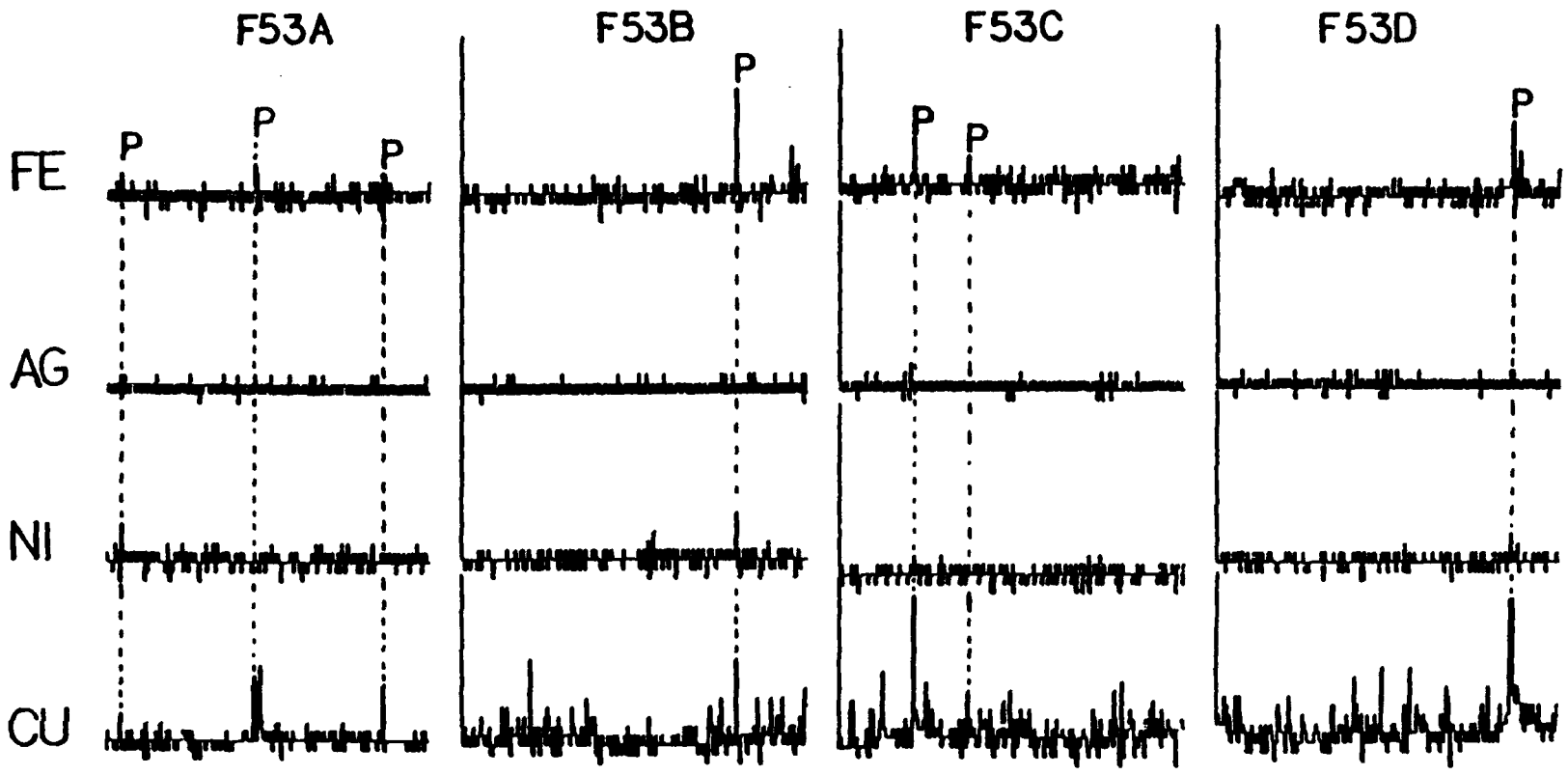

Figure 139. Example Difference Plots (2 Sec) of the Multichannel Capacitor System Connected to the Fe, Ag, Ni and Cu Channels for the F53A-D Used MIL-L-23699 Oil Samples Produced by the Direct Analysis Method on the A/E35U-1 Spectrometer

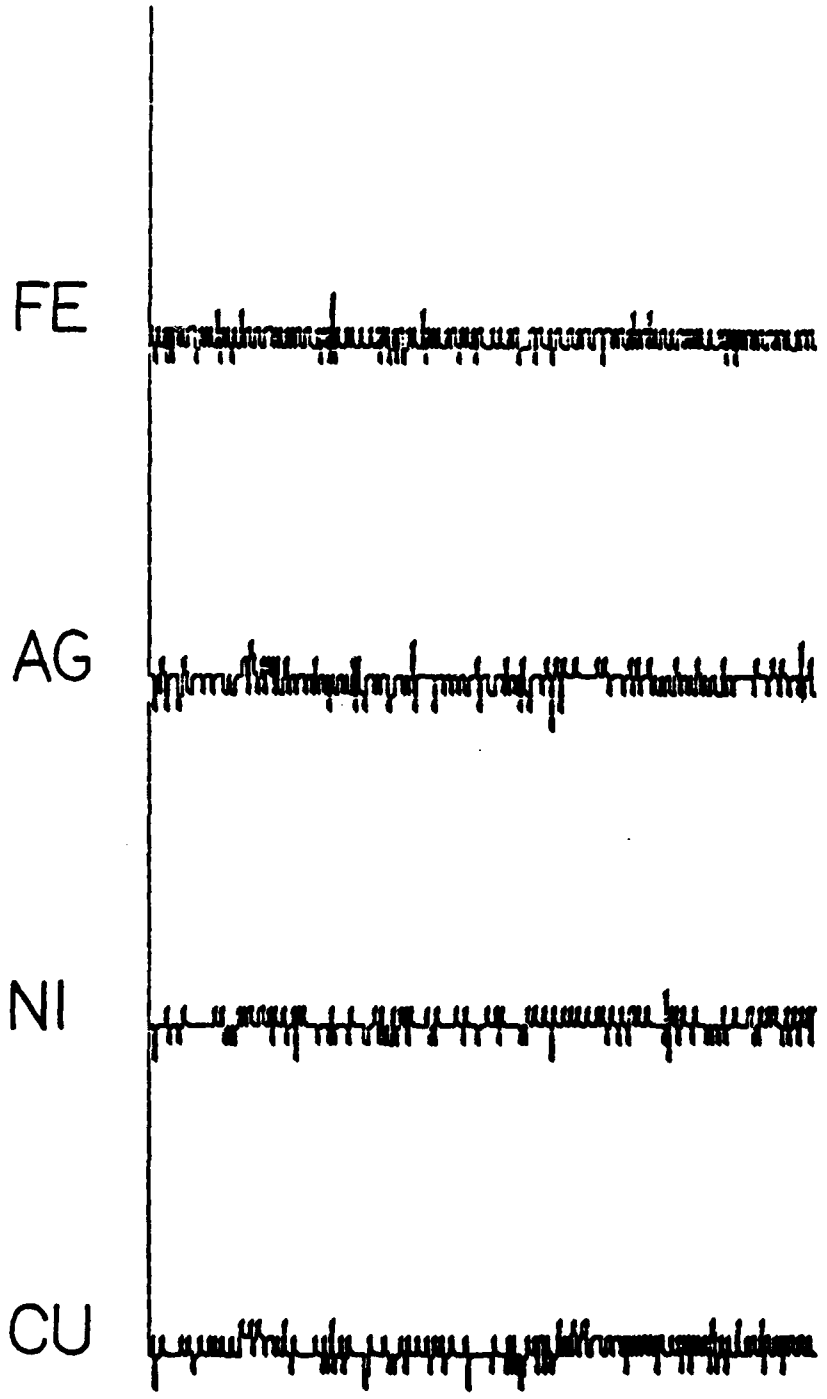

Figure 140. Example Difference Plots (2 Sec) of the Multichannel Capacitor System Connected to the Fe, Ag, Ni and Cu Channels for the C12-10 Standard Produced by the Direct Analysis Method on the A/E35U-1 Spectrometer

wear modes are occurring while the percent RUL evaluations are indicative of a normal wear mode.

(c) Hit Oil Sample Series Analyses

To determine if there is a relationship between the RUL of an oil sample and the moderate wear modes causing OAP recommended engine removals, the H95A-C, H97A-E, H98A-D, H99A-D and H100A-D oil sample series obtained prior to OAP recommended engine removal were analyzed. The H95, H97 and H98 series are used MIL-L-23699 oil samples and the H99 and H100 series are used MIL-L-7808 oil samples. The percent RUL versus engine operating time (hours) prior to engine removal plots for the Hit sample series are shown in Figure 141.

The percent RUL versus operating time plots show that two situations are occurring for the Hit sample series. For the H95A-C and H97A-E sample series, the oils have 0% RUL several samples prior to engine removal. Whereas the percent RUL plots of the H98A-D, H99A-D and H100A-D sample series undergo a rapid decrease prior to the engine removal. In fact, the H98D sample obtained after engine removal has 0% RUL.

To determine if the engines were experiencing abnormal wear prior to engine removal, particle size distribution and particle composition analyses of the wear debris present in the Hit sample series were determined using the multichannel capacitor system modified A/E35U-1 spectrometer. The difference plots of the voltage buildups produced by the photomultiplier outputs for the Fe and Cu channels are shown in Figures 142-146 for the H95A-C, H97A-E, H98A-D, H99A-D and H100A-D series, respectively. No peaks were observed in the difference plots of the Ag and Ni channels, and consequently, the Ag and Ni channels' difference plots were not included in Figures 142-146.

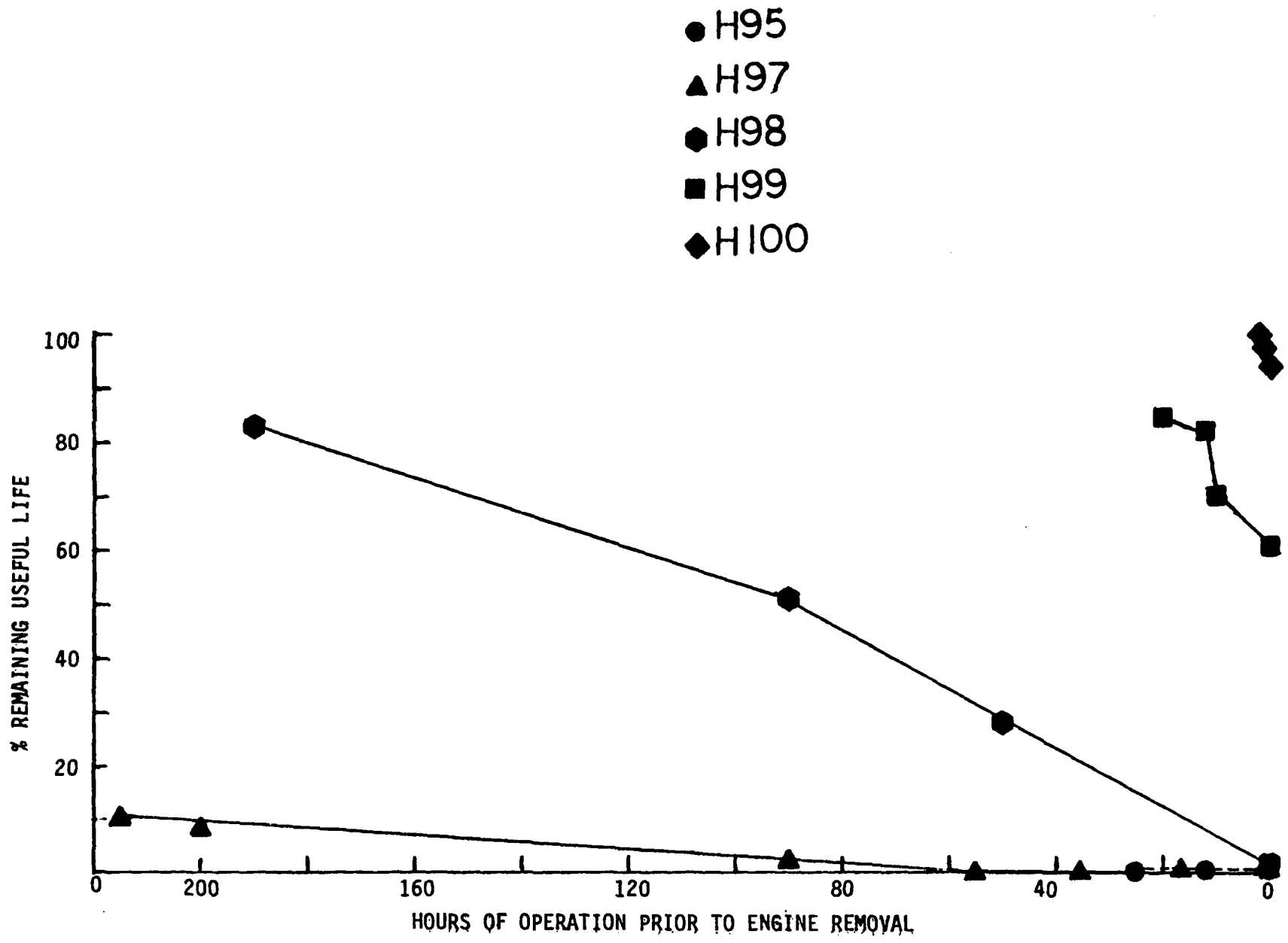

Figure 141. Plots of the % Remaining Useful Life Versus Hours of Operation Prior to Engine Removal (Air Force OAP Recommended) for the Used MIL-L-7808 (H99 and H100) and MIL-L-23699 (H95, H97 and H98) Oil Sample Series

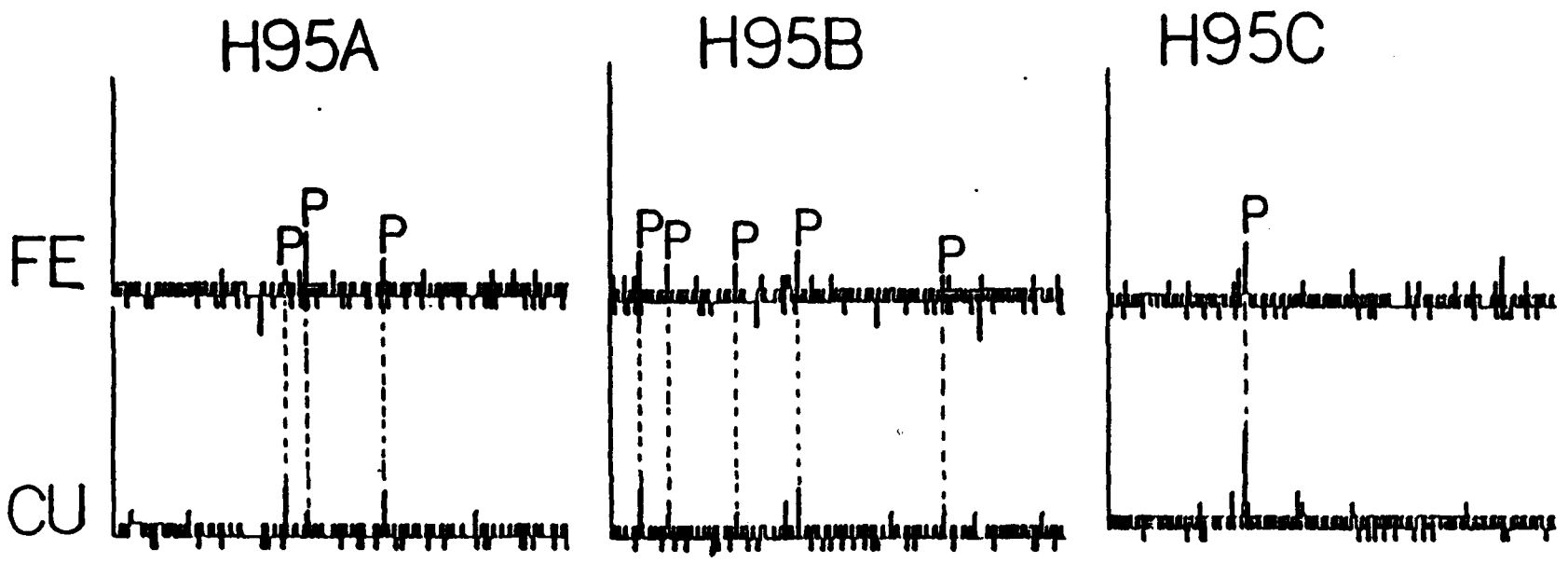

Figure 142. Example Difference Plots (2 Sec) of the Multichannel Capacitor System Connected to the Fe and Cu Channels for the H95A-C Used MIL-L-23699 Oil Samples Produced by the Direct Analysis Method on the A/E35U-1 Spectrometer

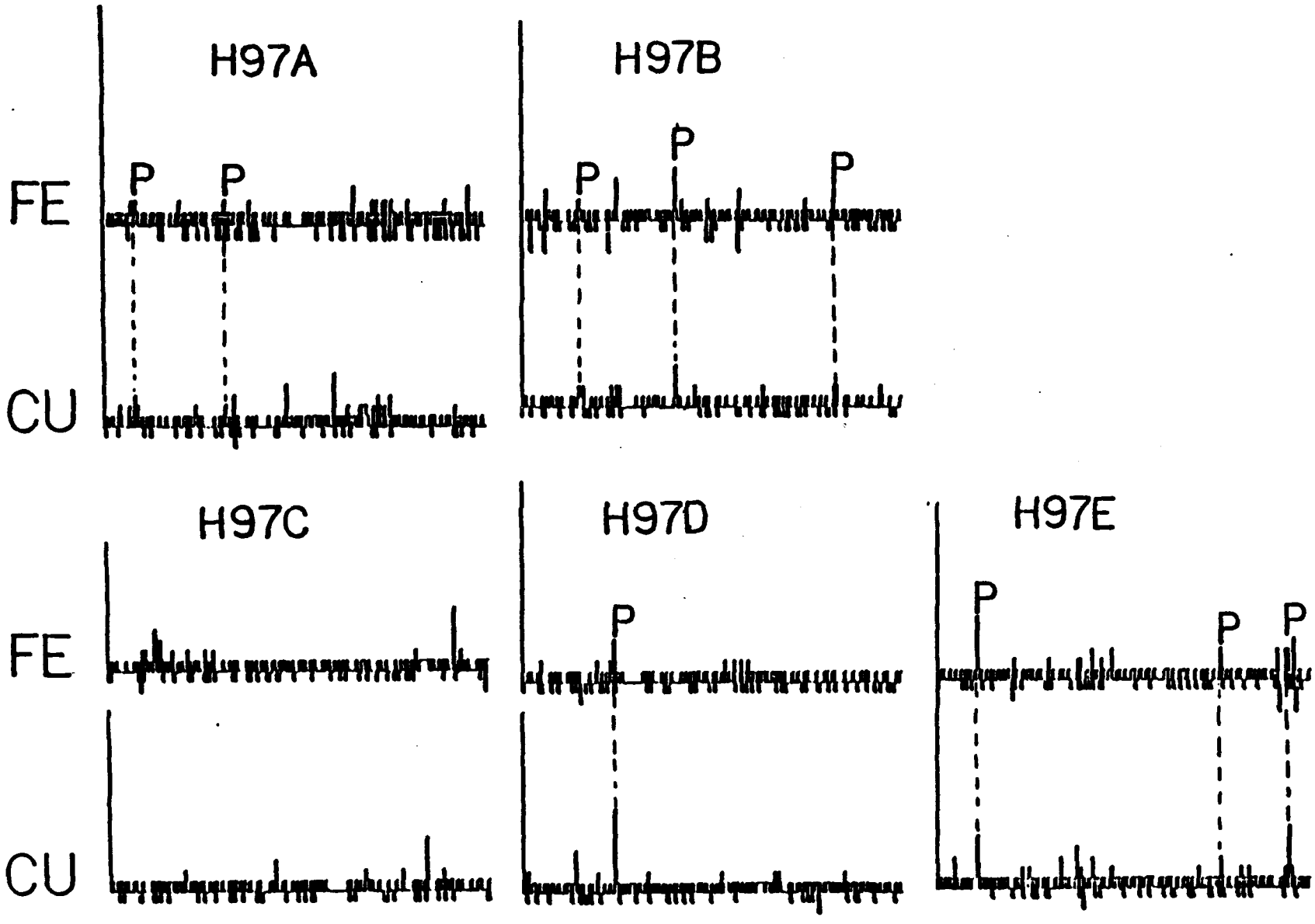

Figure 143. Example Difference Plots (2 Sec) of the Multichannel Capacitor System Connected to the Fe and Cu Channels for the H97A-D Used MIL-L-23699 Oil Samples Produced by the Direct Analysis Method on the A/E35U-1 Spectrometer

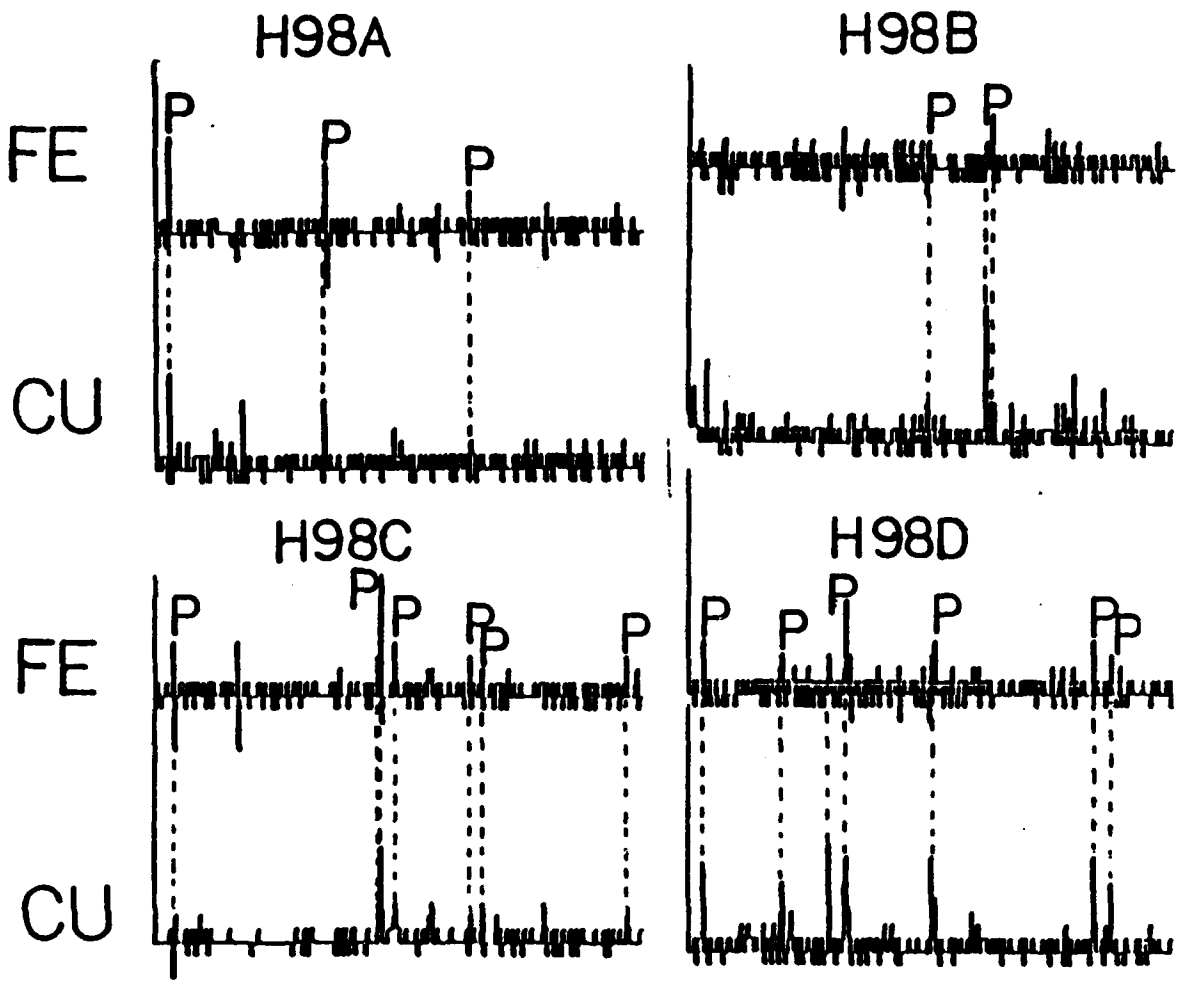

Figure 144. Example Difference Plots (2 Sec) of the Multichannel Capacitor System Connected to the Fe and Cu Channels for the H98A-D Used MIL-L-23699 Oil Samples Produced by the Direct Analysis Method on the A/E35U-1 Spectrometer

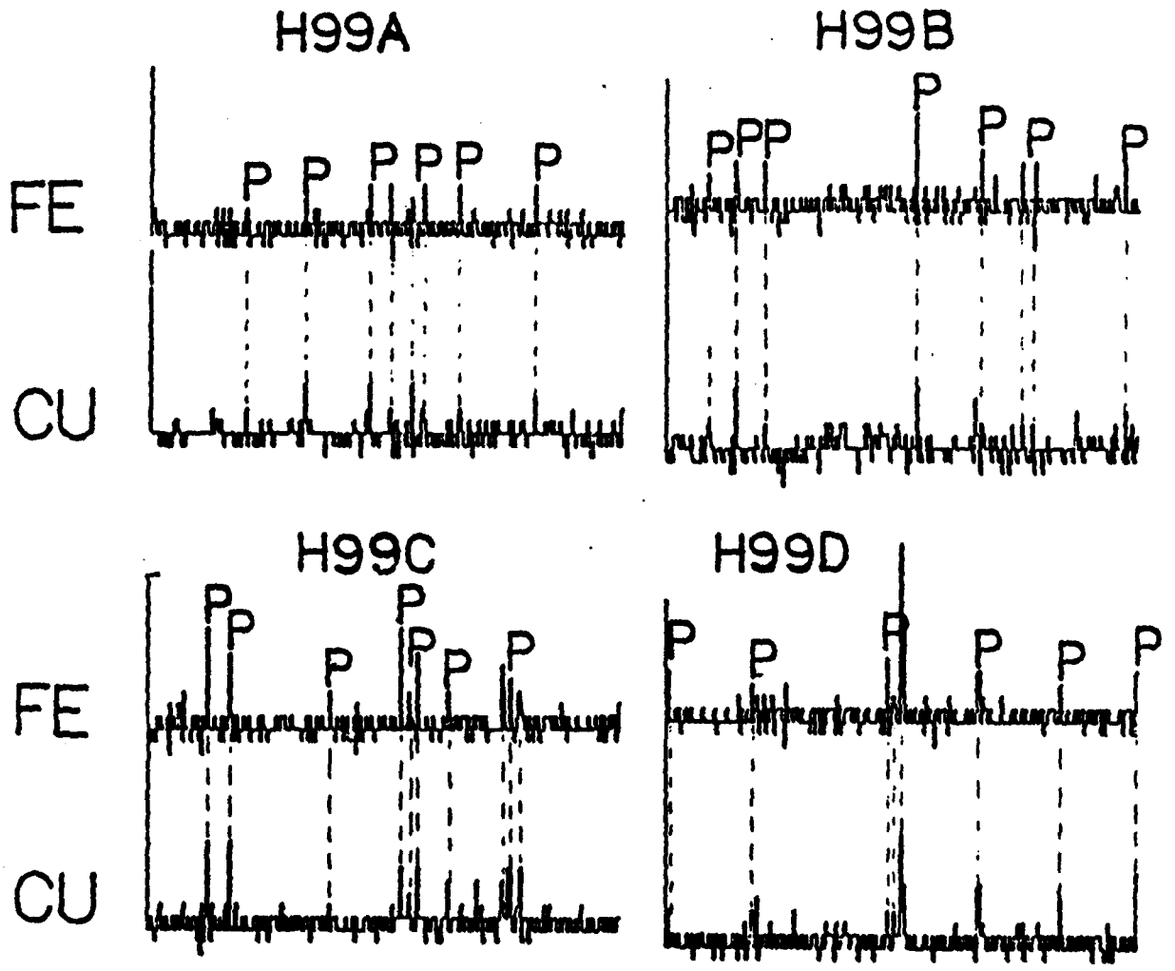

Figure 145. Example Difference Plots (2 Sec) of the Multichannel Capacitor System Connected to the Fe and Cu Channels for the H99A-D Used MIL-L-7808 Oil Samples Produced by the Direct Analysis Method on the A/E35U-1 Spectrometer

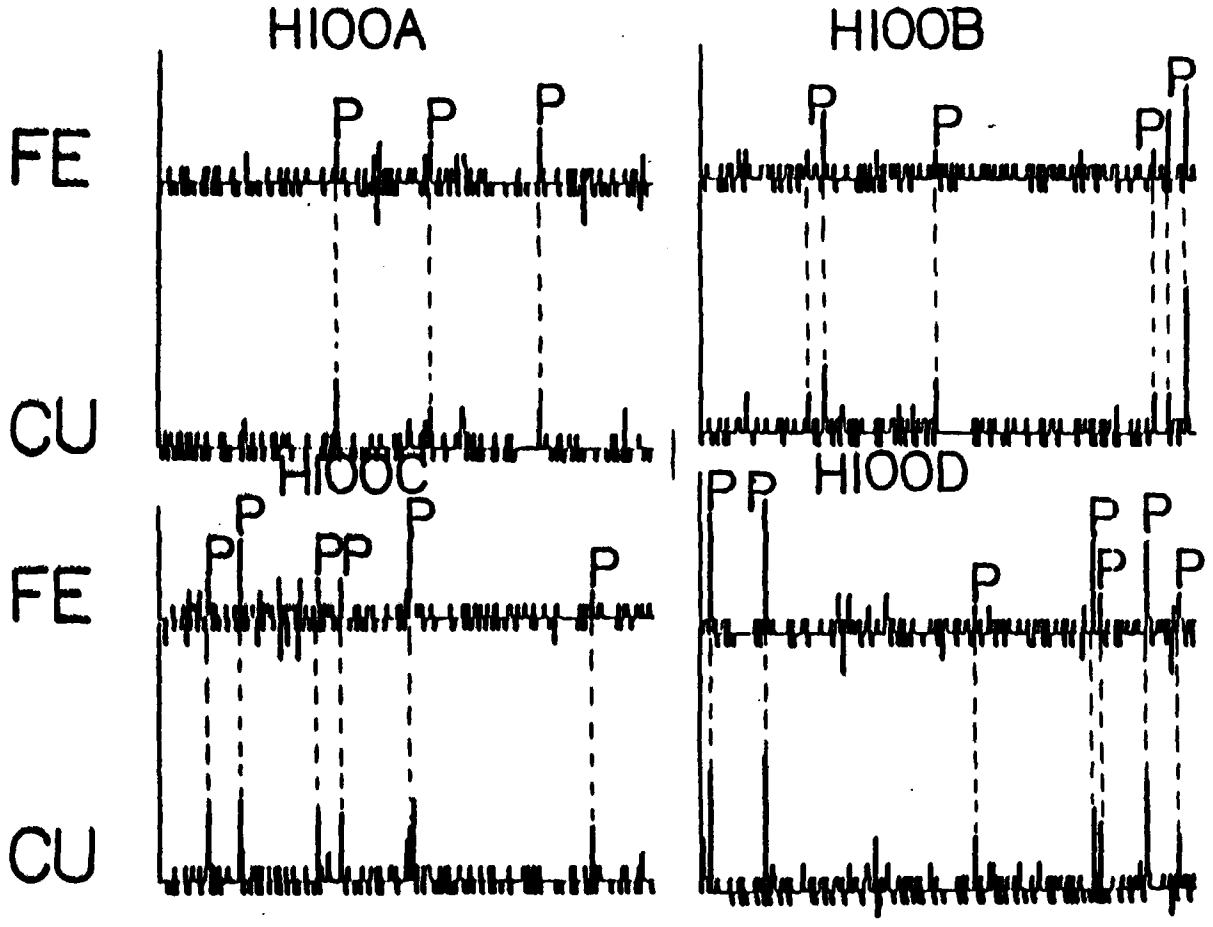

Figure 146. Example Difference Plots (2 Sec) of the Multichannel Capacitor System Connected to the Fe and Cu Channels for the H100A-D Used MIL-L-7808 Oil Samples Produced by the Direct Analysis Method on the A/E35U-1 Spectrometer

For every Hit sample series, the difference plots of the Fe and Cu channels contain numerous peaks (P in Figures 142-146) which are much larger than those in the difference plots produced by the C12-10 standard (Figure 140). For the H95 and H97 series in Figures 142 and 143, respectively, the wear debris were estimated to be in the -3 micron size range and for the H98, H99, and H100 sample series in Figures 144-146, respectively, the wear debris were estimated to be in the -8 micron size range (similar to Failure samples in Figures 137-138). The corresponding and noncorresponding peaks in the Fe and Cu difference plots for the Hit sample series indicate that the wear debris in the Hit samples are Fe and Cu, Fe, or Cu containing particles.

The difference plots of the Hit sample series indicate that the engines were experiencing moderate to severe wear modes several samples prior to the engine removals. The percent RUL data for the same samples presented in Figure 141 also decreased at a significant rate. The data seem to indicate that there is a relationship between some type of wear and the rate of lube degradation.

(d) Routine Oil Sample Series Analyses

To determine the relationship between the RUL of an oil sample and the normal operating conditions of an engine, a series of used MIL-L-7808 oil samples obtained from a normal operating T56-A-5A turboshaft engine test stand was analyzed. The percent RUL versus hours of operation plot for the used MIL-L-7808 oil sample series is shown in Figure 147. The plots of the viscosity (40^{o}C) and total acid number measurements versus hours of operation for the series of used MIL-L-7808 oil samples are also included.

The percent RUL versus hours of operation plot shows that for a normal operating engine, the percent RUL of the obtained samples

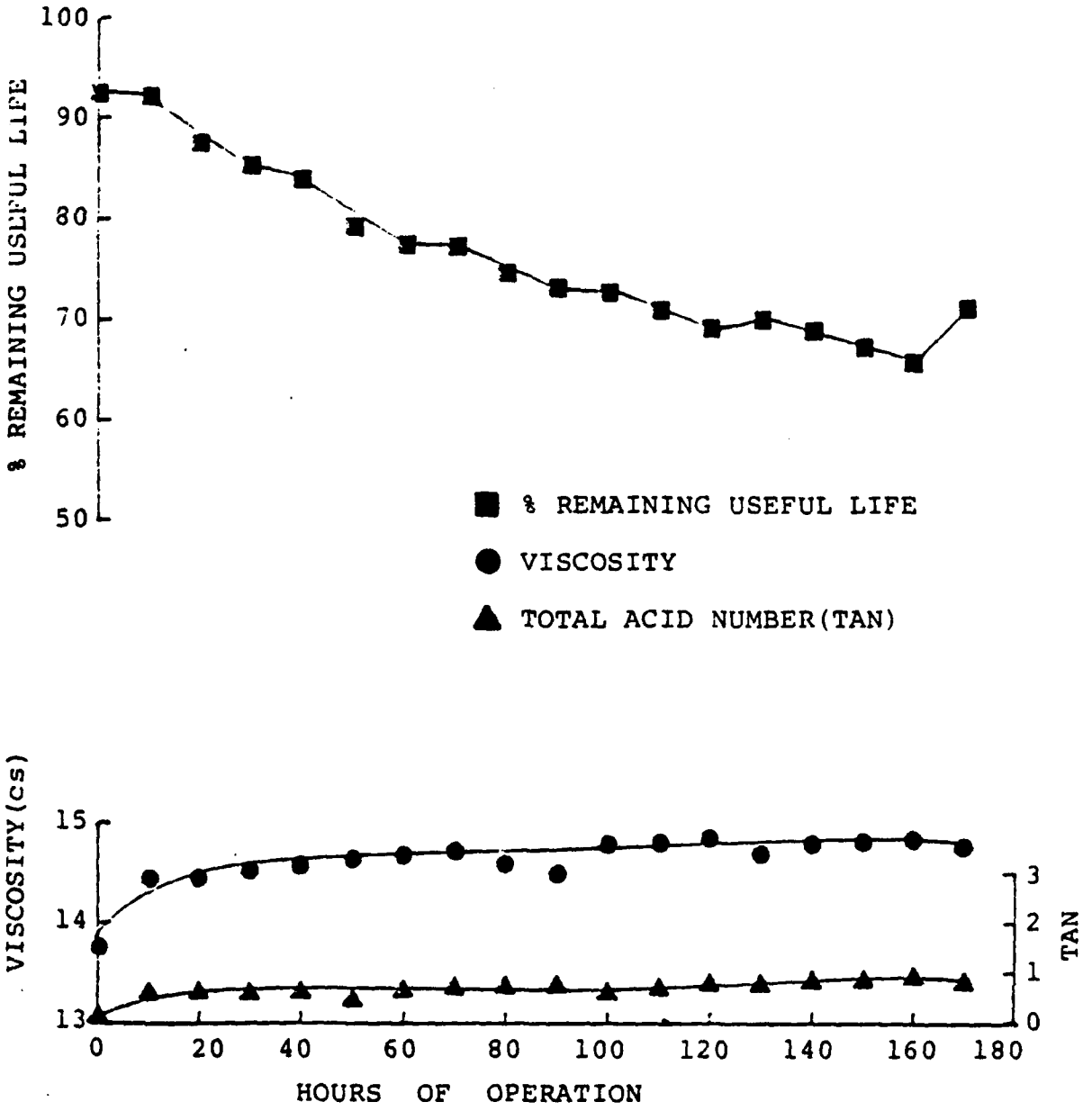

Figure 147. Plots of the Percent Remaining Useful Life, Viscosity (40°C) and Total Acid Number (TAN) Measurements Versus the Hours of Operation for the MIL-L-7808J Oil Samples Obtained from a Normal Operating Test Stand Engine

decrease at a moderate, fairly constant rate during the testing period of 175 hours. The inflection points present in the percent RUL plot (especially at 175 hours) are indicative of oil additions. The viscosity and total acid number plots are fairly level throughout the test confirming that the oil's useful life had not been exceeded.

To further confirm the presence of normal operating conditions for the studied sample series, particle size distribution and particle composition analyses of the wear debris in the used oil samples were performed using the multichannel capacitor system modified A/E35U-1 emission spectrometer. The difference plots of the voltage buildups produced by the photomultiplier outputs for the Fe and Cu channels are shown in Figure 148 for the 10, 60, 110, and 170 hours stressed oil samples. The difference plots of the Ag and Ni channels did not contain peaks and were not included in Figure 148.

For all of the oil samples, regardless of sampling time, no Fe containing wear metal particles were detected (no peaks in difference plots in Figure 148). In contrast to the Fe difference plots, the Cu difference plots show that the particle size distribution of the Cu containing particles increased with test time. The Cu containing particles in the 170 hour sample are similar in size to the Cu containing particles in the Hit samples. Unfortunately, the significance of the Cu containing wear debris could not be determined from the limited information provided on these samples.

(e) Summary

The results of this study indicate that there may be a relationship between the percent RUL evaluations of the SBV-IIe candidate and the wear mode experienced by the sampled engine. In numerous cases, the

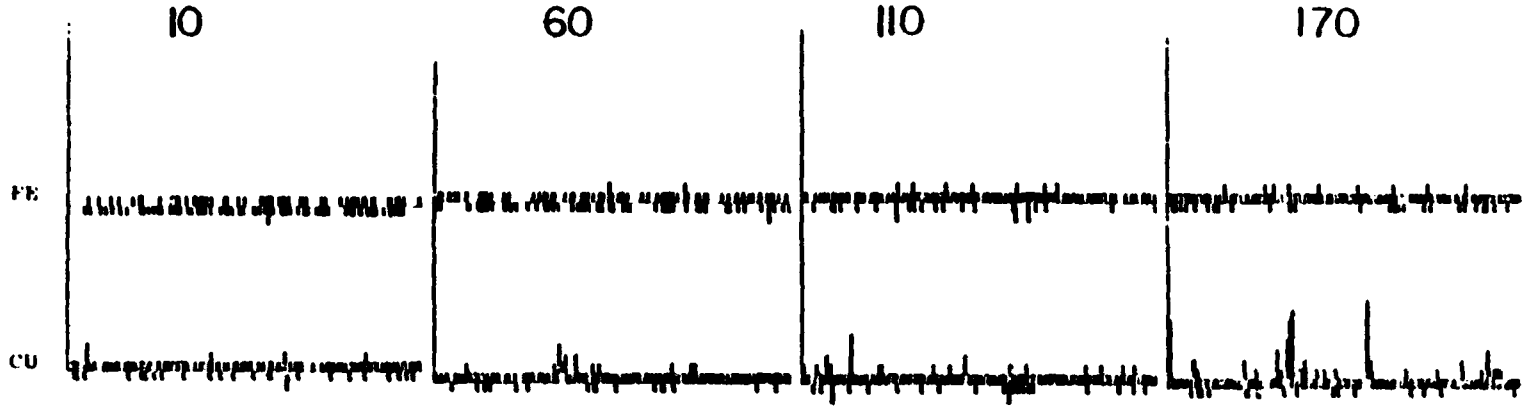

Figure 148. Example Difference Plots (2 Sec) of the Multichannel Capacitor System Connected to the Fe and Cu Channels for the 10, 60, 110 and 170 Hours Stressed (Test Stand Engine) MIL-L-7808 Oil Samples Produced by the Direct Analysis Method on the A/E35U-1 Spectrometer

percent RUL plots decrease at a significant rate several samples prior to engine failure or removal regardless of the oil formulation, MIL-L-7808 or MIL-L-23699. In the cases of the H95 and H97 sample series, the used oil samples had 0% RUL several hours of operation prior to engine removal.

In contrast to the Failure and Hit samples, the percent RUL plots decreased at a moderate, fairly constant rate for the Routine oil samples obtained from a normal operating engine.

Whether the moderate to severe wear modes were the cause or were caused by the significant decreases in the samples' RUL could not be established at this time. However, in the case of the F53 sample series, the severe wear mode did not result in a decrease in the oil samples' RUL.

Therefore, these results indicate that the RULLER candidate may have the potential of improving the Air Force's oil analysis program by assisting in the detection of abnormal operating conditions (seal damage, etc.) which rapidly degrade the oil and by determining the correct oil change intervals for the different type engines used by the Air Force.

b. Production and Evaluation of RULLER Demonstration Devices

(1) Introduction

Once the research to develop the RULLER candidate was completed, research was performed to produce RULLER demonstration devices for field testing at selected Air Force bases. The research concentrated on miniaturizing the data management system of the RULLER demonstration devices and on enabling the SBV to be compatible with all types of microcomputers. Manuals describing the setup and operation of the RULLER demonstration devices were also written. As an initial evaluation of the produced RULLER demonstration devices, used oil samples of unknown formulations obtained from Navy aircraft and Army helicopters were analyzed.

(2) Production of the RULLER Demonstration Devices

The miniaturization of the RULLER demonstration devices was accomplished by replacing the Apple IIe microcomputer and associated floppy disk drive, monitor, 80 column printer, and interfacing cables with the SBV, a Laser 128 microcomputer and a small, 40 column thermal printer. The Laser 128 computer was chosen for incorporation into the RULLER demonstration devices due to its low cost and compactness (floppy disk drive and interface for SBV built into sides of Laser 128).

The SBV used in the RULLER demonstration devices was redesigned to make it compatible with any microcomputer containing a parallel expansion port. Thus, previously purchased microcomputer systems could be used with the RULLER. The universal single board voltammograph (USBV) was achieved by adding analog-to-digital (A/D) and digital-to-analog (D/A) microchips to the analog circuitry of the single board voltammograph. The A/D and D/A microchips also decreased the cost of the RULLER demonstration device (microchips approximately $30 per chip versus circuit boards approximately $250 - $1000 per board).

The electrode system of the RULLER demonstration device was manufactured from a glassy carbon voltammetry electrode and two platinum wires which were encased in heat shrink tubing as described in the Experimental Section.

To simplify the set-up of the RULLER demonstration devices and to prevent damage to the USBV-Laser 128 microcomputer interface during shipping, the USBV was plugged into the parallel expansion port of the Laser 128 microcomputer prior to packaging. The USBV-Laser 128 microcomputer system was then attached to a piece of plywood to make the devices more rugged. The electrode system was attached to the USBV and the thermal

printer was plugged into the Laser 128 microcomputer to further simplify the set-up of the RULLER demonstration device. The power plugs of the USBV, Laser 128 microcomputer, and thermal printer were plugged into an outlet strip also attached to the plywood. The use of an outlet strip improves the ease of operation of the RULLER demonstration devices since the entire system is turned on with one switch. To minimize the effects of solvent spills, a tray was attached to the plywood in front of the USBV. The electrode system vial, cleaning solution vial, and analysis bag holding vial were then attached inside the tray to finalize the packaging of the RULLER demonstration devices. The produced RULLER demonstration device and packaged USBV are shown in Figures 149 and 150.

(3) Evaluation of the RULLER Demonstration Devices

As an initial evaluation of the optimized RULLER demonstration devices, used gas turbine oil samples obtained from Army helicopters and Navy jets were analyzed.

The Army's helicopter oil samples were taken from the transmissions, engines and gear boxes of CH-47D, UH-1H and OV-1 aircraft and were of unknown specification, e.g. MIL-L-7808, MIL-L-23699, etc. The RUL evaluations of the 100 samples from the helicopters ranged from 85 to 105% (fresh O-77-15 MIL-L-23699 oil: 100% standard) and did not appear to be related to the monitored component. The hours of operation since oil change ranged from 18 to 890 hours for the various oil samples and did not trend with the RUL values, i.e., 18 hour sample = 92% life while 890 hour sample = 98% life. Since the oil dilution rates and the previous oil samples of the different monitored components were not provided, the relationships among the RUL evaluations, the health of the monitored components, and the degradation rates of the oils could not be evaluated.

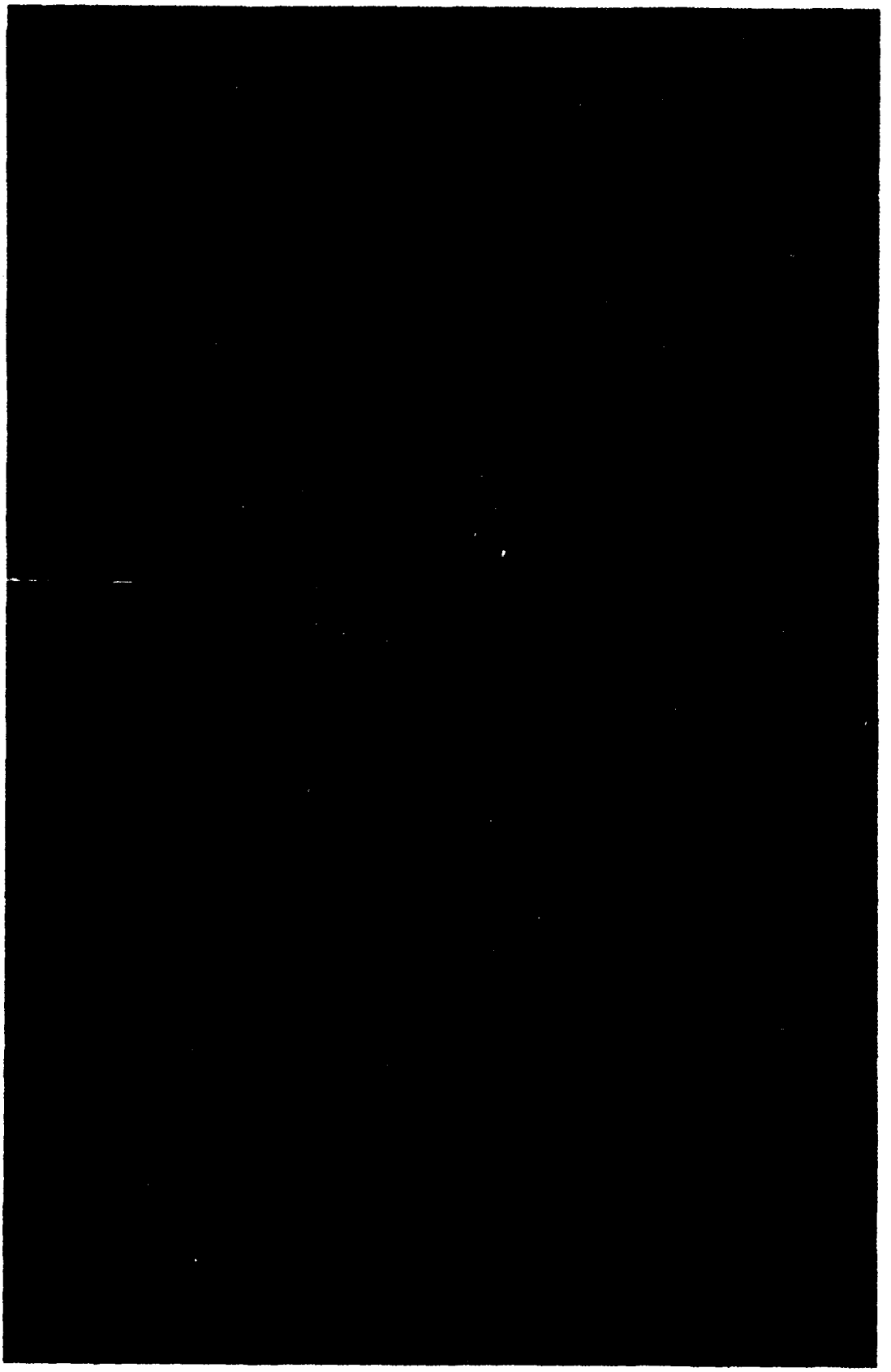

Figure 149. Photograph of RULLER - Microcomputer System Setup

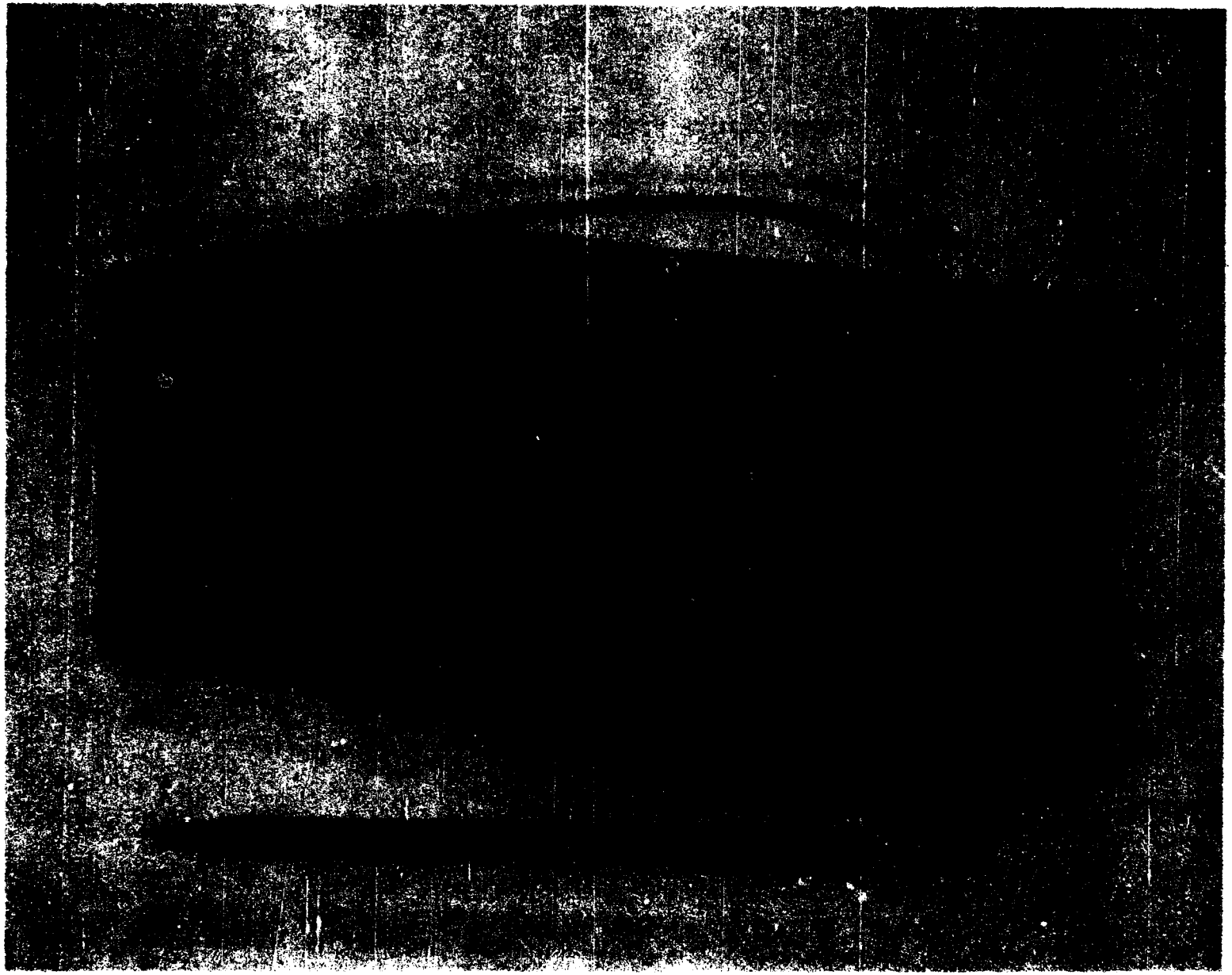

Figure 150. Photograph of RULLER Box (Packaged Universal Single Board Voltammograph) and Developed Electrode System

The Navy's jet oil samples were taken from J60, F404 and J52 engines and were MIL-L-23699 specification. The RUL evaluations of the 10 samples from the Navy jet aircraft ranged from 95 to 102% (fresh O-77-15 MIL-L-23699 oil: 100% standard) and did not trend with operational time (hours since oil change ranged from 10 to 800 hours). Since the oil dilution rates and the previous oil samples of the monitored engines were not provided, the relationships among the RUL evaluations, the health of the monitored components, and the degradation rates of the oils could not be evaluated.

(4) Summary

The initial evaluation of the optimized RULLER demonstration devices showed that the RULLER is able to evaluate the remaining useful lubricant lives of slightly degraded used oil samples regardless of the oil's formulation or the monitored equipment.

c. Field Testing of RULLER Demonstration Devices

(1) Introduction

As a final evaluation of the RULLER demonstration devices for use by the Air Force, devices were placed at three selected Air Force bases. To further evaluate the value of the RULLER for use by the Air Force, other used oil samples were obtained and analyzed by UDRI personnel.

(2) Air Force Base "A" RULLER Results

The used oil samples analyzed with the RULLER demonstration device at AFB "A" were obtained from operating A-10, T-37 and KC-135 aircraft. During the three months of testing, 1111 samples were obtained from approximately 200 different engines representing different type aircraft. The remaining useful life (RUL) values of the different oil samples series (1-9 samples per series) ranged from 96-102% (Fresh O-77-15

MIL-L-23699 oil: 100% standard) for approximately 200 of the engines and from 90 to 95% for 8 engines. The hours of operation since the last oil change (HSOC) ranged from 0 to 3002 hours for the KC-135 aircraft, 0 to 375 hours for the A-10 aircraft, and 15 to 204 hours for the T-37 aircraft. The RUL evaluations did not trend with the HSOC, e.g. 3002 hour sample (KC-135) = 99% RUL while 120 hour sample (KC-135) = 98% RUL.

To compare the percent RUL versus HSOC trends for the A-10 aircraft engines operating at percent RUL values above 95% with those operating at percent RUL values below 95%, the percent RUL versus HSOC plots for representative engines are presented in Figure 151. The percent RUL values for the KC-135 aircraft engines were not presented since the KC-135 samples were limited to 1-2 samples per series. The increases in the percent RUL plots in Figure 151 are indicative of fresh oil additions.

The majority of the samples in Figure 151 having percent RUL values greater than 95% range between 102-97% and the RUL plots exhibit moderate decreases between oil samples. The majority of the samples having percent RUL values less than 95% range between 97-94%. The percent RUL plots of the A-10 engines with serial numbers 205394 and 205625 exhibit rapid decreases between oil samples (Fig. 151) while the percent RUL plot of the other engine having serial number 205929 exhibits only moderate decreases between oil samples.

The oil sample obtained from the 205394 engine at 24 HSOC showed a rapid increase in the iron wear metal concentration by emission spectrometry (Air Force OAP) and the engine was removed for inspection. The maintenance personnel verified that the engine was experiencing abnormal wear and replaced several engine components. The maintenance report on this engine was not given to the personnel operating the RULLER so that the

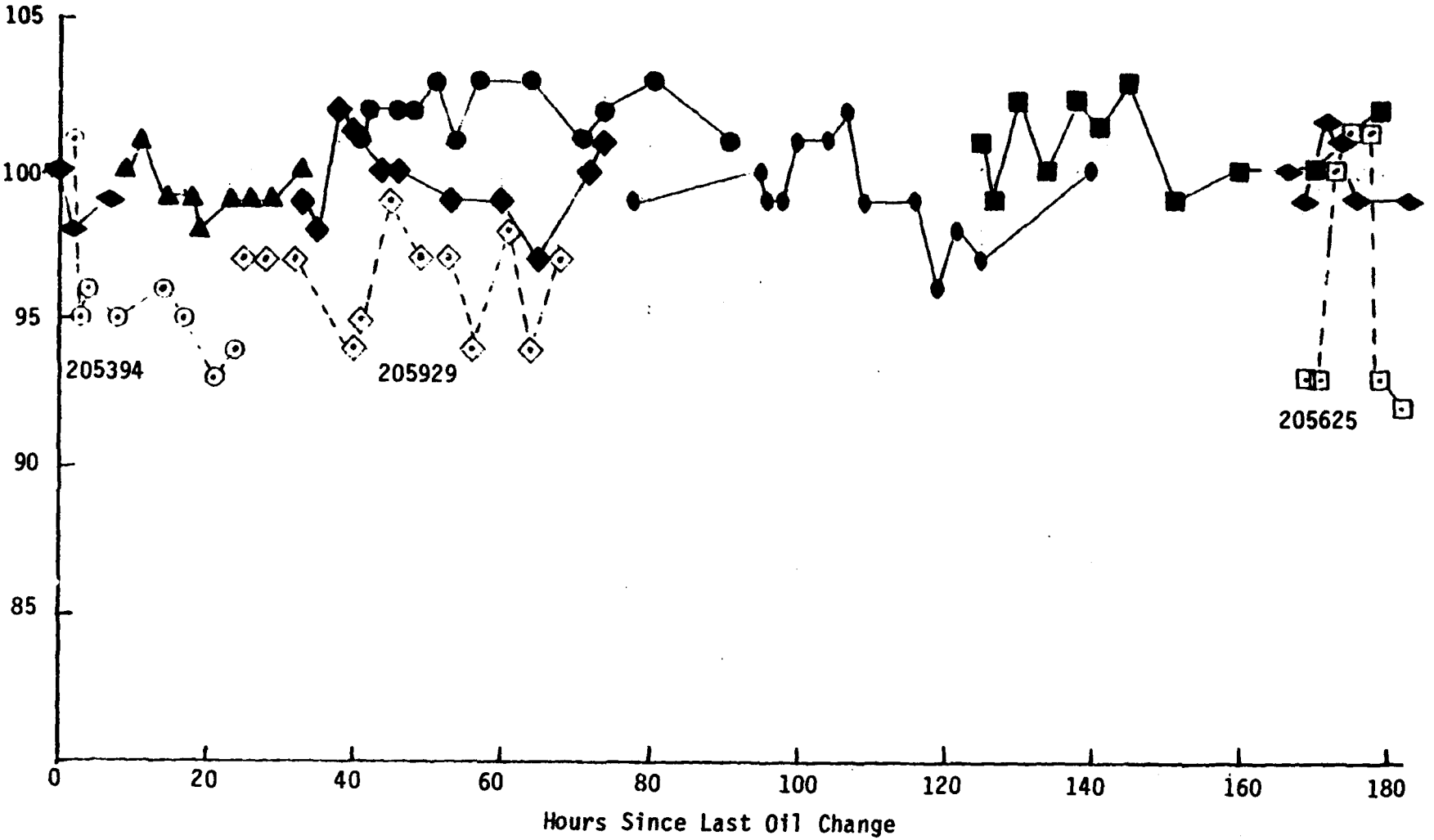

Figure 151. Plots of the Percent Remaining Useful Life Versus the Hours Since Last Oil Change for Used Oil Sample Series Obtained from Normal and Abnormal Operating A-10 Aircraft Engines

components replaced in the 205394 engine are unknown.

The 205625 engine was removed for routine maintenance at 182 HSOC. Whether component repair or replacement was required for this engine is unknown. The 205394 and 205625 engines were not placed back into service during the field test.

(3) UDRI RULLER Results

The used oil samples analyzed by UDRI personnel produced RULLER values similar to those obtained by AFB "A" personnel. During the three months of testing, 1000 samples were obtained from 144 different engines representing T-39, A-7D, C-18B, NC-141, A-10, KC-135E, F-111A and F-4D aircraft. Except for the F-111A and NC-141 aircraft, the RUL values of the oil sample series (1-9 samples per series) ranged from 96-100% regardless of the engine type or HSOC (up to 2643 hours for the KC-135E engines). The RUL values of the oil samples (single samples) obtained from different F-111A aircraft engines ranged from 91 to 99%.

The RUL values of the 29 oil samples (1-3 samples per series) obtained from NC-141 aircraft ranged between 100 and 102 (190 to 240 HSOC). However, the 2 oil samples obtained from the NC-141 aircraft engine serial number 651135 had RUL values of 94 and 95% (190 and 215 HSOC).

The Air Force OAP results for engine, serial number 651135, and another NC-141 aircraft engine, serial number 651634, representative of the engines producing RUL percent values between 100 and 102 are shown in Table 109 with the OAP analyses being well within the normal operating values for NC-141 aircraft engines.

TABLE 109

OAP WEAR METAL CONCENTRATIONS FOR NC-141 AIRCRAFT ENGINES

Engine Ser. No.	HSOC	Fe	Ag	Al	Cu	Mg	Si	Sn	Ti
651634	190	1	0	0	0	0	2	6	1
	214	0	0	0	0	0	0	6	1
651135	190	4	0	0	0	0	2	7	1
	214	4	0	0	0	0	0	6	1

(4) Air Force Base "B" RULLER Results

In contrast to the RULLER values obtained from AFB "A" and UDRI, the RULLER values obtained by AFB "B" personnel were below 90% for several C-130 aircraft engines. The 98 used oil samples analyzed by the RULLER demonstration device during the three months of testing were obtained from over 50 different C-130 aircraft engines. The RUL values of the used oil samples obtained from 96% of the C-130 aircraft engines ranged from 84-103% with the RUL values decreasing slightly with engine operating time (Figure 152). However, the used oil sample series obtained from 2 engines with serial numbers of AE100166 and AE100972 had RUL values between 29-45% and 64-80%, respectively which decreased rapidly with engine operating time.

The AE100166 engine was removed for inspection at 195 HSOC by AFB "B" maintenance personnel. The maintenance personnel discovered that the back carbon seal on the AE100166 engine was cracked. The cracked seal could account for the rapid degradation of the oil (rapid decrease in RULLER values) since hot air would be able to interact with the oil accelerating its thermal-oxidation. The seal was repaired and the AE100166 engine was placed back into service. The percent RUL value for the AE100166 engine was 93% at 30 HSOC further indicating the cracked seal was the cause of the low percent

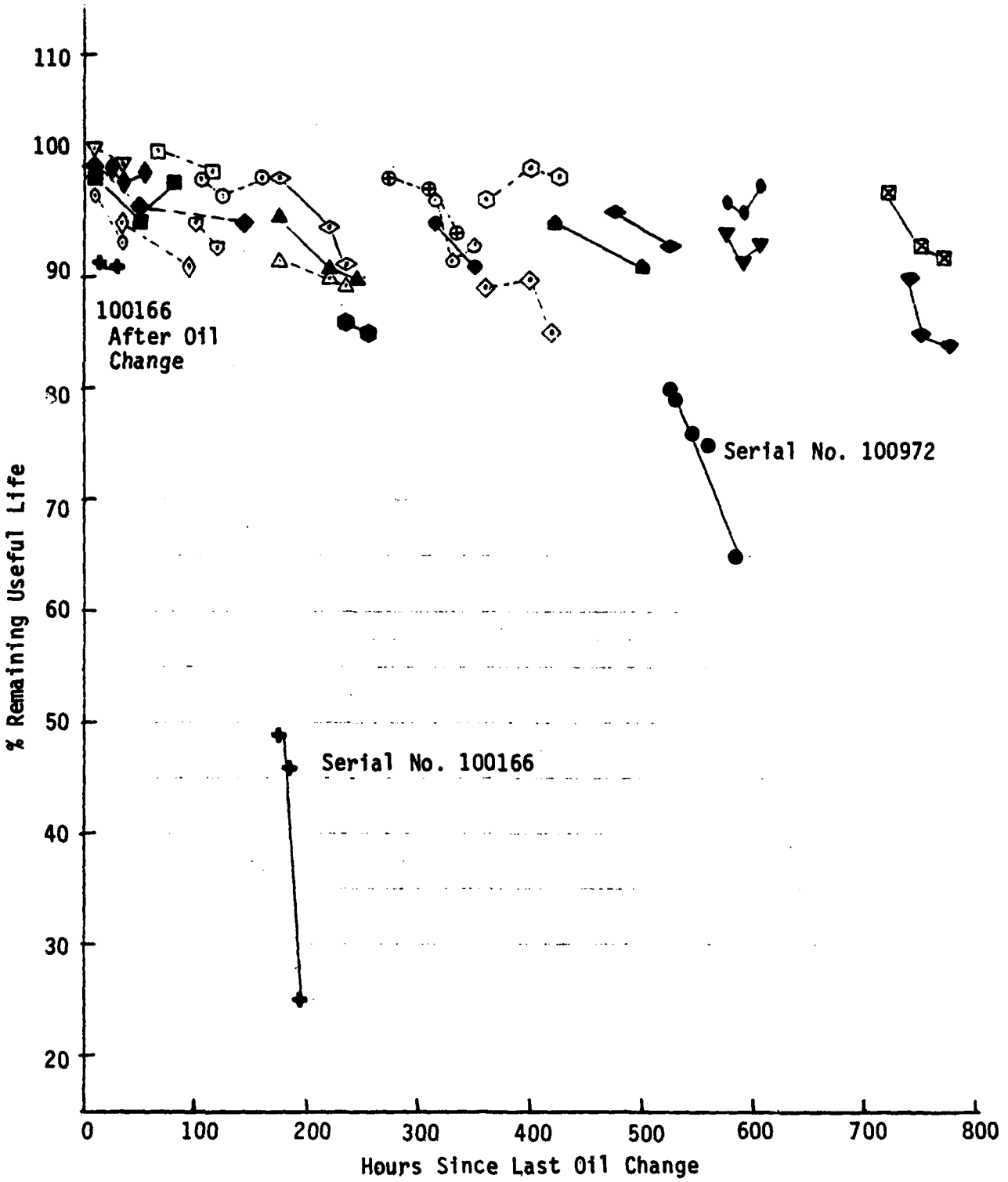

Figure 152. Plots of the Percent Remaining Useful Life Versus the Hours Since Last Oil Change for Used Oil Sample Series Obtained from C-130 Aircraft Engines

RUL values.

(5) AFWAL/POSL C-130 RULLER Results

In addition to the C-130 aircraft engine oil samples analyzed by AFB "B" personnel, AFWAL/POSL supplied to UDRI personnel for RULLER analysis four oil samples obtained from failed C-130 engines. Since the HSOC were unknown for the C-130 oil samples and the oil samples were from different C-130 aircraft engines, no trending information could be obtained for the used oil samples. The percent RUL values obtained for the failed C-130 aircraft engine oil samples were 66, 79, 87 and 99. Through comparison with Figure 152, it can be seen that the percent RUL values of 66 and 79 are abnormal regardless of the C-130 engines' HSOC. The HSOC and oil dilution rate information would be needed for the other two engines to determine if the 87 and 99% RUL values are abnormal or normal.

(6) Air Force Base "C" RULLER Results

Less than 30 oil samples were analyzed with the RULLER demonstration device at this base. The reported percent RUL ranged from 92-101% for the analyzed oil samples.

(7) Summary

The results of the initial RULLER field tests have shown that the RULLER demonstration devices are base level in operation with base personnel operating the devices without further assistance from UDRI personnel. Limited data collected to date for the C-130 aircraft indicate that the RULLER has the potential as a supplementary tool to OAP techniques. The significance of the abnormal operating conditions for the A-10 and NC-141 aircraft engines will be evaluated as additional used oil samples are obtained from the identified engines and analyzed by the RULLER and atomic emission spectrometry (wear metal analysis).

The RULLER results also showed that the oil change intervals for some aircraft engines are very conservative since the samples had percent RUL values of 96-102% prior to oil change. Whether the RULLER has potential for monitoring the operating conditions of the other aircraft used by the Air Force could not be determined since no OAP Hits (abnormal engines detected by Air Force OAP) or engine failures occurred for other types of aircraft during the field test period.

d. Conclusions

The results described herein have shown that a compact inexpensive RULLER has been developed which is base level in operation and provides formulation independent RUL evaluations of used MIL-L-7808 and MIL-L-23699 lubricating oils. Therefore, the developed RULLER is suitable for use by the Air Force and has the potential to supplement the OAP by detecting engines experiencing accelerated lubricant degradation prior to component malfunction and by assisting in establishing correct oil change intervals for normally operating engines.

SECTION IX

RECOMMENDATIONS

The summaries and conclusions given at the end of each subsection of the various tasks are specific, technically oriented and address the effort conducted within the specific section without consideration of other similar studies or tests. The following recommendations are made considering similar areas of study and are oriented towards assessment of the various areas of research with respect to providing similar type information and lubricant test data, the need for continued research for specific tests or lubricant evaluation procedures and the development and the incorporation of selected lubricant evaluation procedures in lubricant specifications. These recommendations along with appropriate discussions are given for each task as follows.

SECTION II Development of Improved Methods for Measuring Lubricant Performance

This task covered four primary areas of research involving lubricant stability, additive analyses, lubricant deposition and lubricant foaming. Two completely different type lubricants (normal ester base and high temperature polyphenyl ethers) were involved in the various studies.

Lubricant stability studies of the ester base lubricants involved oxidative stability testing using DERD Method No. 9, corrosiveness and oxidation stability testing using Federal Test Method Std. 791, Method 5307 and confined heat stability testing using DERD Method No. 1. The major difference between the two oxidation tests are sample size, airflow rates and the use of metal corrosion test specimens and condensate return with Method 5307. This research has shown that a single type test using one test

temperature does not define the complete oxidation stability of ester base lubricants. Various test temperatures and test times must be utilized in providing the required information for developing Arrhenius plots which describe lubricant performance in terms of selected test oil properties such as TAN and viscosity increases and percent lubricant loss. This study has also shown that testing with and without condensate return is also required since some lubricants have greater stability without condensate return while other lubricants have greater stability with condensate return. DERD Method No. 9 modified to use metal test specimens with and without condensate return is recommended as the test for developing Arrhenius plots which describe the effective lubricant life in terms of time, temperature and selected limiting values of changes in lubricant properties. Although current turbine lubricants possess adequate oxidative stability for current turbine engines, the trend of future engines operating at higher oil temperatures with smaller oil capacity systems will increase the oxidative stressing of the lubricant. The modified DERD Method No. 9 should be considered as a qualification test to ensure adequate oxidative stability under these conditions.

ASTM Test Method D 4871 conducted with and without intermediate sampling and DERD Test Method No. 9 modified to include metal test specimens and condensate return were used to investigate the corrosiveness and oxidative stability of high temperature polyphenyl ether lubricants. The two methods give similar results with each test having certain advantages depending on the purpose of the oxidation testing. ASTM Test Method D 4871 with intermediate sampling requires less sample and less actual test analysis time for developing Arrhenius plots which describe the effective life of the lubricant in terms of time and temperature. The modified Method DERD No. 9 requiring much less sample would be preferred or even required when

determining the stability of samples where only small quantities are available or when investigating the effects of other materials or pretest conditions such as used fluids from the four-ball wear test, dilution materials, etc. Either of these tests would be recommended over Fed. Test Method 791, Method 5307 as is currently required by specification MIL-L-87100 covering polyphenyl ether base lubricants.

The confined heat stability test DERD Method No. 1 defines the effective life of ester base lubricants under conditions of restricted oxygen availability. As this study has shown, lubricants having the best corrosiveness and oxidation stability may not have the best stability under the confined heat test conditions. The use of this test should be considered as a qualification test requirement for ester base lubricants since the environments within some areas of turbine engines closely resemble confined heat test conditions and due to the increased thermal and oxidative stress placed upon the lubricants by future engines using ester base lubricants.

Additive analyses such as infrared spectroscopy, chromatography techniques and spectrometric techniques are very important in determining the changes occurring in polyphenyl ether lubricants during use and in determining the remaining useful life of the lubricant. The use of various analytical and instrumental techniques for the evaluation of changes occurring in high temperature lubricants should be continued in the evaluation of these fluids and for the development of satisfactory lubricant monitoring techniques.

Lubricant deposition studies were conducted using the AFAPL Static Coker, the Micro Carbon Residue Tester (MCRT) and the Rolls-Royce Ltd. Coking Propensity Test. These tests provide information relative to the deposit forming characteristics of lubricants under conditions of no oil flow and

high temperatures such which can occur in turbine engines upon shutdown. As expected, the three tests are volatility oriented to various degrees and each test ranks the various classes of the ester base lubricants (3, 5 and 7.5 cSt) in the same order although some differences in ranking of the lubricants occur within each class of fluids. The MCRT gives the highest deposit values which would be expected since this test would have a lower evaporation rate and very little oxygen availability. The static coker having a larger surface area and a thin film of lubricant would have a greater volatility rate and also greater oxygen availability which, overall, gives lower deposits. Slightly thermally and oxidatively stressed lubricants give much higher deposit levels. These higher deposits values are very formulation dependent with some stressed lubricants showing larger deposit increases with the AFAPL Static Coker while other stressed lubricants give much larger deposit increases with the MCRT. Studies should be continued using both the MCRT and the AFAPL Static Coker on new and stressed ester base lubricants and polyphenyl ether lubricants. These studies should include investigating the degree of correlation between the MCRT and Static Coker test deposits with the deposit ratings of specific areas of "test stand" engines used for lubricant (ester base) qualification and with existing field experience relating to thin film coking under little or no oil flow conditions.

Lubricant foaming studies conducted on various lubricants using Fed. Test Method 791, Method 3213 and the small volume foam test showed correlation only for those lubricants having little or no aeration characteristics. Therefore, the small volume test should not be considered as a replacement for Method 3213 required by MIL-L-7808 lubricant specification. Studies of the foaming and aeration characteristics of high temperature fluids such as polyphenyl ethers should be continued using the small volume

foam test and metal spargers at temperatures nearer the expected operating temperatures of these fluids instead of the normal 80°C test temperature required by Method 3213.

SECTION III Development of Improved Lubrication System Health Monitoring Techniques

One of the three areas investigated in this task was improving the sensitivity of the atomic emission spectrometer for the complete detection of wear metals in used lubricating oils. The ashing technique and the sample pin stand offered several advantages relative to conventional systems by improving the particle detection capability. This system could be incorporated in the oil analysis program.

The second area of investigation was determining the impact of microfiltration on oil analysis. This work has shown that even though the level of contaminants is appreciably decreased, it was possible to detect wear by spectrometric methods in samples that have passed through the 3 micron filter. However, further work is needed to investigate the capabilities and limitations of current spectrometric techniques in analyzing oils from engines using microfiltration systems. Oil samples from operational gas turbine engines are needed to establish threshold values for engines using microfiltration systems.

The third effort under this task was to determine the capability of a portable wear particle analyzer. Our findings reveal that the WPA is not entirely quantitative for analyzing magnetic wear debris but it is an adequate tool that can be used to supplement oil analysis techniques since oil samples from engines experiencing severe wear contain particles greater than 1 to 3 microns. Magnetic particles above this range can be readily detected by the WPA and trending techniques can be established for early

detection of engines experiencing severe wear. This advantage coupled with its portability and simplicity of use warrant its field testing as a screening device to identify incipient engine failure.

SECTION IV Investigation of Lubricant Monitoring Techniques

This task involved an investigation into the relationship of various electrochemical properties of lubricants and their chemical properties. Devices used for analysis included the complete oil breakdown rate analyzer (COBRA) and those for measuring conductivity, dielectric constant and dielectric breakdown strengths. Lubricants analyzed included MIL-L-7808 and MIL-L-23699 ester based lubricants and, to a lesser extent, polyphenyl ethers.

Analysis of oxidatively degraded ester lubricants gave similar results and trends when analyzed by either the COBRA or a conductivity meter suggesting a dependence on a molecular charge carrying mechanism. Although the complexity of lubricant oxidation did not allow identification of specific charge carriers, there is evidence to support additives (especially antioxidants) as being the source. It was also shown that the dielectric constant of the lubricant can greatly influence the effect of charge carriers on COBRA readings. These observations account for the variability in the relationship between the COBRA readings of MIL-L-7808 lubricants and their degree of oxidative degradation. Similar variations would be expected to occur in monitoring of engine lubricants, depending on the formulation or mixtures thereof. As a result, the COBRA would be expected to be a generally useful device for detecting abnormally operating engines but not for prediction of lubricant life or oil change intervals. The COBRA has not demonstrated any usefulness for the monitoring of polyphenyl ethers.

Investigation of the dielectric constant properties of ester based

lubricants revealed a useful correlation with the degree of lubricant oxidative degradation, as long as volatilization weight loss was minimal, and a much less useful correlation with simulated metallic wear debris. Unfortunately, this device requires a fresh lubricant to be available for comparison. Since their is a large variation in the dielectric constant of various formulation as well as intermixing of these formulations in an engine, the dielectric constant device is impractical as a field monitoring device. Limited analysis of polyphenyl ethers indicates that this device may be useful as a monitoring device for these high temperature lubricants, but further investigation is needed.

An oil maintenance tester, which measures current decay in the lubricant after application of a DC step voltage, and a dielectric breakdown strength tester were also investigated as monitoring devices for ester lubricants. Neither device displayed a useful correlation with lubricant condition and no further investigation is warranted.

SECTIONS V AND VI Lubricant Load Carrying Capability Test Assessment and Development of Specification Wear Test

A literature survey was conducted and wear tests developed to measure the wear prevention characteristics of synthetic ester based turbine lubricants. The four-ball test was extensively investigated during this study. It is recommended that the standard four-ball test (ASTM D 4172-82) procedure be modified for use in testing ester base lubricants. The modification involves conducting the test for 20 hours duration instead of one hour. The extended test provides a better evaluation of lubricants' wear prevention properties.

In addition to the wear scar size, wear rate measured in mm^3/min was obtained using LVDT data with the BOS and Feng equations. The volumetric

wear rate varied linearly with time and load up to a transition period and then decreased by several orders of magnitude. Transition periods were only noted for oils with TCP.

SECTION VII Development of Lube Data Storage and Retrieval System

A microcomputer software was developed and a user's manual was written to store, retrieve, correlate and evaluate lubricant test data. This system was mainly developed for MIL-L-7808 lubricants and its use is recommended for the newly developed high temperature lubricants.

SECTION VIII RULLER Development

During this contract a compact, inexpensive, and easy to operate RULLER (Remaining Useful Lubricant Life Evaluation Rig) was developed and successfully field tested at several Air Force bases. Based on the proven capability of the RULLER to detect abnormal operating C-130 aircraft engines prior to component failure, it is recommended that the Air Force consider using the RULLER to monitor its C-130 aircraft fleet. The fact that the SOAP has proven ineffective for the C-130 aircraft fleet further increases the potential of the RULLER to greatly improve the reliability of the Air Force's C-130 aircraft fleet.

APPENDIX A

LUBRICANT PERFORMANCE TEST DATA

Appendix A contains lubricant test data obtained during the development of improved methods for measuring lubricant performance and presented in Section II of this report. This test data is tabulated as follows;

TABLE A-1. SQUIRES OXIDATIVE TEST DATA

Table A-1 contains all the Squires Oxidative test data arranged as follows:

a. Lubricants listed in order of specification and lubricant code number sequence.

b. Each lubricant's test data listed in order of increasing temperatures.

c. Lubricants listed in order of specification and lubricant code number sequence using condensate return.

TABLE A-2. SQUIRES CONFINED HEAT TEST DATA

Table A-2 contains all the Squires Confined Heat test data and is arranged in the same order as described for Table A-1.

TABLE A-3. AFAPL STATIC COKER TEST DATA

Table A-3 contains all the AFAPL Static Coker test data arranged in test number sequence.

TABLE A-4. MCRT COKING DATA

Table A-4 contains all the MCRT coking data and is arranged in test number sequence.

TABLE A-5. LUBRICANT FOAMING TEST DATA

Table A-5 contains all lubricant foaming test data arranged in test number sequence.

TABLE A-6. VARIABLE AIRFLOW FOAMING TEST DATA

Table A-6 contains all variable airflow foaming test data arranged in test number sequence.

TABLE A-1

SQUIRES OXIDATIVE TEST DATA

LUBRICANT AND TEST TEMP.	LUBRICANT PROPERTY	TEST HOURS						
		New Oil	96	192	456	528	576	648
	Weight Loss, %		7.0	12.6	31.1	35.8	37.1	ND
O-71-6	COBRA Reading	2	28	43	50	43	82	ND
(a)	Total Acid No.	0.06	0.38	0.81	1.07	1.60	1.66	1.68
190°C	Viscosity @100°C,cs	4.95	5.40	5.63	6.35	6.58	6.72	ND
	Viscosity Change, %		9.1	13.7	28.3	32.9	35.8	ND
	Toluene Insol, % wt	ND	ND	ND	ND	ND	ND	ND
	Visual Appearance of Deposits		Slight Varnish	Slight Varn. and Deposits	Brown crystals, sl. varn.	Sl. Varn. and Deposits	Varnish Crystals Stain	ND

LUBRICANT AND TEST TEMP.	LUBRICANT PROPERTY	TEST HOURS						
		New Oil	672	720				
	Weight Loss, %		ND	52.2				
O-71-6ex	COBRA Reading	2	ND	57				
	Total Acid No.	0.06	1.55	2.44				
190°C	Viscosity @100°C,cs	4.95	ND	6.70				
	Viscosity Change, %		ND	35.4				
	Toluene Insol, % wt	ND	ND	0.03				
	Visual Appearance of Deposits		ND	Coke,varn Stain crystals				

LUBRICANT AND TEST TEMP.	LUBRICANT PROPERTY	TEST HOURS						
		New Oil	168	264	360			
	Weight Loss, %		19.6	31.0	40.9			
O-71-6	COBRA Reading	2	41	36	36			
	Total Acid No.	0.06	1.12	1.84	2.40			
200°C	Viscosity @100°C,cs	4.95	6.01	6.68	7.93			
	Viscosity Change, %		21.4	35.0	60.2			
	Toluene Insol, % wt	ND	ND	ND	0.04			
	Visual Appearance of Deposits		Brown Crystals Sl. Varn.	Brown Crystals Sl. Varn.	Brown Crystals Sl. Varn.			

(a) - see O-71-6ex for extended testing results.

SQUIRES OXIDATIVE TEST DATA

LUBRICANT AND TEST TEMP.	LUBRICANT PROPERTY	TEST HOURS						
		New Oil	24	48	120	168		
	Weight Loss, %		4.8	8.7	19.8	27.9		
O-71-6	COBRA Reading	2	20	30	39	53		
	Total Acid No.	0.06	0.35	0.74	1.21	7.84		
205°C	Viscosity @100°C,cs	4.95	5.46	5.65	6.07	7.80		
	Viscosity Change, %		10.3	14.1	22.6	57.6		
	Toluene Insol, % wt	ND	ND	ND	ND	0.03		
	Visual Appearance of Deposits		None	None	None	Varnish		

LUBRICANT AND TEST TEMP.	LUBRICANT PROPERTY	TEST HOURS						
		New Oil	72	168	384	456	528	672
	Weight Loss, %		4.6	10.5	23.1	26.8	32.1	48.6
O-77-15	COBRA Reading	2	37	79	103	81	81	74
	Total Acid No.	0.43	0.45	0.73	1.47	1.23	1.77	1.88
190°C	Viscosity @100°C,cs	4.95	5.52	5.58	6.14	6.36	6.81	8.30
	Viscosity Change, %		11.5	12.7	24.0	28.5	37.6	67.7
	Toluene Insol, % wt	ND	ND	ND	ND	ND	ND	0.04
	Visual Appearance of Deposits		None	Varnish	Crystals Slight Varnish	Crystals Dark Varnish	Brown Crystals Varnish	Dark Crystals Varnish

LUBRICANT AND TEST TEMP.	LUBRICANT PROPERTY	TEST HOURS						
		New Oil	168	264	360			
	Weight Loss, %		17.1	28.3	38.8			
O-77-15	COBRA Reading	2	80	57	52			
	Total Acid No.	0.43	1.95	2.13	2.70			
200°C	Viscosity @100°C,cs	4.95	5.99	6.86	8.09			
	Viscosity Change, %		21.0	38.6	63.4			
	Toluene Insol, % wt	ND	ND	ND	0.04			
	Visual Appearance of Deposits		Brown crystals sl. varn.	Brown crystals sl. varn.	Brown crystals sl. varn.			

SQUIRES OXIDATIVE TEST DATA

LUBRICANT AND TEST TEMP.	LUBRICANT PROPERTY	TEST HOURS						
		New Oil	24	48	168	216	264	
	Weight Loss, %		4.1	7.3	22.5	50.6	58.2	
O-77-15	COBRA Reading	2	32	59	63	54	27	
	Total Acid No.	0.43	0.74	0.52	2.21	5.96	6.29	
205°C	Viscosity @100°C,cs	4.95	5.32	5.50	6.46	20.64	ND	
	Viscosity Change, %		7.5	11.1	30.5	417.0	N/A	
	Toluene Insol, % wt	ND	ND	ND	ND	ND	0.06	
	Visual Appearance of Deposits		None	White Crystals	White and Brown Crystals	Slight Coke	Clear Deposit	

LUBRICANT AND TEST TEMP.	LUBRICANT PROPERTY	TEST HOURS						
		New Oil	24	48	168	264	360	528
	Weight Loss, %		3.7	7.3	19.4	34.8	47.6	60.6
O-79-18	COBRA Reading	3	37	58	143	78	76	82
	Total Acid No.	0.07	0.37	0.90	0.66	1.24	1.17	2.45
205°C	Viscosity @100°C,cs	5.29	5.44	5.57	6.09	7.03	7.99	ND
	Viscosity Change, %		2.8	5.3	14.1	32.9	51.0	N/A
	Toluene Insol, % wt	ND	ND	ND	ND	ND	ND	0.02
	Visual Appearance of Deposits		None	White Crystals	White Crystals	Crystals	White Crystals	Clear Crystals

LUBRICANT AND TEST TEMP.	LUBRICANT PROPERTY	TEST HOURS						
		New Oil	24	168	285			
	Weight Loss, %		5.6	22.7	51.2			
O-79-18	COBRA Reading	3	32	100	81			
	Total Acid No.	0.07	0.58	1.61	2.91			
210°C	Viscosity @100°C,cs	5.29	5.51	6.47	9.12			
	Viscosity Change, %		4.2	22.3	72.4			
	Toluene Insol, % wt	ND	ND	ND	0.01			
	Visual Appearance of Deposits		None	Clear Deposit	White Crystals			

SQUIRES OXIDATIVE TEST DATA

LUBRICANT AND TEST TEMP.	LUBRICANT PROPERTY	TEST HOURS						
		New Oil	24	72	144			
	Weight Loss, %		6.8	20.9	39.5			
0-79-18	COBRA Reading	3	65	92	73			
	Total Acid No.	0.07	0.91	1.60	2.49			
215°C	Viscosity @100°C,cs	5.29	5.43	6.14	7.74			
	Viscosity Change, %		2.6	16.1	46.4			
	Toluene Insol, % wt	ND	ND	ND	ND			
	Visual Appearance of Deposits		White deposit	Clear Crystals	Clear crystals, sl. var.			

LUBRICANT AND TEST TEMP.	LUBRICANT PROPERTY	TEST HOURS						
		New Oil	24	48	120	168	216	360
	Weight Loss, %		7.1	13.8	32.7	42.8	51.6	ND
0-85-1	COBRA Reading	8	36	63	109	119	110	110
	Total Acid No.	0.02	0.12	0.33	0.67	0.96	1.53	2.54
205°C	Viscosity @100°C,cs	4.04	4.14	4.23	4.55	5.03	5.22	9.94
	Viscosity Change, %		2.5	4.7	12.6	24.5	29.2	146.0
	Toluene Insol, % wt	ND	ND	ND	ND	ND	ND	ND
	Visual Appearance of Deposits		None	Tacky Crystals	White Crystals	Crystals	Crystals	Crystals and Varnish

LUBRICANT AND TEST TEMP.	LUBRICANT PROPERTY	TEST HOURS						
		New Oil	24	68	116	168		
	Weight Loss, %		9.4	26.1	44.8	57.7		
0-85-1	COBRA Reading	8	50	97	123	113		
	Total Acid No.	0.02	0.33	1.00	1.70	2.90		
210°C	Viscosity @100°C,cs	4.40	4.15	4.44	4.94	5.86		
	Viscosity Change, %		2.7	9.9	22.3	45.0		
	Toluene Insol, % wt	ND	ND	ND	ND	0.04		
	Visual Appearance of Deposits		White Deposits	Clear Deposit	White and Clear Deposits	Light Crystals		

SQUIRES OXIDATIVE TEST DATA

LUBRICANT AND TEST TEMP.	LUBRICANT PROPERTY	TEST HOURS						
		New Oil	24	48	72	144		
	Weight Loss, %		13.5	24.7	35.2	76.7		
O-85-1	COBRA Reading	8	66	104	115	57		
	Total Acid No.	0.02	0.91	1.20	1.86	10.46		
215°C	Viscosity @100°C,cs	4.04	4.23	4.46	4.73	ND		
	Viscosity Change, %		4.7	10.4	17.0	N/A		
	Toluene Insol, % wt	ND	ND	ND	ND	0.04		
	Visual Appearance of Deposits		Clear Crystals Sl. Varn.	Clear Crystals	Clear Crystals	Clear Crystals Sl. Varn.		

LUBRICANT AND TEST TEMP.	LUBRICANT PROPERTY	TEST HOURS						
		New Oil	24	72	120			
	Weight Loss, %		9.9	28.6	44.8			
O-86-2	COBRA Reading	10	61	94	129			
	Total Acid No.	0.07	0.35	1.12	2.05			
210°C	Viscosity @100°C,cs	4.01	4.19	4.50	5.03			
	Viscosity Change, %		4.5	12.2	25.4			
	Toluene Insol, % wt	ND	ND	ND	0.03			
	Visual Appearance of Deposits		None	Clear Crystal	Clear Crystal			

LUBRICANT AND TEST TEMP.	LUBRICANT PROPERTY	TEST HOURS						
		New Oil	72	96	120			
	Weight Loss, %		14.4	19.1	37.4			
O-87-3	COBRA Reading	16	10	10	67			
	Total Acid No.	0.13	1.38	1.66	12.53			
200°C	Viscosity @100°C,cs	4.02	4.48	4.60	8.27			
	Viscosity Change, %		11.4	14.4	105.7			
	Toluene Insol, % wt							
	Visual Appearance of Deposits		None oil dark	None oil dark	None oil orange			

SQUIRES OXIDATIVE TEST DATA

LUBRICANT AND TEST TEMP.	LUBRICANT PROPERTY	TEST HOURS						
		New Oil	48	72	96			
	Weight Loss, %		13.0	33.5	44.7			
0-87-3	COBRA Reading	16	11	56	47			
	Total Acid No.	0.13	1.34	10.54	10.51			
205°C	Viscosity @100°C,cs	4.02	4.44	7.84	9.62			
	Viscosity Change, %		10.4	95.0	139.3			
	Toluene Insol, % wt							
	Visual Appearance of Deposits		None oil dark	None oil orange	None oil dark			

LUBRICANT AND TEST TEMP.	LUBRICANT PROPERTY	TEST HOURS						
		New Oil	24	48	48	72	72	
	Weight Loss, %		8.4	24.6	27.4	38.6	38.0	
0-87-3	COBRA Reading	16	10	40	37	45	35	
	Total Acid No.	0.13	1.13	7.79	5.90	3.42	4.33	
210°C	Viscosity @100°C,cs	4.02	4.33	6.11	6.51	8.25	7.79	
	Viscosity Change, %		7.7	52.0	61.9	105.2	93.8	
	Toluene Insol, % wt							
	Visual Appearance of Deposits		None oil dark	None oil orange	None oil dark	None oil dark	None oil dark	

LUBRICANT AND TEST TEMP.	LUBRICANT PROPERTY	TEST HOURS						
		New Oil	72					
	Weight Loss, %		38.5					
0-79-18wCR (a)	COBRA Reading	3	200					
	Total Acid No.	0.07	17.60					
205°C	Viscosity @100°C,cs	5.29	ND					
	Viscosity Change, %		N/A					
	Toluene Insol, % wt	ND	ND					
	Visual Appearance of Deposits		None, oil very viscous					

(a) - Samples oxidatively stressed using condensate return.

SQUIRES OXIDATIVE TEST DATA

LUBRICANT AND TEST TEMP.	LUBRICANT PROPERTY	TEST HOURS						
		New Oil	24	48				
	Weight Loss, %		8.3	39.8				
O-79-18wCR	COBRA Reading	3	200	200				
(a)	Total Acid No.	0.07	1.85	4.77				
215°C	Viscosity @100°C,cs	5.29	5.62	11.02				
	Viscosity Change, %		6.2	108.3				
	Toluene Insol, % wt	ND	ND	ND				
	Visual Appearance of Deposits		none	none				

LUBRICANT AND TEST TEMP.	LUBRICANT PROPERTY	TEST HOURS						
		New Oil	72					
	Weight Loss, %		13.6					
O-85-1w/CR	COBRA Reading	8	200					
(b)	Total Acid No.	0.02	4.99					
205°C	Viscosity @100°C,cs	4.04	4.24					
	Viscosity Change, %		5.0					
	Toluene Insol, % wt	ND	ND					
	Visual Appearance of Deposits		none					

LUBRICANT AND TEST TEMP.	LUBRICANT PROPERTY	TEST HOURS						
		New Oil	24	48	72			
	Weight Loss, %		9.8	14.7	26.1			
O-85-1w/CR	COBRA Reading	8	71	161	200			
(c)	Total Acid No.	0.02	0.47	1.77	3.84			
215°C	Viscosity @100°C,cs	4.04	4.13	4.23	4.62			
	Viscosity Change, %		2.2	4.7	14.4			
	Toluene Insol, % wt	ND	ND	ND	ND			
	Visual Appearance of Deposits		none	clear crystals	none			

(a) - Samples oxidatively stressed using condensate return.
(b) - Samples oxidatively stressed using condensate return.
(c) - Samples oxidatively stressed using condensate return.

TABLE A-2

SQUIRES CONFINED HEAT TEST DATA

LUBRICANT AND TEST TEMP.	LUBRICANT PROPERTY	TEST HOURS						
		New Oil	168	192	264			
	Weight Loss, %		0.0	0.0	0.0			
TEL-7043	COBRA Reading	2	19	21	51			
	Total Acid No.	0.03	2.97	3.77	4.64			
190°C	Viscosity @100°C,cs	5.06	5.28	5.30	5.25			
	Viscosity Change, %		4.3	4.7	3.8			
	Toluene Insol, % wt	ND	ND	ND	ND			
	Visual Appearance of Deposits		Slight Stain	Stain Varnish	Stain Varnish			

LUBRICANT AND TEST TEMP.	LUBRICANT PROPERTY	TEST HOURS						
		New Oil	96	144	192			
	Weight Loss, %		0.0	0.0	0.0			
TEL-7043	COBRA Reading	2	8	18	26			
	Total Acid No.	0.03	2.90	4.27	5.84			
195°C	Viscosity @100°C,cs	5.06	5.23	5.46	5.33			
	Viscosity Change, %		3.3	7.9	5.3			
	Toluene Insol, % wt	ND	ND	ND	ND			
	Visual Appearance of Deposits		Slight Stain	Stain	Stain Varnish Oil Globs			

LUBRICANT AND TEST TEMP.	LUBRICANT PROPERTY	TEST HOURS						
		New Oil	24	48	72	96		
	Weight Loss, %		0.0	0.0	0.0	0.0		
O-71-6	COBRA Reading	2	4	6	11	25		
	Total Acid No.	0.06	1.23	2.73	3.86	6.62		
205°C	Viscosity @100°C,cs	4.95	5.12	5.17	5.22	5.21		
	Viscosity Change, %		3.4	4.4	5.4	5.2		
	Toluene Insol, % wt	ND	ND	ND	ND	0.04		
	Visual Appearance of Deposits		None	Slight Sediment	None	None		

SQUIRES CONFINED HEAT TEST DATA

LUBRICANT AND TEST TEMP.	LUBRICANT PROPERTY	TEST HOURS						
		New Oil	120	192	264	336		
	Weight Loss, %		0.0	0.0	0.0	0.0		
0-77-15	COBRA Reading	2	27	36	57	89		
	Total Acid No.	0.43	2.18	3.06	3.05	6.97		
190°C	Viscosity @100°C,cs	4.95	5.16	5.21	5.27	5.33		
	Viscosity Change, %		4.2	5.2	6.5	7.7		
	Toluene Insol, % wt	ND	ND	ND	ND	0.05		
	Visual Appearance of Deposits		Oil Globlets	Oil Globlets	None	None		

LUBRICANT AND TEST TEMP.	LUBRICANT PROPERTY	TEST HOURS						
		New Oil	72	96	144	168		
	Weight Loss, %		0.0	0.0	0.0	0.0		
0-77-15	COBRA Reading	2	20	26	45	56		
	Total Acid No.	0.43	1.98	2.33	4.74	6.19		
195°C	Viscosity @100°C,cs	4.95	5.13	5.18	5.21	5.19		
	Viscosity Change, %		3.6	4.7	5.3	4.8		
	Toluene Insol, % wt	ND	ND	ND	ND	0.05		
	Visual Appearance of Deposits		None	Sl. Coke, Stain	None	Stain Varnish		

LUBRICANT AND TEST TEMP.	LUBRICANT PROPERTY	TEST HOURS						
		New Oil	24	48	72			
	Weight Loss, %		0.0	0.0	0.0			
0-77-15	COBRA Reading	2	12	24	40			
(a)	Total Acid No.	0.43	1.63	3.42	5.72			
205°C	Viscosity @100°C,cs	4.95	5.22	5.15	5.32			
	Viscosity Change, %		5.4	4.0	5.6			
	Toluene Insol, % wt	ND	ND	ND	0.05			
	Visual Appearance of Deposits		None	None	Slight Stain			

(a) - (TEL 6021)

SQUIRES CONFINED HEAT TEST DATA

LUBRICANT AND TEST TEMP.	LUBRICANT PROPERTY	TEST HOURS						
		New Oil	24	48	72	120		
	Weight Loss, %		0.0	0.1	0.4	0.2		
0-79-18	COBRA Reading	3	15	22	37	73		
(a)	Total Acid No.	.07	0.38	0.83	2.25	5.01		
205°C	Viscosity @100°C, cs	5.29	5.28	5.34	5.33	5.33		
	Viscosity Change, %		-0.2	0.9	0.7	0.7		
	Toluene Insol, % wt	ND	ND	ND	ND	0.00		
	Visual Appearance of Deposits		None	None	None	None		

LUBRICANT AND TEST TEMP.	LUBRICANT PROPERTY	TEST HOURS						
		New Oil	24	68	120	192		
	Weight Loss, %		0.0	0.4	0.1	0.3		
0-79-18	COBRA Reading	3	11	27	91	128		
	Total Acid No.	0.07	0.60	2.31	5.36	8.96		
210°C	Viscosity @100°C, cs	5.29	5.30	5.39	5.50	5.53		
	Viscosity Change, %		0.2	1.9	4.0	4.5		
	Toluene Insol, % wt	ND	ND	ND	ND	0.11		
	Visual Appearance of Deposits		None	None	None	None		

LUBRICANT AND TEST TEMP.	LUBRICANT PROPERTY	TEST HOURS						
		New Oil	49	96	120			
	Weight Loss, %		0.0	0.0	1.0			
0-79-18	COBRA Reading	3	20	45	51			
	Total Acid No.	0.07	1.61	4.67	5.88			
215°C	Viscosity @100°C, cs	5.29	5.37	5.39	5.40			
	Viscosity Change, %		1.5	1.9	2.1			
	Toluene Insol, % wt	ND	ND	ND	0.03			
	Visual Appearance of Deposits		None	None	None			

(a) - (TEL 6022)

SQUIRES CONFINED HEAT TEST DATA

LUBRICANT AND TEST TEMP.	LUBRICANT PROPERTY	TEST HOURS						
		New Oil	24	48	96	192	288	
	Weight Loss, %		0.0	0.0	0.8	0.5	1.0	
0-85-1	COBRA Reading	8	32	31	53	76	140	
	Total Acid No.	0.02	0.08	0.90	2.41	4.47	10.01	
205°C	Viscosity @100°C, cs	4.04	4.04	3.87	4.04	4.10	4.08	
	Viscosity Change, %		0.0	-4.2	0.0	1.5	1.0	
	Toluene Insol, % wt	ND	ND	ND	ND	ND	ND	
	Visual Appearance of Deposits		None	None	None	None	None	

LUBRICANT AND TEST TEMP.	LUBRICANT PROPERTY	TEST HOURS						
		New Oil	68	116	168			
	Weight Loss, %		0.0	0.1	0.4			
0-85-1	COBRA Reading	8	42	74	99			
	Total Acid No.	0.02	2.36	5.19	6.93			
210°C	Viscosity @100°C, cs	4.04	4.06	4.08	4.11			
	Viscosity Change, %		0.5	1.0	1.7			
	Toluene Insol, % wt	ND	ND	ND	0.03			
	Visual Appearance of Deposits		None	None	None			

LUBRICANT AND TEST TEMP.	LUBRICANT PROPERTY	TEST HOURS						
		New Oil	49	72	120			
	Weight Loss, %		0.0	0.0	1.4			
0-85-1	COBRA Reading	8	55	48	84			
	Total Acid No.	0.02	2.43	2.86	5.63			
215°C	Viscosity @100°C, cs	4.04	4.07	4.06	4.10			
	Viscosity Change, %		0.7	0.5	1.5			
	Toluene Insol, % wt	ND	ND	ND	0.05			
	Visual Appearance of Deposits		None	None	None			

SQUIRES CONFINED HEAT TEST DATA

LUBRICANT AND TEST TEMP.	LUBRICANT PROPERTY	TEST HOURS						
		New Oil	72	120	168			
	Weight Loss, %		0.0	0.1	0.0			
0-86-2	COBRA Reading	10	42	72	99			
	Total Acid No.	0.07	2.71	4.87	6.76			
210°C	Viscosity @100°C,cs	4.01	4.04	4.05	4.10			
	Viscosity Change, %		0.7	1.0	2.2			
	Toluene Insol, % wt	ND	ND	ND	0.01			
	Visual Appearance of Deposits		None	None	None			

LUBRICANT AND TEST TEMP.	LUBRICANT PROPERTY	TEST HOURS						
		New Oil	72	120	168			
	Weight Loss, %		0.0	0.9	0.1			
0-87-3	COBRA Reading	16	4	7	7			
	Total Acid No.	0.13	2.03	4.54	5.48			
200°C	Viscosity @100°C,cs	4.02	4.07	4.04	4.07			
	Viscosity Change, %		1.2	0.5	1.2			
	Toluene Insol, % wt							
	Visual Appearance of Deposits		Slight stain at oil level	Slight stain at oil level	Slight stain at oil level			

LUBRICANT AND TEST TEMP.	LUBRICANT PROPERTY	TEST HOURS						
		New Oil	48	98	168			
	Weight Loss, %		0.0	0.0	0.1			
0-87-3	COBRA Reading	16	4	6	9			
	Total Acid No.	0.13	1.83	3.57	5.54			
205°C	Viscosity @100°C,cs	4.02	4.06	4.06	4.14			
	Viscosity Change, %		1.0	1.0	3.0			
	Toluene Insol, % wt							
	Visual Appearance of Deposits		Slight stain at oil level	Slight stain at oil level	None			

SQUIRES CONFINED HEAT TEST DATA

LUBRICANT AND TEST TEMP.	LUBRICANT PROPERTY	TEST HOURS						
		New Oil	48	96	144			
	Weight Loss, %		0.0	0.0	0.1			
0-87-3	COBRA Reading	16	5	8	9			
	Total Acid No.	0.13	2.42	4.46	5.57			
210°C	Viscosity @100°C,cs	4.02	4.05	4.08	4.09			
	Viscosity Change, %		0.7	1.5	1.7			
	Toluene Insol, % wt							
	Visual Appearance of Deposits		Slight stain at oil level	Slight stain at oil level	Slight stain at oil level			

LUBRICANT AND TEST TEMP.	LUBRICANT PROPERTY	TEST HOURS						
		New Oil						
	Weight Loss, %							
	COBRA Reading							
	Total Acid No.							
	Viscosity @100°C,cs							
	Viscosity Change, %							
	Toluene Insol, % wt							
	Visual Appearance of Deposits							

LUBRICANT AND TEST TEMP.	LUBRICANT PROPERTY	TEST HOURS						
		New Oil						
	Weight Loss, %							
	COBRA Reading							
	Total Acid No.							
	Viscosity @100°C,cs							
	Viscosity Change, %							
	Toluene Insol, % wt							
	Visual Appearance of Deposits							

TABLE A-3

AFAPL STATIC COKER TEST DATA

Test No.	Sample	Coker No.	Test Temp. °C	Test Time min.	Type Test Specimen	Sample Size gm	Deposit mg/gm Oil	Description of Deposit
739	O-86-2	1	315	180	Shim Stock	1.0367	24.8	Hard black glossy wavy deposit
740	O-86-2	2	315	180	Shim Stock	1.0209	21.9	Hard black glossy wavy deposit
741	O-86-2	3	315	180	Shim Stock	1.0271	29.5	Hard black glossy wavy deposit
742	O-86-2	4	315	180	Shim Stock	1.0480	24.0	Hard black glossy wavy deposit
743	O-86-2	1	315	180	Shim Stock	1.0149	28.4	Hard black glossy wavy flaky deposit
744	O-86-2	2	315	180	Shim Stock	1.0015	27.3	Hard black glossy wavy flaky deposit
745	O-86-2	3	315	180	Shim Stock	0.9862	23.7	Hard black glossy wavy flaky deposit
746	O-86-2	4	315	180	Shim Stock	1.0064	28.8	Hard black glossy wavy flaky deposit
747	OP-369	1	315	180	Shim Stock	1.0125	39.6	Hard black shiny wavy deposit
748	OP-369	2	315	180	Shim Stock	1.0121	41.1	Hard black shiny wavy deposit
749	OP-369	3	315	180	Shim Stock	1.0131	37.2	Hard black shiny wavy deposit
750	OP-369	4	315	180	Shim Stock	1.0282	39.3	Hard black shiny wavy deposit

AFAPL STATIC COKER TEST DATA

Test No.	Sample	Coker No.	Test Temp. °C	Test Time min.	Type Test Specimen	Sample Size gm	Deposit mg/gm Oil	Description of Deposit
751	OP-369	1	300	180	Shim Stock	1.0277	47.8	Hard black shiny wavy deposit
752	OP-369	2	300	180	Shim Stock	1.0225	43.2	Hard black shiny wavy deposit
753	OP-369	3	300	180	Shim Stock	0.9891	43.6	Hard black shiny wavy deposit
754	OP-369	4	300	180	Shim Stock	1.0022	45.1	Hard black shiny wavy deposit
755	OP-369	1	260	180	Shim Stock	1.0275	83.5	Hard brown to black shiny wavy deposit
756	OP-369	2	260	180	Shim Stock	1.0170	74.6	Hard brown to black shiny wavy deposit
757	OP-369	3	260	180	Shim Stock	0.9836	67.6	Seal leaked
758	OP-369	4	260	180	Shim Stock	0.9993	75.0	Hard brown to black shiny wavy deposit
759	OP-369	1	245	180	Shim Stock	0.9937	114.1	Hard brown to black shiny wavy deposit
760	OP-369	2	245	180	Shim Stock	0.9901	119.9	Hard brown to black shiny wavy deposit
761	OP-369	3	245	180	Shim Stock	0.9788	109.4	Hard brown to black shiny wavy deposit
762	OP-369	4	245	180	Shim Stock	1.0093	111.3	Hard brown to black shiny wavy deposit

AFAPL STATIC COKER TEST DATA

Test No.	Sample	Coker No.	Test Temp. °C	Test Time min.	Type Test Specimen	Sample Size gm	Deposit mg/gm Oil	Description of Deposit
763	OP-369	1	280	180	Shim Stock	0.9813	58.5	Hard black shiny wavy deposit
764	OP-369	2	280	180	Shim Stock	0.9878	56.0	Hard black shiny wavy deposit
765	OP-369	3	280	180	Shim Stock	0.9752	57.5	Hard black shiny wavy deposit
766	OP-369	4	280	180	Shim Stock	0.9991	55.5	Hard black shiny wavy deposit
767	O-79-16	1	315	180	Brass	0.9314	13.0	Hard black semi-glossy wavy deposit
768	O-79-16	2	315	180	Brass	0.9380	13.2	Hard black semi-glossy wavy deposit
769	O-79-16	3	315	180	Brass	0.9511	11.4	Hard black semi-glossy wavy deposit
770	O-79-16	4	315	180	Brass	0.9522	13.6	Hard black semi-glossy wavy deposit
771	O-82-2	1	315	180	Brass	0.9231	9.3	Hard brown to black semi-glossy wavy deposit
772	O-82-2	2	315	180	Brass	0.9345	12.2	Hard brown to black semi-glossy wavy deposit
773	O-82-2	3	315	180	Brass	0.9396	9.6	Hard brown to black semi-glossy wavy deposit
774	O-82-2	4	315	180	Brass	0.9447	14.8	Hard brown to black semi-glossy wavy deposit

AFAPL STATIC COKER TEST DATA

Test No.	Sample	Coker No.	Test Temp. °C	Test Time min.	Type Test Specimen	Sample Size gm	Deposit mg/gm Oil	Description of Deposit
775	RR-A	1	315	180	Shim Stock	1.0253	39.4	Hard black shiny wavy deposit
776	RR-A	2	315	180	Shim Stock	1.0782	34.1	Hard black shiny wavy deposit
777	RR-A	3	315	180	Shim Stock	1.0358	39.7	Controller problem
778	RR-A	4	315	180	Shim Stock	1.0191	36.7	Hard black shiny wavy deposit
779	RR-B	1	315	180	Shim Stock	0.9274	16.6	Hard black shiny wavy flaky deposit
780	RR-B	2	315	180	Shim Stock	0.9322	16.6	Hard black shiny wavy deposit
781	RR-B	3	315	180	Shim Stock	0.9409	15.5	Hard black shiny wavy flaky deposit
782	RR-B	4	315	180	Shim Stock	0.9547	15.6	Hard black shiny wavy flaky deposit
783	RR-C	1	315	180	Shim Stock	1.0170	34.7	Hard black shiny wavy deposit
784	RR-C	2	315	180	Shim Stock	1.0136	28.2	Hard black shiny wavy deposit
785	RR-C	3	315	180	Shim Stock	0.9679	26.9	Hard black shiny wavy deposit
786	RR-C	4	315	180	Shim Stock	0.9856	28.0	Hard black shiny wavy deposit

AFAPL STATIC COKER TEST DATA

Test No.	Sample	Coker No.	Test Temp. °C	Test Time min.	Type Test Specimen	Sample Size gm	Deposit mg/gm Oil	Description of Deposit
787	RR-D	1	315	180	Shim Stock	0.9858	14.7	Hard black shiny smooth deposit
788	RR-D	2	315	180	Shim Stock	0.9360	15.5	Hard black shiny smooth deposit
789	RR-D	3	315	180	Shim Stock	0.9452	11.4	Hard black shiny smooth deposit
790	RR-D	4	315	180	Shim Stock	0.9645	13.8	Hard black shiny smooth deposit
791	RR-E	1	315	180	Shim Stock	0.8225	29.7	Hard black wavy deposit
792	RR-E	2	315	180	Shim Stock	1.0293	34.7	Hard black wavy deposit
793	RR-E	3	315	180	Shim Stock	1.0069	31.5	Hard black wavy deposit
794	RR-E	4	315	180	Shim Stock	0.9776	34.6	Hard black wavy deposit
795	RR-F	1	315	180	Shim Stock	1.0742	33.5	Hard black shiny deposit
796	RR-F	2	315	180	Shim Stock	1.0502	33.6	Hard black shiny deposit
797	RR-F	3	315	180	Shim Stock	1.0433	30.3	Hard black shiny deposit
798	RR-F	4	315	180	Shim Stock	1.0179	35.4	Hard black shiny deposit

AFAPL STATIC COKER TEST DATA

Test No.	Sample	Coker No.	Test Temp. °C	Test Time min.	Type Test Specimen	Sample Size gm	Deposit mg/gm Oil	Description of Deposit
799	RR-G	1	315	180	Shim Stock	0.9772	8.6	Hard black thin smooth semi-glossy deposit
800	RR-G	2	315	180	Shim Stock	0.9376	8.6	Hard black thin smooth semi-glossy deposit
801	RR-G	3	315	180	Shim Stock	0.8657	8.2	Hard black thin smooth semi-glossy deposit
802	RR-G	4	315	180	Shim Stock	0.8733	6.8	Hard black thin smooth semi-glossy deposit
803	RR-H	1	315	180	Shim Stock	0.9519	36.2	Hard black shiny wavy deposit
804	RR-H	2	315	180	Shim Stock	0.9516	37.2	Hard black shiny wavy deposit
805	RR-H	3	315	180	Shim Stock	0.9649	33.4	Hard black shiny wavy deposit
806	RR-H	4	315	180	Shim Stock	0.9707	32.7	Hard black shiny wavy deposit
807	RR-E	1	315	180	Shim Stock	0.9453	8.0	Hard black shiny smooth deposit
808	RR-E	2	315	180	Shim Stock	0.9164	6.0	Hard black shiny smooth deposit
809	RR-E	3	315	180	Shim Stock	0.9221	6.3	Hard black shiny smooth deposit
810	RR-E	4	315	180	Shim Stock	0.8583	7.0	Hard black shiny smooth deposit

AFAPL STATIC COKER TEST DATA

Test No.	Sample	Coker No.	Test Temp. °C	Test Time min.	Type Test Specimen	Sample Size gm	Deposit mg/gm Oil	Description of Deposit
811	TEL-6031	1	315	360	Shim Stock	0.9343	15.3	Hard black very flaky deposit
812	TEL-6031	2	315	360	Shim Stock	0.9475	9.8	Hard black very flaky deposit
813	TEL-6031	3	315	360	Shim Stock	0.9668	13.0	Hard black very flaky deposit
814	TEL-6031	4	315	360	Shim Stock	0.9538	12.3	Hard black very flaky deposit
815	TEL-7042	1	315	180	Shim Stock	0.9905	34.8	Hard black shiny wavy deposit
816	TEL-7042	2	315	180	Shim Stock	0.9955	39.2	Vacuum malfunction
817	TEL-7042	3	315	180	Shim Stock	0.9911	31.9	Hard black shiny wavy deposit
818	TEL-7042	4	315	180	Shim Stock	1.0014	34.6	Hard black shiny wavy deposit
819	RR-E	1	315	180	Shim Stock	0.9115	8.0	Hard black smooth semi-glossy deposit
820	RR-E	2	315	180	Shim Stock	0.9072	8.8	Hard black smooth semi-glossy deposit
821	TEL-7042	3	315	180	Shim Stock	0.9887	36.3	Hard black shiny wavy deposit
822	TEL-7042	4	315	180	Shim Stock	0.9887	36.3	Hard black shiny wavy deposit

AFAPL STATIC COKER TEST DATA

Test No.	Sample	Coker No.	Test Temp. °C	Test Time min.	Type Test Specimen	Sample Size gm	Deposit mg/gm Oil	Description of Deposit
823	O-79-20	1	315	180	Brass	1.0359	17.0	Hard black shiny wavy deposit
824	O-79-20	2	315	180	Brass	0.9567	11.6	Hard black shiny wavy deposit
825	O-82-14	3	315	180	Brass	0.9670	16.9	Hard black shiny wavy slightly flaky deposit
826	O-82-14	4	315	180	Brass	0.9571	17.9	Hard black shiny very flaky deposit
827	TEL-7043	1	315	180	Shim Stock	1.0291	36.9	Hard black shiny wavy deposit
828	TEL-7043	2	315	180	Shim Stock	1.0135	34.2	Temperature suspect
829	O-71-6 Low TAN	3	315	180	Shim Stock	0.9174	25.0	Test suspect
830	O-71-6 Low TAN	4	315	180	Shim Stock	0.9627	26.7	Test suspect
831	O-71-6 Low TAN	1	315	180	Shim Stock	0.9886	30.8	Hard black shiny wavy deposit
832	O-71-6 Low TAN	2	315	180	Shim Stock	0.9912	33.8	Hard black shiny wavy deposit
833	TEL- 7043	3	315	180	Shim Stock	1.0239	28.3	Hard black shiny wavy deposit
834	TEL-7043	4	315	180	Shim Stock	1.0045	34.2	Hard black shiny wavy deposit

AFAPL STATIC COKER TEST DATA

Test No.	Sample	Coker No.	Test Temp. °C	Test Time min.	Type Test Specimen	Sample Size gm	Deposit mg/gm Oil	Description of Deposit
835	O-86-2 560 ppm Wear Part.	1	315	180	Shim Stock	0.9599	34.4	Hard black partially shiny wavy grainy deposit
836	O-86-2 560 ppm Wear Part.	2	315	180	Shim Stock	0.9047	25.4	Hard black partially shiny wavy grainy deposit
837	O-86-2 560 ppm Wear Part.	3	315	180	Shim Stock	0.9724	31.7	Hard black partially shiny wavy grainy deposit
838	O-86-2 560 ppm Wear Part.	4	315	180	Shim Stock	-	-	Balance problem
839	O-85-1	1	230	180	Shim Stock	0.9468	51.6	Sample contaminated
840	O-85-1	2	230	180	Shim Stock	0.9445	46.9	Dark brown sticky viscous deposit
841	O-85-1	3	230	180	Shim Stock	0.9689	46.4	Dark brown sticky viscous deposit
842	O-85-1	4	230	180	Shim Stock	0.9495	40.5	Dark brown sticky viscous deposit
843	O-85-1	1	215	180	Shim Stock	0.9545	75.0	Dark brown soft tacky tar-like deposit
844	O-85-1	2	215	180	Shim Stock	0.9630	87.7	Dark brown soft tacky tar-like deposit
845	O-85-1	3	215	180	Shim Stock	0.9531	64.2	Sample spilled
846	O-85-1	4	215	180	Shim Stock	0.9797	80.5	Dark brown soft tacky tar-like deposit

AFAPL STATIC COKER TEST DATA

Test No.	Sample	Coker No.	Test Temp. °C	Test Time min.	Type Test Specimen	Sample Size gm	Deposit mg/gm Oil	Description of Deposit
847	O-85-1	1	215	300	Shim Stock	0.9773	53.1	Deposits oily and tacky
848	O-85-1	2	215	300	Shim Stock	0.9993	43.9	Deposits oily and tacky
849	O-85-1	3	215	300	Shim Stock	1.0309	40.4	Deposits oily and tacky
850	O-85-1	4	215	300	Shim Stock	1.0417	44.3	Deposits oily and tacky
851	O-85-1	1	215	480	Shim Stock	0.9322	34.9	Tacky deposit
852	O-85-1	2	215	480	Shim Stock	0.9750	33.6	Tacky deposit
853	O-85-1	3	215	480	Shim Stock	0.9076	36.2	Tacky deposit
854	O-85-1	4	215	480	Shim Stock	0.9493	39.6	Tacky deposit
855	O-87-3	1	315	180	Shim Stock	0.9745	18.6	Hard black glossy wavy deposit
856	O-87-3	2	315	180	Shim Stock	0.9610	18.9	Hard black glossy wavy deposit
857	O-87-3	3	315	180	Shim Stock	0.9770	15.1	Hard black glossy wavy deposit
858	O-87-3	4	315	180	Shim Stock	0.9425	18.6	Hard black glossy wavy deposit

AFAPL STATIC COKER TEST DATA

Test No.	Sample	Coker No.	Test Temp. °C	Test Time min.	Type Test Specimen	Sample Size gm	Deposit mg/gm Oil	Description of Deposit
859	O-85-1	1	230	300	Shim Stock	0.9645	27.2	Tacky black non-uniform deposit
860	O-85-1	2	230	300	Shim Stock	1.0733	33.8	Tacky black non-uniform deposit
861	O-85-1	3	230	300	Shim Stock	1.0365	33.0	Tacky black non-uniform deposit
862	O-85-1	4	230	300	Shim Stock	0.9845	31.9	Tacky black non-uniform deposit
863	O-87-3	1	300	180	Shim Stock	0.9812	17.5	Hard black shiny wavy deposit
864	O-87-3	2	300	180	Shim Stock	0.9514	18.1	Hard black shiny wavy deposit
865	O-87-3	3	300	180	Shim Stock	0.9337	14.9	Hard black shiny wavy deposit
866	O-87-3	4	300	180	Shim Stock	0.9416	19.9	Hard black shiny wavy deposit
867	O-87-3	1	245	180	Shim Stock	0.9818	12.6	Tacky dark brown non-uniform deposit
868	O-87-3	2	245	180	Shim Stock	0.9426	8.0	Tacky dark brown non-uniform deposit
869	O-87-3	3	245	180	Shim Stock	0.9437	8.2	Tacky dark brown non-uniform deposit
870	O-87-3	4	245	180	Shim Stock	0.9446	8.0	Tacky dark brown non-uniform deposit

AFAPL STATIC COKER TEST DATA

Test No.	Sample	Coker No.	Test Temp. °C	Test Time min.	Type Test Specimen	Sample Size gm	Deposit mg/gm Oil	Description of Deposit
871	O-87-3	1	285	180	Shim Stock	0.9841	18.1	Hard dark brown to black shiny wavy deposit
872	O-87-3	2	285	180	Shim Stock	0.9564	17.6	Hard dark brown to black shiny wavy deposit
873	O-87-3	3	260	180	Shim Stock	0.9355	23.1	Dark brown soft non-uniform deposit
874	O-87-3	4	260	180	Shim Stock	0.9505	23.7	Dark brown soft non-uniform deposit
875	O-87-3	1	215	180	Shim Stock	0.9764	238.1	Viscous oil slightly darkened
876	O-87-3	2	215	180	Shim Stock	0.9445	270.1	Viscous oil slightly darkened
877	O-87-3	3	230	180	Shim Stock	0.9338	108.5	Very viscous oily residue dark spots
878	O-87-3	4	230	180	Shim Stock	0.9431	73.6	Part of the sample spilled
879	O-85-1	1	245	480	Shim Stock	1.0032	24.4	Hard dark brown non-uniform deposit
880	O-85-1	2	245	480	Shim Stock	0.9797	24.8	Hard dark brown non-uniform deposit
881	O-85-1	3	230	480	Shim Stock	0.9583	37.9	Soft brown non-uniform deposit
882	O-85-1	4	230	480	Shim Stock	0.9619	30.6	Soft brown non-uniform deposit

AFAPL STATIC COKER TEST DATA

Test No.	Sample	Coker No.	Test Temp. °C	Test Time min.	Type Test Specimen	Sample Size gm	Deposit mg/gm Oil	Description of Deposit
883	O-85-1	1	245	300	Shim Stock	0.9947	30.6	Hard dark brown shiny wavy deposit
884	O-85-1	2	245	300	Shim Stock	0.9748	30.8	Hard dark brown shiny wavy deposit
885	O-85-1	3	300	300	Shim Stock	0.9550	25.1	Hard black shiny wavy deposit
886	O-85-1	4	300	300	Shim Stock	0.9603	25.4	Hard black shiny wavy deposit
887	O-87-3	1	245	300	Shim Stock	0.9813	7.4	Soft dark brown non-uniform deposit
888	O-87-3	2	245	300	Shim Stock	0.9514	6.3	Soft dark brown non-uniform deposit
889	O-87-3	3	315	300	Shim Stock	0.9660	24.5	Hard black shiny wavy deposit
890	O-85-1	4	315	300	Shim Stock	0.9660	25.4	Hard black shiny wavy deposit
891	O-85-1	1	300	480	Shim Stock	1.0331	27.0	Hard black shiny wavy deposit
892	O-85-1	2	300	480	Shim Stock	0.9425	24.1	Hard black shiny wavy deposit
893	O-85-1	3	315	480	Shim Stock	0.9932	21.2	Hard black shiny wavy deposit
894	O-85-1	4	315	480	Shim Stock	1.0047	23.4	Hard black shiny wavy deposit

AFAPL STATIC COKER TEST DATA

Test No.	Sample	Coker No.	Test Temp. °C	Test Time min.	Type Test Specimen	Sample Size gm	Deposit mg/gm Oil	Description of Deposit
895	O-85-1	1	260	300	Shim Stock	1.0700	39.3	Hard dark brown shiny wavy deposit
896	O-85-1	2	260	300	Shim Stock	1.0383	33.1	Hard dark brown shiny wavy deposit
897	O-85-1	3	260	480	Shim Stock	1.0155	28.3	Hard dark brown shiny wavy deposit
898	O-85-1	4	260	480	Shim Stock	0.9998	26.9	Hard dark brown shiny wavy deposit
899	O-85-1	1	260	180	Shim Stock	0.9948	37.9	Hard dark brown shiny wavy deposit
900	O-85-1	2	260	180	Shim Stock	0.9701	39.0	Hard dark brown shiny wavy deposit
901	O-87-3	3	260	180	Shim Stock	0.9444	25.3	Hard dark brown shiny wavy deposit
902	O-87-3	4	260	180	Shim Stock	0.9412	26.7	Hard dark brown shiny wavy deposit
903	O-85-1 48 CH 205 C	1	315	180	Shim Stock	0.9813	28.9	Hard black shiny wavy deposit
904	O-85-1 48 CH 205 C	2	315	180	Shim Stock	0.8626	27.8	Hard black shiny wavy deposit
905	O-85-1 96 CH 205 C	3	315	180	Shim Stock	0.9778	20.5	Seal leaked
906	O-85-1 96 CH 205 C	4	315	180	Shim Stock	0.9587	29.5	Hard black shiny wavy deposit

AFAPL STATIC COKER TEST DATA

Test No.	Sample	Coker No.	Test Temp. °C	Test Time min.	Type Test Specimen	Sample Size gm	Deposit mg/gm Oil	Description of Deposit
907	O-85-1 48 OX 205 C	1	315	180	Shim Stock	0.9702	33.5	Hard black shiny wavy deposit
908	O-85-1 48 OX 205 C	2	315	180	Shim Stock	0.9942	32.1	Hard black shiny wavy deposit
909	O-85-1 168 OX 205 C	3	315	180	Shim Stock	0.9687	45.2	Hard black shiny wavy deposit
910	O-85-1 168 OX 205 C	4	315	180	Shim Stock	1.0069	48.4	Hard black shiny wavy deposit
911	O-85-1	1	260	300	Shim Stock	1.0275	29.3	Hard dark brown to black shiny wavy deposit
912	O-85-1	2	260	300	Shim Stock	0.9818	30.4	Hard dark brown to black shiny wavy deposit
913	O-85-1	3	230	480	Shim Stock	0.9516	33.4	Soft brown non-uniform deposit
914	O-85-1	4	230	480	Shim Stock	0.9863	33.3	Soft brown non-uniform deposit
915	O-85-1	1	215	960	Shim Stock	0.9920	41.8	Brown to black very tacky deposit
916	O-85-1	2	215	960	Shim Stock	0.9788	42.3	Brown to black very tacky deposit
917	O-85-1	3	215	960	Shim Stock	0.9868	41.4	Brown to black very tacky deposit
918	O-85-1	4	215	960	Shim Stock	0.9989	33.9	Brown to black very tacky deposit

AFAPL STATIC COKER TEST DATA

Test No.	Sample	Coker No.	Test Temp. °C	Test Time min.	Type Test Specimen	Sample Size gm	Deposit mg/gm Oil	Description of Deposit
919	O-85-1	1	245	960	Shim Stock	0.9882	18.1	Hard brown to black deposit
920	O-85-1	2	245	960	Shim Stock	0.9611	18.5	Hard brown to black deposit
921	O-85-1	3	260	960	Shim Stock	0.9837	19.8	Hard brown to black deposit
922	O-85-1	4	260	960	Shim Stock	0.9904	26.3	Hard brown to black deposit
923	O-87-3	1	300	300	Shim Stock	1.1536	15.9	Hard black deposit
924	O-87-3	2	300	300	Shim Stock	0.9534	18.1	Hard black deposit
925	O-87-3	3	315	300	Shim Stock	0.9684	12.4	Hard black deposit
926	O-87-3	4	315	300	Shim Stock	0.9649	15.0	Hard black deposit
927	O-85-1	1	300	960	Shim Stock	0.9733	18.4	Hard black deposit
928	O-85-1	2	300	960	Shim Stock	0.9895	19.9	Hard black deposit
929	O-85-1	3	315	960	Shim Stock	1.0052	15.6	Hard black deposit
930	O-85-1	4	315	960	Shim Stock	1.0056	19.1	Hard black deposit

AFAPL STATIC COKER TEST DATA

Test No.	Sample	Coker No.	Test Temp. °C	Test Time min.	Type Test Specimen	Sample Size gm	Deposit mg/gm Oil	Description of Deposit
931	O-87-3	1	230	300	Shim Stock	0.9800	9.0	Soft dark brown tacky deposit
932	O-87-3	2	230	300	Shim Stock	0.9558	8.3	Soft dark brown tacky deposit
933	O-87-3	3	215	300	Shim Stock	0.9683	6.1	Oily dark brown deposit
934	O-87-3	4	215	300	Shim Stock	0.9621	7.5	Oily dark brown deposit
935	O-85-1	1	230	960	Shim Stock	0.9936	23.1	Hard dark brown non-uniform deposit
936	O-85-1	2	230	960	Shim Stock	0.9940	21.9	Hard dark brown non-uniform deposit
937	O-85-1	3	230	960	Shim Stock	1.0113	18.1	Deposit loss on removal
938	O-85-1	4	230	960	Shim Stock	1.0121	24.3	Hard dark brown non-uniform deposit
939	O-87-3	1	260	300	Shim Stock	0.9541	20.1	Hard brown to black shiny wavy deposit
940	O-87-3	2	260	300	Shim Stock	0.9562	18.6	Hard brown to black shiny wavy deposit
941	O-87-3	3	285	300	Shim Stock	0.9712	16.7	Hard black shiny wavy deposit
942	O-87-3	4	285	300	Shim Stock	0.9770	19.0	Hard black shiny wavy deposit

AFAPL STATIC COKER TEST DATA

Test No.	Sample	Coker No.	Test Temp. °C	Test Time min.	Type Test Specimen	Sample Size gm	Deposit mg/gm Oil	Description of Deposit
943	O-67-1 Teflon Seal	1	355	300	Shim Stock	0.2774	11.5	Very soft light gold to brown deposit
944	O-67-1 Teflon Seal	2	355	300	Shim Stock	0.3158	10.8	Very soft light gold to brown deposit
945	O-67-1 Stainless Steel Seal	3	355	300	Shim Stock	0.3300	6.4	Very soft light gold to brown deposit
946	O-67-1 Stainless Steel Seal	4	355	300	Shim Stock	0.2488	10.4	Very soft light gold to brown deposit
947	O-67-1 Teflon Seal	1	355	300	Shim Stock	0.6076	3.5	Very soft light golden deposit
948	O-67-1 Teflon Seal	2	355	300	Shim Stock	0.6255	3.7	Very soft light golden deposit
949	O-67-1 Stainless Steel Seal	3	355	300	Shim Stock	0.6293	3.0	Very soft light golden deposit
950	O-67-1 Stainless Steel Seal	4	355	300	Shim Stock	0.6085	3.1	Very soft light golden deposit
951	O-67-1 240 O/C 320 C Tef.	1	355	300	Shim Stock	0.3166	30.0	Hard brown to black shiny wavy non-uniform deposit
952	O-67-1 240 O/C 320 C Tef.	2	355	300	Shim Stock	0.3097	27.4	Hard brown to black shiny wavy non-uniform deposit
953	O-67-1 240 O/C 320 C S.S.	3	355	300	Shim Stock	0.2811	11.4	Thin gray to black non-uniform deposit and coke to varnish on seal
954	O-67-1 240 O/C 320 C S.S.	4	355	300	Shim Stock	0.2655	10.5	Thin gray to black non-uniform deposit and coke to varnish on seal

AFAPL STATIC COKER TEST DATA

Test No.	Sample	Coker No.	Test Temp. °C	Test Time min.	Type Test Specimen	Sample Size gm	Deposit mg/gm Oil	Description of Deposit
955	O-67-1 168 O/C 320 C Tef.	1	355	300	Shim Stock	0.2967	15.5	Hard dark gray thin non-uniform deposit
956	O-67-1 168 O/C 320 C Tef.	2	355	300	Shim Stock	0.2889	14.2	Hard light to dark gray thin non-uniform deposit
957	O-67-1 168 O/C 320 C S.S.	3	355	300	Shim Stock	0.2843	7.4	Light to dark gray very thin deposit
958	O-67-1 168 O/C 320 C S.S.	4	355	300	Shim Stock	0.2660	10.9	Light to dark gray gold very thin deposit
959	O-87-3	1	245	480	Shim Stock	0.9425	21.1	Hard dark brown to black shiny wavy deposit
960	O-87-3	2	245	480	Shim Stock	0.9666	18.6	Hard dark brown to black shiny wavy deposit
961	O-87-3	3	260	480	Shim Stock	0.9902	15.6	Hard dark brown to black shiny wavy deposit
962	O-87-3	4	260	480	Shim Stock	0.9530	18.4	Hard dark brown to black shiny wavy deposit
963	O-87-3	1	215	480	Shim Stock	0.9606	4.3	Thin brown tacky uniform deposit
964	O-87-3	2	215	480	Shim Stock	0.8911	8.5	Thin brown tacky uniform deposit
965	O-87-3	3	230	480	Shim Stock	0.9759	4.4	Thin light to dark brown hard non-uniform deposit
966	O-87-3	4	230	480	Shim Stock	0.9749	5.1	Thin light to dark brown hard non-uniform deposit

AFAPL STATIC COKER TEST DATA

Test No.	Sample	Coker No.	Test Temp. °C	Test Time min.	Type Test Specimen	Sample Size gm	Deposit mg/gm Oil	Description of Deposit
967	0-87-3	1	245	480	Shim Stock	0.9852	17.6	Hard dark brown to black uneven deposits
968	0-87-3	2	245	480	Shim Stock	0.9333	13.3	Seal leaked
969	0-87-3	3	285	480	Shim Stock	1.0013	12.0	Seal leaked
970	0-87-3	4	285	480	Shim Stock	0.9522	15.8	Hard dark brown to black uneven deposits
971	0-87-3	1	245	180	Shim Stock	0.9474	38.1	Soft slightly tacky dark brown non-uniform deposit
972	0-87-3	2	245	180	Shim Stock	0.9445	37.6	Soft slightly tacky dark brown non-uniform deposit
973	0-87-3	3	245	300	Shim Stock	0.9865	26.3	Soft dark brown non-uniform deposit
974	0-87-3	4	245	300	Shim Stock	0.9519	23.4	Soft dark brown non-uniform deposit
975	0-87-3	1	215	300	Shim Stock	0.9459	40.9	Oily light to dark brown deposit
976	0-87-3	2	215	300	Shim Stock	0.9437	44.8	Oily light to dark brown deposit
977	0-87-3	3	230	300	Shim Stock	1.0064	10.2	Tacky light brown to dark brown deposit
978	0-87-3	4	230	300	Shim Stock	0.9545	9.7	Tacky light brown to dark brown deposit

AFAPL STATIC COKER TEST DATA

Test No.	Sample	Coker No.	Test Temp. °C	Test Time min.	Type Test Specimen	Sample Size gm	Deposit mg/gm Oil	Description of Deposit
979	O-87-3	1	300	480	Shim Stock	0.9438	11.1	Hard black shiny wavy deposit
980	O-87-3	2	300	480	Shim Stock	0.9378	9.7	Hard black shiny wavy deposit
981	O-87-3	3	315	480	Shim Stock	0.9996	8.2	Hard black shiny wavy deposit
982	O-87-3	4	315	480	Shim Stock	1.0001	13.4	Hard black shiny wavy deposit
983	O-87-3	1	230	300	Shim Stock	0.9229	5.1	Tacky light to dark brown non-uniform deposit
984	O-87-3	2	230	300	Shim Stock	0.9217	6.0	Tacky light to dark brown non-uniform deposit
985	O-87-3	3	230	300	Shim Stock	0.9497	7.5	Tacky light to dark brown non-uniform deposit
986	O-87-3	4	230	300	Shim Stock	0.9752	9.4	Tacky light to dark brown non-uniform deposit
987	O-85-1 72 OX 215 C	1	315	180	Shim Stock	1.0078	39.4	Hard black shiny wavy deposit
988	O-85-1 72 OX 215 C	2	315	180	Shim Stock	0.9799	37.0	Hard black shiny wavy deposit
989	O-85-1 72 OX w/CR 215 C	3	315	180	Shim Stock	1.0126	20.6	Hard black shiny wavy deposit
990	O-85-1 72 OX w/CR 215 C	4	315	180	Shim Stock	1.0013	24.8	Hard black shiny wavy deposit

AFAPL STATIC COKER TEST DATA

Test No.	Sample	Coker No.	Test Temp. °C	Test Time min.	Type Test Specimen	Sample Size gm	Deposit mg/gm Oil	Description of Deposit
991	D-87-3	1	215	300	Shim Stock	0.9163	22.4	Light to dark brown oily and tacky deposit
992	D-87-3	2	215	300	Shim Stock	0.9403	7.0	Light to dark brown oily and tacky deposit
993	D-87-3	3	215	300	Shim Stock	0.9480	27.9	Light to dark brown very oily deposit
994	D-87-3	4	215	300	Shim Stock	0.9790	9.(	Light to dark brown oily and tacky deposit
995	D-87-3	1	215	300	Shim Stock	0.9459	36.7	Light to dark brown oil and deposit
996	D-87-3	2	215	300	Shim Stock	0.9434	9.2	Light to dark brown oil and deposit
997	D-87-3	3	215	300	Shim Stock	0.9527	44.5	Light to dark brown oil and deposit
998	D-87-3	4	215	300	Shim Stock	0.9831	28.9	Light to dark brown oil and deposit
999	D-87-3	1	215	300	Shim Stock	0.9515	27.8	Light to dark brown oily and tacky deposit
1000	D-87-3	2	215	300	Shim Stock	0.9399	12.2	Light to dark brown oily and tacky deposit
1001	D-87-3	3	215	300	Shim Stock	0.9585	53.0	Light to dark brown oily and tacky deposit
1002	D-87-3	4	215	300	Shim Stock	0.9840	38.3	Light to dark brown oily and tacky deposit

AFAPL STATIC COKER TEST DATA

Test No.	Sample	Coker No.	Test Temp. °C	Test Time min.	Type Test Specimen	Sample Size gm	Deposit mg/gm Oil	Description of Deposit
1003	D-79-18 24 CH 205 C	1	315	180	Shim Stock	1.0018	44.4	Hard black shiny wavy deposit
1004	D-79-18 24 CH 205 C	2	315	180	Shim Stock	0.9828	41.2	Temperature suspect
1005	D-79-18 72 CH 205 C	3	315	180	Shim Stock	1.0133	43.3	Hard black shiny wavy deposit
1006	D-79-18 72 CH 205 C	4	315	180	Shim Stock	0.9833	43.6	Hard black shiny wavy deposit
1007	D-79-18 168 OX 205 C	1	315	180	Shim Stock	0.9475	57.8	Hard black shiny wavy deposit
1008	D-79-18 168 OX 205 C	2	315	180	Shim Stock	0.9266	60.2	Hard black shiny wavy deposit
1009	D-79-18 24 OX w/CR 215 C	3	315	180	Shim Stock	1.0039	46.9	Hard black shiny wavy deposit
1010	D-79-18 24 OX w/CR 215 C	4	315	180	Shim Stock	0.9891	44.9	Hard black shiny wavy deposit

TABLE A-4

MCRT COKING TEST DATA

Test No.	Sample	Test Temp. °C	Test Time Hrs	Sample Size g.	Deposit Ave. Percent	Std. Dev.	Notes
1	O-79-18	275	30	0.5	23.12	0.63	No drier on air line
2	O-79-18	275	30	0.5	24.06	0.54	No drier on air line
3	RR-A	275	30	0.5	27.11	0.15	No drier on air line
4	RR-A	275	30	0.5	27.37	0.19	
5	RR-B	275	30	0.5	13.70	0.35	
6	RR-C	275	30	0.5	25.69	0.23	
7	RR-D	275	30	0.5	12.08	0.39	
8	RR-E	275	30	0.5	9.68	0.19	
9	RR-F	275	30	0.5	22.16	0.29	
10	RR-G	275	30	0.5	11.98	0.20	11 determinations
11	RR-H	275	30	0.5	24.56	0.36	
12	TEL-6031	275	30	0.5	18.42	0.41	

MCRT COKING TEST DATA

Test No.	Sample	Test Temp. °C	Test Time Hrs	Sample Size g.	Deposit Ave. Percent	Std. Dev.	Notes
13	TEL-6032	275	30	0.5	12.16	0.24	
14	O-71-6	275	30	0.5	21.67	0.35	11 determinations, Unused oil with high TAN.
15	TEL-7042	275	30	0.5	21.92	0.40	
16	O-77-15	275	30	0.5	24.20	0.58	10 determinations
17	OP-369	275	30	0.5	26.95	0.36	
18	O-79-16	275	30	0.5	12.51	0.29	
19	O-85-1	275	30	0.5	14.81	0.48	
20	O-79-17	275	30	0.5	10.11	0.23	
21	O-71-6	275	30	0.5	21.95	0.29	Low TAN
22	TEL-7043	275	30	0.5	22.05	0.41	
23	O-79-20	275	30	0.5	11.44	0.46	
24	O-82-3	275	30	0.5	7.37	0.35	

MCRT COKING TEST DATA

Test No.	Sample	Test Temp. °C	Test Time Hrs	Sample Size g.	Deposit Ave. Percent	Std. Dev.	Notes
25	0-82-14	275	30	0.5	18.51	0.47	
26	0-82-2	275	30	0.5	17.28	0.33	
27	0-86-2	275	30	0.5	15.25	0.50	
28	0-79-16, 48 hrs. CH @ 205 C	275	30	0.5	12.76	0.33	6 determinations
29	0-82-14, 48 hrs. CH @ 205 C	275	30	0.5	20.74	0.34	6 determinations
30	0-77-15, 48 hrs. CH @ 205 C	275	30	0.5	25.43	0.39	6 determinations
31	0-79-18, 48 hrs. CH @ 205 C	275	30	0.5	28.01	0.96	6 determinations
32	0-79-16, 24 hrs. OX @ 205 C	275	30	0.5	15.20	0.53	6 determinations
33	0-82-14, 24 hrs. OX @ 205 C	275	30	0.5	20.41	0.33	6 determinations
34	0-77-15, 24 hrs. OX @ 205 C	275	30	0.5	26.96	0.22	6 determinations
35	0-79-18, 24 hrs. OX @ 205 C	275	30	0.5	27.84	0.65	6 determinations
36	0-86-2 plus 500 ppm P.D.D. Wear Debris	275	30	0.5	16.71	0.26	

MCRT COKING TEST DATA

Test No.	Sample	Test Temp. °C	Test Time Hrs	Sample Size g.	Deposit Ave. Percent	Std. Dev.	Notes
37	O-87-3	275	30	0.5	16.72	0.78	11 determinations
38	O-87-3	275	30	0.5	16.73	1.10	
39	O-85-1, 48 hr CH 205 C	275	30	0.5	15.22	0.35	6 determinations
40	O-85-1, 96 hr CH 205 C	275	30	0.5	15.48	0.42	6 determinations
41	O-85-1, 48 hr OX 205 C	275	30	0.5	16.09	0.18	6 determinations
42	O-85-1, 168 hr OX 205 C	275	30	0.5	19.04	0.50	6 determinations
43	O-79-18, 168 hr OX 205 C	275	30	0.5	27.62	0.30	6 determinations
44	O-79-18, 72 hr CH 205 C	275	30	0.5	26.75	0.68	6 determinations
45	O-79-18, 24 hr OX 215 C W/CR	275	30	0.5	25.62	0.68	6 determinations
46	O-85-1, 72 hr OX 215 C W/CR	275	30	0.5	13.58	0.44	6 determinations
47	O-85-1, 72 hr OX 215 C W/CR	275	30	0.5	13.58	0.28	
48	O-79-18, 24 hr OX 215 C	275	30	0.5	26.71	0.55	11 determinations

MCRT COKING TEST DATA

Test No.	Sample	Test Temp. °C	Test Time Hrs	Sample Size g.	Deposit Ave. Percent	Std. Dev.	Notes
49	O-85-1, 72 hrs., OX @ 215 C	275	30	0.5	18.51	0.39	6 determinations
50	O-79-18, 48 hrs., OX @ 205 C	275	30	0.5	27.41	1.09	6 determinations
51	O-79-18, 48 hrs. CH @ 205 C	275	30	0.5	28.82	0.38	6 determinations
52	O-79-20, 48 hrs. CH @ 205 C	275	30	0.5	13.86	0.45	6 determinations
53	O-82-2 48 hrs. CH @ 205 C	275	30	0.5	19.83	0.25	6 determinations
54	O-82-3 48 hrs. CH @ 205 C	275	30	0.5	9.24	0.31	6 determinations
55	O-77-15 24 hrs. CH @ 205 C	275	30	0.5	25.13	0.45	6 determinations
56	O-79-20 48 hrs. OX @ 205 C	275	30	0.5	15.71	0.40	6 determinations
57	O-79-17 48 hrs. CH @ 201 C	275	30	0.5	11.73	0.35	6 determinations
58	O-79-17 48 hrs. OX @ 205 C	275	30	0.5	14.69	0.37	6 determinations
59	O-79-18 168 hrs. OX @ 205 C	275	30	0.5	27.49	0.36	6 determinations
60	O-79-18 24 hrs. OX w/CR @ 215 C	275	30	0.5	24.48	0.48	6 determinations

MCRT COKING TEST DATA

Test No.	Sample	Test Temp. °C	Test Time Hrs	Sample Size g.	Deposit Ave. Percent	Std. Dev.	Notes
61	O-82-2 48 hrs. OX @ 205 C	275	30	0.5	22.89	0.37	6 determinations
62	O-82-3 48 hrs. OX @ 205 C	275	30	0.5	15.81	0.54	6 determinations
63	O-67-1 168 hrs. O/C @ 320 C	350	30	0.5	4.32	0.29	6 determinations
64	O-67-1 240 hrs. O/C @ 320 C	350	30	0.5	8.69	1.44	6 determinations
65	O-67-1	350	30	0.5	2.39	0.52	6 determinations
66	O-67-1 Can B, Top	375	30	0.5	1.15	0.05	11 determinations

TABLE A-5

LUBRICANT FOAMING TEST DATA

Test No	Test Lubricant	Type Air Diffuser	Test Cylinder Size (ml)	Sample Volume (ml)	Oil Volume at Maximum Foam Height (ml)	Foam Volume (ml)	Foam Collapse Time (sec)
202	O-79-17 3ppm DC-200,500cs	ASTM-1A	500	200	230[a] (225)[b]	180[a] (60)[b]	67[a] (64)[b]
203	O-79-17 3ppm DC-200,500cs	ASTM-1A	250	25	10 (40)	102 (16)	22 (11)
204	O-79-17 3ppm DC-200,500cs	13/16" Sparger #1 (5 micron)	250	25	14 (38)	88 (18)	38 (-)
205	O-79-17 3ppm DC-200,500cs	11/16" Sparger (5 micron)	250	25	34 (34)	20 (10)	14 (8)
206	O-79-17 3ppm DC-200,500cs	ASTM-1A	500	200	218 (220)	210 (100)	50 (32)
207	O-79-17 3ppm DC-200,500cs	ASTM-1A	250	25	32 (36)	24 (6)	23 (8)
208	O-79-17 3ppm DC-200,500cs	13/16" Sparger (5 micron)	250	25	10 (34)	102 (22)	40 (32)
209	O-79-17 3ppm DC-200,500cs	11/16" Sparger (5 micron)	250	25	36 (34)	18 (6)	14 (8)
210	O-79-17 3ppm DC-200,500cs	ASTM-1A	500	200	215 (220)	185 (110)	50 (35)
211	O-79-17 3ppm DC-200,500cs	ASTM-1A	250	25	34 (34)	68 (28)	18 (9)
212	O-79-17 3ppm DC-200,500cs	13/16" Sparger (5 micron)	250	25	12 (30)	88 (30)	37 (24)
213	O-79-17 3ppm DC-200,500cs	11/16" Sparger (5 micron)	250	25	38 (38)	22 (8)	31 (8)

a - Airflow of 1000 cc/minute
b - Airflow of 500 cc/minute

LUBRICANT FOAMING TEST DATA

Test No	Test Lubricant	Type Air Diffuser	Test Cylinder Size (ml)	Sample Volume (ml)	Oil Volume at Maximum Foam Height (ml)	Foam Volume (ml)	Foam Collapse Time (sec)
214	O-79-17 3ppm DC-200,500cs	ASTM-1A	250	25	30[a] (36)[b]	54[a] (12)[b]	16[a] (10)[b]
215	O-76-1 3ppm DC-200,20cSt	ASTM-1A	250	25	36 (36)	22 (10)	29 (25)
216	O-76-1 3ppm DC-200,20cSt	13/16" Sparger (5 micron)	250	25	32 (28)	28 (20)	48 (38)
217	O-76-1 3ppm DC-200,20cSt	11/16" Sparger (5 micron)	250	25	34 (32)	10 (8)	10 (8)
218	O-76-1 3ppm DC-200,20cSt	ASTM-1A	250	25	38 (38)	20 (10)	35 (-)
219	O-76-1 3ppm DC-200,20cSt	13/16" Sparger (5 micron)	250	25	28 (32)	28 (10)	35 (27)
220	O-76-1 3ppm DC-200,20cSt	11/16" Sparger (5 micron)	250	25	32 (32)	18 (8)	26 (21)
221	O-76-1 3ppm DC-200,20cSt	13/16" Sparger (5 micron)	250	25	34 (32)	22 (14)	32 (25)
222	O-76-1 3ppm DC-200,20cSt	ASTM-1A	250	25	18 (32)	56 (18)	32 (27)
223	O-76-1 3ppm DC-200,20cSt	11/16" Sparger (5 micron)	250	25	32 (32)	16 (10)	34 (25)
224	O-76-5 1.5% PANA 1.5% TCP	13/16" Sparger (5 micron)	250	25	10 (18)	134 (54)	6 (6)
225	O-76-5 1.5% PANA 1.5% TCP	ASTM-1A	250	25	10 (32)	114 (34)	4 (3)

a - Airflow of 1000 cc/minute
b - Airflow of 500 cc/minute

LUBRICANT FOAMING TEST DATA

Test No	Test Lubricant	Type Air Diffuser	Test Cylinder Size (ml)	Sample Volume (ml)	Oil Volume at Maximum Foam Height (ml)	Foam Volume (ml)	Foam Collapse Time (sec)
226	O-76-5 1.5% PANA 1.5% TCP	ASTM-1A	250	25	12[a] (28)[b]	112[a] (34)[b]	4[a] (3)[b]
227	O-76-5 1.5% PANA 1.5% TCP	ASTM-1A	500	200	25	295	70
228	O-76-5 1.5% PANA 1.5% TCP	13/16" Sparger (5 micron)	500	200	235	295	10
229	O-76-5 1.5% PANA 1.5% TCP	13/16" Sparger (5 micron)	500	200	245	315	15
230	O-76-5 1.5% PANA 1.5% TCP	ASTM-1A	500	200	350	325	34
231	O-76-5 1.5% PANA 1.5% TCP	13/16" Sparger (5 micron)	250	25	10	126	5
232	O-76-5 1.5% PANA 1.5% TCP	11/16" Sparger (5 micron)	250	25	72 (48)	58 (16)	5 (4)
233	O-67-21	ASTM-1A	500	200	25	>500	-
234	O-67-21	13/16" Sparger (5 micron)	250	25	10	176	33
235	O-67-21	ASTM-1A	250	25	6	166 (102)	92 (73)
236	O-67-21	11/16" Sparger (5 micron)	250	25	8	142 (74)	70 (54)
237	75% O-67-21 + 25% O-79-17	ASTM-1A	500	200	25 (215)	465 (80)	56 (49)

a - Airflow of 1000 cc/minute
b - Airflow of 500 cc/minute

LUBRICANT FOAMING TEST DATA

Test No	Test Lubricant	Type Air Diffuser	Test Cylinder Size (ml)	Sample Volume (ml)	Oil Volume at Maximum Foam Height (ml)	Foam Volume (ml)	Foam Collapse Time (sec)
238	75% O-67-21 + 25% O-79-17	13/16" Sparger (5 micron)	250	25	6[a] (12)[b]	176[a] (80)[b]	64[a] (53)[b]
239	75% O-67-21 + 25% O-79-17	11/16" Sparger (5 micron)	250	25	8 (16)	144 (54)	54 (52)
240	O-82-2	ASTM-1A	500	200	255	10	5
241	O-82-2	13/16" Sparger (5 micron)	250	25	14	62	12
242	O-79-20	ASTM-1A	500	200	255	20	6
243	O-79-20	13/16" Sparger (5 micron)	250	25	16 (40)	62 (10)	6 (3)
244	O-79-17 (3ppm DC-200-500cs	ASTM-1A	500	200	225	195	56
245	O-76-1 (3ppm DC-200-20cs)	ASTM-1A	500	200	225	150	46
246	O-76-5 1.5% PANA 1.5% TCP	ASTM-1A	500	200	255	310	6
247	O-76-5 1.5% PANA 1.5% TCP	ASTM-1A	500	200	255	310	13
248	O-79-16	ASTM-1A	500	200	260	50	5
249	O-79-16	13/16" Sparger (5 micron)	250	25	10	98	5

a - Airflow of 1000 cc/minute
b - Airflow of 500 cc/minute

LUBRICANT FOAMING TEST DATA

Test No	Test Lubricant	Type Air Diffuser	Test Cylinder Size (ml)	Sample Volume (ml)	Oil Volume at Maximum Foam Height (ml)	Foam Volume (ml)	Foam Collapse Time (sec)
250	O-82-3	ASTM-1A	500	200	245[a] / 0[b]	15[a] / [b]	4[a] / [b]
251	O-82-3	13/16" Sparger (5 micron)	250	25	40	12	4
252	O-82-14	ASTM-1A	500	200	245	105	10
253	O-82-14	13/16" Sparger (5 micron)	250	25	10	136	11
254	O-79-20	11/16" Sparger (5 micron)	250	25	34	14	15
255	O-82-14	13/16"Sparger (5 micron)	500	200	240 (235)	120 (20)	16 (20)
256	O-79-16	ASTM-1A	250	25	10 (32)	88 (28)	9 (7)

a - Airflow of 1000 cc/minute
b - Airflow of 500 cc/minute

TABLE A-6

VARIABLE AIRFLOW FOAMING TEST DATA

Test No	Lubricant	Type Air Diffuser	Sample Volume (ml)	Airflow Rate (cc/min)	Oil Volume at Maximum Foam Height (ml)	Foam Volume (ml)	Remarks
1	O-76-5 1.5% PANA 1.5% TCP	13/16" Sparger (5 micron)	25	1000	10	110	Foam
"	"	"	"	800	12	88	"
"	"	"	"	600	14	66	"
"	"	"	"	400	20	38	"
2	O-82-2	"	25	1000	20	44	All Aeration
"	"	"	"	900	38	22	Oil/foam interface
"	"	"	"	800	38	14	"
"	"	"	"	500	38	10	"
3	O-82-2	11/16" Sparger (5 micron)	"	1000	32	24	Oil/foam interface
"	"	"	"	900	32	16	"
"	"	"	"	800	34	14	"
"	"	"	"	500	32	10	"

VARIABLE AIRFLOW FOAMING TEST DATA

Test No	Lubricant	Type Air Diffuser	Sample Volume (ml)	Airflow Rate (cc/min)	Oil Volume at Maximum Foam Height (ml)	Foam Volume (ml)	Remarks
4	0-79-20	ASTM # 1A	200	1200	205	20	-
"	"	"	"	1000	260	20	-
5	0-82-14	13/16" Sparger (5 micron)	25	1000	10	128	All foam and aeration
"	"	"	"	900	12	114	"
"	"	"	"	800	12	98	"
"	"	"	"	500	36	28	Oil/foam interface
6	0-82-14	11/16" Sparger (5 micron)	25	1000	10	114	All foam and aeration
"	"	"	"	800	12	90	"
"	"	"	"	500	30	28	Oil/foam interface
7	0-79-20	13/16" Sparger (5 micron)	25	1000	18	50	All foam and aeration
"	"	"	"	800	40	14	Oil/foam interface
"	"	"	"	500	46	8	"

VARIABLE AIRFLOW FOAMING TEST DATA

Test No	Lubricant	Type Air Diffuser	Sample Volume (ml)	Airflow Rate (cc/min)	Oil Volume at Maximum Foam Height (ml)	Foam Volume (ml)	Remarks
8	0-82-14	ASTM # 1A	200	1100	195	270	Oil/foam interface
"	"	"	"	1000	250	100	"
"	"	"	"	800	250	40	"
"	"	"	"	500	240	20	"
9	0-79-16	11/16" Sparger (5 micron)	25	1000	12	94	All foam and aeration
"	"	"	"	800	16	66	"
"	"	"	"	500	30	22	Oil/foam interface
10	0-79-16	13/16" Sparger (5 micron)	"	1000	10	118	All foam and aeration
"	"	"	"	800	14	80	Oil/foam interface questionable
"	"	"	"	500	20	40	Oil/foam interface
"	0-82-2	ASTM # 1A	25	1000	30	42	Oil/foam interface
"	"	"	"	750	38	16	"

VARIABLE AIRFLOW FOAMING TEST DATA

Test No	Lubricant	Type Air Diffuser	Sample Volume (ml)	Airflow Rate (cc/min)	Oil Volume at Maximum Foam Height (ml)	Foam Volume (ml)	Remarks
11 (Cont'd)	0-82-2	ASTM # 1A	25	500	37	11	Oil/foam interface
12	0-82-2	13/16" Sparger (5 micron)	200	1000	250	17	Oil/foam interface
"	"	"	"	750	237	13	"
"	"	"	"	500	230	10	"
13	0-79-16	13/16" Sparger (5 micron)	200	1000	267	58	"
"	"	"	"	750	243	22	"
"	"	"	"	500	241	14	"
14	0-82-14	13/16" Sparger (5 micron)	200	1000	243	124	Oil/foam interface
"	"	"	"	750	255	47	"
"	"	"	"	500	235	23	"
15	0-79-20	13/16" Sparger (5 micron)	200	1000	247	16	Oil/foam interface
"	"	"	"	750	237	13	"

VARIABLE AIRFLOW FOAMING TEST DATA

Test No	Lubricant	Type Air Diffuser	Sample Volume (ml)	Airflow Rate (cc/min)	Oil Volume at Maximum Foam Height (ml)	Foam Volume (ml)	Remarks
15 (Cont'd)	0-79-20	13/16" Sparger (5 micron)	200	500	232	10	Oil/foam interface
16	0-79-20	13/16" Sparger (5 micron)	25	1000	17	56	All foam and aeration
"	"	"	"	900	35	27	Oil/foam interface
"	"	"	"	800	38	18	"
"	"	"	"	500	38	10	"
17	0-82-3	11/16" Sparger (5 micron)	25	1000	34	11	Oil/foam interface
"	"	"	"	750	33	9	"
"	"	"	"	500	32	8	"
18	0-82-3	13/16" Sparger (5 micron)	200	1000	236	15	Oil/foam interface
"	"	"	"	800	236	13	"
"	"	"	"	500	228	12	"
19	0-76-1 6ppm DC-200-20 cSt	13/16" Sparger (5 micron)	25	1000	14	72	All foam and aeration

VARIABLE AIRFLOW FOAMING TEST DATA

Test No	Lubricant	Type Air Diffuser	Sample Volume (ml)	Airflow Rate (cc/min)	Oil Volume at Maximum Foam Height (ml)	Foam Volume (ml)	Remarks
19 (Cont'd)	0-76-1 6ppm DC-200-20 cSt	13/16" Sparger (5 micron)	25	800	14	72	All foam and aeration
"	"	"	"	650	16	72	"
"	"	"	"	500	20	62	"
20	0-76-1 3 ppm DC-200-20 cSt	13/16" Sparger (5 micron)	25	1200	38	30	Oil/foam interface
"	"	"	"	1000	40	20	"
"	"	"	"	800	40	14	"
"	"	"	"	500	40	10	"
21	5K3L6	13/16" Sparger (5 micron)	25	1000	5	153	All foam and aeration
"	"	"	"	800	9	121	"
"	"	"	"	500	15	67	"
22	0-76-5 2% PANA 2% TCP	13/16" Sparger (5 micron)	25	1000	5	175	All foam and aeration (milkshaking)
"	"	"	"	800	5	149	"

VARIABLE AIRFLOW FOAMING TEST DATA

Test No	Lubricant	Type Air Diffuser	Sample Volume (ml)	Airflow Rate (cc/min)	Oil Volume at Maximum Foam Height (ml)	Foam Volume (ml)	Remarks
22 (Cont'd)	0-76-5 2% PANA 2% TCP	13/16" Sparger (5 micron)	25	500	12	88	All foam and aeration (milkshaking)
23	0-79-17 3 ppm DC-200-500 cSt	13/16" Sparger (5 micron)	25	1000	12	80	All foam and aeration (milkshaking)
"	"	"	"	800	16	60	"
"	"	"	"	500	36	15	Oil/foam interface
24	0-79-17	13/16" Sparger (5 micron)	25	1000	78	63	All foam and aeration
"	"	"	"	800	64	46	"
"	"	"	"	700	56	20	Oil/foam interface
"	"	"	"	500	48	10	"
25	0-79-17	11/16" Sparger (5 micron)	25	1000	45	8	Oil/foam interface
"	"	"	"	800	43	7	"
"	"	"	"	500	41	7	"

APPENDIX B

IRON CONCENTRATIONS AND PARTICLE SIZE DISTRIBUTIONS OF MICROFILTRATION SAMPLES

Appendix B contains spectrometric oil analysis results for iron concentrations and particle size distributions in samples obtained from six microfiltration tests.

TABLE B-1

SUMMARY OF VARIOUS ANALYTICAL TECHNIQUES
USED TO EVALUATE EFFECT OF MICROFILTRATION
ON IRON CONCENTRATION

Test No. 1
Fe Concentration, ppm

Sample	AA	AE	ADM	PWMA	WPA
A-1[a]	8	25	27	60	6
A-1	8	25	31	-	-
A-2	5	14	10	9	3
B-1	6	16	13	-	-
B-2	6	13	10	-	-
C-1	6	13	11	-	-
C-2	5	12	11	-	-
D-1	5	13	11	-	-
D-2	5	13	10	-	-

[a]Sample "pre-filter" directly from tank, all subsequent "pre-filter" samples taken from sampling valve.

Test No. 2
Fe Concentration, ppm

Sample	AA	AE	ADM	PWMA	WPA
A-1	15	93	61	61	18
A-2	12	54	28	34	-
B-1	14	62	36	-	-
B-2	13	51	28	-	-
C-1	13	62	32	-	-
C-2	13	51	28	-	-

Test No. 3
Fe Concentration, ppm

Sample	AA	AE	ADM	PWMA	WPA
A-1	9	32	13	15	2
A-2	8	27	1	13	1
B-1	9	28	12	-	1
B-2	8	26	11	-	1
C-1	8	28	12	-	-
C-2	8	26	11	-	-

Test No.4

Fe Concentration, ppm

Sample	AA	AE	ADM	PWMA	WPA
A-1	3	17	32	40	5(12)[a]
A-2	1	0	1	2	1
B-1	2	5	11	13	2(8)[a]
B-2	0	0	2	1	1
C-1	-	-	-	-	-
C-2	0	0	1	1	1
D-1	1	2	4	4	1
D-2	0	0	1	0	1

Test No. 5

Sample	AA	AE	ADM	PWMA	WPA
A-1	89	110	121	54	8(13)[a]
A-2	86	108	116	49	4(4)[a]
B-1	86	121	117	54	-
B-2	82	110	108	52	-
C-1	90	119	114	54	-
C-2	83	107	110	52	-
D-1	85	100	110	46	-
D-2	87	95	111	43	-

[a]WPA fast flow rate

Test No. 6
Fe Concentration, ppm

Sample	AA	AE	ADM	PWMA	WPA
A-1	5	13	9	10	3(2)[a]
A-2	4	11	6	5	1(1)[a]
B-1	4	12	6	7	-
B-2	4	10	6	5	-
C-1	4	11	6	5	-
C-2	4	10	5	4	-
D-1	4	10	6	5	-
D-2	4	10	6	4	-

[a]WPA fast flow rate

TABLE B-2

PARTICLE SIZE DISTRIBUTION OF IRON PARTICLES FROM MICROFILTRATION TESTS AS DETERMINED BY ADM, PWMA AND AE

Test No. 1
Fe Concentration, ppm

Sample (<μm)	ADM	PWMA	AE
A-1	27	60	25
A-1, 12	16	35	-
10	16	33	-
8	15	28	-
5	13	30	21
3	11	14	15
2	13	14	12
1	8	10	12
0.4	3	4	5
A-2	10	9	14
A-2, 12	8	9	-
10	9	9	-
8	9	9	-
5	9	9	12
3	8	8	14
2	10	7	13
1	8	5	10
0.4	4	2	6

Test No. 2
Fe Concentration, ppm

Sample (<μm)	ADM	PWMA	AE
A-1	61	61	91
A-1, 12	52	34	96
10	53	35	89
8	50	32	87
5	46	31	77
3	40	23	73
2	33	21	63
1	25	14	48
0.4	8	3	11
A-2	27	34	54
A-2, 12	27	33	52
10	26	33	50
8	27	34	49
5	26	33	54
3	28	38	38
2	24	34	44
1	18	23	32
0.4	5	4	7

Test No.3
Fe Concentration, ppm

Sample (<μm)	ADM	PWMA	AE
A-1	13	15	32
A-1, 12	12	14	32
10	11	14	28
8	12	15	33
5	12	11	31
3	11	17	30
2	13	14	33
1	10	17	28
0.4	1	1	3
A-2	11	13	27
A-2, 12	12	12	25
10	12	11	25
8	12	13	29
5	11	12	25
3	9	11	27
2	10	12	28
1	10	10	23
0.4	2	1	1

Test No. 4
Fe Concentration, ppm

Sample (<μm)	ADM	AE
A-1	32	17
A-1, 12	17	16
10	14	14
8	12	14
5	8	8
3	5	7
2	-	-
1	-	-
0.4	-	-
A-2	1	0
A-2, 12	2	0
10	-	-
8	-	-
5	-	-
3	2	0
2	2	0
1	1	0
0.4	2	0

Test No. 5
Fe Concentration, ppm

Sample	(<μm)	ADM	AE
A-1		121	110
A-1,	12	122	ND
	10	112	112
	8	113	ND
	5	112	104
	3	130	105
	2	94	89
	1	-	-
	0.4	-	-
A-2		116	108
A-2,	12	99	101
	10	102	109
	8	103	85
	5	104	84
	3	109	90
	2	105	87
	1	-	-
	0.4	-	-

Test No. 6
Fe Concentration, ppm

Sample	(<μm)	ADM	PWMA	AE
A-1		9	12	13
A-1,	12	-	-	-
	10	-	-	-
	8	-	-	-
	5	7	9	14
	3	7	8	13
	2	6	6	12
	1	5	6	10
	0.4	2	1	2
A-2		6	5	11
A-2,	12	-	-	-
	10	-	-	-
	8	-	-	-
	5	6	7	10
	3	6	5	10
	2	6	5	10
	1	6	4	9
	0.4	3	1	2

APPENDIX C

SCHEMATIC FOR RULLER CANDIDATE

Appendix C contains schematic and diagrams of universal single board voltammograph for the RULLER candidate.

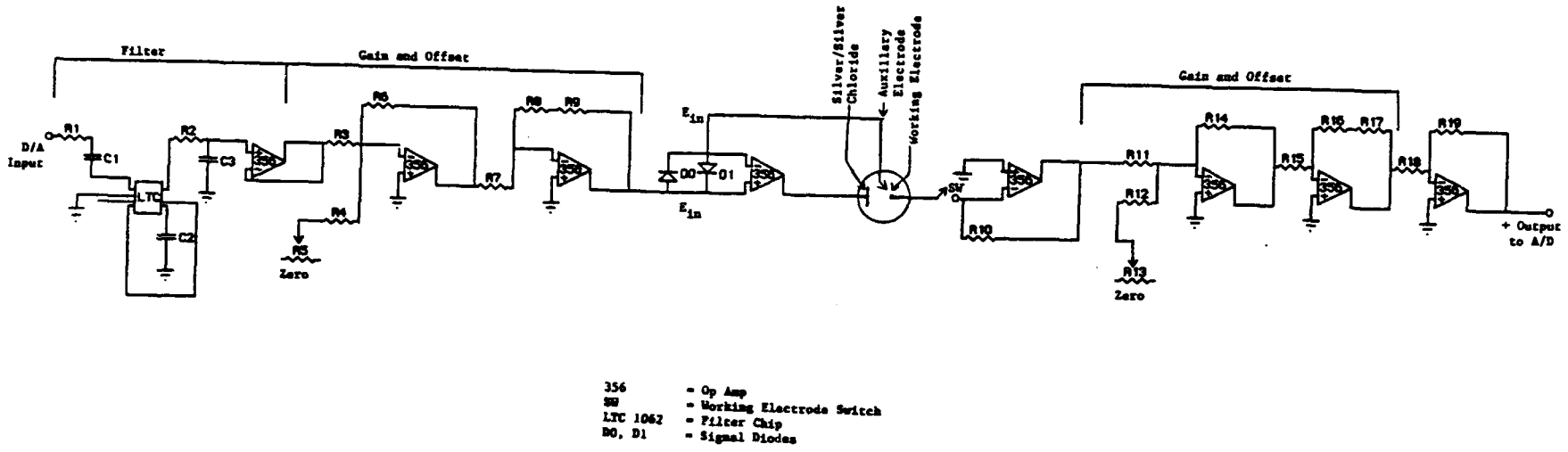

Figure C-1. Schematic of Universal Single Board Voltammograph

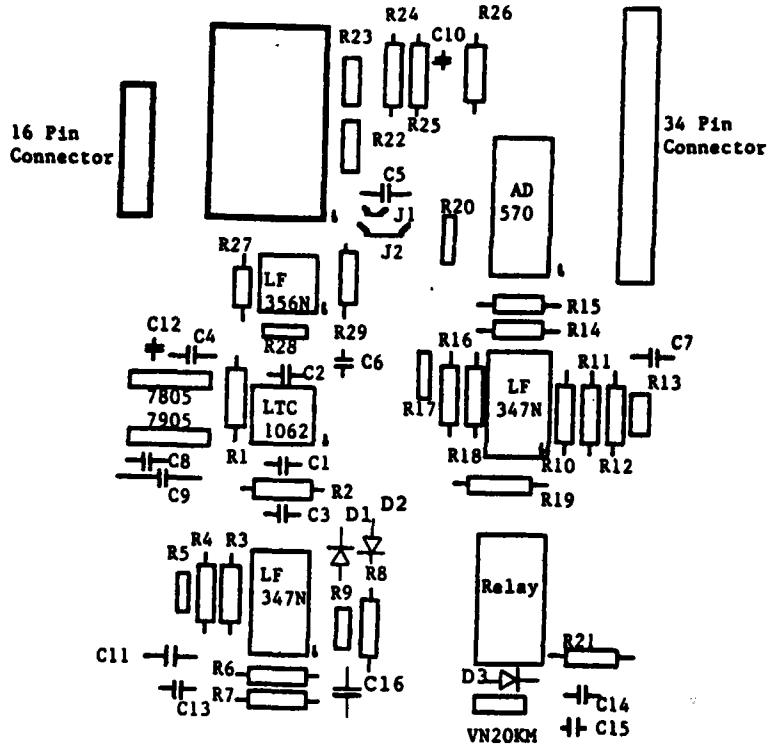

D1, D2, D3 = 1N4150 Diodes

R1 = 16.2 KΩ

R2 = 1 MΩ

R3, R6, R7, R10, R11, R14, R15, R18, R19 = 10 KΩ

R4, R24 = 100 KΩ

R5, R13, R17, R28 = 10 KΩ Trimpot

R8 = 11.5 KΩ

R9 = 2 K Trimpot

R12 = 24.9 KΩ

R16 = 95.3 KΩ

R20 = 200 Ω Trimpot

R21 = 68 Ω

R22 = 100Ω Trimpot

R23 = 50 KΩ Trimpot

R25, R26 = 100 KΩ

R27 = 681 Ω

R29 = 2.49 KΩ

C1, C5, C10, C11, C12, C13, C14, C15 = .1 μF

C4, C9 = 100 μF

C3 = 150 pF

C2, C7, C16 = 220 pF

J1, J2 = Jumpers

Figure C-2. Parts Diagram of Universal Single Board Voltammograph

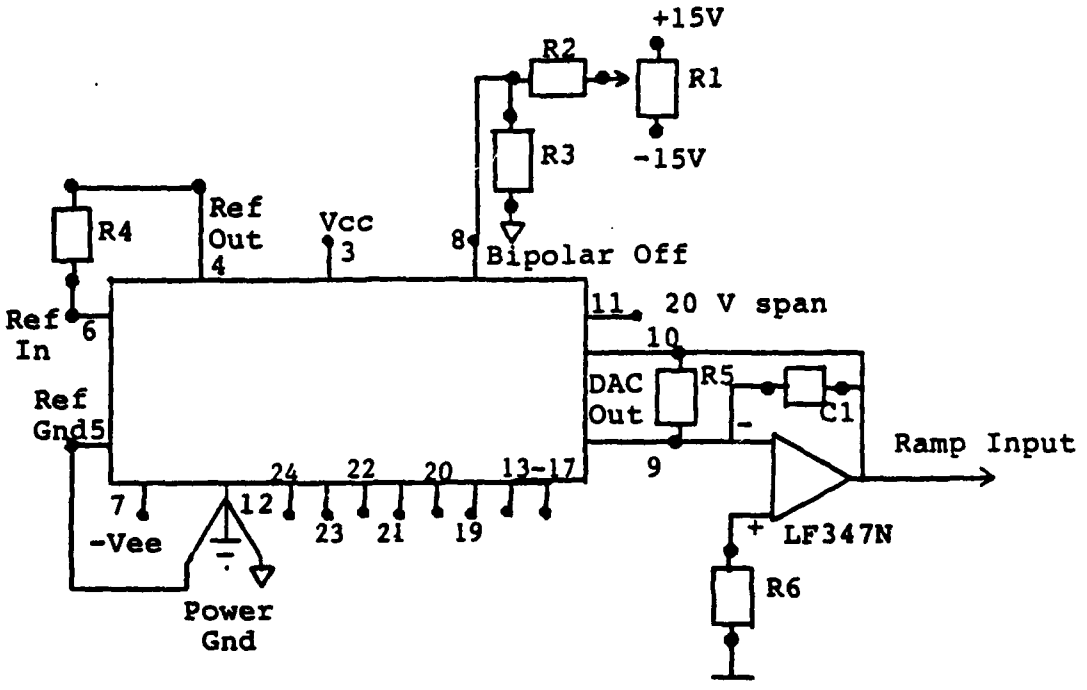

R1		= 50 KΩ
R2,	R3, R4	= 100 KΩ
R5		= 680 Ω
R6		= 2.4 KΩ
C1		= 10 pF

Figure C-3. Wiring Diagram of the Digital-to-Analog Microchip Connected to the Input of the Universal Single Board Voltammograph

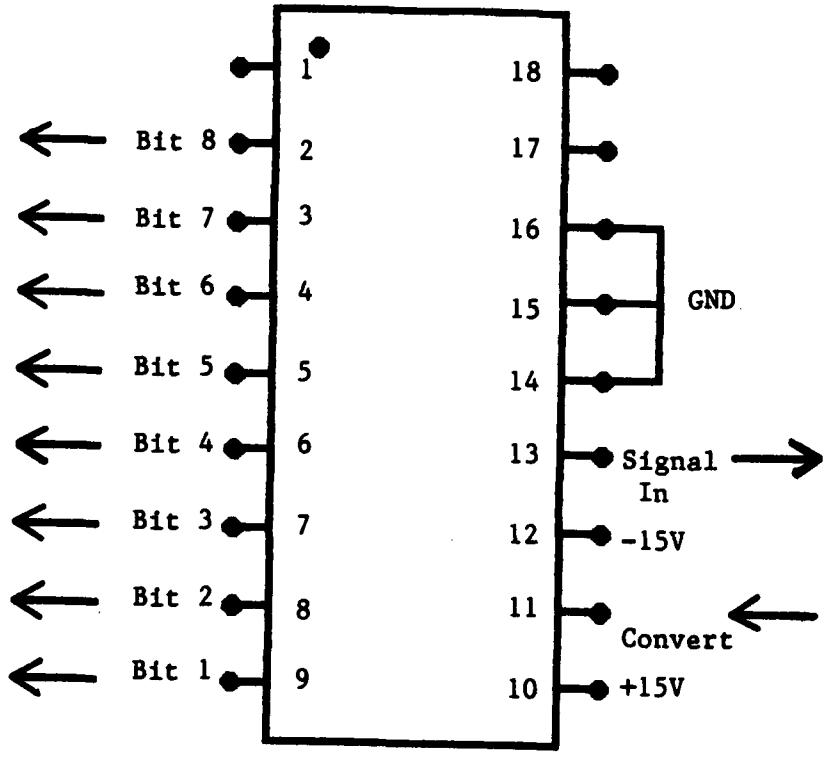

Figure C-4. Wiring Diagram of the Analog-to-Digital Microchip Connected to the Output of the Universal Single Board Voltammograph

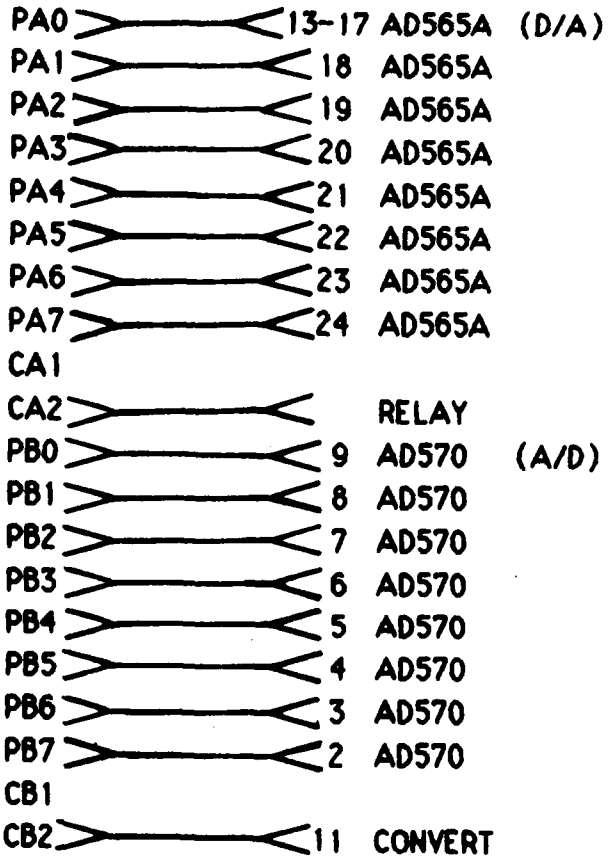

Figure C-5. Wiring Connections of the Parallel Interface Connected to the Digital-to-Analog (AD565A) and Analog-to-Digital (AD570) Microchips and to the Electrode Switch (Relay) of the Universal Single Board Voltammograph

Figure C-6

Laser Microcomputer Memory Map

Location		Description
Hex	Decimal	
$4000		Start data (Same as Apple)
$5200		End Data (Same as Apple)
$C0F1	-16143	Start A/D 12 Bit Conversion -5V-+5V SLOT=7
$C0F1	-16143	Read MSB A/D
$C0F0	-16144	Read LSB Data=MSB*16+LSB/16
$C0FA	-16134	LSB D/A
$C0FB	-16133	MSB D/A Writes Data to Port 0-10V 12 Bits
$C0F2	-16142	1 Bit TTL Poke 16 $10

APPENDIX D

CHARACTERIZATION OF STRESSED MIL-L-23699 TYPE OIL SAMPLES FOR RULLER STUDIES

1. INTRODUCTION

To develop the RULLER candidates, sets of stressed oil samples were prepared from the O-71-6, O-77-15, O-79-18 and TEL-7004 MIL-L-23699 type lubricating oils using Federal Test Method Standard 791B Method 5307.1 at a stressing temperature of 370°F as discussed in Section II.3. The stressed oil samples were thoroughly characterized by viscosity (40°C), total acid number (TAN), and COBRA measurements. The antioxidants in the stressed oil samples were identified and quantified by gas chromatography using a thermionic specific (nitrogen-phosphorous) detector.

The physical properties and antioxidant concentrations of the O-71-6, O-77-15, O-79-18 and TEL-7004 MIL-L-23699 type oils were then plotted versus stressing time at 370°F to determine the useful lives of the fresh oils. The relationships that exist among the physical properties, antioxidant concentrations, and the RUL of the different MIL-L-23699 type oils were then plotted.

2. PHYSICAL PROPERTIES OF THE MIL-L-23699 TYPE OILS STRESSED AT 370°F

a. O-71-6, O-77-15, and TEL-7004 Oils

The plots of the viscosity (40°C) and TAN versus stressing time are shown in Figure D-1 for the fresh and stressed O-71-6 and O-77-15 MIL-L-23699 type lubricating oils and in Figure D-2 for the fresh and stressed TEL-7004 MIL-L-23699 type lubricating oils. The plots of the COBRA readings did not exhibit breakpoints, and consequently, were not included in Figures D-1 and D-2.

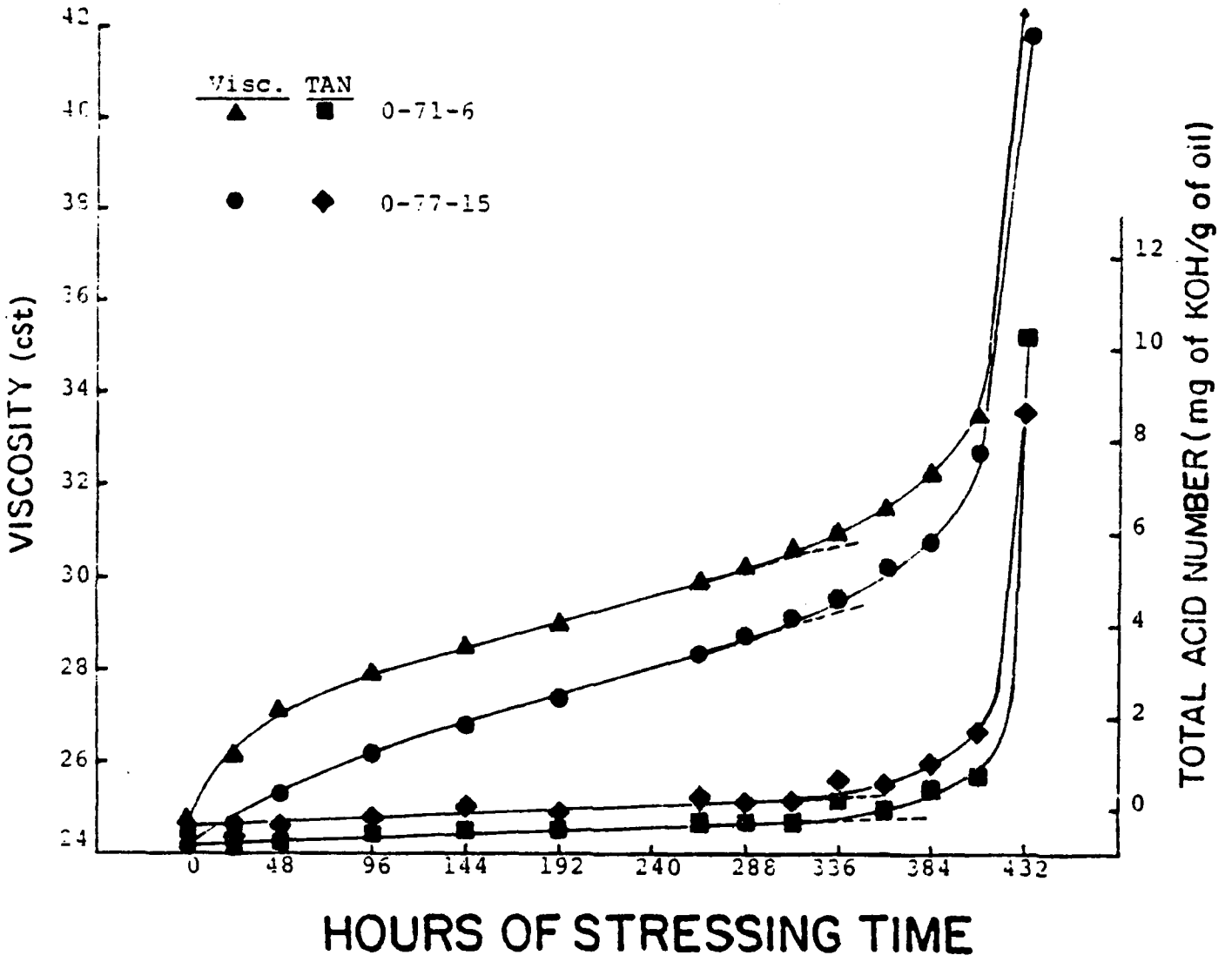

Figure D-1. Plots of the Viscosity (40°C) and Total Acid Number (TAN) Versus Hours of Stressing Time at 370°F for the Fresh and Stressed 0-71-6 and 0-77-15 MIL-L-23699 Type Oils

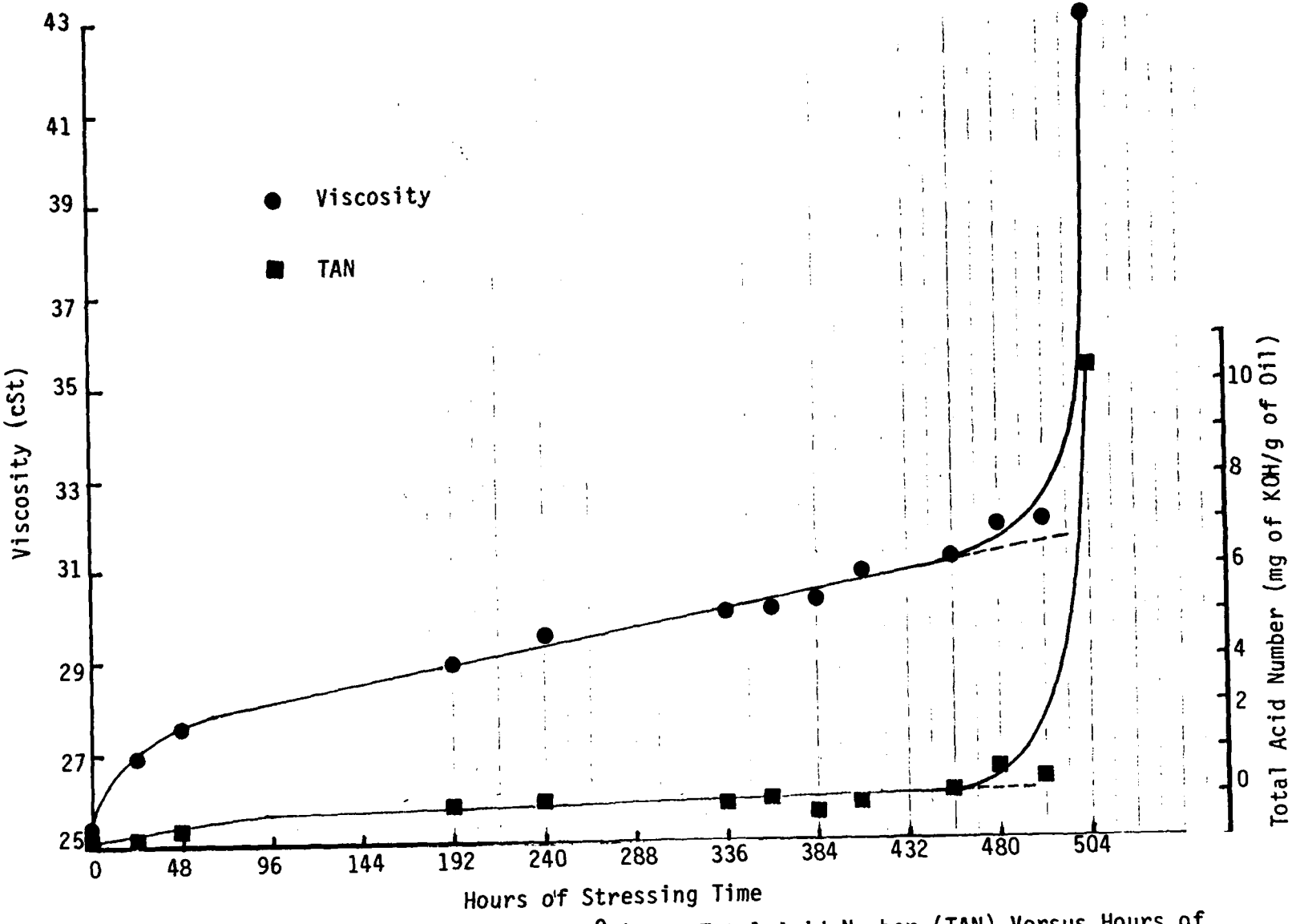

Figure D-2. Plots of the Viscosity (40°C) and Total Acid Number (TAN) Versus Hours of Stressing Time at 370°F for the Fresh and Stressed TEL-7004 MIL-L-23699 Type Oil

As seen in Figures D-1 and D-2, during the early hours of oxidative stressing the values of the oils' physical properties increase at moderate rates. After the initial rises in Figures D-1 and D-2, the values of the physical properties increase at much slower, steady rates up to the times of the dramatic rate increases that occur at the ends of the oils' useful lives.

To determine the stressing time at which the breakpoint occurs (oil's useful life ends), the flat portion of each physical property plot was extrapolated to a stressing time past the dramatic rate increase as shown in Figures D-1 and D-2. The stressing time at which the physical property plot diverges from the extrapolated plot is defined (for this study) as the breakpoint of the physical property plot. The useful lives of the fresh O-71-6, O-77-15 and TEL-7004 MIL-L-23699 type oils at 370°F [defined by the breakpoints of the viscosity (40°C) and TAN versus stressing time plots in Figures D-1 and D-2] were estimated to be 336, 336, and 456 hours respectively.

b. O-79-18 Oil

The plots of the viscosity (40°C) and TAN versus stressing time are shown in Figure D-3 for the fresh and stressed O-79-18 MIL-L-23699 type lubricating oils. COBRA readings also showed a breakpoint (Table 12) but were not included in Figure D-3.

As seen in Figure D-3, the values of the O-79-18 oils' physical properties increase at a moderate rate during the early hours of oxidative stressing. After the initial rise, the values of the TAN plot in Figure D-3 increase at a much slower, steady rate up to the stressing time of 672 hours. At 696 hours of stressing the TAN value of the stressed O-79-18 oil increases dramatically. Thus, extrapolation is not needed to determine the breakpoint of the TAN plot and a useful life of 672 hours at 370°F is assigned to the

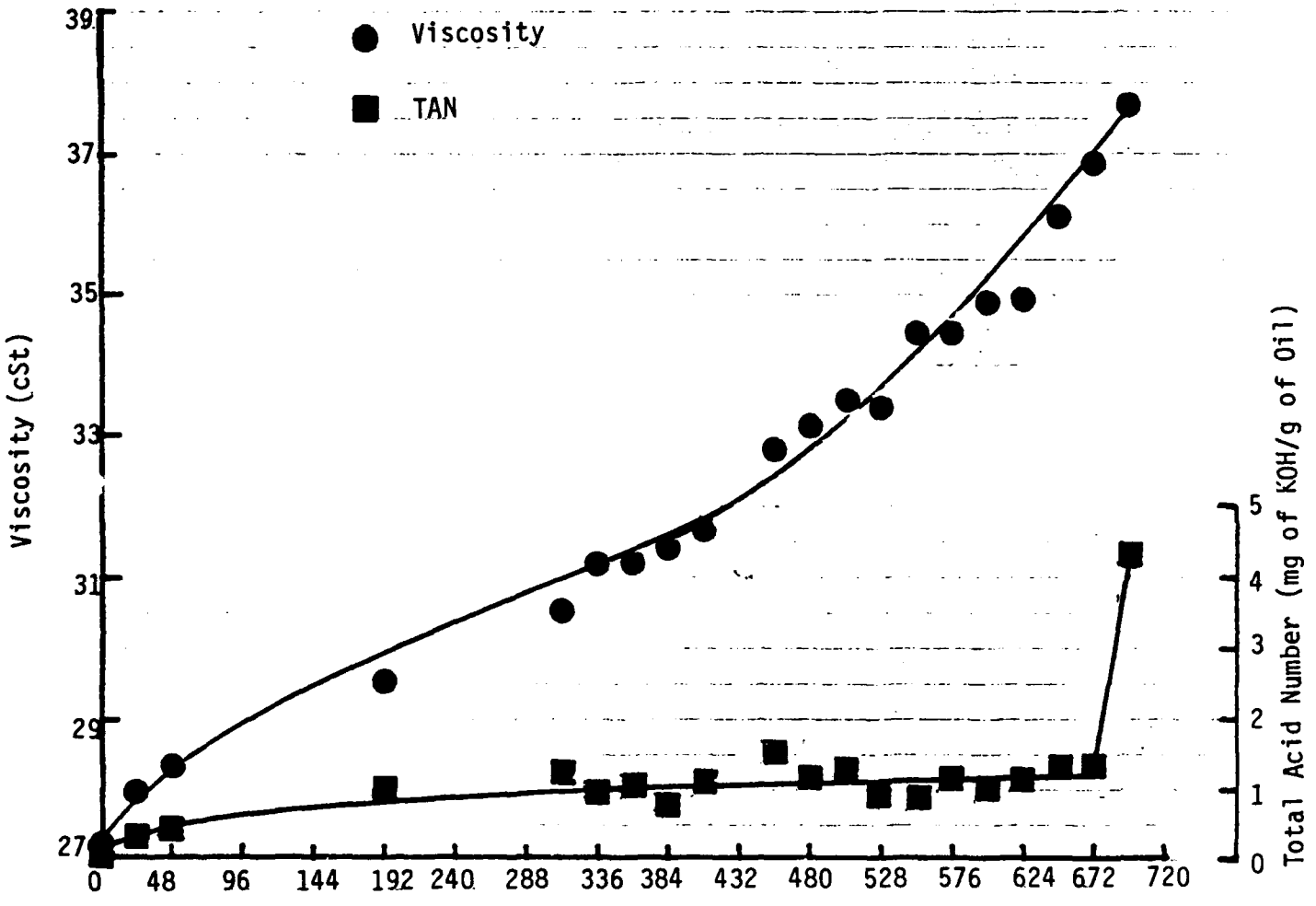

Figure D-3. Plots of the Viscosity (40°C) and Total Acid Number (TAN) Versus Hours of Stressing Time at 370°F for the Fresh and Stressed O -79-18 MIL-L-23699 Type Oil

fresh O-79-18 oil from the TAN plot.

In contrast to the TAN plot in Figure D-3 and the TAN and viscosity plots in Figures D-1 and D-2, the viscosity plot of the O-79-18 oils in Figure D-3 increases at a moderate rate during the entire oxidative stressing test. Therefore, an accurate useful life based on viscosity change cannot be determined from the viscosity property plots in Figure D-3. The TAN plot in Figure D-3 indicates that the useful life of the fresh O-79-18 oil is approximately 672 hours at 370°F.

3. SUMMARY OF THE MIL-L-23699 TYPE OILS' CHARACTERIZATION

The investigation to prepare and characterize the MIL-L-23699 type oils showed that the O-71-6, O-77-15, and TEL-7004 MIL-L-23699 type oils contain similar antioxidant systems resulting in similar useful lives at a stressing temperature of 370°F. The breakpoints of the viscosity and TAN plots in Figures D-1 and D-2 were used to estimate the useful lives of the O-71-6, O-77-15, and TEL-7004 MIL-L-23699 type oils to be 336, 336, and 456 hours at 370°F, respectively.

The investigation also showed that the antioxidant system of the O-79-18 oil is very different from those used in the other MIL-L-23699 type oils. The useful life of the O-79-18 oil is much greater than the useful lives of the other MIL-L-23699 type oils. However, the absence of a breakpoint in the viscosity plot of the O-79-18 oil (Figure D-3) and the wide scatter in the antioxidant analyses for the O-79-18 oil samples with greater than 336 hours of stressing time make the assignment of an exact useful life to the O-79-18 oil at 370°F uncertain. The results indicate that the useful life for the O-79-18 MIL-L-23699 type oil at 370°F is approximately 672 hours based on TAN breakpoint.

REFERENCES

1. Saba, C.S., Smith, H.A., Keller, M.A., Jain, V.K. and Kauffman, R.E., "Lubricant Performance and Evaluation," Interim Technical Report AFWAL-TR-87-2025, DDC No. AD A183881, June 1987.

2. Military Specification, MIL-L-87100 (USAF) Lubricating Oil, Aircraft Turbine Engine, Polyphenyl Ether Base

3. Cuellar, J.P. and Baber, B.B., "Evaluation Study of the Oxidation-Corrosion Characteristics of Aircraft Turbine Engine Lubricants," Report No. AFAPL-TR-70-10, Volumes I and II, May 1970.

4. Cundiff, R.H. and Markunas, P.C., "Tetrabutylammonium Hydroxide as Titrant for Acids in Nonaqueous Solutions," Anal. Chem., 28, p 792 (1956).

5. Wilson, G., Smith, J. and Stemniski, J., "Mechanism of Oxidation of Polyphenyl Ethers," AFML-TDR-64-98, December, 1963.

6. Stemniski, J.R., Wilson, G.R., Smith J.O. and McHugh, K.L., "Antioxidants for High Temperature Lubricants," ASLE Trans., 7, p 43 (1964).

7. Ravner, H., Russ, E.R. and Timmons, C.O.,"Antioxidant Action of Metals and Metal-Organic Salts in Fluoroesters and Polyphenyl Ethers," J. Chem. and Eng. Data, 8, p 591 (1963).

8. Ravner, H., Moniz, W. and Blachly, C., "High-Temperature Stabilization of Polyphenyl Ethers by Inorganic Salts," ASLE Transactions, 15, p 45 (1971).

9. Archer, W.L. and Bozer, K.B., "Oxidative Degradation of the Polyphenyl Ethers," Ind. Eng. Chem. Prod. Res. Develop., pp 145-149 (1966).

10. Ravner, H. and Kaufman, S., "High-Temperature Stabilization of Polyphenyl Ethers by Soluble Metal-Organic Salts," ASLE Trans., 18, p 1, (1975).

11. Butler, R.D., and Hoptins, V., "Research for Lubricant Evaluation Techniques, Lubricant-Bearing Evaluation," Midwest Research Institute Report No. MRI 3271-E, February 1972.

12. Bochartz, W., "Carbon Residue Studies with a Micro Carbon Residue Tester," Report No. AFWAL-TR-85-2099 (June 1986).

13. Worthington, K.I., "Evaluation of the Alcor Micro Carbon Residue Tester (MCRT)," Rolls-Royce Report No. ESL 11474, 20 May 1986.

14. Rhine, W.E., Saba, C.S., Kauffman, R.E., Brown, J.R. and Fair, P.S., "Evaluation of Plasma Source Spectrometers for the Air Force Oil Analysis Program," Report No. AFWAL-TR-82-4017, February 1982.

15. Jones, Jr., W.R. and Lowenthal, S.H., "Analysis of Wear Debris from Full-Scale Bearing Fatigue Tests Using the Ferrograph," ASLE Trans., 24, p 323 (1980).

16. Eisentraut, K.J., Newman, R.W., Saba, C.S., Kauffman, R.E. and Rhine, W.E., "Spectrometric Oil Analysis," Anal. Chem., 56, p 1086A (1984).

17. Rhine, W.E., Saba, C.S. and Kauffman, R.E., "Spectrometer Sensitivity Investigations on the Spectrometric Oil Analysis Program," Report No. NAEC-92-169, April 1983.

18. Lynch, C.W. and Cooper, R.B., "The Development of a Three-Micron Absolute Main Oil Filter for the T53 Gas Turbine," ASME Journal of Lubrication Technology, 93, p 430 (1971).

19. Tauber, T., Hudgins, W.A. and Lee, R.S., "Oil Debris Assessment and Fine Filtration in Helicopter Propulsion Systems," Oil Analysis Workshop-Symposium, Pensacola, Florida, May 1983.

20. Wansong, J.F., "T700 Engine-Designed for the Pilot and Mechanic" Presented at the 39th Annual Forum of the American Helicopter Society, May 9-11, 1983.

21. Quinn, M.J., "New Device for Analysis of Metal Particles in Oil, Wear, 120, pp 369-381 (1987).

22. Rhine, W.E., Saba, C.S. and Kauffman, R.E., "Metal Particle Detection Capabilities of Rotating Disk Emission Spectrometer," Lubr. Engin., 42, p 755 (1986).

23. Lewis, R.T., "The Wear Particle Analyzer," Presented at the 41st Meeting of the Mechanical Failures Prevention Group. Oct 28-30, 1986, Patuxent River, Maryland.

24. Lewis, R.T., "Analysis of Ferrous Wear Debris," Proceedings of an International Conference on Condition Monitoring Held at the University College of Swansea, 31st March - 3rd April, 1987, Ed. Mervin H. Jones, p. 360.

25. Lewis, R.T., "Application of Magnetization Measurements to Wear Analysis," Presented at the International Conference of Wear of Materials, San Francisco, CA, March 30-April 1, 1981.

26. Kauffman, R.E., Saba, C.S., Rhine, W.E. and Eisentraut, K.J., "Quantitative Multielement Determination of Metallic Wear Species in Lubricating Oils and Hydraulic Fluids," Anal. Chem., 54, p 975 (1982).

27. Kauffman, R.E., Saba, C.S., Rhine, W.E. and Eisentraut, K.J., "Chemical Nature of Wear Debris," STLE Trans., 28, p 400 (1985).

28. Westcott, V.C. and Seifert, W.W., "Investigation of Iron Content of Lubricating Oil Using a Ferrograph and an Emission Spectrometer," Wear, 23, p 239 (1973).

29. Rhine, W.E., Saba, C.S., Kauffman, R.E., Brown, J.R. and Fair, P.S., "Research and Development on Wear Metal Analysis," AFWAL-TR-81-4184, January 1982.

30. "Handbook of Chemistry and Physics," CRC Press Inc., Boca Raton, 64th Edition (1985), Ed. Weast, Robert C.

31. Smith, H.A., "Lubricant Monitoring Using the Complete Oil Breakdown Rate Analyzer (COBRA)," Report No. AFAPL-TR-82-2109, DDC No. AD B073132, March 1983.

32. Bronshtein, L.A., Shekhter, Yo. N. and Shkol'nikov, V.M., "Mechanism of Electrical Conduction in Lubricating Oils (Review)," Khim Tekhnol. topl. Masel, 5, pp 36-40 (1979).

33. Andrews, L.J., "Aromatic Molecular Complexes of the Electron Donor-Acceptor Type," Chem. Rev., 54, pp 713-776 (1954).

34. Parine, V.P., "Organic Charge-Transfer Complexes," Russ. Chem. Rev., 31, pp 408-417 (1962).

35. Rao, N., Maciejewski, A. and Senholzi, D., "Precision Measurement of Gear Lubricant Load-Carrying Capacity (Feasibility Study)," Report No. AFWAL-TR-81-2107, (DTIC AD-A110289), November, 1981.

36. Voitik, R.M. and Heerdt, L.R., "Wear and Friction Evaluation of Gear Lubricants by Bench Test," Lubri. Eng., 40, p 719 (1984).

37. Zaskal'ko, P.P., Nekrasdu, V.I. and Terekhou, A.S., "Correlation Indices of Extreme-Pressure Properties of Oils when Evaluated in Four-Ball Friction Tester and in IAE Gear Machine," Translated from Khimiya: Tekhnologiya Topliv i. Masel, No. 4, pp 40-44, April 1978.

38. Jain, V.K., Wright, M.S. and Saba, C.S., "Evaluation of Ester Base Lubricants Using a Four Ball Machine," Presented at the STLE Annual Meeting May 9-12, Cleveland, OH, Preprint No. 88-AM-8D-1.

39. Bos, A., "Wear in the Four-Ball Apparatus: Relationship Between the Displacement of the Upper Ball and the Diameter of the Wear Scars on the Lower Balls," Wear, 41, pp 191-194 (1977).

40. Feng, I-Ming, "A New Approach in Interpreting the Four Ball-Wear Results," Wear, 5, pp 275-288 (1962).

41. Willermet, P.A., and Kandah, S.K., "Wear Asymmetry - A Comparison of the Wear Volumes of the Rotating and Stationary Balls in the Four-Ball Machine," ASLE Trans., 26, pp 173-178 (1983).

42. Anderson, J.E., et al., "Inexpensive Microprocessor - Based Technology," American Laboratory, 13, p 21 (1981).

43. Anderson, J.E. and Bond, A.M., "Microprocessor - Controlled Instrument for the Simultaneous Generation of Square Wave, Alternating Current, Direct Current, and Pulse Polarograms," Anal. Chem., 55, p 1934. (1983).

44. Myers, R.L. and Shain, I., "A Solid-State Signal Generator for Electroanalytical Experiments," Chem. Instrumentation, 2, p 203 (1969).

45. Naval Air Systems Command Report No. NA 17-15-50 of 1 May 1977: Joint Oil Analysis Program Laboratory Manual.

46. Kauffman, R.E. and Rhine, W.E., "Characterization of the Arc/ Spark Excitation Sources Used in the Spectrometric Oil Analysis Program," Report No. NAEC-92-191, October 1987.

47. Kauffman, R.E. and Rhine, W.E., "Assessment of Remaining Lubricant Life," Report No. AFWAL-TR-86-2024, November 1986.

*U.S.Government Printing Office: 1989 — 648-056/04327